International Journal of
Molecular Sciences

Special Issue Reprint

Advances in Neurodegenerative Diseases Research and Therapy

Third Edition

Edited by
Sumonto Mitra

mdpi.com/journal/ijms

MDPI

Advances in Neurodegenerative Diseases Research and Therapy—Third Edition

Advances in Neurodegenerative Diseases Research and Therapy—Third Edition

Guest Editor

Sumonto Mitra

MDPI

Basel • Beijing • Wuhan • Barcelona • Belgrade • Novi Sad • Cluj • Manchester

Guest Editor
Sumonto Mitra
NVS Department
Karolinska Institutet
Huddinge
Sweden

Editorial Office
MDPI AG
Grosspeteranlage 5
4052 Basel, Switzerland

This is a reprint of the Special Issue, published open access by the journal *International Journal of Molecular Sciences* (ISSN 1422-0067), freely accessible at: https://www.mdpi.com/journal/ijms/special_issues/1SIE1D4849.

For citation purposes, cite each article independently as indicated on the article page online and as indicated below:

Lastname, A.A.; Lastname, B.B. Article Title. *Journal Name* **Year**, *Volume Number*, Page Range.

ISBN 978-3-7258-9275-4 (Hbk)
ISBN 978-3-7258-9276-1 (PDF)
https://doi.org/10.3390/books978-3-7258-9276-1

© 2026 by the authors. Articles in this reprint are Open Access and distributed under the Creative Commons Attribution (CC BY) license. The reprint as a whole is distributed by MDPI under the terms and conditions of the Creative Commons Attribution-NonCommercial-NoDerivs (CC BY-NC-ND) license (https://creativecommons.org/licenses/by-nc-nd/4.0/).

Contents

About the Editor . . . . . **vii**

Sumonto Mitra
Special Issue "Advances in Neurodegenerative Diseases Research and Therapy—Third Edition"
Reprinted from: *Int. J. Mol. Sci.* **2026**, *27*, 8267, https://doi.org/10.3390/ijms27188267 . . . . . **1**

Ida Manna, Selene De Benedittis and Danilo Porro
A Comprehensive Examination of the Role of Epigenetic Factors in Multiple Sclerosis
Reprinted from: *Int. J. Mol. Sci.* **2024**, *25*, 8921, https://doi.org/10.3390/ijms25168921 . . . . . **5**

Davide Pietrafesa, Alessia Casamassa, Barbara Benassi, Massimo Santoro, Massimo Marano, Claudia Consales, et al.
Investigating the Impact of the Parkinson's-Associated GBA1 E326K Mutation on β-Glucocerebrosidase Dimerization and Interactome Dynamics Through an In Silico Approach
Reprinted from: *Int. J. Mol. Sci.* **2024**, *25*, 11443, https://doi.org/10.3390/ijms252111443 . . . . . **26**

Lorenza Brusini, Giorgio Dolci, Lorenzo Pini, Federica Cruciani, Fabrizio Pizzagalli, Paolo Provero, et al.
Morphometric Similarity Patterning of Amyloid-β and Tau Proteins Correlates with Transcriptomics in the Alzheimer's Disease Continuum
Reprinted from: *Int. J. Mol. Sci.* **2024**, *25*, 12871, https://doi.org/10.3390/ijms252312871 . . . . . **43**

Melissa Vos, Fabian Ott, Hawwi Gillo, Giuliana Cesare, Sophie Misera, Hauke Busch and Christine Klein
Endoplasmic Reticulum Proteins Impact Penetrance in a *Pink1*-Mutant *Drosophila* Model
Reprinted from: *Int. J. Mol. Sci.* **2025**, *26*, 979, https://doi.org/10.3390/ijms26030979 . . . . . **59**

Ewelina Palasz, Anna Gasiorowska-Bien, Patrycja Drapich, Wiktor Niewiadomski and Grazyna Niewiadomska
Steady Moderate Exercise Confers Resilience Against Neurodegeneration and Neuroinflammation in a Mouse Model of Parkinson's Disease
Reprinted from: *Int. J. Mol. Sci.* **2025**, *26*, 1146, https://doi.org/10.3390/ijms26031146 . . . . . **72**

Piotr Alster and Natalia Madetko-Alster
The Genetic Background of the Immunological and Inflammatory Aspects of Progressive Supranuclear Palsy
Reprinted from: *Int. J. Mol. Sci.* **2025**, *26*, 3927, https://doi.org/10.3390/ijms26093927 . . . . . **97**

Dominika Przewodowska, Piotr Alster and Natalia Madetko-Alster
Role of the Intestinal Microbiota in the Molecular Pathogenesis of Atypical Parkinsonian Syndromes
Reprinted from: *Int. J. Mol. Sci.* **2025**, *26*, 3928, https://doi.org/10.3390/ijms26093928 . . . . . **107**

Gonzalo Olmedo-Saura, Eugenio Bernardi, Lidia Bojtos, Saül Martínez-Horta, Javier Pagonabarraga, Jaime Kulisevsky and Jesús Pérez-Pérez
Update on the Symptomatic Treatment of Huntington's Disease: From Pathophysiology to Clinical Practice
Reprinted from: *Int. J. Mol. Sci.* **2025**, *26*, 6220, https://doi.org/10.3390/ijms26136220 . . . . . **131**

María Martín-Rico, Blanca Salgado, Inés Beamonte, Isabel Sastre, María J. Bullido and Jesús Aldudo
Impact of HSV-1 Infection on Alzheimer's Disease Neurodegeneration Markers: Insights from LUHMES 2D and 3D Neuronal Models
Reprinted from: *Int. J. Mol. Sci.* **2026**, *27*, 642, https://doi.org/10.3390/ijms27020642 . . . . . **163**

About the Editor

Sumonto Mitra

Sumonto Mitra is an academic researcher currently serving as a Researcher at the Department of Neurobiology, Care Sciences and Society (NVS), Karolinska Institutet, Stockholm, Sweden. He is a biochemist and neuroscientist by training, and his primary research centers on neurotrophin metabolism, the cholinergic system, and therapy development in the context of Alzheimer's disease.

International Journal of
Molecular Sciences

MDPI

Editorial

Special Issue "Advances in Neurodegenerative Diseases Research and Therapy—Third Edition"

Sumonto Mitra

Division of Clinical Geriatrics, Center for Alzheimer Research, Department of NVS, Karolinska Institutet, 141 52 Huddinge, Sweden; sumonto.mitra@ki.se

Neurodegenerative diseases remain among the most pressing biomedical challenges of the twenty-first century. Despite decades of research, disorders such as Alzheimer's disease (AD), Parkinson's disease (PD), progressive supranuclear palsy (PSP), multiple sclerosis (MS), Huntington disease (HD) and related neurodegenerative conditions continue to affect millions of individuals worldwide, while effective disease-modifying therapies remain limited. Traditionally, these disorders have been defined by distinct pathological hallmarks, including amyloid-β and tau aggregates in AD and α-synuclein inclusions in PD and related synucleinopathies. However, growing evidence suggests that these pathological signatures represent only one dimension of a far more complex biological landscape involving cellular homeostasis, neuroimmune regulation, environmental exposures, and systemic biological interactions [1–5].

There is a growing recognition that disruptions of intracellular homeostasis represent common drivers of neurodegenerative disease. Increasing evidence implicates autophagy, lysosomal degradation, protein trafficking, mitochondrial maintenance, and endoplasmic reticulum (ER) function as central determinants of neuronal health [4,5]. The study by Martín-Rico et al. (Contribution 1), investigating Herpes simplex virus type 1 (HSV-1) infection in human 2D and 3D LUHMES in vitro neuronal models, exemplifies this concept by demonstrating that viral infection induces intracellular amyloid accumulation, tau hyperphosphorylation, and impairment of the autophagy–lysosome pathway. These observations not only provide mechanistic support for environmental contributions to neurodegeneration but also highlight the vulnerability of neuronal clearance mechanisms to external biological stressors.

Equally important is the recognition that neurodegeneration is fundamentally a multicellular process. While early disease models focused primarily on neuronal dysfunction, contemporary research has increasingly demonstrated the participation of astrocytes, microglia, oligodendrocytes, vascular cells, and peripheral immune systems in disease progression [6–8]. The imaging-transcriptomic study by Brusini et al. (Contribution 2) illustrates this paradigm by linking amyloid-β and tau-associated cortical remodelling to gene-expression profiles enriched in immune pathways and glial cell signatures among AD patients. The identification of astrocytes, microglia, and oligodendrocyte precursor cells as key biological correlates of structural brain alterations further supports the concept that neurodegeneration emerges from coordinated dysfunction across multiple cell populations rather than neuronal pathology alone.

Complementing these findings, the analysis by Vos et al. (Contribution 3) of reduced penetrance in Pink1-mutant Drosophila identifies ER-associated proteins as modifiers of disease expression, emphasizing that cellular stress-response pathways can actively

influence disease outcomes. Collectively, these studies reinforce a growing consensus that failures in proteostasis and intracellular quality-control networks constitute a common biological foundation across seemingly distinct neurodegenerative disorders. Similarly, Pietrafesa et al. (Contribution 4) reported the molecular dynamics investigation of the Parkinson's disease-associated genetic mutation in GBA1 E326K variant and demonstrates how subtle alterations in lysosomal protein interactions may have consequences that extend far beyond enzymatic activity alone. By affecting interactions with α-synuclein, saposin C, and LIMP-2, this study highlights the importance of intracellular trafficking and lysosomal organization in disease pathogenesis. This perspective is further strengthened by the review examining the genetic background of inflammatory mechanisms in PSP (Alster and Madetko-Alster (Contribution 5)). Although PSP has historically been considered primarily a tauopathy, accumulating evidence suggests that microglial activation and immune-related pathways may play central roles in disease susceptibility and progression.

Increasingly, neurodegenerative diseases are recognized as the product of complex interactions between genetic susceptibility and environmental exposures. This concept is exemplified by the HSV-1 study (Martín-Rico et al.), which highlights the potential consequences of viral infection on neuronal homeostasis and modifying AD pathological markers, and by the comprehensive review exploring the role of the gut microbiota in atypical Parkinsonian syndromes (Przewodowska et al. (Contribution 6)). Through its effects on immune regulation, metabolism, vitamin synthesis, and gut–brain communication, the intestinal microbiome has emerged as a potentially important modulator of neurodegenerative processes. These observations are consistent with growing evidence that the gut–brain axis contributes to neurological disease through bidirectional interactions involving microbial metabolites, inflammatory signalling, and neural pathways [9,10].

The review by Manna et al. (Contribution 7) addressing epigenetic mechanisms in MS further expands this framework by emphasizing the importance of gene–environment interactions. Epigenetic regulation may provide a mechanistic bridge between inherited susceptibility and environmental influences, contributing to disease heterogeneity and progression. Together, these contributions suggest that future models of neurodegeneration must account not only for central nervous system pathology but also for the cumulative influence of infectious exposures, microbiome dynamics, immune responses, metabolism, lifestyle, and aging. In this context, the concept of an individual's neurological exposome may offer a useful framework for understanding disease risk across the lifespan.

Historically, neurodegenerative disease research has focused on identifying mechanisms that drive neuronal injury and death. However, an equally important question is increasingly gaining prominence: why do certain individuals or neuronal populations remain resistant despite substantial pathological burden? Understanding resilience may ultimately prove as important as understanding disease itself.

The study by Palasz et al. (Contribution 8) demonstrating that moderate aerobic exercise confers neuroprotection in an MPTP model of Parkinson's disease provides an important example. By preserving dopaminergic neurons, enhancing BDNF and GDNF levels, and suppressing inflammation, moderate exercise produced robust neuroprotective effects comparable to those observed following more intense training paradigms. These findings are particularly encouraging because they suggest that clinically feasible interventions can meaningfully influence disease-relevant biological pathways. Likewise, the identification of ER-associated modifiers that reduce phenotypic expression in Pink1-deficient flies illustrates that endogenous protective mechanisms can substantially alter disease outcomes. Together, these studies shift attention from pathology alone toward a more balanced understanding of vulnerability and resilience. Another review by Olmedo-Saura et al. (Contribution 9)

https://doi.org/10.3390/ijms27188267

represents the current landscape of the various aspects of available treatments and clinical considerations for HD, including physical interventions and pharmacological approaches.

Future therapeutic strategies may increasingly focus on enhancing resilience mechanisms rather than exclusively attempting to eliminate pathological proteins. Neurotrophic signalling, metabolic adaptation, immune homeostasis, stress resistance, and adaptive network plasticity may emerge as critical therapeutic targets. In the coming years, biomarkers of resilience may become as valuable as biomarkers of pathology, enabling earlier and more individualized interventions aimed at preserving neuronal function before irreversible degeneration occurs.

Beyond their biological insights, the studies in this Special Issue collectively highlight the technological transformation currently reshaping neuroscience. Human-relevant 3D neuronal cultures, imaging transcriptomics, computational modelling, molecular dynamics simulations, and systems-level analyses are providing unprecedented opportunities to investigate disease mechanisms across multiple scales of biological organization. The 3D LUHMES platform for studying virus-induced neurodegeneration, the integration of neuroimaging and transcriptomics to characterize AD-related cortical remodelling, and the computational interrogation of Parkinson's disease-associated mutations all exemplify how technological innovation is accelerating mechanistic discovery. Distinct diseases may ultimately be stratified according to shared patterns of proteostatic dysfunction, neuroimmune activation, environmental exposure, or resilience. Such a framework offers the potential to transform diagnosis, improve patient stratification, and facilitate the development of targeted disease-modifying therapies.

The contributions assembled in "Advances in Neurodegenerative Diseases Research and Therapy—Third Edition" collectively illustrate a major conceptual shift occurring across the field. Rather than viewing neurodegenerative diseases as isolated clinical entities, the studies included in this Special Issue reveal convergence across multiple biological networks that regulate neuronal vulnerability and resilience. Together, they support an emerging systems-level framework in which neurodegeneration is understood as the consequence of dynamic interactions among various processes. Simultaneously, growing recognition of resilience mechanisms is shifting the focus from why neurons die toward how they can be protected. The studies assembled in this Special Issue contribute meaningfully to this evolution and underscore the exciting opportunities that lie ahead for neurodegenerative disease research and therapy.

Acknowledgments: The Special Issue Guest Editor sincerely appreciates the efforts from all the authors in preparing their manuscript, reviewers for their insightful comments in a timely and constructive manner, and to the *IJMS* editorial team for their support.

Conflicts of Interest: The author declares no conflicts of interest.

List of Contributions

1. Martín-Rico, M.; Salgado, B.; Beamonte, I.; Sastre, I.; Bullido, M.J.; Aldudo, J. Impact of HSV-1 Infection on Alzheimer's Disease Neurodegeneration Markers: Insights from LUHMES 2D and 3D Neuronal Models. *Int. J. Mol. Sci.* 2026, *27*, 642. https://doi.org/10.3390/ijms27020642.
2. Brusini, L.; Dolci, G.; Pini, L.; Cruciani, F.; Pizzagalli, F.; Provero, P.; Menegaz, G.; Galazzo, I.B. Morphometric Similarity Patterning of Amyloid-β and Tau Proteins Correlates with Transcriptomics in the Alzheimer's Disease Continuum. *Int. J. Mol. Sci.* 2024, *25*, 12871. https://doi.org/10.3390/ijms252312871.
3. Vos, M.; Ott, F.; Gillo, H.; Cesare, G.; Misera, S.; Busch, H.; Klein, C. Endoplasmic Reticulum Proteins Impact Penetrance in a *Pink1*-Mutant *Drosophila* Model. *Int. J. Mol. Sci.* 2025, *26*, 979. https://doi.org/10.3390/ijms26030979.
4. Pietrafesa, D.; Casamassa, A.; Benassi, B.; Santoro, M.; Marano, M.; Consales, C.; Rosati, J.; Arcangeli, C. Investigating the Impact of the Parkinson's-Associated GBA1 E326K Mutation on

β-Glucocerebrosidase Dimerization and Interactome Dynamics Through an In Silico Approach. *Int. J. Mol. Sci.* 2024, *25*, 11443. https://doi.org/10.3390/ijms252111443.
5. Alster, P.; Madetko-Alster, N. The Genetic Background of the Immunological and Inflammatory Aspects of Progressive Supranuclear Palsy. *Int. J. Mol. Sci.* 2025, *26*, 3927. https://doi.org/10.3390/ijms26093927.
6. Przewodowska, D.; Alster, P.; Madetko-Alster, N. Role of the Intestinal Microbiota in the Molecular Pathogenesis of Atypical Parkinsonian Syndromes. *Int. J. Mol. Sci.* 2025, *26*, 3928. https://doi.org/10.3390/ijms26093928.
7. Manna, I.; De Benedittis, S.; Porro, D. A Comprehensive Examination of the Role of Epigenetic Factors in Multiple Sclerosis. *Int. J. Mol. Sci.* 2024, *25*, 8921. https://doi.org/10.3390/ijms25168921.
8. Palasz, E.; Gasiorowska-Bien, A.; Drapich, P.; Niewiadomski, W.; Niewiadomska, G. Steady Moderate Exercise Confers Resilience Against Neurodegeneration and Neuroinflammation in a Mouse Model of Parkinson's Disease. *Int. J. Mol. Sci.* 2025, *26*, 1146. https://doi.org/10.3390/ijms26031146.
9. Olmedo-Saura, G.; Bernardi, E.; Bojtos, L.; Martínez-Horta, S.; Pagonabarraga, J.; Kulisevsky, J.; Pérez-Pérez, J. Update on the Symptomatic Treatment of Huntington's Disease: From Pathophysiology to Clinical Practice. *Int. J. Mol. Sci.* 2025, *26*, 6220. https://doi.org/10.3390/ijms26136220.

References

1. Hardy, J.; Selkoe, D.J. The amyloid hypothesis of Alzheimer's disease: Progress and problems on the road to therapeutics. *Science* **2002**, *297*, 353–356. [CrossRef] [PubMed]
2. Spillantini, M.G.; Schmidt, M.L.; Lee, V.M.; Trojanowski, J.Q.; Jakes, R.; Goedert, M. Alpha-synuclein in Lewy bodies. *Nature* **1997**, *388*, 839–840. [CrossRef] [PubMed]
3. Heneka, M.T.; van der Flier, W.M.; Jessen, F.; Hoozemanns, J.; Thal, D.R.; Boche, D.; Brosseron, F.; Teunissen, C.; Zetterberg, H.; Jacobs, A.H.; et al. Neuroinflammation in Alzheimer disease. *Nat. Rev. Immunol.* **2025**, *25*, 321–352. [CrossRef] [PubMed]
4. De Strooper, B.; Karran, E. The Cellular Phase of Alzheimer's Disease. *Cell* **2016**, *164*, 603–615. [CrossRef] [PubMed]
5. Nixon, R.A. The role of autophagy in neurodegenerative disease. *Nat. Med.* **2013**, *19*, 983–997. [CrossRef] [PubMed]
6. Mitchener, V.F.T.; Thackray, M.J.; Arancibia-Carcamo, I.L. The glia-immune network: Astrocytes and oligodendrocytes as microglial co-ordinators in health and disease. *J. Physiol.* **2026**, *604*, 1558–1574. [CrossRef] [PubMed]
7. Latour, Y.L.; McGavern, D.B. Immune signaling and function in neurodegeneration. *J. Clin. Investig.* **2026**, *136*, e199850. [CrossRef] [PubMed]
8. Wilson, D.M., III; Cookson, M.R.; Van Den Bosch, L.; Zetterberg, H.; Holtzman, D.M.; Dewachter, I. Hallmarks of neurodegenerative diseases. *Cell* **2023**, *186*, 693–714. [CrossRef] [PubMed]
9. Sampson, T.R.; Debelius, J.W.; Thron, T.; Janssen, S.; Shastri, G.G.; Ilhan, Z.E.; Challis, C.; Schretter, C.E.; Rocha, S.; Gradinaru, V.; et al. Gut Microbiota Regulate Motor Deficits and Neuroinflammation in a Model of Parkinson's Disease. *Cell* **2016**, *167*, 1469–1480.e.12. [CrossRef] [PubMed]
10. Cryan, J.F.; O'Riordan, K.J.; Cowan, C.S.M.; Sandhu, K.V.; Bastiaanssen, T.F.S.; Boehme, M.; Codagnone, M.G.; Cussotto, S.; Fulling, C.; Golubeva, A.V.; et al. The Microbiota-Gut-Brain Axis. *Physiol. Rev.* **2019**, *99*, 1877–2013. [CrossRef] [PubMed]

Disclaimer/Publisher's Note: The statements, opinions and data contained in all publications are solely those of the individual author(s) and contributor(s) and not of MDPI and/or the editor(s). MDPI and/or the editor(s) disclaim responsibility for any injury to people or property resulting from any ideas, methods, instructions or products referred to in the content.

International Journal of
Molecular Sciences

MDPI

Review

A Comprehensive Examination of the Role of Epigenetic Factors in Multiple Sclerosis

Ida Manna [1,*], Selene De Benedittis [2] and Danilo Porro [3]

[1] Institute of Bioimaging and Complex Biological Systems (IBSBC), National Research Council (CNR), Section of Catanzaro, 88100 Catanzaro, Italy
[2] Institute for Biomedical Research and Innovation (IRIB), National Research Council (CNR) Cosenza, 88100 Catanzaro, Italy
[3] Institute of Bioimaging and Complex Biological Systems (IBSBC), National Research Council (CNR), Segrate, 20054 Milan, Italy
* Correspondence: ida.manna@cnr.it

Abstract: According to various research, the risk of multiple sclerosis (MS) is strongly influenced by genetic variations. Population, familial, and molecular studies provide strong empirical support for a polygenic pattern of inheritance, mainly due to relatively common allelic variants in the general population. The strongest MS susceptibility locus, which was unmistakably identified in tested populations, is the major histocompatibility complex on chromosome 6p21.3. However, the effect of a given predisposing variant remains modest, so there is the possibility that multiple gene–gene and/or gene–environment interactions could significantly increase the contribution of specific variants to the overall genetic risk. Furthermore, as is known, susceptibility genes can be subject to epigenetic modifications, which greatly increase the complexity of MS heritability. Investigating epigenetic and environmental factors can provide new opportunities for the molecular basis of the MS, which shows complicated pathogenesis. Although studies of epigenetic changes in MS only began in the last decade, a growing body of literature suggests that these may be involved in the development of MS. Here, we summarize recent studies regarding epigenetic changes related to MS initiation and progression. Furthermore, we discuss how current studies address important clinical questions and how future studies could be used in clinical practice.

Keywords: multiple sclerosis; epigenetic modifications; environmental factors; biomarkers

1. Introduction

Multiple sclerosis (MS) is a disorder of the central nervous system (CNS), characterized by both inflammatory and neurodegenerative features. Autoreactive CD4 T cells are thought to be the primary cause of MS pathogenesis. Activated in the peripheral, these cells cross the blood–brain barrier (BBB) to enter the CNS along with activated myeloid cells and B lymphocytes [1]. Following their reactivation in the CNS, invading cells and immune cells that spread in the brain create an inflammatory environment that causes axon demyelination and neuronal death. Demyelinating lesions, which affects the myelin sheath surrounding the axon, causing axonal degeneration and neuronal loss in the brain, are a hallmark of MS [2]. By destroying the myelin sheath, this disease compromises the transmission of nerve impulses which are followed by neurological episodes that compromise their function and cause disability [3]. MS can present in four different clinical phenotypes which are important not only to predict the course of the disease, but also to decide on the appropriate therapeutic approach: (1) relapsing–remitting multiple sclerosis (RR-MS); (2) primary–progressive multiple sclerosis (PP-MS); (3) secondary–progressive multiple sclerosis (SP-MS); and (4) progressive–relapsing multiple sclerosis (PR-MS). Each form of MS has a different symptom pattern and course of the disease [4]. Neurological dysfunctional episodes may occur in RR-MS patients with or without residual damage.

Of the several patterns, RR-MS is the most common clinical type of the disease. It is characterized by repeated episodes of remission brought on by the immune system shutting down and relapse brought on by autoimmune aggressiveness [5,6]. In total, 15% to 30% of patients with RRMS will proceed to secondary progressive MS, which causes progressive disability. Last but not least, 15% of people have primary progressive MS, which impairs neurologic function from the moment symptoms arise without relapses or remissions [7]. Several clinical investigations, including clinical examination, magnetic resonance imaging, measurement of cerebrospinal fluid, and electrophysiology, are crucial for the diagnosis and monitoring of MS. Although the precise etiology of MS is still unknown, it is thought to be caused by an aberrant immune response to one or more myelin antigens that appear in genetically vulnerable people following exposure to an as-yet-unidentified causative agent. The genetic predisposition to MS is polygenic. The major histocompatibility complex (MHC), also called the human leukocyte antigen (*HLA*) system, was the first to be linked to the disease. More than 200 polymorphic variations associated with MS were found using genome-wide association studies, with the haplotype HLA-DRB1*15:01 having the most impact. Although MS risk loci confer only modest individual effects, they do converge into pathways that are significant for T cell and adaptive immunity activities. In addition, cigarette smoking, mononucleosis, the pathogenic Epstein–Barr virus (EBV), and low vitamin D levels were all repeatedly linked to an increased risk of MS [8]. Furthermore, compared to the effects of each genetic risk factor alone, smoking was demonstrated to interact with HLA-DRB1*15:01, *HLA-A2*, and *NAT1*, significantly increasing the probability of developing MS [9]. Hypovitaminosis D was proposed as a potential risk factor for MS based on study findings from the past few decades about the relationship between MS and vitamin D status. MS susceptibility was linked to certain gene variations encoding proteins involved in vitamin D metabolism, transport, and activity, which are responsible for changes in vitamin D status [10]. The first study conducted to evaluate the possible influence of different SNPs in vitamin D-related genes on the severity of MS did not highlight any association between the SNPs investigated and the progression of MS [11]. Other case-control studies did not show any association between selected SNPs and susceptibility to MS [12–14]. Overall, these studies do not offer sufficient results to say whether vitamin D-related genetic variants influence MS risk or not. However, several statistical data suggest that the contribution of all MS-associated variations discovered to date may only account for up to 48% of the heritability of the disease, highlighting the possible role of interactions between environmental and genetic factors [15]. In addition to environmental and genetic factors, epigenetic factors also influence the risk of onset and can mediate part of the risk associated with environmental factors by altering gene expression. Epigenetics also might be the link between environmental variables and MS susceptibility (Figure 1).

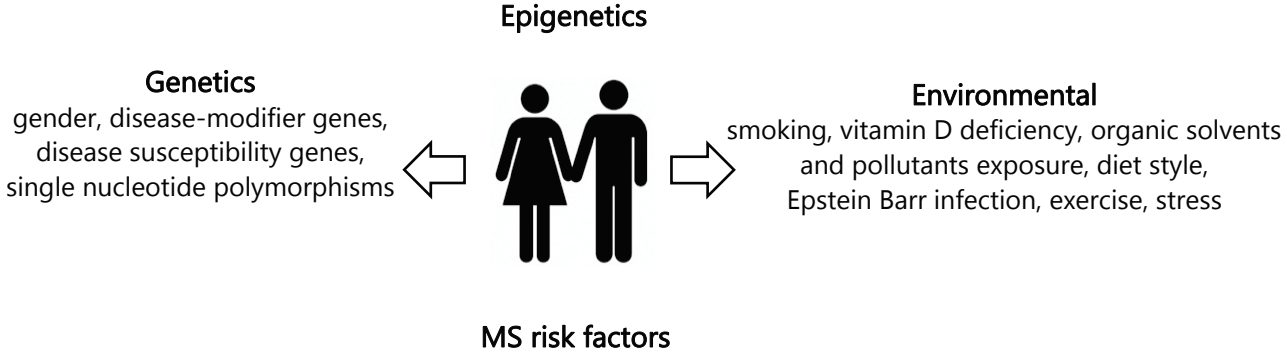


Figure 1. Risk factors of multiple sclerosis.

To further understand the molecular mechanisms of MS, epigenetic modifications should also be investigated. The field of epigenetics investigates how a person's age and exposure to environmental elements, such as chemicals and physical hazards, food, and

physical exercise, can affect their lifetime and vary depending on the type of cell or tissue they are in.

Epigenetic marks are heritable, independent of changes in DNA sequence, and modulate gene expression. Indeed, these changes can trigger or influence critical cellular responses that may be crucial in determining disease phenotype. Various environmental factors, including food, smoking, and stressful conditions, can impact the epigenome's plasticity and play a role in epigenetic regulation. A schematic diagram of the different types of epigenetic mechanisms is illustrated in Figure 2.

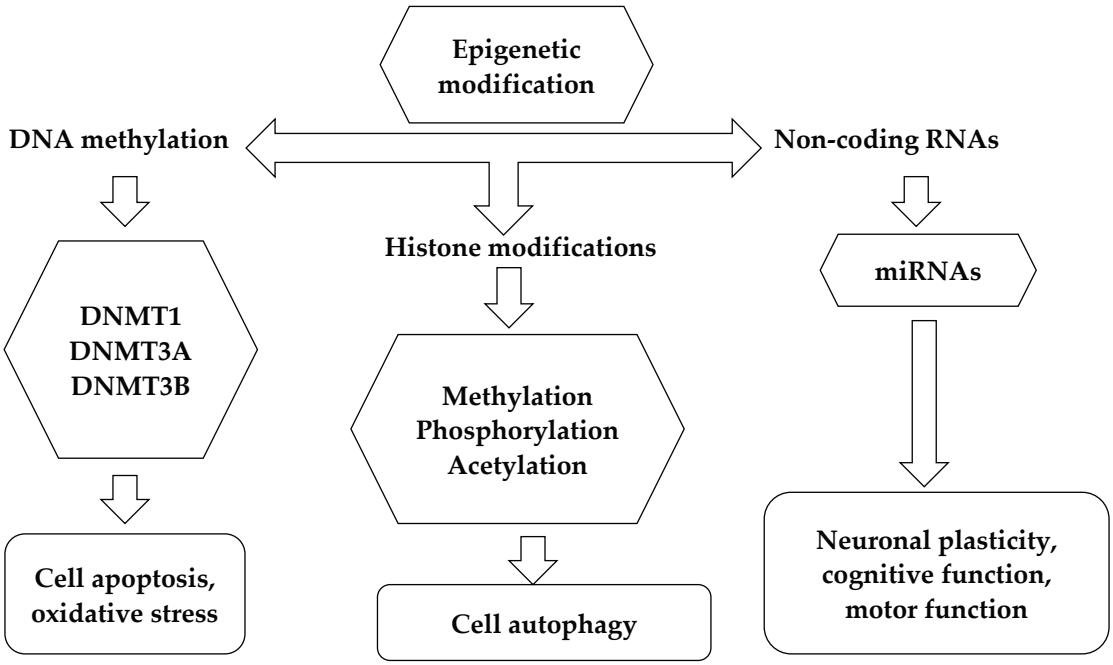


Figure 2. Epigenetic mechanisms.

Briefly, DNA methylation consists of the addition of a methyl group (-CH3) to a base, such as methylation at the carbon-5 level of cytosine, which constitutes almost all methylation of eukaryotic DNA. 5-methyl-cytosine (5mC) is found almost exclusively in the cytosine-phosphate-guanine (CpG) dinucleotide in the coding region of genes [16]. The main function of DNA methylation is associated with the inactivation of gene expression and could also contribute to transcriptional regulation by influencing chromatin remodeling [17], and alternative splicing [18]. The process is produced by a family of enzymes called DNA-methyl-transferase (DNMT). In the genome, almost 80% of CpG sequences are methylated [19]. The transfer of a methyl group is catalyzed by three DNA methyltransferases: DNMT1, DNMT3A, and DNMT3B. While DNMT3a and DNMT3b, together with their coactivator DNMT3L, are engaged in de novo DNA methylation and in DNA methylation maintenance, DNMT1 is in charge of methylating hemimethylated DNA and thereby maintaining DNA methylation [20]. More recently, a fourth DNA methyltransferase enzyme, called DNMT3C, was discovered by Barau et al., in mouse germ cells. This enzyme is responsible for methylating the promoters of evolutionarily young retrotransposons and its activity is required for mouse fertility. In addition to expanding knowledge of the mechanisms involved in the epigenetic regulation of retrotransposons, the identification of DNMT3C highlights the plasticity of the DNA methylation system [21]. Methylation of cytosine residues causes gene silencing possibly by blocking the binding of transcription factors to promoters; however, in some cases, methylated DNA motifs can also be specifically recognized by transcription activators [22].

Another well-known fundamental epigenetic mechanism, which controls gene expression without altering the genetic material, is the modifications of the histone tails. When

we talk about histone modification we refer to the addition of chemical groups to histones, the proteins around which the long strand of DNA wraps itself so that it is "packaged" and contained in the nucleus of the cell [23]. There are five types of histones in eukaryotic cells: H1, H2A, H2B, H3, and H4. Two copies of histones H2A, H2B, H3, and H4 form a protein complex called a histone octamer, around which the double strand of DNA wraps. The fifth type of histone, H1, stabilizes the binding of DNA to histones in chromatin. Histones can undergo various modifications, among which the most common are acetylation (addition of an acetyl group) and methylation, which lead to variations in the structure of chromatin, making it more or less accessible to RNA polymerase, resulting in activation or repression of genes associated with the modified histone [24]. The best-understood histone modification is acetylation and deacetylation at the lysine residues that are carried out by histone acetyltransferases (HAT) and histone deacetylases (HDAC), respectively. Acetylation of histones is usually associated with upregulated transcriptional activity of the associated gene, whereas deacetylation of histones contributes to transcriptional silencing. In fact, modifications such as acetylation and methylation of the tails, in specific amino acid residues of specific histones, have the effect of activating or inhibiting transcription, according to a real histone code [25]. Indeed, the functional consequences of these changes on transcription depend on the type of change and the location of the targeted amino acid residue within the histone tail.

An additional mechanism of epigenetic control can also be achieved at the post-transcriptional level by small non-coding RNAs (ncRNAs). Among ncRNAs, microRNAs (miRNAs) are small endogenous single-stranded molecules that modulate messenger RNA activity. The role of miRNAs is to negatively regulate gene expression through binding to the target mRNA to cause transcriptional repression and/or mRNA degradation without modifying the gene sequence [26]. It is interesting to note that miRNAs typically change the activity of pathways since they can regulate the synthesis of multiple downstream targets not only a single mRNA [27]. miRNAs were shown to regulate more than 60% of protein-coding genes. Since this complex "network" is normally very finely regulated, alteration in microRNA expression can lead to the development of various diseases [28]. The abundance of miRNAs in the CNS can impact a variety of cellular activities, including differentiation, growth, proliferation, plasticity, and development [29]. miRNAs can be considered epigenetic components involved in immune regulation and MS pathogenesis due to their ability to alter gene expression, and their role in physiology and numerous pathological processes. Immune cells also exhibit high expression of miRNAs. Furthermore, miRNAs are detectable in a wide variety of body fluids [30], and consequently, peripheral circulating miRNAs may be employed as biomarkers for MS diagnosis, MS subtype differentiation, and MS prognosis prediction.

In the development of MS, the interaction between hereditary determinants and cell-specific epigenetic alterations may be extremely important. Epigenome modifications caused by environmental risk factors for MS create a connection between environmental exposure and changes in gene expression [31]. An increasing amount of research points to the importance of dietary nutrients in inducing epigenetic modifications for health and disease prevention, particularly for neurodegenerative illnesses. Folic acid, vitamin B12, and dietary polyphenols were demonstrated in numerous studies to interact with epigenetic pathways and ultimately gene regulation [32]. Epigenetic changes were also implicated in developmental myelination and remyelination [33]. The complex genetic profile of MS and its epidemiological traits led us to hypothesize that the balance between the genetic and epigenetic components may be crucial for disease susceptibility, onset, and progression. Finally, studying the epigenome in MS provides valuable insights into the pathophysiology of disease progression and repair. Although the mechanisms involved in the development of MS are not yet fully defined, understanding the salient characteristics of the evolution of lesions in the different areas and phases of the disease is the basis for the development of increasingly targeted and effective therapies. For this purpose, considering the cellular specificity of epigenetic changes, in this review, we discuss the most relevant

findings to date in different tissues of MS patients. Finally, we examine their potential implications for the future application of epigenetic advances in the field of MS.

2. DNA Methylation: Contribution in Patients with MS

DNA methylation is a crucial epigenetic process that controls gene expression in a dynamic and reversible manner. The transcription of genes is typically activated or repressed depending on whether a methyl group is present or absent on CpG dinucleotides. DNA methylation is modulated by environmental variables, including nutrition, stress, and exposure to the environment [34]. Recent studies connected neurological illnesses to changes in DNA methylation [35]. These epigenetic modifications function as simple tools for controlling the expression of the vital gene networks that mediate physiological processes. The specific pathophysiological mechanisms mediating the relationship between environmental risk factors and MS susceptibility remain unknown, and DNA methylation may provide information on these mechanisms [36]. This epigenetic pathway contributes to various MS pathophysiological processes, such as demyelination and remyelination, inflammatory response, and the collapse of the BBB [37]. It is also linked to chronic inflammatory states. DNA methylation appears to play a major role in the epigenetics of MS, as aberrant methylation in the promoter regions of the genome may be the cause of many processes involved in the beginning and development of MS. Since DNA methylation is involved in many neurodegenerative diseases, modifying DNA methylation may be a useful therapeutic approach in treating these conditions. It was described that methylation of CpG dinucleotides in gene promoter regions could be responsible for the immune properties of MS, with the dominance of T helper 1 cell immunity, associated with the cytokine interferon-γ, compared to T helper 2 cell immunity. The promoter region of IFN-γ within T helper cells showed aberrant patterns of DNA methylation, which could be associated with the predominance of TH1 immunity over TH2 immunity in MS [38]. The BBB, which is thought to be composed of endothelial cells and intercellular adhesion molecules, is known to allow the passage of self-reactive proinflammatory cells, a pathogenic characteristic of multiple sclerosis. It was demonstrated that in RR-MS patients, a hypermethylated E-cadherin (*CDH1*) profile can increase blood–brain barrier permeability, allowing lymphocyte infiltration into the brain and, ultimately, the progression of the disease [39]. Referring to the *ICAM* family, namely *ICAM-1*, which is essential for T cell proliferation, Ligget et al., note that cell-free plasma DNA of RR-MS patients have an *ICAM1* hypermethylation pattern in response to clinical remission, and the observed differences mostly correlated with the disease process. Significant differences in concentration and the methylation patterns of cell-free plasma DNA were detected in all three comparisons: RRMS patients in remission versus healthy controls; RRMS patients in exacerbation versus healthy controls; and RRMS patients in exacerbation versus those in remission [40]. These results may have important therapeutic ramifications since methylation patterns that distinguish patients from healthy individuals may serve as biomarkers for the identification and diagnosis of disease. Moreover, a predictive biomarker for exacerbation may result from variations in the methylation patterns of patients in remission and/or exacerbation. Remyelination failure in the advanced stage of MS is ultimately caused by the impaired differentiation of oligodendrocyte precursor cells (OPCs). Using postmortem brain tissue, genome-wide DNA methylation and transcriptional patterns were examined between matched normal-appearing white matter (NAWM) and chronically demyelinated MS lesions. Using pyrosequencing, it was confirmed that DNA methylation variations in laser-captured OPCs were exclusive to cell type and negatively linked with mRNA expression of the respective genes. Through the application of epigenetic editing to alter the DNA methylation status of particular CpGs within the promoter region of the myelin basic protein gene (*MBP*), it was demonstrated that the CRISPR–dCas9–DNMT3a/TET1 system may be used to bidirectionally influence myelination and cellular differentiation in vitro [41].

Recently, Tiane et al. [41,42] looked into the possibility that a blood-borne biomarker for demyelination may be found in the blood methylomic profile of myelin-related genes, and

that this profile might be systemically changed in advancing MS stages. Their preliminary research showed that patients with progressive MS differed from controls in the blood methylation state of key myelin-related genes: *MBP*, myelin-associated glycoprotein (*MAG*), contactin 2 (*CNTN2*), brain-enriched myelin-associated protein 1 (*BCAS1*), partitioning defective 3 homolog (*PARD3*). Among the five genes, three (*MBP*, *MAG*, and *CNTN2*), in particular, displayed a methylation pattern that differed significantly between the control and MS samples. It is interesting to note that these genes' methylation profiles matched the pattern found in the central nervous system, indicating systemic hypermethylation of these genes in MS patients with progressing disease. This suggests that a panel of peripheral markers, useful for assessing demyelination in the course of MS disease, could employ the DNA methylation profile of these genes. Although, these findings were not confirmed in further independent patient cohorts [42]. More longitudinal research on bigger cohorts of diverse ethnic backgrounds, including both patient and control groups, would be necessary to fully test the findings of these investigations.

Research on how DNA methylation affects MS in rodent models, especially in mice with experimental autoimmune encephalomyelitis (EAE), demonstrated significant potential for application to human MS patients [43]. The majority of attempts to identify variations in DNA methylation throughout the genome fall into two categories: genome-wide methylation investigations and candidate gene approaches, which involve selecting specific genetic loci and examining their DNA methylation patterns.

Additionally, combinations of these methods can be used [44]. To date, several researchers linked the methylation status of specific genes to MS. In particular, Kumagai et al. observed of the promoter of tyrosine phosphatase (*SHP-1*) a negative regulator of proinflammatory signaling in peripheral blood mononuclear cells (PBMCs) of MS patients compared to healthy controls. Hypomethylation results in decreased *SHP-1* expression and thus increased lymphocyte-mediated inflammatory activity [45]. In another work, Janson et al., analyzed CD4+ T cells in a cohort of RR-MS patients and observed that the regulatory T cell transcription factor *FOXP3* was demethylated in these patients. Demethylation of *FOXP3* stimulates regulatory T cells and Th17 cells while inhibiting the development of Th1 and Th2 cells. The proper balance of these cells is linked to DNA methylation [46]. In addition, hypomethylation of the promoter of the gene encoding *IL-17A*, a proinflammatory cytokine, mainly secreted by activated T cells, was reported [47]. In the work of Mastronardi et al., during white matter demyelination in MS patients, the authors observed demethylation of the peptidyl arginine deiminase 2 (*PAD-2*) promoter and thus *PAD-2* overexpression in the brain. *PAD-2* leads to the loss of stability of *MBP* due to the enzymatic conversion of arginine to citrulline. This process leads the *MBP* protein to act as an antigen for T cells. The authors observed a 25% reduction in white matter *PAD-2* promoter methylation in patients compared to healthy controls. Of note, these changes were not seen in patients with other neurological diseases such as Alzheimer's disease, Parkinson's disease, and Huntington's disease [48].

Literature data report genome-wide DNA methylation profiling in MS patients, brain tissues, whole blood, and immune cells. Because CD4+ and CD8+ immune cells are the most prevalent cell populations, with a well-documented role in the genesis and progression of MS, they were examined more frequently than other immune cell types. Although the precise role of DNA methylation in MS is not fully understood, several studies reported differentially methylated regions in both immune cells and brain tissue collected from both MS patients and healthy controls. The ability to identify the neurotoxic and pro-inflammatory mechanisms causing neuronal vulnerability in MS progression made the study of glial cell populations particularly interesting [49]. This could lead to the eventual restoration of brain repair mechanisms that support neuroprotection and remyelination. Oligodendrocytes, which are more prevalent in the white matter (WM) than the grey matter (GM) due to their capacity to produce myelin, give neurons structural and trophic support by regulating the myelination of axons [50]. Numerous minor differences between the bulk NAWM of MS patients and controls were found by previous case-control methylome

studies of brain tissue. In the work of Huynh et al., genome-wide RNA-sequencing analysis helped to further identify the transcriptional effects of differential DNA methylation, and it was confirmed in two separate cohorts of brain samples from patients with multiple sclerosis and healthy controls. In brains affected by MS, genes controlling oligodendrocyte survival, such as *BCL2L2* and *NDRG1*, were expressed at lower levels and showed hypermethylation compared to controls. Conversely, increased levels of hypomethylation and expression were seen in genes associated with proteolytic processing, such as *LGMN* and *CTSZ*. According to their findings, there may be a trend toward hypomethylation in genes linked to immune-related activity and hypermethylation in genes involved in oligodendrocyte function [51]. Chomyk et al. looked at whether demyelination in the MS hippocampal region affected DNA methylation. When MS patients' demyelinated and myelinated hippocampi were compared, abnormal epigenetic alterations linked to the dysregulation of a few select genes were found. The demyelinated MS hippocampal region exhibits hyper-methylation in 10 genes and hypo-methylation in 6 upstream sequences according to comparative methylation profiling [52]. Recent research of Kular et al., using DNA methylation analysis of neuronal nuclei, revealed functionally significant alterations, such as decreased activity of the transcription factor *CREB*, linked to neuro-axonal dysfunction in MS patients relative to controls. The two cohorts' pathway studies revealed dysregulation of genes related to synaptic plasticity and axonal guidance, and a meta-analysis confirmed that the most significantly enriched route underlying these processes is CREB signaling [53]. Recently, using the Illumina Infinium MethylationEPIC BeadChip, Kular et al., profiled DNA methylation in the nuclei of non-neuronal cells isolated from 38 post-mortem NAWM specimens of MS patients (n = 8) in comparison to the white matter of control individuals (n = 14) in order to capture relevant molecular changes underlying MS neuropathology. They found 1226 significantly differentiably methylated sites (DMPs) between MS patients and controls (genome-wide adjusted p-value < 0.05). The modified DMP-genes' functional annotation revealed changes in metabolic processes, cytoskeleton dynamics, cellular motility, synaptic support, neuroinflammation, and signaling, including Wnt and TGF-β pathways. Their results clearly imply that even in the absence of lesional damage, NAWM glial cells are significantly changed, showing a multicellular response to widespread inflammation [54].

Several studies showed an aberrant DNA methylation profile in RR and progressive MS forms [55]. Kiselev et al., to identify differential methylation profiles of CpG sites in the DNA of CD14+ monocytes from patients with primary progressive MS, a genome-wide analysis of DNA methylation in patients compared to healthy subjects was conducted. The study highlighted 169 differentially methylated positions (DMPs), 90.5% of which were hypermethylated in PPMS patients [56]. In recent years, many research teams examined the impact of aberrant DNA methylation on MS characteristics, and they reached a variety of conclusions. However, to date, the results of published genome-wide DNA methylation studies are not consistent and may be associated with the choice of non-uniform criteria, such as heterogeneity of the groups studied, sample size, different methodologies, and statistical strategies used. In addition, further research indicates that sample storage may affect DNA methylation patterns selectively, which could make epigenetic analysis less accurate. As a result, while choosing samples for biomarker research, sample storage period should be taken into account. Indeed, regarding the selection of the group of patients with MS, not only naive patients are included in the various studies, but also patients who received various immunomodulatory drugs before and/or during blood sampling, when it is well known that drug therapy affects the level of methylation in blood cells [57]. Comparing the DNA methylation profiles of other cell groups from the same individuals may help to address some of these issues and provide more accurate information on the pathophysiology of MS.

About it, little research the literature conducted on DNA methylation analysis takes into account various immune cell populations obtained from the same MS patients. Ewing et al., investigated DNA methylation changes in four immune cell types, i.e., CD4+ and CD8+ T cells, CD14+ monocytes, and CD19+ B cells, in a cohort of patients with RRMS and SPMS and healthy controls. They found 1511, 666, and 30 significant differentially methylated positions (DMPs) in CD19+, CD14+, and CD8+ cells, respectively, between RRMS, SPMS, and HC individuals, with two significant DMRs mapping to *HLA-DRB1* and *SLFN12* genes [58]. Recently, Kiselev et al., considering cell populations key in triggering pathological processes underlying the development of MS, performed pairwise DNA methylation profiling in CD4+ T lymphocytes and CD14+ monocytes. They observed significant changes in the DNA methylation profiles among these cell populations, and they highlighted that in CD4+ cells of MS patients, most of the DMPs were hypomethylated, while in CD14+ cells they were hypermethylated. However, they observed that approximately 20% of the identified DMPs were shared between the two cell populations from treatment-naïve RR-MS patients and healthy subjects [59]. Although these findings suggest that differential DNA methylation in immune cells could contribute to MS, further studies are needed to validate these findings and especially to understand their functional significance. In genome-wide association studies, the strongest association between MS and differential DNA methylation occurs at the *HLA-DRB* locus. Despite the HLA genes being among the highest genetic predictors of MS risk for more than 40 years, the precise causative genes and the processes by which they affect MS susceptibility remain unknown.

Graves et al., provide the findings of a genome-wide link between CD4+ cell methylation levels and susceptibility to MS. The significant differential methylation signal at CpG sites throughout the MHC complex, particularly the hypomethylation of eight closely clustered sites in *HLA-DRB1*, was the study's most notable observation. The hypomethylation at *DRB1* may be a key epigenetic locus for MS, and this is the first instance of aberrant methylation at HLA being linked to MS [60]. Recently, to understand the biological effects of inheritance of MS risk alleles and show that DNA methylation influences risk of developing MS, Kular et al. examined DNA methylation in MS patients in the context of genetic diversity and gene expression. In particular, the protective HLA variant (rs9267649) and the strongest MS risk variant (HLA-DRB1*1501) have an impact on *HLA-DRB1* expression and the risk of MS through DNA methylation. Their findings highlight that the region containing exon 2 of *DRB1*15:01* is regulated by DNA methylation, and hypomethylated *DRB1*15:01* has a capacity to promote increased gene expression. Therefore, *DRB1*1501*'s hypomethylation and predominant expression may be a possible mechanism by which MS risk is conferred [61]. More recently, Xavier et al., confirmed prior findings that DNA methylation acts as a mediator of the HLA-DRB1*1501 allele and provided evidence that this occurs early in disease pathology rather than as a result of treatment or long-standing disease by using a large dataset of MS cases early in their diagnosis with age/sex/location-matched controls. They examined the relationship between methylation and expression levels of *HLA-DRB1* in monocytes, CD19+ B cells, and CD4+ T cells, and found a strong negative correlation between gene expression and methylation at *DMR-2* located in exon 2 of *HLA-DRB1*. These data indicate that hypomethylation at this locus was associated with increased gene expression in these immune cell subtypes [62]. Furthermore, in their study they examined whole blood DNA methylation profiles of a large group of MS subjects compared to those of healthy control subjects, thus highlighting that methylation differences in patients occur independently of genetic risk loci, subsequently proving that they differentiated the disease more strongly than known genetic risk loci. Table 1 lists the studies discussed in the manuscript.

Table 1. DNA methylation changes in MS patients.

Tissue	Cohort	Method	Findings	Reference
cell-free plasma DNA	RRMS in remission vs. HC; RRMS in exacerbation vs. HC; and RRMS in exacerbation vs. remission	microarray-based assay	RR-MS patients have an ICAM1 hypermethylation pattern in response to clinical remission, the observed differences mostly correlated with the disease process.	Ligget et al., 2010 [40]
Brain tissue	Matched NAWM and chronically demyelinated MS lesions	pyrosequencing	DNA methylation status in the promoter region of MBP, may be used to bidirectionally influence myelination and cellular differentiation in vitro.	Tiane et al., 2023 [41]
Blood	RRMS and SPMS vs. NNC	pyrosequencing	MBP, MAG, and CNTN2 showed a significant difference in methylation pattern between the control and MS sample.	Tiane et al., 2024 [42]
Buffy coat	69 MS (7 PPMS, 50 RRMS, 12 SPMS; 49 F, 20 M), 19 HC	cloning BS-sequencing	Increased DNA methylation level of SHP-1 promoter 2 in MS compared with HC. No relationships between DNA methylation and MS clinical parameters (EDSS, disease duration, phase).	Kumagai et al., 2012 [45]
CD4+ T cells	17 RRMS (10 MS tysabri, 3 glatiramer acetate, 2 IFN-1b treated, 2 nontreated), 7 HC	cloning BS-sequencing	No difference in DNA methylation level of FOX3P and IL-17A between MS tysabri-treated patients and HC. Demethylation of FOX3P and IL-17A loci in tysabri untreated patients compared with HC.	Janson et al., 2011 [46]
Brain NAWM	DC: 28 MS; VC: 10 MS, 20 NNC	Illumina 450 K array	220 hypomethylated DMRs (1235 CpGs) and 319 hypermethylated DMRs (1292 CpGs) at oligodendrocyte specific genes (BCL2L2, HAGHL, NDRG1, CTSZ, andLGMN). Correlation with expression of a portion of corresponding genes.	Huynh et al., 2014 [51]
Hippocampus	myelinated (n = 8) or demyelinated MS (n = 7)	Illumina 450 K array	Hyper-methylation in 10 genes and hypo-methylation in 6 genes.	Chomyk et al., 2017 [52]
Brain tissue	active lesion, chronic active lesion, chronic inactive lesion and NAWM vs. HC	Illumina 450 K array	Decreased activity of the transcription factor CREB, linked to neuro-axonal dysfunction in MS patients vs. controls.	Kular et al., 2019 [53]
Brain tissue	active lesion, chronic active lesion, chronic inactive lesion and NAWM vs. HC	Illumina 450 K array	A total of 1226 significantly differentiably methylated sites between MS and NNC.	Kular et al., 2022 [54]
CD14+ monocytes	PPMS vs. HC	Illumina 450 K array	A total of 169 DMPs, 90.5% of which were hypermethylated in PPMS patients.	Kiselev et al., 2020 [55]
CD4+ and CD8+ T cells, CD14+ monocytes and CD19+ B cells	RRMS, SPMS and HC	EWAS	A total of 1511, 666, and 30 significant DMPs in CD19+, CD14+, and CD8+ cells, respectively, between RRMS, SPMS, and HC.	Ewing et al., 2019 [58]
CD4+ T lymphocytes and CD14+ monocytes	treatment-naïve RR-MS patients and HC	EWAS	In CD4+ cells of MS patients, most of the DMPs were hypomethylated, while in CD14+ cells they were hypermethylated.	Kiselev et al., 2022 [59]

Table 1. *Cont.*

Tissue	Cohort	Method	Findings	Reference
CD4+ T cells	30 RRMS (interferons, glatiramer acetate, natalizumab or fingolimod treated), 28 HC	Illumina 450 K array	Correlation of HLA-DRB1 DNA methylation status and HLA-DRB1*15:01 haplotype. Differently methylated CpG sites (19) inside of MHC region and 55 outside.	Graves et al., 2014 [60]
Blood,	MS vs. HC	EWAS	Negative correlation between gene expression, and methylation at DMR-2	Xavier et al., 2023 [62].

HC, healthy controls; RRMS, relapsing-remitting multiple sclerosis; SPMS, secondary progressive multiple sclerosis; PPMS, primary progressive multiple sclerosis; NNC, nonneurological controls; EDSS, expanded disability status scale; DC, discovery cohort; VC, validation cohort; IFN-1b, interferon beta-1b; NAWM, normal appearing white matter; BS, bisulfite; MBP, myelin basic protein gene; DMRs, Differentially methylated regions; DMPs, differentially methylated positions; and EWAS, epigenome-wide association study.

In conclusion, the genome-wide DNA methylation changes in whole blood and isolated cell types were the subject of numerous studies. Even though results are inconsistent and limited by heterogeneous cell populations, disease heterogeneity, the use of a wide variety of disease-modifying therapies (DMTs), or small sample sizes, there is no doubt that DNA methylation is influenced by genotype and environment, making it an important molecular interface for researching disease etiology and progression.

3. Post-Translational Histone Modifications: Contribution to MS

Post-translational modifications (PTMs), which occur when proteins are translated into the cytoplasm, are crucial for the folding and functionality of proteins [63]. Among the most common histone changes are histone acetylation/deacetylation, and histone methylation. Two opposing enzymatic activities regulate histone acetylation: histone acetyl transferase o HAT, and histone deacetylase or HDAC. HATs add acetyl groups on lysine residues, while HDACs remove them.

According to growing data, epigenetic changes may hold the key to understanding the partial heredity of MS risk. Indeed, epigenetic pathways are thought to mediate the response to a variety of environmental factors, including geographic location, Epstein–Barr virus (EBV) infection, smoking, and vitamin D deficiency, which are known to affect the development of the disease [64–67]. It is well known that *HLA-DR* expression was shown to be suppressed from *HDAC1*. The connection between inflammation and neurodegeneration and *HDAC/HAT* imbalance may have an effect on MS mechanisms. HDAC mRNAs were previously demonstrated to be higher in immune cells that were activated, indicating their possible uses as therapeutic targets or activation markers [68]. This suggests that the MS susceptibility loci are related to histone regulation. In the work of Pedre et al. the authors observe increased levels of histone H3 acetylation in chronic lesions of MS patients compared to healthy controls. Notably, they point out that in oligodentroglia cells, changes were associated with higher transcript levels of inhibitors of oligodendrocyte differentiation. Interestingly, deacetylation was evident in early MS lesions, unlike in chronic lesions. This observation highlights the important role of the acetylation/deacetylation balance in the demyelinating and remyelinating processes in the early stages of the disease [69]. Furthermore, regarding changes in histone H3 methylation, the latter linked to mitochondrial alterations in MS. Singhal et al., in a study, measured the concentrations of methionine metabolites, histone H3 methylation patterns, and markers of mitochondrial respiration in gray matter from postmortem MS and control cortical samples. They found decreases in both respiratory markers and concentrations of methionine metabolites in the gray matter of MS [70]. In another work, the study group of Singhal et al., demonstrated that methyl donor betaine is reduced in MS and is linked to decreases in histone H3 trimethylation (H3K4me3). They also observed that betaine increases histone methyltransferase activity by activating chromatin-bound betaine homocysteine S-methyltransferase (BHMT) [71]. In a recent study, Singhal et al. linked histone PTMs to communication between energetically

impaired neurons and oligodendrocytes to promote remyelination in MS. They observed reduced levels of the metabolite N-acetylaspartate (NAA) in MS patients that correlated with reduced levels of the myelin component in apparently NAWM [72]. This finding is in agreement with previous work related to neuronal metabolic dysfunction, linked to a marked decrease in NAA metabolite in postmortem multiple sclerosis cortex, that precedes neuronal atrophy and can be reversed in disease remission conditions. Reduced NAA and neuronal mitochondrial dysfunction in MS may influence the epigenetic changes of histones, which in turn mediates regulatory signals in oligodendrocytes. In the end, altered myelin lipid content and oligodendrocyte gene expression may make axons more susceptible to demyelination as a result of decreased NAA synthesis in neurons and catabolism in oligodendrocytes [73].

In a more recent work, Sternbach et al. investigated the role of the BHMT-betaine methylation in oligodendrocytes. They determined the presence of the BHMT enzyme in oligodendrocytes and the role of the BHMT–betaine pathway in chromatin regulation and HMT/DNMT activity in oligodendrocyte progenitor cells. This is the first work involving the study of *BHMT* expression in oligodendrocytes and where the authors suggest that *BHMT* is present in oligodendrocytes in both rats and humans, specifically in human MS tissue. They found that oxidative stress increases *BHMT* expression and showed that, in an oxidative environment, betaine can stimulate the expression of the oligodendrocyte maturation genes *SOX10* and *NKX-2.2*. Collectively, these data underscore that regulation of transcription factors required for oligodendrocyte differentiation by betaine could modulate oligodendrocyte maturation, likely impacting epigenetic changes including histone PTMs [74].

Another PTM of histones is citrullination, which represents the hydrolytic conversion from peptidyl-arginine to peptidyl-citrulline, catalyzed by enzymes belonging to the family of peptidylarginine deiminases (*PAD*). Citrullination plays an essential role in physiological processes, such as regulation of gene expression, apoptosis, and plasticity, while aberrant citrullination may be involved in the initiation and/or progression of autoimmune disorders such as MS.

Mastronardi et al. looked at white matter from healthy subjects and NAWM tissue from MS brains to identify metabolic alterations that would make these areas more prone to eventual lesion development. To determine whether elevated nuclear *PAD-4* was accompanied by citrullination of nuclear proteins, they used a citrulline-specific monoclonal antibody (F95) to stain normal and MS white matter sections. They observed an increased *PAD4* with increased citrullination of histone H3 and TNF-α in MS NAWM and in the brains of animal models of demyelination. The mechanism involves nuclear translocation of PAD-4 [75]. This alteration may modify transcription and chromatin structure by altering the degree of methylation on arginine residues [76]. It is noteworthy that enzymatic inhibitors of this post-translational alteration can improve disease progression in mice models of demyelination, despite the fact that the functional relevance of histone citrullination has to be better understood.

Recently, Faigle et al., to better understand whether citrullination is implicated in distinct pathogenetic mechanisms in MS, i.e., whether structural proteins and/or those involved in inflammatory processes are citrullinated, with a proteomic approach, studied the role of citrullination in the brain tissue of patients affected by MS. However, based on their findings, they concluded that citrullination could be a side effect of an immunological or inflammatory response rather than having a key role in activating a T cell response [77].

Finally, there is emerging evidence that histone proteins post-translational modifications have roles in a number of fundamental MS-related processes (such as aging and neurodegeneration) and are susceptible to environmental variables. PTMs were suggested to be a mediator between oxidative stress, inflammation, and aging. Published data on PTMs in many age-related disorders, such as neurodegenerative diseases, provide evidence for a connection between histone PTMs and aging. Histone variations, DNA methylation, PTMs of histones, positioning of histones on the DNA sequence, and non-coding RNAs are

some of the elements that contribute to the complicated process known as epigenome dysregulation that occurs with aging [78]. Future research should focus on intricate interactions between heritable and environmental factors that contribute to MS illness heterogeneity in order to better understand how histone PTMs variations affect these processes.

In conclusion, it is important to consider that histone modifications could act sequentially or in combination to form a recognizable "code" that increases the information of the genetic code [79,80], and decoding the complexity of histone marks is a challenge. Routinely antibody-based methods are used to investigate specific PTMs. However, these methods present some important limitations; for example, they are limited to confirming the existence of modifications and they are unable to identify unknown PTMs [81]. The mass spectrometry (MS) is progressively becoming an effective tool for studying histones. Recently, De Benedittis et al., using a top-down MS approach were able to quantify and identify, at the same time, several histone PTMs in the human lymphoblastoid cell line [82]. In the future, the development of technologies useful for a more in-depth and global screening of histone PTMs could have a profound impact on understanding their role in physiological and pathological processes.

4. miRNAs: Contribution in Patients with MS

Small ncRNAs, which have a broad ability to influence gene expression in conjunction with chromatin remodeling complexes, can also play a role in mediating epigenetic control. The ability of miRNAs to regulate the expression of hundreds of genes and consequently have an impact on a number of cellular processes makes them of particular interest among ncRNAs [83]. miRNAs are important participants in many biological processes and dysfunction of these molecules can affect the immune system, cause the release of inflammatory cytokines, and trigger the formation of autoantibodies, thus contributing to the pathogenesis of MS. It is becoming clear that miRNAs are essential regulators of both innate and adaptive immune responses, and their altered expression and/or function was linked to a variety of human diseases, including inflammatory conditions. The innate immune system is activated through toll-like receptors (TLRs), which by recognizing pathogen-associated molecular patterns, attract adapter proteins to the receptor and activate downstream signaling pathways. By governing the growth and activation of T and B cells, miRNAs were linked to adaptive immunity in addition to their function in innate immune system regulation [84]. It is well known that dysregulation or upregulation of proinflammatory/or neurotoxic miRNAs and/or downregulation of anti-inflammatory and neuroprotective miRNAs could contribute to MS onset and progression. An overview of the impact of different miRNAs and mediators on the pathophysiology of MS is presented in the work of Mohammed et al. [85].

Given that MS is the most prevalent chronic inflammatory and neurodegenerative disease, many research teams are looking for miRNAs that can predict the occurrence and course of the disease, and most of the studies examined miRNAs in immune tissues. However, altered miRNA profiles within both the central nervous system and the immune system were observed in the disease.

A comprehensive review examined the results of 61 papers investigating small noncoding RNAs in immune compartments and CNS tissue of MS patients, highlighting the most frequently dysregulated miRNAs across studies (dysregulated in at least four independent studies). miR-142-3p, miR-146a/b, miR-145, miR-155, miR-22, miR223/-3p, miR-326, and miR-584 were consistently found to be upregulated, while members of the miR-103, miR-15, miR-548, and let-7 families and miR-140 showed predominant downregulation in MS patients [86]. miRNAs dysregulation can result in altered levels of gene expression in many cell types involved in this disease.

Most of the studies examined miRNAs in a case-control study, and used high-throughput miRNA profiling to identify dysregulated miRNAs.

Furthermore, different RNA resources were used to study miRNAs expression, such as whole blood, as well as serum and PBMC, including lymphocytes [87]. The investigation of

miRNA expression performed in 59 naïve MS patients (PPMS, SPMS, and RRMS) displayed that miR-17 and miR-20a were the most significantly different, and down regulated, in all MS groups vs. controls. Interestingly, gene expression analysis revealed that both miRNAs may regulate genes involved in T cell activation [88]. Investigating the expression of 365 miRNAs in lymphocyte, Lindberg et al., evidenced different miRNA expression profiles in CD4+, CD8+ T cells, and B cells of RRMS patients compared to controls. In particular, miR-17-5p was up-regulated in CD4+ cells of MS patients. The subsequent pathway analysis of potential miR-17 target genes further indicated that one of the most prevalent pathways was that of PI3K/Akt [89], which is known to be involved in lymphocyte development, activation, and survival [90,91]. In a subsequent study, a Taqman array of 667 miRNAs shed light on miRNA levels in subpopulations if not activated naïve CD4+ and in memory CD4+ T cells.

Comparing naïve T cells from MS patients to healthy controls, miR-128 and miR-27b are significantly higher in patients, while memory T cells show an increase in miR-340. Further, through the repression of their target genes, B lymphoma Mo-MLV insertion region 1 homolog (BMI1) and interleukin-4 (IL4), these miRNAs could induce inhibition of Th2 cell development and promote pro-inflammatory Th1 responses [92]. As it is known, a pro-inflammatory response is the main cause of the development of MS, where immune cells, such as T helper and cytotoxic T cells, B cells, and macrophages, infiltrate the central nervous system through the temporarily disrupted BBB. These cells, together with microglia and activated astrocytes, damage oligodendrocytes and myelin through the secretion of cytokines and chemokines that promote phagocytosis, ROS production, energetic crisis, and cytotoxic T cell activity, which then may cause myelin loss and or axon loss [93]. In the last ten years, several studies showed deregulated miRNA expression, both in blood cells and in CNS lesions, lineage-specific in particular cell populations, or at particular MS stages or subtypes. Further, during both relapse and remission periods, differential expression of various miRNAs was observed in PBMC of MS patients [94].

A better knowledge of the aetiology of multiple sclerosis as well as new alternative techniques for the diagnosis and treatment of the disease can be derived from the analysis of miRNA dysregulation and associated changes at the level of the miRNA/protein interaction [95]. Neurotrophic variables influencing neuroplasticity and neuroprotection in the CNS are known to be more important in neurodegenerative diseases such as MS.

When neuroprotective factors, such as nerve growth factor, brain-derived neurotrophic factor (*BDNF*), neurotrophin 3 (*NT-3*), and neurotrophin 4/5 (*NT-4/5*) are deficient in MS patients, the influx of PBMC cells to the CNS can make up for this, slowing the rate of cerebral atrophy. The protective impact on neuronal axons in the course of MS was linked to the *BDNF* factor released by PBMCs [91]. Heat shock proteins (HSPs) were demonstrated to have a neuroprotective effect by triggering anti-apoptotic pathways in addition to inhibiting the aggregation of misfolded proteins. The inflammatory process seen in the early stages of MS serves as a trigger for glial cells to express HSPs and release them into the extracellular environment, protecting nerve cells in the disease's later neurodegenerative stages. Overexpression of most HSPs caused by inflammation and oxidative stress was seen in lesions in the CNS of MS patients and in an animal model of MS disease [96]. A class of histone deacetylases known as sirtuins (*SIRTs*) is controlled and dependent on the nicotinamide adenine dinucleotide. They participate in numerous processes that improve cell survival, while *SIRT1* preferentially inhibits genes linked to apoptosis and inflammation. In an animal model of MS, SIRT1 activation by SRT501 reduces brain dysfunction and stops neuronal death [97].

There is no information, however, on the function of miRNAs in controlling the level of expression of neuroprotective proteins, such as neurotrophies, heat shock proteins, and sirtuins, during the onset of multiple sclerosis.

In a recent work, Piotrzkowska et al., studied the effect of miRNAs on the expression levels of neuroprotective proteins, and some selected miRNAs. They specifically note a decrease in the expression of the *BDNF* and *SIRT1* genes, and an increase in the expression

of miR-132-3p, miR-34a, and miR-132 in PBMCs, of MS patients, suggesting that the investigated miRNAs may regulate the expression-level genes under study. This drives the immune system towards the chronic inflammation seen in MS. The findings imply that the levels of selected neurotrophins (*BDNF* and *NT4/5*), heat shock proteins (*HSP70* and *HSP27*), *SIRT1*, and selected miRNAs in PBMC cells may function as biomarkers of inflammation in the CNS and neurodegenerative processes in MS patients. Investigations using animal models of neurodegenerative and demyelinating disorders demonstrated that *SIRT1* activation can slow the progression of the illness. *SIRT1* is a prospective novel target for MS treatment intervention as well as a potential biomarker of relapses. *SIRT1* modulation might be a useful strategy for MS treatment or prevention [98].

Dysregulation of miRNA expression and function may be related to MS diagnosis and pathogenesis, and miRNA-related pathways may also be used as a potential therapeutic target for MS. In the recent work of Erkal et at., they identify miRNA biomarkers for MS illness by in silico data analysis. They identify and analyze in detail four miRNAs (mir-212-3p, mir-98-5p, mir-142-3p, and mir-629-5p), and their target genes and related pathways were searched using different tools. For this investigation, immunological and neurological system-related pathways were given priority. They found that miR-142-3p, miR-98-5p, and miR-629-5p were upregulated and miR-212-3p was downregulated, and all were statistically significant. Their results demonstrate that miR-212-3p pathways (such as Toll-like receptor, neurotrophin signaling pathway, and cytokine–cytokine receptor interaction) and their common target genes *MAPK1*, *PIK3R3*, and *PIK3R1* have an effective role in the regulation of immune- and nervous-related systems. Compared to controls, they discovered that mir-98 has a greater expression level. According to their study, mir-98–5p is crucial for the JAK-STAT, ErbB, TGF-beta, and MAPK signaling pathways. Target genes of the mir-142-3p-associated pathways include *PIK3R5*, *PIK3CD*, *RAC1*, *AKT2*, and *PIK3R2*. Additionally, it was shown that these genes were connected to the PI3K-Akt signaling pathway. This pathway is involved in T cell responses. mir-142-3p, mir-98-5p, mir-629-5p, and mir-212-3p were shown to be statistically significant in the all-silico data analysis used to identify miRNA biomarkers for MS disease. Their target pathways and genes may also be useful in the pathophysiology of MS and aid in the diagnosis, prognosis, and therapy procedures [99]. Table 2 lists the studies discussed in the manuscript.

Table 2. Studies that detailed alterations in miRNA expression levels associated with multiple sclerosis.

Sources	Methodology	Cohort	Upregulated miRNAs	Downregulated miRNAs	Reference
N.A.	comprehensive literature review (61 papers)	N.A.	miR-142-3p, miR-146a/b, miR-145, miR-155, miR-22, miR223/-3p, miR-326, miR-584	miR-103, miR-15, miR-548, let-7, miR-140	Piket et al., 2019 [86]
Whole blood	microarray analysis	59 treatment naïve MS patients (18 PPMS, 17 SPMS, 24 RRMS) vs. 37 HC		miR-17 and miR-20a	COX et al., 2010 [88]
$CD4^+$	qRT-PCR	8 RRMS patients vs. 10 HC (discovery cohort) 23 RRMS patients vs. 20 HC (validation cohort)	miR-485-3p, miR-376a, miR-497, miR-193a, miR-126, miR-17-5p	miR-34a	Lindberg et al., 2010 [89]
naïve CD4+ T cells, memory CD4+ T cells	qRT-PCR	22 treatment naïve MS patients (5 PPMS, 5 SPMS, 12 RRMS) vs. 16 HC	miR-128, miR-27b (naïve CD4+ T cells), miR-340 (memory CD4+ T cells)		Guerau-de-Arellano et al., 2011 [92]

Table 2. *Cont.*

Sources	Methodology	Cohort	Upregulated miRNAs	Downregulated miRNAs	Reference
PBMC	qRT-PCR	28 MS patients (15 SPMS, 13 RRMS) vs. 33 HC	miR-132, miR-21-5p, miR-181b-5p, miR-34a, miR-132-3p	miR-134	Piotrzkowska et al., 2021 [98]
PBMC	Datasets analysis (from GEO)	66 MS patients vs. 185 HC	mir-142-3p, mir-98, mir-629	hsa-mir-212	Erkal et al., 2022 [99]

N.A., not applicable; GEO, NCBI Gene Expression Omnibus; HC, healthy controls; RRMS, relapsing-remitting multiple sclerosis; SPMS, secondary progressive multiple sclerosis; and PPMS, primary progressive multiple sclerosis.

In conclusion, research assessed the miRNAs present in blood, biological fluids, or cells of MS patients, revealing specific miRNAs that differ between MS and healthy controls. While there is a lack of replication in the literature regarding miRNAs as biomarkers and conflicting results from various forms of research, several miRNAs were found with proven roles in inflammatory signaling, including regulation of lymphocyte subsets. Finally, some studies addressed the impact of therapy on miRNA expression by comparing naïve to treated patients [100]. However, collecting samples free from the effects of therapy is one of the challenges in MS research and the impact of therapy on miRNA expression that has to be take in account in biomarkers discovery.

5. Remarks on the Interaction of Epigenetic Changes

More and more evidence was given for epigenetic mechanisms being the bridge between genetics and environment in the pathogenesis of MS. The three epigenetic alterations (DNA methylation, histone modification, and miRNA regulation) that are currently best understood interact with one another. An increasing body of research demonstrates how these systems all interact. For instance, miRNA expression is controlled by DNA methylation [101], histone modification [102], and miRNAs themselves [103]. The recruitment of DNA methyltransferase 3A by histone modification, and connections between methylated DNA and histone deacetylases are two other interactions [104]. In summary, the evidence described here suggests that miRNAs and the epigenetic apparatus are both regulated in a reciprocal manner. Epigenetic regulation is carried out by miRNAs as part of the epigenetic machinery. The expression of miRNAs was epigenetically controlled by DNA methylations, and histone modifications. At promoter CpG islands, DNA methylation is frequently established, which limits the expression of miRNAs. Histone modification now has the power to promote and suppress miRNA translation activation. Enzymes involved in epigenetics can also be miRNA targets. By controlling the activity of epigenetics-related enzymes, miRNAs control how DNA methylation and histone modification are expressed. Additionally, it was discovered that some miRNAs are controlled by epigenetic regulators and, as a result, have an impact on the epigenetic machinery. Finally, these interactions imply that the epigenomic modifications are controlled not just by individual mechanisms, but also by intricate and poorly understood interactions between these fundamental mechanisms. However, given the possible significance of epigenetic modifications in MS, a deeper comprehension of these pathways and how they interact with other elements of the illness will be essential to comprehending and ultimately treating MS.

Further research in this area should occur soon given the growing array of tools available to manipulate and evaluate the effects of epigenetic modifications, such as oligonucleotide-modified miRNA profiles, histone modification via histone deacetylase inhibitors, and DNA methylation silencing via DNA methyltransferase inhibitors. Thus far, research demonstrated that autoimmune disorders possess a noteworthy epigenetic foundation, primarily attributable to the impact of environmental variables that modulate the immune system. Understanding the specific epigenetic modifications that take place in a patient's genome can aid in determining which genes may require regulation and by what

epigenetic regulatory pathways. Today, there is consensus that personalized epigenetics has the potential to transform the diagnostic, prognostic, and therapeutic approach for the treatment of autoimmune disorders such as MS. The interindividual differences in various epigenetic signatures, such as DNA methylation, histone modifications, and microRNAs, are the fundamental components of personalized epigenetics. Moreover, computational epigenetics opened up new avenues to use complex epigenomic data in patient diagnosis, prognosis, and treatment.

The potential application of epigenetic modifications and their regulation could definitely lead to the development of an entirely new field of methodology for the treatment and probable cure of MS.

6. Conclusions and Future Prospective

MS is a chronic condition that is influenced by both environmental and genetic factors. Despite the fact that the cause of the condition is unknown, epigenetic factors, such as DNA methylation and miRNA-based gene expression regulation, as well as histone modification, were linked to the pathogenesis of MS. Most MS-related genes are controlled by epigenetic processes in both immunological and central nervous system cells. Analysis of epigenetic modifications represents a useful strategy to decipher genome activity and its effect on the cellular and tissue dysfunction underlying MS. We summarized here the results of studies investigating epigenetic modifications. A large amount of research emphasized the significance of epigenetic mechanisms in the pathogenesis of MS, and studies so far made some progress in determining the involvement of epigenetics in MS. Several cellular processes including apoptosis, differentiation, and evolution can be modified along with epigenetic changes. Some alternations are associated with epigenetic mechanisms in MS patients and these changes can become key points for MS therapy. Indeed, knowledge of epigenetic modifications involved in the pathogenesis of MS opens a new avenue of research for identification of potential biomarkers, as well as finding new therapeutic targets. Although epigenetic therapy is still in its early stages, further research on the topic can be expected to reveal a new approach to understanding the phenotypic variations of MS. Drugs that can change abnormal histone modification, methylation, or miRNA expression in MS patients are the basis of epigenetic therapy [105].

Despite the lack of curative drugs capable of preventing the degeneration of nervous tissue, current therapies for MS are based on immunomodulatory and anti-inflammatory treatments. The goal of current MS treatments is to prevent further immune-mediated myelin degradation. Patients may still have progressive disability despite the widespread use of immunomodulatory treatments due to myelin regeneration failure and neuronal loss. Although these drugs reduce relapse rates, they fail to slow long-term disease progression of the disease or prevent neurodegeneration, and the long-term effects of early immunomodulatory intervention are not yet clear. Immunomodulatory drugs, such as interferons beta and glatiramer acetate, are used to treat MS; in particular, they reduce clinical attacks and the number of lesions [106]. However, these drugs can only be injected and have dangerous adverse effects. Furthermore, humanized monoclonal antibodies and oral drugs used to treat patients with MS exhibited several serious side effects, such as progressive multifocal leukoencephalopathy [107].

Patients with MS who are receiving therapy showed a variety of reactions. In order to direct these patients toward more efficacious treatments, predictive testing should be performed on them within the context of personalized medicine. In addition to the progress made in medication development, it is appropriate to select a therapy that considers each patient's distinct genetic background. Thus, the discovery of genetic markers that impact the effectiveness of existing MS treatments can be viewed as a promising beginning that may lead to other discoveries down the road.

As epigenetic abnormalities, especially those that contribute to the etiology of autoimmune diseases, are better defined, it will be possible to find new epigenetic markers for early diagnosis and identification of new therapeutic targets. Importantly, epigenetic modi-

fications are regulatory, stable, and reversible. Therefore, studying epigenetic mechanisms could represent a promising approach to better understand the mechanisms underlying MS and other diseases with similar complex etiology and improve therapeutic solutions. In conclusion, numerous studies established the importance of epigenetics in the pathogenesis of MS, and as a result, scientists are working to develop MS drugs with the fewest possible side effects. This can be accomplished by figuring out the specific mechanisms of epigenetics that contribute to MS pathogenesis. Further investigation into the epigenetic pathways underlying MS will undoubtedly open the door to creating novel diagnostic criteria, tracking disease activity, and designing epigenetically valid treatment strategies.

Author Contributions: I.M.: Conceptualization, writing—original draft. S.D.B.: data curation. D.P.: and supervision. All authors contributed to the article and approved the submitted version. All authors have read and agreed to the published version of the manuscript.

Funding: This research received no external funding.

Conflicts of Interest: The authors declare no conflicts of interest.

References

1. Dendrou, C.A.; Fugger, L.; Friese, M.A. Immunopathology of multiple sclerosis. *Nat. Rev. Immuno.* **2015**, *15*, 545–558. [CrossRef]
2. Franklin, R.J.; Ffrench-Constant, C. Remyelination in the CNS: From biology to therapy. *Nat. Rev. Neurosci.* **2008**, *9*, 839–855. [CrossRef]
3. Yamout, B.I.; Alroughani, R. Multiple Sclerosis. *Semin. Neurol.* **2018**, *38*, 212–225.
4. Kuhlmann, T.; Moccia, M.; Coetzee, T.; Cohen, J.A.; Correale, J.; Graves, J.; Marrie, R.A.; Montalban, X.; Yong, V.W.; Thompson, A.J.; et al. International Advisory Committee on Clinical Trials in Multiple Sclerosis. Multiple sclerosis progression: Time for a new mechanism-driven framework. *Lancet Neurol.* **2023**, *22*, 78–88. [CrossRef] [PubMed]
5. Zettl, U.K.; Stuve, O.; Patejd, R. Immune-mediated CNS diseases: A review on nosological classification and clinical features. *Autoimmun. Rev.* **2012**, *11*, 167–173. [CrossRef]
6. Lassmann, H.; van Horssen, J.; Mahad, D. Progressive multiple sclerosis: Pathology and pathogenesis. *Nat. Rev. Neurol.* **2012**, *8*, 647–656. [CrossRef] [PubMed]
7. Miller, D.H.; Leary, S.M. Primary-progressive multiple sclerosis. *Lancet Neurol.* **2007**, *6*, 903–912. [CrossRef]
8. Olsson, T.; Barcellos, L.F.; Alfredsson, L. Interactions between genetic, lifestyle and environmental risk factors for multiple sclerosis. *Nat. Rev. Neurol.* **2017**, *13*, 25–36. [CrossRef] [PubMed]
9. Briggs, F.B.; Acuna, B.; Shen, L.; Ramsay, P.; Quach, H.; Bernstein, A.; Bellesis, K.H.; Kockum, I.S.; Hedström, A.K.; Alfredsson, L.; et al. Smoking and risk of multiple sclerosis: Evidence of modification by NAT1 variants. *Epidemiology* **2015**, *25*, 605–614. [CrossRef]
10. Scazzone, C.; Agnello, L.; Bivona, G.; Lo Sasso, B.; Ciaccio, M. Vitamin D and Genetic Susceptibility to Multiple Sclerosis. *Biochem. Genet.* **2021**, *59*, 1–30. [CrossRef]
11. Agnello, L.; Scazzone, C.; Sasso, B.L.; Vidali, M.; Giglio, R.V.; Ciaccio, A.M.; Ragonese, P.; Salemi, G.; Ciaccio, M. Role of Multiple Vitamin D-Related Polymorphisms in Multiple Sclerosis Severity: Preliminary Findings. *Genes* **2022**, *13*, 1307. [CrossRef] [PubMed]
12. Scazzone, C.; Agnello, L.; Lo Sasso, B.; Salemi, G.; Gambino, C.M.; Ragonese, P.; Candore, G.; Ciaccio, A.M.; Giglio, R.V.; Bivona, G.; et al. FOXP3 and GATA3 Polymorphisms, Vitamin D3 and Multiple Sclerosis. *Brain Sci.* **2021**, *11*, 415. [CrossRef] [PubMed]
13. Scazzone, C.; Agnello, L.; Sasso, B.L.; Ragonese, P.; Bivona, G.; Realmuto, S.; Iacolino, G.; Gambino, C.M.; Bellia, C.; Salemi, G.; et al. Klotho and vitamin D in multiple sclerosis: An Italian study. *Arch. Med. Sci.* **2019**, *16*, 842–847. [CrossRef] [PubMed]
14. Agnello, L.; Scazzone, C.; Lo Sasso, B.; Bellia, C.; Bivona, G.; Realmuto, S.; Brighina, F.; Schillaci, R.; Ragonese, P.; Salemi, G.; et al. VDBP, CYP27B1, and 25-Hydroxyvitamin D Gene Polymorphism Analyses in a Group of Sicilian Multiple Sclerosis Patients. *Biochem. Genet.* **2017**, *55*, 183–192. [CrossRef] [PubMed]
15. Sawcer, S.; Hellenthal, G.; Pirinen, M.; Spencer, C.C.A.; Patsopoulos, N.A.; Moutsianas, L.; Dilthey, A.; Su, Z.; Freeman, C.; Hunt, S.E.; et al. Genetic risk and a primary role for cell-mediated immune mechanisms in multiple sclerosis. *Nature* **2011**, *476*, 214–219.
16. Goll, M.G.; Bestor, T.H. Eukaryotic cytosine methyltransferases. *Annu. Rev. Biochem.* **2005**, *74*, 481–514. [CrossRef]
17. Lorincz, M.C.; Dickerson, D.R.; Schmitt, M.; Groudine, M. Intragenic DNA methylation alters chromatin structure and elongation efficiency in mammalian cells. *Nat. Struct. Mol. Biol.* **2004**, *11*, 1068–1075. [CrossRef] [PubMed]
18. Shukla, S.; Kavak, E.; Gregory, M.; Imashimizu, M.; Shutinoski, B.; Kashlev, M.; Oberdoerffer, P.; Sandberg, R.; Oberdoerffer, S. CTCF-promoted RNA polymerase II pausing links DNA methylation to splicing. *Nature* **2011**, *479*, 74–79. [CrossRef]
19. Okano, M.; Bell, D.W.; Haber, D.A.; Li, E. DNA methyltransferases Dnmt3a and Dnmt3b are essential for de novo methylation and mammalian development. *Cell* **1999**, *99*, 247–257. [CrossRef]
20. Castillo-Aguilera, O.; Depreux, P.; Halby, L.; Arimondo, P.B.; Goossens, L. DNA Methylation Targeting: The DNMT/HMT Crosstalk Challenge. *Biomolecules* **2017**, *7*, 3. [CrossRef]

21. Barau, J.; Teissandier, A.; Zamudio, N.; Roy, S.; Nalesso, V.; Hérault, Y.; Guillou, F.; Bourc'his, D. The DNA methyltransferase DNMT3C protects male germ cells from transposon activity. *Science* **2016**, *354*, 909–912. [CrossRef] [PubMed]
22. Greenberg, M.V.C.; Bourc'his, D. The diverse roles of DNA methylation in mammalian development and disease. *Nat. Rev. Mol. Cell Biol.* **2019**, *20*, 590–607. [CrossRef] [PubMed]
23. Kouzarides, T. Chromatin modifications and their function. *Cell* **2007**, *128*, 693–705. [CrossRef] [PubMed]
24. Yun, M.; Wu, J.; Workman, J.L.; Li, B. Readers of histone modifications. *Cell Res.* **2011**, *21*, 564–578. [CrossRef] [PubMed]
25. Shahbazian, M.D.; Grunstein, M. Functions of site-specific histone acetylation and deacetylation. *Annu. Rev. Biochem.* **2007**, *76*, 75–100. [CrossRef] [PubMed]
26. Bartel, D.P. MicroRNAs: Genomics, biogenesis, mechanism, and function. *Cell* **2004**, *116*, 281–297. [CrossRef]
27. Backes, C.; Meese, C.E.; Lenhof, H.P.; Keller, A. A dictionary on microRNAs and their putative target pathways. *Nucleic Acids Res.* **2010**, *38*, 4476–4486. [CrossRef] [PubMed]
28. Lombardi, G.; Perego, S.; Sansoni, V.; Banfi, G. Circulating miRNA as fine regulators of the physiological responses to physical activity: Pre-analytical warnings for a novel class of biomarkers. *Clin. Biochem.* **2016**, *49*, 1331–1339. [CrossRef] [PubMed]
29. Iyengar, B.R.; Choudhary, A.; Sarangdhar, M.A.; Venkatesh, K.V.; Gadgil, C.J.; Pillai, B. Non-coding RNA interact to regulate neuronal development and function. *Front. Cell. Neurosci.* **2014**, *8*, 47. [CrossRef]
30. Jin, X.F.; Wu, N.; Wang, L.; Li, J. Circulating microRNAs: A novel class of potential biomarkers for diagnosing and prognosing central nervous system diseases. *Cell. Mol. Neurobiol.* **2013**, *33*, 601–613. [CrossRef]
31. Liu, J.; Sandoval, J.; Doh, S.T.; Cai, L.; López-Rodas, G.; Casaccia, P. Epigenetic modifiers are necessary but not sufficient for reprogramming non-myelinating cells into myelin gene-expressing cells. *PLoS ONE* **2010**, *5*, e13023. [CrossRef]
32. Mao, X.Y.; Yin, X.X.; Guan, Q.W.; Xia, Q.X.; Yang, N.; Zhou, H.H.; Liu, Z.Q.; Jin, W.L. Dietary nutrition for neurological disease therapy: Current status and future directions. *Pharmacol. Ther.* **2021**, *226*, 107861. [CrossRef]
33. Copray, S.; Huynh, J.L.; Sher, F.; Casaccia-Bonnefil, P.; Boddeke, E. Epigenetic mechanisms facilitating oligodendrocyte development, maturation, and aging. *Glia* **2009**, *57*, 1579–1587. [CrossRef] [PubMed]
34. Li, E.; Zhang, Y. DNA methylation in mammals. *Cold Spring Harb. Perspect. Biol.* **2014**, *6*, a019133. [CrossRef]
35. Xu, Z.; Li, X. DNA methylation in neurodegenerative disorders. *Curr. Geriatr. Rep.* **2012**, *1*, 199–205. [CrossRef]
36. Landgrave-Gomez, J.; Mercado-Gomez, O.; Guevara-Guzman, R. Epigenetic mechanisms in neurological and neurodegenerative diseases. *Front. Cell. Neurosci.* **2015**, *9*, 58.
37. Hojati, Z. Molecular Genetic and Epigenetic Basis of Multiple Sclerosis. *Adv. Exp. Med. Biol.* **2017**, *958*, 65–90. [PubMed]
38. Kürtüncü, M.; Tüzün, E. Multiple sclerosis: Could it be an epigenetic disease? *Med. Hypotheses* **2008**, *71*, 945–947. [CrossRef]
39. On, N.H.; Kiptoo, P.; Siahaan, T.J.; Miller, D.W. Modulation of blood-brain barrier permeability in mice using synthetic E-cadherin peptide. *Mol. Pharm.* **2014**, *11*, 974–981. [CrossRef]
40. Liggettt, T.; Melnikov, A.; Tilwalli, S.; Yi, Q.; Chen, H.; Replogle, C.; Feng, X.; Reder, A.; Stefoski, D.; Balabanov, R.; et al. Methylation patterns of cell-free plasma DNA in relapsing-remitting multiple sclerosis. *J. Neurol. Sci.* **2010**, *290*, 16–21. [CrossRef]
41. Tiane, A.; Schepers, M.; Reijnders, R.A.; van Veggel, L.; Chenine, S.; Rombaut, B.; Dempster, E.; Verfaillie, C.; Wasner, K.; Grünewald, A.; et al. From methylation to myelination: Epigenomic and transcriptomic profiling of chronic inactive demyelinated multiple sclerosis lesions. *Acta Neuropathol.* **2023**, *146*, 283–299. [CrossRef]
42. Tiane, A.; Somers, V.; Hellings, N.; van den Hove, D.L.A.; Vanmierlo, T. The Impact of Sample Storage on Blood Methylation: Towards Assessing Myelin Gene Methylation as a Biomarker for Progressive Multiple Sclerosis. *Int. J. Mol. Sci.* **2024**, *25*, 3468. [CrossRef]
43. Sokratous, M.; Dardiotis, E.; Tsouris, Z.; Bellou, E.; Michalopoulou, A.; Siokas, V.; Arseniou, S.; Stamati, T.; Tsivgoulis, G.; Bogdanos, D.; et al. Deciphering the role of DNA methylation in multiple sclerosis: Emerging issues. *Autoimmun. Highlights* **2016**, *7*, 12. [CrossRef] [PubMed]
44. Levenson, V.V.; Melnikov, A.A. DNA methylation as clinically useful biomarkers-light at the end of the tunnel. *Pharmaceuticals* **2012**, *5*, 94. [CrossRef] [PubMed]
45. Kumagai, C.; Kalman, B.; Middleton, F.A.; Vyshkina, T.; Massa, P.T. Increased promoter methylation of the immune regulatory gene SHP-1 in leukocytes of multiple sclerosis subjects. *J. Neuroimmunol.* **2012**, *246*, 51–57. [CrossRef]
46. Janson, P.C.; Linton, L.B.; Bergman, E.A.; Marits, P.; Eberhardson, M.; Piehl, F.; Malmström, V.; Winqvist, O. Profiling of CD4+ T cells with epigenetic immune lineage analysis. *J. Immunol.* **2011**, *186*, 92–102. [CrossRef]
47. Koch, M.W.; Metz, L.M.; Kovalchuk, O. Epigenetic changes in patients with multiple sclerosis. *Nat. Rev. Neurol.* **2013**, *9*, 35–43. [CrossRef] [PubMed]
48. Mastronardi, F.G.; Noor, A.; Wood, D.D.; Paton, T.; Moscarello, M.A. Peptidyl arginine deiminase 2 CpG island in multiple sclerosis white matter is hypomethylated. *J. Neurosci. Res.* **2007**, *85*, 2006–21016. [CrossRef]
49. Ransohoff, R.M. How neuroinflammation contributes to neurodegeneration. *Science* **2016**, *353*, 777–783. [CrossRef]
50. Von Bartheld, C.S.; Bahney, J.; Herculano-Houzel, S. The search for true numbers of neurons and glial cells in the human brain: A review of 150 years of cell counting. *J. Comp. Neurol.* **2016**, *524*, 3865–3895. [CrossRef]
51. Huynh, J.L.; Garg, P.; Thin, T.H.; Yoo, S.; Dutta, R.; Trapp, B.D.; Haroutunian, V.; Zhu, J.; Donovan, M.J.; Sharp, A.J.; et al. Epigenome-wide differences in pathology-free regions of multiple sclerosis-affected brains. *Nat. Neurosci.* **2014**, *17*, 121–130. [CrossRef] [PubMed]

52. Chomyk, A.M.; Volsko, C.; Tripathi, A.; Deckard, S.A.; Trapp, B.D.; Fox, R.J.; Dutta, R. DNA methylation in demyelinated multiple sclerosis hippocampus. *Sci. Rep.* **2017**, *7*, 8696. [CrossRef] [PubMed]
53. Kular, L.; Needhamsen, M.; Adzemovic, M.Z.; Kramarova, T.; Gomez-Cabrero, D.; Ewing, E.; Piket, E.; Tegnér, J.; Beck, S.; Piehl, F.; et al. Neuronal methylome reveals CREB-associated neuro-axonal impairment in multiple sclerosis. *Clin. Epigenet.* **2019**, *11*, 86. [CrossRef] [PubMed]
54. Kular, L.; Ewing, E.; Needhamsen, M.; Pahlevan Kakhki, M.; Covacu, R.; Gomez-Cabrero, D.; Brundin, L.; Jagodic, M. DNA methylation changes in glial cells of the normal-appearing white matter in Multiple Sclerosis patients. *Epigenetics* **2022**, *17*, 1311–1330. [CrossRef]
55. Celarain, N.; Tomas-Roig, J. Aberrant DNA methylation profile exacerbates inflammation and neurodegeneration in multiple sclerosis patients. *J. Neuroinflamm.* **2020**, *17*, 21. [CrossRef]
56. Kiselev, I.S.; Kulakova, O.G.; Baturina, O.A.; Kabilov, M.R.; Boyko, A.N.; Favorova, O.O. DNA Methylation Profile of CD14+ Monocytes Changes in Primary Progressive Multiple Sclerosis. *Mol. Biol.* **2023**, *57*, 819–826. [CrossRef]
57. Maltby, V.E.; Lea, R.A.; Ribbons, K.A.; Sanders, K.A.; Kennedy, D.; Min, M.; Scott, R.J.; Lechner-Scott, J. DNA methylation changes in CD4+ T cells isolated from multiple sclerosis patients on dimethyl fumarate. *Mult. Scler. J. Exp. Transl. Clin.* **2018**, *4*, 2055217318787826. [CrossRef]
58. Ewing, E.; Kular, L.; Fernandes, S.J.; Karathanasis, N.; Lagani, V.; Ruhrmann, S.; Tsamardinos, I.; Tegner, J.; Piehl, F.; Gomez-Cabrero, D.; et al. Combining evidence from four immune cell types identifies DNA methylation patterns that implicate functionally distinct pathways during multiple sclerosis progression. *EBioMedicine* **2019**, *43*, 411–423. [CrossRef]
59. Kiselev, I.; Danilova, L.; Baulina, N.; Baturina, O.; Kabilov, M.; Boyko, A.; Kulakova, O.; Favorova, O. Genome-wide DNA methylation profiling identifies epigenetic changes in CD4+ and CD14+ cells of multiple sclerosis patients. *Mult. Scler. Relat. Disord.* **2022**, *60*, 103714. [CrossRef]
60. Graves, M.C.; Benton, M.; Lea, R.A.; Boyle, M.; Tajouri, L.; Macartney-Coxson, D.; Scott, R.J.; Lechner-Scott, J. Methylation differences at the HLA-DRB1 locus in CD4+ T-Cells are associated with multiple sclerosis. *Mult. Scler.* **2014**, *20*, 1033–1041. [CrossRef]
61. Kular, L.; Liu, Y.; Ruhrmann, S.; Zheleznyakova, G.; Marabita, F.; Gomez-Cabrero, D.; James, T.; Ewing, E.; Lindén, M.; Górnikiewicz, B.; et al. DNA methylation as a mediator of HLA-DRB1*15:01 and a protective variant in multiple sclerosis. *Nat. Commun.* **2018**, *9*, 2397. [CrossRef] [PubMed]
62. Xavier, A.; Maltby, V.E.; Ewing, E.; Campagna, M.P.; Burnard, S.M.; Tegner, J.N.; Slee, M.; Butzkueven, H.; Kockum, I.; Kular, L.; et al. DNA Methylation Signatures of Multiple Sclerosis Occur Independently of Known Genetic Risk and Are Primarily Attributed to B Cells and Monocytes. *Int. J. Mol. Sci.* **2023**, *24*, 12576. [CrossRef]
63. Ramazi, S.; Allahverdi, A.; Zahiri, J. Evaluation of post-translational modifications in histone proteins: A review on histone modification defects in developmental and neurological disorders. *J. Biosci.* **2020**, *45*, 135. [CrossRef]
64. Huynh, J.L.; Casaccia, P. Epigenetic mechanisms in multiple sclerosis: Implications for pathogenesis and treatment. *Lancet Neurol.* **2013**, *12*, 195–206. [CrossRef] [PubMed]
65. Niller, H.H.; Wolf, H.; Minarovits, J. Epigenetic dysregulation of the host cell genome in Epstein-Barr virus-associated neoplasia. *Semin. Cancer Biol.* **2009**, *19*, 158–164. [CrossRef] [PubMed]
66. Wan, E.S.; Qiu, W.; Baccarelli, A.; Carey, V.J.; Bacherman, H.; Rennard, S.I.; Agusti, A.; Anderson, W.; Lomas, D.A.; Demeo, D.L. Cigarette smoking behaviors and time since quitting are associated with differential DNA methylation across the human genome. *Hum. Mol. Genet.* **2012**, *21*, 3073–3082. [CrossRef]
67. Pereira, F.; Barbáchano, A.; Singh, P.K.; Campbell, M.J.; Muñoz, A.; Larriba, M.J. Vitamin D has wide regulatory effects on histone demethylase genes. *Cell Cycle* **2012**, *11*, 1081–1089. [CrossRef]
68. Gray, S.G.; Dangond, F. Rationale for the use of histone deacetylase inhibitors as a dual therapeutic modality in multiple sclerosis. *Epigenetics* **2006**, *1*, 67–75. [CrossRef]
69. Pedre, X.; Mastronardi, F.; Bruck, W.; López-Rodas, G.; Kuhlmann, T.; Casaccia, P. Changed histone acetylation patterns in normal-appearing white matter and early multiple sclerosis lesions. *J. Neurosci.* **2011**, *31*, 3435–3445. [CrossRef]
70. Singhal, N.K.; Li, S.; Arning, E.; Alkhayer, K.; Clements, R.; Sarcyk, Z.; Dassanayake, R.S.; Brasch, N.E.; Freeman, E.J.; Bottiglieri, T.; et al. Changes in Methionine Metabolism and Histone H3 Trimethylation Are Linked to Mitochondrial Defects in Multiple Sclerosis. *J. Neurosci.* **2015**, *35*, 15170–15186. [CrossRef]
71. Singhal, N.K.; Freeman, E.; Arning, E.; Wasek, B.; Clements, R.; Sheppard, C.; Blake, P.; Bottiglieri, T.; McDonough, J. Dysregulation of methionine metabolism in multiple sclerosis. *Neurochem. Int.* **2018**, *112*, 1–4. [CrossRef] [PubMed]
72. Singhal, N.K.; Huang, H.; Li, S.; Clements, R.; Gadd, J.; Daniels, A.; Kooijman, E.E.; Bannerman, P.; Burns, T.; Guo, F.; et al. The neuronal metabolite NAA regulates histone H3 methylation in oligodendrocytes and myelin lipid composition. *Exp. Brain Res.* **2017**, *235*, 279–292. [CrossRef]
73. Li, S.; Clements, R.; Sulak, M.; Gregory, R.; Freeman, E.; McDonough, J. Decreased NAA in gray matter is correlated with decreased availability of acetate in white matter in postmortem multiple sclerosis cortex. *Neurochem. Res.* **2013**, *38*, 2385–2396. [CrossRef]
74. Sternbach, S.; West, N.; Singhal, N.K.; Clements, R.; Basu, S.; Tripathi, A.; Dutta, R.; Freeman, E.J.; McDonough, J. The BHMT-betaine methylation pathway epigenetically modulates oligodendrocyte maturation. *PLoS ONE* **2021**, *16*, e0250486. [CrossRef]

75. Mastronardi, F.G.; Wood, D.D.; Mei, J.; Raijmakers, R.; Tseveleki, V.; Dosch, H.M.; Probert, L.; Casaccia-Bonnefil, P.; Moscarello, M.A. Increased citrullination of histone H3 in multiple sclerosis brain and animal models of demyelination: A role for tumor necrosis factor-induced peptidylarginine deiminase 4 translocation. *J. Neurosci.* **2006**, *26*, 11387–11396. [CrossRef]
76. Zhang, J.; Jing, L.; Li, M.; He, L.; Guo, Z. Regulation of histone arginine methylation/demethylation by methylase and demethylase (Review). *Mol. Med. Rep.* **2019**, *19*, 3963–3971. [CrossRef]
77. Faigle, W.; Cruciani, C.; Wolski, W.; Roschitzki, B.; Puthenparampil, M.; Tomas-Ojer, P.; Sellés-Moreno, C.; Zeis, T.; Jelcic, I.; Schaeren-Wiemers, N.; et al. Brain Citrullination Patterns and T Cell Reactivity of Cerebrospinal Fluid-Derived CD4+ T Cells in Multiple Sclerosis. *Front. Immunol.* **2019**, *10*, 540. [CrossRef] [PubMed]
78. Dubey, S.K.; Dubey, R.; Kleinman, M.E. Unraveling Histone Loss in Aging and Senescence. *Cells* **2024**, *13*, 320. [CrossRef]
79. Strahl, B.D.; Allis, C.D. The language of covalent histone modifications. *Nature* **2000**, *403*, 41–45. [CrossRef]
80. Liu, R.; Wu, J.; Guo, H.; Yao, W.; Li, S.; Lu, Y.; Jia, Y.; Liang, X.; Tang, J.; Zhang, H. Post-translational modifications of histones: Mechanisms, biological functions, and therapeutic targets. *MedComm* **2023**, *4*, e292. [CrossRef] [PubMed]
81. Sidoli, S.; Bhanu, N.V.; Karch, K.R.; Wang, X.; Garcia, B.A. Complete Workflow for Analysis of Histone Post-translational Modifications Using Bottom-up Mass Spectrometry: From Histone Extraction to Data Analysis. *J. Vis. Exp.* **2016**, *111*, 54112.
82. De Benedittis, S.; Gaspari, M.; Magariello, A.; Spadafora, P.; Citrigno, L.; Romeo, N.; Qualtieri, A. LC-MALDI-TOF ISD MS analysis is an effective, simple and rapid method of investigation for histones characterization: Application to EBV lymphoblastoid cell lines. *J. Mass Spectrom.* **2021**, *56*, e4712. [CrossRef] [PubMed]
83. Catalanotto, C.; Cogoni, C.; Zardo, G. MicroRNA in Control of Gene Expression: An Overview of Nuclear Functions. *Int. J. Mol. Sci.* **2016**, *17*, 1712. [CrossRef] [PubMed]
84. Raisch, J.; Darfeuille-Michaud, A.; Nguyen, H.T. Role of microRNAs in the immune system, inflammation and cancer. *World, J. Gastroenterol.* **2013**, *19*, 2985–2996. [CrossRef]
85. Mohammed, E.M. Environmental Influencers, MicroRNA, and Multiple Sclerosis. *J. Cent. Nerv. Syst. Dis.* **2020**, *12*, 1179573519894955. [CrossRef] [PubMed]
86. Piket, E.; Zheleznyakova, G.Y.; Kular, L.; Jagodic, M. Small non-coding RNAs as important players, biomarkers and therapeutic targets in multiple sclerosis: A comprehensive overview. *J. Autoimmun.* **2019**, *101*, 17–25. [CrossRef] [PubMed]
87. de Faria, O., Jr.; Moore, C.S.; Kennedy, T.E.; Antel, J.P.; Bar-Or, A.; Dhaunchak, A.S. MicroRNA dysregulation in multiple sclerosis. *Front. Genet.* **2013**, *3*, 311.
88. Cox, M.B.; Cairns, M.J.; Gandhi, K.S.; Carroll, A.P.; Moscovis, S.; Stewart, G.J.; Broadley, S.; Scott, R.J.; Booth, D.R.; Lechner-Scott, J. ANZgene Multiple Sclerosis Genetics Consortium. MicroRNAs miR-17 and miR-20a inhibit T cell activation genes and are under-expressed in MS whole blood. *PLoS ONE* **2010**, *5*, e12132. [CrossRef]
89. Lindberg, R.L.; Hoffmann, F.; Mehling, M.; Kuhle, J.; Kappos, L. Altered expression of miR-17-5p in CD4+ lymphocytes of relapsing-remitting multiple sclerosis patients. *Eur. J. Immunol.* **2010**, *40*, 888–898. [CrossRef]
90. Juntilla, M.M.; Koretzky, G.A. Critical roles of the PI3K/Akt signaling pathway in T cell development. *Immunol. Lett.* **2008**, *116*, 104–110. [CrossRef]
91. Fruman, D.A.; Bismuth, G. Fine tuning the immune response with PI3K. *Immunol. Rev.* **2009**, *228*, 253–272. [CrossRef] [PubMed]
92. Guerau-de-Arellano, M.; Smith, K.M.; Godlewski, J.; Liu, Y.; Winger, R.; Lawler, S.E.; Whitacre, C.C.; Racke, M.K.; Lovett-Racke, A.E. Micro-RNA dysregulation in multiple sclerosis favours pro-inflammatory T-cell-mediated autoimmunity. *Brain* **2011**, *134 Pt 12*, 3578–3589. [CrossRef]
93. Mahad, D.H.; Trapp, B.D.; Lassmann, H. Pathological mechanisms in progressive multiple sclerosis. *Lancet Neurol.* **2015**, *14*, 183–193. [CrossRef]
94. Yousuf, A.; Qurashi, A. Non-coding RNAs in the Pathogenesis of Multiple Sclerosis. *Front. Genet.* **2021**, *12*, 717922. [CrossRef] [PubMed]
95. Huang, H.Y.; Lin, Y.C.; Li, J.; Huang, K.Y.; Shrestha, S.; Hong, H.C.; Tang, Y.; Chen, Y.G.; Jin, C.N.; Yu, Y.; et al. miRTarBase 2020: Updates to the experimentally validated microRNA-target interaction database. *Nucleic Acids Res.* **2020**, *48*, D148–D154. [CrossRef] [PubMed]
96. Welch, W.J. Heat shock proteins functioning as molecular chaperones: Their roles in normal and stressed cells. *Philos. Trans. R. Soc. Lond. B Biol. Sci.* **1993**, *339*, 327–333.
97. Nimmagadda, V.K.; Makar, T.K.; Chandrasekaran, K.; Sagi, A.R.; Ray, J.; Russell, J.W.; Bever, C.T., Jr. SIRT1 and NAD+ precursors: Therapeutic targets in multiple sclerosis a review. *J. Neuroimmunol.* **2017**, *304*, 29–34. [CrossRef]
98. Piotrzkowska, D.; Miller, E.; Kucharska, E.; Niwald, M.; Majsterek, I. Association of miRNA and mRNA Levels of the Clinical Onset of Multiple Sclerosis Patients. *Biology* **2021**, *10*, 554. [CrossRef]
99. Erkal, B.; Vural Korkut, S. Identification of miRNAs and their potential effects on multiple sclerosis related pathways using ın silico analysis. *Mult. Scler. Relat. Disord.* **2022**, *59*, 103642. [CrossRef]
100. Waschbisch, A.; Atiya, M.; Linker, R.A.; Potapov, S.; Schwab, S.; Derfuss, T. Glatiramer acetate treatment normalizes deregulated microRNA expression in relapsing remitting multiple sclerosis. *PLoS ONE* **2011**, *6*, e24604. [CrossRef]
101. Han, L.; Witmer, P.D.; Casey, E.; Valle, D.; Sukumar, S. DNA methylation regulates MicroRNA expression. *Cancer Biol. Ther.* **2007**, *6*, 1284–1288. [CrossRef] [PubMed]
102. Scott, G.K.; Mattie, M.D.; Berger, C.E.; Benz, S.C.; Benz, C.C. Rapid alteration of microRNA levels by histone deacetylase inhibition. *Cancer Res.* **2006**, *66*, 1277–1281. [CrossRef] [PubMed]

103. Zhao, S.; Wang, Y.; Liang, Y.; Zhao, M.; Long, H.; Ding, S.; Yin, H.; Lu, Q. MicroRNA-126 regulates DNA methylation in CD4+ T cells and contributes to systemic lupus erythematosus by targeting DNA methyltransferase 1. *Arthritis Rheum.* **2011**, *63*, 1376–1386. [CrossRef] [PubMed]
104. Yao, Q.; Chen, Y.; Zhou, X. The roles of microRNAs in epigenetic regulation. *Curr. Opin. Chem. Biol.* **2019**, *51*, 11–17. [CrossRef] [PubMed]
105. van der Star, B.J.; Vogel, D.Y.; Kipp, M.; Puentes, F.; Baker, D.; Amor, S. In vitro and in vivo models of multiple sclerosis. *CNS Neurol. Disord. Drug Targets* **2012**, *11*, 570–588. [CrossRef] [PubMed]
106. Lalive, P.H.; Neuhaus, O.; Benkhoucha, M.; Burger, D.; Hohlfeld, R.; Zamvil, S.S.; Weber, M.S. Glatiramer acetate in the treatment of multiple sclerosis: Emerging concepts regarding its mechanism of action. *CNS Drugs* **2011**, *25*, 401–414. [CrossRef] [PubMed]
107. Kang, C.; Blair, H.A. Ofatumumab: A Review in Relapsing Forms of Multiple Sclerosis. *Drugs* **2022**, *82*, 55–62. [CrossRef]

Disclaimer/Publisher's Note: The statements, opinions and data contained in all publications are solely those of the individual author(s) and contributor(s) and not of MDPI and/or the editor(s). MDPI and/or the editor(s) disclaim responsibility for any injury to people or property resulting from any ideas, methods, instructions or products referred to in the content.

International Journal of
Molecular Sciences

MDPI

Article

Investigating the Impact of the Parkinson's-Associated GBA1 E326K Mutation on β-Glucocerebrosidase Dimerization and Interactome Dynamics Through an In Silico Approach

Davide Pietrafesa [1,2], Alessia Casamassa [3], Barbara Benassi [4], Massimo Santoro [4], Massimo Marano [5,6], Claudia Consales [4], Jessica Rosati [3,7] and Caterina Arcangeli [4,*]

1 Department of Biology, University of Rome Tor Vergata, Via della Ricerca Scientifica 1, 00133 Rome, Italy; davide.pietrafesa@uniroma2.it
2 PhD Program in Materials for Health, Environment and Energy, University of Rome Tor Vergata, Via della Ricerca Scientifica 1, 00133 Rome, Italy
3 Cellular Reprogramming Unit, Fondazione IRCCS Casa Sollievo della Sofferenza, Viale dei Cappuccini 1, 71013 San Giovanni Rotondo, Italy; a.casamassa@css-mendel.it (A.C.); j.rosati@css-mendel.it or jessicadiana.rosati@unicamillus.org (J.R.)
4 Division of Biotechnologies, Department for Sustainability, Italian National Agency for New Technologies, Energy and Sustainable Economic Development (ENEA), Via Anguillarese 301, 00123 Rome, Italy; barbara.benassi@enea.it (B.B.); massimo.santoro@enea.it (M.S.); claudia.consales@enea.it (C.C.)
5 Unit of Neurology, Neurophysiology, Neurobiology and Psychiatry, Department of Medicine, University Campus Biomedico, Via Alvaro del Portillo 200, 00128 Rome, Italy; m.marano@policlinicocampus.it
6 Fondazione Policlinico Universitario Campus Biomedico, Via Alvaro del Portillo 200, 00128 Rome, Italy
7 Departmental Faculty of Medicine, UniCamillus, Saint Camillus International University of Health Sciences, Via di Sant'Alessandro 8, 00131 Rome, Italy
* Correspondence: caterina.arcangeli@enea.it; Tel.: +39-(06)-3048-6898

Abstract: Heterozygous mutations or genetic variants in the *GBA1* gene, which encodes for the β-glucocerebrosidase (GCase), a lysosomal hydrolase enzyme, may increase the risk of Parkinson's disease (PD) onset. The heterozygous E326K form is one of the most common genetic risk factors for PD worldwide, but, to date, the underlying molecular mechanisms remain unclear. Here, we investigate the effect of the E326K on the structure, stability, dimerization process, and interaction mode with some proteins of the interactome of GCase using multiple molecular dynamics (MD) simulations at pH 5.5 and pH 7.0 to mimic the lysosomal and endoplasmic reticulum environments, respectively. The analysis of the MD trajectories highlights that the E326K mutation did not significantly alter the structural conformation of the catalytic dyad but significantly makes the structure of the dimeric complexes unstable, especially at lysosomal pH, potentially impacting the organization of the quaternary structure. Furthermore, the E326K mutation significantly impacts protein interactions by altering the binding mode with the activator Saposin C (SapC), reducing the binding affinity with the inhibitor α-Synuclein (α-Syn), and increasing the affinity for the Lysosomal integral membrane protein-2 (LIMP-2) transporter.

Keywords: molecular dynamics simulation; Gaucher disease; GCase dimer structure; pH effect; Sap C; α-Syn; LIMP-2

1. Introduction

The correlation between the risk of developing Parkinson's disease (PD) and mutations in the *GBA1* gene has been known since the 1990s, when PD cases were first observed in Ashkenazi Jewish (AJ) patients with Gaucher's disease (GD) and in their family members [1,2]. GD is the most common autosomal recessive lysosomal storage disorder, in which the glycolipid substrate accumulates in cells. GD is caused by the defective activity of the *GBA1*-encoded β-glucocerebrosidase (GCase), a lysosomal enzyme. GCase is a

glycoprotein synthesized in the endoplasmic reticulum (ER), where it interacts with the lysosomal integral membrane protein 2 (LIMP-2) through hydrophobic interfaces, facilitating its transport to the lysosome. Here, GCase catalyzes the hydrolysis of glucosylceramide (GlcCer) into ceramide and glucose with the help of the activator protein Saposin C (SapC). SapC, a glycoprotein derived by proteolytic cleavage of Prosaposin [3], facilitates the interaction of GCase with its natural substrates and induces a conformational change that directly stimulates the enzyme's activity [4,5]. The structure of the glycoprotein GCase is characterized by three discontinuous domains (Figure 1A). Domain I is an antiparallel β-sheet flanked by a loop, while domain II forms an eight-stranded β-barrel organized in a manner reminiscent of the folding assumed by immunoglobulins [6]. Domain II plays a regulatory and structural function, even though most of the mutations associated with GD are situated in domain III, which is composed of a (β/α)-8-barrel of triose phosphate isomerase (TIM). This latter domain contains the catalytic dyad consisting of two glutamic residues: E340, acting as the nucleophile, and E235, functioning as the acid/base catalyst. At the entrance of the active catalytic site, there are five exposed loops [7–9]. The rearrangements of these loops, pH conditions, and specific residue interactions collectively influence the accessibility of the catalytic site, determining the active and inactive states of the GCase [10].

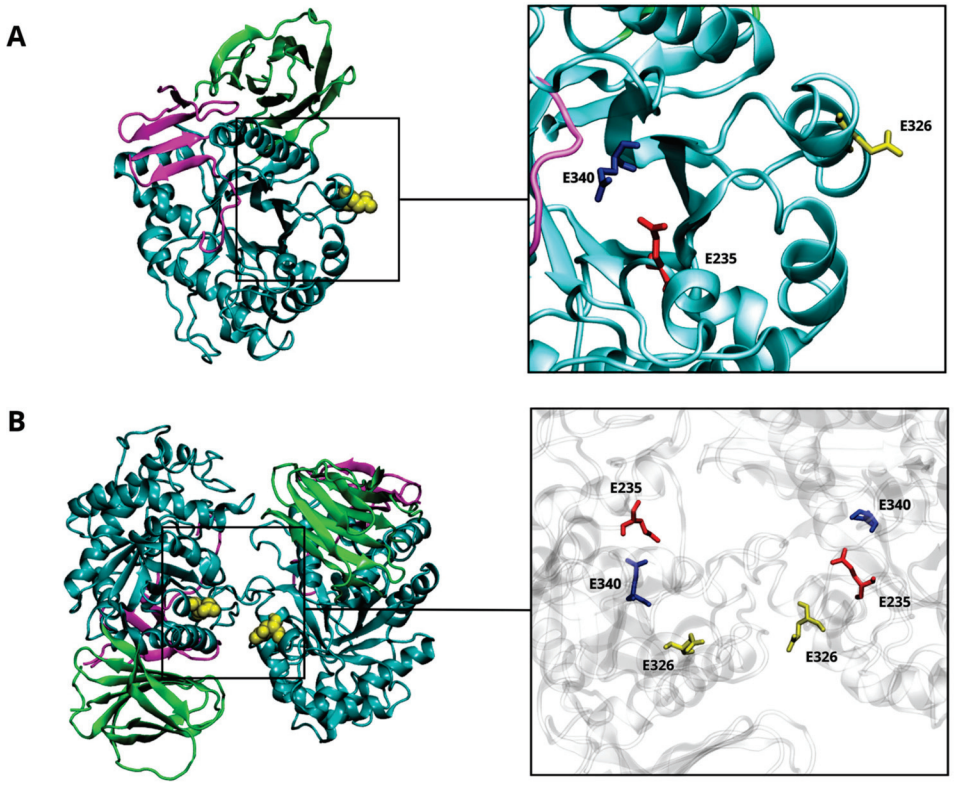


Figure 1. β-glucocerebrosidase (GCase) structure. The 3D structure of the GCase (PDB-ID: 3GXI) showing domain I (magenta), domain II (green), and domain III (cyan). The catalytic dyad is highlighted by a squared box showing the E235 (red) and the E340 (blue) residues. The site of mutation (E326) is also highlighted in yellow (**A**). The 3D structure of the wild-type CGase dimer. The interaction's interface between the two monomers is highlighted by a squared box that shows the E235 (red), the E340 (blue), and the E326 (yellow) residues (**B**).

More than 490 *GBA1* mutations are known to be associated with GD, but only a few of them (20–30%) have been so far associated with PD [11]. Mutations linked to a pathological outcome are spread throughout the GCase structure. Many are located far from the active site but still ensure a certain degree of enzymatic activity. Other mutations are situated close to the regions responsible for interaction with either the SapC activator or the LIMP-2

transporter. Nevertheless, a clear correlation between the location of mutation and the severity of the diseases has not been established yet. E326K, E388K, and T369M *GBA1* mutations do not cause GD but have been specifically associated with an increased risk (i.e., "risk" variants) of developing aggressive α-synucleinopathies, such as PD and dementia with Lewy bodies. Specifically, E326K is situated far from the catalytic site (Figure 1A) and predisposes to PD onset in both homozygous and heterozygous forms [12–14], thus increasing the risk by up to 10 times [11]. Some heterozygous GCase mutations promote PD pathogenesis through a gain-of-function mechanism that may include ER stress [15]. This implies a multifactorial GBA/PD-based molecular mechanism that does not depend solely on the deficient lysosomal activity. Recent in vitro findings demonstrated that the E326K mutation in human fibroblasts does not significantly reduce enzymatic activity, whereas it stimulates the aggregation of insoluble α-Synuclein (α-Syn) fibrils and lipid droplet formation [16], a set of structural modifications typically characterizing human PD neurons [17–19]. Moreover, the accumulation of a high amount of GlcCer may contribute to α-Syn aggregation, leading to decreased GCase activity [11]. Despite in vitro experimental evidence supporting the occurrence of a specific α-Syn-GCase complex, no data have been provided in terms of identification of the molecular mechanism(s) underlying such interaction. A direct interaction of the α-Syn's C-terminus has been postulated to occur with specific residues of the GCase in its monomeric form to promote lysosomal degradation of α-Syn or inhibit its excessive accumulation [20,21]. The wild-type GCase displays a more stable and functional structure as a dimer, where the active sites are partially buried [22]. The GCase dimer has a butterfly-shaped structure (Figure 1B), and the dimer interface provides an allosteric binding pocket [22,23]. It was suggested that dimerization could be an important process for GCase activation [23]. Considering the translocation of the GCase from the ER to the lysosome, other studies highlighted the presence of dimers at neutral and acidic pHs both in vitro [23] and in vivo [24]. The equilibrium is mainly altered by interaction with SapC, shifting toward the monomeric form [24]. It is not clear whether SapC acts by dissociating the GCase dimer or by binding the free monomer, preventing self-association.

Despite efforts to find relationships between mutations, protein structure, GD manifestation, and enzymatic activity in the literature, our understanding of how specific mutations alter GCase's tertiary and quaternary structure and its interaction with other proteins and influence the risk of developing PD remains incomplete. To such an extent, a computational approach based on molecular dynamics (MD) simulations can help in understanding the differences in the structural and functional behavior of a protein due to mutations. Here, to gain insight into the effect of the E326K mutation on the tertiary and quaternary structure of GCase, we employed several classical MD simulations. They act as a computational microscope able to capture the behavior of biomolecules and dynamically map their interactions in full atomic detail [25]. Heterodimeric, wild-type, and mutated homodimeric complexes of GCase were modeled and simulated at both pH 5.5 and 7.0, mimicking the lysosomal and ER environments, respectively. The potential effects of E326K mutation on the active site of the GCase, the stability of its dimerization, and its interaction dynamics with LIMP-2, SapC, and α-Syn were investigated and evaluated through interaction energy characterization. Our computational approach revealed that the E326K mutation does not affect the structural integrity of the catalytic site but reduces binding affinity with the inhibitor α-Syn and destabilizes dimeric complexes, particularly under lysosomal pH conditions.

2. Results

Here, we report a comprehensive analysis of the structure stability and interactome dynamics of wild-type and mutated GCase dimers by exploiting classical MD simulations, which provide unique and useful insights into the structural stability and dynamics of several biological systems [25–28].

2.1. The E326K Mutation Does Not Affect the Catalytic Dyad's Structure

The site of mutation is sufficiently far from the catalytic dyad (Figure 1), and this might have no direct effect on it. To verify this hypothesis, we monitored throughout the simulations at pH 5.5 (i) the distances between the mutation site (residue 326) and the two catalytic residues (E340 and E235), as well as (ii) the distance between the two residues that form the catalytic dyad; their averaged values are reported in Table 1. The average distances between site 326 and residue E235 are comparable in wild-type and mutant monomers; in the mutated one, a higher distance between K326 and E340 is observed compared to the wild-type monomer. This may be attributed to the mutation, which affects the accessibility of the catalytic site, potentially increasing its available surface area. Nevertheless, the mutation does not significantly affect the average distance between the two catalytic residues (E235 and E340). The preservation of this distance can be considered a reliable indicator of the structural integrity and retention of catalytic competence in GCase.

Table 1. Time-averaged distances (nm) between specific residues. Notes: data are presented as mean ± standard deviation. For comparison, the average values obtained when the enzyme is in its inactive state at pH 7.0 are provided in Table S1 of the Supplementary Materials.

Simulation at pH 5.5	Wild-Type	E326K
E/K326-E235	2.04 ± 0.08	2.13 ± 0.08
E/K326-E340	2.03 ± 0.06	2.38 ± 0.08
E235-E340	0.73 ± 0.06	0.77 ± 0.04

We further analyzed the effect of the E326K mutation on the catalytic dyad by monitoring the side chain orientations of residues W348 and R395 relative to E340 and E235. These residues are known to adopt different orientations depending on the activity state of GCase [10]. In the inactive state at a neutral pH, W348 blocks the catalytic dyad by pointing toward the active site, while R395 faces E340. At an acidic lysosomal pH, W348 shifts toward the active site, and R395 points outward. As shown in Figure 2, the side chain orientations of W348 and R395, in both wild-type and mutated monomers (at acidic pH), are in agreement with data reported in the literature [29], indicating that the E326K mutation does not impair GCase functionality in the lysosome. Interestingly, in the inactive state at pH 7.0 (Figure 3), R395 behaves as expected in the wild-type monomer, while in the mutated one, its orientation deviates. This suggests that catalytic E340 residue may not be properly blocked, potentially compromising the inactive form of GCase at a neutral pH.

We monitored specific hydrogen bonds that play crucial roles in GCase activation, focusing on the Y313-E235 bond at pH 7.0 and the Y313-E340 bond at an acidic pH (Table 2, Figure S1). At a neutral pH, the Y313-E235 bond acts as a gate, keeping the active site closed [6,9]. As expected, such a bond is present in the wild-type GCase with over 47% persistence, but it disappears in the mutated protein at pH 7.0. Upon GlcCer substrate binding at lysosomal pH, Y313 shifts to bind with E340 in the active site, suggesting an induced-fit mechanism for GCase near the active site [6,9]. In simulations at an acidic pH without the substrate, the Y313-E340 bond is absent in the wild-type protein, as anticipated, but unexpectedly, it is present in the mutated GCase, persisting for over 47% of the simulation (Table 2, Figure S1).

Table 2. Hydrogen bonds between specific residues of the active site.

Pair Residues, pH	Wild-Type	E326K
Y313-E235, pH 7.0	67.70 [a]	--
Y313-E340, pH 5.5	--	47.80

[a] The number indicates the percentage (%) of persistence of hydrogen bonds throughout the concatenated simulation. The value was calculated as the average of the persistence percentages of individual replicas that are reported in Table S2. Only the hydrogen bonds with a persistence of over 45% were considered. These hydrogen bonds are depicted in Figure S1.

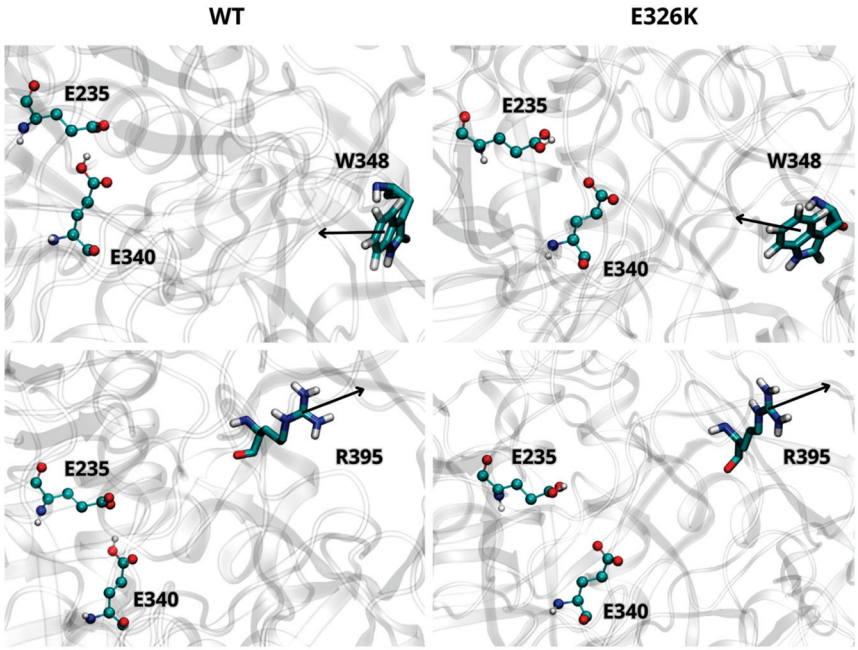


Figure 2. Orientation of W348 and R395 residues in wild-type (WT) and mutated GCase at pH 5.5. Arrows indicate the direction of the side chain. The images are representative snapshots from the simulations. Color codes for the selected residues: carbon, cyan; hydrogen, white; nitrogen, blue; oxygen, red.

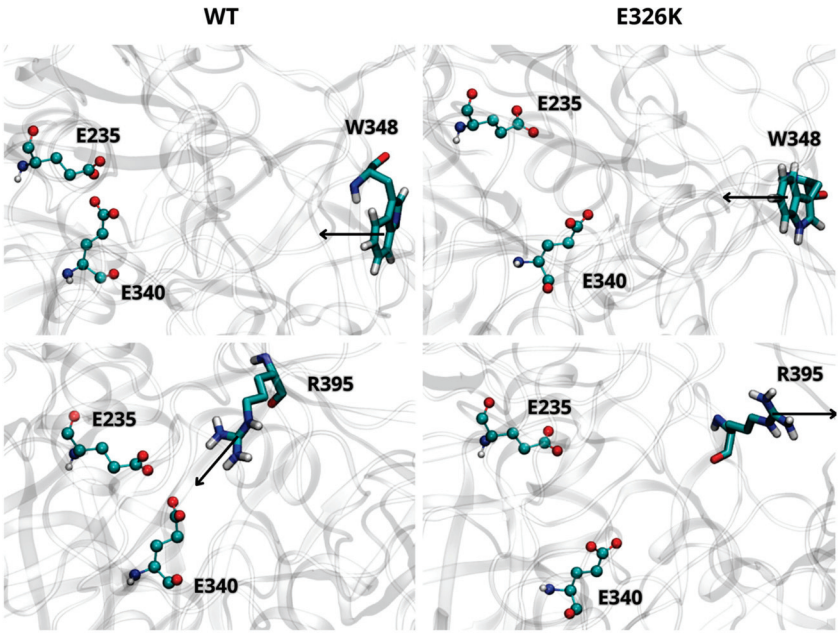


Figure 3. Orientation of residues W348 and R395 in WT and mutated GCase at pH 7.0. Arrows indicate the direction of the side chain. The images are representative snapshots from the simulations. Color codes for the selected residues: carbon, cyan; hydrogen, white; nitrogen, blue; oxygen, red.

At a neutral pH, the E326 residue forms three stable hydrogen bonds with a persistence of over 70% during the simulation. The mutation from E to K triggers the loss of two of them (Table 3, Figure S2). Despite this change, the total number of hydrogen bonds is higher in the mutant than in the wild-type form at both pH 7.0 and pH 5.5 (Table 4).

Table 3. Hydrogen bonds involving the mutation site, residue 326 at neutral pH.

pH 7.0	Wild-Type	E326K
Residue/Residue	E326	K326
H328	70.82 [a]	--
R329	82.43	--
L330	76.72	80.78

[a] The number indicates the percentage (%) of persistence of hydrogen bonds throughout the concatenated simulation. The value was calculated as the average of the persistence percentages of individual replicas that are reported in Table S3. Only the hydrogen bonds with a persistence of over 70% were considered. These hydrogen bonds are depicted in Figure S2.

Table 4. Time-averaged number of intrachain hydrogen bonds.

pH	Wild-Type	E326K
pH 5.5	37 ± 0.17 [a]	48 ± 0.05
pH 7.0	46 ± 0.15	50 ± 0.10

[a] Data are presented as mean ± standard deviation. The number only considers the hydrogen bonds with more than 85% persistence during the simulation.

2.2. GCase Dimerization Is Disfavoured by the E326K Mutation

It has been proposed that dimerization may play a crucial role in the functioning and activation of GCase, with the dimeric form proving to be more stable and functional than the monomeric one [22–24]. To assess the impact of the E326K mutation on dimer stability, we monitored the interchain hydrogen bond pattern at an acidic (Table 5) and neutral pH (Table 6). While residue 326 is located at the dimer interface (Figure 1), it does not directly contribute to the intrachain hydrogen bond network in any of the simulations analyzed. At an acidic pH (Table 5), notably, in the homodimer wild-type, residue R395 forms a hydrogen bond with E349, part of loop 1 at the entrance of monomer B's binding site. This bond is absent in the mutated dimers. As reported in Table 5, the mutation significantly reduces the number of hydrogen bonds, indicating destabilization of the mutated homodimer in the lysosomal environment. At pH 7.0, however, the mutated homodimer shows an increase in hydrogen bond interactions compared to the wild-type dimer (Table 6).

Table 5. Hydrogen bond pattern at the interface of the wild-type (WT-WT) and mutated (E326K-E326K) homodimer and of the heterodimer (WT-E326K) at pH 5.5.

Residue of Chain A	Residue of Chain B	WT-WT	E326K-E326K	WT-E326K
S12	S242	--	46.00 [a]	--
Y244	F347	36.63	--	--
W348	Y244	37.84	--	--
E349	S242	--	--	60.02
E349	G243	--	--	44.07
E349	Y244	46.97	--	--
E350	G243	--	--	64.75
E350	S345	--	--	35.44
D358	S242	--	88.59	--
R395	E349	35.55	--	--
F397	F347	38.85	--	--
Number of total hydrogen bonds		5	2	4

[a] The number indicates the percentage (%) of persistence of hydrogen bonds throughout the concatenated simulation. The value was calculated as the average of the persistence percentages of individual replicas that are reported in Table S4. Only the hydrogen bonds with a persistence of over 35% were considered. The residues involved in these hydrogen bonds are depicted in Figure S3.

Table 6. Hydrogen bond pattern at the dimer's interface at pH 7.0.

Residue of Chain A	Residue of Chain B	WT-WT	E326K-E326K	WT-E326K
N192	D358	--	36.40 [a]	--
S242	D358	44.20	43.20	43.94
Y244	Y313	--	--	42.20
Y244	F347	--	--	47.95
Y244	E349	42.25	--	--
E254	S464	--	44.75	39.82
E254	S465	--	--	37.25
E284	D315	--	--	39.18
Y291	D445	--	35.40	--
K293	D443	--	44.76	--
V294	D443	--	41.63	--
V295	D443	--	42.15	--
D315	L240	45.32	--	--
D315	G243	--	45.57	--
L317	A320	--	--	37.18
D358	S242	55.15	--	--
Number of total hydrogen bonds		4	8	7

[a] The number indicates the percentage (%) of persistence of hydrogen bonds throughout the concatenated simulation. The value was calculated as the average of the persistence percentages of individual replicas that are reported in Table S5. Only the hydrogen bonds with a persistence of over 35% were considered. The residues involved in these hydrogen bonds are depicted in Figure S3.

The instability of the E326K homodimer at pH 5.5 is further supported by PCA-based conformational analysis (Figure S4), which shows that, while the wild-type homodimer predominantly occupies a single stable conformational state with minimal variability, the E326K homodimer exhibits a broader spread along PC1. This suggests increased flexibility and a potentially less stable state.

The strength of interaction between monomers in the complexes was estimated by calculating the binding free energy (ΔG) for each system, with the results listed in Table 7. At pH 5.5, the wild-type homodimer exhibits significantly lower binding energy values (higher affinity) compared to those at pH 7.0, in line with the literature [23,24], which suggests stronger monomer interactions at an acidic pH to support the protein's hydrolytic function. The E326K mutation has a destabilizing effect on the mutated homodimer, particularly at pH 5.5, where the binding energy is substantially less favorable (-14.55 ± 0.43 kcal/mol) than that of the wild-type homodimer (-18.89 ± 0.43 kcal/mol) and the heterodimer (-16.88 ± 0.22 kcal/mol). At pH 7.0, the wild-type homodimer again shows the highest binding affinity (-15.70 ± 0.16 kcal/mol), followed by the WT-E326K heterodimer (-14.99 ± 0.24 kcal/mol) and the mutated E326K-E326K homodimer (-14.72 ± 0.25 kcal/mol). This may have a negative effect on the trafficking of dimeric GCase in neutral pH vesicles [23].

Table 7. Predicted binding free energies of GCase dimers at acidic and neutral pH, calculated using the PRODIGY server. Data are presented as mean ± standard deviation.

Dimers	ΔG (kcal/mol) at pH 5.5	ΔG (kcal/mol) at pH 7.0
WT-WT	-18.89 ± 0.43	-15.70 ± 0.16
E326K-E326K	-14.55 ± 0.18	-14.72 ± 0.25
E326K-WT	-16.88 ± 0.22	-14.99 ± 0.24

2.3. The Effects of E326K on GCase Interactome

The potential impact of the E326K mutation on the dynamics of interaction between GCase and its interactor proteins (LIMP-2, SapC, and α-Syn) was investigated. Evidence

from both in vivo and in vitro studies suggests that GCase exists as a dimer in both the ER and lysosome [24]. To date, it is unclear whether these interacting proteins bind GCase in its monomeric or multimeric form. Experimental findings indicate that GCase binds to LIMP-2 and SapC in a 1:1 stoichiometry [24,30] and that SapC may disrupt the multimer by binding near the active site [24]. Additionally, therapeutic chaperones [22,23] act as dimer stabilizers, which seems to enhance enzymatic activity, even in the presence of mutations. A plausible hypothesis, therefore, is that interactome proteins might bind dimeric GCase through a mechanism where the ligand competes with one of the monomers. In our docking simulations, we used the monomer extracted from the dimeric structure, followed by molecular dynamics, allowing the proteins to further refine their interaction interface. A visual inspection of the molecular configurations sampled by the complexes is shown in Figures 4–6 at different points of the concatenated trajectories.

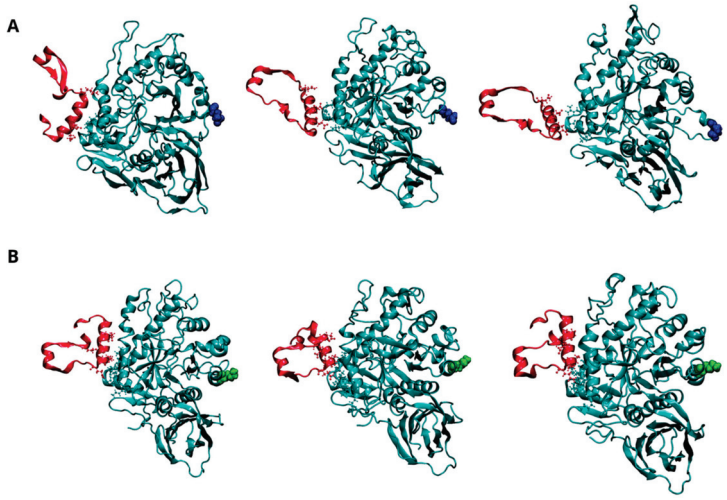


Figure 4. Dynamics of interaction between GCase and Lysosomal integral membrane protein-2 (LIMP-2) at pH 7.0. Representative snapshots from the concatenated molecular dynamics (MD) trajectories of the WT-LIMP-2 complex (**A**) and the E326K-LIMP-2 complex (**B**). GCase is shown in cyan, and LIMP-2 is in red, both depicted in a New Cartoon representation. Key residues involved in the interaction between the two proteins are displayed in the CPK model. The mutation site, residue 326, is highlighted in blue for the wild-type GCase and green for the mutated GCase, represented in the VDW model. For clarity, the water molecules are not shown, and only the LIMP-2 region interacting with GCase is shown here; the full complex can be viewed in Figure S5 of the Supplementary Materials.

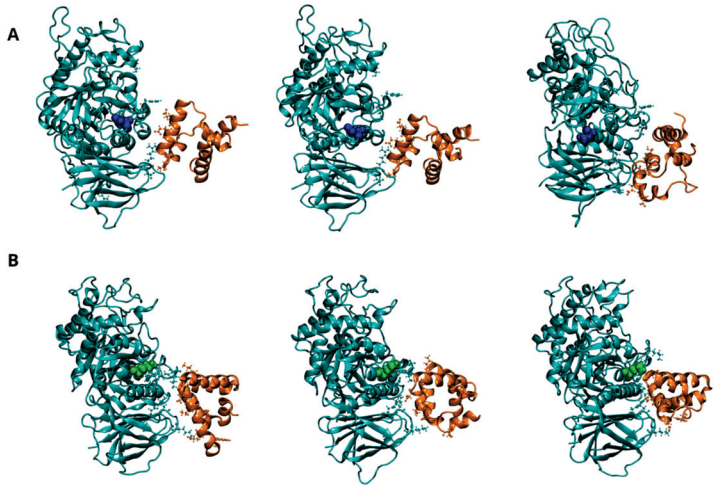


Figure 5. Dynamics of interaction between GCase and Saposin C (SapC) at pH 5.5. Representative snapshots from the concatenated MD trajectories of the WT-SapC complex (**A**) and the E326K-SapC

complex (**B**). GCase is shown in cyan and SapC-2 in orange, both depicted in a New Cartoon representation. Key residues involved in the interaction between the two proteins are displayed in the CPK model. The mutation site, residue 326, is highlighted in blue for the wild-type GCase and green for the mutated GCase, represented in the VDW model. For clarity, the water molecules are not shown.

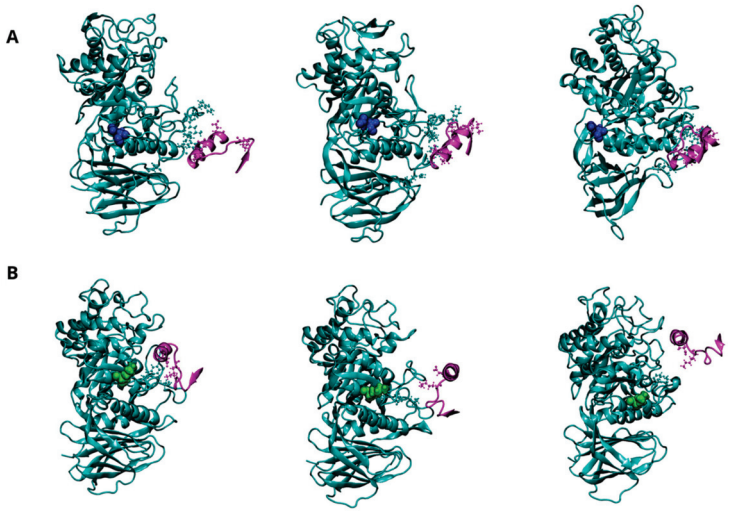


Figure 6. Dynamics of interaction between GCase and α-Synuclein (α-Syn) at pH 5.5. Representative snapshots from the concatenated MD trajectories of the WT-α-Syn complex (**A**) and the E326K-α-Syn complex (**B**). GCase is shown in cyan, and α-Syn is in purple, both depicted in a New Cartoon representation. Key residues involved in the interaction between the two proteins are displayed in the CPK model. The mutation site, residue 326, is highlighted in blue for the wild-type GCase and green for the mutated GCase, represented in the VDW model. For clarity, the water molecules are not shown.

Figure 4A (and Figure S5A) shows the dynamic behavior of the interaction interface between LIMP-2 and the wild-type GCase monomer at pH 7.0. As reported in the literature, the interaction involves residues from 152 to 175 of LIMP-2 and several segments of GCase (86–96, 99–110, and 150–168) [30], all located on the opposite side from the mutation site at position 326. As shown in Figure 4B (and Figure S5B), the E326K monomer interacts with a greater number of residues, indicating a stronger and more stable interaction with LIMP-2.

This observation is reinforced by the analysis of intermolecular interactions (hydrogen bonds and salt bridges) shown in Table 8 and Figure S6. The data show an increased number of hydrogen bonds between the mutant and LIMP-2, although a salt bridge between R163 of GCase and E149 of LIMP-2 is lost.

At the lysosomal level, GCase interacts with the activator SapC to catalyze the hydrolysis of GlcCer [4,5]. Although the exact interaction interface between GCase and SapC is not fully defined, experimental and computational studies suggest that residues 441–445, 463–466, and 487 of GCase are critical for binding SapC [29]. SapC has two key binding domains: domain 1 (residues 6–34) and domain 2 (residues 41–70), with domain 2 known to bind GCase with significantly higher affinity [31,32]. Figure 5A shows the potential interaction interface between SapC and wild-type GCase, showing that most interactions occur with domain 2 of SapC (residues 44 to 70). The E326K changes the interaction pattern, leading to increased interactions with domain 1 (residues 6–27) of SapC. The hydrogen bond patterns between chains, as detailed in Table 9 and Figure S7, support this finding and suggest that the mutation may alter the mode of interaction with SapC.

Table 8. Intermolecular interactions (hydrogen bonds and salt bridges) between GCase monomers at pH 7.0 and Lysosomal integral membrane protein-2 (LIMP-2).

GCase Residue	LIMP-2 Residue	Wild-Type	E326K
L94	K153	--	10.96 [a]
A95	K153	--	12.92
Q101	K153	--	27.79
Q101	Q 156	--	41.23
N102	Q156		80.61
N102	E146	32.97	--
K106	E146	23.19	--
R163	**E149**	**64.37** [b]	**--**
R163	A154	--	13.50
R163	Q156	--	17.80
Q166	E175	--	11.10
Number of total hydrogen bonds		3	8
Number of total salt bridges		1	0

[a] The number indicates the percentage (%) of persistence of hydrogen bond throughout the concatenated simulation. The value was calculated as the average of the persistence percentages of individual replicas that are reported in Table S6. Only the hydrogen bonds with a persistence of over 10% were considered. [b] Bold text highlights residue pairs that form stable salt bridges.

Table 9. Intermolecular interactions (hydrogen bonds and salt bridges) between GCase monomers at pH 5.5 and Saposin C (SapC).

GCase Residue	SapC Residue	Wild-Type	E326K
G10	Y53	--	17.35 [a]
R44	E48	12.95	--
R44	D51	--	20.14
S237	*E8* [b]	*19.86*	--
K321	*E13*	--	*11.12*
R329	C77	--	38.05
K346	***E24***	**--**	***53.65*** [c]
F347	L76	16.67	--
W348	S55	--	13.31
E 349	*Y3*	*16.59*	--
R353	D51	--	48.53
D358	*K25*	--	*26.66*
Q362	*E24*	--	*24.62*
D443	*T15*	--	*10.90*
D443	*K16*		*20.31*
D443	S55	28.89	--
D445	*K16*	--	*12.32*
D463	***D19***	**--**	***88.08***
D463	S59	11.18	--
S465	E63		18.55
K466	*E8*	--	*15.00*
Number of total hydrogen bonds		6	14
Number of total salt bridges		0	2

[a] The number indicates the percentage (%) of persistence of hydrogen bonds throughout the concatenated simulation. The value was calculated as the average of the persistence percentages of individual replicas that are reported in Table S7. Only the hydrogen bonds with a persistence of over 10% were considered. [b] Italic text highlights residues belonging to domain 1 (residues 6–34) of SapC. [c] Bold text highlights residue pairs that form stable salt bridges.

Three putative regions of GCase (223, 273–328, and 344–349) are thought to interact with the C-terminus of α-Syn (residues 118 to 137). Although a direct interaction with GCase has been proposed to promote lysosomal degradation of α-Syn or inhibit its excessive accumulation, it is still unclear which of these regions plays a predominant role in the interaction or the specific mechanism through which GCase interacts with α-Syn.

Figure 6A illustrates the potential interaction interface between wild-type GCase and α-Syn, indicating that the 344–349 region is directly involved in the interaction. Interestingly, these interactions become extremely weak in the mutant, suggesting that the mutation at position 326 severely affects GCase's ability to stably bind α-Syn (Figure 6B). The significant loss of affinity for α-Syn can be clearly attributed to the reduction of several hydrogen bonds and two salt bridges, which are the driving forces behind intermolecular interactions, as shown in Table 10 and Figure S8.

Table 10. Intermolecular interactions (hydrogen bonds and salt bridges) between GCase monomers at pH 5.5 and α-Synuclein (α-Syn).

GCase Residue	α-Syn Residue	Wild-Type	E326K
Y11	P133	16.40 [a]	--
Y11	E138	17.27	--
R48	**E130**	**31.80** [b]	**--**
Y313	E131	--	21.32
S345	K127	--	12.06
K346	**E131**	**31.07**	**--**
W348	L121	21.50	--
S351	E138	18.81	--
R353	E138	22.11	--
Number of total hydrogen bonds		7	2
Number of total salt bridges		2	0

[a] The number indicates the percentage (%) of persistence of hydrogen bonds throughout the concatenated simulation. The value was calculated as the average of the persistence percentages of individual replicas that are reported in Table S8. Only the hydrogen bonds with a persistence of over 10% were considered. [b] Bold text highlights residue pairs that form stable salt bridges.

To quantify the strength of the interaction between GCase and LIMP-2, SapC, and α-Syn, the binding free energy (ΔG) for each system was predicted using the PRODIGY server. The results, presented in Table 11, demonstrate that the GCase mutant significantly decreases its binding affinity for α-Syn (-7.47 ± 0.50 kcal/mol) compared to the wild-type form (-9.21 ± 0.21 kcal/mol), while it appears to have lower binding energy values, therefore higher affinity, with LIMP-2. In contrast, the ΔG values for the interaction with SapC are comparable.

Table 11. Predicted binding free energies of the GCase monomer at neutral pH in complex with LIMP-2 and at acidic pH in complex with SapC and α-Syn, calculated using the PRODIGY server. Data are presented as mean ± standard deviation.

	ΔG (kcal/mol) Wild-Type	ΔG (kcal/mol) E326K
LIMP-2	-6.73 ± 0.14	-7.07 ± 0.12
SapC	-7.60 ± 0.21	-7.86 ± 0.14
α-Syn	-9.31 ± 0.21	-7.47 ± 0.50

3. Discussion

GBA1 mutations are the leading genetic risk factor for the development of PD [11,33]. Here, we focused on the E326K mutation, which is recognized for increasing the susceptibility to PD in affected individuals [33]. However, to date, the impact of such mutation on the protein structure, as well as on physiological functions, remains unclear. MD simulation is acknowledged for its ability to evaluate the stability, flexibility, and dynamics of molecular systems at both temporal and spatial resolutions, making it a powerful investigative tool [25–28]. In this study, we employed classical MD simulations to identify the pathological mechanism, at the structural level, of the E326K mutation of the *GBA1* gene. We accounted for the heterozygous condition by simulating three distinct GCase dimers:

a mutant heterodimer, as well as wild-type and mutant homodimers. To the best of our knowledge, we present the first computational study addressing i) the characterization of the structural, dynamical, and physicochemical features of these dimers at two different pH levels—representing the lysosomal (acid pH) and ER (neutral pH) environments—as well as ii) the interaction models between GCase and its interactome. Our findings demonstrate that the proposed computational approach serves as a valuable tool for assessing the structural features of the GCase in physiological aqueous solutions, along with their conformational rearrangements at an atomic resolution.

The structural analysis of the GCase monomers shows that the E326K mutation does not significantly affect the catalytic dyad (E235-E340), consistent with experimental in vitro findings by Smith et al. (2022) [16], which showed that the E326K mutation in human fibroblasts does not substantially reduce enzymatic activity. But, significantly, the E326K mutation may compromise the inactive state of GCase at a neutral pH. It has been observed that E326K does not affect the orientation of residues W348 and R395, which plays a crucial role at specific pH levels during GCase function. Notably, the orientation of these two residues at an acidic pH is not influenced. On the contrary, the side chain orientation of R395 deviates from the observed orientation [8,9,29] under neutral pH conditions. Based on this result, it could be hypothesized that the transition of GCase from an inactive to an active form and vice versa, regulated by various cellular factors, does not occur, potentially because the enzyme is in continuous activity. The lack of the Y313-E235 hydrogen bond, which acts as a gate, in the mutated GCase does not allow the inactive form of the GCase to be maintained at a neutral pH.

Given the uncertainty about whether the enzyme exists as a monomer or dimer in the cellular context [23], we focused attention on the formation of dimers, observing the mutation's influence on the spatial arrangement of the systems. Overall, the results suggest a potential mutation-induced destabilizing effect on dimeric structure. At the structural level, the mutated homodimer appears disadvantaged compared with the wild-type one. This effect becomes more pronounced with a decreasing pH from neutral to acidic, as indicated by hydrogen bond analysis. This result suggests that the E326K mutation has a major impact under lysosomal conditions, i.e., when GCase both explicates its enzymatic activity and interacts with other proteins.

Since GCase interacts with various proteins during its journey from the ER to the lysosome and within the lysosomal environment, in this study, we simulated the dynamics of interaction between GCase and its interactome to reveal if the mutation causes gain-of-function and loss-of-function effects. Taken together, our results suggest that the mutation exerts a dual gain-of-function and loss-of-function mechanism. The LIMP-2 transporter may retain the mutated form of GCase, which exhibits greater affinity than the wild type (gain-of-function), potentially inducing endoplasmic reticulum stress. Simultaneously, a loss-of-function mechanism is triggered due to the significantly reduced interaction between mutant GCase and α-Syn, leading to α-Syn accumulation and the disruption of its physiological competition with SapC. This loss of direct GCase-α-Syn interaction may explain the aggregation of insoluble α-Syn fibrils caused by the E326K mutation, as observed in in vitro experiments on human fibroblasts [16]. Additionally, the interaction with its activator, SapC, also seems to be affected by the presence of the mutation. We would like to stress that in this study, we focused on simulating interactions between interactome proteins and the monomeric form of GCase. However, it is possible that interactome proteins interact with dimeric GCase via a competitive mechanism, wherein proteins like α-Syn, SapC, or LIMP-2 may compete with one of the monomers. This competition suggests that interactome proteins might disrupt the dimer, effectively replacing one GCase monomer, as has been reported in the literature for SapC [24]. Consequently, the complexes we simulated represent a plausible state following the dissociation of one monomer. Further research would be valuable to investigate whether interactome proteins stabilize this dissociation or bind directly in a way that destabilizes the dimer, potentially shedding light on a dynamic equilibrium between monomeric and dimeric forms in cellular environments.

If experimentally validated, these findings provide the groundwork to explore molecular mechanisms underlying the correlation between the E326 mutation and PD onset.

4. Materials and Methods

4.1. Structures' Preparation

The 3D structure of the wild-type dimeric GCase (Uniprot ID P04062) was obtained by selecting the A and B chains of the 3GXI crystal (X-ray resolution: 1.34 Å) [6]. To model the heterozygous condition, two additional dimeric complexes were prepared: the mutant homodimer and the heterodimer, in which the E326K mutation was introduced, through the CHARMM-GUI platform (https://www.charmm-gui.org/, accessed on 11 January 2024) [34–36]. The mutation was introduced in both the chains for the homodimer and in only the A chain for the heterodimer. The protonation states of titratable amino acids at pH 5.5 and pH 7.0 were predicted and determined with PROPKA 3.1 by means of the Play Molecule tool (https://open.playmolecule.org/, accessed on 11 January 2024) [37] and listed in Supplementary Table S9. The wild-type and mutated GCase monomers at pH 5.5 were docked against the 3D structure of SapC (Uniprot ID P07602) in the open conformation (PDB id: 2QYP, chain A) [38] and of α-Syn (Uniprot ID P37840) fused to the maltose binding protein (PDB id: 3Q27) [39] to create complexes that simulate lysosomal interactions. At neutral pH, the wild-type and mutated GCase monomers were docked with the 3D structure of LIMP-2 (Uniprot ID Q14108, PDB id: 4F7B) [40] to model their interaction in the endoplasmic reticulum. Docking calculations were performed using the HADDOCK version 2.4 protein–protein docking algorithm [41], incorporating known active residues as data restraints to guide simulations. Table 12 summarizes the prepared systems: a total of twelve (12) complexes were set up as starting systems for the classical MD simulations.

Table 12. Summary of simulations performed.

Simulation Name	Description of the System	Simulation Length
WT-WT_pH5	Wild-type GCase homodimer at pH 5.5	1000 ns, 2 replicas [a]
E326K-E326K_pH5	Mutated GCase homodimer at pH 5.5	1000 ns, 2 replicas
WT-E326K_pH5	GCase heterodimer at pH 5.5	1000 ns, 2 replicas
WT-WT_pH7	Wild-type GCase homodimer at pH 7.0	1000 ns, 2 replicas
E326K-E326K_pH7	Mutated GCase homodimer at pH 7.0	1000 ns, 2 replicas
WT-E326K_pH7	GCase heterodimer at pH 7.0	1000 ns, 2 replicas
WT-LIMP2	Wild-type GCase monomer at pH 7.0 in complex with LIMP-2 (endoplasmic reticulum interaction)	200 ns, 3 replicas [b]
E326K-LIMP2	Mutated GCase monomer at pH 7.0 in complex with LIMP-2 (endoplasmic reticulum interaction)	200 ns, 3 replicas
WT-SapC	Wild-type GCase monomer at pH 5.5 in complex with Saposin C (lysosomal interaction)	200 ns, 3 replicas
E326K-SapC	Mutated GCase monomer at pH 5.5 in complex with Saposin C (lysosomal interaction)	200 ns, 3 replicas
WT-α-Syn	Wild-type GCase monomer at pH 5.5 in complex with α−Synuclein (lysosomal interaction)	200 ns, 3 replicas
E326K-α-Syn	Muated GCase monomer at pH 5.5 in complex with α-Synuclein (lysosomal interaction)	200 ns, 3 replicas

[a] Replicas' frames were concatenated to form a single continuous trajectory for each system after discharging the first 400 ns of simulation (equilibration phase). [b] Replicas' frames were concatenated to form a single continuous trajectory for each system after discharging the first 50 ns of simulation (equilibration phase).

4.2. MD Simulations

All the MD simulations were performed by using Gromacs version 2019 [42,43] with the GROMOS 53a6 united-atoms force field [44]. The systems were solvated by using TIP3P model [45], neutralized with NaCl (0.15 M), and energy-minimized by using 5000 steps of the steepest descent method [46]. Periodic boundary conditions (PBC) were applied to avoid edge effects and to better describe the full hydration conditions. Systems were equilibrated for the first 200 ps under the NVT ensemble at 100 K, followed by further 200 ps under NPT ensemble at 310 K, following the protocol shown in Supplementary Table S10. The time step was set to 2 fs. The V-rescale algorithm [47] with a time constant of 0.1 was used to keep the temperature constant. The average pressure was kept constant to 1 bar by using the Parrinello–Rahman barostat [48]. The LINCS algorithm [49] was used to constrain all the bonds throughout the equilibration process. Unrestrained replica MD simulations with a time step of 2 fs were carried out for each system (Table 12). The replicates are simulations of identical structures with identical parameters where only the initial velocities are created randomly according to a Maxwell–Boltzmann distribution. Long-range electrostatic interactions were computed using the Particle Mesh Ewald (PME) method [50]. A residue-based cutoff of 1 nm was used for the short-range electrostatic and van der Waals interactions. All MD simulations were performed using High Parallel Computing (HPC) provided by the computational infrastructure ENEAGRID/CRESCO (Computational RESearch Center of COmplex systems) [51] site in the ENEA Research Centre of Portici, Italy.

4.3. Analysis of the Trajectories

The first 400 ns of each dimer's replica were excluded as equilibration phase. The remaining frames were concatenated to form a continuous trajectory for each system. Similarly, for the GCase-protein interactor complexes, the first 50 ns of each trajectory were discarded before concatenation. The concatenated trajectories were analyzed using modules included in the GROMACS suite to extract various structural, dynamic, and energetic features. The *mindist* module was employed to monitor the minimum distance between the center of mass of the A and B chains and between specific residues. Cluster analysis was conducted using the *cluster* module and by using the gromos method [52]. A matrix of atom positional RMSD was calculated for the Cα atoms of the proteins. Structural similarity was assessed using a positional RMSD cutoff value determined from the RMSD distribution curve for each system. The structures identified by the most populated clusters were used as representative snapshots for the visualization analysis and for $\Delta G_{binding}$ analysis using the PRODIGY (PROtein binDIng enerGY prediction) server (https://rascar.science.uu.nl/prodigy/, accessed on 19 June 2024) [53], which provides a quantitative estimate of the binding affinity between the A and B chains of the complexes by analyzing intermolecular contacts and desolvation effects. It specifically evaluates the number of contacts between the binding partners within a defined distance threshold, factoring in temperature as a correction. The free energy (ΔG) is then calculated based on the number and type of intermolecular contacts (ICs) at the interface, classifying them into polar, apolar, and charged interactions. This method relies on statistical models derived from experimental data, offering a reliable prediction of binding affinities while acknowledging the inherent approximations of empirical approaches [53]. Hydrogen bonds and the salt bridges were identified with the *H-bonds* and *Salt Bridge* VMD version 1.9.3 plugins, respectively [54]. A hydrogen bond was assumed to exist if the donor to acceptor distance was shorter than 0.35 nm and the hydrogen donor–acceptor angle was lower than 30°. The hydrogen bond persistence throughout a simulation was calculated for evaluating the duration, or "lifetime", of specific hydrogen bonds. In our analysis, we specifically considered hydrogen bonds that persisted beyond a defined percentage of the simulation time, as specified in the legend of tables. A salt bridge was assumed to exist if the distance between the side-chain oxygen (O) of Asp or Glu and the side-chain nitrogen (N) of Lys, Arg, or His was less than 0.50 nm. Principal component analysis (PCA) of the covariance

matrix of the positional fluctuations of the Cα atoms [55] was performed by using the *covar* module. The covariance matrix was built from each replica trajectory of the dimers, from which the overall rotational and translational motions were removed. The *anaeig* module was used to calculate the 2D projections with respect to the first two eigenvectors. All graphical representations were generated using VMD version 1.9.3 [54].

Supplementary Materials: The following supporting information can be downloaded at: https://www.mdpi.com/article/10.3390/ijms252111443/s1.

Author Contributions: D.P.: Formal analysis, Investigation, Methodology, Visualization, Writing—original draft, Writing—review and editing. A.C.: Investigation, Methodology. B.B.: Conceptualization, Supervision, Writing—review and editing. M.S.: Investigation, Methodology. M.M.: Investigation. C.C.: Conceptualization, Investigation, Methodology. J.R.: Conceptualization, Investigation, Methodology, Supervision, Resources, Writing—original draft, Writing—review and editing. C.A.: Conceptualization, Data curation, Formal analysis, Investigation, Methodology, Supervision, Resources, Writing—original draft, Writing—review and editing. All authors have read and agreed to the published version of the manuscript.

Funding: This research received no external funding.

Institutional Review Board Statement: Not applicable.

Informed Consent Statement: Not applicable.

Data Availability Statement: The dataset is available on request from the authors.

Acknowledgments: The computing resources and the related technical support used for this work have been provided by CRESCO/ENEAGRID high-performance computing infrastructure and his staff. Specifically, we thank Guido Guarnieri and Simone Giusepponi for their technical support. CRESCO/ENEAGRID high-performance computing infrastructure is funded by ENEA, the Italian National Agency for New Technologies, Energy and Sustainable Economic Development and by Italian and European research programmers (see http://www.cresco.enea.it/english for information).

Conflicts of Interest: The authors declare no conflicts of interest.

References

1. Neudorfer, O.; Giladi, N.; Elstein, D.; Abrahamov, A.; Turezkite, T.; Aghai, E.; Reches, A.; Bembi, B.; Zimran, A. Occurrence of Parkinson's Syndrome in Type 1 Gaucher Disease. *QJM* **1996**, *89*, 691–694. [CrossRef] [PubMed]
2. Tayebi, N. Gaucher Disease with Parkinsonian Manifestations: Does Glucocerebrosidase Deficiency Contribute to a Vulnerability to Parkinsonism? *Mol. Genet. Metab.* **2003**, *79*, 104–109. [CrossRef] [PubMed]
3. Kolter, T.; Sandhoff, K. Lysosomal Degradation of Membrane Lipids. *FEBS Lett.* **2010**, *584*, 1700–1712. [CrossRef]
4. Berent, S.L.; Radin, N.S. Mechanism of Activation of Glucocerebrosidase by CO-β-Glucosidase (Glucosidase Activator Protein). *Biochim. Biophys. Acta (BBA)—Lipids Lipid Metab.* **1981**, *664*, 572–582. [CrossRef]
5. Sun, Y.; Qi, X.; Grabowski, G.A. Saposin C Is Required for Normal Resistance of Acid β-Glucosidase to Proteolytic Degradation. *J. Biol. Chem.* **2003**, *278*, 31918–31923. [CrossRef]
6. Lieberman, R.L.; D'aquino, J.A.; Ringe, D.; Petsko, G.A. Effects of pH and Iminosugar Pharmacological Chaperones on Lysosomal Glycosidase Structure and Stability. *Biochemistry* **2009**, *48*, 4816–4827. [CrossRef]
7. Dvir, H.; Harel, M.; McCarthy, A.A.; Toker, L.; Silman, I.; Futerman, A.H.; Sussman, J.L. X-ray Structure of Human Acid-β-glucosidase, the Defective Enzyme in Gaucher Disease. *EMBO Rep.* **2003**, *4*, 704–709. [CrossRef] [PubMed]
8. Lieberman, R.L.; Wustman, B.A.; Huertas, P.; Powe, A.C.; Pine, C.W.; Khanna, R.; Schlossmacher, M.G.; Ringe, D.; Petsko, G.A. Structure of Acid β-Glucosidase with Pharmacological Chaperone Provides Insight into Gaucher Disease. *Nat. Chem. Biol.* **2007**, *3*, 101–107. [CrossRef]
9. Lieberman, R.L. A Guided Tour of the Structural Biology of Gaucher Disease: Acid- *β*-Glucosidase and Saposin C. *Enzym. Res.* **2011**, *2011*, 973231. [CrossRef]
10. Smith, L.; Mullin, S.; Schapira, A.H.V. Insights into the Structural Biology of Gaucher Disease. *Exp. Neurol.* **2017**, *298*, 180–190. [CrossRef]
11. Behl, T.; Kaur, G.; Fratila, O.; Buhas, C.; Judea-Pusta, C.T.; Negrut, N.; Bustea, C.; Bungau, S. Cross-Talks among GBA Mutations, Glucocerebrosidase, and α-Synuclein in GBA-Associated Parkinson's Disease and Their Targeted Therapeutic Approaches: A Comprehensive Review. *Transl. Neurodegener.* **2021**, *10*, 4. [CrossRef] [PubMed]
12. Duran, R.; Mencacci, N.E.; Angeli, A.V.; Shoai, M.; Deas, E.; Houlden, H.; Mehta, A.; Hughes, D.; Cox, T.M.; Deegan, P.; et al. The Glucocerobrosidase E326K Variant Predisposes to Parkinson's Disease, but Does Not Cause Gaucher's Disease. *Mov. Disord.* **2013**, *28*, 232–236. [CrossRef] [PubMed]

13. Horowitz, M.; Pasmanik-Chor, M.; Ron, I.; Kolodny, E.H. The Enigma of the E326K Mutation in Acid β-Glucocerebrosidase. *Mol. Genet. Metab.* **2011**, *104*, 35–38. [CrossRef] [PubMed]
14. Marano, M.; Zizzo, C.; Malaguti, M.C.; Bacchin, R.; Cavallieri, F.; De Micco, R.; Spagnolo, F.; Bentivoglio, A.R.; Schirinzi, T.; Bovenzi, R.; et al. Increased Glucosylsphingosine Levels and Gaucher Disease in GBA1-Associated Parkinson's Disease. *Park. Relat. Disord.* **2024**, *124*, 107023. [CrossRef]
15. Gegg, M.E.; Burke, D.; Heales, S.J.R.; Cooper, J.M.; Hardy, J.; Wood, N.W.; Schapira, A.H.V. Glucocerebrosidase Deficiency in Substantia Nigra of Parkinson Disease Brains. *Ann. Neurol.* **2012**, *72*, 455–463. [CrossRef]
16. Smith, L.J.; Bolsinger, M.M.; Chau, K.-Y.; Gegg, M.E.; Schapira, A.H.V. The *GBA* Variant E326K Is Associated with Alpha-Synuclein Aggregation and Lipid Droplet Accumulation in Human Cell Lines. *Human Mol. Genet.* **2022**, *32*, 773–789. [CrossRef]
17. Stefanis, L. α-Synuclein in Parkinson's Disease. *Cold Spring Harb. Perspect. Med.* **2012**, *2*, a009399. [CrossRef]
18. Logan, T.; Bendor, J.; Toupin, C.; Thorn, K.; Edwards, R.H. α-Synuclein Promotes Dilation of the Exocytotic Fusion Pore. *Nat. Neurosci.* **2017**, *20*, 681–689. [CrossRef]
19. Wakabayashi, K.; Tanji, K.; Mori, F.; Takahashi, H. The Lewy Body in Parkinson's Disease: Molecules Implicated in the Formation and Degradation of A-synuclein Aggregates. *Neuropathology* **2007**, *27*, 494–506. [CrossRef]
20. Yap, T.L.; Velayati, A.; Sidransky, E.; Lee, J.C. Membrane-Bound α-Synuclein Interacts with Glucocerebrosidase and Inhibits Enzyme Activity. *Mol. Genet. Metab.* **2013**, *108*, 56–64. [CrossRef]
21. Yap, T.L.; Jiang, Z.; Heinrich, F.; Gruschus, J.M.; Pfefferkorn, C.M.; Barros, M.; Curtis, J.E.; Sidransky, E.; Lee, J.C. Structural Features of Membrane-Bound Glucocerebrosidase and α-Synuclein Probed by Neutron Reflectometry and Fluorescence Spectroscopy. *J. Biol. Chem.* **2015**, *290*, 744–754. [CrossRef]
22. Zheng, J.; Chen, L.; Skinner, O.S.; Ysselstein, D.; Remis, J.; Lansbury, P.; Skerlj, R.; Mrosek, M.; Heunisch, U.; Krapp, S.; et al. β-Glucocerebrosidase Modulators Promote Dimerization of β-Glucocerebrosidase and Reveal an Allosteric Binding Site. *J. Am. Chem. Soc.* **2018**, *140*, 5914–5924. [CrossRef] [PubMed]
23. Benz, J.; Rufer, A.C.; Huber, S.; Ehler, A.; Hug, M.; Topp, A.; Guba, W.; Hofmann, E.C.; Jagasia, R.; Rodríguez Sarmiento, R.M. Novel β-Glucocerebrosidase Activators That Bind to a New Pocket at a Dimer Interface and Induce Dimerization. *Angew. Chem. Int. Ed.* **2021**, *60*, 5436–5442. [CrossRef] [PubMed]
24. Gruschus, J.M.; Jiang, Z.; Yap, T.L.; Hill, S.A.; Grishaev, A.; Piszczek, G.; Sidransky, E.; Lee, J.C. Dissociation of Glucocerebrosidase Dimer in Solution by Its Co-Factor, Saposin C. *Biochem. Biophys. Res. Commun.* **2015**, *457*, 561–566. [CrossRef]
25. Hollingsworth, S.A.; Dror, R.O. Molecular Dynamics Simulation for All. *Neuron* **2018**, *99*, 1129–1143. [CrossRef] [PubMed]
26. Arcangeli, C.; Cantale, C.; Galeffi, P.; Rosato, V. Structure and Dynamics of the Anti-AMCV scFv(F8): Effects of Selected Mutations on the Antigen Combining Site. *J. Struct. Biol.* **2008**, *164*, 119–133. [CrossRef]
27. Arcangeli, C.; Lico, C.; Baschieri, S.; Mancuso, M. Characterization Of Blood–Brain Barrier Crossing And Tumor Homing Peptides By Molecular Dynamics Simulations. *Int. J. Nanomed.* **2019**, *14*, 10123–10136. [CrossRef]
28. Innamorati, G.; Pierdomenico, M.; Benassi, B.; Arcangeli, C. The Interaction of DNMT1 and DNMT3A Epigenetic Enzymes with Phthalates and Perfluoroalkyl Substances: An in Silico Approach. *J. Biomol. Struct. Dyn.* **2023**, *41*, 1586–1602. [CrossRef]
29. Romero, R.; Ramanathan, A.; Yuen, T.; Bhowmik, D.; Mathew, M.; Munshi, L.B.; Javaid, S.; Bloch, M.; Lizneva, D.; Rahimova, A.; et al. Mechanism of Glucocerebrosidase Activation and Dysfunction in Gaucher Disease Unraveled by Molecular Dynamics and Deep Learning. *Proc. Natl. Acad. Sci. USA* **2019**, *116*, 5086–5095. [CrossRef]
30. Zunke, F.; Andresen, L.; Wesseler, S.; Groth, J.; Arnold, P.; Rothaug, M.; Mazzulli, J.R.; Krainc, D.; Blanz, J.; Saftig, P.; et al. Characterization of the Complex Formed by β-Glucocerebrosidase and the Lysosomal Integral Membrane Protein Type-2. *Proc. Natl. Acad. Sci. USA* **2016**, *113*, 3791–3796. [CrossRef]
31. Qi, X.; Qin, W.; Sun, Y.; Kondoh, K.; Grabowski, G.A. Functional Organization of Saposin C: DEFINITION OF THE NEUROTROPHIC AND ACID β-GLUCOSIDASE ACTIVATION REGIONS (∗). *J. Biol. Chem.* **1996**, *271*, 6874–6880. [CrossRef] [PubMed]
32. Weiler, S.; Tomich, J.M.; Kishimoto, Y.; O'Brien, J.S.; Barranger, J.A. Identification of the Binding and Activating Sites of the Sphingolipid Activator Protein, Saposin C, with Glucocerebrosidase. *Protein Sci.* **1995**, *4*, 756–764. [CrossRef] [PubMed]
33. Riboldi, G.M.; Di Fonzo, A.B. GBA, Gaucher Disease, and Parkinson's Disease: From Genetic to Clinic to New Therapeutic Approaches. *Cells* **2019**, *8*, 364. [CrossRef] [PubMed]
34. Jo, S.; Kim, T.; Iyer, V.G.; Im, W. CHARMM-GUI: A Web-Based Graphical User Interface for CHARMM. *J. Comput. Chem.* **2008**, *29*, 1859–1865. [CrossRef] [PubMed]
35. Brooks, B.R.; Bruccoleri, R.E.; Olafson, B.D.; States, D.J.; Swaminathan, S.; Karplus, M. CHARMM: A Program for Macromolecular Energy, Minimization, and Dynamics Calculations. *J. Comput. Chem.* **1983**, *4*, 187–217. [CrossRef]
36. Lee, J.; Cheng, X.; Swails, J.M.; Yeom, M.S.; Eastman, P.K.; Lemkul, J.A.; Wei, S.; Buckner, J.; Jeong, J.C.; Qi, Y.; et al. CHARMM-GUI Input Generator for NAMD, GROMACS, AMBER, OpenMM, and CHARMM/OpenMM Simulations Using the CHARMM36 Additive Force Field. *J. Chem. Theory Comput.* **2016**, *12*, 405–413. [CrossRef]
37. Martínez-Rosell, G.; Giorgino, T.; De Fabritiis, G. PlayMolecule ProteinPrepare: A Web Application for Protein Preparation for Molecular Dynamics Simulations. *J. Chem. Inf. Model.* **2017**, *57*, 1511–1516. [CrossRef]
38. Rossmann, M.; Schultz-Heienbrok, R.; Behlke, J.; Remmel, N.; Alings, C.; Sandhoff, K.; Saenger, W.; Maier, T. Crystal Structures of Human Saposins C and D: Implications for Lipid Recognition and Membrane Interactions. *Structure* **2008**, *16*, 809–817. [CrossRef]

39. Zhao, M.; Cascio, D.; Sawaya, M.R.; Eisenberg, D. Structures of Segments of α-Synuclein Fused to Maltose-Binding Protein Suggest Intermediate States during Amyloid Formation. *Protein Sci.* **2011**, *20*, 996–1004. [CrossRef]
40. Neculai, D.; Schwake, M.; Ravichandran, M.; Zunke, F.; Collins, R.F.; Peters, J.; Neculai, M.; Plumb, J.; Loppnau, P.; Pizarro, J.C.; et al. Structure of LIMP-2 Provides Functional Insights with Implications for SR-BI and CD36. *Nature* **2013**, *504*, 172–176. [CrossRef]
41. Honorato, R.V.; Trellet, M.E.; Jiménez-García, B.; Schaarschmidt, J.J.; Giulini, M.; Reys, V.; Koukos, P.I.; Rodrigues, J.P.G.L.M.; Karaca, E.; Van Zundert, G.C.P.; et al. The HADDOCK2.4 Web Server for Integrative Modeling of Biomolecular Complexes. *Nat. Protoc.* **2024**. [CrossRef] [PubMed]
42. Van Der Spoel, D.; Lindahl, E.; Hess, B.; Groenhof, G.; Mark, A.E.; Berendsen, H.J.C. GROMACS: Fast, Flexible, and Free. *J. Comput. Chem.* **2005**, *26*, 1701–1718. [CrossRef] [PubMed]
43. Abraham, M.J.; Murtola, T.; Schulz, R.; Páll, S.; Smith, J.C.; Hess, B.; Lindahl, E. GROMACS: High Performance Molecular Simulations through Multi-Level Parallelism from Laptops to Supercomputers. *SoftwareX* **2015**, *1–2*, 19–25. [CrossRef]
44. Oostenbrink, C.; Villa, A.; Mark, A.E.; Van Gunsteren, W.F. A Biomolecular Force Field Based on the Free Enthalpy of Hydration and Solvation: The GROMOS Force-field Parameter Sets 53A5 and 53A6. *J. Comput. Chem.* **2004**, *25*, 1656–1676. [CrossRef] [PubMed]
45. Jorgensen, W.L.; Chandrasekhar, J.; Madura, J.D.; Impey, R.W.; Klein, M.L. Comparison of Simple Potential Functions for Simulating Liquid Water. *J. Chem. Phys.* **1983**, *79*, 926–935. [CrossRef]
46. Petrova, S.S.; Solov'ev, A.D. The Origin of the Method of Steepest Descent. *Hist. Math.* **1997**, *24*, 361–375. [CrossRef]
47. Bussi, G.; Donadio, D.; Parrinello, M. Canonical Sampling through Velocity Rescaling. *J. Chem. Phys.* **2007**, *126*, 014101. [CrossRef]
48. Parrinello, M.; Rahman, A. Polymorphic Transitions in Single Crystals: A New Molecular Dynamics Method. *J. Appl. Phys.* **1981**, *52*, 7182–7190. [CrossRef]
49. Hess, B.; Bekker, H.; Berendsen, H.; Fraaije, J. LINCS: A Linear Constraint Solver for Molecular Simulations. *J. Comput. Chem.* **1998**, *18*, 1463–1472. [CrossRef]
50. Essmann, U.; Perera, L.; Berkowitz, M.L.; Darden, T.; Lee, H.; Pedersen, L.G. A Smooth Particle Mesh Ewald Method. *J. Chem. Phys.* **1995**, *103*, 8577–8593. [CrossRef]
51. Iannone, F.; Ambrosino, F.; Bracco, G.; De Rosa, M.; Funel, A.; Guarnieri, G.; Migliori, S.; Palombi, F.; Ponti, G.; Santomauro, G.; et al. CRESCO ENEA HPC Clusters: A Working Example of a Multifabric GPFS Spectrum Scale Layout. In Proceedings of the 2019 International Conference on High Performance Computing & Simulation (HPCS), Dublin, Ireland, 15–19 July 2019; IEEE: Piscataway, NJ, USA, 2020; pp. 1051–1052.
52. Daura, X.; Gademann, K.; Jaun, B.; Seebach, D.; Van Gunsteren, W.F.; Mark, A.E. Peptide Folding: When Simulation Meets Experiment. *Angew. Chem. Int. Ed.* **1999**, *38*, 236–240. [CrossRef]
53. Honorato, R.V.; Koukos, P.I.; Jiménez-García, B.; Tsaregorodtsev, A.; Verlato, M.; Giachetti, A.; Rosato, A.; Bonvin, A.M.J.J. Structural Biology in the Clouds: The WeNMR-EOSC Ecosystem. *Front. Mol. Biosci.* **2021**, *8*, 729513. [CrossRef] [PubMed]
54. Humphrey, W.; Dalke, A.; Schulten, K. VMD: Visual Molecular Dynamics. *J. Mol. Graph.* **1996**, *14*, 33–38. [CrossRef]
55. Amadei, A.; Linssen, A.B.; Berendsen, H.J. Essential dynamics of proteins. *Proteins* **1993**, *17*, 412–425. [CrossRef] [PubMed]

Disclaimer/Publisher's Note: The statements, opinions and data contained in all publications are solely those of the individual author(s) and contributor(s) and not of MDPI and/or the editor(s). MDPI and/or the editor(s) disclaim responsibility for any injury to people or property resulting from any ideas, methods, instructions or products referred to in the content.

International Journal of
Molecular Sciences

MDPI

Article

Morphometric Similarity Patterning of Amyloid-β and Tau Proteins Correlates with Transcriptomics in the Alzheimer's Disease Continuum

Lorenza Brusini [1,*], Giorgio Dolci [1,2], Lorenzo Pini [3], Federica Cruciani [1,4], Fabrizio Pizzagalli [5], Paolo Provero [5], Gloria Menegaz [1] and Ilaria Boscolo Galazzo [1,†] for the Alzheimer's Disease Neuroimaging Initiative

[1] Department of Engineering for Innovation Medicine, University of Verona, 37134 Verona, Italy
[2] Department of Computer Science, University of Verona, 37134 Verona, Italy
[3] Department of Neuroscience, University of Padova, 35121 Padova, Italy
[4] Istituto Fondazione Oncologia Molecolare Ente del Terzo Settore (IFOM ETS)–The Associazione Italiana per la Ricerca sul Cancro (AIRC) Institute of Molecular Oncology, 20139 Milano, Italy
[5] Department of Neurosciences "Rita Levi Montalcini", University of Turin, 10126 Turin, Italy
* Correspondence: lorenza.brusini@univr.it
† Data used in preparation of this article were obtained from the Alzheimer's Disease Neuroimaging Initiative (ADNI) database (adni.loni.usc.edu). As such, the investigators within the ADNI contributed to the design and implementation of ADNI and/or provided data but did not participate in analysis or writing of this report. A complete listing of ADNI investigators can be found at: http://adni.loni.usc.edu/wp-content/uploads/how_to_apply/ADNI_Acknowledgement_List.pdf

Abstract: Bridging the gap between cortical morphometric remodeling and gene expression can help to clarify the effects of the selective brain accumulation of Amyloid-β (Aβ) and tau proteins occurring in the Alzheimer's disease (AD). To this aim, we derived morphometric similarity (MS) networks from 126 Aβ- and tau-positive (Aβ+/tau+) and 172 A$\beta-$/tau$-$ subjects, and we investigated the association between group-wise regional MS differences and transcriptional correlates thanks to an imaging transcriptomics approach grounded in the Allen Human Brain Atlas (AHBA). The expressed gene with the highest correlation with MS alterations was *BCHE*, a gene related to Aβ homeostasis. In addition, notably, among the most promising results derived from the enrichment analysis, we found the immune response to be a biological process and astrocytes, microglia, and oligodendrocyte precursors for the cell types. In summary, by relating cortical MS and AHBA-derived transcriptomics, we were able to retrieve findings suggesting the biological mechanisms underlying the Aβ- and tau-induced cortical MS alterations in the AD continuum.

Keywords: T1-weighted MRI; diffusion MRI; ADNI; partial least squares; gene expression; enrichment analysis

1. Introduction

Imaging techniques enabling the possibility to observe, in vivo, the prints of the biological processes acting on the brain are of extreme importance. In particular, finding imaging markers able to reflect specific pathological mechanisms is valuable especially in clinics. Positron emission tomography (PET) has enabled the detection of Amyloid-β (Aβ) and tau protein accumulation, the molecular hallmarks of Alzheimer's disease (AD), demonstrating that Aβ plaques and neurofibrillary tangles formed from phosphorylated tau protein can be detected several years before the onset of clinical symptoms [1]. Consequently, the risk of developing AD or an early diagnosis can potentially be identified during pre-clinical stages, allowing for timely intervention through therapies aimed at preventing, slowing, or even halting disease progression.

In addition to being valuable in aiding clinical practice and drug development, in vivo imaging markers sensitive enough to detect changes in the AD continuum would also be

relevant in understanding its pathophysiology. Indeed, a comprehensive picture of alterations in AD is essential to understand the complexity of modifications occurring during the disease. Vilkaite et al. [2] illustrated the potential of linking omics data (genomics, proteomics, and transcriptomics) to molecular imaging to uncover the mechanisms relating Aβ and tau in AD. Omics information can be related to different scales of imaging and not ultimately standard non-invasive in vivo magnetic resonance imaging (MRI) of the whole brain. By taking advantage of the Allen Human Brain Atlas (AHBA) and PET-MRI with different tracers to distinctively capture Aβ and tau, Yu and colleagues [3] were able to confirm the existence of a specific sensibility to these two AD hallmarks depending on the spatial location on the brain. In fact, AHBA provides the gene expression profiles for 20,736 genes encoding proteins for each brain region, thus enabling the discovery of the possible relationships between genetics and imaging at a higher spatial resolution. Studying the imaging transcriptomics of these pathological mechanisms with other MRI modalities may bring to light novel insights for the understanding of AD.

To the best of our knowledge, works attempting to investigate the imaging transcriptomics relationship to explain the role and behaviour of Aβ and tau in AD mainly rely on PET [2–6]. On top of this, no work exists on imaging transcriptomics for studying Aβ and tau in the AD continuum based on cortical morphometric similarity (MS). Typically, in vivo morphometric features of the brain tissue are derived from the conventional T1-weighted (T1w) MRI. Cortical volume, surface area, and thickness are the most known, and they have been extensively used in the literature for characterizing brain variations in both healthy and pathological individuals. T1w-MRI in AD is proven to be able to show signs of the atrophy encountered by patients along with the disease's progression [7], generally in the late stage. While T1w-MRI captures macroscopic characteristics of the brain tissue, diffusion (d)MRI, instead targeting the diffusion of water molecules, can indirectly reveal microscopic insights about geometry, architecture, and topology [8]. Recent studies have shown that microstructural abnormalities in gray matter can be detected in cognitively unimpaired (CN) or mild cognitively impaired (MCI) individuals depending on the Aβ and/or tau positivity [9,10]. Moreover, Spotorno et al. [9] demonstrated that the dMRI-derived microscopic alterations occurred before brain atrophy arises, evidenced by T1w-MRI. Thus, relying on features derived from both T1w-MRI and dMRI, an MS network (MSN) representing patterns of similarity between regions can be constructed at a single subject's level. The biological meaning of the MSN is grounded in evidence that cortical areas showing a similar cytoarchitecture are probably more anatomically connected [11,12].

Linking MSN and transcriptomics has already been proven to be able to boost research in several fields. Through such an approach, Morgan et al. [13] shed light on the biological mechanisms underlying schizophrenia, showing that MS was reduced in patients compared to controls and highlighting that the pattern was associated with the expression of genes enriched for processes including the development of the nervous system and synaptic signaling. In [14], Li et al. studied the biological mechanisms relating genetics with MS alterations in generalized epilepsy, while Lei and colleagues [15] and Martins et al. [16] studied those in pediatric bipolar disorder and in chronic pain. Generally, the method also proved to be effective in contributing to knowledge on the advancement of post-traumatic stress disorder [17], Parkinson's disease [18], and COVID-19 [19]. Notably, only one work attempted to do such an investigation in AD [20]. In detail, Zhang et al. compared MS between advanced AD patients and healthy subjects. The differences found included an increased MS in the frontal cortex and occipital cortex and a decreased MS in the temporal and parietal cortex. The authors also found an association between these alterations and memory function, and among the biological processes enriched, the most significant term was related to synaptic transmission.

To summarize, for the first time, with the present work, we aim at characterizing cortical MS on the AD continuum by developing MSNs relying on both macro- and microscopic features of the brain tissue of individuals from the pre-clinical to the MCI stage, categorized as Aβ-positive/tau-positive (Aβ+/tau+) and Aβ-negative/tau-negative (A$\beta-$/tau$-$). Fur-

thermore, by establishing the link with transcriptomics, we will reach our second aim of finding the viable biological mechanisms underlying these two processes (i.e., Aβ and tau).

The categorizations Aβ+/tau+ and A$\beta-$/tau$-$ do not consider more complex cases (Aβ+/tau$-$ and A$\beta-$/tau+), but they maximize the effects due to the presence of the AD hallmarks. Moreover, such a strategy will also maximize the probability of investigating cortical MS patterning due to the effects of Aβ and tau in the specific pre-clinical condition of AD.

2. Results

2.1. Regional Morphometric Similarity Group-Wise Differences

Figure 1 shows the differences in regional MS between Aβ+/tau+ and A$\beta-$/tau$-$ groups. More precisely, eight out of thirty-four brain regions had a significant regional MS difference ($p < 0.05$, uncorrected for multiple comparisons). Regional MS was increased in Aβ+/tau+ compared to A$\beta-$/tau$-$ in the caudal anterior cingulate and in the lateral occipital cortex, suggesting an increased similarity with the other brain areas in terms of morphometric and microstructural features. Conversely, MS decreased in Aβ+/tau+ compared to A$\beta-$/tau$-$ in the caudal middle frontal cortex, in the cuneus, in the pars triangularis, in the pericalcarine, in the posterior cingulate, and in the supramarginal cortex. No region was retained after multiple comparisons correction with false discovery rate (FDR), although p_{FDR} was close to significance ($p_{FDR} = 0.07$) in the caudal anterior cingulate, in the lateral occipital cortex, in the cuneus, and in the pars triangularis.

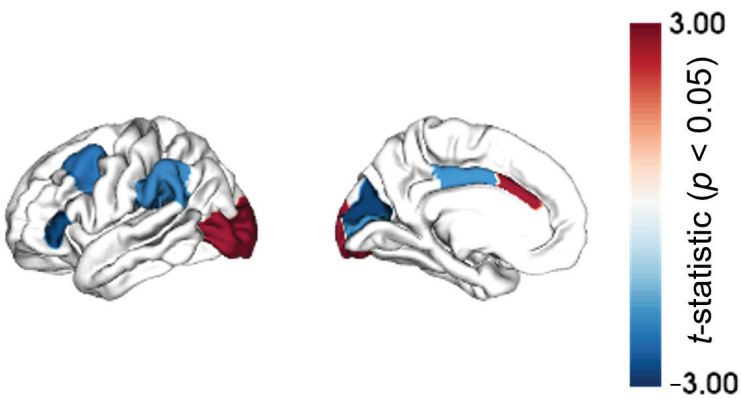


Figure 1. Differences in regional morphometric similarity between Aβ+/tau+ and A$\beta-$/tau$-$ represented on cortical maps and quantified as *t*-statistics. Only brain regions with a *p*-value < 0.05 are highlighted. Note: No region was retained after false discovery rate correction.

2.2. Regional Morphometric Similarity and Transcriptomics Relationship

The association between regional MS changes in Aβ+/tau+ versus A$\beta-$/tau$-$ and brain transcriptomics profiles as investigated with partial least squares (PLS) was deemed significant by the permutation test ($p = 0.039$). The PLS scores related to the weighted gene expression values were positively correlated with the differences in regional MS expressed as t-statistics ($r = 0.474$, $p = 0.005$) (Figure 2, panel A). Such a relationship translates for a high expression of genes with a positive PLS weight in regions where MS was increased, and conversely, genes with a negative PLS weight were highly expressed in regions where MS decreased.

The gene ranking was based on significant *z*-scores derived from bootstrapping ($p_{FDR} < 0.05$), and the subsequent selection obtained with threshold values of ± 3 ended in a PLS+ set including 1474 genes and a PLS$-$ set with 1223 genes. A complete list of the significant genes is provided in Supplementary Materials, Table S1. The highest positive and significant *z*-score was associated with the butyrylcholinesterase (*BCHE*) gene, while the microtubule-associated serine/threonine-protein kinase 4 (*MAST4*) gene represented the opposite extreme. The first gene encodes for an enzyme involved in Aβ binding, while the

second gene encodes for proteins with a domain giving the kinase the capacity to shape its own scaffold for controlling its activities (Figure 2, panel B).

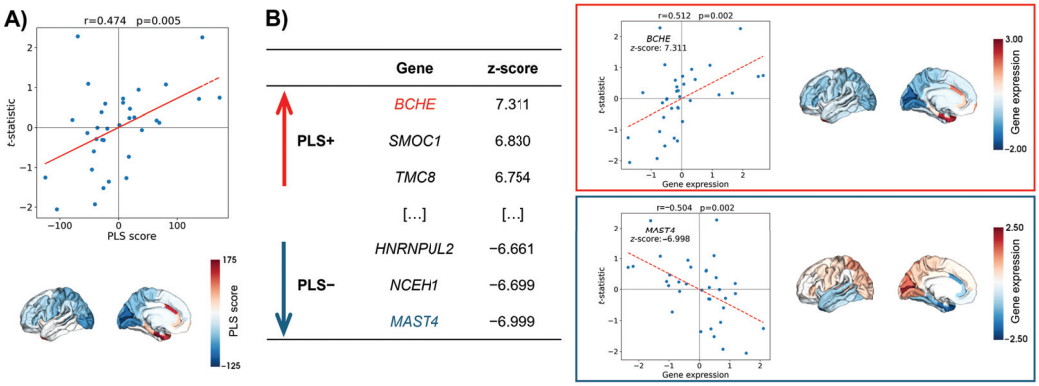


Figure 2. Transcriptomic profiles related to differences in morphometric similarity between Aβ+/tau+ and Aβ−/tau−. (**A**) Weighted gene expression profiles calculated as partial least squares (PLS) regression-derived scores shown (i) in association with the regional MS group-wise differences in the scatter plot on the upper part of the panel and (ii) on cortical maps on the lower one. (**B**) The left part of the panel shows the table summarizing the top three genes and related *z*-scores positively and negatively impacting the PLS regression, respectively; the right part of the panel, instead, shows the scatter plot with gene expression profiles versus regional MS group-wise differences and gene expression-related cortical maps for both the most positively (*BCHE*, at the top) and the most negatively (*MAST4*, at the bottom) impactful genes.

2.3. Enrichment Analysis

Figure 3 shows the gene set enrichment analyses and summarizes the significant Gene Ontology biological processes (GO BP) terms and Kyoto Encyclopaedia of Genes and Genomes (KEGG) pathways ($p_{FDR} < 0.05$). In general, 363 GO BP terms and 18 KEGG pathways were found for PLS+, whereas 17 GO BP terms and 5 KEGG pathways were found for PLS−. Note that, for ease of visualization, only the top 20 GO BP terms based on the adjusted p-value are shown for PLS+ in Figure 3 (a complete list is provided in Supplementary Materials, Table S2). Concerning PLS+, the highest enrichment term based on p_{FDR} was the immune response GO BP ($p_{FDR} = 5.94 \times 10^{-10}$), which was also the third term overall based on the number of overlapping genes with the input set (=172). Regarding PLS−, the top enrichment term based on the adjusted p-value was the transmembrane transport GO BP ($p_{FDR} = 1.86 \times 10^{-6}$), which was also the second term overall based on the number of overlapping genes with the input set (=149).

The protein–protein interaction (PPI) network based on the PLS+ gene set resulted in 1360 nodes and 4011 edges, which is 726 interactions more than what would be expected by chance (PPI enrichment $p < 1.0 \times 10^{-16}$). Similarly, the PPI network based on the PLS− gene set resulted in a number of edges significantly higher than the number of interactions expected by chance (PPI enrichment $p < 1.62 \times 10^{-14}$). Indeed, the network had 1176 nodes and 1556 edges, whereas 1275 were expected by chance. A representation of the two networks is provided in Figure 4. The greater presence of clusters is immediately evident in the PLS+-derived PPI network compared to the PLS−-derived PPI network. This was also supported by the higher average node degree and the average local clustering coefficient reached by the first gene set compared to the second one (i.e., 5.90 and 0.413 for PLS+ and 2.65 and 0.356 for PLS−). Additional evidence of the higher level of clusterization of the PPI network built upon the PLS+ gene set was also provided via the detection of significant local clusters, whereas none was found for the PPI network based on the PLS− gene set. In detail, for the PLS+ gene set, the local network cluster with the highest significance was the cluster of the cytoplasmic ribosomal proteins (FDR-corrected p-value = 1.43×10^{-10}).

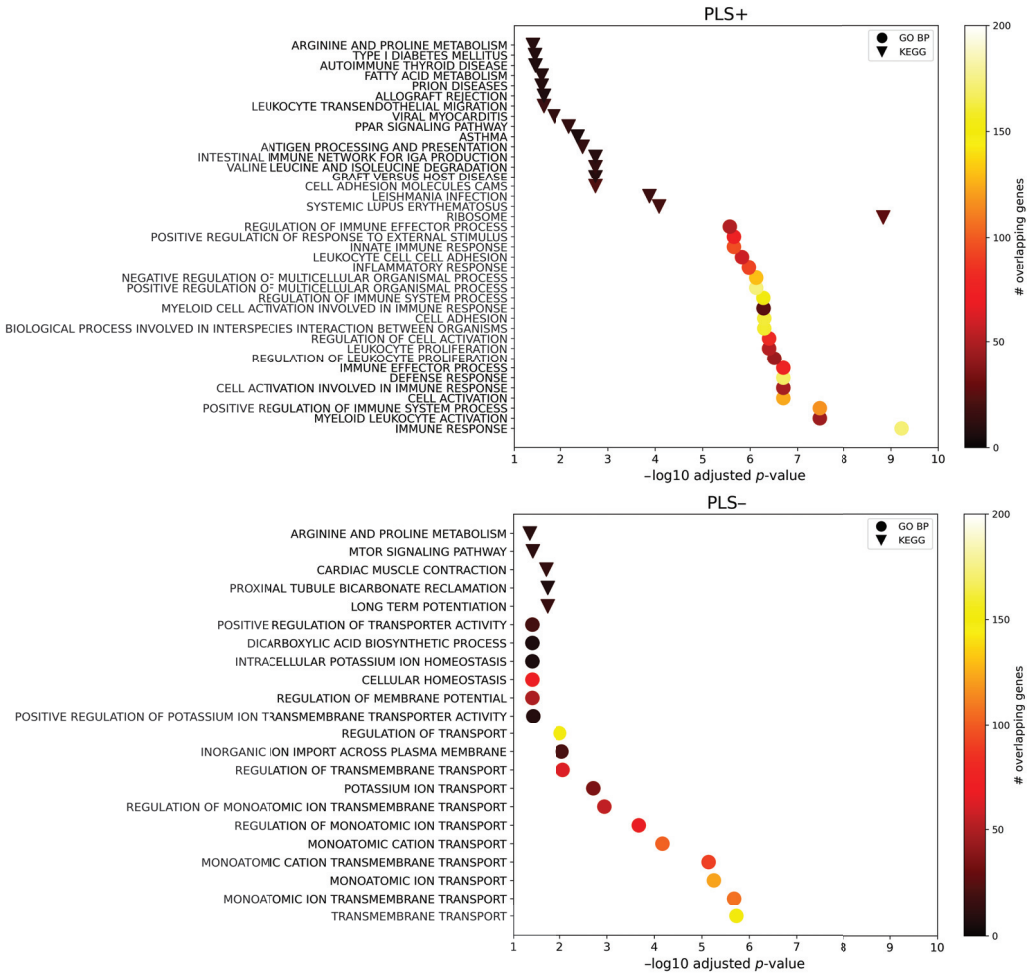


Figure 3. Gene set enrichment analysis of the top genes positively (PLS+, upper part) and negatively (PLS−, bottom part) associated with regional morphometric similarity differences in Aβ+/tau+ and Aβ−/tau− conditions. Overall, only terms with p-values surviving the correction for multiple comparisons are shown, and a further selection of the top 20 Gene Ontology biological processes (GO BP) terms is made for PLS+ for the purposes of clearer visualization. The triangles indicate the Kyoto Encyclopaedia of Genes and Genomes (KEGG) pathways, while the circles indicate GO BP terms. The color scale indicates the number of input genes overlapping with the tested gene sets.

Figure 5 shows the results of the enrichment analysis for gene expression in different brain cell types. Statistically significant enrichment ($p_{FDR} < 0.05$) was found for genes belonging to the PLS+ set, typically expressed in astrocytes, microglia, and oligodendrocytes precursors, while the significantly enriched genes of the PLS− set were those typically expressed in excitatory and inhibitory neurons.

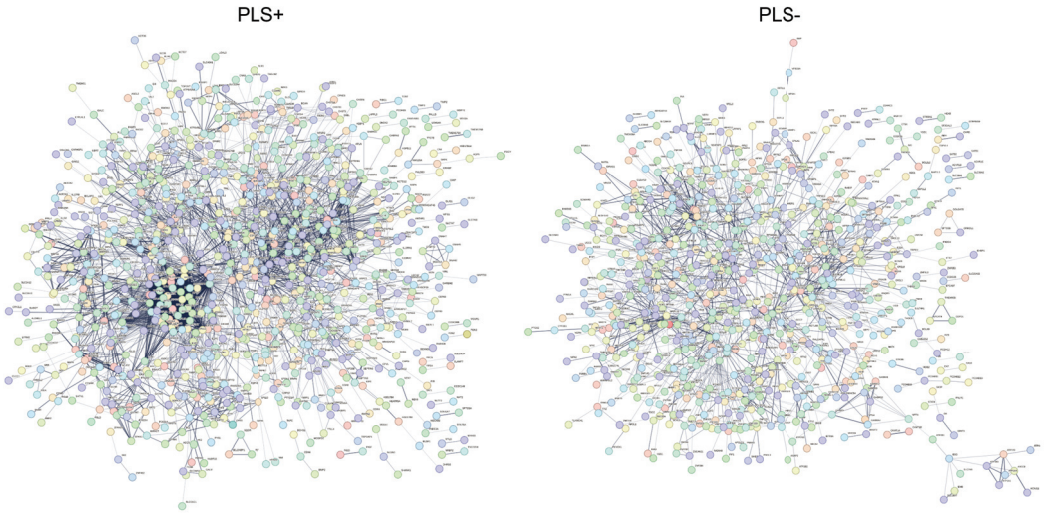


Figure 4. Protein–protein networks from STRING. Maps of interactions between proteins derived from PLS+ (**left**) and PLS− (**right**) sets of genes.

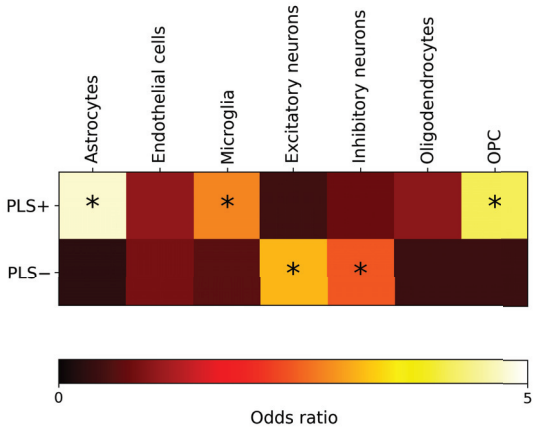


Figure 5. Cell-type enrichment analysis of the top genes positively (PLS+) and negatively (PLS−) associated with regional morphometric similarity differences in Aβ+/tau+ and Aβ−/tau− conditions. The color scale represents the enrichment quantified via odds ratios (ORs), where a high OR indicates high enrichment in genes of a specific cell class. Asterisks denote cell classes for which significant enrichment has been found ($p_{FDR} < 0.05$). FDR = false discovery rate. OPC = Oligodendrocyte precursors.

Finally, the enrichment analysis for genes related to AD was found to be significant for the PLS+ gene set (odds ratio, OR = 1.84, $p = 8.0 \times 10^{-4}$) but not for the PLS− one (OR = 0.99, $p = 0.5$). Notably, one of the most common AD-related genes is the Apolipoprotein E (*APOE*) gene, and this was included in the PLS+ gene set.

3. Discussion

In this study, we aimed at characterizing the regional MS alterations possibly driven by the brain's accumulation of Aβ and tau proteins along the AD continuum. Moreover, we showed that such a remodeling is associated with the brain's expression of genes, which can be related to AD and to Aβ homeostasis. We also highlighted their relationships with cell classes and biological pathways, suggesting possible targets for the assessment of future treatments. To the best of our knowledge, this has not yet been investigated in the current literature, as previous studies on imaging transcriptomics in AD have not focused

on biologically defined subtypes nor on assessing the association of brain morphometric changes induced by Aβ and tau accumulation with gene expression.

Despite not surviving the correction for multiple comparisons, the brain regions showing a significant regional MS difference in Aβ+/tau+ compared to A$\beta-$/tau$-$ revealed a trend of alteration resembling the late stages of amyloid and tau depositions [21]. Braak and Braak [21] examined eighty-three ex vivo brains from dementia and non-dementia subjects and established the neocortex modification as the last two steps of the six indicated for AD neuropathological degeneration. In a more recent work, Grothe et al. [22] confirmed the neuropathological findings by conducting an in vivo staging of the regional amyloid deposition through a multiregional analysis of florbetapir (18F-AV45)–PET data from 667 subjects in the Alzheimer's Disease Neuroimaging Initiative (ADNI) database. They proposed a four-stage model, according to which, again, the neocortex starts to be involved in the last stages of amyloid progression. Interestingly, by following such a staging model, the caudal anterior cingulate region here found as having a significantly increased MS in Aβ+/tau+ compared to A$\beta-$/tau$-$ should be the region exposed for the longest time to amyloid deposition. Our work also evidenced significantly increased MS of the lateral occipital cortex in Aβ+/tau+ compared to A$\beta-$/tau$-$. Notably, in a very different context from pathology staging, Hwang and colleagues [23] developed an accurate deep generative model to predict the amyloid positivity of CN individuals from structural MR images and other demographic and cognitive information, and the lateral occipital cortex was among the three most relevant regions for the success of the task as disclosed by the integrated gradient explainability method.

The regional MS group-wise differences were correlated, through a PLS fitting, with brain gene expressions as provided by AHBA, resulting in a significant association between the cortical remodeling and the transcription of genes documented to be involved in the late onset of AD [24]. To date, such a phenotype of AD is supposed to be due to many factors, and their precise genetic relationship is still to be fully uncovered [24]. Attempting this goal, genome-wide association studies have identified many susceptibility genes/loci for late-onset AD risk related to Aβ homeostasis [24]. Some of these genes are reported in [24] and are deemed as significant in our work (refer to Supplementary Materials, Table S1). More specifically, in addition to *APOE* and *SORL1*, which are linked to Aβ trafficking, we found *CD33* and *RIN3*, known to be transcripted in the endosomal–lysosomal system for Aβ degradation. Excepting *SORL1*, these genes were significantly expressed in regions with increased MS in Aβ+/tau+ versus A$\beta-$/tau$-$ individuals. Some of our significantly expressed genes can also be found in studies that specifically focus on phosphorylated tau interactomes (phosphorylated tau is the abnormal state of the protein preceding the neurofibrillary tangles in AD) [25]. Among genes with a positive z-score, Drummond et al. [25] showed that *UBA52* encodes for a form of ubiquitin that is one of the most relevant phosphorylated tau interactors. As further confirmation, phosphorylated tau is well known to be ubiquitinated [25]. On the other hand, *HSPA12A* and *PSMD11* highlighted a negative z-score in our analysis, and the same genes were found to have highly significant interactions with phosphorylated tau too [25]. The first is considered a novel interactor and is a neuron-specific protein, while the second is related through enrichment to the ubiquitin-proteasome system [25].

Our results show that *BCHE* was the highest expressed gene in regions where MS increased in Aβ+/tau+ compared to A$\beta-$/tau$-$ (i.e., caudal anterior cingulate, lateral occipital cortex), and it is related to Aβ binding. *BCHE* translates for an enzyme found to be associated to Aβ protein in the final steps of the neuritic plaque maturation process in AD brain tissues [26]. However, in 1997, it was still not known how *BCHE* participates in the process. It was in 2001 that Darvesh et al. [27] demonstrated the interaction of *BCHE* with trypsin, consisting of the enhancement of trypsin catalytic activity depending on *BCHE* concentration. The opposite was not true. This is of interest because serine peptidases similar to trypsin are present in the brain, and the finding suggests that altered *BCHE* may

not be able to regulate such catalytic activity anymore, leading to the formation of neuritic plaques.

On the contrary, *MAST4* was the most expressed gene in the regions showing a decreased MS in the Aβ+/tau+ subjects with respect to the A$\beta-$/tau$-$ individuals (e.g., pars triangularis, posterior cingulate, and pericalcarine). Interestingly, the protein encoded from *MAST4* is a microtubule-associated kinase, whereas tau (from which the neurofibrillary tangles typical in AD originate) is a microtubule-binding protein [20]. Moreover, *MAST4* has been found among the 107 differentially expressed genes in atypical cases of frontotemporal lobar degeneration with fused sarcoma inclusions [28]. Some of the 107 proteins were also associated with other proteomic studies in AD, but *MAST4*, in particular, was shown to be expressed in the prefrontal cortex without knowing the biological pathway to which it belongs. Further comparisons of these proteomic studies with similar ones on AD would be needed to identify proteins and the ways they are related to dementia.

Based on our enrichment analysis, the immune response was the biological process most impacting the regional MS changes shown between Aβ+/tau+ and A$\beta-$/tau$-$. Indeed, by focusing on the results obtained for the PLS+ set that was found to be significantly enriched for genes related to AD, many of the processes discovered were associated with the immune response. The immune response has been already documented as being influenced by several genes involved in late-onset AD [24]. For example, the innate immune response was also included among our findings, and it can induce the death of the cells in many different modalities that may lead, in AD, to chronic neuroinflammation linked to the neurodegenerative disease [29]. Strengthening this outcome, our results for the PLS+ set comprised the inflammation response as well. Moreover, microglia and astrocytes are the brain's immunological cells [30,31], and we observed that they were significantly enriched when looking for PLS+ genes expression in different brain cell types. Single-cell studies have revealed that alterations in inflammatory responses in microglia and astrocytes returned from a complex neuroimmune interplay related to AD pathophysiology [32–34].

An additional result from the PLS+ gene enrichment analysis was the involvement of the cytoplasmic ribosomal proteins constituting the most significant cluster found in the corresponding PPI network. Notably, Evans et al. [35] demonstrated the alteration of ribosomal function due to the expression of tau, and particularly in the case of tau mutations due to frontotemporal dementia, as an example of neurodegenerative disease.

The analysis conducted on PLS+ genes further ended in significant enrichment of the oligodendrocyte precursor cell type. Concerning this cell, recently, Zeng and colleagues [36] reported the results from their brain tissue analysis of an AD mouse model exhibiting amyloidosis, tauopathy, and neurodegeneration. These findings were obtained through a new method, namely, STARmap PLUS, combining high-resolution spatial transcriptomics and protein detection. In their work, Zeng et al. unexpectedly observed that oligodendrocyte precursors were enriched at an intermediate spatio-temporal distance from the appearance of the Aβ plaques. Such an enrichment potentially subtends localized proliferation and differentiation of the oligodendrocyte precursors to mature oligodendrocytes. The authors of [36] suggested that many layers arise and surround the plaques, and oligodendrocyte precursors and oligodendrocytes may constitute one of the last layers after those composed of reactive microglia.

On the other hand, the PLS$-$ set did not show any significant local clusters in the derived PPI network, and it was not significantly enriched for genes related to AD, even though we found significant enrichment for biological processes related to transmembrane transport and for both excitatory and inhibitory neuron cell types. This may be linked to the main limitation of our work, consisting in the low number of subjects retained in our cohort. Indeed, a higher number of individuals would probably give greater statistical power to the cortical MS patterns captured in this study, also representing a cascade of benefits for the imaging transcriptomics associations disclosed. In addition, we included MCI patients in the control cohort to increase the sample size and better match the clinical severity of the Aβ+/tau+ group. However, a subset of MCI patients with A$\beta-$/tau$-$ status

may exhibit different pathophysiological mechanisms. Further research is needed to assess the influence of these individuals on the imaging transcriptomics relationship. However, in an attempt to control these issues, we maintained a balanced numerosity of the two groups under investigation, and we used the Mini-Mental State Examination (MMSE) as the covariate. Future works will increase the resolution of the investigation by including Aβ+/tau− and Aβ−/tau+ groups. This will entail the uncovering of distinct mechanisms underlying the two pathways, perhaps providing support for understanding the different theories underlying AD [1].

4. Materials and Methods

4.1. Data Cohort

The data used in the preparation of this article were obtained from the ADNI database (adni.loni.usc.edu). The ADNI was launched in 2003 as a public–private partnership, led by Principal Investigator Michael W. Weiner, MD. The primary goal of ADNI has been to test whether serial MRI, PET, other biological markers, and clinical and neuropsychological assessment can be combined to measure the progression of MCI and early AD.

A total of 298 subjects from ADNI-3 were selected among those diagnosed as CN, significant memory concern (SMC), and MCI (Stages I–III), excluding patients with dementia (Stages IV–VI) [37], in order to selectively capture Aβ and tau transcriptomic signatures in AD pre-clinical conditions. Of note, when the present study was initiated, ADNI-4 was just starting to enroll participants, and their number was negligible for this investigation. ADNI is IRB-approved, and all participants signed their informed consent. For every subject, we collected a 3D T1w-MR image and single-shell dMRI volumes along with information on age, gender, years of education, MMSE score, and concentrations of Aβ and tau protein in the cerebrospinal fluid. All these participants had their MRI taken and their Aβ and tau concentrations collected within 12 months from each other.

Concerning MRI, the following acquisition parameters were used: (i) 3D T1w-MRI: sagittal accelerated MPRAGE, TR/TE = shortest, TI = 900 ms, FOV = 208 $\times$ 240 $\times$ 256 mm^3, flip angle = 9°, resolution = 1 $\times$ 1 $\times$ 1 mm^3; (ii) dMRI: TR/TE = 7200/56 ms, FOV = 232 $\times$ 232 $\times$ 160 mm^3, resolution = 2 $\times$ 2 $\times$ 2 mm^3, b = 0 and 1000 s/mm^2. Note that, while the dMRI protocol of ADNI-3 includes both single- and multi-shell acquisitions, only the former was considered here [38].

The subjects were categorized as Aβ−/tau− if [Aβ] $\geq$ 980 pg/mL and [tau] $\leq$ 24 pg/mL and vice versa for Aβ+/tau+ [39].

Table 1 summarizes the main sociodemographic and clinical information about the cohort under investigation.

Table 1. Demographic, social, and clinical details of the study cohort. The mean value and the standard deviation [mean (SD)] are reported for age and education years (Y) and mini-mental state examination (MMSE) score. Gender is reported as count of males over females (M/F). The p-value was retrieved from the Mann–Whitney non-parametric U-test for age, education, and MMSE, and from the χ^2 test for gender.

Covariate	Aβ−/tau−	Aβ+/tau+	p-Value
Age [Y]	71.05 (7.10)	77.18 (7.92)	4×10^{-11}
Gender [M/F]	71/101	60/66	0.148
Education [Y]	16.70 (2.38)	16.01 (2.54)	0.016
MMSE	28.85 (1.47)	26.06 (4.62)	2×10^{-11}

4.2. Magnetic Resonance Imaging Data Processing

The T1w-MR images were minimally preprocessed by using *fsl_anat* tool (FSL, version 6.0, https://fsl.fmrib.ox.ac.uk/fsl/fslwiki/ (accessed on 25 November 2024)) [40] to correct for bias field artifacts and to linearly register them to the 2 mm MNI space. FreeSurfer (version 7.0, https://surfer.nmr.mgh.harvard.edu/ (accessed on 25 November 2024)) [41]

was then employed to extract 84 regions of interest (ROIs) for each subject by referring to the Desikan–Killiany atlas. Subcortical ROIs were discarded together with ROIs belonging to the right hemisphere for coherence of analysis, with the data coming from AHBA (http://human.brain-map.org/ (accessed on 25 November 2024)) [42]. Please refer to Section 4.4 for details. Then, 7 different morphometric descriptors were considered for the 34 cortical ROIs in the left hemisphere. These included area, fold index, curvature index, Gaussian curvature, mean curvature, thickness, and volume.

FSL [43] was used to extract the brain and to correct for Eddy current artifacts in the dMRI data. The Python *dipy* library (https://dipy.org/ (accessed on 25 November 2024)) [44] was subsequently employed to denoise data by performing a principal component analysis and by automatically classifying the partial components relying on the Marcenko–Pastur distribution (3D sliding window radius set to 2) [45]. For each subject, the dMRI volumes corresponding to $b = 0$ were averaged, the resulting image was registered to the T1w volume of the subject by taking advantage of the *epi_reg* routine in FSL [46], and it followed a linear alignment to the MNI space thanks to the *fsl_anat*-derived transformation. Then, all the dMRI volumes were linearly transformed by applying the transformations obtained from the average *b0* processing. Finally, the result obtained for each subject was corrected for EPI-induced currents through a non-linear registration to the MNI space [47] with ANTs software (version 2.3, http://stnava.github.io/ANTs/ (accessed on 25 November 2024)) [48], and the direction of the gradients was rotated accordingly. The diffusion tensor model [49] in the *dipy* library was used to derive the standard mean diffusivity, radial diffusivity, fractional anisotropy, and the three diffusion tensor's eigenvalue microstructural maps [49]. Finally, the indices' mean value for each of the aforementioned 34 ROIs was calculated.

4.3. Regional Morphometric Similarity Group-Wise Differences

For each subject, the 13 features calculated for each of the 34 ROIs, including both morphometric measures from T1w images and microstructural descriptors from dMRI data, were used to construct the individual MSN. More specifically, all the features were separately normalized by subtracting the mean and dividing by the standard deviation across all ROIs. Pearson's correlation coefficient was then calculated for each pair of ROIs, leading to a subject-specific MSN (i.e., a 34×34 symmetric matrix). Each regional MS was thus computed by calculating the sum of the absolute value of all the correlation coefficients obtained for the considered ROI with all the other ROIs and dividing by the number of all the ROIs except for the one considered.

The differences in regional MS between the Aβ+/tau+ and A$\beta-$/tau$-$ groups were assessed by fitting, for each ROI, a linear model considering the sociodemographic and clinical information described in Table 1 as covariates. *t*-statistics were used as variables for the analysis detailed in Section 4.5, while *p*-values were adjusted for multiple comparisons through a FDR threshold (<0.05). The analyses were performed in Python, taking advantage of the *statsmodels* (https://www.statsmodels.org/stable/ (accessed on 25 November 2024)) and *SciPy* packages (https://docs.scipy.org/doc/scipy-1.14.0/ (accessed on 25 November 2024)).

4.4. Gene Expression: Allen Human Brain Atlas

The AHBA dataset includes post-mortem brain-wide gene expression data from 6 donors [age = 42.5 (13.38) years, male/female = 5/1] [42]. The data were processed and mapped to 84 parcellated brain regions from the Desikan–Killiany atlas by employing the *abagen* toolbox (https://github.com/netneurolab/abagen (accessed on 25 November 2024)) [50], but only the left hemisphere (i.e., 34 ROIs) was considered in the current work due to the fact that only two of the six donors effectively presented the right hemisphere [51]. The reannotation of the microarray probes was performed by using data from [51] and discarding those not matching a valid Entrez ID. The probes were subsequently filtered based on the intensity value of their expression relative to the background noise. When

more than one probe was related to the expression of the same gene, the probe's selection was based on the differential stability criterion, which points at the probe showing a pattern of regional variation mostly consistent across the 6 subjects. These steps led to 15633 probes, each one corresponding to a single gene. Then, based on the tissue sample MNI coordinates, the brain region corresponding to each sample was identified as the nearest within a 2 mm radius. In the event that no match was found, the nearest sample to the centroid of the region was chosen. The average value for each sample assigned to the same brain region was calculated for every donor. Then, the values of the gene expression were normalized separately for each of the 6 subjects over the regions by relying on a robust sigmoid function and rescaling to the unit. Finally, the gene expression values were averaged across donors ending in a resultant matrix of dimensions 34 × 15633 (i.e., ROIs × genes).

4.5. Regional Morphometric Similarity and Transcriptomics Relationship

The Aβ+/tau+ and A$\beta-$/tau$-$ differences in regional MS, represented by the *t*-statistics previously calculated, were associated with the transcriptomics data through a PLS regression [13]. More specifically, the regional MS differences represented the response variables predicted by the measurements of the gene expression (i.e., the predictors). PLS regression allows us to find the best linear combination of gene expression values based on the maximum covariance they present with the regional MS variations induced by Aβ/tau conditions. The PLS regression was performed by using the Python *scikit-learn* package (https://scikit-learn.org/stable/ (accessed on 25 November 2024)) and specifying one latent component to search for after the standardization of the predictors. The PLS model's significance was then assessed through a permutation test performed by permuting the response variables 10^4 times [52].

The contribution of each gene in the PLS model was calculated by bootstrapping [13]. In detail, such a contribution was quantified based on the *z*-score, calculated for every gene as the ratio of the corresponding PLS weight and the standard error obtained by resampling the 34 ROIs with replacements. Highly positive *z*-scores correspond to genes with a great positive contribution to PLS, meaning that they are overexpressed in ROIs with increased MS. Conversely, highly negative *z*-scores identify the genes with a great negative contribution to PLS that translates to an overexpression in ROIs with decreased MS. The genes were then ranked according to their *z*-score and selected after the FDR correction based on the *p*-value ($p_{FDR} < 0.05$). A further selection was made by deriving the list of genes with $z > 3$ (PLS+) and the list of genes with $z < -3$ (PLS$-$). Both lists underwent an enrichment analysis as described in the following section.

4.6. Enrichment Analysis

The *GENE2FUNC* tool of the Functional Mapping and Annotation of Genome-Wide Association Studies (FUMA GWAS, https://fuma.ctglab.nl/ (accessed on 25 November 2024)) platform [53] was used to investigate the GO and KEGG databases to find the pathways and the BP involving PLS+ and PLS$-$ genes, respectively. The background genes used were those belonging to the final list coming from the processing described in Section 4.4 (i.e., 15633 genes), and the results of the gene set enrichments were FDR-corrected.

STRING (version 12.0, https://string-db.org/ (accessed on 25 November 2024)) [54] was employed to build the PLS+ and the PLS$-$ protein–protein functional interaction networks. We did not include text mining among the possible active interaction sources, and we set the minimum required interaction score to the default (i.e., 0.400).

To investigate the enrichment of PLS+ and PLS$-$ genes for specific types of brain cells, as in [55], we compiled the data coming from 5 single-cell studies employing postmortem cortical samples in human postnatal subjects [56–60]. All the 5 study-specific gene lists were merged by cell type, and we avoided duplicates and removed genes not present in the AHBA dataset. In detail, the neuron-related gene sets from [56,60] were discarded because the authors did not provide any specific distinction between the excitatory and inhibitory neurons as the others did, while the gene set related to pericyte was excluded because such a

cell type was considered only in [58]. The whole process ended in 7 gene sets corresponding to genes specifically expressed in microglia, endothelial cells, oligodendrocyte precursors, oligodendrocytes, astrocytes, excitatory and inhibitory neurons. The cell-class enrichment analyses were performed in R, using the *GeneOverlap* package (version 1.40.0) [61]. The same background used in the enrichment analysis and consisting of the 15633 AHBA genes was kept unaltered for this analysis. The overlap between the individual PLS+ and PLS− gene sets and each of the 7 cell-specific gene sets was tested through Fisher's exact test. The FDR correction for the number of cell types was applied to identify significant overlaps ($p_{FDR} < 0.05$). Finding a significant overlap means that the overlap between the two sets of genes is greater than the overlap that can be obtained with a random selection of a set of the same number of genes from the background.

Finally, *GeneOverlap* was also used to inspect the enrichment of PLS+ and PLS− genes for AD-related genes. The sources for defining such an AD-related genes list were (i) all the genes having loci with genetic evidence and all the AD risk/protective causal genes as compiled by the AD sequencing project gene verification committee and cleaned of duplicates (https://adsp.niagads.org/gvc-top-hits-list/ (accessed on 25 November 2024)); (ii) all the AD-associated genes retrieved in [62] through the employment of HETIONET (https://het.io/ (accessed on 25 November 2024)); (iii) and the genes involved in AD collected in DisGeNET (https://disgenet.com/ (accessed on 25 November 2024)) [63]. The three lists were merged, duplicates were avoided, and those genes that were not present among the 15633 AHBA genes used in this study were discarded, leading to a total number of 245 AD-related genes. PLS+ and PLS− gene sets were individually tested for overlapping with such a gene set by specifying the 15633 AHBA genes as the background.

5. Conclusions

Regional MS differences between Aβ+/tau+ and Aβ−/tau− along the AD continuum were assessed in this work for the first time. The alterations correlating with gene expression in the brain as provided by AHBA, resulting in *BCHE*, a gene involved in Aβ binding, had the most impact. Moreover, the enrichment analysis suggested that the immune response, astrocytes, microglia, and oligodendrocyte precursors are the biological process and cell types possibly leading to the cortical MS remodeling experienced by individuals before AD diagnosis when the Aβ/tau status changes from negative to positive.

Supplementary Materials: The following supporting information can be downloaded at https://www.mdpi.com/article/10.3390/ijms252312871/s1.

Author Contributions: Conceptualization, L.B. and I.B.G.; methodology, L.B., L.P., P.P., G.M. and I.B.G.; software, L.B., G.D., F.C. and F.P.; formal analysis, L.B., G.D., F.C. and I.B.G.; investigation, L.B., F.C. and I.B.G.; resources, G.M.; data curation, L.B.; writing—original draft preparation, L.B.; writing—review and editing, L.B., G.D., L.P., F.C., F.P., P.P., G.M. and I.B.G.; visualization, L.B.; supervision, G.M. and I.B.G.; project administration, L.B., G.M. and I.B.G.; funding acquisition, L.B., G.M. and I.B.G. All authors have read and agreed to the published version of the manuscript.

Funding: This work was supported in part by the Ministero dell'Università e della Ricerca (Bando Progetti di Rilevante Interesse Nazionale, PRIN 2022, "AI4BRAVE: AI for modeling of the Brain-Heart Axis in aging" project-reference code 202292PHR2) and in part by the Ministero dell'Istruzione e del Merito (MIUR D.M. 737/2021, "AI4Health: empowering neurosciences with eXplainable AI methods" project).

Institutional Review Board Statement: ADNI is IRB-approved (adni.loni.usc.edu).

Informed Consent Statement: All participants signed their informed consent (adni.loni.usc.edu).

Data Availability Statement: The data employed in this work were obtained from a third-party organization: ADNI. All ADNI data are shared through the LONI Image and Data Archive (IDA), a secure research data repository. Interested scientists may obtain access to ADNI imaging, clinical, genomic, and biomarker data for the purposes of scientific investigation, teaching, or planning

clinical research studies. Access is contingent on adherence to the ADNI Data Use Agreement and the publication policies outlined in the documents listed at the following link: https://adni.loni.usc.edu/.

Acknowledgments: We sincerely thank Lucrezia Vetro and Benedetta Visonà for all the efforts invested, in order that this work could take shape. Further thanks are also extended to the University of Verona for their provision of funds for open access publications. Data collection and sharing for this project was funded by the Alzheimer's Disease Neuroimaging Initiative (ADNI) (National Institutes of Health Grant U01 AG024904) and DOD ADNI (Department of Defense award number W81XWH-12-2-0012). ADNI is funded by the National Institute on Aging, the National Institute of Biomedical Imaging and Bioengineering, and the generous contributions from the following: AbbVie, Alzheimer's Association; Alzheimer's Drug Discovery Foundation; Araclon Biotech; BioClinica, Inc.; Biogen; Bristol-Myers Squibb Company; CereSpir, Inc.; Cogstate; Eisai Inc.; Elan Pharmaceuticals, Inc.; Eli Lilly and Company; EuroImmun; F. Hoffmann-La Roche Ltd and its affiliated company Genentech, Inc.; Fujirebio; GE Healthcare; IXICO Ltd.; Janssen Alzheimer Immunotherapy Research & Development, LLC.; Johnson & Johnson Pharmaceutical Research & Development LLC.; Lumosity; Lundbeck; Merck & Co., Inc.; Meso Scale Diagnostics, LLC.; NeuroRx Research; Neurotrack Technologies; Novartis Pharmaceuticals Corporation; Pfizer Inc.; Piramal Imaging; Servier; Takeda Pharmaceutical Company; and Transition Therapeutics. The Canadian Institutes of Health Research provides funds to support ADNI clinical sites in Canada. Private sector contributions are facilitated by the Foundation for the National Institutes of Health (www.fnih.org (accessed on 25 November 2024)). The grantee organization is the Northern California Institute for Research and Education, and this study was coordinated by the Alzheimer's Therapeutic Research Institute at the University of Southern California. ADNI data are disseminated by the Laboratory for Neuro Imaging at the University of Southern California.

Conflicts of Interest: The authors declare no conflicts of interest.

Abbreviations

The following abbreviations are used in this manuscript:

MRI	Magnetic resonance imaging
PET	Positron emission tomography
Aβ	Amyloid-β
AD	Alzheimer's disease
T1w	T1-weighted
dMRI	Diffusion MRI
AHBA	Allen Human Brain Atlas
MS	Morphometric similarity
CN	Cognitively unimpaired
MCI	Mildly cognitively impaired
MSN	MS network
SMC	Significant memory concern
Aβ+/tau+	Aβ-positive/tau-positive
A$\beta-$/tau$-$	Aβ-negative/tau-negative
ADNI	AD Neuroimaging Initiative
MMSE	Mini-mental state examination
ROI	Region of interest
FDR	False discovery rate
PLS	Partial least squares
FUMA GWAS	Functional Mapping and Annotation of Genome-Wide Association Studies
KEGG	Kyoto Encyclopedia of Genes and Genomes
GO BP	Gene Ontology biological process
PPI	Protein–protein interaction
OR	Odds ratio

References

1. Frisoni, G.B.; Altomare, D.; Thal, D.R.; Ribaldi, F.; van der Kant, R.; Ossenkoppele, R.; Blennow, K.; Cummings, J.; van Duijn, C.; Nilsson, P.M.; et al. The probabilistic model of Alzheimer disease: The amyloid hypothesis revised. *Nat. Rev. Neurosci.* **2022**, *23*, 53–66. [CrossRef] [PubMed]
2. Vilkaite, G.; Vogel, J.; Mattsson-Carlgren, N. Integrating amyloid and tau imaging with proteomics and genomics in Alzheimer's disease. *Cell Rep. Med.* **2024**, *5*, 101735. [CrossRef] [PubMed]
3. Yu, M.; Risacher, S.L.; Nho, K.T.; Wen, Q.; Oblak, A.L.; Unverzagt, F.W.; Apostolova, L.G.; Farlow, M.R.; Brosch, J.R.; Clark, D.G.; et al. Spatial transcriptomic patterns underlying amyloid-β and tau pathology are associated with cognitive dysfunction in Alzheimer's disease. *Cell Reports* **2024**, *43*, 113691. [CrossRef] [PubMed]
4. Grothe, M.J.; Sepulcre, J.; Gonzalez-Escamilla, G.; Jelistratova, I.; Schöll, M.; Hansson, O.; Teipel, S.J. Molecular properties underlying regional vulnerability to Alzheimer's disease pathology. *Brain* **2018**, *141*, 2755–2771. [CrossRef] [PubMed]
5. Mattsson, N.; Palmqvist, S.; Stomrud, E.; Vogel, J.; Hansson, O. Staging β-Amyloid Pathology with Amyloid Positron Emission Tomography. *JAMA Neurol.* **2019**, *76*, 1319–1329. [CrossRef]
6. Sanchez-Rodriguez, L.M.; Khan, A.F.; Adewale, Q.; Bezgin, G.; Therriault, J.; Fernandez-Arias, J.; Servaes, S.; Rahmouni, N.; Tissot, C.; Stevenson, J.; et al. In-vivo neuronal dysfunction by Aβ and tau overlaps with brain-wide inflammatory mechanisms in Alzheimer's disease. *Front. Aging Neurosci.* **2024**, *16*, 1383163. [CrossRef]
7. Pini, L.; Pievani, M.; Bocchetta, M.; Altomare, D.; Bosco, P.; Cavedo, E.; Galluzzi, S.; Marizzoni, M.; Frisoni, G.B. Brain atrophy in Alzheimer's Disease and aging. *Ageing Res. Rev.* **2016**, *30*, 25–48. [CrossRef]
8. Le Bihan, D.; Mangin, J.-F.; Poupon, C.; Clark, C.A.; Pappata, S.; Molko, N.; Chabriat, H. Diffusion tensor imaging: Concepts and applications. *J. Magn. Reson. Imaging* **2001**, *13*, 534–546. [CrossRef]
9. Spotorno, N.; Strandberg, O.; Vis, G.; Stomrud, E.; Nilsson, M.; Hansson, O. Measures of cortical microstructure are linked to amyloid pathology in Alzheimer's disease. *Brain* **2022**, *146*, 1602–1614. [CrossRef]
10. Brusini, L.; Cruciani, F.; Dall'Aglio, G.; Zajac, T.; Boscolo Galazzo, I.; Zucchelli, M.; Menegaz, G. XAI-Based Assessment of the AMURA Model for Detecting Amyloid-β and Tau Microstructural Signatures in Alzheimer's Disease. *IEEE J. Transl. Eng. Health Med.* **2024**, *12*, 569–579. [CrossRef]
11. Bassett, D.S.; Bullmore, E.; Verchinski, B.A.; Mattay, V.S.; Weinberger, D.R.; Meyer-Lindenberg, A. Hierarchical Organization of Human Cortical Networks in Health and Schizophrenia. *J. Neurosci.* **2008**, *28*, 9239–9248. [CrossRef] [PubMed]
12. Seidlitz, J.; Vasa, F.; Shinn, M.; Romero-Garcia, R.; Whitaker, K.J.; Vértes, P.E.; Wagstyl, K.; Kirkpatrick Reardon, P.; Clasen, L.; Liu, S.; et al. Morphometric Similarity Networks Detect Microscale Cortical Organization and Predict Inter-Individual Cognitive Variation. *Neuron* **2018**, *97*, 231–247.e7. [CrossRef] [PubMed]
13. Morgan, S.E.; Seidlitz, J.; Whitaker, K.J.; Romero-Garcia, R.; Clifton, N.E.; Scarpazza, C.; van Amelsvoort, T.; Marcelis, M.; van Os, J.; Donohoe, G.; et al. Cortical patterning of abnormal morphometric similarity in psychosis is associated with brain expression of schizophrenia-related genes. *Proc. Natl. Acad. Sci. USA* **2019**, *116*, 9604–9609. [CrossRef] [PubMed]
14. Li, J.; Keller, S.S.; Seidlitz, J.; Chen, H.; Li, B.; Weng, Y.; Meng, Y.; Yang, S.; Xu, Q.; Zhang, Q.; et al. Cortical morphometric vulnerability to generalised epilepsy reflects chromosome- and cell type-specific transcriptomic signatures. *Neuropathol. Appl. Neurobiol.* **2023**, *49*, e12857. [CrossRef]
15. Lei, W.; Xiao, Q.; Wang, C.; Gao, W.; Xiao, Y.; Dai, Y.; Lu, G.; Su, L.; Zhong, Y. Cell-type-specific genes associated with cortical structural abnormalities in pediatric bipolar disorder. *Psychoradiology* **2022**, *2*, 56–65. [CrossRef]
16. Martins, D.; Dipasquale, O.; Veronese, M.; Turkheimer, F.; Loggia, M.L.; McMahon, S.; Howard, M.A.; Williams, S.C.R. Transcriptional and cellular signatures of cortical morphometric remodelling in chronic pain. *Pain* **2022**, *163*, e759–e773. [CrossRef]
17. Xiao, Y.; Chen, F.; Lei, W.; Ke, J.; Dai, Y.; Qi, R.; Lu, G.; Zhong, Y. Transcriptional signal and cell specificity of genes related to cortical structural differences of post-traumatic stress disorder. *J. Psychiatr. Res.* **2023**, *160*, 28–37. [CrossRef]
18. Wang, Y.; Xiao, Y.; Xing, Y.; Yu, M.; Wang, X.; Ren, J.; Liu, W.; Zhong, Y. Morphometric similarity differences in drug-naive Parkinson's disease correlate with transcriptomic signatures. *CNS Neurosci. Ther.* **2024**, *30*, e14680. [CrossRef]
19. Long, J.; Li, J.; Xie, B.; Jiao, Z.; Shen, G.; Liao, W.; Song, X.; Le, H.; Xia, J.; Wu, S. Morphometric similarity network alterations in COVID-19 survivors correlate with behavioral features and transcriptional signatures. *Neuroimage Clin.* **2023**, *39*, 103498. [CrossRef] [PubMed]
20. Zhang, Y.; Ma, M.; Xie, Z.; Wu, H.; Zhang, N.; Shen, J. Bridging the Gap Between Morphometric Similarity Mapping and Gene Transcription in Alzheimer's Disease. *Front. Neurosci.* **2021**, *15*, 731292. [CrossRef]
21. Braak, H.; Braak, E. Neuropathological stageing of Alzheimer-related changes. *Acta Neuropathol.* **1991**, *82*, 239–259. [CrossRef] [PubMed]
22. Grothe, M.J.; Barthel, H.; Sepulcre, J.; Dyrba, M.; Sabri, O.; Teipel, S.J. In vivo staging of regional amyloid deposition. *Neurology* **2017**, *89*, 2031–2038. [CrossRef]
23. Hwang, U.; Kim, S.W.; Jung, D.; Kim, S.; Lee, H.; Seo, S.W.; Seong, J.K.; Yoon, S. Real-world prediction of preclinical Alzheimer's disease with a deep generative model. *Artif. Intell. Med.* **2023**, *144*, 102654. [CrossRef] [PubMed]
24. Hampel, H.; Hardy, J.; Blennow, K.; Chen, C.; Perry, G.; Kim, S.H.; Villemagne, V.L.; Aisen, P.; Vendruscolo, M.; Iwatsubo, T.; et al. The Amyloid-β Pathway in Alzheimer's Disease. *Mol. Psychiatry* **2021**, *26*, 5481–5503. [CrossRef]
25. Drummond, E.; Pires, G.; MacMurray, C.; Askenazi, M.; Nayak, S.; Bourdon, M.; Safar, J.; Ueberheide, B.; Wisniewski, T. Phosphorylated tau interactome in the human Alzheimer's disease brain. *Brain* **2020**, *143*, 2803–2817. [CrossRef]

26. Guillozet, A.L.; Mesulam, M.M.; Smiley, J.F.; Mash, D.C. Butyrylcholinesterase in the life cycle of amyloid plaques. *Ann. Neurol.* **1997**, *42*, 909–918. [CrossRef]
27. Darvesh, S.; Kumar, R.; Roberts, S.; Walsh, R.; Martin, E. Butyrylcholinesterase-Mediated Enhancement of the Enzymatic Activity of Trypsin. *Cell. Mol. Neurobiol.* **2001**, *21*, 285–296. [CrossRef] [PubMed]
28. Martins-de-Souza, D.; Guest, P.C.; Mann, D.M.; Roeber, S.; Rahmoune, H.; Bauder, C.; Kretzschmar, H.; Volk, B.; Baborie, A.; Bahn, S. Proteomic Analysis Identifies Dysfunction in Cellular Transport, Energy, and Protein Metabolism in Different Brain Regions of Atypical Frontotemporal Lobar Degeneration. *J. Proteome Res.* **2012**, *11*, 2533–2543. [CrossRef]
29. Rajesh, Y.; Kanneganti, T.D. Innate Immune Cell Death in Neuroinflammation and Alzheimer's Disease. *Cells* **2022**, *11*, 1885. [CrossRef]
30. Norris, G.T.; Kipnis, J. Immune cells and CNS physiology: Microglia and beyond. *J. Exp. Med.* **2018**, *216*, 60–70. [CrossRef]
31. Preman, P.; Alfonso-Triguero, M.; Alberdi, E.; Verkhratsky, A.; Arranz, A.M. Astrocytes in Alzheimer's Disease: Pathological Significance and Molecular Pathways. *Cells* **2021**, *10*, 540. [CrossRef] [PubMed]
32. Olah, M.; Menon, V.; Habib, N.; Taga, M.F.; Ma, Y.; Yung, C.J.; Cimpean, M.; Khairallah, A.; Coronas-Samano, G.; Sankowski, R.; et al. Single cell RNA sequencing of human microglia uncovers a subset associated with Alzheimer's disease. *Nat. Commun.* **2020**, *11*, 6129. [CrossRef] [PubMed]
33. Alsema, A.M.; Jiang, Q.; Kracht, L.; Gerrits, E.; Dubbelaar, M.L.; Miedema, A.; Brouwer, N.; Hol, E.M.; Middeldorp, J.; van Dijk, R.; et al. Profiling Microglia From Alzheimer's Disease Donors and Non-demented Elderly in Acute Human Postmortem Cortical Tissue. *Front. Mol. Neurosci.* **2020**, *13*, 134. [CrossRef] [PubMed]
34. Habib, N.; McCabe, C.; Medina, S.; Varshavsky, M.; Kitsberg, D.; Dvir-Szternfeld, R.; Green, G.; Dionne, D.; Nguyen, L.; Marshall, J.L.; et al. Disease-associated astrocytes in Alzheimer's disease and aging. *Nat. Neurosci.* **2020**, *23*, 701–706. [CrossRef] [PubMed]
35. Evans, H.T.; Taylor, D.; Kneynsberg, A.; Bodea, L.G.; Götz, J. Altered ribosomal function and protein synthesis caused by tau. *Acta Neuropathol. Commun.* **2021**, *9*, 110. [CrossRef]
36. Zeng, H.; Huang, J.; Zhou, H.; Meilandt, W.J.; Dejanovic, B.; Zhou, Y.; Bohlen, C.J.; Lee, S.-H.; Ren, J.; Liu, A.; et al. Integrative in situ mapping of single-cell transcriptional states and tissue histopathology in a mouse model of Alzheimer's disease. *Nat. Neurosci.* **2023**, *26*, 430–446. [CrossRef]
37. Cohen, S.; Cummings, J.; Knox, S.; Potashman, M.; Harrison, J. Clinical Trial Endpoints and Their Clinical Meaningfulness in Early Stages of Alzheimer's Disease. *J. Prev. Alzheimer's Dis.* **2022**, *9*, 507–522. [CrossRef]
38. Zavaliangos-Petropulu, A.; Nir, T.M.; Thomopoulos, S.I.; Reid, R.I.; Bernstein, M.A.; Borowski, B.; Jack Jr., C.R.; Weiner, M.W.; Jahanshad, N.; Thompson, P.M. Diffusion MRI Indices and Their Relation to Cognitive Impairment in Brain Aging: The Updated Multi-protocol Approach in ADNI3. *Front. Neuroinformatics* **2019**, *13*, 2. [CrossRef]
39. Thomas, K.R.; Bangen, K.J.; Rotblatt, L.J.; Weigand, A.J.; Edwards, L.; Tosun, D.; Galasko, D. Self- and study partner–reported cognitive decline in older adults without dementia: The role of α-synuclein and amyloid biomarkers in the Alzheimer's Disease Neuroimaging Initiative. *Alzheimer's Dement.* **2024**, *20*, 7777–7787. [CrossRef]
40. Jenkinson, M.; Beckmann, C.F.; Behrens, T.E.; Woolrich, M.W.; Smith, S.M. FSL. *NeuroImage* **2012**, *62*, 782–790. [CrossRef]
41. Fischl, B.; Salat, D.H.; Busa, E.; Albert, M.; Dieterich, M.; Haselgrove, C.; van der Kouwe, A.; Killiany, R.; Kennedy, D.; Klaveness, S.; et al. Whole brain segmentation: Automated labeling of neuroanatomical structures in the human brain. *Neuron* **1991**, *33*, 341–355. [CrossRef] [PubMed]
42. Hawrylycz, M.J.; Lein, E.S.; Guillozet-Bongaarts, A.L.; Shen, E.H.; Ng, L.; Miller, J.A.; van de Lagemaat, L.N.; Smith, K.A.; Ebbert, A.; Riley, Z.L.; et al. An anatomically comprehensive atlas of the adult human brain transcriptome. *Nature* **2012**, *489*, 391–399. [CrossRef] [PubMed]
43. Andersson, J.L.; Sotiropoulos, S.N. An integrated approach to correction for off-resonance effects and subject movement in diffusion MR imaging. *NeuroImage* **2016**, *125*, 1063–1078. [CrossRef]
44. Garyfallidis, E.; Brett, M.; Amirbekian, B.; Rokem, A.; Van Der Walt, S.; Descoteaux, M.; Nimmo-Smith, I. Dipy, a library for the analysis of diffusion MRI data. *Front. Neuroinformatics* **2014**, *8*, 8. [CrossRef]
45. Veraart, J.; Fieremans, E.; Novikov, D.S. Diffusion MRI noise mapping using random matrix theory. *Magn. Reson. Med.* **2016**, *76*, 1582–1593. [CrossRef]
46. Jenkinson, M.; Bannister, P.; Brady, M.; Smith, S. Improved Optimization for the Robust and Accurate Linear Registration and Motion Correction of Brain Images. *NeuroImage* **2002**, *17*, 825–841. [CrossRef] [PubMed]
47. Nir, T.M.; Jahanshad, N.; Villalon-Reina, J.E.; Isaev, D.; Zavaliangos-Petropulu, A.; Zhan, L.; Leow, A.D.; Jack Jr., C.R.; Weiner, M.W.; Thompson, P.M. Fractional anisotropy derived from the diffusion tensor distribution function boosts power to detect Alzheimer's disease deficits. *Magn. Reson. Med.* **2017**, *78*, 2322–2333. [CrossRef]
48. Avants, B.B.; Tustison, N.J.; Stauffer, M.; Song, G.; Wu, B.; Gee, J.C. The Insight ToolKit image registration framework. *Front. Neuroinformatics* **2014**, *8*, 44. [CrossRef]
49. Basser, P.J.; Pierpaoli, C. Microstructural and Physiological Features of Tissues Elucidated by Quantitative-Diffusion-Tensor MRI. *J. Magn. Reson. Ser. B* **1996**, *111*, 209–219. [CrossRef]
50. Markello, R.D; Arnatkeviciute, A.; Poline, J.-B.; Fulcher, B.D; Fornito, A.; Misic, B. Standardizing workflows in imaging transcriptomics with the abagen toolbox. *eLife* **2021**, *10*, e72129. [CrossRef]
51. Arnatkeviciute, A.; Fulcher, B.D.; Fornito, A. A practical guide to linking brain-wide gene expression and neuroimaging data. *NeuroImage* **2019**, *189*, 353–367. [CrossRef] [PubMed]

52. McIntosh, A.R.; Lobaugh, N.J. Partial least squares analysis of neuroimaging data: Applications and advances. *NeuroImage* **2004**, *23*, S250–S263. [CrossRef]
53. Watanabe, K.; Taskesen, E.; van Bochoven, A.; Posthuma, D. Functional mapping and annotation of genetic associations with FUMA. *Nat. Commun.* **2017**, *8*, 1826. [CrossRef]
54. Szklarczyk, D.; Kirsch, R.; Koutrouli, M.; Nastou, K.; Mehryary, F.; Hachilif, R.; Gable, A.L.; Fang, T.; Doncheva, N.T.; Pyysalo, S.; et al. The STRING database in 2023: Protein–protein association networks and functional enrichment analyses for any sequenced genome of interest. *Nucleic Acids Res.* **2022**, *51*, D638–D646. [CrossRef]
55. Seidlitz, J.; Nadig, A.; Liu, S.; Bethlehem, R.A.I.; Vertes, P.E.; Morgan, S.E.; Vasa, F.; Romero-Garcia, R.; Lalonde, F.M.; Clasen, L.S.; et al. Transcriptomic and cellular decoding of regional brain vulnerability to neurogenetic disorders. *Nat. Commun.* **2020**, *11*, 3358. [CrossRef] [PubMed]
56. Darmanis, S.; Sloan, S.A.; Zhang, Y.; Enge, M.; Caneda, C.; Shuer, L.M.; Hayden Gephart, M.G.; Barres, B.A.; Quake, S.R. A survey of human brain transcriptome diversity at the single cell level. *Proc. Natl. Acad. Sci. USA* **2015**, *112*, 7285–7290. [CrossRef]
57. Habib, N.; Avraham-Davidi, I.; Basu, A.; Burks, T.; Shekhar, K.; Hofree, M.; Choudhury, S.R.; Aguet, F.; Gelfand, E.; Ardlie, K.; et al. Massively parallel single-nucleus RNA-seq with DroNc-seq. *Nat. Methods* **2017**, *14*, 955–958. [CrossRef]
58. Lake, B.B.; Chen, S.; Sos, B.C.; Fan, J.; Kaeser, G.E.; Yung, Y.C.; Duong, T.E.; Gao, D.; Chun, J.; Kharchenko, P.V.; Zhang, K. Integrative single-cell analysis of transcriptional and epigenetic states in the human adult brain. *Nat. Biotechnol.* **2018**, *36*, 70–80. [CrossRef] [PubMed]
59. Li, M.; Santpere, G.; Imamura Kawasawa, Y.; Evgrafov, O.V.; Gulden, F.O.; Pochareddy, S.; Sunkin, S.M.; Li, Z.; Shin, Y.; Zhu, Y.; et al. Integrative functional genomic analysis of human brain development and neuropsychiatric risks. *Science* **2018**, *362*, eaat7615. [CrossRef]
60. Zhang, Y.; Sloan, S.A.; Clarke, L.E.; Caneda, C.; Plaza, C.A.; Blumenthal, P.D.; Vogel, H.; Steinberg, G.K.; Edwards, M.S.B.; Li, G.; et al. Purification and Characterization of Progenitor and Mature Human Astrocytes Reveals Transcriptional and Functional Differences with Mouse. *Neuron* **2016**, *89*, 37–53. [CrossRef]
61. Shen, L. *GeneOverlap: Test and Visualize Gene Overlaps*; R package version 1.40.0; 2024. [CrossRef]
62. Himmelstein, D.S.; Baranzini, S.E. Heterogeneous Network Edge Prediction: A Data Integration Approach to Prioritize Disease-Associated Genes. *PLoS Comput. Biol.* **2015**, *11*, e1004259. [CrossRef] [PubMed]
63. Pinero, J.; Ramirez-Anguita, J.; Sauch-Pitarch, J.; Ronzano, F.; Centeno, E.; Sanz, F.; Furlong, L.I. The DisGeNET knowledge platform for disease genomics: 2019 update. *Nucleic Acids Res.* **2019**, *48*, D845–D855. [CrossRef]

Disclaimer/Publisher's Note: The statements, opinions and data contained in all publications are solely those of the individual author(s) and contributor(s) and not of MDPI and/or the editor(s). MDPI and/or the editor(s) disclaim responsibility for any injury to people or property resulting from any ideas, methods, instructions or products referred to in the content.

International Journal of
Molecular Sciences

MDPI

Article

Endoplasmic Reticulum Proteins Impact Penetrance in a *Pink1*-Mutant *Drosophila* Model

Melissa Vos [1,*], Fabian Ott [2], Hawwi Gillo [1], Giuliana Cesare [1], Sophie Misera [1], Hauke Busch [2] and Christine Klein [1,*]

[1] Institute of Neurogenetics, University of Luebeck, UKSH (Universitätsklinikum Schleswig-Holstein, Campus Lübeck), Ratzeburger Allee 160, Building 67 (BMF), 23562 Luebeck, Germany
[2] Medical Systems Biology Division, Lübeck Institute of Experimental Dermatology, University of Luebeck, 23562 Luebeck, Germany
* Correspondence: melissa.vos@uni-luebeck.de (M.V.); christine.klein@uni-luebeck.de (C.K.)

Abstract: Parkinson's disease (PD) is a neurodegenerative disorder with a high variability of age at onset, disease severity, and progression. This suggests that other factors, including genetic, environmental, or biological factors, are at play in PD. The loss of PINK1 causes a recessive form of PD and is typically fully penetrant; however, it features a wide range in disease onset, further supporting the existence of protective factors, endogenous or exogenous, to play a role. The loss of Pink1 in *Drosophila melanogaster* results in locomotion deficits, also observed in PINK1-related PD in humans. In flies, Pink1 deficiency induces defects in the ability to fly; nonetheless, around ten percent of the mutant flies are still capable of flying, indicating that advantageous factors affecting penetrance also exist in flies. Here, we aimed to identify the mechanisms underlying this reduced penetrance in Pink1-deficient flies. We performed genetic screening in *pink1*-mutant flies to identify RNA expression alterations affecting the flying ability. The most important biological processes involved were transcriptional and translational activities, endoplasmic reticulum (ER) regulation, and flagellated movement and microtubule organization. We validated two ER-related proteins, zonda and windbeutel, to positively affect the flying ability of Pink1-deficient flies. Thus, our data suggest that these processes are involved in the reduced penetrance and that influencing them may be beneficial for Pink1 deficiency.

Keywords: Parkinson's disease; reduced penetrance; Pink1; *Drosophila melanogaster*; endoplasmic reticulum

1. Introduction

Parkinson's disease (PD) features a wide variability in disease signs and symptoms, severity, progression, and age at onset [1], suggesting elements exist that alter disease development. Furthermore, the identification of a surprisingly large number of carriers of allegedly pathogenic variants remaining free of disease or developing a mild form indicates the existence of reduced penetrance [2]. The best-studied example in the field of PD is LRRK2-linked PD: the autosomal dominant PD-causing mutation G2019S in *LRRK2* is the most commonly known genetic cause of PD; however, it has a low penetrance that is affected by environmental and genetic factors [3–7]. In this manuscript, we focus on the mechanisms of Pink1-related penetrance on the basis of unique findings in a Pink1 *Drosophila* model [8]. The recessively inherited forms of PD, caused by mutations in *pink1* and *Parkin*, are typically highly (to fully) penetrant, yet they come with an extensive range of ages at onset, supporting external factors to be pivotal [3,9]. For instance, studies show

that smoking or caffeine intake reduces the risk of PD [10,11]. Furthermore, the progression of PD can be delayed with a protective diet, such as the Mediterranean diet, combined with physical exercise [12,13], further underscoring the importance of external factors in the progression of PD.

Several mechanisms were found to be linked to PD. One of the more recent findings is the impact of the 'gut-brain' axis on PD [14] (cite a review article here?). In PD patients, gut bacteria appear to be pro-inflammatory via modulation of lipid metabolism that, in turn, may induce neuroinflammation [14,15]. Interestingly, infection of the intestines exacerbates PD-like signs in Pink1-deficient mice [16], reinforcing the importance of the gut–brain axis. Of further note, PINK1 is a mitochondrial protein that also localizes to the ER–mitochondrial contact sites [17–19]. These ER–mitochondrial contact sites play an important role in calcium homeostasis, mitophagy, and lipid metabolism, i.e., processes that are defective in PD [17,18,20,21]. Notably, in this context, PINK1 plays a direct role in mitophagy [17,22]. In addition, the ER is responsible for properly folding newly synthesized proteins. When these proteins are folded incorrectly, they accumulate in the ER, leading to ER stress and activating the unfolded protein response (UPR), both of which are related to PD [23,24]. Finally, mitochondrial dysfunction and a defective sphingolipid metabolism have been identified to play a role in the pathogenesis of PD [25–27]. Thus, elements affecting the penetrance of PD are most likely involved in these cellular processes. For example, a recent study on homozygous twins discordant for idiopathic PD links mitochondrial integrity to altered disease penetrance [28]. However, the underlying mechanisms remain elusive. Hence, additional studies are required to understand the mechanisms that result in reduced penetrance.

Studies in *Drosophila melanogaster* have significantly contributed to our current knowledge of the mechanisms implicated in PD [29]. Research using the fruit fly was the first to highlight a common pathway between Pink1 and Parkin [30,31]. This finding was confirmed in human cellular systems [32,33]. Interestingly, in *Drosophila melanogaster*, reduced penetrance is observed concerning the flying phenotype in *pink1*-mutant flies. Previous studies show that the loss of Pink1 in flies results in a variable flying ability with a mean of around 10% [8,27,34], even though all these flies carry the same loss of function deletion in Pink1. Thus, the fruit fly is a suitable model to study mechanisms underlying altered penetrance.

Here, we performed a transcriptome analysis in *pink1*-mutant flies to identify alterations in RNA expression levels that affect the flying ability. The most significant upregulation of biological processes was observed primarily in pathways associated with transcriptional and translational activities and endoplasmic reticulum (ER) regulation. Conversely, downregulated pathways were linked to flagellated movement and microtubule organization. In addition, four genes were tested for validation, of which two, zonda (Zda) and windbeutel (wbl), were confirmed to be beneficial and involved in autophagy and ER stress, supporting a role of reduced penetrance for these cellular mechanisms.

2. Results

2.1. Lack of Flying Ability of Pink1-Deficient Flies Shows a Pattern of Reduced Penetrance

The average flying ability of general *pink1*^{B9}-mutant fly stock is around ten percent [8], suggesting that a protective mechanism allows these ten percent of flies to fly. To analyze genetic factors that play a role in this reduced penetrance, we set up a group of 200 parent pairs consisting of one male and one virgin female fly to reduce the genetic variability of the offspring. One hundred and twenty-five parent pairs resulted in Pink1-deficient offspring and were tested for their flying ability. The offspring showed substantial variability in the ability to fly, ranging from a complete inability to fly to a flying ability of 60% (Figure 1A).

Although we reduced the genetic variability by combining only one male and one female, the offspring of these parent pairs are not genetically identical, explaining that not all offspring of a specific parent pair display the same flying ability. This provides a direct tool to analyze the existing reduced penetrance, and our screen allows for the identification of genetic factors impacting the penetrance of the flying phenotype.

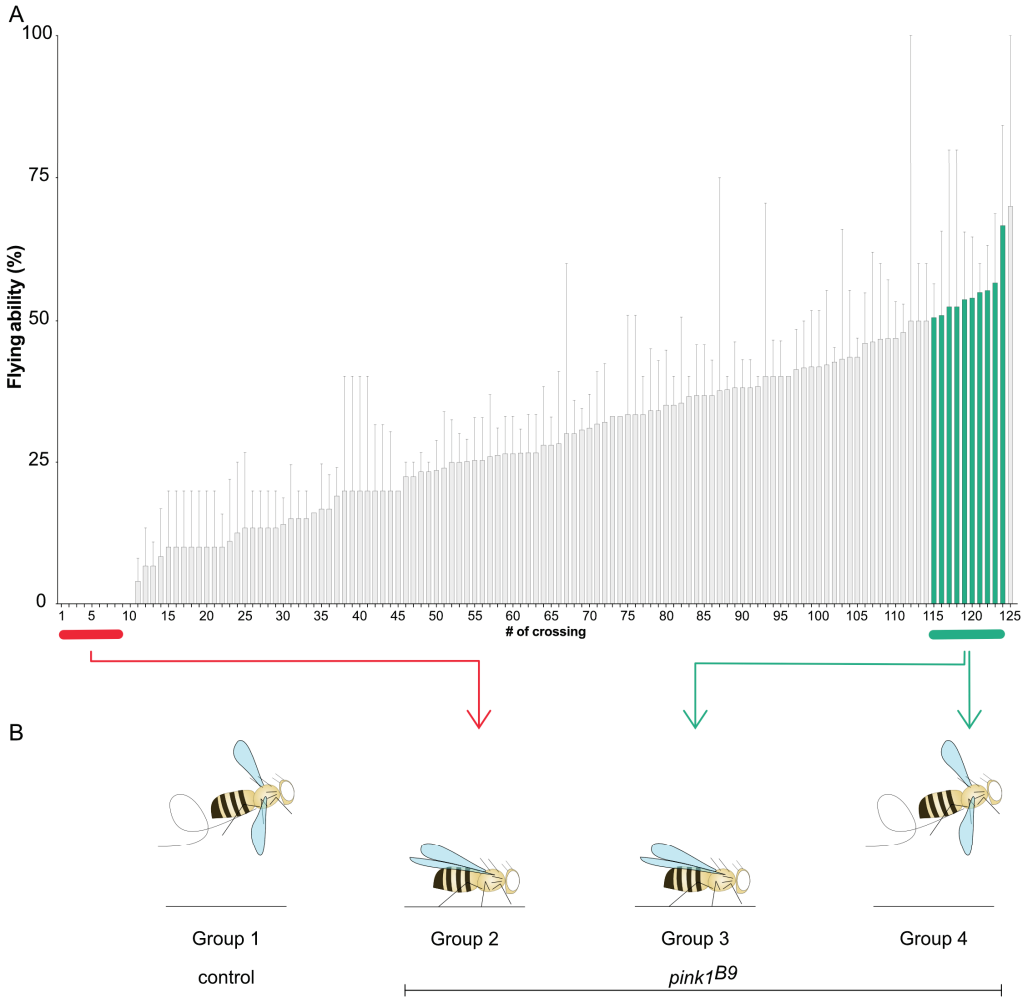


Figure 1. Reduced penetrance of the lack of flying ability of Pink1-deficient flies. (**A**) The flying ability of the offspring of 125 parent pairs of *pink1*-mutant flies. (**B**) Scheme to identify the different groups on which RNA sequencing analyses were performed. Data are percentages with sem; n > 5.

2.2. RNA Sequencing Analysis Identifies Genes Involved in Reduced Penetrance

To identify genes that play a role in reduced penetrance, we performed RNA sequencing analyses on four different groups (Figure 1B): 1. control flies ($pink1^{RV}$); 2. $pink1^{B9}$-mutant flies, of which none of the offspring could fly; 3. $pink1^{B9}$-mutant flies that could not fly; 4. 'siblings' of group 3 that could fly (group 4). Thus, groups 3 and 4 were offspring of the same parent pair and had the lowest genetic variability; hence, differential RNA expression between those two groups may be the most relevant in the context of reduced penetrance.

In our group analysis, genes were designated differentially expressed with an absolute effect size (beta-value) > 1 and an adjusted *p*-value < 0.05. Notably, we identified 350, 611, and 650 differentially expressed genes (DEGs) when comparing the control group against groups two, three, and four, respectively (cf. volcano plots in Figure 2). When considering genes with human orthologs only, the gene count was substantially reduced, resulting in 144, 226, and 261 DEGs for the control comparison against groups two, three, and four.

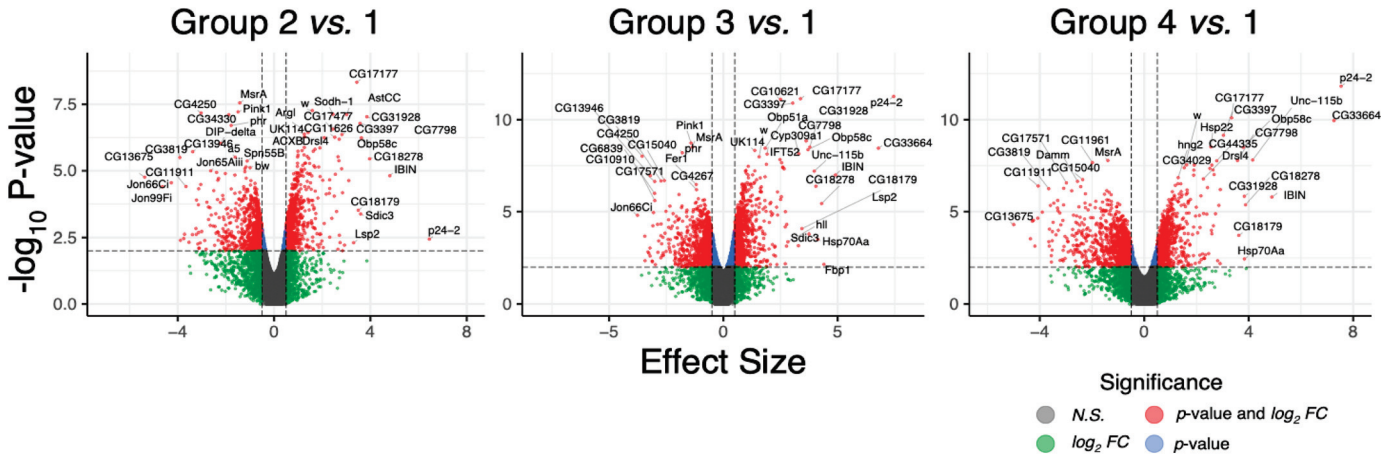


Figure 2. Volcano plots showing groupwise differentially regulated genes. The x- and y-axes denote the effect size (beta-value) and negative $\log_{10}$ values of the *p*-value corrected for multiple testing, respectively. Values are based on the likelihood-ratio test using sleuth. Significantly regulated genes (adj. *p*-value < 0.05; |effect size| > 1.0) are shown in red and annotated with their gene symbol.

While we found many differentially regulated genes when comparing groups 2–4 to group 1, few significant DEGs were identified when comparing groups 2–4 to each other. A principal component analysis (PCA) further confirms gene expression similarity among these groups (Figure 3). Using the 2000 most variable transcripts based on transcripts per million (TPM) values across all samples, the three mutated groups clustered closely, as depicted by the ellipses encircling each group. Only the samples from group 1 are positioned further apart (red dots, Figure 3). Overall, we identified 12 genes that displayed significant RNA expression differences between groups 3 and 4, i.e., Pink1-deficient flies that cannot fly vs. those that can fly coming from the same parent pair.

To assess the penetrance of the loss of Pink1, we examined genes differentially regulated in controls and mutants that retained their flying ability compared to non-flying mutants. The comparison of the established groups (Flying, MutatedFlying, and Mutant) with the multiple regression model from limma revealed 3396 genes that were significantly reduced to 1692 genes when filtered for human orthologs. Additionally, we refined our gene selection criteria to include only those that exhibited either up- or down-regulation in both groups when compared to mutated, non-flying fruit flies. To enhance specificity and eliminate non-penetrance-related noise, we restricted the magnitude of expression changes between these groups to a factor of 3. Consequently, we successfully identified 124 genes, as detailed in Table S2.

2.3. Validation of the Protective Effects of Single Hits

Pathway analyses revealed a significant enrichment of transcriptional and translational activities and regulation of (endo)membranes and ER, as well as a decrease in pathways related to flagellated movement and microtubule organization. The ER is known to be linked to neurodegeneration [35]; however, the underlying processes are not fully understood. Hence, we selected four ER-linked genes, which were also significant in the ANOVA test and that were readily available for testing: Torsin, KdelR, and winbeutel (wbl), which showed increased differential expression levels, and zonda (Zda), which displayed lower differential expression levels (Figure 4A), approaching control expression levels. The overexpression of KdelR and Torsin in Pink1-deficient flies failed to elicit an effect on the flying ability of *pink1*-mutant flies (Figure 4B,D), while the overexpression of wbl and two independent alleles of heterozygous loss of Zda improved the flying ability (Figure 4C,E).

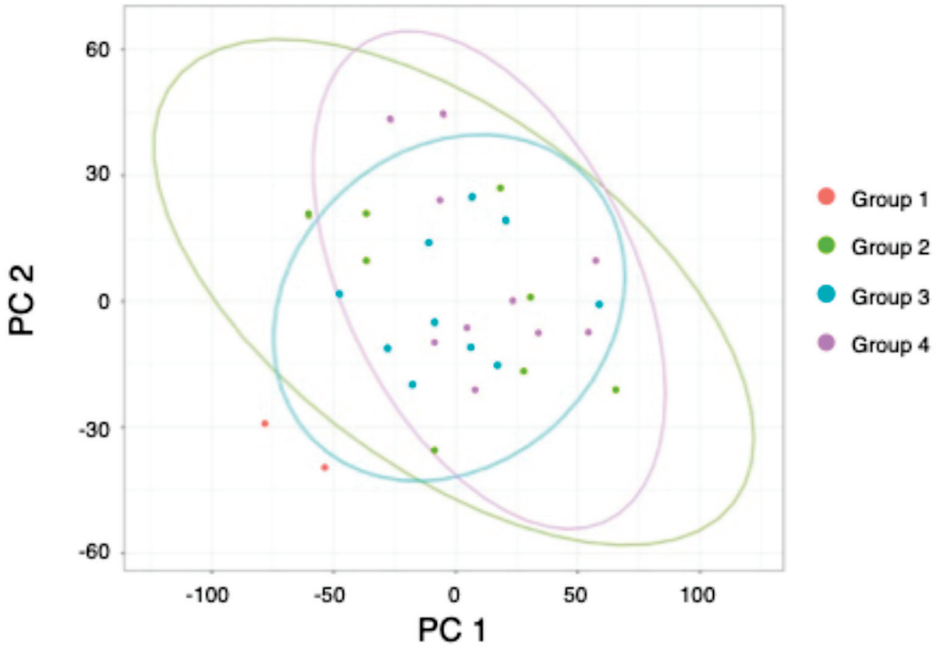


Figure 3. Principal component analysis showing the first two principal components (PC1/2) using TPM values of the 2000 most variable genes. Colors represent the different groups, as shown in the legend, while the ellipses encapsulating the groups assume a multivariate t-distribution of the data.

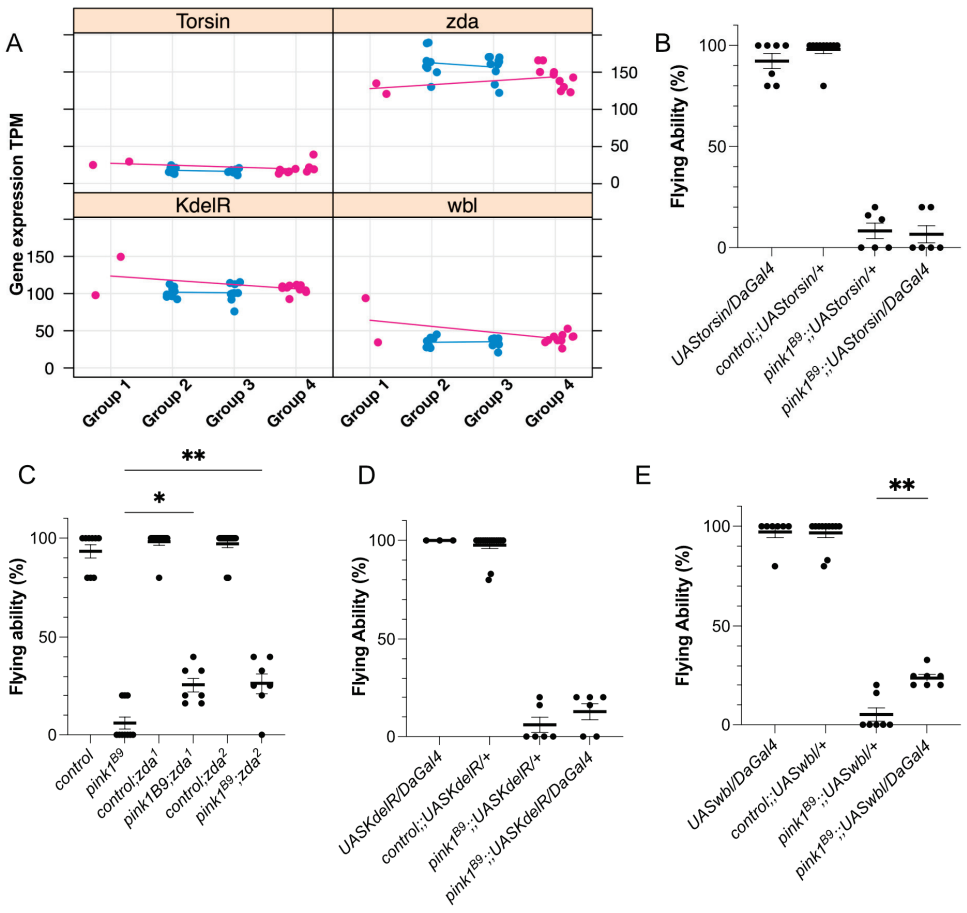


Figure 4. Validation of the protective effects of selected positive hits. (**A**) Gene expression of relevant hits from the multiple regression analysis. Normalized gene expression is plotted for the different

groups, where the points for control and the mutated flyable offspring are colored in pink, while the data points of parents and non-flyable offspring are colored in blue. The genes selected showed annealing of mean gene expression for flyable offspring to the control level, while the mutated group remained higher/lower than the expression of the controls. (**B**–**E**) Flying ability of over-expression using the ubiquitous driver Daughterless Gal4 (DaGal4) of Torsin (**B**), KdelR (**D**), and wbl (**E**) or heterozygous loss of Zda (**C**) in a *pink1*-mutant background to validate the identified hits. Data are single data points of percentages with sem; n $\geq$ 3. *: $p < 0.05$; **: $p < 0.01$.

3. Discussion

In this work, we showed the presence of reduced penetrance in Pink1-deficient flies and performed RNA expression analyses to elucidate possible mechanisms underlying this observation. Via gene ontology and pathway analyses, we identified several molecular mechanisms that appear to be involved in the penetrance of loss of Pink1, including ER-related activity. Finally, we confirmed a beneficial effect of lower Zda and higher wbl levels on the flying phenotype of *pink1*-mutant flies, suggesting that ER-linked autophagy and ER stress play an essential role in the penetrance of a PD-like phenotype in our *Drosophila* model.

The low genetic variability between the parents and offspring groups is to be expected since we assume that the genetic background should still be relatively close to its progenitor individuals. Additionally, the offspring groups were sampled from the same time point, resulting in an even higher genetic resemblance. In an attempt to circumvent this, we decided that a multiple linear regression would be the most fitting model, only focusing on the flying ability of the different sample groups. This also enabled us to work with a rather small control group of two sequencing samples since limma is fit for handling small sample sizes, and the multiple linear regression grouped the controls with the flying mutants, allowing us to pinpoint potential genetic variables that could affect the penetrance of the flying phenotype. By applying our set criteria for candidate genes (relevant pathways, significant ANOVA hits, same direction of logFC, human ortholog), we identified 124 genes that approach control expression levels in our mutants. Most genes in Table S2 still need to be identified, which makes them potential candidates for the modulation of penetrance that is challenging to evaluate experimentally.

The comparison of DEGs between groups 3 (*pink1*-mutant flies that cannot fly) and 4 (*pink1*-mutant flies that can fly and are 'siblings' of group 3) revealed twelve candidate genes to be altered, suggesting that these genes affect the reduced penetrance of the flying ability. Nonetheless, we did not validate these genes due to the assumption that it is unlikely that one gene can regulate penetrance. Instead, (minor) alterations in biological processes or cellular mechanisms are more likely to affect the penetrance. One of the identified pathways entails transcriptional and translational activities. Previously, PARIS, a Parkin-interacting substrate, was found to be accumulating following a loss of Parkin, exerting a detrimental effect on rRNA transcription [36].

Furthermore, the structure and function of mitochondrial ribosomes play a crucial role in determining oxidative phosphorylation efficiency. This feature is commonly affected in PD [37], providing possible explanations of how these biological processes impact the penetrance. Microtubule organization, another identified pathway, is key for the structural support of the cytoskeleton, facilitates intracellular transport, and contributes to the organization of cellular organelles. The dysfunction of microtubules is strongly associated with PD; however, it remains unclear whether this dysfunction is a cause or a consequence of PD [38]. Our data support that these pathways are involved in the reduced penetrance of the Pink1-deficient flying phenotype; however, how and to what extent remain elusive.

The ER is another biological process that plays a role in the reduced penetrance of the ability of *pink1*-mutant flies to fly. The ER has apparent links to neurodegeneration via its function in protein quality control and folding, mitophagy, and lipid homeostasis [21, 23,24]. Poor function or dysregulation of one of these processes induces ER stress and can lead to neuronal cell death and, thus, neurodegeneration, such as Alzheimer's disease and PD [35]. Therefore, we tested four genes, each showing significant transcriptional alterations separately, and will discuss these candidates in more detail below.

One of the proteins involved in ER stress is KDELR. KDELR plays key roles in maintaining ER homeostasis, protein trafficking, ER stress regulation, and autophagy [39,40]. Interestingly, KDELR is upregulated upon ER stress, which is also observed in PD [35,39,41], resulting in autophagy induction [39]. Furthermore, autophagy is a process that is affected in (Pink1-related) PD [25,27,42], suggesting that KDELR upregulation can be beneficial to overcome defective autophagy upon PD. This is in line with the findings of our initial screen, in which higher expression levels improve the flying ability. However, we were not able to reproduce these findings by overexpressing KDELR. One possible explanation could lie in the limitations of the applied GAL4/UAS system. This system overexpresses a protein beyond physiological levels [43] and is temperature-sensitive [44]. In our experimental setup, we grew the flies at 25 °C, which supports an efficient activation of the GAL4/UAS system, while the increased expression levels identified are only tenfold higher. These data suggest that too much KDELR abolishes the positive effect in *pink1*-mutant flies and that there is a small therapeutic window.

Interestingly, wbl is linked to KDELR, further supporting the involvement of KDELR and its processes in the penetrance of PD symptoms. Wbl is a protein disulfide isomerase (PDI)-related chaperone [45,46] that contains a C-terminal ER retention motif KDEL [47]. This motif interacts with KDELR to retrieve these ER chaperones from the Golgi [48,49]. The human ortholog for wbl is the endoplasmic reticulum protein of 29 kDA (ERp29), which is ubiquitously expressed [49]. ERp29 binds to misfolded proteins to facilitate proper folding or target them for degradation. Similar to the KDELR, ERp29 is upregulated upon ER stress to mitigate the accumulation of misfolded proteins and reduce cellular damage. Dysregulation of ERp29 is linked to several cancers and may serve as a biomarker for the progression of the tumor [50]. Furthermore, ERp29 is elevated following a dopamine exposure-related PD model, suggesting that ER stress occurs in the early stages of PD [51]. Our data show that increased ERp29 levels benefit the Pink1-deficient flying phenotype, supporting the notion that ER stress and its associated elevated ER proteins are a compensatory mechanism in this Pink1-related PD model.

TorsinA, the human ortholog for Torsin, is an AAA ATPase localized to the ER and the nuclear envelope. TorsinA maintains proteostasis and lipid metabolism and regulates intracellular vesicle trafficking [52–54]. TorsinA is encoded by the *TOR1A* gene, a mutation that causes early-onset dystonia [55]. Furthermore, impaired protein folding and increased ER stress due to TorsinA dysfunction [56] may contribute to neurodegeneration. Previously, Torsin has been linked to PD via its presence in the Lewy bodies [57,58]. Furthermore, in *C. elegans*, increased Torsin exerts a protective effect in a 6-hydroxydopamine (6-OHDA) PD model [59], supporting the findings from our screen where higher Torsin expression is beneficial for the flying phenotype in Pink1-deficient flies. However, via the GAL4/UAS system, we were unable to confirm these results, while overexpression in *C. elegans* did lead to a rescue. Unfortunately, these data are difficult to directly compare due to the unknown expression efficiency and the difference in the human disease and phenotypes observed in animal models. Hence, while increased Torsin levels have the potential to be protective, further investigations are required to determine the exact effect of Torsin, its relationship to the ER function, and its effect on PD.

Zda is an immunophilin localized at the ER. Zda is required for starvation-induced autophagy and interacts with the autophagy genes Atg1, Atg6, and Vps34 (vacuolar sorting protein) to activate the autophagy-specific activation of Vps34 and thus the initial stages of autophagy [60]. The human ortholog of Zda is FKBP8, an anti-apoptotic protein that assists in protein folding and the stabilization of proteins. FKBP8 is implicated in cardiovascular diseases, and studies in mammals suggest developmental abnormalities [61,62]. Furthermore, FKBP8 contains a microtubule-associated protein 1 light chain 3 (LC3)-interacting region (LIR) motif. It recruits LC3 to the mitochondria to induce Parkin-independent mitophagy while escaping degradation [63]. Autophagy or mitochondrial-specific mitophagy are processes that are affected in PD. Namely, PINK1 functions in mitophagy [25,27,32,64], suggesting that the beneficial effect of Zda lies in its mitophagy function. Previous studies showed that lowering mitophagy activity is beneficial for PINK1-dependent PD [27,42]. Thus, decreased Zda expression provokes lower mitophagy levels in an attempt to improve the *pink1*-mutant flying phenotype. In addition, under stress conditions, FKBP8 equally plays a role in mitochondrial fragmentation. Via its LIR-motif-like sequence (LIRL), FKBP8 binds to OPA1, mediating fragmentation and enabling mitophagy [65]. Reversely, the knockdown of FKBP8 enlarges the mitochondria to form its natural tubular network. Interestingly, the loss of Pink1 induces mitochondrial accumulation and loss of the tubular network [8,31]. Thus, decreased Zda levels could induce a more tubular mitochondrial network, allowing the mitochondria to function more efficiently. Therefore, the beneficial role of reducing Zda levels may extend to a dual role in inhibiting mitophagy and mitochondrial dynamics.

This study is the first to identify possible cellular mechanisms involved in the penetrance of the flying ability in a PD model. The fly model proved to be of excellent value for investigating and identifying biological processes involved in reduced penetrance. Nonetheless, we were not able to validate all the selected candidates, possibly due to the limitations of the applied genetic tools. Lowering the incubation temperature ensures a less efficient UAS-Gal4 system and, hence, lowers the UAS lines' overexpression. However, as the alterations in RNA expression are rather minor, the reduced overexpression would still be too high to mimic the results of RNA expression. Alternatively, a genomic construct could be created to overcome this.

Furthermore, with this setup, we could not validate if these biological processes equally affect other phenotypes in *pink1*-mutant flies, nor did we test their relevance to patients. For this validation in a clinical context, our data should first be tested in a higher species model, such as patient-derived dopaminergic neurons. In these cells, the effect of manipulation of the ER to influence ER stress can be assessed for its evolutionary conservation and to test if reducing ER stress is a valid therapeutic target to affect the penetrance of PD in as yet unaffected pathogenic variant carriers. In conclusion, our data further point to the ER implicated in PD and its penetrance in a genetic PD fly model that needs further validation in a patient-relevant context. In addition, further investigation into the exact underlying mechanism is necessary so that this pathway can be modulated to alter the penetrance for PD.

4. Materials and Methods

4.1. Fly Genetics

w pink1^{B9} null mutants and controls (*w pink1*^{RV}) were kindly provided by Jeehye Park and Jongkyeong Chung (Korea Advanced Institute of Science and Technology) [30]. y[1] w[*]; M{RFP[3xP3.PB] w[+mC]=UAS-KDELR-RFP}ZH-22A (UASKdelR) were generously shared by the Katanaev laboratory (Department of Pharmacology and Toxicology, University of Lausanne) [66]. Two independent lines of Zda (w1118; PBac{IT.GAL4}zda0818-G4

(Zda^1) and y1 w67c23; P{EPgy2}zdaEY08359 (Zda^2)) and *daughterless Gal4* (DaGal4) were purchased from the Bloomington Stock Center (Indianapolis, United States of America). M[UAS-Torsin.ORF.3xHA.GW]ZH-86Fb (UASTorsin) and M[UAS-Wbl.ORF.3xHA.GW] (UASWbl) were purchased from the FlyORF stock center (Zurich, Switzerland).

4.2. Flight Assay

One-day-old male flies were collected and tested for their flying ability. Flies were placed in an empty vial that was gently tapped. Flies able or unable to fly were scored one and zero, respectively [8]. For the sequencing analyses, the offspring of each parent pair that was able to fly (group 4) was separately collected from those that were not able to fly (group 3).

4.3. RNA Sequencing and Analyses

RNA sequencing was performed on four different groups. Group 1 is control flies (*pink1*^{RV}), group 2 is *pink1*^{B9}-mutant flies of which none of the offspring were able to fly, and groups 3 and 4 are *pink1*^{B9}-mutant flies that are offspring from the same parent; however, in group 3, none of the flies were able to fly, while in group 4, all the flies were able to fly. RNA was isolated from five flies via a standard procedure (Qiagen, Venlo, The Netherlands), and RNA sequencing was performed by the genomics core UZ Leuven (Belgium) using an Illumina Hiseq system.

The fastq files underwent preprocessing using fastp (version 0.23.4) [67], wherein reads with less than 30% of bases possessing a quality PHRED score under 15 were selectively retained. Subsequently, reads were pseudoaligned to the *Drosophila melanogaster* genome assembly BDGP6.46 through kallisto (version 0.44.0). The alignment metrics are detailed in Table S1.

Differential expression and pathway analyses were executed in R (version 4.2.2), primarily employing sleuth (version 0.30.1) [68] or limma (version 3.54.2) [69]. Sleuth was utilized for straightforward group comparisons, while limma and its extension of ANOVA tests were applied for more intricate model computations. Gene annotation was derived from the genome-wide annotation for *Drosophila melanogaster* package org.Dm.eg.db (version 3.16.0), encompassing entries for HGNC and flybase nomenclature, GO terms, and Homo sapiens gene homology.

Expression data analysis with limma was performed on kallisto's abundance levels, which were transformed into length-scaled count values using tximport (version 1.26.1) [70]. Pathway analysis was conducted using GAGE (version 2.48.0) [71], incorporating either the $\log_2$ fold changes from differential expression or sleuth's beta values. We corrected differential gene expression and pathway significance for multiple testing using the BH correction. The cutoff for the adjusted *p*-value was set to 0.05 in all our analyses.

To investigate penetrance, we combined the sample groups into flying, mutated, and non-flying and looked for co-regulation between the two flying groups when compared to the mutated non-flying group with multiple comparison testing. Specifically, the Flying group consisted of samples from the controls (group 1) and the offspring with flying ability (group 4). The MutatedFlying group only encapsulated the flying offspring (group 4), while the Mutated group combined the samples from offspring that were unable to fly (group 2 and 3). Using this design, we calculated the DEGs between Flying versus Mutated and MutatedFlying versus Mutated and subsequently called the limma equivalent of an ANOVA and these multiple comparisons.

Supplementary Materials: The supporting information can be downloaded at: https://www.mdpi.com/article/10.3390/ijms26030979/s1.

Author Contributions: Conceptualization: M.V., H.B., and C.K.; methodology: M.V., F.O., H.G., G.C., and S.M.; software: F.O. and H.B.; validation: M.V., H.B., and C.K.; formal analysis: M.V. and F.O.; data curation: H.B.; writing—original draft preparation: M.V. and F.O.; writing—review and editing: H.G., G.C., S.M., H.B., and C.K.; visualization: M.V. and F.O.; supervision: M.V., H.B., and C.K.; project administration: M.V. All authors have read and agreed to the published version of the manuscript.

Funding: F.O. and H.B. acknowledge funding through the German Reseearch Foundation (BU 2487/6-2) and Germany's Excellence Strategy (EXC 2167-390884018).

Institutional Review Board Statement: Not Applicable.

Informed Consent Statement: Not applicable.

Data Availability Statement: The data has been uploaded to Gene Expression Omnibus (GEO) and is available under the accession ID GSE287758.

Conflicts of Interest: CK has served as a consultant for Centogene, Retromer Therapeutics, and Lundbeck and received speakers' honoraria from Desitin and Bial and research funding from DFG, MJFF, and ASAP.

References

1. Bloem, B.R.; Okun, M.S.; Klein, C. Parkinson's disease. *Lancet* **2021**, *397*, 2284–2303. [CrossRef]
2. Höglinger, G.U.; Adler, C.H.; Berg, D.; Klein, C.; Outeiro, T.F.; Poewe, W.; Postuma, R.; Stoessl, A.J.; Lang, A.E. A biological classification of Parkinson's disease: The SynNeurGe research diagnostic criteria. *Lancet Neurol.* **2024**, *23*, 191–204. [CrossRef]
3. Morais, V.A.; Vos, M. Reduced penetrance of Parkinson's disease models. *Med. Genet.* **2022**, *34*, 117–124. [CrossRef]
4. Healy, D.G.; Falchi, M.; O'Sullivan, S.S.; Bonifati, V.; Durr, A.; Bressman, S.; Brice, A.; Aasly, J.; Zabetian, C.P.; Goldwurm, S.; et al. Phenotype, genotype, and worldwide genetic penetrance of LRRK2-associated Parkinson's disease: A case-control study. *Lancet Neurol.* **2008**, *7*, 583–590. [CrossRef]
5. Luciano, M.S.; Tanner, C.M.; Meng, C.; Marras, C.; Goldman, S.M.; Lang, A.E.; Tolosa, E.; Schüle, B.; Langston, J.W.; Brice, A.; et al. Nonsteroidal Anti-inflammatory Use and LRRK2 Parkinson's Disease Penetrance. *Mov. Disord.* **2020**, *35*, 1755–1764. [CrossRef]
6. Lee, A.J.; Wang, Y.; Alcalay, R.N.; Mejia-Santana, H.; Saunders-Pullman, R.; Bressman, S.; Corvol, J.C.; Brice, A.; Lesage, S.; Mangone, G.; et al. Penetrance estimate of LRRK2 p.G2019S mutation in individuals of non-Ashkenazi Jewish ancestry. *Mov. Disord.* **2017**, *32*, 1432–1438. [CrossRef]
7. Chittoor-Vinod, V.G.; Nichols, R.J.; Schüle, B. Genetic and Environmental Factors Influence the Pleomorphy of LRRK2 Parkinsonism. *Int. J. Mol. Sci.* **2021**, *22*, 1045. [CrossRef]
8. Vos, M.; Esposito, G.; Edirisinghe, J.N.; Vilain, S.; Haddad, D.M.; Slabbaert, J.R.; Van Meensel, S.; Schaap, O.; De Strooper, B.; Meganathan, R.; et al. Vitamin K2 is a mitochondrial electron carrier that rescues pink1 deficiency. *Science* **2012**, *336*, 1306–1310. [CrossRef]
9. Kasten, M.; Hartmann, C.; Hampf, J.; Schaake, S.; Westenberger, A.; Vollstedt, E.J.; Balck, A.; Domingo, A.; Vulinovic, F.; Dulovic, M.; et al. Genotype-Phenotype Relations for the Parkinson's Disease Genes Parkin, PINK1, DJ1: MDSGene Systematic Review. *Mov. Disord.* **2018**, *33*, 730–741. [CrossRef]
10. Gabbert, C.; König, I.R.; Lüth, T.; Kolms, B.; Kasten, M.; Vollstedt, E.J.; Balck, A.; Grünewald, A.; Klein, C.; Trinh, J. Coffee, smoking and aspirin are associated with age at onset in idiopathic Parkinson's disease. *J. Neurol.* **2022**, *269*, 4195–4203. [CrossRef]
11. Lüth, T.; König, I.R.; Grünewald, A.; Kasten, M.; Klein, C.; Hentati, F.; Farrer, M.; Trinh, J. Age at Onset of LRRK2 p.Gly2019Ser Is Related to Environmental and Lifestyle Factors. *Mov. Disord.* **2020**, *35*, 1854–1858. [CrossRef]
12. Zhen, K.; Zhang, S.; Tao, X.; Li, G.; Lv, Y.; Yu, L. A systematic review and meta-analysis on effects of aerobic exercise in people with Parkinson's disease. *Npj Park. Dis.* **2022**, *8*, 146. [CrossRef]
13. Chromiec, P.A.; Urbaś, Z.K.; Jacko, M.; Kaczor, J.J. The Proper Diet and Regular Physical Activity Slow Down the Development of Parkinson Disease. *Aging Dis.* **2021**, *12*, 1605. [CrossRef]
14. Menozzi, E.; Macnaughtan, J.; Schapira, A.H.V. The gut-brain axis and Parkinson disease: Clinical and pathogenetic relevance. *Ann. Med.* **2021**, *53*, 611. [CrossRef]
15. Pereira, P.A.B.; Trivedi, D.K.; Silverman, J.; Duru, I.C.; Paulin, L.; Auvinen, P.; Scheperjans, F. Multiomics implicate gut microbiota in altered lipid and energy metabolism in Parkinson's disease. *Npj Park. Dis.* **2022**, *8*, 39. [CrossRef]
16. Matheoud, D.; Cannon, T.; Voisin, A.; Penttinen, A.M.; Ramet, L.; Fahmy, A.M.; Ducrot, C.; Laplante, A.; Bourque, M.J.; Zhu, L.; et al. Intestinal infection triggers Parkinson's disease-like symptoms in *Pink1*$^{-/-}$ mice. *Nature* **2019**, *571*, 565–569. [CrossRef]

17. Barazzuol, L.; Giamogante, F.; Brini, M.; Calì, T. PINK1/Parkin Mediated Mitophagy, Ca^{2+} Signalling, and ER–Mitochondria Contacts in Parkinson's Disease. *Int. J. Mol. Sci.* **2020**, *21*, 1772. [CrossRef]
18. Chidambaram, R.; Kumar, K.; Parashar, S.; Ramachandran, G.; Chen, S.; Ferro-Novick, S. PINK1 controls RTN3L-mediated ER autophagy by regulating peripheral tubule junctions. *J. Cell Biol.* **2024**, *223*, e202407193. [CrossRef]
19. Gelmetti, V.; De Rosa, P.; Torosantucci, L.; Marini, E.S.; Romagnoli, A.; Di Rienzo, M.; Arena, G.; Vignone, D.; Fimia, G.M.; Valente, E.M. PINK1 and BECN1 relocalize at mitochondria-associated membranes during mitophagy and promote ER-mitochondria tethering and autophagosome formation. *Autophagy* **2017**, *13*, 654–669. [CrossRef]
20. Vance, J.E. MAM (mitochondria-associated membranes) in mammalian cells: Lipids and beyond. *Biochim. Biophys. Acta (BBA)-Mol. Cell Biol. Lipids* **2014**, *1841*, 595–609. [CrossRef]
21. Geisler, S.; Holmström, K.M.; Skujat, D.; Fiesel, F.C.; Rothfuss, O.C.; Kahle, P.J.; Springer, W. PINK1/Parkin-mediated mitophagy is dependent on VDAC1 and p62/SQSTM1. *Nat. Cell Biol.* **2010**, *12*, 119–131. [CrossRef]
22. Narendra, D.P.; Youle, R.J. Targeting mitochondrial dysfunction: Role for PINK1 and Parkin in mitochondrial quality control. *Antioxid. Redox Signal.* **2011**, *14*, 1929–1938. [CrossRef]
23. Colla, E.; Coune, P.; Liu, Y.; Pletnikova, O.; Troncoso, J.C.; Iwatsubo, T.; Schneider, B.L.; Lee, M.K. Endoplasmic reticulum stress is important for the manifestations of α-synucleinopathy in vivo. *J. Neurosci.* **2012**, *32*, 3306–3320. [CrossRef] [PubMed]
24. Wang, D.; Qu, S.; Zhang, Z.; Tan, L.; Chen, X.; Zhong, H.J.; Chong, C.M. Strategies targeting endoplasmic reticulum stress to improve Parkinson's disease. *Front. Pharmacol.* **2023**, *14*, 1288894. [CrossRef]
25. Vos, M.; Klein, C.; Hicks, A.A. Role of Ceramides and Sphingolipids in Parkinson's Disease. *J. Mol. Biol.* **2023**, *435*, 168000. [CrossRef]
26. Mandik, F.; Vos, M. Neurodegenerative Disorders: Spotlight on Sphingolipids. *Int. J. Mol. Sci.* **2021**, *22*, 11998. [CrossRef]
27. Vos, M.; Dulovic-Mahlow, M.; Mandik, F.; Frese, L.; Kanana, Y.; Diaw, S.H.; Depperschmidt, J.; Böhm, C.; Rohr, J.; Lohnau, T.; et al. Ceramide accumulation induces mitophagy and impairs β-oxidation in PINK1 deficiency. *Proc. Natl. Acad. Sci. USA* **2021**, *118*, e2025347118. [CrossRef]
28. Dulovic-Mahlow, M.; König, I.R.; Trinh, J.; Diaw, S.H.; Urban, P.P.; Knappe, E.; Kuhnke, N.; Ingwersen, L.C.; Hinrichs, F.; Weber, J.; et al. Discordant Monozygotic Parkinson Disease Twins: Role of Mitochondrial Integrity. *Ann. Neurol.* **2021**, *89*, 158–164. [CrossRef]
29. Vos, M.; Klein, C. The Importance of Drosophila melanogaster Research to UnCover Cellular Pathways Underlying Parkinson's Disease. *Cells* **2021**, *10*, 579. [CrossRef]
30. Park, J.; Lee, S.B.; Lee, S.; Kim, Y.; Song, S.; Kim, S.; Bae, E.; Kim, J.; Shong, M.; Kim, J.-M.; et al. Mitochondrial dysfunction in Drosophila PINK1 mutants is complemented by parkin. *Nature* **2006**, *441*, 1157–1161. [CrossRef]
31. Clark, I.E.; Dodson, M.W.; Jiang, C.; Cao, J.H.; Huh, J.R.; Seol, J.H.; Yoo, S.J.; Hay, B.A.; Guo, M. Drosophila pink1 is required for mitochondrial function and interacts genetically with parkin. *Nature* **2006**, *441*, 1162–1166. [CrossRef]
32. Narendra, D.; Tanaka, A.; Suen, D.F.; Youle, R.J. Parkin-induced mitophagy in the pathogenesis of Parkinson disease. *Autophagy* **2009**, *5*, 706–708. [CrossRef]
33. Narendra, D.P.; Jin, S.M.; Tanaka, A.; Suen, D.F.; Gautier, C.A.; Shen, J.; Cookson, M.R.; Youle, R.J. PINK1 is selectively stabilized on impaired mitochondria to activate Parkin. *PLoS Biol.* **2010**, *8*, e1000298. [CrossRef] [PubMed]
34. Vos, M.; Geens, A.; Böhm, C.; Deaulmerie, L.; Swerts, J.; Rossi, M.; Craessaerts, K.; Leites, E.P.; Seibler, P.; Rakovic, A.; et al. Cardiolipin promotes electron transport between ubiquinone and complex I to rescue PINK1 deficiency. *J. Cell Biol.* **2017**, *216*, 695–708. [CrossRef]
35. Lindholm, D.; Wootz, H.; Korhonen, L. ER stress and neurodegenerative diseases. *Cell Death Differ.* **2006**, *13*, 385–392. [CrossRef]
36. Kang, H.; Shin, J.H. Repression of rRNA transcription by PARIS contributes to Parkinson's disease. *Neurobiol. Dis.* **2015**, *73*, 220–228. [CrossRef]
37. Gonçalves, A.M.; Pereira-Santos, A.R.; Esteves, A.R.; Cardoso, S.M.; Empadinhas, N. The Mitochondrial Ribosome: A World of Opportunities for Mitochondrial Dysfunction Toward Parkinson's Disease. *Antioxid. Redox Signal.* **2021**, *34*, 694–711. [CrossRef]
38. Bhardwaj, K.; Roy, A.; Guha, L.; Kumar, H. Evaluating the Role of Lin-11, Isl-1, and Mec-3 Kinases in Dopaminergic Neurodegeneration in a Subacute 1-Methyl-4-phenyl-1,2,3,6-tetrahydropyridine Model of Parkinson's Disease. *ACS Pharmacol. Transl. Sci.* **2024**, *7*, 3879–3888. [CrossRef]
39. Wang, P.; Li, B.; Zhou, L.; Fei, E.; Wang, G. The KDEL receptor induces autophagy to promote the clearance of neurodegenerative disease-related proteins. *Neuroscience* **2011**, *190*, 43–55. [CrossRef]
40. Yamamoto, K.; Hamada, H.; Shinkai, H.; Kohno, Y.; Koseki, H.; Aoe, T. The KDEL receptor modulates the endoplasmic reticulum stress response through mitogen-activated protein kinase signaling cascades. *J. Biol. Chem.* **2003**, *278*, 34525–34532. [CrossRef]
41. Wires, E.S.; Trychta, K.A.; Kennedy, L.M.; Harvey, B.K. The Function of KDEL Receptors as UPR Genes in Disease. *Int. J. Mol. Sci.* **2021**, *22*, 5436. [CrossRef]
42. Vos, M.; Klein, C. Ceramide-induced mitophagy impairs ß-oxidation-linked energy production in PINK1 deficiency. *Autophagy* **2022**, *18*, 703–704. [CrossRef]

43. Her, Y.; Pascual, D.M.; Goldstone-Joubert, Z.; Marcogliese, P.C. Variant functional assessment in Drosophila by overexpression: What can we learn? *Genome* **2024**, *67*, 158–167. [CrossRef]
44. Nagarkar-Jaiswal, S.; Lee, P.T.; Campbell, M.E.; Chen, K.; Anguiano-Zarate, S.; Gutierrez, M.C.; Busby, T.; Lin, W.W.; He, Y.; Schulze, K.L.; et al. A library of MiMICs allows tagging of genes and reversible, spatial and temporal knockdown of proteins in Drosophila. *eLife* **2015**, *4*, e05338. [CrossRef] [PubMed]
45. Sen, J.; Goltz, J.S.; Konsolaki, M.; Schüpbach, T.; Stein, D. Windbeutel is required for function and correct subcellular localization of the Drosophila patterning protein Pipe. *Development* **2000**, *127*, 5541–5550. [CrossRef]
46. Konsolaki, M.; Schüpbach, T. *windbeutel*, a gene required for dorsoventral patterning in Drosophila, encodes a protein that has homologies to vertebrate proteins of the endoplasmic reticulum. *Genes Dev.* **1998**, *12*, 120–131. [CrossRef]
47. Pelham, H.R.B. The retention signal for soluble proteins of the endoplasmic reticulum. *Trends Biochem. Sci.* **1990**, *15*, 483–486. [CrossRef]
48. Yamamoto, K.; Fujii, R.; Toyofuku, Y.; Saito, T.; Koseki, H.; Hsu, V.W.; Aoe, T. The KDEL receptor mediates a retrieval mechanism that contributes to quality control at the endoplasmic reticulum. *EMBO J.* **2001**, *20*, 3082–3091. [CrossRef]
49. Brecker, M.; Khakhina, S.; Schubert, T.J.; Thompson, Z.; Rubenstein, R.C. The Probable, Possible, and Novel Functions of ERp29. *Front. Physiol.* **2020**, *11*, 574339. [CrossRef]
50. Zhang, D.; Richardson, D.R. Endoplasmic reticulum protein 29 (ERp29): An emerging role in cancer. *Int. J. Biochem. Cell Biol.* **2011**, *43*, 33–36. [CrossRef]
51. Dukes, A.A.; Van Laar, V.S.; Cascio, M.; Hastings, T.G. Changes in endoplasmic reticulum stress proteins and aldolase A in cells exposed to dopamine. *J. Neurochem.* **2008**, *106*, 333–346. [CrossRef]
52. Granata, A.; Watson, R.; Collinson, L.M.; Schiavo, G.; Warner, T.T. The Dystonia-associated Protein TorsinA Modulates Synaptic Vesicle Recycling. *J. Biol. Chem.* **2008**, *283*, 7568–7579. [CrossRef]
53. Kakazu, Y.; Koh, J.Y.; Ho, K.W.D.; Gonzalez-Alegre, P.; Harata, N.C. Synaptic vesicle recycling is enhanced by torsinA that harbors the DYT1 dystonia mutation. *Synapse* **2012**, *66*, 453–464. [CrossRef]
54. Grillet, M.; Gonzalez, B.D.; Sicart, A.; Pöttler, M.; Cascalho, A.; Billion, K.; Diaz, S.H.; Swerts, J.; Naismith, T.V.; Gounko, N.V.; et al. Torsins Are Essential Regulators of Cellular Lipid Metabolism. *Dev. Cell* **2016**, *38*, 235–247. [CrossRef]
55. Slominsky, P.A.; Markova, E.D.; Shadrina, M.I.; Illarioshkin, S.N.; Miklina, N.I.; Limborska, S.A.; Ivanova-Smolenskaya, I.A. A common 3-bp deletion in the DYT1 gene in Russian families with early-onset torsion dystonia. *Hum. Mutat.* **1999**, *3*, 269. [CrossRef]
56. Beauvais, G.; Rodriguez-Losada, N.; Ying, L.; Zakirova, Z.; Watson, J.L.; Readhead, B.; Gadue, P.; French, D.L.; Ehrlich, M.E.; Gonzalez-Alegre, P. Exploring the Interaction Between eIF2α Dysregulation, Acute Endoplasmic Reticulum Stress and DYT1 Dystonia in the Mammalian Brain. *Neuroscience* **2018**, *371*, 455–468. [CrossRef] [PubMed]
57. Shashidharan, P.; Good, P.F.; Hsu, A.; Perl, D.P.; Brin, M.F.; Olanow, C.W. TorsinA accumulation in Lewy bodies in sporadic Parkinson's disease. *Brain Res.* **2000**, *877*, 379–381. [CrossRef]
58. Sharma, N.; Hewett, J.; Ozelius, L.J.; Ramesh, V.; McLean, P.J.; Breakefield, X.O.; Hyman, B.T. A close association of torsinA and alpha-synuclein in Lewy bodies: A fluorescence resonance energy transfer study. *Am. J. Pathol.* **2001**, *159*, 339–344. [CrossRef]
59. Cao, S.; Gelwix, C.C.; Caldwell, K.A.; Caldwell, G.A. Torsin-Mediated Protection from Cellular Stress in the Dopaminergic Neurons of *Caenorhabditis elegans*. *J. Neurosci.* **2005**, *25*, 3801–3812. [CrossRef]
60. Melani, M.; Valko, A.; Romero, N.M.; Aguilera, M.O.; Acevedo, J.M.; Bhujabal, Z.; Perez-Perri, J.; De La Riva-Carrasco, R.V.; Katz, M.J.; Sorianello, E.; et al. Zonda is a novel early component of the autophagy pathway in Drosophila. *Mol. Biol. Cell* **2017**, *28*, 3070. [CrossRef]
61. Misaka, T.; Murakawa, T.; Nishida, K.; Omori, Y.; Taneike, M.; Omiya, S.; Molenaar, C.; Uno, Y.; Yamaguchi, O.; Takeda, J.; et al. FKBP8 protects the heart from hemodynamic stress by preventing the accumulation of misfolded proteins and endoplasmic reticulum-associated apoptosis in mice. *J. Mol. Cell. Cardiol.* **2018**, *114*, 93–104. [CrossRef] [PubMed]
62. Bulgakov, O.V.; Eggenschwiler, J.T.; Hong, D.H.; Anderson, K.V.; Li, T. FKBP8 is a negative regulator of mouse sonic hedgehog signaling in neural tissues. *Development* **2004**, *131*, 2149–2159. [CrossRef]
63. Bhujabal, Z.; Birgisdottir, Å.B.; Sjøttem, E.; Brenne, H.B.; Øvervatn, A.; Habisov, S.; Kirkin, V.; Lamark, T.; Johansen, T. FKBP8 recruits LC3A to mediate Parkin-independent mitophagy. *EMBO Rep.* **2017**, *18*, 947–961. [CrossRef]
64. Narendra, D.; Tanaka, A.; Suen, D.-F.; Youle, R.J. Parkin is recruited selectively to impaired mitochondria and promotes their autophagy. *J. Cell Biol.* **2008**, *183*, 795–803. [CrossRef]
65. Yoo, S.M.; Yamashita, S.I.; Kim, H.; Na, D.H.; Lee, H.; Kim, S.J.; Cho, D.H.; Kanki, T.; Jung, Y.K. FKBP8 LIRL-dependent mitochondrial fragmentation facilitates mitophagy under stress conditions. *FASEB J.* **2020**, *34*, 2944–2957. [CrossRef] [PubMed]
66. Solis, G.P.; Bilousov, O.; Koval, A.; Lüchtenborg, A.M.; Lin, C.; Katanaev, V.L. Golgi-Resident Gαo Promotes Protrusive Membrane Dynamics. *Cell* **2017**, *170*, 939–955.e24. [CrossRef]
67. Chen, S.; Zhou, Y.; Chen, Y.; Gu, J. fastp: An ultra-fast all-in-one FASTQ preprocessor. *Bioinformatics* **2018**, *34*, i884–i890. [CrossRef]

68. Pimentel, H.; Bray, N.L.; Puente, S.; Melsted, P.; Pachter, L. Differential analysis of RNA-seq incorporating quantification uncertainty. *Nat. Methods* **2017**, *14*, 687–690. [CrossRef]
69. Ritchie, M.E.; Phipson, B.; Wu, D.; Hu, Y.; Law, C.W.; Shi, W.; Smyth, G.K. *limma* powers differential expression analyses for RNA-sequencing and microarray studies. *Nucleic Acids Res.* **2015**, *43*, e47. [CrossRef]
70. Soneson, C.; Love, M.I.; Robinson, M.D. Differential analyses for RNA-seq: Transcript-level estimates improve gene-level inferences. *F1000Research* **2016**, *4*, 1521. [CrossRef]
71. Luo, W.; Friedman, M.S.; Shedden, K.; Hankenson, K.D.; Woolf, P.J. GAGE: Generally applicable gene set enrichment for pathway analysis. *BMC Bioinform.* **2009**, *10*, 161. [CrossRef]

Disclaimer/Publisher's Note: The statements, opinions and data contained in all publications are solely those of the individual author(s) and contributor(s) and not of MDPI and/or the editor(s). MDPI and/or the editor(s) disclaim responsibility for any injury to people or property resulting from any ideas, methods, instructions or products referred to in the content.

International Journal of
Molecular Sciences

MDPI

Article

Steady Moderate Exercise Confers Resilience Against Neurodegeneration and Neuroinflammation in a Mouse Model of Parkinson's Disease

Ewelina Palasz [1,†], Anna Gasiorowska-Bien [2,†], Patrycja Drapich [2], Wiktor Niewiadomski [2] and Grazyna Niewiadomska [2,3,*]

[1] Department of Cellular Signalling, Mossakowski Medical Research Institute, Polish Academy of Sciences, 02-106 Warsaw, Poland; epalasz@imdik.pan.pl
[2] Clinical and Research Department of Applied Physiology, Mossakowski Medical Research Institute, Polish Academy of Sciences, 02-106 Warsaw, Poland; agasiorowska@imdik.pan.pl (A.G.-B.); pdrapich@imdik.pan.pl (P.D.); wniewiadomski@imdik.pan.pl (W.N.)
[3] Nencki Institute of Experimental Biology, Polish Academy of Sciences, 02-093 Warsaw, Poland
* Correspondence: g.niewiadomska@nencki.edu.pl; Tel.: +48-22-608-6612
† These authors contributed equally to this work.

Abstract: Intensive aerobic exercise slows the progression of movement disorders in Parkinson's disease (PD) and is therefore recommended as an important component of treatment for PD patients. Studies in animal models of PD have shown that vigorous exercise has neuroprotective effects, and emerging evidence suggests that it may be a disease-modifying treatment in humans. However, many people with PD may not be able to participate in vigorous exercise because of multiple medical conditions that severely limit their physical activity. In this study, we have shown that chronic MPTP treatment in sedentary mice resulted in loss of dopaminergic neurons in the SNpc, decreased levels of neurotrophins, BDNF and GDNF, and increased levels of inflammatory markers and pro-inflammatory changes in immunocompetent cells. Moderate exercise, initiated both before and after chronic MPTP treatment, significantly attenuated the loss of dopaminergic neurons and increased BDNF and GDNF levels even above those in sedentary control mice. No signs of inflammation were observed in MPTP-treated mice, either when training began before or after MPTP treatment. Training induced beneficial changes in the dopaminergic system, increased levels of neurotrophins and suppression of inflammation were similar for both steady moderate (present data) and intense training (our previously published data). This suggests that there is a kind of saturation when the percentage of rescued dopaminergic neurons reaches the highest possible value, and therefore further increases in exercise intensity do not enhance neuroprotection. In conclusion, our present results compared with the previous data show that increasing exercise intensity beyond the level used in this study does not increase the neuroprotective effect of aerobic training in a mouse model of Parkinson's disease.

Keywords: Parkinson's disease; exercise intensity; MPTP animal model; inflammation; neuroprotection; neurotrophins; PD therapy

1. Introduction

Parkinson's disease (PD) is a degenerative disorder of the central nervous system whose primary symptom is movement disorders resulting from the degeneration of dopaminergic neurons in the nigrostriatal pathway. The etiology of the disease is not

fully understood due to the complex underlying mechanisms. Existing therapies only alleviate the symptoms of the disease and become less effective as the disease progresses [1]. Therefore, it is extremely important to search for new therapies to support drug treatment. Increasing attention is being paid to the effects of exercise on improving or maintaining normal brain function. Studies in healthy elderly populations without central nervous system disorders have shown that regular aerobic activity induces changes related to neuroplasticity, including synaptogenesis, increased glucose consumption, angiogenesis, and neurogenesis. Exercise improves brain function by inhibiting inflammation, reducing oxidative stress, stabilizing calcium homeostasis, and stimulating the release of endogenous neurotrophins [2]. The importance of training and exercise is currently being studied extensively in animal models of PD. Many of these studies suggest that exercise may have a neuroprotective effect, slowing or even stopping neurodegenerative processes and restoring disrupted signaling pathways [3]. Based on the findings in humans and animal models of PD, physical activity has been found to improve motor behavior patterns and enhance angiogenesis, synaptogenesis, and neurogenesis in the brain. It also increases levels of neurotrophic factors and reduces the severity of inflammatory processes [4].

Physical activity has been shown to have beneficial effects on both motor and non-motor symptoms in PD. The mechanisms involved in these effects are neuroendocrine and neurotransmitter regulation, enhancement of neuronal insulin signaling, upregulation of neurotrophins and the myokine irisin, attenuation of inflammatory and oxidative responses, enhancement of pro-survival and anti-apoptosis effects, and optimization of the autophagy process. Exercise has also been shown to have beneficial effects on a number of intracellular signaling pathways involving Ca^{2+}, cyclic AMP-responsive element-binding protein (CREB), nuclear factor kappa B (NF-κB) and peroxisome proliferator-activated receptor gamma coactivator 1-alpha (PGC-1α), protein chaperones, neurotrophic factors, DNA repair proteins, mitochondrial biogenesis (for a review of this, see [5,6]). Therefore, the question of whether exercise, particularly vigorous exercise, can be used as a disease-modifying therapy in people with PD remains central to clinical management. Uhrbrand et al. [7] and Gamborg et al. [8] reviewed randomized controlled trials assessing the functional effects of different types of vigorous exercise in PD patients. All types of exercise were found to be safe and feasible, did not worsen PD symptoms, and were recognized as beneficial adjunctive rehabilitation strategies for this disease. Schenkman et al. [9] compared the functional effects of intensive treadmill exercise to those of moderate-intensity treadmill exercise and found that only the former significantly slowed the time-dependent decline in motor function observed in PD. Based on data from a number of studies, Alberts and Rosenfeldt [10] published an article recommending the inclusion of vigorous regular aerobic exercise in the treatment of patients with PD. However, Parkinson's disease may discourage or even prevent participation in intensive training due to muscle weakness, which is a primary symptom in PD [11], sympathetic denervation of the heart, which reduces cardiac contractility [12], debilitating and persistent fatigue, apathy, which is often reported in PD, and increased fatigability, which may be caused by reduced cardiorespiratory fitness [13]. In light of the above, it is important to consider the following questions: What is the role of exercise intensity in the mechanism that modifies the effect of exercise on the course of PD?

It is clear that one of the most useful, if imperfect, ways of investigating these questions at present is in animal models of PD. A considerable number of studies have shown that exercise has neuroprotective effects on dopaminergic neurons in rodent models of PD [14], and the results have been summarized in several reviews [15,16]. However, the effects of the type of exercise and its dose, in terms of either intensity or volume, have not been systematically investigated. An example of such a study is the work of Gerecke et al. [17],

who investigated the neuroprotection against 1-Methyl-4-phenyl-1,2,3,6-tetrahydropyridine (MPTP) intoxication provided by exercise performed prior to neurotoxin administration. The authors found that there is a certain distance of daily running in mice on a running wheel that completely prevents neuronal loss. However, 2/3 of this distance provides only partial protection, and 1/3 of the distance run has no neuroprotective effect. We are not aware of similar studies of exercise-induced neuroprotection when exercise was performed during or after MPTP application.

Our previous study [18] looked at the time of the onset of exercise (before or after intoxication) required for the induction of neuroprotection in a mouse model of PD induced by MPTP. A clear effect of exercise on neuronal survival, neuroinflammation, and the expression of a number of growth factors was observed after high-intensity training. As the role of exercise intensity as a variable that may be relevant to the disease-modifying effects of exercise in PD has been highlighted in human studies, we decided to present our results of what exercise intensity is necessary to induce neuroprotection in an environmental model of PD. The current study analyzes the neuroprotective effect of less intense exercise. To address the question of whether the neuroprotective effect of physical exercise depends on the intensity of the training, the current study was conducted using exercise of moderate intensity. The results of moderately trained mice are compared to an untreated and untrained control group and an MPTP-treated and untreated group, which are the same as those in both previous and current studies. As a result, the only difference between the previously published data and those of the present study was the intensity of the exercise. By comparing the results of this and the previous experiment, it is possible to assess the effect of changing just one variable—exercise intensity.

2. Results

2.1. Treadmill Exercise Neuroprotects the Nigrostriatal Dopaminergic System in a Chronic MPTP Mouse Model of Parkinson's Disease

MPTP is a well-known neurotoxin responsible for the extensive and relatively selective destruction of dopaminergic neurons in the nigrostriatal pathway [19,20]. To assess changes in dopaminergic projections in the nigrostriatal pathway in a mouse model of Parkinsonism, immunohistochemical staining against tyrosine hydroxylase (or tyrosine 3-monooxygenase; EC 1.14.16.2; TH) and a computer-assisted densitometric analysis of TH-ir neurons in the SNpc and the target dopaminergic projection in the striatum were performed. TH is an enzyme of the hydroxylase group, responsible for converting the amino acid L-tyrosine to dihydroxyphenylalanine (DOPA). This is an important step in the biosynthesis of dopamine in neuronal cells. This enzyme is highly substrate-specific, and TH is therefore considered a useful marker for dopaminergic neurons.

A significant decrease in staining intensity was observed in the SNpc as well as in the ST, which receives dopaminergic projections from the SNpc, after MPTP administration in untrained mice (MPTP group) (Figure 1, microphotographs on the left and right vertical panels). There was a significant reduction of 66% in the number of TH-ir neurons in the SNpc in untrained MPTP mice compared to control mice not receiving neurotoxin (group C). The application of moderate-intensity treadmill training in MPTP-treated mice resulted in a lower loss of TH-positive neurons in the SNpc. The reduction in TH-ir neurons reached 27% in the MPTP-TE group and 18% in the MPTP-TL group compared to the untrained control group (group C). It should be emphasized that this difference in the number of TH-ir neurons was not statistically significant, which may indicate a beneficial neuroprotective effect of exercise. Unexpectedly, the number of TH-ir neurons was lower (by 13%) in the trained control group (C-T) compared to the non-exercise group C, but this difference was not statistically significant. Therefore, the differences in the number of TH-ir neurons in

the MPTP-TE and MPTP-TL groups were less pronounced compared to the C-T group, by 16% and 6%, respectively. Again, these differences were not statistically significant. The analysis also showed that the time of training onset did not significantly affect the number of TH-ir cells in the SNpc in the MPTP-TE and MPTP-TL groups (Figure 1A).

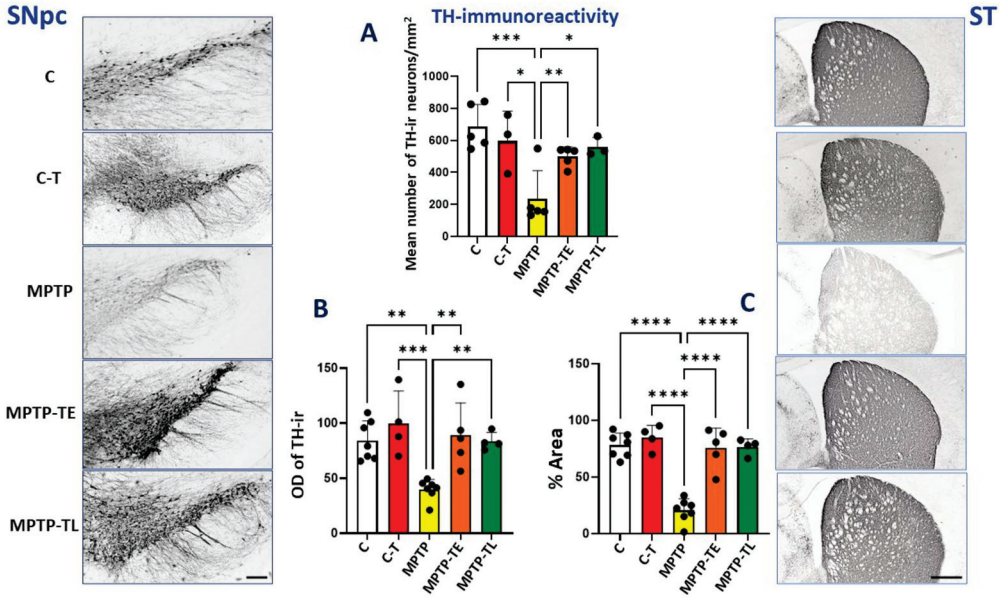


Figure 1. Tyrosine hydroxylase (TH) immunohistochemistry in the substantia nigra pars compacta (SNpc) and striatum (ST) of control mice (C, n = 5 in SNpc and n = 7 in ST), trained control mice (C-T, n = 3 in SNpc and n = 4 in ST), untrained mice with induced Parkinsonism (MPTP, n = 5 in SNpc and n = 7 in ST), mice with induced Parkinsonism that underwent early-onset training (MPTP-TE, n = 5 in SNpc and n = 5 in ST), and mice with induced Parkinsonism that underwent late-onset training (MPTP-TL, n = 3 in SNpc and n = 4 in ST). Representative images of the TH immunohistochemical staining in SNpc (SNpc left panel) and in the striatum (ST right panel). Magnification of microphotographs by 100 times for SNpc and 40 times for the striatum. (**A**) Mean number of TH-immunoreactive neurons in SNpc, (**B**) optical density (OD) of TH-immunoreactivity, and (**C**) % of immunoreactive area (%Area) in the dorsal striatum. Values are presented as the mean ± SD with scatter plots of individual data. (**A**) For TH-immunoreactive neurons in the SNpc, a one-way ANOVA confirmed a significant main effect of Group ($F(4, 16) = 7.623$; $p = 0.0012$). MPTP mice presented strongly reduced TH labeling relative to both control groups. While the mean number of the TH-ir neurons was reduced in MPTP relative to control groups, this reduction was restrained when physical exercise was administered. Both early-onset and late-onset treadmill training favorably affected the preservation of the dopaminergic phenotype of neurons in the SNpc. (**B**) For TH labeling in the striatum, statistical analysis yielded the main effect of Group for OD ($F(4, 22) = 8.225$; $p = 0.0003$) and (**C**) for %Area ($F(4, 22) = 31.93$; $p < 0.0001$). Neurotoxin administration reduced the density of dopaminergic afferents in the striatum, while exercise counteracted this reduction, regardless of when it was applied. Statistical significance between the groups was calculated using the Newman–Keuls test (* $p < 0.05$, ** $p < 0.01$, *** $p < 0.001$, and **** $p < 0.0001$). Scale bars: 100 µm for SNpc and 500 µm for ST.

In the striatum, TH expression was assessed by the OD and %Area. A significant reduction of 53% in OD and 73% in %Area was observed in the group of untrained MPTP-treated mice (MPTP) compared to untreated and untrained control mice (C). Treadmill training applied to untreated control mice (C-T) increased OD (by 18%) and %Area (by 8%) compared to untreated controls (C), but the difference was not significant. The application of training to MPTP-treated mice resulted in the preservation of TH staining intensity. Early-onset training (MPTP-TE) resulted in a 6% increase in OD and a 3% increase in %Area, while late-onset training (MPTP-TL) resulted in a 1% decrease in OD and a 2%

decrease in %Area compared to group C. These differences were not statistically significant. There were also no significant differences between the MPTP groups treated with early- or late-onset training. Thus, in the striatum, similar to the SNpc, training prevented the decrease in TH staining induced by MPTP (Figure 1B,C).

DRD2 dopamine receptors play a key role in the function of direct and indirect pathways in the striatum, which connect to peripheral output systems to influence motor behavior. The direct pathway is associated with movement activation, while the indirect pathway is associated with movement inhibition. The presence of only one type of dopamine receptor in a single brain region is rare, and one such structure is the dorsal striatum in mice, which has only DRD2 dopamine receptors [21]. Therefore, the assessment of DRD2 receptor expression levels may be a good marker for abnormalities in the projection of dopaminergic neurons in the nigrostriatal pathway.

In our study, DRD2 immunohistochemical staining in the striatum showed the strongest intensity in untrained MPTP-treated mice (MPTP group) and was significantly stronger than in all other groups (Figure 2A). In the MPTP group, DRD2 immunoreactivity was statistically significantly higher by 64% in OD and 37% in %Area compared to group C. Training alone did not significantly affect the intensity of DRD2 immunoreactivity; there were slight decreases in OD and %Area (3% and 2%, respectively) in the C-T group compared to group C. Training in MPTP mice prevented the increase in DRD2-ir staining intensity. There were no significant differences between untreated control groups (C and C-T) and trained MPTP groups (MPTP-TE and MPTP-TL). There was only a 2% increase in OD and a 2% increase in %Area in the MPTP-TE group compared to group C, and there was a 5% increase in OD and a 4% increase in %Area compared to the C-T group. Late-onset training (MPTP-TL group) resulted in a 15% increase in OD and a 13% increase in %Area compared to group C as well as a 19% increase in OD and a 14% increase in %Area compared to the C-T group (Figure 2B,C).

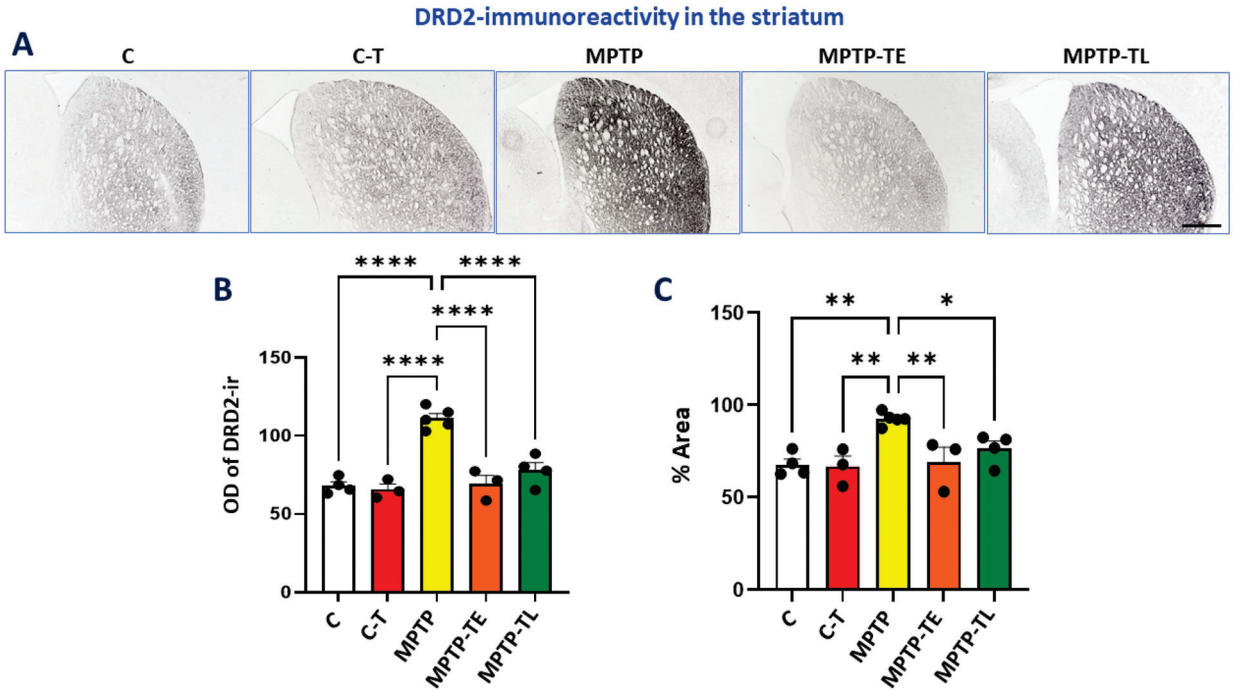


Figure 2. Dopamine receptor D2 (DRD2) immunohistochemistry in the striatum of control mice (C, n = 4), trained control mice (C-T, n = 3), untrained mice with induced Parkinsonism (MPTP, n = 5), mice with induced Parkinsonism that underwent early-onset training (MPTP-TE, n = 3), and mice with induced Parkinsonism that underwent late-onset training (MPTP-TL, n = 4). (**A**) Representative

images of the DRD2 immunohistochemical staining in the striatum. Magnification of microphotographs by 40 times. (**B**) Optical density (OD) of DRD2-immunoreactivity and (**C**) % of the immunoreactive area (%Area) in the dorsal striatum. Values are presented as the mean ± SD with scatter plots of individual data. (**B**) For DRD2 labeling in the striatum, statistical analysis yielded the main effects of Group for OD ($F(4, 14) = 28.25$; $p < 0.0001$) and (**C**) for %Area ($F(4, 14) = 7.409$; $p = 0.0020$). Neurotoxin administration increased striatal DRD2 expression in MPTP mice (relative to C and to C-T), while physical training normalized DRD2 levels, as measured by OD and %Area. Statistical significance between the groups was calculated using the Newman–Keuls test (* $p < 0.05$, ** $p < 0.01$, and **** $p < 0.0001$). Scale bar: 500 µm.

2.2. Effect of Treadmill Exercise and the Administration of MPTP on the Levels of Endogenous Neurotrophic Factors

Studies suggest the involvement of trophic factors such as BDNF and GDNF, which have a protective effect on dopaminergic neurons. It is noteworthy that physical activity may influence neuroplasticity mechanisms in PD related to neurotransmission in the dopaminergic and glutamatergic systems [22–24]. Therefore, the effects of physical training and MPTP administration on BDNF and GDNF levels were investigated by immunohistochemistry in the SNpc and striatum and by an ELISA assay in the midbrain and striatum.

Anti-BDNF staining in the SNpc showed the strongest intensity in the MPTP-trained groups, while the weakest intensity was present in the MPTP-untrained group (Figure 3, left vertical panel). The ELISA assay showed that in the midbrain, BDNF levels were 14% lower in untrained MPTP-treated mice compared to untreated mice (group C), but this difference was not significant. Exercise alone (C-T vs. group C) resulted in a 22% increase in the BDNF concentration, which was not significant. Physical training combined with MPTP administration significantly increased the upregulation of BDNF by 81% in MPTP-TE and 74% in MPTP-TL compared to the untrained control (group C) and by 49% in MPTP-TE and 43% in MPTP-TL compared to the C-T group. However, the timing of training did not matter as both early- and late-onset training resulted in similar increases in BDNF concentrations in the MPTP-TE and MPTP-TL groups (Figure 3B).

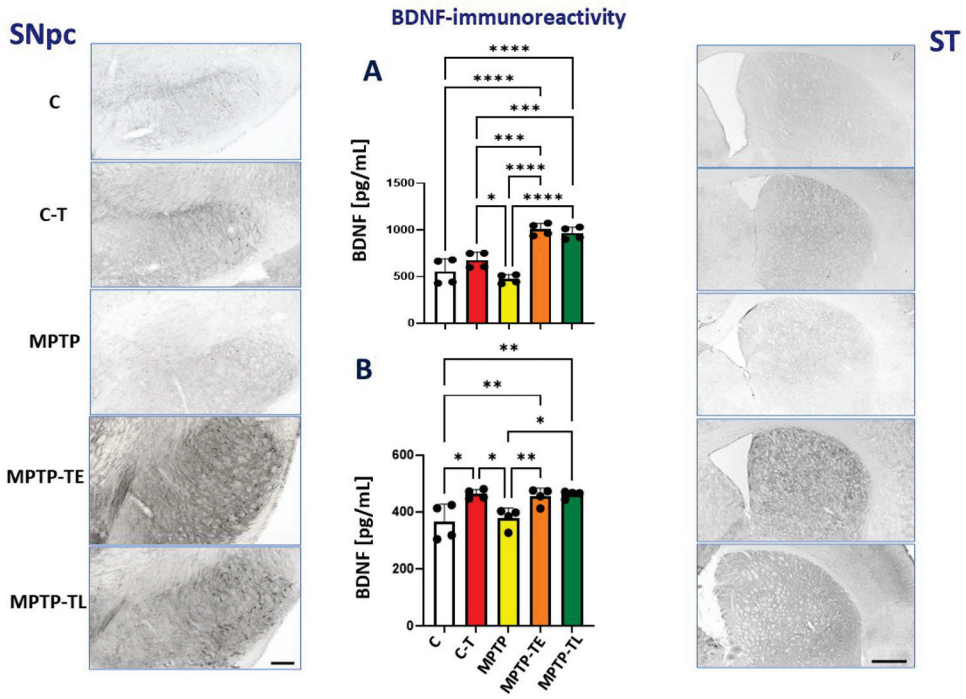


Figure 3. Brain-derived neurotrophic factor (BDNF) immunohistochemistry in the substantia nigra pars compacta (SNpc) and striatum (ST) of control mice (C, n = 4), trained control mice (C-T, n = 4),

untrained mice with induced Parkinsonism (MPTP, n = 4), mice with induced Parkinsonism that underwent early-onset training (MPTP-TE, n = 4), and mice with induced Parkinsonism that underwent late-onset training (MPTP-TL, n = 4). Representative images of the BDNF immunohistochemical staining in SNpc (SNpc left panel) and the striatum (ST right panel). Magnification of microphotographs by 100 times for SNpc and 40 times for the striatum. Quantitative analysis of the levels of BDNF by ELISA in the midbrain (**A**) and the striatum (**B**). Values are presented as the mean ± SD with scatter plots of individual data. (**A**) Quantitative analysis of the BDNF level in the midbrain with one-way ANOVA confirmed a significant main effect of Group ($F(4, 15) = 31.49$; $p < 0.0001$). Untrained MPTP mice did not show a strongly reduced BDNF level compared to the control group (group C), whereas BDNF levels were elevated when physical exercise was administered in the control (C-T) and reached even higher levels when training was combined with MPTP treatment (MPTP-TE and MPTP-TL). (**B**) Quantitative analysis of the BDNF level in the striatum with one-way ANOVA yielded the main effects of Group ($F(4, 15) = 7.357$; $p = 0.0017$). Similarly, as observed in the midbrain, untrained MPTP mice did not show a strongly reduced BDNF level compared to control group (group C), whereas BDNF levels were similarly elevated when physical exercise was administered in the control (C-T) and when training was combined with MPTP treatment (MPTP-TE and MPTP-TL). Statistical significance between the groups was calculated using the Newman–Keuls test (* $p < 0.05$, ** $p < 0.01$, *** $p < 0.001$, and **** $p < 0.0001$). Scale bars: 100 μm for SNpc and 500 μm for ST.

Similar to the SNpc, anti-BDNF staining in the striatum was strongest in the trained MPTP groups and weakest in the untrained MPTP group (Figure 3, right vertical panel). The ELISA assay showed that BDNF levels in the striatum of untrained MPTP mice (MPTM group) were similar to those observed in untreated mice (group C). When training was applied to animals not treated with neurotoxin (C-T group), the concentration of BDNF increased significantly by 27% compared to the untrained group (group C). The application of training to MPTP groups also caused a significant increase in BDNF concentration, reaching 24% and 27% in MPTP-TE and MPTP-TL, respectively, compared to untrained control mice (group C). In contrast to the midbrain, MPTP treatment did not potentiate the training-induced upregulation of BDNF levels in the striatum. BDNF levels were similar in the C-T, MPTP-TE, and MPTP-TL groups (Figure 3B).

Anti-GDNF staining in the midbrain was strongest in the MPTP-TE and MPTP-TL groups and weakest in the untrained MPTP group (Figure 4, left vertical panel). The ELISA test showed that the midbrain GDNF level was 4% lower in the untrained MPTP group compared to untreated mice (group C). This difference was not statistically significant. However, when training was applied to the control group (C-T group), the GDNF level was significantly higher than in the untrained MPTP group. MPTP treatment combined with training increased the GDNF level, which was similar to the level in the C-T group and significantly higher than that in the MPTP group without training. The timing of training application (early- vs. late-onset of training) did not result in differences between the MPTP-TE and MPTP-TL groups with regard to GDNF levels (Figure 4A).

As in the midbrain, anti-GDNF staining in the striatum was most intense in the MPTP-TE and MPTP-TL groups and weakest in untrained MPTP mice (group C) (Figure 4, right vertical panel). Compared to the midbrain, MPTP administration caused a significantly greater decrease in GDNF levels in the striatum in untrained MPTP mice (by 4% in the midbrain vs. 13% in the striatum) (Figure 4A,B), and the decrease in GDNF levels was significant compared to group C. The pro-trophic effect of exercise was enhanced in mice receiving MPTP. Training significantly increased GDNF levels by 9% in C-T groups, 28% in MPTP-TE, and 22% in MPTP-TL compared to untrained control mice (C). Consequently, GDNF levels were also significantly higher in the MPTP-TE group and the MPTP-TL group, by 17% and 12%, respectively, compared to treadmill-exercising control mice (C-T). Similar to the midbrain, the timing of training application did not result in differences between the MPTP-TE and MPTP-TL groups with regard to GDNF levels (Figure 4B).

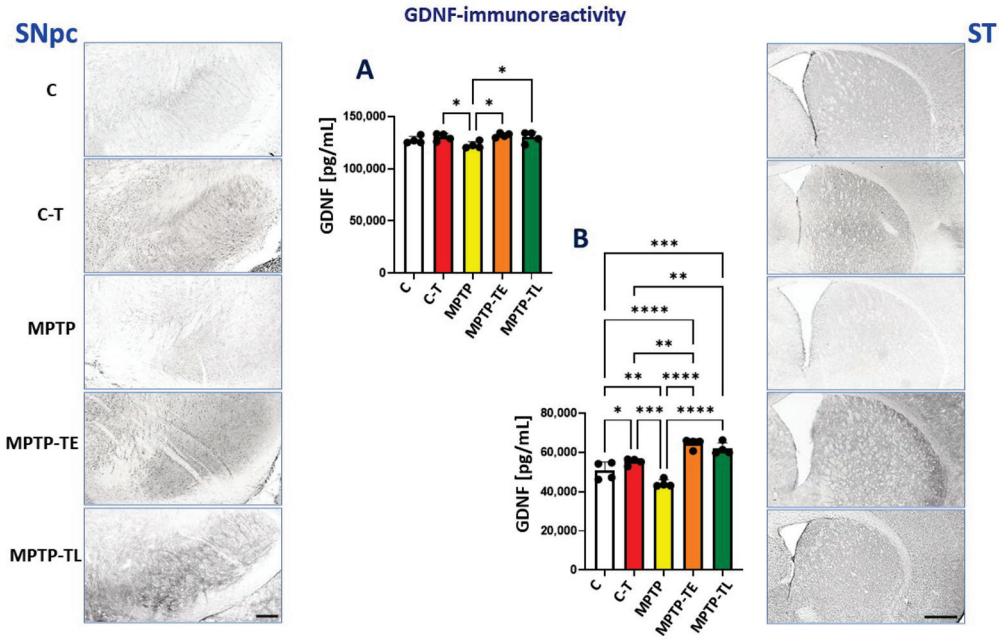


Figure 4. Glial-derived neurotrophic factor (GDNF) immunohistochemistry in the substantia nigra pars compacta (SNpc) and striatum (ST) of control mice (C, n = 4), trained control mice (C-T, n = 4), untrained mice with induced Parkinsonism (MPTP, n = 4), mice with induced Parkinsonism that underwent early-onset training (MPTP-TE, n = 4), and mice with induced Parkinsonism that underwent late-onset training (MPTP-TL, n = 4). Representative images of the GDNF immunohistochemical staining in SNpc (SNpc left panel) and the striatum (ST right panel). Magnification of microphotographs by 100 times for SNpc and 40 times for the striatum. Quantitative analysis of the levels of GDNF by ELISA in the midbrain (**A**) and the striatum (**B**). Values are presented as the mean ± SD with scatter plots of individual data. (**A**) Quantitative analysis of the GDNF level in the midbrain with one-way ANOVA showed a significant main effect of Group (F (4, 15) = 3.976; $p = 0.0215$). MPTP mice showed a non-significantly decreased GDNF level compared to the control group (group C). GDNF levels were not reduced in trained MPTP mice when compared to control groups (C, C-T). (**B**) Quantitative analysis of the GDNF level in the striatum with one-way ANOVA yielded the main effects of Group (F (4, 15) = 31.76; $p < 0.0001$). Unlike in the SNpc, untrained MPTP mice showed significantly decreased GDNF levels compared to control groups, whereas GDNF levels were elevated when physical exercise was administered in both control and MPTP-treated mice. The pro-trophic effect of exercise was particularly pronounced in mice receiving MPTP, both in the early-onset and late-onset training groups. Statistical significance between the groups was calculated using the Newman–Keuls test (* $p < 0.05$, ** $p < 0.01$, *** $p < 0.001$, and **** $p < 0.0001$). Scale bars: 100 μm for SNpc and 500 μm for ST.

2.3. Pro-Inflammatory Activation of Glial Cells After the Administration of MPTP Is Attenuated After Physical Training

Chronic inflammation plays an important role in the development of PD. On the other hand, it is not yet clear whether inflammation is a primary or secondary phenomenon, i.e., a consequence of neuronal death [25]. Characteristic features of neuroinflammation include activated microglia and reactive astrocytes, which are known to produce cytokines, chemokines, prostaglandins, protein complement cascades, and reactive oxygen and nitrogen species [26]. Our present study involved an immunohistochemical analysis of GFAP, Iba-1b, and integrin CD11b in the SNpc and striatum to assess the neuroinflammation evoked by MPTP and the potential neuroprotective influence of applied training on astrocytes and microglia.

Significant staining intensity for GFAP, Iba-1b, and integrin CD11b in the SNpc and ST was observed in sedentary MPTP mice (Figure 5A,B). Immunofluorescence staining for GFAP showed increased recruitment of astrocytes in the SNpc and ST of the seden-

tary MPTP mice compared to all other groups. In addition, microglial recruitment was observed in mice with induced Parkinsonism. Immunofluorescence for CD11b and Iba-1b, markers of microglia, also showed higher intensity in the SNpc and ST in MPTP-untrained mice compared to results obtained in controls (C and C-T groups) and both MPTP-treated and treadmill-trained groups (MPTP-TE and MPTP-TL groups) (Figure 5A,B). In addition, in the MPTP-treated group, higher magnification of anti-Iba-1b and anti-CD11b staining in both the SNpc and ST indicated the morphological transformation of resting microglia into activated cells resembling pro-inflammatory amoeboid phagocytic cells (Figure 5A,B insertions).

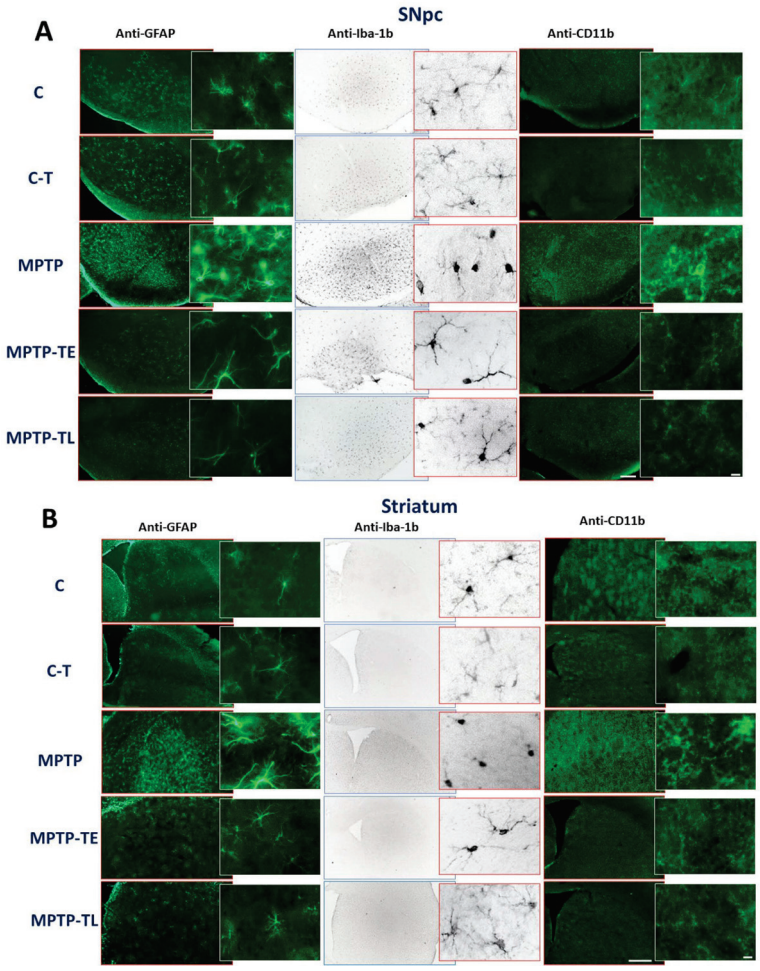


Figure 5. Immunohistochemical staining against glial fibrillary acid protein (GFAP), ionized calcium-binding adaptor molecule 1 (Iba-1b), and integrin CD 11b in the (**A**) substantia nigra pars compacta (SNpc) and (**B**) striatum (ST) of control mice (C), trained control mice (C-T), untrained mice with induced Parkinsonism (MPTP), mice with induced Parkinsonism that underwent early-onset training (MPTP-TE), and mice with induced Parkinsonism that underwent late-onset training (MPTP-TL). Representative images of GFAP, Iba-1b, and CD11b immunohistochemical staining in SNpc and ST. Scale bars: 100 μm for SNpc, 500 μm for ST, and 10 μm for insertions.

In contrast, we found that exercise appeared to prevent the development of inflammatory processes mediated by astrocytes and microglia cells, despite MPTP intoxication. Microscopic analysis revealed a significantly lower intensity of staining against GFAP in the SNpc and ST in the MPTP-TE and MPTP-TL treadmill-trained groups of mice compared to the untrained MPTP group, comparable to the staining in the control groups, especially when compared to the C-T group (Figure 5A,B). Iba-1b-ir and CD11b-ir in the SNpc and ST of the MPTP-TE and MPTP-TL groups were similar to those observed in the C and

C-T groups, and the morphology of the microglial cells resembled that of non-activated microglial cells (Figure 5A,B, insertions in the anti-Iba-1b and anti-CD11b panels).

High levels of inflammatory markers and pro-inflammatory changes in the morphology of immunocompetent cells were observed only in MPTP-treated sedentary mice. No signs of inflammation were seen in MPTP-treated mice when training started either before or after MPTP administration. Thus, the persistent inflammation induced by MPTP was abolished by physical exercise.

3. Discussion

The results presented above confirm observations that physical activity counteracts damage to midbrain dopaminergic neurons in an animal model of PD [17,18,27] and that this effect is accompanied by an increase in GDNF and BDNF levels in the substantia nigra pars compacta and striatum [28–30] and a reduction in the development of inflammation in dopaminergic structures [31–35]. Our data are of clinical relevance as they provide important evidence that exercise training may be a beneficial form of therapy in patients with Parkinson's syndrome, even if it is not characterized by high exercise intensity.

3.1. Steady Moderate Physical Training Attenuates the Loss of Dopaminergic Neurons Induced by the Chronic Administration of MPTP

Our study showed that a steady moderate 10-week exercise regimen applied immediately after chronic 5-week MPTP treatment significantly attenuated the loss of dopaminergic neurons in the SNpc and normalized DRD2 receptor levels and the density of dopaminergic innervation in the striatum, similar to the same 10-week exercise regimen initiated 1 week prior to such MPTP treatment in mice.

The neuroprotective effects of exercise on the nigrostriatal system have been demonstrated in animal models of PD [36]. Numerous studies in these models have confirmed that high physical activity attenuates the damaging effects of the dopaminergic neurotoxins 6-OHDA and MPTP, has neuroprotective effects on dopaminergic neurons in the SNpc, and normalizes the integrity of dopaminergic terminals in the striatum. An analysis of the number of dopaminergic neurons in the midbrain confirmed the neuroprotective effect of exercise in most [17,37,38], but not all, studies [39,40]. The neuroprotective effect was found to be dose-, duration-, and intensity-dependent, with each of these elements having an effect on neurochemical measures, neuronal counts, and motor symptoms of Parkinsonism [17,37]. In contrast, our previously published results [18] demonstrated that the training, which began before the administration of the neurotoxin and was applied after the end of the intoxication, (1) almost completely preserved the number of dopaminergic neurons in the SNpc and ventral tegmental area (VTA), (2) increased the BDNF level in the midbrain and the GDNF level in the striatum to a similar degree, and (3) entirely prevented inflammatory responses evoked by chronic MPTP treatment.

3.2. Neurotrophins Are Involved in the Neuroprotective Effects of Steady Moderate Exercise in a Mouse Model of Parkinson's Disease

Steady moderate physical training for 10 weeks increased BDNF in the midbrain and striatum in trained non-MPTP-treated mice. Chronic MPTP treatment in sedentary mice decreased the levels of this neurotrophin. Training that started both before and after chronic MPTP treatment increased BDNF levels not only above those of non-MPTP-treated sedentary mice but also above those found in the midbrain of trained non-MPTP-treated mice.

For GDNF levels, the greatest differences induced by training were observed in the striatum. Training increased the level of GDNF in non-MPTP-treated mice above the level observed in sedentary non-MPTP-treated mice. Chronic MPTP treatment in sedentary mice

decreased the levels of this neurotrophin. Surprisingly, in the striatum, MPTP treatment potentiated the effect of training as GDNF levels in trained MPTP-treated mice increased even above those observed in trained non-MPTP-treated mice. However, in the midbrain, MPTP treatment did not potentiate the effect of training on GDNF levels, but training in MPTP groups maintained midbrain GDNF levels similar to those observed in the trained non-MPTP-treated group.

The available literature supports the central role of the neurotrophic factors BDNF and GDNF in exercise-induced neuroprotection. In addition to the fact that exercise increases the levels of neurotrophic factors, it is also known that supplementation with exogenous BDNF or GDNF alone is sufficient to prevent the loss of dopaminergic neurons following the damaging effects of toxins, as demonstrated both in vitro and in animal model studies [41–43].

In contrast, the reduced synthesis of GDNF or BDNF after the knock-out of their genes or silencing of their expression by antisense oligonucleotides results in a progressive loss of TH-positive neurons in the SNpc of mice and increases their sensitivity to MPTP [44,45]. Exercise also fails to protect against MPTP-induced neurotoxicity in mice heterozygous for the BDNF gene ($BDNF^{+/-}$) [17,24]. It has also been shown that the application of a TrkB receptor antagonist causes physical activity to lose its protective effect on dopaminergic neurons [43]. These results suggest that physical activity may reduce the sensitivity of dopaminergic neurons to toxins via the activation of signaling cascades triggered by the increased availability of BDNF and GDNF. The increased number of immunohistochemically labeled GDNF cells observed in exercising mice may indicate exercise-induced mobilization of glial cells and the activation of anti-inflammatory processes.

3.3. Anti-Inflammatory Effect of Steady Moderate Exercise in a Mouse Model of Parkinson's Disease

Immunohistochemical detection of increased levels of GFAP, Iba-1b, and CD11b may indicate that both astroglia and microglia are involved in the inflammatory response or pathological changes in nigrostriatal structures in mice receiving MPTP. High levels of inflammatory markers and pro-inflammatory changes in immunocompetent cells were observed only in MPTP-treated sedentary mice. The signs of inflammation were still present four weeks after the end of MPTP treatment, but they were absent in the early-onset training group examined at the same time point, i.e., also four weeks after the end of neurotoxin treatment. Thus, the persistent inflammation induced by MPTP was abolished by exercise.

Iba-1b and CD11b proteins are among the markers of immune cells and, in the context of microglia, are specific markers for these cells [46]. Increased expression of Iba-1b and CD11b indicates that microglia may be activated in a given tissue area, which may be indicative of inflammation, immune response, or neuroinflammatory processes, as both proteins are associated with phagocytic functions and inflammatory cell activity [47].

CD11b, together with other transmembrane and surface proteins, is the first line of defense against pathogens. It is involved in adhesion processes and the uptake of complement-coated molecules [48]. It has been reported that increased CD11b expression in various neuroinflammatory diseases corresponds to the severity of microglial activation [49]. Morphologically, microglial activation is associated with intense branching and cytoskeletal rearrangement, with changes in shape and motility correlating with an increased expression of CD11b [50]. During this activation process, the cytoplasmic domain of CD11b is thought to interact increasingly with cytoskeletal proteins [51].

The most commonly used protein marker of microglial activation is also an elevated level of Iba1. This is a member of the calcium-binding protein group. Iba1 is an intracellular protein, and its functions are related to the reorganization of the microglial cytoskeleton

and the support of the phagocytosis process. The latter is possible thanks to its ability to bind actin molecules [52]. This protein is one of the most widely studied in inflammatory processes due to its conservative amino acid sequence and stability of antigenic epitopes across species, including humans [53].

Current knowledge of the mechanisms involved in the anti-inflammatory effects of exercise training in PD is based on data obtained in animal models [54], and these studies are not very numerous. The results obtained by Sconce et al. [55] show that animals treated with increasing doses of MPTP for 4 weeks had significantly increased levels of GFAP in the SNpc, suggesting that astrocytosis processes were activated. Interestingly, the MPTP-treated and exercising groups also had elevated GFAP levels compared to the control group, but this was significantly lower than the group of mice treated with MPTP but not exercising. This suggests that exercise may suppress the inflammatory response in the brain, including the attenuation of astrocytosis. Another study, also in a mouse model using the neurotoxin 6-OHDA [32], showed that both aerobic treadmill training and resistance training have neuroprotective effects, probably by stimulating sirtuin 1 activity. This can regulate both mitochondrial function and neuroinflammatory processes through the deacetylation of NF-κB. Both forms of training also reduced levels of nitric oxide (NO), TNF-α (tumor necrosis factor alfa), IFN-γ (interferon gamma, a type 2 interferon produced by leukocytes), IL-1β (interleukin beta 1), and TGF-β1 (transforming growth factor beta 1) in mice receiving 6-OHDA. The regulation of NO levels may also be the mechanism by which exercise training affects the magnitude of the inflammatory response induced by 6-OHDA administration.

It is reasonable to suggest that the exercise-induced reduction in the inflammatory response may be the result of a direct effect on systemic immune processes. Contracting skeletal muscles secrete cytokines (myokines), in particular interleukin-6 (IL-6), which mediates the metabolic changes that occur during exercise [56,57]. IL-6 release from muscles increases up to 100-fold during exercise contraction, resulting in an increased systemic production of anti-inflammatory cytokines, including interleukin-10 (IL-10) and interleukin-1 (IL-1) receptor antagonists, and decreased production of TNF-α and IL-1β [58,59]. Exercise-induced improvements in the inflammatory profile may also result from the modulation of intracellular signaling pathways and cellular functions mediated by NO and reactive oxygen species (ROS). The induction of anti-inflammatory defense mechanisms involves an increase in the expression levels of genes encoding antioxidant enzymes and heat shock proteins [60,61].

Although physical activity is effective in reducing the risk of many chronic diseases [62], acute training that is inappropriate in terms of intensity and duration for the capacity of the trainee can cause damage to muscle and connective tissue, typically manifested by the infiltration of inflammatory cells into the damaged tissue and the presence of pro-inflammatory cytokines in the peripheral blood [56]. The inflammatory response to exercise is attenuated when exercise is repeated at moderate intensity as the body adapts to the overload that occurs. Regular moderate exercise leads to a reduction in the baseline levels of circulating inflammatory markers as well as a reduction in the inflammatory response to intense exercise [61].

3.4. Equipotent Neuroprotective Effect of Steady Moderate and Intensive Physical Training

We compared the currently presented results, in which we used steady moderate exercise, to our previously published data [18], in which mice with induced Parkinsonism were subjected to high-intensity exercise. When subjected to steady moderate exercise, mice ran 360 m/day, whereas mice subjected to intensive exercise [18] ran 450 m daily. Importantly, the run velocity was constant (15 cm/s) during moderate exercise, while

during intensive exercise [18], the velocity was variable (10–25 cm/s) and its mean value was 18.75 cm/s. There was a 25% difference between constant speed during moderate-intensity training and average speed during high-intensity training. Given the same daily training time (40 min), this also means a 25% difference in the distance run. Such a difference approximately corresponds to the difference between moderate and intensive exercise in human studies.

Comparing the results of the moderate-intensity training groups to those of the high-intensity training groups shows that the neuroprotection provided by the former type of training was at least as effective as that provided by the latter type of training. MPTP treatment in sedentary mice reduced the number of TH-ir neurons in the SNpc by 66%. Interestingly, the loss of dopaminergic neurons was less in the moderate-intensity training groups than in the high-intensity training mice (27 vs. 31% after early-onset training and 18 vs. 26% after late-onset training), although these differences were not significant (Figure S1).

BDNF levels in the midbrain, as well as the striatum, were non-significantly lower in untrained MPTP-treated mice compared to untrained and untreated control mice. Both moderate- and high-intensity training elevated the BDNF level in MPTP-untreated mice. In the midbrain, treatment with MPTP significantly potentiated the effects of both moderate- and high-intensity training as the BDNF level was significantly higher in MPTP-trained groups than in non-treated trained groups (Figure S2).

MPTP-treated sedentary mice had non-significantly reduced GDNF levels in the midbrain and significantly reduced GDNF levels in the striatum compared to untrained and trained controls. The effect of training and its intensity on GDNF levels was more pronounced in the striatum than in the midbrain. In the striatum, high-intensity training caused a significantly greater increase in GDNF in trained MPTP-untreated mice than moderate-intensity training. Similarly, high-intensity exercise caused a greater increase in GDNF levels than moderate exercise in MPTP-treated mice, but the difference was only present between the early-onset training groups (Figure S3).

It is also reasonable to suggest that the exercise-induced reduction in the inflammatory response may be the result of the activation of trophic factor-dependent signaling pathways triggered by an increased availability of neurotrophins [43]. For example, the anti-inflammatory activated microglia show increased expression of cytokines recognized as anti-inflammatory, such as IL-10, TGFβ, IGF-1, NGF, and BDNF [63,64]. Astrocytes, like microglia, also secrete anti-inflammatory agents into the environment, including neurotrophic factors (e.g., GDNF, BDNF, and mesencephalic astrocyte-derived neurotrophic factor (MANF)), which stimulate the survival and resuscitation of damaged dopaminergic neurons [65,66]. In addition, endogenous IL-1β has been shown to induce GDNF gene expression, synthesis, and secretion under in vitro conditions [67,68]. It is possible that exercise training in Parkinsonian MPTP mice induces an alternative neuroprotective activation of microglia rather than reducing pro-inflammatory glial activation.

On the other hand, it can be assumed that there is no increased pro-inflammatory proliferation and activation of glial cells as a result of prolonged exercise because neurotrophin-protected dopaminergic neurons do not degenerate and thus do not send signals that mobilize the inflammatory response system [7].

3.5. Importance of Exercise Intensity in Exercise-Induced Neuroprotection

The conclusion of a number of human studies is that only intensive exercise performed by PD patients slows motor deterioration [7,8], whereas there are not many publications confirming the beneficial effects of intensive exercise on the functionality of rescued dopaminergic neurons in the substantia nigra and the protection of nigrostriatal terminals

in the putamen. Zigmond et al. [69] presented results obtained in three rhesus monkeys injected unilaterally with MPTP, with the other side of the brain serving as a control. One monkey was sedentary, the second performed treadmill running at 60% of the maximum heart rate (HRmax), and the third performed running at 80% HRmax. Running lasted 12 weeks before MPTP and 5 weeks after MPTP. The levels of TH, vesicular monoamine transporter 2 [VMAT2], and dopamine transporter (DAT) were undetectable in the caudate and putamen of the MPTP-treated hemisphere in the sedentary monkey; in the monkey running at 60% HRmax, only TH was barely detectable in this hemisphere. Running at 80% HRmax maintained TH, VMAT2, and DAT at levels similar to the control hemisphere.

The results of the study by de Laat et al. [70] bear some resemblance to the results described above in rhesus monkeys, in that the intensive exercise performed by PD patients improved the functionality of the remaining dopaminergic neurons in the substantia nigra and protected the nigrostriatal terminals in the putamen. Ten patients with mild and early PD exercised above the moderate intensity level, i.e., their heart rate was above 60–65% of their individual HRmax, often reaching 80% HRmax. This type of exercise increased DAT levels in the substantia nigra and putamen, as measured by PET imaging. This increase was found to be statistically significant when compared to the expected decrease previously measured by Delva et al. [71]. The authors also found that intense exercise reversed the expected decrease in neuromelanin concentration in the substantia nigra, as assessed by MRI. Neuromelanin is produced in the cytosol from dopamine and other catecholamines, and its concentration in dopaminergic neurons increases linearly with age in healthy subjects [72]. In PD patients, neuromelanin concentration decreases significantly in the early years of the disease; so, an increase, rather than a decrease, in neuromelanin concentration can be interpreted as a renormalization of dopaminergic neuron activity.

The study cited above only looked at the effects of vigorous exercise; so, the question arises as to whether only vigorous exercise can reverse the progression of PD in sedentary PD patients. An indirect answer to this question is provided by the study by Schenkman et al. [9]. The authors compared the change in Unified Parkinson's Disease Rating Scale (UPDRS) motor score caused by intensive treadmill exercise (80–85% HRmax) and moderate-intensity treadmill exercise (60–65% HRmax) for six months, 3 days per week. The mean change in UPDRS motor score was 0.3 (slight deterioration) in the high-intensity group, 2.0 in the moderate-intensity group, and 3.2 in the control group. Based on these results, the authors accepted the hypothesis that high-intensity exercise was associated with a significant attenuation of motor decline and rejected the hypothesis that moderate-intensity exercise could produce such a result.

If, in fact, very intensive exercises have to be used to positively modify the course of PD, this type of intervention will remain restricted to a limited number of Parkinson's patients. It may become increasingly difficult to recruit truly sedentary people with PD and those in more advanced stages of the disease to systematically participate in intensive exercise. It should also be borne in mind that, according to current knowledge, intensive exercise can only slow the progression of the disease such that even people who exercise intensively will progress to a more advanced stage of PD.

As mentioned in the Introduction section, people with PD may find it difficult or impossible to participate in vigorous exercise. Muscle weakness in PD is a primary symptom [11] and exacerbates the normal age-related loss of maximal isometric strength, making people with PD weaker than healthy people of similar age [73]. Both maximal voluntary contraction and the rate of force development are reduced in PD, which may lead to a decrease in force production [74]. Sympathetic denervation reduces cardiac contractility, which may affect exercise capacity in patients with PD [70]. Fatigue is a debilitating and persistent symptom commonly reported in PD. Physical activity is also impaired in PD due

to increased fatigability. This increase may be caused by reduced cardiorespiratory fitness, resulting in reduced oxygen delivery and utilization and leading to increased reliance on anaerobic metabolism [13].

It is also important to remember that exercise puts a strain on the body, especially the cardiovascular system. For example, exercise increases blood pressure. The extent to which blood pressure rises during exercise is determined by the brain's pressure-regulating center. The increase in blood pressure in response to the same exercise is specific to each individual, and a certain percentage of exercisers, including patients with PD, will experience an above-average increase in arterial pressure [75]. A high increase in arterial pressure during exercise has been shown to be associated with a higher risk of cardiac events [76]. Although a cause-and-effect relationship between an exaggerated pressor response to exercise and cardiac events has not been established, individuals who experience particularly large increases in arterial pressure during exercise are systematically exposed to high cardiovascular stress.

It should be also taken into consideration that acute training that is inappropriate in terms of intensity and duration for the capacity of the trainee can cause damage to muscle and connective tissue, typically manifested by the infiltration of inflammatory cells into the damaged tissue and the presence of pro-inflammatory cytokines in the peripheral blood [56]. The inflammatory response to exercise is attenuated when exercise is repeated at moderate intensity as the body adapts to the overload that occurs. Regular moderate exercise leads to a reduction in the baseline levels of circulating inflammatory markers, as well as a reduction in the inflammatory response to intense exercise [61]. However, it should also be considered that very intense exercise may increase the risk of common infections and the anti-inflammatory response due to a downregulation of pro-inflammatory cytokines, together with the stimulation of anti-inflammatory cytokines [77].

The currently presented results obtained with steady moderate training and previously presented results from high-intensity training [18] show that increasing the intensity of exercise above the level applied in this study did not enhance the neuroprotective effect of aerobic training in this particular mouse model of PD induced by a series of MPTP injections. This suggests that there is a kind of saturation where the effect (% of neurons saved) has reached its highest possible value and further increases in exercise intensity do not produce a further increase in neuroprotection. Translating this finding into clinical practice means that it may not be rational to strive for maximum intensity of exercise as this may not enhance neuroprotection but may be detrimental and lead to the exclusion of many, if not the majority of, PD patients.

We think it is likely that the relationship between the intensity of exercise and neuroprotection could be a sigmoidal one. In such a case, in addition to saturation, which occurs when exercise intensity is high, there is also a sub-threshold range where this intensity is low and its change within this range has no effect on neuroprotection. The range between threshold and saturation is the range in which a change in exercise intensity will produce a change in neuroprotection. This range can be quite narrow, i.e., if the intensity of exercise falls below the level that still confers maximum neuroprotection, one would observe a disproportionate increase in neuronal loss. This seems to be the case in the study by Gerecke et al. [17]. Bearing in mind that they studied the neuroprotective effect of exercise applied before MPTP intoxication, the loss of dopaminergic neurons in the SNpc was 9.2% after a full distance run, while a 2/3 full distance run resulted in a loss of 30.7%, and a 1/3 full distance run resulted in a loss of 35.6% of neurons, which is close to the 41.5% loss in sedentary mice.

4. Materials and Methods

4.1. Experimental Groups: Drugs and Treatments

In the present study, we compared changes in the dopaminergic system, expression levels of trophic factors, and inflammatory processes under moderate-intensity training to those observed in a previous study in which mice with induced Parkinsonism were subjected to high-intensity training. The experiments were performed on cohorts of mice from the same generations of the breeding program, under the same conditions, by the same experimenter, and using the same methods of tissue processing and evaluation.

All procedures used in this study were approved by the First Local Ethics Committee for Animal Experiments in Warsaw and were performed in accordance with the Polish Law on the Protection of Animals and the National Institute of Health's Guide for the Care and Use of Laboratory Animals (Publication No. 85-23, revised 1985) and the European Union Council Directive (63/2010/EU). Studies were performed in 12-week-old male C57BL/6J mice, purchased from the Medical University of Bialystok (Poland) and delivered to the Nencki Institute of Experimental Biology 1 month before the experiments. In this study, 35 control (vehicle-treated) and 52 mice treated with MPTP were used. Mice were kept on a 12:12 h light/dark cycle, with temperature and humidity maintained at 23 ± 1 °C and 55 ± 5%, respectively; food and water were freely available. With regards to the chronic MPTP administration protocol, mice were given 10 subcutaneous doses of MPTP 12.5 mg/kg dissolved in saline (Santa Cruz Biotechnology, San Diego, CA, USA, Cat No sc-206178; Axon Medchem, Groningen, The Netherlands, Cat No 1075) in combination with the intraperitoneal application of probenecid (250 mg/kg dissolved in dimethyl sulfoxide (DMSO); Sigma-Aldrich, St. Louis, MO, USA, Cat No P8761) injections for 5 weeks. The purpose of probenecid administration was to inhibit the rapid excretion and disintegration of MPTP and its metabolites from the brain and kidney; probenecid alone has no significant neurotoxic effect, but in combination, it potentiates the neurotoxicity of MPTP [78]. Control mice received saline and DMSO injections only. The mice were thus divided as follows: 19 mice in a control group (group C), 16 mice in a control treadmill training group (C-T), 19 mice in an MPTP-injected group (MPTP), 17 mice in an MPTP-injected trained group that started treadmill training 1 week before the induction of Parkinsonism (MPTP-TE, i.e., MPTP + early-onset treadmill training), and 16 mice in an MPTP-injected trained group that started treadmill training immediately after the induction of Parkinsonism (MPTP-TL, i.e., MPTP + late-onset treadmill training) (Figure 6). The treadmill training lasted 40 min/day at 15 cm/s (360 m/day) and was performed 5 days/week for 10 weeks.

4.2. Animal Sacrifice and Brain Tissue Collection

Animals were initially induced into a sedative state with a mixture of ketamine (75 mg/kg; i.p.) and medetomidine (0.5 mg/kg; i.p.) and then deeply anesthetized (loss of corneal reflexes) by the intraperitoneal administration of Vetbutal at a dose of 1 mL/kg body weight. Intra-aortic perfusion was started when there was no reflex to skin stimulation. The tissues were rinsed with cold (4 °C) 0.1 M phosphate-buffered saline (PBS) containing 5 IU of heparin per 1 mL of buffer (50 mL within 5 min) and fixed with 4% paraformaldehyde in 0.1 M PBS (50 mL within 5 min). Tissues were cryoprotected with 5% glycerol and 2% DMSO in 0.1M PBS (50 mL within 5 min). Fluids were administered through a cannula connected to a peristaltic pump. After perfusion, the brains were removed, placed in fixative for 1 h, and then immersed in 10% glycerol and 2% DMSO (24 h) for cryoprotection, followed by 20% glycerol and 2% DMSO (24 h). The brains were kept at −80 °C until used for staining. Mouse brains were delivered on dry ice and cooled in a cryostat (Leica CM1850,

Leica Bioststems, Deer Park, IL, USA) at −27 °C for 45 min. Frozen brains were fixed to the cryostat stage with a tissue freezing medium and sectioned coronally at 40 µm thickness.

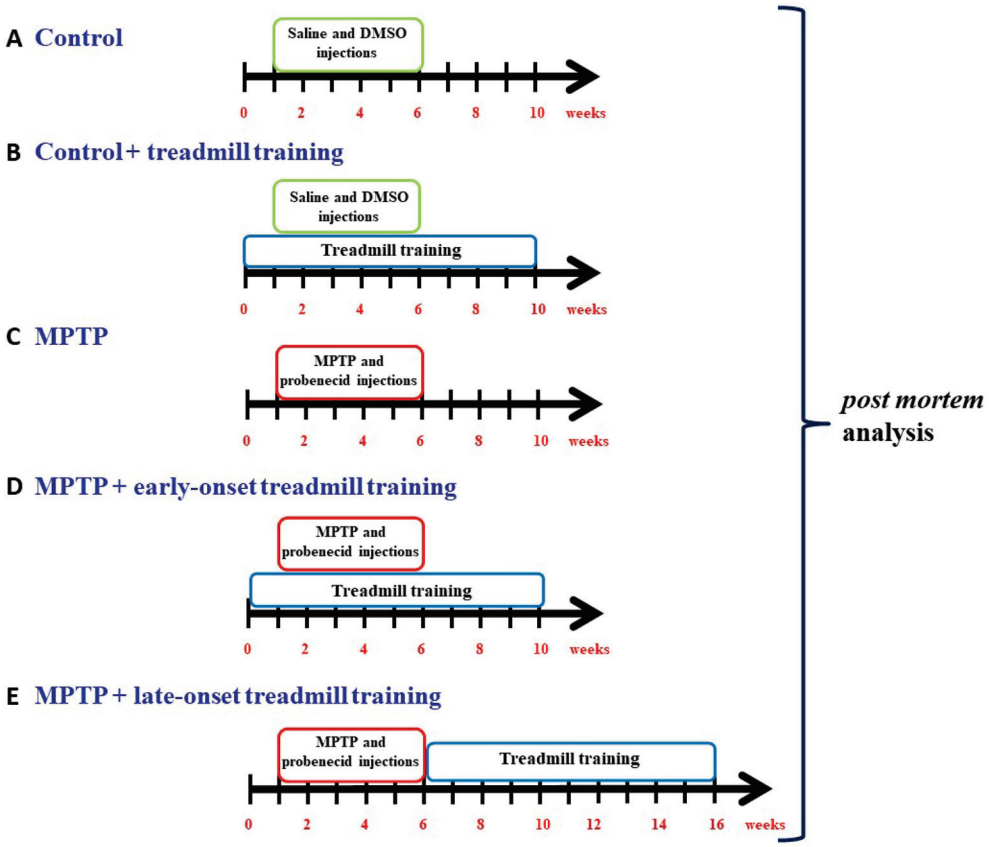


Figure 6. Schematic diagram of the study design. A detailed description of the research protocol can be found in the Methods section. MPTP—1-N-Methyl-4-phenyl-1,2,3,6-tetrahydropyridine, a precursor to the neurotoxin 1-Methyl-4-phenylpyridinium (MPP^+) and DMSO—dimethyl sulfoxide.

4.3. Staining

4.3.1. Nissl Staining

Sections were mounted in 0.03 M PB on gelled slides and dried at room temperature (RT) for several days. Sections were dewaxed by incubation for 3 min in the following ethanol solutions: 96%, 80%, and 70% acidified with acetic acid. This was followed by rinsing with distilled water and staining with 0.1% cresyl violet in acetate buffer for 15 min. After rinsing with distilled water, differentiation was carried out in a 70% ethanol solution with 10% acetic acid until no excess dye was present. The sections were then dehydrated in increasing concentrations of alcohol (one change of 80%, two changes of 96%, two changes of absolute alcohol). Next, the sections were incubated twice in the mixture of absolute alcohol and xylene (mixture I: 2 parts of absolute alcohol for 2 parts of xylene and mixture II: 1 part of absolute alcohol for 2 parts of xylene) and in 3 xylene solutions (3 min in each solution). The sections were finally mounted in a DePeX medium. Nissel-stained sections were used as reference labels for the identification of the brain structures that were to be analyzed.

4.3.2. Immunohistochemistry for TH, DRD2, BDNF, and GDNF

For each individual antibody, all brain sections were processed simultaneously in the same reagents during the same labeling reaction. The sections were rinsed three times for 5 min with 0.1 M PBS. The sections were then incubated with 1% H_2O_2 solution in 0.1 M PBS to block the activity of endogenous peroxidases. The tissue material was

then rinsed three times with 0.1 M PBS and incubated with 5% normal goat serum (NGS; Vector Laboratories, Inc., Newark, CA, USA) in 0.1 M PBS containing 0.3% TritonX-100 for one hour at RT. This was followed by incubation with primary antibodies in a solution containing 5% NGS, 1% bovine serum albumin (BSA), and 0.3% TritonX100 in 0.1 M PBS for one hour at RT and then overnight at 4 °C with continuous shaking. The following primary antibodies were used: anti-dopamine D2 receptor (DRD2, Invitrogen, Waltham, MA, USA; Cat #PA5-115142) at a dilution of 1:200, anti-glial cell line-derived neurotrophic factor (GDNF, Santa Cruz Biotechnology, Cat No sc-328) at a dilution of 1:500, anti-brain-derived neurotrophic factor (BDNF, Santa Cruz Biotechnology, Cat No sc-20981) at a dilution of 1:500, and anti-tyrosine hydroxylase (TH, MERCK, Darmstadt, Germany: Cat No AB152) at a dilution of 1:1000. After three washes with 0.1 M PBS, brain sections were incubated for 1 h at RT with secondary antibody solution (Biotinylated Goat Anti-Rabbit IgG Antibody, Vector Laboratories, Cat No BA-1000) (5% NGS, 1% BSA, and 0.3% TritonX100 in 0.1 M PBS) at a dilution of 1:200. The formulations were rinsed three times with 0.1 M PBS and then incubated with the Vectastain ABC Kit (Vector Laboratories, Inc., Newark, CA, USA) for 1 h at RT. To visualize primary–secondary antibody complexes, sections were incubated in PBS containing 3,3′-diaminobenzidine tetrahydrochloride (DAB, Sigma-Aldrich, Merck KGaA, Darmstadt, Germany), H_2O_2, and $NiSO_4$ at concentrations of 0.025%, 0.0125%, and 0.04%, respectively. Stained sections were mounted, air-dried, and cover-slipped. The specificity of the immunostaining was checked by running some slides through the entire procedure without the primary antibody (first control) or secondary antibody (second control). No specific staining was observed in any of the control slides.

4.3.3. Immunohistochemistry for Iba-1b

Brain sections were rinsed in 0.1 M PBS for 3 × 5 min, incubated with 1% H_2O_2 solution in 0.1 M PBS, and blocked with 5% normal rabbit serum (NRS; Vector Laboratories Inc., Newark, CA, USA) in 0.1 M PBS containing 0.3% TritonX100 for one hour at RT. The sections were then incubated with primary antibody against ionized calcium-binding adaptor molecule 1 (Iba-1b, Abcam Limited, Cambridge, UK; Cat No ab5076) diluted (1:500) in 0.1 M PBS containing 5% NRS, 1% BSA, and 0.3% TritonX100 for 1 h at RT and then overnight at 4 °C with continuous shaking. This was followed by 3 × 5 min PBS washes and one hour of incubation at RT with the solution of rabbit anti-goat IgG and horseradish peroxidase (HRP) conjugate. The secondary antibody was diluted (1:500) in 0.1 M PBS containing 5% NRS, 1% BSA, and 0.3% TritonX100. DAB was used as a chromogen to visualize the reaction. The stained sections were mounted, air-dried, and cover-slipped. Controls for immunohistochemistry were performed as described above.

4.3.4. Immunofluorescence Staining for GFAP and CD11b

Free-floating sections were rinsed three times in 0.1 M PBS, incubated in 1% H_2O_2 solution in 0.1 M PBS for 30 min, and in 5% NGS solution (Vector Laboratories) in 0.1 M PBS with 0.3% TritonX-100 for 60 min. The next step was overnight incubation with anti-glial fibrillary acidic protein (GFAP, dilution 1:1000, Dako, Glostrup, Denmark) and anti-integrin subunit alpha M (CD11b, dilution 1:200, Bio-Rad Laboratories, Inc., Hercules, CA, USA) antibody solution in 0.1 M PBS with 0.3% TritonX100, 5% NGS, and 1% BSA. The next day, the sections were rinsed with 0.1 M PBS and transferred to a mixture of secondary antibodies (1:1000, ThermoFisher Scientific Inc., Waltham, MA USA for both GFAP and CD11b). Incubation with fluorescent antibodies was performed in the dark to prevent photobleaching. The sections were mounted on slides and cover-slipped using UltraCruz® Aqueous Mounting Medium with DAPI (Santa Cruz Biotechnology, Inc., Dallas, TX, USA). The details for primary and secondary antibodies used are given in Table S1.

4.3.5. Enzyme-Linked Immunosorbent Assay for BDNF, GDNF, and GFAP

Five mice from each experimental group were decapitated, the brains were quickly removed, and the striatum (ST) and midbrain, including the substantia nigra (SN), were collected and stored at −80 °C until further use. Tissue samples were weighed and homogenized in 20 volumes of ice-cold homogenization buffer against wet tissue weight. After centrifugation, the resulting supernatants were used in an enzyme-linked immunosorbent assay (ELISA) to quantify striatal and midbrain levels of BDNF (ChemiKine Brain Derived Neurotrophic Factor, Sandwich ELISA Kit Cat. No. CYT306, Merck, Darmstadt, Germany), GDNF (Mouse GDNF/Glial Cell Line-Derived Neurotrophic Factor ELISA Kit, Cat No EIAab/e0043m, Filgen Inc., Nagoja, Japan), and GFAP (NS830, Merck Millipore, Darmstadt, Germany). All steps of the assay were performed according to the manufacturer's recommendations.

4.4. Data Analyses

4.4.1. Quantification of the Number of Dopaminergic Neurons in SNpc

The anterior to posterior extent of the SN was determined using the Paxinos and Franklin [79] mouse brain atlas. TH-immunoreactive neurons in the substantia nigra pars compacta (SNpc) (−3.15 to −3.51 posterior to Bregma) were imaged using a Nikon Eclipse Ni-E microscope (Nikon Instruments, Inc., Tokyo, Japan). Brain sections were selected for analysis so that the coronal cross-section through the substantia nigra corresponded to the level of the greatest dopaminergic cell distribution (i.e., between 400 and 700 microns from the rostral to caudal development of the SNpc) [80]. The boundaries of the region of interest (ROI), in this case, the area of the TH-ir neurons and their dendrites, were delineated using the X–Y plotting system of the NIS software (Nikon Instruments, Inc., Tokyo, Japan, https://www.microscope.healthcare.nikon.com/en_EU/products/software/nis-elements), which also measured the square area (in mm^2) of the ROI. TH-immunoreactive neurons were counted under 100× magnification. We only counted neurons in which the neuronal bodies were immunoreactive for TH and the nucleus and proximal segment of one or two dendrites were clearly visible. Afterward, the mean packing density (mPD) of dopaminergic neurons was calculated as a function of the rostrocaudal level and location within the SNpc by using the determined number of cells and the square area of the ROI in each section analyzed. The following equation was used:

$$mPD = \frac{\sum_{i=1}^{n} N_i}{\sum_{i=1}^{n} SA_i}$$

where mPD—mean packing density [mm^{-2}]; N_i—number of neurons counted in the i-TH section (positively stained against tyrosine hydroxylase); and SA_i—square area of the i-TH analyzed ROI [mm^2]. The mean number of TH-ir neurons found in each experimental group was expressed as the mean packing density [number of cells per one square millimeter].

4.4.2. Densitometric Analysis of the Immunostaining of TH and DRD2 in the Striatum

DAB-stained sections were analyzed using a brightfield microscope (Zeiss, AXIO IMAGER.M1, Carl Zeiss Industrielle Messtechnik GmbH, Oberkochen, Germany). Fiji-ImageJ (v. 1.53t, https://fiji.sc/) software was used for quantitative analysis. Relative optical density (OD) was measured in ROI, i.e., the striatum. The digitization of the SNpc microscope images was carried out in a single microscopy session, and the OD measurements were carried out at the same time. In the first step, the observer delineated the ROI. In the second step, OD, i.e., the average level of greyness in the ROI, was calculated using ImageJ software. Mathematically, OD was the sum of the grey values of all pixels within the ROI divided by the number of these pixels. The threshold of OD was then

determined by the observer. ImageJ allows all pixels with an OD below the threshold to be marked in red. In fact, it is possible to find a threshold value such that only the immunospecifically stained tissue is marked red. In order to find a suitable threshold value, the observer had to gradually change its value until all immunolabelled elements within the ROI became red. This procedure was performed once for the selected reference image. This threshold was then used to analyze all the other images. Using the threshold, a new measure was calculated: %Area. Specific OD was calculated as the mean OD of all pixels within the ROI with an OD below the threshold. %Area was calculated as the ratio of the number of pixels within the ROI with an OD below the threshold to the number of all pixels within that area.

4.4.3. Quantification of the Levels of BDNF, GDNF, and GFAP in the Striatum and Midbrain

The optical density of the standards and samples processed in the ELISA test was determined using a microplate reader (ThermoLabsystem, Thermo Fisher Scientific Inc., Waltham, MA, USA) set at a wavelength of 450 nm, and the concentration of the tested samples was read from the standard curve and expressed as pg/mL for BDNF and GDNF and ng/mL for GFAP.

4.4.4. Statistical Analysis

All datasets are expressed as group mean ± SD. A comparison between experimental groups was carried out with the use of a one-way analysis of variance (ANOVA) followed by a post hoc comparison with the Newman–Keuls test using STATISTICA 12 software (StatSoft Polska, Krakow, Poland, https://www.statsoft.pl/). The differences between groups were considered statistically significant for $p \leq 0.05$.

5. Conclusions

Our previously published results [18] and those presented in this article show that there is a threshold of exercise intensity above which increasing exercise intensity no longer results in increased neuroprotection. Consistent with this finding, the increases in the neurotrophins BDNF and GDNF and the attenuation of inflammatory processes induced by steady moderate-intensity exercise were similar to those induced by high-intensity exercise. Future research should use a wide range of exercise intensities to determine how changes in exercise intensity affect neuroprotective efficacy. By examining changes in different processes and phenomena in relation to changes in exercise intensity, key determinants of exercise-induced neuroprotection may be identified.

Supplementary Materials: The following supporting information can be downloaded at: https://www.mdpi.com/article/10.3390/ijms26031146/s1.

Author Contributions: P.D.: investigation and data curation. A.G.-B.: investigation, writing—review and editing, and funding acquisition. E.P.: investigation, project administration, data curation, methodology, manuscript initiation, and writing—review and editing. W.N.: writing—review and editing, funding acquisition, and conceptualization. G.N.: writing—review and editing, writing—original draft, visualization, formal analysis, and conceptualization. All authors contributed to the design of the manuscript, discussed its content, and finalized the manuscript. All authors evaluated and reviewed the manuscript. All authors have read and agreed to the published version of the manuscript.

Funding: This research was supported by the National Science Centre Poland (NCN; https://www.ncn.gov.pl/) under research project funds to A.G-B. (UMO-2011/01/D/NZ7/04405) and by the statutory funds from the Mossakowski Medical Research Institute.

Institutional Review Board Statement: This study was conducted in accordance with the Declaration of Helsinki. All animal experimental procedures used in this study were approved by the First Local Ethics Committee in Warsaw (511/2011 14 December 2011), in compliance with the guidelines of the Directive 22 September 2010 (2010/63/EU) and the Animal Protection Act of Poland (2017) on the protection of animals used for scientific purposes.

Informed Consent Statement: Not applicable.

Data Availability Statement: The data presented in this study are available upon request from the corresponding author. Please refer to the Supplementary Files for additional data supporting the reported results.

Conflicts of Interest: The authors declare that the research was conducted in the absence of any commercial or financial relationships that could be construed as a potential conflict of interest. The funders had no role in the design of this study, the collection, analyses, or interpretation of the data, the writing of the manuscript, or the decision to publish the results.

Abbreviations

The following abbreviations are used in this manuscript:

BDNF	Brain-derived neurotrophic factor
BSA	Bovine serum albumin
C	Control
CD11b	Integrin subunit alpha M
CREB	Cyclic AMP-responsive element-binding protein
C-T	Control treadmill training
CTT	High-intensity trained control mice
DAB	3,3′-diaminobenzidine tetrahydrochloride
DAT	Dopamine transporter
DMSO	Dimethyl sulfoxide
DOPA	Dihydroxyphenylalanine
DOPAC	Dihydroxyphenylacetic acid
DRD2	Dopamine D2 receptor
ELISA	Enzyme-linked immunosorbent assay
GDNF	Glial cell line-derived neurotrophic factor
GFAP	Glial fibrillary acidic protein
HRmax	Maximum heart rate
HRP	Horseradish peroxidase
HVA	Homovanillic acid
Iba-1b	Ionized calcium-binding adaptor molecule 1
IFN-γ	Interferon gamma
IL-1	Interleukin-1
IL-10	Interleukin-10
IL-1β	Interleukin beta 1
IL-6	Interleukin-6
MANF	Mesencephalic astrocyte-derived neurotrophic factor
METT	Early-onset high-intensity training
MLTT	Late-onset high-intensity training
mPD	Mean packing density
MPP+	1-Methyl-4-phenylpyridinium
MPTP	1-Methyl-4-phenyl-1,2,3,6-tetrahydropyridine
MPTP-LE	MPTP + late-onset treadmill training
MPTP-TE	MPTP + early-onset treadmill training
NF-κB	Nuclear factor kappa B
NGS	Normal goat serum

Ni	Number of neurons counted in the i-TH section
NO	Nitric oxide
NRS	Normal rabbit serum
OD	Optical density
PB	Phosphate-buffered
PBS	Phosphate-buffered saline
PD	Parkinson's disease
PGC-1α	Peroxisome proliferator-activated receptor gamma coactivator 1-alpha
ROI	Region of interest
ROS	Reactive oxygen species
RT	Room temperature
SAi	Square area of the i-TH analyzed ROI
SN	Substantia nigra
SNpc	Substantia nigra pars compacta
ST	Striatum
TGFβ	Transforming growth factor beta
TGF-β1	Transforming growth factor beta 1
TH	Tyrosine hydroxylase or tyrosine 3-monooxygenase, EC 1.14.16.2
TNF-α	Tumor necrosis factor alfa
UPDRS	Unified Parkinson's Disease Rating Scale
VMAT2	Vesicular monoamine transporter 2
VTA	Ventral tegmental area

References

1. Emamzadeh, F.N.; Surguchov, A. Parkinson's Disease: Biomarkers, Treatment, and Risk Factors. *Front. Neurosci.* **2018**, *12*, 612. [CrossRef]
2. Hirsch, M.A.; Farley, B.G. Exercise and neuroplasticity in persons living with Parkinson's disease. *Eur. J. Phys. Rehabil. Med.* **2009**, *45*, 215–229. [PubMed]
3. Mitchell, A.K.; Bliss, R.R.; Church, F.C. Exercise, Neuroprotective Exerkines, and Parkinson's Disease: A Narrative Review. *Biomolecules* **2024**, *14*, 1241. [CrossRef] [PubMed]
4. Cotman, C.W.; Berchtold, N.C.; Christie, L.A. Exercise builds brain health: Key roles of growth factor cascades and inflammation. *Trends Neurosci.* **2007**, *30*, 464–472. [CrossRef]
5. Mahalakshmi, B.; Maurya, N.; Lee, S.D.; Bharath Kumar, V. Possible Neuroprotective Mechanisms of Physical Exercise in Neurodegeneration. *Int. J. Mol. Sci.* **2020**, *21*, 5895. [CrossRef]
6. Bhalsing, K.S.; Abbas, M.M.; Tan, L.C.S. Role of Physical Activity in Parkinson's Disease. *Ann. Indian Acad. Neurol.* **2018**, *21*, 242–249. [CrossRef] [PubMed]
7. Uhrbrand, A.; Stenager, E.; Pedersen, M.S.; Dalgas, U. Parkinson's disease and intensive exercise therapy--a systematic review and meta-analysis of randomized controlled trials. *J. Neurol. Sci.* **2015**, *353*, 9–19. [CrossRef]
8. Gamborg, M.; Hvid, L.G.; Dalgas, U.; Langeskov-Christensen, M. Parkinson's disease and intensive exercise therapy—An updated systematic review and meta-analysis. *Acta Neurol. Scand.* **2022**, *145*, 504–528. [CrossRef]
9. Schenkman, M.; Moore, C.G.; Kohrt, W.M.; Hall, D.A.; Delitto, A.; Comella, C.L.; Josbeno, D.A.; Christiansen, C.L.; Berman, B.D.; Kluger, B.M.; et al. Effect of High-Intensity Treadmill Exercise on Motor Symptoms in Patients With De Novo Parkinson Disease: A Phase 2 Randomized Clinical Trial. *JAMA Neurol.* **2018**, *75*, 219–226. [CrossRef]
10. Alberts, J.L.; Rosenfeldt, A.B. The Universal Prescription for Parkinson's Disease: Exercise. *J. Park. Dis.* **2020**, *10*, S21–S27. [CrossRef]
11. Kakinuma, S.; Nogaki, H.; Pramanik, B.; Morimatsu, M. Muscle weakness in Parkinson's disease: Isokinetic study of the lower limbs. *Eur. Neurol.* **1998**, *39*, 218–222. [CrossRef] [PubMed]
12. Nakamura, T.; Hirayama, M.; Yamashita, F.; Uchida, K.; Hama, T.; Watanabe, H.; Sobue, G. Lowered cardiac sympathetic nerve performance in response to exercise in Parkinson's disease. *Mov. Disord.* **2010**, *25*, 1183–1189. [CrossRef] [PubMed]
13. Pechstein, A.E.; Gollie, J.M.; Guccione, A.A. Fatigability and Cardiorespiratory Impairments in Parkinson's Disease: Potential Non-Motor Barriers to Activity Performance. *J. Funct. Morphol. Kinesiol.* **2020**, *5*, 78. [CrossRef]
14. Wang, Y.; Wei, L.; Tan, M.; Yang, Z.; Gao, B.; Li, J.; Liu, Y.; Zikereya, T.; Shi, K.; Chen, W. Aerobic exercise improves motor dysfunction in Parkinson's model mice via differential regulation of striatal medium spiny neuron. *Sci. Rep.* **2024**, *14*, 12132. [CrossRef] [PubMed]

15. Palasz, E.; Niewiadomski, W.; Gasiorowska, A.; Wysocka, A.; Stepniewska, A.; Niewiadomska, G. Exercise-Induced Neuroprotection and Recovery of Motor Function in Animal Models of Parkinson's Disease. *Front. Neurol.* **2019**, *10*, 1143. [CrossRef] [PubMed]
16. Crowley, E.K.; Nolan, Y.M.; Sullivan, A.M. Exercise as a therapeutic intervention for motor and non-motor symptoms in Parkinson's disease: Evidence from rodent models. *Prog. Neurobiol.* **2019**, *172*, 2–22. [CrossRef] [PubMed]
17. Gerecke, K.M.; Jiao, Y.; Pani, A.; Pagala, V.; Smeyne, R.J. Exercise protects against MPTP-induced neurotoxicity in mice. *Brain Res.* **2010**, *1341*, 72–83. [CrossRef]
18. Palasz, E.; Niewiadomski, W.; Gasiorowska, A.; Mietelska-Porowska, A.; Niewiadomska, G. Neuroplasticity and Neuroprotective Effect of Treadmill Training in the Chronic Mouse Model of Parkinson's Disease. *Neural Plast.* **2019**, *2019*, 8215017. [CrossRef] [PubMed]
19. Watanabe, Y.; Himeda, T.; Araki, T. Mechanisms of MPTP toxicity and their implications for therapy of Parkinson's disease. *Med. Sci. Monit.* **2005**, *11*, RA17–RA23.
20. Blesa, J.; Phani, S.; Jackson-Lewis, V.; Przedborski, S. Classic and New Animal Models of Parkinson's Disease. *J. Biomed. Biotechnol.* **2012**, *2012*, 845618. [CrossRef]
21. Gerfen, C.R. Segregation of D1 and D2 dopamine receptors in the striatal direct and indirect pathways: An historical perspective. *Front. Syn. Neurosci.* **2023**, *14*, 1002960. [CrossRef]
22. Paul, G.; Sullivan, A.M. Trophic factors for Parkinson's disease: Where are we and where do we go from here? *Eur. J. Neurosci.* **2019**, *49*, 440–452. [CrossRef]
23. Pałasz, E.; Bąk, A.; Gąsiorowska, A.; Niewiadomska, G. The role of trophic factors and inflammatory processes in physical activity-induced neuroprotection in Parkinson's disease. *Postep. Hig. Med. Dosw.* **2017**, *71*, 713–726. [CrossRef]
24. Gerecke, K.M.; Jiao, Y.; Pagala, V.; Smeyne, R.J. Exercise does not protect against MPTP-induced neurotoxicity in BDNF haploinsufficient mice. *PLoS ONE* **2012**, *7*, e43250. [CrossRef]
25. Tansey, M.G.; Goldberg, M.S. Neuroinflammation in Parkinson's disease: Its role in neuronal death and implications for therapeutic intervention. *Neurobiol. Dis.* **2010**, *37*, 510–518. [CrossRef]
26. Vivekanantham, S.; Shah, S.; Dewji, R.; Dewji, A.; Khatri, C.; Ologunde, R. Neuroinflammation in Parkinson's disease: Role in neurodegeneration and tissue repair. *Int. J. Neurosci.* **2015**, *125*, 717–725. [CrossRef] [PubMed]
27. Jang, Y.; Kwon, I.; Song, W.; Cosio-Lima, L.M.; Lee, Y. Endurance Exercise Mediates Neuroprotection Against MPTP-mediated Parkinson's Disease via Enhanced Neurogenesis, Antioxidant Capacity, and Autophagy. *Neuroscience* **2018**, *379*, 292–301. [CrossRef] [PubMed]
28. Lau, Y.-S.; Patki, G.; Das-Panja, K.; Le, W.-D.; Ahmad, S.O. Neuroprotective effects and mechanisms of exercise in a chronic mouse model of Parkinson's disease with moderate neurodegeneration. *Eur. J. Neurosci.* **2011**, *33*, 1264–1274. [CrossRef] [PubMed]
29. Tajiri, N.; Yasuhara, T.; Shingo, T.; Kondo, A.; Yuan, W.; Kadota, T.; Wang, F.; Baba, T.; Tayra, J.T.; Morimoto, T.; et al. Exercise exerts neuroprotective effects on Parkinson's disease model of rats. *Brain Res.* **2010**, *1310*, 200–207. [CrossRef]
30. Real, C.C.; Ferreira, A.F.B.; Chaves-Kirsten, G.P.; Torrão, A.S.; Pires, R.S.; Britto, L.R.G. BDNF receptor blockade hinders the beneficial effects of exercise in a rat model of Parkinson's disease. *Neuroscience* **2013**, *237*, 118–129. [CrossRef] [PubMed]
31. Goes, A.T.; Souza, L.C.; Filho, C.B.; Del Fabbro, L.; De Gomes, M.G.; Boeira, S.P.; Jesse, C.R. Neuroprotective effects of swimming training in a mouse model of Parkinson's disease induced by 6-hydroxydopamine. *Neuroscience* **2014**, *256*, 61–71. [CrossRef] [PubMed]
32. Tuon, T.; Souza, P.S.; Santos, M.F.; Pereira, F.T.; Pedroso, G.S.; Luciano, T.F.; De Souza, C.T.; Dutra, R.C.; Silveira, P.C.; Pinho, R.A. Physical Training Regulates Mitochondrial Parameters and Neuroinflammatory Mechanisms in an Experimental Model of Parkinson's Disease. *Oxid. Med. Cell. Longev.* **2015**, *2015*, 261809. [CrossRef]
33. Real, C.C.; Garcia, P.C.; Britto, L.R.G. Treadmill Exercise Prevents Increase of Neuroinflammation Markers Involved in the Dopaminergic Damage of the 6-OHDA Parkinson's Disease Model. *J. Mol. Neurosci.* **2017**, *63*, 36–49. [CrossRef]
34. de Almeida, E.J.R.; Ibrahim, H.J.; Chitolina Schetinger, M.R.; de Andrade, C.M.; Cardoso, A.M. Modulation of Inflammatory Mediators and Microglial Activation Through Physical Exercise in Alzheimer's and Parkinson's Diseases. *Neurochem. Res.* **2022**, *47*, 3221–3240. [CrossRef] [PubMed]
35. Strohm, A.O.; Majewska, A.K. Physical exercise regulates microglia in health and disease. *Front. Neurosci.* **2024**, *18*, 1420322. [CrossRef]
36. Ishaq, S.; Shah, I.A.; Lee, S.-D.; Wu, B.-T. Effects of exercise training on nigrostriatal neuroprotection in Parkinson's disease: A systematic review. *Front. Neurosci.* **2025**, *18*, 1464168. [CrossRef]
37. Ahmad, S.O.; Park, J.-H.; Stenho-Bittel, L.; Lau, Y.-S. Effects of endurance exercise on ventral tegmental area neurons in the chronic 1-methyl-4-phenyl-1,2,3,6-tetrahydropyridine and probenecid-treated mice. *Neurosci. Lett.* **2009**, *450*, 102–105. [CrossRef]
38. Tillerson, J.L.; Caudle, W.M.; Reveron, M.E.; Miller, G.W. Exercise induces behavioral recovery and attenuates neurochemical deficits in rodent models of Parkinson's disease. *Neuroscience* **2003**, *119*, 899–911. [CrossRef] [PubMed]

39. Pothakos, K.; Kurz, M.; Lau, Y.-S. Restorative effect of endurance exercise on behavioral deficits in the chronic mouse model of Parkinson's disease with severe neurodegeneration. *BMC Neurosci.* **2009**, *10*, 6. [CrossRef] [PubMed]
40. Petzinger, G.M.; Walsh, J.P.; Akopian, G.; Hogg, E.; Abernathy, A.; Arevalo, P.; Turnquist, P.; Vucković, M.; Fisher, B.E.; Togasaki, D.M.; et al. Effects of treadmill exercise on dopaminergic transmission in the 1-methyl-4-phenyl-1,2,3, 6-tetrahydropyridine-lesioned mouse model of basal ganglia injury. *J. Neurosci.* **2007**, *27*, 5291–5300. [CrossRef] [PubMed]
41. Choi-Lundberg, D.L.; Lin, Q.; Chang, Y.N.; Chiang, Y.L.; Hay, C.M.; Mohajeri, H.; Davidson, B.L.; Bohn, M.C. Dopaminergic Neurons Protected from Degeneration by GDNF Gene Therapy. *Science* **1997**, *275*, 838–841. [CrossRef]
42. Kramer, B.C.; Goldman, A.D.; Mytilineou, C. Glial cell line derived neurotrophic factor promotes the recovery of dopamine neurons damaged by 6-hydroxydopamine in vitro. *Brain Res.* **1999**, *851*, 221–227. [CrossRef] [PubMed]
43. Wu, S.Y.; Wang, T.F.; Yu, L.; Jen, C.J.; Chuang, J.I.; Wu, F.S.; Wu, C.W.; Kuo, Y.M. Running exercise protects the substantia nigra dopaminergic neurons against inflammation-induced degeneration via the activation of BDNF signaling pathway. *Brain Behav. Immun.* **2011**, *25*, 135–146. [CrossRef]
44. Porritt, M.J.; Batchelor, P.E.; Howells, D.W. Inhibiting BDNF expression by antisense oligonucleotide infusion causes loss of nigral dopaminergic neurons. *Exp. Neurol.* **2005**, *192*, 226–234. [CrossRef]
45. Boger, H.A.; Middaugh, L.D.; Huang, P.; Zaman, V.; Smith, A.C.; Hoffer, B.J.; Tomac, A.C.; Granholm, A.C. A partial GDNF depletion leads to earlier age-related deterioration of motor function and tyrosine hydroxylase expression in the substantia nigra. *Exp. Neurol.* **2006**, *202*, 336–347. [CrossRef] [PubMed]
46. Boche, D.; Perry, V.H.; Nicoll, J.A.R. Review: Activation patterns of microglia and their identification in the human brain. *Neuropathol. Appl. Neurobiol.* **2013**, *39*, 3–18. [CrossRef] [PubMed]
47. Butovsky, O.; Weiner, H.L. Microglial signatures and their role in health and disease. *Nat. Rev. Neurosci.* **2018**, *19*, 622–635. [CrossRef] [PubMed]
48. Jeong, H.K.; Ji, K.; Min, K.; Joe, E.H. Brain inflammation and microglia: Facts and misconceptions. *Exp. Neurobiol.* **2013**, *22*, 59–67. [CrossRef] [PubMed]
49. Bortolanza, M.; Cavalcanti-Kiwiatkoski, R.; Padovan-Neto, F.E.; da-Silva, C.A.; Mitkovski, M.; Raisman-Vozari, R.; Del-Bel, E. Glial activation is associated with l-DOPA induced dyskinesia and blocked by a nitric oxide synthase inhibitor in a rat model of Parkinson's disease. *Neurobiol. Dis.* **2015**, *73*, 377–387. [CrossRef] [PubMed]
50. Roy, A.; Jana, A.; Yatish, K.; Freidt, M.B.; Fung, Y.K.; Martinson, J.A.; Pahan, K. Reactive oxygen species up-regulate CD11b in microglia via nitric oxide: Implications for neurodegenerative disease. *Free Radic. Biol. Med.* **2008**, *45*, 686–699. [CrossRef] [PubMed]
51. Jurga, A.M.; Paleczna, M.; Kuter, K.Z. Overview of General and Discriminating Markers of Differential microglia Phenotypes. *Front. Cell. Neurosci.* **2020**, *14*, 198. [CrossRef] [PubMed]
52. Ohsawa, K.; Imai, Y.; Sasaki, Y.; Kohsaka, S. Microglia/macrophage-specific protein Iba1 binds to fimbrin and enhances its actin-bundling activity. *J. Neurochem.* **2004**, *88*, 844–856. [CrossRef]
53. Deininger, M.H.; Meyermann, R.; Schluesener, H.J. The allograft inflammatory factor-1 family of proteins. *FEBS Lett.* **2002**, *514*, 115–121. [CrossRef] [PubMed]
54. Koo, J.H.; Jang, Y.C.; Hwang, D.J.; Um, H.S.; Lee, N.H.; Jung, J.H.; Cho, J.Y. Treadmill exercise produces neuroprotective effects in a murine model of Parkinson's disease by regulating the TLR2/MyD88/NF-κB signaling pathway. *Neuroscience* **2017**, *356*, 102–113. [CrossRef]
55. Sconce, M.D.; Churchill, M.J.; Greenea, A.R.E.; Meshul, C.K. Intervention with Exercise Restores Motor Deficits But Not Nigrostriatal Loss in a Progressive MPTP Mouse Model of Parkinson's Disease. *Neuroscience* **2015**, *299*, 156–174. [CrossRef] [PubMed]
56. Woods, J.A.; Wilund, K.R.; Martin, S.A.; Kistler, B.M. Exercise, inflammation and aging. *Aging Dis.* **2012**, *3*, 130–140. [PubMed]
57. Febbraio, M.A.; Pedersen, B.K. Muscle-derived interleukin-6: Mechanisms for activation and possible biological roles. *FASEB J.* **2002**, *16*, 1335–1347. [CrossRef] [PubMed]
58. Pedersen, M.; Bruunsgaard, H.; Weis, N.; Hendel, H.W.; Andreassen, B.U.; Eldrup, E.; Dela, F.; Pedersen, B.K. Circulating levels of TNF-alpha and IL-6-relation to truncal fat mass and muscle mass in healthy elderly individuals and in patients with type-2 diabetes. *Mech. Ageing Dev.* **2003**, *124*, 495–502. [CrossRef]
59. Starkie, R.; Ostrowski, S.R.; Jauffred, S.; Febbraio, M.; Pedersen, B.K. Exercise and IL-6 infusion inhibit endotoxin-induced TNF-alpha production in humans. *FASEB J.* **2003**, *17*, 884–886. [CrossRef] [PubMed]
60. Brooks, S.V.; Vasilaki, A.; Larkin, L.M.; McArdle, A.; Jackson, M.J. Repeated bouts of aerobic exercise lead to reductions in skeletal muscle free radical generation and nuclear factor kappa B activation. *J. Physiol.* **2008**, *586*, 3979–3990. [CrossRef] [PubMed]
61. Scheele, C.; Nielsen, S.; Pedersen, B.K. ROS and myokines promote muscle adaptation to exercise. *Trends Endocrinol. Metabol.* **2009**, *20*, 95–990. [CrossRef]
62. Beavers, K.M.; Hsu, F.C.; Isom, S.; Kritchevsky, S.B.; Church, T.; Goodpaster, B.; Pahor, M.; Nicklas, B.J. Long-term physical activity and inflammatory biomarkers in older adults. *Med. Sci. Sports Exerc.* **2010**, *42*, 2189–2196. [CrossRef] [PubMed]

63. Ho, M.S. Microglia in Parkinson's Disease. *Adv. Exp. Med. Biol.* **2019**, *1175*, 335–353. [CrossRef] [PubMed]
64. Gao, C.; Jiang, J.; Tan, Y.; Chen, S. Microglia in neurodegenerative diseases: Mechanism and potential therapeutic targets. *Signal Transduct. Target. Ther.* **2023**, *8*, 359. [CrossRef]
65. McGeer, P.L.; McGeer, E.G. Glial reactions in Parkinson's disease. *Mov. Disord.* **2008**, *23*, 474–483. [CrossRef] [PubMed]
66. Lindahl, M.; Saarma, M.; Lindholm, P. Unconventional neurotrophic factors CDNF and MANF: Structure, physiological functions and therapeutic potential. *Neurobiol. Dis.* **2017**, *97*, 90–102. [CrossRef]
67. Tanabe, K.; Nishimura, K.; Dohi, S.; Kozawa, O. Mechanisms of interleukin-1beta-induced GDNF release from rat glioma cells. *Brain Res.* **2009**, *1274*, 11–20. [CrossRef]
68. Fonseca, C.P.; Gama, S.; Saavedra, A.; Baltazar, G. H_2O_2- or $_L$-DOPA-injured dopaminergic neurons trigger the release of soluble mediators that up-regulate striatal GDNF through different signalling pathways. *Biochim. Biophys. Acta* **2014**, *1842*, 927–934. [CrossRef] [PubMed]
69. Zigmond, M.J.; Cameron, J.L.; Hoffer, B.J.; Smeyne, R.J. Neurorestoration by physical exercise: Moving forward. *Park. Relat. Disord.* **2012**, *18* (Suppl. S1), S147–S150. [CrossRef]
70. de Laat, B.; Hoye, J.; Stanley, G.; Hespeler, M.; Ligi, J.; Mohan, V.; Wooten, D.W.; Zhang, X.; Nguyen, T.D.; Key, J.; et al. Intense exercise increases dopamine transporter and neuromelanin concentrations in the substantia nigra in Parkinson's disease. *NPJ Park. Dis.* **2024**, *10*, 34. [CrossRef]
71. Delva, A.; Van Laere, K.; Vandenberghe, W. Longitudinal Positron Emission Tomography Imaging of Presynaptic Terminals in Early Parkinson's Disease. *Mov. Disord.* **2022**, *37*, 1883–1892. [CrossRef]
72. Zecca, L.; Fariello, R.; Riederer, P.; Sulzer, D.; Gatti, A.; Tampellini, D. The absolute concentration of nigral neuromelanin, assayed by a new sensitive method, increases throughout the life and is dramatically decreased in Parkinson's disease. *FEBS Lett.* **2002**, *510*, 216–220. [CrossRef]
73. Falvo, M.J.; Schilling, B.K.; Earhart, G.M. Parkinson's disease and resistive exercise: Rationale, review, and recommendations. *Mov. Disord.* **2008**, *23*, 1–11. [CrossRef]
74. Earhart, G.M.; Falvo, M.J. Parkinson disease and exercise. *Comp. Physiol.* **2013**, *3*, 833–848. [CrossRef]
75. Niewiadomski, W.; Gąsiorowska, A.; Żyliński, M.; Karbowniczek, A.; Cebrat, J.; Stępniewska, A. Exaggerated pressor response to static squats in Parkinson's disease (PD) and healthy subjects is likely an individual trait, not influenced by whole body vibration (WBV). *NeuroRehabilitation* **2023**, *52*, 289–298. [CrossRef] [PubMed]
76. Keller, K.; Stelzer, K.; Ostad, M.A.; Post, F. Impact of exaggerated blood pressure response in normotensive individuals on future hypertension and prognosis: Systematic review according to PRISMA guideline. *Adv. Med. Sci.* **2017**, *62*, 317–329. [CrossRef] [PubMed]
77. Wang, J.; Song, H.; Tang, X.; Yang, Y.; Vieira, V.J.; Niu, Y.; Ma, Y. Effect of exercise training intensity on murine T-regulatory cells and vaccination response. *Scand. J. Med. Sci. Sports* **2012**, *22*, 643–652. [CrossRef]
78. Barber-Singh, J.; Seo, B.B.; Nakamaru-Ogiso, E.; Lau, Y.S.; Matsuno-Yagi, A.; Yagi, T. Neuroprotective effect of long-term NDI1 gene expression in a chronic mouse model of Parkinson disorder. *Rejuven. Res.* **2009**, *12*, 259–267. [CrossRef]
79. Paxinos, G.; Franklin, K.B.J. *The Mouse Brain in Stereotaxic Coordinates*, 2nd ed.; Academic Press: San Diego, CA, USA, 2001.
80. Baquet, Z.C.; Williams, D.; Brody, J.; Smeyne, R.J. A comparison of model-based (2D) and design-based (3D) stereological methods for estimating cell number in the substantia nigra pars compacta (SNpc) of the C57BL/6J mouse. *Neuroscience* **2009**, *161*, 1082–1090. [CrossRef]

Disclaimer/Publisher's Note: The statements, opinions and data contained in all publications are solely those of the individual author(s) and contributor(s) and not of MDPI and/or the editor(s). MDPI and/or the editor(s) disclaim responsibility for any injury to people or property resulting from any ideas, methods, instructions or products referred to in the content.

International Journal of
Molecular Sciences

MDPI

Opinion

The Genetic Background of the Immunological and Inflammatory Aspects of Progressive Supranuclear Palsy

Piotr Alster * and Natalia Madetko-Alster *

Department of Neurology, Medical University of Warsaw, Kondratowicza 8, 03-242 Warsaw, Poland
* Correspondence: piotr.alster@wum.edu.pl (P.A.); natalia.madetko@wum.edu.pl (N.M.-A.);
Tel.: +48223265744 (P.A. & N.M.-A.)

Abstract: Progressive supranuclear palsy (PSP) is a neurodegenerative disease, classified as an atypical Parkinsonian syndrome, that has been pathologically and clinically defined. The histopathological aspects of the disease include tufted astrocytes, while the clinical features involve oculomotor dysfunction, postural instability, akinesia, cognitive impairment, and language difficulties. Although PSP is generally considered a sporadic disease, interest is growing in its genetics, with contemporary research focusing on familial backgrounds and neuroinflammation. Indeed, microglial activation and other inflammatory mechanisms of PSP pathogenesis have been extensively analyzed using genetic examinations to identify the factors impacting neurodegeneration. As such, this review aims to elaborate on recent findings in this field.

Keywords: PSP; MAPT; microglia; genetics; atypical parkinsonism

1. Introduction

Progressive supranuclear palsy (PSP) is a rare neurodegenerative disease characterized by four-repeat tauopathy [1]. Among its crucial pathological elements are tufted astrocytes, with clinical manifestations, including akinesia, postural instability, oculomotor dysfunction, cognitive impairment, and language difficulties [2]. The disease, which has a prevalence of 5.8 to 6.5 per 100,000 [3], is defined within specific domains that distinguish multiple clinical phenotypes. PSP–Richardson's syndrome (PSP-RS) is the most common subtype and features pronounced oculomotor dysfunction, an early presence of falls, and a lack of responsiveness to levodopa. PSP–parkinsonism-predominant (PSP-P) is an entity that, due to its clinical overlap with Parkinson's disease (PD), may be indistinguishable in the early stages [4]. Among the less common PSP subtypes are PSP–pure akinesia with gait freezing (PSP-PAGF), PSP–corticobasal syndrome (PSP-CBS), PSP–behavioral variant of frontotemporal dementia (PSP-bvFTD), PSP–progressive non-fluent aphasia (PSP-PNFA), PSP–frontal-dominant, PSP with predominant cerebellar ataxia, and PSP with oculomotor dysfunction [2].

PSP is characterized by pronounced clinical deterioration; inefficient diagnosis through in vivo diagnostic tools such as magnetic resonance imaging (MRI), positron emission tomography (PET), and single-photon emission computed tomography (SPECT); and a lack of evidence-based treatments. Indeed, in vivo examination only enables a possible or probable diagnosis, with a definite diagnosis dependent on neuropathological evaluation [2]. PSP is generally considered a sporadic disease, although research into a link between familial genetics and increased risk of the disease is evolving alongside investigations into genetic aspects of PSP and inflammation-induced neurodegeneration. Despite multiple studies

on the pathogenesis of PSP indicating a possible impact of glial activation, it is unclear whether inflammation is the cause or consequence of neurodegenerative mechanisms [5,6]. In PSP, the issue of autoimmune mechanisms was brought up based on HLA phenotyping in neuropathologically verified PSP cases [7]. Wang et al., in a preliminary study, showed that epitopes within the tau peptide may have affinity to HLA alleles, which could be detected in a subset of PSP patients. Anti-IGLON5, a disease that clinically partially overlaps with PSP, is associated with the presence of HLA-DRB1*10:01 and HLA-DQB1*05:01 alleles [8]. Certain features of microglial activation and cytokines derived therefrom may be linked with a potentially beneficial impact on clinical impairments, contrary to their role in atrophic changes [5,6,9,10]. Additionally, different clinical subtypes are associated with diverse interleukin and inflammatory factor profiles that, considering the impact of tau loading and its distribution, may be determined by genetics [11–14]. Therefore, the current review provides a perspective on the features linking the genetic and inflammatory aspects of PSP.

2. The Genetic Background of Progressive Supranuclear Palsy—A General Overview

A genome-wide association study (GWAS) by Farrell et al. revealed that factors such as cortical expression of syntaxin 6 (*STX6*), RUNX family transcription factor 2 (*RUNX2*), and myelin-associated oligodendrocyte basic protein (*MOBP*) are linked with increased PSP risk [15]. A transcriptome-wide association analysis in the same study stressed the significance of multiple genes in the *6p21.32* and *17q21.32* loci, including complement C4A (*C4A*), complement C4B (*C4B*), and the microtubule-associated protein tau gene (*MAPT*). As such, the research indicates the existence of cell-specific effects on gene expression in oligodendrocytes.

The PSP tau pathology is linked to ubiquitin-fold modifier-1 (UFM1) substrate modification (UFMylation) through cascade disruption in neurofibrillary-tangle-bearing neurons [16]. Fujioka et al. analyzed 19 descriptions of familial PSP and identified Parkinsonism and oculomotor dysfunction as the most common clinical aspects of familial PSP [17]. Mutations in *MAPT* are considered the most frequent factor associated with familial PSP, while deviations linked with PSP are observed in the *17q21.31* locus and are associated with low copy number repeats accompanied by genomic inversion [18] (Table 1).

Table 1. Crucial features of *MAPT* in progressive supranuclear palsy (PSP).

		Pathogenesis of PSP
Comparison to other genetic factors	⇨	more frequently linked to the early onset of PSP than leucine-rich repeat kinase 2 (*LRRK2*) or dynactin subunit 1 (*DCTN1*)
Clinical implications	⇨	early onset of PSP
	⇨	detected in patients with PSP–Richardson's syndrome who developed features commonly associated with synucleinopathies, including autonomic failure and dream enactment behavior
Other features	⇨	the *MAPT* H1 haplotype is considered to be a risk factor for PSP
	⇨	impact on astrocyte tau distribution

Patients with *MAPT* mutations are affected by the earlier initiation of PSP symptoms than carriers of less common genetic features such as leucine-rich repeat kinase 2 (*LRRK2*) or dynactin subunit 1 (*DCTN1*) [19]. *MAPT* variants are also linked with frontotemporal dementia (FTD). In particular, the mutation N279K associated with region Ex10 is associated with FTDP-17. Furthermore, whole-exome sequencing in a 61-year-old female patient with

a clinical manifestation of PSP revealed the E342K variant of *MAPT* [20], while the homozygosity linked with the *MAPT* H1 haplotype is considered to be a risk factor for PSP and corticobasal degeneration (CBD) [21]. As such, multiple theories exist around the overlapping of neurodegeneration in both tauopathies [22]. *MAPT* mutations (*MAPT c.1024G>A*, *p. Glu342Lys*, and *MAPT c.1217 G>A*, *p. Arg406Gln*) were detected among patients with PSP-RS who developed features commonly associated with synucleinopathies, including autonomic failure and dream enactment behavior [23]. Similarly, as in Alzheimer's disease (AD), PSP pathogenesis involves the joint expression of specific N- and C-terminal *MAPT* isoforms [24].

Recent studies indicated the possible significance of PSP genetic risk factors. An examination of the *17q21.31* chromosome region and extended evaluations of α, β, and γ whole-genome duplications found an association between γ duplications and PSP risk [25].

The characteristic classical PSP phenotype symptoms may be due to entirely different entities mimicking a PSP clinical manifestation. In a case using SPECT to examine a patient with clinical features of the disease, investigators observed pronounced atrophic changes within the midbrain combined with dopamine transporter uptake deficiencies [26]. Meanwhile, a genetic evaluation revealed a novel in-frame deletion/insertion mutation in exon 3 of glial acidic fibrillary protein (*GFAP*).

PSP may be linked with pathogenic sphingomyelin phosphodiesterase 1 (*SMPD1*) variants associated with Niemann–Pick disease types A and B as its recessive cause. A study by Lim et al. presented three unrelated patients affected by the heterogenous form of the gene and a clinical manifestation of PSP-RS [27].

An evaluation of bassoon presynaptic cytomatrix protein (*BSN*) in Japanese patients with neuropathologically verified PSP highlighted two mutations at *p.Thr2542Met* and *p.Glu2759Gly*, with the former associated with cognitive impairment, Parkinsonism, and behavioral changes. On the other hand, the *p.Glu2759Gly* mutation was linked with cognitive impairment, right-dominant motor impairment, right limping gait, and postural instability [28]. The mutations differed in the context of atrophic changes, as *p.Thr2542Met* was associated with hippocampal atrophy and *p.Glu2759Gly* with left-dominant parietal atrophy. Nonetheless, atrophic changes in the midbrain tegmentum were observed in both cases. Interestingly, an analysis of neurofibrillary tangle occurrence revealed different disseminations, with tangles observed in the globus pallidus, subthalamic nucleus, substantia nigra, and CA1 in the first case and the globus pallidus, subthalamic nucleus, substantia nigra, thalamus, putamen, and brainstem tegmentum in the second mutation. However, any interpretation of the general significance of these mutations is limited since the study involved only two cases.

Whole-genome sequencing by Wang et al. found—alongside the genetic loci commonly linked with PSP pathophysiology, such as *MAPT*, *MOBP*, *STX6*, solute carrier organic anion transporter family member 1A2 (*SLCO1A2*), dual-specificity phosphatase 10 (*DUSP10*), and SP1 transcription factor (*SP1*)—signals for apolipoprotein E (*APOE*), FCH and mu domain-containing endocytic adapter 1 (*FCHO1*)/*MAP1S*, *kinesin family member 13A* (*KIF13A*), *tripartite motif-containing 24* (*TRIM24*), *tenascin XB* (*TNXB*), and *ELVOL fatty acid elongase 1* (*ELOVL1*). Interestingly, *APOE* ε2, an allele with a protective role in AD pathogenesis, was linked with increased PSP risk [29–31]. Such discrepancies may be crucial in the context of recently described differences between the tau-mediated inflammatory processes of *APOEε2* and *APOEε4* astrocytes in these two diseases [30–32]. Other studies indicate that the association between *APOE* and PSP risk factors is more ambiguous in the non-Caucasian population [33].

3. Immune Molecular Pathogenesis in Progressive Supranuclear Palsy

Although the PSP pathomechanism pathways remain unclear, hypotheses focusing on immune activation [34] are supported by evidence of the tufted astrocyte pathology being significantly enriched in microglial genes [35] and abnormal microglial transcript upregulation associated with enhanced astrocytic tau. In this context, the outcome of a GWAS by Farrell et al. on the colocalization of abnormal tau species in oligodendrocytes with *C4A* protein, using a novel pattern in deoxyribonucleic acid in PSP analysis, highlights the potential significance of internal immune functioning [15]. Neurodegeneration pathways leading to tauopathies are linked by factors that, contrarily, activate and suppress microglial activation [34]. Rexach et al. employed a weighted gene co-expression analysis to evaluate transgenic models with human mutant *MAPT* and identify co-expressed gene modules in microglia and brain tissue [34]. Their study found 13 co-expressed modules, with 7 containing microglial genes. The modules were sorted according to distinct trajectories with respect to disease progression, including (1) the earliest stages before neuronal loss and present through later stages (M_UP1, M_DOWN1, and M_DOWN2), (2) early periods of neuronal loss (M_UP2 and M_DOWN3), and (3) late-stage neurodegeneration (M_UP3) [34]. The disease periods differed in the context of genes impacting pro-inflammatory (M_UP1) and anti-inflammatory (M_DOWN1) mechanisms, leading to homeostasis deviations. Interestingly, the microglial activation patterns differed between PSP and other tauopathies, such as AD and FTD–Pick's disease. In this context, the evaluation of modules in the area of microglial activation could explain abnormalities in the levels of microglial-derived factors such as interleukin 1-beta, interleukin 6, and interferon gamma [12]. For genetic risk, PSP was matched with EARLY_DOWN1, FTD–Pick's disease with EARLY-DOWN1 and EARLY-UP1, and AD with M_UP3. The study's authors demonstrated a dual-element process involving primary suppression through type II interferon with subsequent pro-inflammatory mechanisms [34]. Follow-up research by Rexach et al. based on the use of snRNAseq and snATACseq showed that PSP astrocytes have high chromatin accessibility in normally hypermethylated regions, indicating de-repressed gene expression [36].

An analysis of module eigengenes showed their varying impact on PSP's pathophysiology, with higher expression of M4, M6, and M12 linked to the disease [37]. Cell enrichment in module M4 was linked with astrocyte genes, and M6 was linked to microglial/endothelial genes. Meanwhile, M3 was associated with oligodendroglia and lower expression in PSP, and M6 coincided with differentially expressed chemokine ligand 3 (*CL3*). An issue with microglial genes was also raised in a study evaluating ABI family member 3 (*ABI3*) and phospholipase C gamma 2 (*PLCG2*) missense variants as neurodegenerative disease risk factors among Caucasians and African Americans. Although the study was primarily based on AD assessment, it included 231 PSP patients [38] and found that microglial gene-enriched co-expression networks increased significantly in AD but not in PSP. Another study showed an association between amyloid beta, but not tau, and microgliosis, microglial activation, and increased *PLCG2* levels in the brain [39]. However, the study showed a link between *PLCG2_rs72824905-G* and tau neuropathology suppression in PSP. Furthermore, *rs72824905-G* was associated with longevity and indicated as a factor in reducing the risk of AD, dementia with Lewy bodies, and FTD but not that of PD [40].

Triggering receptor expressed in myeloid cells 2 (*TREM2*) is generally connected to the microglial-driven phagocytosis of apoptotic neuronal cells, though abnormalities in this gene can be associated with the pathogenesis of neurodegenerative disorders [41]. Indeed, an assessment of microglia-related *TREM2* revealed upregulation in the substantia nigra when 24 neuropathologically confirmed cases of PSP were compared with 14 controls [42]. Additionally, *TREM2* messenger ribonucleic acid (mRNA) corresponded with hyperphosphorylated neuronal tau in the substantia nigra. However, an analysis of

TREM2 in tauopathic mouse models showed an ambiguous role of this gene, with abnormal tau enhancement and accumulation found [43]. *TREM2* variants were also linked with atypical Parkinsonism in multiple pathologies, including synucleinopathies in the context of multiple system atrophy [44]. *TREM2* was also evaluated in PD and FTD, with further assessment revealing that *TREM2* p.R47H substitution can be interpreted as a risk factor for AD, PD, and FTD [41]. On the other hand, an analysis of the frequency of the *TREM2* p.R47H variant using a large cohort comprising AD, FTD, mild cognitive impairment, PSP, CBS, and amyotrophic lateral sclerosis (ALS) cases and controls did not find any significant links between the variant and neurodegenerative diseases other than AD [45]. Carrying p.R47H in the TREM2 gene was associated with mild cognitive impairment, amyloid deposition, and microglial activation in a study on influenza vaccine immune challenge [46]. This variant was found to show ambiguous results in the context of the risk of neurodegenerative diseases. It was indicated as a possible risk factor of sporadic amyotrophic lateral sclerosis (ALS) and essential tremor [47,48]. Contrary studies based on the examination of FTD, PD, and ALS did not show results indicating p.R47H as a definitive risk factor of these diseases [49,50]. In AD, *TREM2* mutations were linked with phosphorylated tau (p-tau)181 and soluble TREM2 and were interpreted as being related to an unfavorable clinical course. Such an analysis has yet to be undertaken for PSP [51].

PSP and CBD involve early/immediate inflammatory responses that result in a p-tau signature [52]. Briel et al. showed that, apart from those for transcription factor EB (TFEB) and nuclear factor IC (NFIC)/T-cell leukemia homeobox 1 (TLX1), the transcription factor site accessibilities are similar in both diseases. The crucial discrepancies are associated with the extent of accessibility alterations, with Jun proto-oncogene (*JUN*) $(B, D)_{HIGH}$, Fos proto-oncogene (*FOS*) $(L1, L2)_{HIGH}$, double homeobox 4 (*DUX4*), KLF transcription factor 5 (*KLF5*), MYC-associated factor X (*MAX*)/MYC proto-oncogene (*MYC*), paired box 6 (*PAX6*), and peroxisome proliferator-activated receptor gamma (*PPARG*) suggesting CBD astrocytes, and decreased *TFEB* and cAMP responsive element-binding protein 1 (*CREB1*) accessibilities indicative of PSP astrocytes [52]. The genetic risk variants of PSP and FTD were mapped to astrocytic chromatin accessibility profiles, suggesting a complex (epi-)genetic link to astrocytic pathology, with, notably, no enrichments in microglial profiles [44].

The shared features of PSP, CBD, PD, and FTD pathogenesis have been described in the context of C-X-C chemokine receptor type 4 (*CXCR4*) [53–55], which is involved in microglial activation and increases the likelihood of developing these diseases. Increased *CXCR4* expression was detected in the ventral thalamus, subthalamus, pontine tegmentum, and cerebellar nuclei, which are partially linked with the structures identified in PSP staging [52–56]. Further analyses highlighted the significance of *CXCR4* in astroglial signaling abnormalities in neurodegenerative processes [55]. Additionally, *CXCR4* interacts with microglia-related cysteine-X-cysteine chemokine ligand 12 (*CXCL12*), toll-like receptor 2 (*TLR2*), RAS-like proto-oncogene B (*RALB*), and C-C motif chemokine receptor 5 (*CCR5*) [55]. Moreover, *CCR5* is associated with blood–brain barrier integrity [55], while *CXCR4* is indicated as impacting cognitive deterioration in neurodegenerative disease within an axis including *CXCL12* and *CXCR7*. Another study highlighted the possible impact of this axis on dopaminergic neuron survival, though it did not focus on PSP [57].

MAPT dysregulation is thought to affect the astrocyte tau distribution in PSP [11], with astrocytic tau buildup found prior to its accumulation in neurons. Experiments using a p-tau antibody (AT8) revealed that AT8+ astrocytes had significantly more *MAPT* transcripts and that deviations in endogenous astrocyte mRNA resulted in increased astrocytic tau accumulation in PSP. Furthermore, this process was not associated with AD. Other genetic variants linked with neuropathologically verified PSP include *STX6* and

eukaryotic translation initiation factor 2 alpha kinase 3 (*EIF2AK3*) [57,58], with upregulated *STX6* expression found in the cerebellum [17].

4. Discussion

The associations between microglial activation and astrocytic tau in PSP and the evaluation of their molecular background raise questions about the causes of the different disease subtypes. To the best of our knowledge, no studies have been performed to genetically examine PSP in the context of its clinical subtypes. Based on the features of genes related to microglial activation, such as deviations in *TREM2* and their impact on cognitive deterioration and differences in cognition between PSP subtypes, it may be assumed that the diversity of these abnormalities plays a role in the clinical evolution of the disease [2,9,55]. However, the mechanism presented does not provide sufficient data to explain the pace of neurodegeneration in PSP compared to other neurodegenerative disorders. Moreover, the variability of immune processes leading to neurodegeneration in PSP raises concern over the repeatability of such mechanisms. Furthermore, the relatively low number of cases evaluated in genetic studies of immune processes in PSP limits an extended analysis of this issue. Nonetheless, some studies highlighting the genetic background in related conditions may be applicable to PSP due to the extent of overlap between such disorders.

5. Conclusions

The inflammatory mechanisms in PSP are an understudied issue in the analysis of the pathomechanisms of this disease (Figure 1). The diversity of paths leading to neurodegeneration in this process has been studied in terms of their causes and consequences. Inevitably, the genetic background of inflammation may partly explain the wider picture of clinical manifestations of PSP. It is not clear why certain cases develop into PSP-RS associated with pronounced clinical deterioration, while others are linked to more gradual evolution. Understanding PSP's pathomechanisms may help to progress research on the treatment of this currently incurable disease, and it seems inevitable that evaluations of the genetic aspects of PSP will be crucial in furthering our understanding.

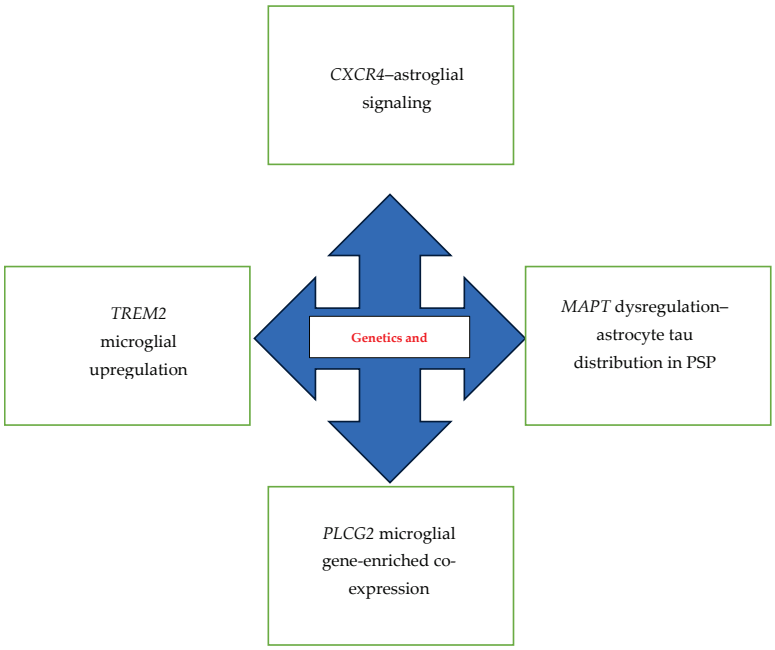


Figure 1. Aspects of immune molecular pathogenesis of progressive supranuclear palsy (PSP).

Author Contributions: P.A.: study design, data analysis, review of the literature, and final acceptance. N.M.-A.: data analysis, review of the literature, and final acceptance. All authors have read and agreed to the published version of the manuscript.

Funding: The study used internal funds.

Conflicts of Interest: The authors declare that the research was conducted without any commercial or financial relationship that could be construed as a potential conflict of interest.

References

1. Yoshida, M. Astrocytic inclusions in progressive supranuclear palsy and corticobasal degeneration. *Neuropathology* **2014**, *34*, 555–570. [CrossRef] [PubMed]
2. Höglinger, G.U.; Respondek, G.; Stamelou, M.; Kurz, C.; Josephs, K.A.; Lang, A.E.; Mollenhauer, B.; Müller, U.; Nilsson, C.; Whitwell, J.L.; et al. Clinical diagnosis of progressive supranuclear palsy: The movement disorder society criteria. *Mov. Disord.* **2017**, *32*, 853–864. [CrossRef] [PubMed] [PubMed Central]
3. Debnath, M.; Dey, S.; Sreenivas, N.; Pal, P.K.; Yadav, R. Genetic and Epigenetic Constructs of Progressive Supranuclear Palsy. *Ann. Neurosci.* **2022**, *29*, 177–188. [CrossRef]
4. Alster, P.; Madetko, N.; Koziorowski, D.; Friedman, A. Progressive Supranuclear Palsy-Parkinsonism Predominant (PSP-P)-A Clinical Challenge at the Boundaries of PSP and Parkinson's Disease (PD). *Front. Neurol.* **2020**, *11*, 180. [CrossRef] [PubMed] [PubMed Central]
5. Alster, P.; Otto-Ślusarczyk, D.; Kutyłowski, M.; Migda, B.; Wiercińska-Drapało, A.; Jabłońska, J.; Struga, M.; Madetko-Alster, N. The associations between common neuroimaging parameters of Progressive Supranuclear Palsy in magnetic resonance imaging and non-specific inflammatory factors—Pilot study. *Front. Immunol.* **2024**, *15*, 1458713. [CrossRef]
6. Chunowski, P.; Otto-Ślusarczyk, D.; Duszyńska-Wąs, K.; Drzewińska, A.; Załęski, A.; Madetko-Alster, N.; Wiercińska-Drapało, A.; Struga, M.; Alster, P. Possible Impact of Peripheral Inflammatory Factors and Interleukin-1β (IL-1β) on Cognitive Functioning in Progressive Supranuclear Palsy-Richardson Syndrome (PSP-RS) and Progressive Supranuclear Palsy-Predominant Parkinsonism (PSP-P). *Int. J. Mol. Sci.* **2024**, *25*, 13211. [CrossRef]
7. Wang, J.; Forrest, S.L.; Dasari, S.; Tanaka, H.; Rogaeva, E.; Tartaglia, M.C.; Fox, S.; Lang, A.E.; Kalyaanamoorthy, S.; Kovacs, G.G. Investigation of the HLA locus in autopsy-confirmed progressive supranuclear palsy. *Immunobiology* **2025**, *230*, 152892. [CrossRef] [PubMed]
8. Gaig, C.; Graus, F.; Compta, Y.; Högl, B.; Bataller, L.; Brüggemann, N.; Giordana, C.; Heidbreder, A.; Kotschet, K.; Lewerenz, J.; et al. Clinical manifestations of the anti-IgLON5 disease. *Neurology* **2017**, *88*, 1736–1743. [CrossRef]
9. Alster, P.; Madetko, N.; Koziorowski, D.; Friedman, A. Microglial Activation and Inflammation as a Factor in the Pathogenesis of Progressive Supranuclear Palsy (PSP). *Front. Neurosci.* **2020**, *14*, 893. [CrossRef]
10. Fernández-Botrán, R.; Ahmed, Z.; Crespo, F.A.; Gatenbee, C.; Gonzalez, J.; Dickson, D.W.; Litvan, I. Cytokine expression and microglial activation in progressive supranuclear palsy. *Parkinsonism Relat. Disord.* **2011**, *17*, 683–688. [CrossRef]
11. Jackson, R.J.; Melloni, A.; Fykstra, D.P.; Serrano-Pozo, A.; Shinobu, L.; Hyman, B.T. Astrocyte tau deposition in progressive supranuclear palsy is associated with dysregulation of MAPT transcription. *Acta Neuropathol. Commun.* **2024**, *12*, 132. [CrossRef]
12. Madetko-Alster, N.; Otto-Ślusarczyk, D.; Wiercińska-Drapało, A.; Koziorowski, D.; Szlufik, S.; Samborska-Ćwik, J.; Struga, M.; Friedman, A.; Alster, P. Clinical Phenotypes of Progressive Supranuclear Palsy-The Differences in Interleukin Patterns. *Int. J. Mol. Sci.* **2023**, *24*, 15135. [CrossRef]
13. Alster, P.; Otto-Ślusarczyk, D.; Wiercińska-Drapało, A.; Struga, M.; Madetko-Alster, N. The potential significance of hepcidin evaluation in progressive supranuclear palsy. *Brain Behav.* **2024**, *14*, e3552. [CrossRef] [PubMed]
14. Kovacs, G.G.; Lukic, M.J.; Irwin, D.J.; Arzberger, T.; Respondek, G.; Lee, E.B.; Coughlin, D.; Giese, A.; Grossman, M.; Kurz, C.; et al. Distribution patterns of tau pathology in progressive supranuclear palsy. *Acta Neuropathol.* **2020**, *140*, 99–119. [CrossRef] [PubMed]
15. Farrell, K.; Humphrey, J.; Chang, T.; Zhao, Y.; Leung, Y.Y.; Kuksa, P.P.; Patil, V.; Lee, W.P.; Kuzma, A.B.; Valladares, O.; et al. Genetic, transcriptomic, histological, and biochemical analysis of progressive supranuclear palsy implicates glial activation and novel risk genes. *Nat. Commun.* **2024**, *15*, 7880, Erratum in *Nat. Commun.* **2024**, *15*, 9828. https://doi.org/10.1038/s41467-024-53617-3. [CrossRef]
16. Parra Bravo, C.; Giani, A.M.; Madero-Perez, J.; Zhao, Z.; Wan, Y.; Samelson, A.J.; Wong, M.Y.; Evangelisti, A.; Cordes, E.; Fan, L.; et al. Human iPSC 4R tauopathy model uncovers modifiers of tau propagation. *Cell* **2024**, *187*, 2446–2464.e22. [CrossRef] [PubMed]
17. Fujioka, S.; Van Gerpen, J.A.; Uitti, R.J.; Dickson, D.W.; Wszolek, Z.K. Familial progressive supranuclear palsy: A literature review. *Neurodegener Dis.* **2014**, *13*, 180–182. [CrossRef] [PubMed]

18. Ressler, H.W.; Humphrey, J.; Vialle, R.A.; Babrowicz, B.; Kandoi, S.; Raj, T.; Dickson, D.W.; Ertekin-Taner, N.; Crary, J.F.; Farrell, K. MAPT haplotype-associated transcriptomic changes in progressive supranuclear palsy. *Acta Neuropathol. Commun.* **2024**, *12*, 135. [CrossRef]
19. Wen, Y.; Zhou, Y.; Jiao, B.; Shen, L. Genetics of Progressive Supranuclear Palsy: A Review. *J. Parkinsons. Dis.* **2021**, *11*, 93–105. [CrossRef] [PubMed] [PubMed Central]
20. Li, H.; Li, Q.; Weng, Q.; Cui, R.; Yen, T.C.; Li, Y. A novel *MAPT* variant (E342K) as a cause of familial progressive supranuclear palsy. *Front. Neurol.* **2024**, *15*, 1372507. [CrossRef] [PubMed] [PubMed Central]
21. Houlden, H.; Baker, M.; Morris, H.R.; MacDonald, N.; Pickering-Brown, S.; Adamson, J.; Lees, A.J.; Rossor, M.N.; Quinn, N.P.; Kertesz, A.; et al. Corticobasal degeneration and progressive supranuclear palsy share a common tau haplotype. *Neurology* **2001**, *56*, 1702–1706. [CrossRef] [PubMed]
22. Respondek, G.; Grimm, M.J.; Piot, I.; Arzberger, T.; Compta, Y.; Englund, E.; Ferguson, L.W.; Gelpi, E.; Roeber, S.; Giese, A.; et al. Validation of the movement disorder society criteria for the diagnosis of 4-repeat tauopathies. *Mov. Disord.* **2020**, *35*, 171–176. [CrossRef] [PubMed] [PubMed Central]
23. Badihian, N.; Ali, F.; Botha, H.; Savica, R.; Machulda, M.M.; Clark, H.M.; Stierwalt, J.A.G.; Pham, N.T.T.; Baker, M.C.; Rademakers, R.; et al. The MAPT p.E342K and p.R406W mutations are associated with progressive supranuclear palsy with atypical features. *Parkinsonism Relat. Disord.* **2024**, *119*, 105962. [CrossRef] [PubMed] [PubMed Central]
24. Sexton, C.E.; Bitan, G.; Bowles, K.R.; Brys, M.; Buée, L.; Maina, M.B.; Clelland, C.D.; Cohen, A.D.; Crary, J.F.; Dage, J.L.; et al. Novel avenues of tau research. *Alzheimer's Dement.* **2024**, *20*, 2240–2261. [CrossRef]
25. Wang, H.; Chang, T.S.; Dombroski, B.A.; Cheng, P.L.; Si, Y.Q.; Tucci, A.; Patil, V.; Valiente-Banuet, L.; Farrell, K.; Mclean, C.; et al. Association of Structural Forms of 17q21.31 with the Risk of Progressive Supranuclear Palsy and *MAPT* Sub-haplotypes. *medRxiv* **2024**. [CrossRef] [PubMed] [PubMed Central]
26. Shiina, A.; Ishikawa, D.; Ishizawa, K.; Kasahara, H.; Fujita, Y.; Mizuta, I.; Yoshida, T.; Ikeda, Y. Alexander disease with a novel GFAP insertion-deletion mutation mimicking progressive supranuclear palsy. *Clin. Neurol. Neurosurg.* **2024**, *240*, 108261. [CrossRef] [PubMed]
27. Lim, S.Y.; Tan, A.H.; Foo, J.N.; Tan, Y.J.; Chew, E.G.; Annuar, A.A.; Closas, A.M.D.; Pajo, A.; Lim, J.L.; Tay, Y.W.; et al. Loss-of-Function Variant in the SMPD1 Gene in Progressive Supranuclear Palsy-Richardson Syndrome Patients of Chinese Ancestry. *J. Mov. Disord.* **2024**, *17*, 213–217. [CrossRef] [PubMed] [PubMed Central]
28. Wakita, M.; Yaguchi, H.; Otuski, M.; Tanikawa, S.; Miki, Y.; Aiba, I.; Yoshida, M.; Nomura, T.; Uwatoko, H.; Mito, Y.; et al. Pathological study of progressive supranuclear palsy the cases with mutations in Bassoon. *Neuropathology* **2024**, *45*, 140–152. [CrossRef]
29. Wang, H.; Chang, T.S.; Dombroski, B.A.; Cheng, P.L.; Patil, V.; Valiente-Banuet, L.; Farrell, K.; Mclean, C.; Molina-Porcel, L.; Rajput, A.; et al. Whole-genome sequencing analysis reveals new susceptibility loci and structural variants associated with progressive supranuclear palsy. *Mol. Neurodegener.* **2024**, *19*, 61, Erratum in *Mol. Neurodegener.* **2024**, *19*, 73. https://doi.org/10.1186/s13024-024-00763-3. [CrossRef]
30. Li, Z.; Shue, F.; Zhao, N.; Shinohara, M.; Bu, G. APOE2: Protective mechanism and therapeutic implications for Alzheimer's disease. *Mol. Neurodegener.* **2020**, *15*, 63. [CrossRef]
31. Jackson, R.J.; Hyman, B.T.; Serrano-Pozo, A. Multifaceted roles of APOE in Alzheimer disease. *Nat. Rev. Neurol.* **2024**, *20*, 457–474. [CrossRef]
32. Mothes, T.; Konstantinidis, E.; Eltom, K.; Dakhel, A.; Rostami, J.; Erlandsson, A. Tau processing and tau-mediated inflammation differ in human *APOEε2* and *APOEε4* astrocytes. *iScience* **2024**, *27*, 111163. [CrossRef] [PubMed]
33. López González, I.; Garcia-Esparcia, P.; Llorens, F.; Ferrer, I. Genetic and Transcriptomic Profiles of Inflammation in Neurodegenerative Diseases: Alzheimer, Parkinson, Creutzfeldt-Jakob and Tauopathies. *Int. J. Mol. Sci.* **2016**, *17*, 206. [CrossRef] [PubMed]
34. Rexach, J.E.; Polioudakis, D.; Yin, A.; Swarup, V.; Chang, T.S.; Nguyen, T.; Sarkar, A.; Chen, L.; Huang, J.; Lin, L.C.; et al. Tau Pathology Drives Dementia Risk-Associated Gene Networks toward Chronic Inflammatory States and Immunosuppression. *Cell Rep.* **2020**, *33*, 108398. [CrossRef] [PubMed]
35. Allen, M.; Wang, X.; Serie, D.J.; Strickland, S.L.; Burgess, J.D.; Koga, S.; Younkin, C.S.; Nguyen, T.T.; Malphrus, K.G.; Lincoln, S.J.; et al. Divergent brain gene expression patterns associate with distinct cell-specific tau neuropathology traits in progressive supranuclear palsy. *Acta Neuropathol.* **2018**, *136*, 709–727. [CrossRef]
36. Rexach, J.E.; Cheng, Y.; Chen, L.; Polioudakis, D.; Lin, L.C.; Mitri, V.; Elkins, A.; Han, X.; Yamakawa, M.; Yin, A.; et al. Cross-disorder and disease-specific pathways in dementia revealed by single-cell genomics. *Cell* **2024**, *187*, 5753–5774.e28. [CrossRef]
37. Min, Y.; Wang, X.; İş, Ö.; Patel, T.A.; Gao, J.; Reddy, J.S.; Quicksall, Z.S.; Nguyen, T.; Lin, S.; Tutor-New, F.Q.; et al. Cross species systems biology discovers glial DDR2, STOM, and KANK2 as therapeutic targets in progressive supranuclear palsy. *Nat. Commun.* **2023**, *14*, 6801. [CrossRef]

38. Conway, O.J.; Carrasquillo, M.M.; Wang, X.; Bredenberg, J.M.; Reddy, J.S.; Strickland, S.L.; Younkin, C.S.; Burgess, J.D.; Allen, M.; Lincoln, S.J.; et al. ABI3 and PLCG2 missense variants as risk factors for neurodegenerative diseases in Caucasians and African Americans. *Mol. Neurodegener.* **2018**, *13*, 53. [CrossRef]
39. Strickland, S.L.; Morel, H.; Prusinski, C.; Allen, M.; Patel, T.A.; Carrasquillo, M.M.; Conway, O.J.; Lincoln, S.J.; Reddy, J.S.; Nguyen, T.; et al. Association of ABI3 and PLCG2 missense variants with disease risk and neuropathology in Lewy body disease and progressive supranuclear palsy. *Acta Neuropathol. Commun.* **2020**, *8*, 172. [CrossRef]
40. Van Der Lee, S.J.; Conway, O.J.; Jansen, I.; Carrasquillo, M.M.; Kleineidam, L.; van den Akker, E.; Hernández, I.; Van Eijk, K.R.; Stringa, N.; Chen, J.A.; et al. A nonsynonymous mutation in PLCG2 reduces the risk of Alzheimer's disease, dementia with Lewy bodies and frontotemporal dementia, and increases the likelihood of longevity. *Acta Neuropathol.* **2019**, *138*, 237–250, Erratum in *Acta Neuropathol.* **2020**, *139*, 959–962. https://doi.org/10.1007/s00401-019-02107-8. [CrossRef]
41. Rayaprolu, S.; Mullen, B.; Baker, M.; Lynch, T.; Finger, E.; Seeley, W.W.; Hatanpaa, K.J.; Lomen-Hoerth, C.; Kertesz, A.; Bigio, E.H.; et al. TREM2 in neurodegeneration: Evidence for association of the p.R47H variant with frontotemporal dementia and Parkinson's disease. *Mol. Neurodegener.* **2013**, *8*, 19. [CrossRef] [PubMed]
42. Sánchez-Ruiz de Gordoa, J.; Erro, M.E.; Vicuña-Urriza, J.; Zelaya, M.V.; Tellechea, P.; Acha, B.; Zueco, S.; Urdánoz-Casado, A.; Roldán, M.; Blanco-Luquin, I.; et al. Microglia-Related Gene Triggering Receptor Expressed in Myeloid Cells 2 (TREM2) Is Upregulated in the Substantia Nigra of Progressive Supranuclear Palsy. *Mov. Disord.* **2020**, *35*, 885–890. [CrossRef] [PubMed]
43. Bemiller, S.M.; McCray, T.J.; Allan, K.; Formica, S.V.; Xu, G.; Wilson, G.; Kokiko-Cochran, O.N.; Crish, S.D.; Lasagna-Reeves, C.A.; Ransohoff, R.M.; et al. TREM2 deficiency exacerbates tau pathology through dysregulated kinase signaling in a mouse model of tauopathy. *Mol. Neurodegener.* **2017**, *12*, 74. [CrossRef]
44. Leńska-Mieciek, M.; Madetko-Alster, N.; Alster, P.; Królicki, L.; Fiszer, U.; Koziorowski, D. Inflammation in multiple system atrophy. *Front. Immunol.* **2023**, *14*, 1214677. [CrossRef]
45. Ayer, A.H.; Wojta, K.; Ramos, E.M.; Dokuru, D.; Chen, J.A.; Karydas, A.M.; Papatriantafyllou, J.D.; Agiomyrgiannakis, D.; Kamtsadeli, V.; Tsinia, N.; et al. Frequency of the TREM2 R47H Variant in Various Neurodegenerative Disorders. *Alzheimer Dis. Assoc. Disord.* **2019**, *33*, 327–330. [CrossRef]
46. Cousins, O.; Schubert, J.J.; Chandra, A.; Veronese, M.; Valkimadi, P.; Creese, B.; Khan, Z.; Arathimos, R.; Hampshire, A.; Rosenzweig, I.; et al. Microglial activation, tau and amyloid deposition in TREM2 p.R47H carriers and mild cognitive impairment patients: A multi-modal/multi-tracer PET/MRI imaging study with influenza vaccine immune challenge. *J. Neuroinflammation* **2023**, *20*, 272. [CrossRef] [PubMed]
47. Cady, J.; Koval, E.D.; Benitez, B.A.; Zaidman, C.; Jockel-Balsarotti, J.; Allred, P.; Baloh, R.H.; Ravits, J.; Simpson, E.; Appel, S.H.; et al. TREM2 variant p.R47H as a risk factor for sporadic amyotrophic lateral sclerosis. *JAMA Neurol.* **2014**, *71*, 449–453. [CrossRef]
48. Ortega-Cubero, S.; Lorenzo-Betancor, O.; Lorenzo, E.; Agúndez, J.A.; Jiménez-Jiménez, F.J.; Ross, O.A.; Wurster, I.; Mielke, C.; Lin, J.J.; Coria, F.; et al. TREM2 R47H variant and risk of essential tremor: A cross-sectional international multicenter study. *Parkinsonism Relat. Disord.* **2015**, *21*, 306–309. [CrossRef]
49. Ruiz, A.; Dols-Icardo, O.; Bullido, M.J.; Pastor, P.; Rodríguez-Rodríguez, E.; de Munain, A.L.; de Pancorbo, M.M.; Pérez-Tur, J.; Álvarez, V.; Antonell, A.; et al. Assessing the role of the TREM2 p.R47H variant as a risk factor for Alzheimer's disease and frontotemporal dementia. *Neurobiol. Aging* **2014**, *35*, e1–e444. [CrossRef]
50. Lill, C.M.; Rengmark, A.; Pihlstrøm, L.; Fogh, I.; Shatunov, A.; Sleiman, P.M.; Wang, L.S.; Liu, T.; Lassen, C.F.; Meissner, E.; et al. The role of TREM2 R47H as a risk factor for Alzheimer's disease, frontotemporal lobar degeneration, amyotrophic lateral sclerosis, and Parkinson's disease. *Alzheimer's Dement.* **2015**, *11*, 1407–1416. [CrossRef]
51. McQuade, A.; Blurton-Jones, M. Microglia in Alzheimer's Disease: Exploring How Genetics and Phenotype Influence Risk. *J. Mol. Biol.* **2019**, *431*, 1805–1817. [CrossRef] [PubMed]
52. Briel, N.; Ruf, V.C.; Pratsch, K.; Roeber, S.; Widmann, J.; Mielke, J.; Dorostkar, M.M.; Windl, O.; Arzberger, T.; Herms, J.; et al. Single-nucleus chromatin accessibility profiling highlights distinct astrocyte signatures in progressive supranuclear palsy and corticobasal degeneration. *Acta Neuropathol.* **2022**, *144*, 615–635. [CrossRef]
53. Yokoyama, J.S.; Karch, C.M.; Fan, C.C.; Bonham, L.W.; Kouri, N.; Ross, O.A.; Rademakers, R.; Kim, J.; Wang, Y.; Höglinger, G.U.; et al. Shared genetic risk between corticobasal degeneration, progressive supranuclear palsy, and frontotemporal dementia. *Acta Neuropathol.* **2017**, *133*, 825–837. [CrossRef]
54. Didonna, A. Tau at the interface between neurodegeneration and neuroinflammation. *Genes Immun.* **2020**, *21*, 288–300. [CrossRef] [PubMed]
55. Bonham, L.W.; Karch, C.M.; Fan, C.C.; Tan, C.; Geier, E.G.; Wang, Y.; Wen, N.; Broce, I.J.; Li, Y.; Barkovich, M.J.; et al. *CXCR4* involvement in neurodegenerative diseases. *Transl. Psychiatry* **2018**, *8*, 73. [CrossRef] [PubMed]
56. Planche, V.; Mansencal, B.; Manjon, J.V.; Meissner, W.G.; Tourdias, T.; Coupé, P. Staging of progressive supranuclear palsy-Richardson syndrome using MRI brain charts for the human lifespan. *Brain Commun.* **2024**, *6*, fcae055. [CrossRef]

57. Sarallah, R.; Jahani, S.; Soltani Khaboushan, A.; Moaveni, A.K.; Amiri, M.; Majidi Zolbin, M. The role of CXCL12/CXCR4/CXCR7 axis in cognitive impairment associated with neurodegenerative diseases. *Brain Behav. Immun. Health* **2024**, *43*, 100932. [CrossRef]
58. Höglinger, G.U.; Melhem, N.M.; Dickson, D.W.; Sleiman, P.M.; Wang, L.S.; Klei, L.; Rademakers, R.; de Silva, R.; Litvan, I.; Riley, D.E.; et al. Identification of common variants influencing risk of the tauopathy progressive supranuclear palsy. *Nat. Genet.* **2011**, *43*, 699–705. [CrossRef] [PubMed] [PubMed Central]

Disclaimer/Publisher's Note: The statements, opinions and data contained in all publications are solely those of the individual author(s) and contributor(s) and not of MDPI and/or the editor(s). MDPI and/or the editor(s) disclaim responsibility for any injury to people or property resulting from any ideas, methods, instructions or products referred to in the content.

International Journal of
Molecular Sciences

MDPI

Review

Role of the Intestinal Microbiota in the Molecular Pathogenesis of Atypical Parkinsonian Syndromes

Dominika Przewodowska *, Piotr Alster and Natalia Madetko-Alster *

Department of Neurology, Medical University of Warsaw, Kondratowicza 8, 03-242 Warsaw, Poland; piotr.alster@wum.edu.pl
* Correspondence: dominika.przewodowska@wum.edu.pl (D.P.); natalia.madetko@wum.edu.pl (N.M.-A.)

Abstract: The role of the intestinal microbiota and its influence on neurodegenerative disorders has recently been extensively explored, especially in the context of Parkinson's disease (PD). In particular, its role in immunomodulation, impact on inflammation, and participation in the gut–brain axis are under ongoing investigations. Recent studies have revealed new data that could be important for exploring the neurodegeneration mechanisms connected with the gut microbiota, potentially leading to the development of new methods of treatment. In this review, the potential roles of the gut microbiota in future disease-modifying therapies were discussed and the properties of the intestinal microbiota—including its impacts on metabolism and short-chain fatty acids and vitamins—were summarized, with a particular focus on atypical Parkinsonian syndromes. This review focused on a detailed description of the numerous mechanisms through which the microbiota influences neurodegenerative processes. This review explored potentially important connections between the gut microbiota and the evolution and progression of atypical Parkinsonian syndromes. Finally, a description of recently derived results regarding the microbiota alterations in atypical Parkinsonian syndromes in comparison with results previously described in PD was also included.

Keywords: atypical Parkinsonian syndromes; Parkinson disease; neurodegeneration; intestinal microbiota; systemic inflammation; gut–brain axis; α-synuclein; tau; short-chain fatty acids; vitamin B12

1. Introduction

Atypical Parkinsonian syndromes (APSs) comprise various neurodegenerative disorders characterized by rapid progression, poor levodopa responsiveness and shorter life expectancy when compared to Parkinson's disease (PD) [1]. Among them, Progressive Supranuclear Palsy (PSP), Multiple System Atrophy (MSA), Corticobasal Syndrome (CBS) and Frontotemporal Dementia (FTD) can be distinguished. Although all of the above entities are classified as neurodegenerative diseases caused by the accumulation of abnormal proteins, the compositions of these deposits differ. PSP and CBS are grouped with the FTD-related disorders due to their underlying tau pathology, while MSA and PD are described as α-synucleinopathies [2].

Frontotemporal dementia (FTD), first described by Pick in 1892, is a clinical manifestation of neuronal degeneration in the frontal and temporal lobes. As these structures are mainly responsible for speech and behavior control, loss of neurons leads to progressive aphasia and cognitive and behavioral dysfunction [3]. Pathologically, it is recognized by a tau- and TDP-43-based pathology [4]. In some cases, patients initially diagnosed with FTD

develop additional symptoms, such as gait disturbance, increased falls and supranuclear palsy [4]. In this case, the behavioral FTD variant of PSP should be diagnosed (PSP-bvFTD). It is worth mentioning that, among the various PSP subtypes, PSP-Parkinsonism predominant (PSP-P) and PSP-Richardson Syndrome (PSP-RS) are the most common. Pseudobulbar and horizontal gaze palsy concomitant with axial rigidity and postural instability are described as the core clinical features of PSP. In PSP-P, tremor, rigidity and bradykinesia are typical symptoms, while a reduction in horizontal eye movement, gait instability, falls and profoundly progressing cognitive decline is described in the context of PSP-RS [4].

The main symptom of MSA is dysautonomia (dysfunction of the autonomic system) concomitant with cerebellar signs (MSA-C) or Parkinsonism (MSA-P) [5]. The chronic progression of clinical symptoms with transient, poor or no levodopa response and relatively rare cognitive decline are characteristic of the disease.

Neurocognitive dysfunction—often misdiagnosed as AD—is a common sign of CBS. Coincidentally, it is also characterized by alien limb phenomena, described as asymmetric rigidity, hypokinesia and dystonia with numerous uncontrolled limb movements [2]. At present, there are no data concerning dysbiosis in corticobasal degeneration (CBD), which could be (at least partially) explained by the rarity of the disease and the need for neuropathological examination in order to obtain a diagnosis. CBS, which can be diagnosed based on the clinical syndrome, is very diverse in the context of neuropathology, which could explain the lack of studies concerning the gut microbiota with respect to this disease.

The criteria for diagnosing particular forms of atypical Parkinsonism are constantly being modified in response to the results of new studies. The final and only certain way to make the right diagnosis is a post-mortem examination of the brain. Making the most probable diagnosis as soon as possible is crucial, as standard methods of therapy are not satisfactory in patients with APSs. Modern researchers are trying to find as many potential factors as possible that contribute to neurodegeneration in patients with APSs in the hope of determining possible drug targets for use in future therapies. The data from APS studies have indicated differences in the type of protein accumulated in the CNS, the levels of individual inflammatory markers, the degree of reaction to pain, and the expression levels of genes leading to the development of pathology in the brain [3,4,6,7].

While the prevalence of Parkinson's disease is expected to increase from 76 (in 2021) to 267 cases per 100,000 in 2050, the prevalence of APS tends to remain stable over time and has been estimated as less than 10 per 10,000 [8,9]. At present, the exact pathomechanism of neurodegeneration in APS remains unknown, although there is likely a multitudinous combination of endo- and exogenic factors generally affecting the pace of neurodegeneration [10]. The genetic background of neuronal deterioration, as well as its correlation with toxin exposure or brain injury, have been broadly described in the literature, although an "enriched environment" due to anti-oxidative properties seems to act as another factor impacting the number of neuronal cell deaths [10,11]. Among multiple theories explaining the mechanisms of neurodegeneration, the involvement of inflammatory processes is certain, although it has still not been definitively established whether it this a cause or result of the disease. Recognizing the human body as a combination of interconnected systems, the search for factors influencing the exacerbation of inflammation is one of the most widespread topics in the contemporary literature.

Although Braak's dual-hit hypothesis of sporadic PD development has been widely recognized for nearly 20 years, its accuracy remains a subject of debate. According to Braak's idea, the process of neurodegeneration within the central nervous system (CNS) remains strictly dependent on the conditions of the digestive tract, being the expanded system connecting the external environment with the brain. When potential pathogens (virus, bacteria) achieve access to the olfactory bulb, they can also pass through the nasal

cavity and into the digestive tract after being swallowed. Through the promotion of regional inflammation and intestinal barrier disruption, these pathogens stimulate local α-synuclein accumulation, which then could be transported by the vagal nerve into the CNS [12]. Braak's theory remains only partially in line with that of Horsager, who has proposed another mechanism of PD development and highlighted its two phenotypes [13]. While Braak's theory applies to PD and α-synuclein, it is not known whether and to what extent it can be extended to tauopathies. The previously mentioned model of α-synuclein accumulation starts with non-specific inflammation in the gastrointestinal tract and assumes its further dispersion into the CNS. According to Horsager, this is described as a body-first phenotype, linked with an increased risk of motor/dysautonomic symptoms, clinically distinguished from the second, brain-first phenotype by the presence of rapid eye movement (REM) sleep behavior disorder (RBD). According to this theory, the disease can start initially in the CNS—on the level of the substantia nigra pars compacta dopaminergic neurons—and then spread within the cortex. This model is more common in patients with *LRRK2* mutations [14]. Due to clinical similarities, it could be assumed that the mechanisms underlying APSs might resemble one another. Beside the fact that inflammation is present even before protein accumulation, the number of involved immunological pathways is so wide that it seems to be impossible to choose only one factor strictly related to the initiation of inflammatory processes and eventual progression. While diet, aging, infections and gut dysbiosis (imbalance in the gut microflora), among other factors, seem to represent environmental modulators, the roles of genetics and endogenic mediators have also been strictly discussed.

According to McGeers' hypothesis, a local inflammatory reaction within the brain can promote microglial activation, resulting in enhanced oxidative stress reactions. Increased expression levels of IL-1, IL-6 and TNF-alpha in cerebral tissue concurrent with increased complement system activity provides evidence for the possible role of regional inflammation when explaining the pathogenesis of PD [15]. The exact role of inflammation in initiating neurodegeneration or its potential reactive character still requires more extensive evaluation.

The existence of neuro-inflammatory processes in neurodegenerative disorders is not in doubt and has been observed in in vivo trials [16]. Furthermore, multiple studies have provided data supporting the potential role of inflammation in the course of the disease; for example, Madetko-Alster et al. described differences between the cytokine profiles in blood and CSF among patients with PSP-P and PSP-RS. Significant differences between IL-1 and IL-6 concentrations with respect to PSP-P and PSP-RS patients could be explained by microglial activity and IL release, with a potential impact on the progression of the disease [17].

The inflammatory processes present during neurodegeneration are generalized and can be reflected by unspecific peripheral parameters. Investigations of the serum lymphocyte-to-monocyte ratio (LMR), neutrophil-to-lymphocyte ratio (NLR) and neutrophil-to-high density lipoprotein ratio (NHR) revealed higher parameters of NLR and NHR concurrently with lower LMR in patients with PD in comparison with HC, in correspondence with the severity of the disease [18]. Madetko-Alster et al. reported increased levels of NLR as well as another parameter—the platelet-to-lymphocyte ratio (PLR)—in PD (in comparison with HC), with no statistically significant differences in NLR and PLR between patients with PD and MSA-P. In MSA-P patients, only NLR was significantly higher when compared with HC [19]. Although no explanation for this observation has been fully established, the intestinal microbiota and its bacterial composition could act as potential factors triggering inflammation, thus resulting in different levels of inflammatory enhancement.

This paper provides a narrative review concerning the potential roles of the gut microbiota in the pathogenesis of atypical Parkinsonian syndromes. The PubMed and Google Scholar databases were searched for papers related to the molecular mechanisms of bacterial activity in the context of atypical Parkinsonian syndromes. The following medical subject headings were used: "atypical parkinsonian syndromes—role of intestinal microbiota", "molecular mechanisms of neurodegeneration", "microbiota activity", "gut-brain axis activity", "gut–brain axis modulation" and "role of bacteria in neuroinflammation". All search results were manually reviewed prior to inclusion in this review. This review focuses mostly on original papers published within the past 5 years and/or studies that are highly relevant to the topic of the gut microbiota in Parkinsonian syndromes. Pilot studies and case reports were excluded from the analysis.

2. Role of the Intestinal Microbiota in Inflammation and PD Pathogenesis

The human digestive tract is a commonly known area of existence for about 100 trillion micro-organisms, including more than 160 bacterial species. The term "microbiota" refers to the group of living organisms existing in a certain environment, comprising bacteria, archaea, fungi, protists and algae, while not including phages, viruses, plasmids, prions, viroids, and free DNA [2]. Regarding bacteria, *Firmicutes*, *Bacteroidetes*, *Actinobacteria*, *Fusobacteria*, *Proteobacteria* and *Verrucomicrobia* make up the majority (i.e., up to 90%) of the intestinal microenvironment, with their concentration, composition and proportion differing among individuals, depending, i.e., on their localization in the gastrointestinal (GI) tract. The highest bacterial concentration is observed in the distal region (colon) [20]. At least 30% of the microbiota composition remains as a constant core group, while the remaining part is related to numerous factors such as lifestyle (stress, diet) and environment, as mentioned before [20,21].

The microbiota participates in crosstalk with the human body, forming an overarching system called a holobiont: the human digestive tract serves as a suitable environment for the sustainable development of bacteria and the production of numerous substances enabling the maintenance of homeostasis [22]. Interestingly, specific changes in the composition of microflora has been associated with the precise exacerbation of the clinical symptoms of PD—both cognitive and motor [23].

The availability of oxygen in the singular sections of the digestive tract strictly defines the type of bacteria living in that space. While *Lactobacillus* strains constitute the majority in the duodenum, anaerobic *Ruminococcaceae* and *Lachnospiraceae* predominate in the large intestine. Moreover, due to the presence of the intestinal barrier, bacteria that multiply and live in the intestinal lumen (LM) or in the mucous membrane (MAM) can be distinguished. Luminal bacteria in the duodenum are responsible for carbohydrate metabolism, while mucosal bacteria play a major role in endocrine system coordination. Large intestine luminal bacteria are focused mainly on lipid metabolism, while mucosal bacteria focus on general interactions with the host [24].

Inflammation—in addition to its undeniable impact in terms of increasing the permeability of the intestinal barrier—influences the selection of bacteria that are able to grow in the non-physiological conditions of this environment. Similarly to the blood–brain barrier, the integrity of the intestinal layer seems to act as a crucial factor protecting against pathogens and limiting the risk of toxic molecule absorption. The intestinal microbiota remains a key factor engaged with gut–brain axis activity. At present, numerous products of bacterial metabolic paths are being researched as factors that may reduce the risk of systemic inflammation and additional neurodegeneration [25].

Although the results of studies based on *Akkermansia* species remain contradictory, they are known as mucin-degrading bacteria, provoking a loss of intestinal barrier function while promoting gut inflammation and endotoxemia [26]. Nevertheless, in animal models, *Akkermansia muciniphila* has been shown to regulate the activity of T regulatory cells, short-chain fatty acid (SCFA) production and intestinal passage prolongation, as well as improving cognitive function by inhibiting the pro-inflammatory IL-6-dependent pathway [26,27]. Furthermore, the concentration of *Actinobacteria*—comprising, i.e., *Bifidobacterium* species—has been proven to be positively correlated with pro-inflammatory parameters, including white blood cells (WBCs) or the percentage of neutrophils and monocytes in the blood [28]. As these bacteria participate in histidine degradation and proline synthesis, they lead to increased glutamate levels in both pathways—thus promoting neuronal excitation—and increase the risk of excitotoxicity and neuronal cell death. Proline metabolism imbalance has been mentioned as a cause of alterations in neuronal activity and is linked with CNS diseases [29]. Arginine synthesis is strictly correlated with proline and glutamate acid concentrations. Its increased metabolism leads to the formation of putrescine and spermidine—molecules related to the degree of gut barrier permeability. Metagenomic studies have indicated that norspermidine enhances the aggregation of α-synuclein, while increased allantoin degradation could be a result of the inflammatory-based uric acid production, suggesting an increased risk of oxidative stress among PD patients [30]. Furthermore, some *Bifidobacteria* species contain succinate-semialdehyde dehydrogenase or glutamate decarboxylase, both resulting in an increased concentration of GABA, which is known as a promoter of PD motor symptoms [31].

The additional breakdown of connections between epithelial cells leads to increased exposure to lipopolysaccharides (LPS); that is, elements of the cellular wall of bacteria from the *Proteobacteria* group. This leads to a systemic pro-inflammatory reaction and the progression of neurodegeneration [32]. The excessive release of LPS and other bacterial metabolic products into the bloodstream could result in systemic inflammation progression, leading to disruption of the blood–brain barrier (BBB) and increasing the risk of enhanced transfer of inflammatory cells to the CNS, resulting in an increased risk of neuroinflammation and degeneration [16]. Recent data showed that LPS also increases the risk of vascular wall integrity disruption, leading to renal insufficiency and cardiovascular disease [33]. *Escherichia coli* and *Salmonella* are equipped with special fibers called Curli, which are the main proteinaceous component of their extracellular matrix (ECM) [34]. By binding with laminin and fibronectin, they provide contact with the host; however, they also bind t-PA, which activates plasminogen and leads to destruction of local tissue according to its protease property [35,36]. It is suspected that the Curli subunit CsgA (extracellular bacterial amyloid protein) interacts with mammalian proteins in so-called cross-seeding, promoting α-synuclein accumulation [37]. Interestingly, Curli belongs to the biofilm-associated proteins (BAPs) group, described as molecules that are responsible not only for the maintenance of biofilm integrity but also amyloid-like fibril accumulation, relentlessly leading to neurodegeneration [38].

Cells damaged by inflammation act as a great source of the host-derived immune-activating damage-associated molecular patterns (DAMPs), which are present in the blood and stimulate epithelial repair processes [39]. DAMPs show affinity with several types of receptors, such as toll-like receptors (TLRs), RIG-1-like receptors (RLS) and the Nod-like receptor family, triggering mechanisms of innate immunity. By stimulating myeloid-differentiation factor-88 and the NLRP3 inflammasome, they contribute to the activation of caspases and the release of pro-inflammatory interleukins, such as TNF-α, IL-1, IL-6, IL-8, and IL-12 via myeloid-differentiation factor-88 stimulation and IL-1β and IL-18 in the NLRP3 inflammasome [40].

Blood samples from PD patients have revealed increased levels of, i.e., IL-1β, IL-6 and TNF-α, while dysbiosis was also suspected to cause higher IFN-γ concentrations [41]. Comparing APS and idiopathic Parkinson's disease (iPD) patients, the former revealed higher serum concentrations of IL-2, IL-4, IL-6, TNF-α, and IFN-γ, while the level of IL-10 was the lowest in APS patients [42].

Animal model-based research has revealed that a stress environment (water avoidance stress) leading to the inhibition of the NOD-like receptor and pyrin domain containing (NLRP)-6 inflammasome resulted in not only inflammatory enhancement, but also fundamental dysbiosis in mice [43].

A few articles have underlined the health-promoting role of inhalation of hydrogen sulfide (H2S), a substance produced mainly by *Prevotellaceae* (part of the *Proteobacteria* family) [44]. It is supposed to cause such a positive effect through the indirect expression of heme oxygenase-1 and glutamate-cysteine ligase, as well as anti-inflammatory properties [44]. However, trials in PD patients have shown that H2S enhances α-synuclein accumulation and could be triggered by *Desulfovibrionaceae*, as well as other bacteria, exposing PD patients to increased concentrations of this substance [45]. *Prevotellaceae* has been reported to decrease toxic polyglutamine (polyQ) aggregation and promote intestinal motility [46]. Some such species can also produce magnetite (Fe3O4), which collectively leads to excessive cytochrome c release in mitochondria, promotes iron accumulation and increases the level of reactive oxygen species production [47]. It has been postulated that rhamnolipid (RL)—an active element of the cellular surface produced by *Pseudomonas aeruginosa* (included in the *Proteobacteria* family)—could interact with α-synuclein molecules and indirectly modulate the risk of neurodegeneration in PD models [48]. Pseudomonas species also express genes for esterase PA2949, sharing a similar structure with the human membrane-bound α/β-hydrolase domain 6 (ABHD6) protein, leading to 2-arachidonylglycerol (2-AG) hydrolysis and endocannabinoid signaling impairment. As endocannabinoid receptors are mostly expressed on the surface of basal ganglia, their inhibition can result in impaired interactions with other pathways (including GABAergic and dopaminergic paths), increasing the risk of occurrence of neurodegeneration symptoms [49,50].

By reducing access to oxygen, anaerobic bacteria obtain optimal conditions to live and develop. The presence of *Actinobacteria* and *Enterococcus* species (e.g., *Olsenella*, *E. faecalis*) is associated with an increased level of the tyrosine metabolite p-cresol [51]. In a mouse model, p-cresol sulphate caused not only a decrease in circulating BDNF but also increased corticosterone and repressor element-1 silencing transcription factor (REST), leading to the development of depression-like, anxiety-like and cognitive impairment symptoms, including memory and learning difficulties [52]. Tyrosine decarboxylase (TyrDC) leads to premature synthesis of dopamine in the intestine, which is unable to cross the BBB and, thus, cannot have a beneficial effect in terms of alleviating the clinical symptoms of PD. Decreased levels of tyrosine, increased levels of α-synuclein, impaired sodium transport and higher succinate levels in feces and serum have been described in a mouse model of PD, notably revealing an increased concentration of *Alistipes* species [53].

Accordingly, isopropanol can have toxic effects on neuronal cells, being an alcohol that penetrates the CNS more effectively than ethanol and acting as a nervous system depressant [54]. Inhibition of its production concomitantly with alleviation of pyruvate fermentation to propanoate I have been shown to be facilitated by *Lactobacillus* (from phylum *Firmicutes*) [28]. As vitamin B12 is responsible for, i.e., propanoate breakdown, its potential protective role against inflammation and cell death, concomitantly with synaptic hippocampal support, has been shown in a rat model of AD [55].

A limited concentration of propanoate, caused by the mitochondrial unfolded protein response (mitoUPR) due to α-synuclein accumulation, has been shown to impede lipid and

protein metabolism and impair energy production, which is crucial for effective gut–brain communication [56].

Ruminococcaceae bacteria (included in phylum Firmicutes) also exhibit numerous activities related to metabolic alterations [57]. They are predominantly responsible for α-linolenic acid (ALA) production, stimulating the Wnt/β-catenin signaling pathway and resulting in enhanced proliferation of intestinal stem cells [58]. *Ruminococcaceae* CPB6 have been found to express the LDH gene and promote apoptosis of microglial cells [59,60]. Apart from lactate modifications, CPB6 is also engaged in n-caproic acid (CA) production, involving other molecules, including acyl carrier protein (ACP) and coenzyme A (CoA) [61].

Toxins produced by particular *Clostridium* species (part of *Firmicutes*)—namely, through the inhibition of potassium channels—have been shown to lead to mitochondrial hyperpolarization, cellular death and increased intestinal permeability [62]. In a murine model, *Clostridium orbiscindens* has been shown to produce desaminotyrosine (DAT), which is also responsible for mucosal barrier maintenance and inflammatory attenuation. It is derived from tyrosine and flavonoid metabolism, and exhibits antiviral activity due to enhancement of the type I interferon signal-dependent pathway [63]. Reported data have indicated no significant change in microbiota diversity after levodopa treatment, although a reduced number of group IV *Clostridioides* bacteria has been described in patients showing significant motor improvement after levodopa initiation [64]. Similarly, regarding *Bifidobacteria*, participation in numerous metabolic paths related to amino acids allows *Lactobacillus* species to act as an important immunomodulatory element. The presence of *Lactobacillus* (belonging to *Firmicutes*) has been shown to correspond to the intensity of pyruvate fermentation to propanoate I and is negatively associated with isopropanol synthesis [28]. The ability of *L. plantarum* CCFM405 to promote the production of branched-chain amino acids (BCAAs)—including valine, leucine and isoleucine—has been proven to modify the composition of the intestinal microbiota, reduce inflammation (by decreasing IL-1β, IL-6 and TNF-α concentrations) and attenuate neuronal death [65]. Furthermore, it has been shown that another Lactobacillus representative (*L. plantarum PS128*) regulates improper microRNA (miR155-5p) expression and promotes the activity of a cytokine signaling inhibitor (SOCS1), exhibiting anti-inflammatory properties. While the gut microflora seems to be associated with the expression of numerous PD-related genes regulated by miRNAs, it is suspected that its diversity could act as a potential factor influencing the course of this disease [66].

The number of activities in which intestinal bacteria are involved emphasizes the importance of maintaining their proper composition, avoidance of dysbiosis and the provision of essential nutrients. Bacteria are involved in the formation of microbe–microbe and host–microbe interactions, indirectly contributing to the exacerbation or inhibition of neurodegeneration processes [67]. Through their local action, bacteria contribute to maintenance of the continuity of the intestinal barrier. Moreover, both direct molecules included in the bacterial cell membrane, as well as products of their metabolism, participate in numerous processes that are responsible for sustaining the energy balance—for example, lipid and carbohydrate metabolism, as well as immunomodulation and protection of the body against pathogens. SCFAs are synthesized through the fermentation processes carried out by bacteria; among these, acetate is involved in lipogenesis and gluconeogenesis, while butyrate and propionate are associated with the maintenance of physiological processes and regulation of the immune system [68].

Bacterial activity that is potentially important in the context of parkinsonian syndrome neurodegeneration is summarized in Table 1.

Table 1. Bacterial activity potentially influencing neurodegeneration.

Bacteria	Activity	Effect
Akkermansia	degrades mucin regulates T regulatory cell activity regulates SCFA production inhibits IL-6 dependent pathway	intestinal passage prolongation cognitive function improvement
Actinobacteria	increases glutamate level, promoting neuronal excitation forms putrescine and spermidine	enhancement of aggregation of α-synuclein risk of increased oxidative stress
Desulfovibrionaceae	produces magnetite (Fe_3O_4)	excessive cytochrome c release in mitochondria iron accumulation and increase in the level of reactive oxygen species production
Proteobacteria	rhamnolipid (RL) interacts with α-synuclein molecules disables endocannabinoid receptors	risk of neurodegeneration symptoms occurrence
Prevotellaceae	decreases toxic polyglutamine (polyQ) aggregation	decreased constipation
Firmicutes (*type*) *Bacilli* (*class*) *Lactobacillus* *Enterococcus* *Streptococcaceae* *Clostridium* (*class*) *Lachnospiraceae* *Ruminococcaceae*	inhibits isopropanol production ferments pyruvate to propanoate I promotes BCAAs production produces p-cresol decreases circulating BDNF disrupts intercellular connections inhibits potassium channels produces SCFAs produces secondary bile acids produces α-linolenic acid (ALA)	potential protective role against inflammation and cell death (in AD) intestinal microbiota composition modification inflammation reduction depression-like, anxiety-like and cognitive impairment symptoms development increased intestinal permeability increased cellular death and intestinal permeability enteric pathogen inhibition mucosal immunity regulation apoptosis of microglial cells

Legend: AD—Alzheimer's Disease, ALA—α-Linolenic Acid, BCAAs—Branched-Chain Amino Acids, BDNF—Brain-Derived Neurotrophic Factor, IL-6—Interleukin-6, p-cresol—Para-Cresol, polyQ—Polyglutamine, RL—Rhamnolipid, SCFAs—Short-Chain Fatty Acids.

3. Role of the Intestinal Microbiota in Metabolism

3.1. SCFAs

Acetic acid (C2), propionic acid (C3) and butyric acid (C4) are the most abundant SCFAs in the human GI tract, with their concentrations being higher in its proximal part [51]. They occur in a ratio of 60:20:20 (C2:C3:C4), with C3 and C4 requiring the additional presence of the Firmicutes and Bacteroides family members within the intestine [69]. SCFAs serve as a crucial component regulating the microbiota–gut–brain axis, due to their numerous properties [70]. Butyrate's beta-oxidation in mitochondria of intestinal epithelial cells ensures the continuity of intestinal barrier maintenance, providing, i.e., protection against pathogens [71,72]. SCFAs regulate the expression of genes encoding proteins (zonulin, occludin, claudin) that are part of tight junctions between enterocytes and stimulate the production of glycoproteins of the mucous layer [71]. They act as crucial factors coordinating processes involved in energy production and oxygen exploitation, regulating the level of hypoxia-inducible factor (HIF) and decreasing the risks of ROS synthesis, oxidative stress and intestinal barrier disruption [71]. Through regulation of the activities of enzymes such as tyrosine hydroxylase and tryptophan 5-hydroxylase 1, they take part in intermediate stages of the synthesis of tyrosine-related neurotransmitters—in particular, dopamine, adrenaline and noradrenaline—and are responsible for the conversion of tryptophan to serotonin [73]. In the available literature, 5-HT is known to impact lipid metabolism, regulate mitochondrial biogenesis and modulate the diversity of the intestinal microbiota [62]. The involvement of tyrosine metabolites, such as p-cresol and 4-ethylphenyl sulfate, in the gut–brain pathway has been described in the literature [74,75]. Tryptophan is mostly

converted along the kynurenine pathway, which limits the extent to which it is metabolized into 5-HT. Once kynurenine has formed, it can act as a predictor of neuroprotection or neurotoxicity, as kynurenine's metabolites—quinolinic and kynurenic acid—are NMDA receptor ligands reflecting opposite effects [76]. Tryptophan can also be metabolized into substances that stimulate Pregnane X receptors (PXRs), which participate in glucose and lipid metabolism processes and are indirectly activated by macrophages during inflammation [77–79]. Another tryptophan-derived substance is melatonin, which is responsible for coordination of the circadian rhythm and NF-κB-mediated immunomodulation [80,81].

SCFAs inhibit the accumulation of lipids in adipose tissue and participate in the regulation of carbohydrate metabolism, improving glucose tolerance [82]. They also possess neuroactive properties, and research in animal models has indicated the involvement of these acids in the maturation of microglial cells and maintaining the integrity of the BBB [73]. Through the regulation of neurotrophic factor levels, SCFAs have an impact on neurogenesis [83]. The concentration of brain-derived neurotrophic factor (BDNF) is proportionally related to the level of lactates, which are produced mainly by Lactobacillus and Bifidobacterium bacteria [83,84]. As LA increases the excitability of glutamatergic (NMDA) receptors, it contributes to an increase in intracellular calcium concentration and promotes the synthesis of BDNF [84]. Quinolinic acid, which participates in immune reactions, seems to modulate the astrocytic glutamate–glutamine cycle, simultaneously stimulating NMDA receptors and inhibiting glutamine synthetase [69]. It has been reported that neuronal activity enhanced by kainic acid (KA) receptors can be attenuated by melatonin in animal models, which could potentially become a future therapeutic approach in human trials [85].

SCFAs promote the differentiation of naive T lymphocytes into anti-inflammatory Tr1 and macrophage polarization into the M2 phenotype, sharing similar properties [86]. Through free fatty acid receptors (FFARs), they facilitate the reduction in pro-inflammatory iNOS and TNF-alpha [72]. They regulate gene expression, having the ability to inhibit histone deacetylases (HDACs), and are responsible for cellular signal transduction when attached to G protein-coupled receptors. It is suspected that they act as ligands of the aryl-hydrocarbon receptor—in animal models, AhR has been shown to be expressed on the surface of intraepithelial lymphocytes and is required to localize them to the skin and gut [71,72,87].

In terms of pathologic protein accumulation, another molecule called nerve growth factor (NGF) has been found to inhibit the hyperphosphorylation of tau protein in both in vitro and in vivo investigations, whereas glial cell line-derived neurotrophic factor (GDNF) is suspected to provide a therapeutic impact in PD patients, based on animal trials [73,88,89]. Notably, both of these factors are modulated by SCFAs [73].

Previous studies have shown that both the composition of the intestinal microbiota and the distribution of specific SCFAs differ depending on the biological age of the subjects [90]. This is undoubtedly influenced by the type of food consumed; for example, the composition of the intestinal microflora of breastfed infants differs significantly from that of humans on an adult diet mainly consisting of solid products [90,91]. With the end of the milk diet, the concentration of bacteria in the Firmicutes and Bacteroidetes phyla gradually increases, contributing to increases in the concentrations of propionate and butyrate [92]. Species of the genera Roseburia and Blautia—included in the Lachnospiraceae family (part of Firmicutes)—have been reported to participate in the process of intestinal maturation and exhibit immunomodulatory properties [41,93–95]. Lachnospiraceae are also responsible for secondary bile acid production and enteric pathogen inhibition [96].

3.2. Glucose and Lipid Metabolism

Existing data suggest that bacteria could influence both glucose and lipid metabolism. Interestingly, it is suspected that processes related to the transformation of carbohydrates are not always only a consequence of the implementation of overweight or anti-obesity treatments. Indirect intestinal bacterial activities mediated by SCFAs and succinate production could exhibit numerous metabolic effects [97].

A decreased level of insulin receptor phosphorylation, similar to the insulin receptor substrate (IRS) and Akt, could result in impaired insulin signaling, while some bacteria exhibit enzymatic activity including, i.e., glycoside hydrolases and carbohydrate esterases [98]. As SCFAs have been previously described to be molecules responsible for proper glucose metabolism, they also play a significant role in the regulation of lipid concentrations in the blood. Propionic acid, similar to commonly known statins, is known to inhibit 3-hydroxy-3-methyl glutaryl-coenzyme A synthase activity. Furthermore, a decreased concentration of reabsorbed bile salts in the liver resulting from the enzymatic activity of Lactobacilli species could impact the increased demand for bile salts and lead to enhanced cholesterol transformation, concurrently providing decreased blood cholesterol levels [98]. Data from ALS and AD revealed that the microbiota is also involved in polyunsaturated fatty acids (PUFAs), exhibiting both pro- and anti-inflammatory activity [99].

3.3. Vitamins

The intestinal microbiota creates a network exhibiting cross-feeding properties [100]. Available data suggest that at least 40% of gut species produce one of eight B-vitamins and are able to exchange vitamins among each other by complementary matching [101]. B vitamins are crucial not only for the production of ATP but also one-carbon (1C) metabolism, supporting the synthesis of purines (elements of nucleic acids) and the formation of amino acids (e.g., glycine, serine and methionine) [102].

As vitamin B1 (thiamine) participates in processes connected with ATP production and modulation of the immune system, there is a strong suspicion of its potential role in immunometabolism [103]. Research using a mouse model has revealed that thiamine deficiency—mostly produced by Prevotella, Desulfovibrio and Bacteroides—results in a significant reduction in Peyer's patches and the number of B cells [102].

According to the significant number of vitamin B6 (pyridoxin) transporters in the large intestine, it is one of the few vitamins that is largely absorbed only in the distal part of the digestive tract [104]. It is responsible for the coordination of mucus production in the intestine, and acts as an antioxidant and cofactor in the production of neurotransmitters [105].

Vitamin B12 (VB12) is produced by only 20% of the intestinal microbiota [102]. It modulates the activity of epithelial cells and microbial functions in the intestines, exhibiting anti-inflammatory properties. It activates the HIF-1alpha pathway and, by enhancing mitochondrial processes, decreases the concentration of free oxygen within the intestines, creating a suitable environment for anaerobic bacteria and limiting the intensity of epithelial oxygenation [106]. VB12 also controls cellular proliferation, and its deficiency results in reduced villus height and a disruption of intestinal barrier maintenance [107]. A lack of VB12 leads to increases in kynurenine and homocysteine, resulting in increased inflammatory parameters [107,108].

Although there is no direct relationship between specific bacterial flora and the concentration of produced vitamin K, some studies have indicated a correlation between specific enterotypes (Prevotella and Bacteroides) and an increased amount of menaquinone in the stool [109]. Vitamin K and its active metabolites have been shown to reduce the concentrations of cytokines such as IL-1, IL-6 and TNF-alpha in both in vitro and in vivo investigations, indicating their potential anti-inflammatory properties [110]. The activa-

tion of Gla proteins affected the NF-kB/Nrf2 pathway (nuclear factor kappa-light-chain-enhancer of activated B cells (NF-kB)/nuclear factor erythroid 2-related factor 2) and decreased the risk of vascular inflammation in DM2 patients [111,112]. Additionally, it enabled carboxylation of the Gas6 protein (growth arrest-specific gene product 6), inhibiting neurodegeneration-related processes and limiting the cellular accumulation of free radicals. It indirectly inhibited certain aging processes (inflammaging) and epigenetic dysregulation, thus protecting against genomic instability [113,114].

The intestinal microbiota can also convert dietary vitamin A precursors into retinoic acid (RA), exhibiting immunomodulatory properties and acting as a regulator of gene expression [100,115]. The γt-orphan receptor related to the RA-receptor (RAR)—ROR—is expressed concurrently with AhR on the surface of lymphoid tissue-inducer cells, which are responsible for lymphoid development [116].

Impacts of bacterial metabolites on neurotransmitter production, microglial activation and blood–brain barrier integrity is summarized in Figure 1.

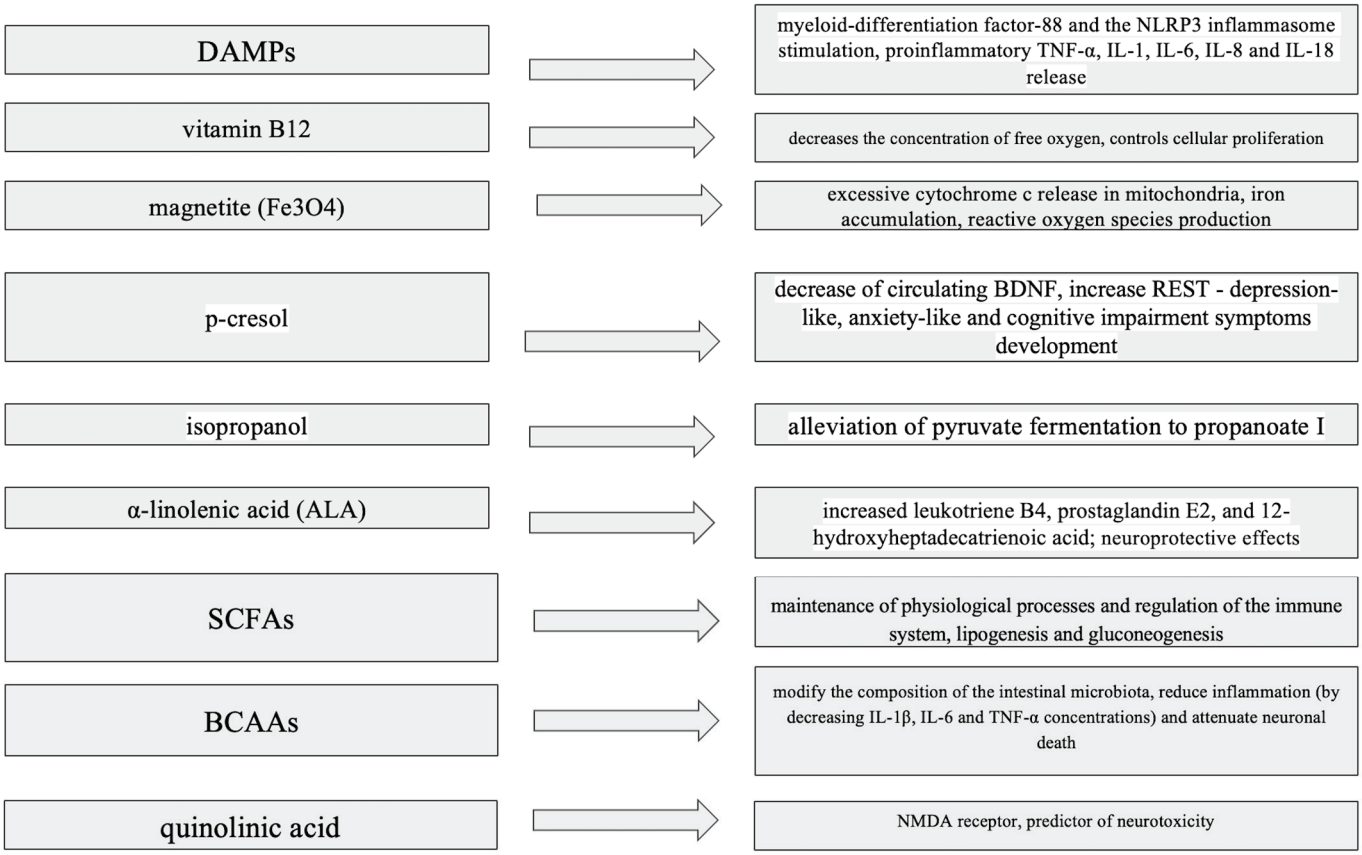


Figure 1. Impact of bacterial metabolites on neurotransmitter production, microglial activation and blood–brain barrier integrity. ALA—α-Linolenic Acid, BCAAs—Branched-Chain Amino Acids, BDNF—Brain-Derived Neurotrophic Factor, DAMPs—Damage-Associated Molecular Patterns, IL-1—Interleukin-1, IL-6—Interleukin-6, IL-8—Interleukin-8, IL-18—Interleukin-18, NLRP3—NOD-like Receptor Protein 3, NMDA—N-Methyl-D-Aspartate, p-cresol—Para-Cresol, REST—Repressor Element-1 Silencing Transcription Factor, SCFAs—Short-Chain Fatty Acids, TNF-α—Tumor Necrosis Factor Alpha.

4. Role of the Intestinal Microbiota in Atypical Parkinsonian Syndromes

As mentioned before, limited data on divergence in the microbiota of APS patients has been described so far. According to the undoubted similarity when it comes to the clinical profiles of PD and APSs, comparisons of the microbiota profiles between these

populations and those of HCs have been conducted. While the majority of these results overlapped, subtle differences were also found. Following Barichella et al., in the context of PD, Lachnospiraceae (in MSA) and Lactobacillaceae (in PSP) concentrations remained similar to those in HC, while Prevotellaceae (in MSA) and Streptococcaceae (in PSP) were decreased [23].

Results obtained in animal models have underlined the undeniable connection between immune system activity and neurodegeneration. Enhanced microgliosis and astrogliosis concurrent with the influx of T cells have been confirmed to play a role in tau-related neurodegeneration [117]. N6-carboxymethyllysine (CML)—one of the numerous microbial metabolites—is suspected to promote the enhancement of oxidative stress in microglia, resulting in mitochondrial impairment and the progression of intestinal permeability [118].

In vitro studies have revealed that the Gram-negative bacterium *Erwinia carotovora* 15 (Ecc15) could lead to regional inflammation, resulting in the release of numerous cytokines, activation of Janus kinase (JAK) receptors and subsequent promotion of the signal transducer and activator of transcription (STAT) signaling pathway. This leads to increased claudin-2 expression, which is involved in cellular tight junction regulation and increasing intestinal permeability via pore promotion [119,120].

Inhibition of Programmed Death protein 1 (PD-1), encoded by *Pdcd1*, has been reported to support long-term potentiation (LTP) and memory in hippocampal neurons [121]. Recent data have suggested that the suppression of PDCD1 could limit tauopathy-related neurodegeneration, while recent in vivo trials have revealed that the microbiota plays a role in the PD-1/PD-L1 pathway and exhibits immunomodulatory properties mediated by anti-PD1 molecules [122,123].

The *Streptococcaceae* concentration in PSP was found to be reduced, while there was no significant change in *Lactobacillaceae* [23]. Although the broad evaluation of fecal microbiota transplantation (FMT) treatments in PD patients has demonstrated the undeniable impact of the intestinal flora in immunomodulation and inflammatory alleviation, there has only been one published clinical trial suggesting a similar effect in PSP cases.

Existing studies point to the lack of a clear answer to the question regarding the mechanism of action of bacteria contributing to neuroprotection and inhibition of the accumulation of abnormal proteins. Studies in animal models have reported promising results, emphasizing the low risk of including human patients in similar studies. The results obtained to date have indicated a variety of results depending on the form of administration of the bacteria, which can be both oral and enteral [124].

After oral FMT in eight patients, a stool investigation revealed increased *Lactobacillaceae*, *Limnochordaceae* and *Peptostreptococcaceae* concentrations one week after therapy. One month after FMT, the patients reported improvements in areas such as motor performance, sleep quality and constipation; however, these improvements did not persist in later observations, which most likely indicates the need for regular FMTs in order to maintain the expected effects [124,125].

The results of FMT in the form of an oral capsule administered weekly for 3 weeks divided patients into responders and non-responders, according to the results described in terms of clinical scores. As a novel observation, the responders revealed increased concentrations of *Eubacterium*, *Clostridia* and *Roseburia* genera, similar to the donor's microbiota diversity. The authors suggested that the response to FMT and engraftment success could be linked with (so far) unknown factors and underlined the importance of potential future biomarkers for the assessment of therapeutic effectiveness [126]. Intraintestinal microbiota administration indicated that FMT could also result in a decreased levodopa equivalent daily dose (LEDD) [127].

Restoring the healthy microbiota in PSP patients contributed to the alleviation of both motor and non-motor symptoms. While increased concentrations of *Escherichia-Shigella*, *Lactobacillus* and *Klebsiella* (in comparison with healthy controls, HC) were associated with a higher score in the PSPRS evaluation, PSP-RS patients also revealed decreased levels of *Faecalibacterium*, *Blautia*, *Agathobacter* (*Lachnospiraceae*), *Romboutsia* (*Peptostreptococcus*) and *Roseburia* species in comparison with HCs [128]. Nonetheless, the correlations between tau alterations and environmental factors such as dysbiosis still remain limited and further investigations in this context are required [117]. The precise link between microbiota and tauopathies can be described as misunderstood at present.

Under normal conditions, α-synuclein (α-Syn) is a presynaptically based unfolded protein divided into three regions, of which its central part presents hydrophobic properties and remains strictly fibrillogenic [129]. It is now known that improper forms of molecules, especially their aggregates, have a strong influence on microglial activation and could impede microglial autophagy [99]. The cyclic GMP–AMP synthase (cGAS)–stimulator of interferon genes (STING) signaling pathway, Toll-like receptor 4 (TLR4)-dependent p38 mitogen-activated protein kinase (MAPK) and AKT-mTOR cascade, tyrosine kinase-binding protein (TYROBP), triggering receptor expressed on myeloid cells 2-apolipoprotein E (TREM2-APOE) pathway, spleen tyrosine kinase (SYK), classical complement system, purinergic system, sialic acid binding immunoglobin-like lectins (Siglecs; CD22 and CD33), TAM system, and mechanosensor Piezo1 are only some of the potential mechanisms responsible for the regulation of microglial activity [99,129]. An increased concentration of isoamylamine (IAA)—related, i.e., with an increased abundance of *Ruminococcaceae*—consequently leads to deconfiguration of S100A8's protein hairpin structure, enabling enhanced p53 activity [99]. Based on research in an animal model, the nucleotide-binding oligomerization domain leucine-rich repeat and pyrin domain-containing protein 3 (NLRP3) inflammasome also could potentially act as a molecule modulating the inflammatory response [99]. Decreased inflammasome-related caspase-1 concentration, concomitantly with decreased α-Syn, were found in all investigated PD cases, while their levels were positively correlated with monocyte activities [130].

α-Syn remains one of multiple factors responsible for monocyte activation. While it has not been profoundly explored, it exhibits a pro-inflammatory effect and differentiated cellular responses, possibly due to unexplored mechanisms [131]. Its level seems to be linked with the concentration of bacterial endotoxins and, although LPS can activate microglia and the pro-inflammatory M1 response, it can also induce the cellular death of astrocytes [130,132]. Monocyte Human Leukocyte Antigen (HLA)-DR expression has been found to be negatively correlated with motor and cognitive outcomes in PD patients [130].

The role of α-synuclein accumulation in MSA has been deeply investigated. As its strains are believed to cause disease-specific neurodegeneration, researchers have suggested the existence of a potential oligodendrocyte–neuron–α-Syn interplay, contributing to the development of MSA [133]. It is suspected that oligodendroglia cytoplasmic inclusions (GCIs) exhibit a distinct level of toxicity and their varied placement could serve as evidence of multiple symptoms. Interestingly, the amplification profile of α-synuclein derived from CSF in PD and MSA patients revealed different secondary structures, while its strains in DLB reflected traits of the 'fibrils' strain—in opposition to the 'ribbons' strain described previously in α-synucleinopathies.

Interestingly, recent studies have revealed that the E46K mutation in the α-synuclein gene inhibits neuropropagation of its self-templating prion conformation [134]. Animal studies have also shown that tau protein forms connections with α-synuclein, intensifying the process of their accumulation in PD [135].

MSA patients were found to have higher concentrations of *Prevotellaceae* concurrently with unchanged *Lachnospiraceae* levels [23]. A study in American MSA patients revealed higher *Clostridiaceae* and *Rikenellaceae* concentrations, while *Lachnospiraceae* (genera *Ruminococcus*, *Roseburia* and *Coprococcus*) and *Ruminococcaceae* (genus *Faecalibacterium*) were reduced [136]. An MSA patient in an ethnic Chinese population of Malaysia presented an increased level of *Bacteroides* and less-abundant *Paraprevotella* [137].

The described results seem to be inconclusive, due to the limited available patient groups as a result of their high morbidity and the rarity of the considered diseases [138]. Potential connections between gut microbiota and neurodegeneration are summarized in Figure 2.

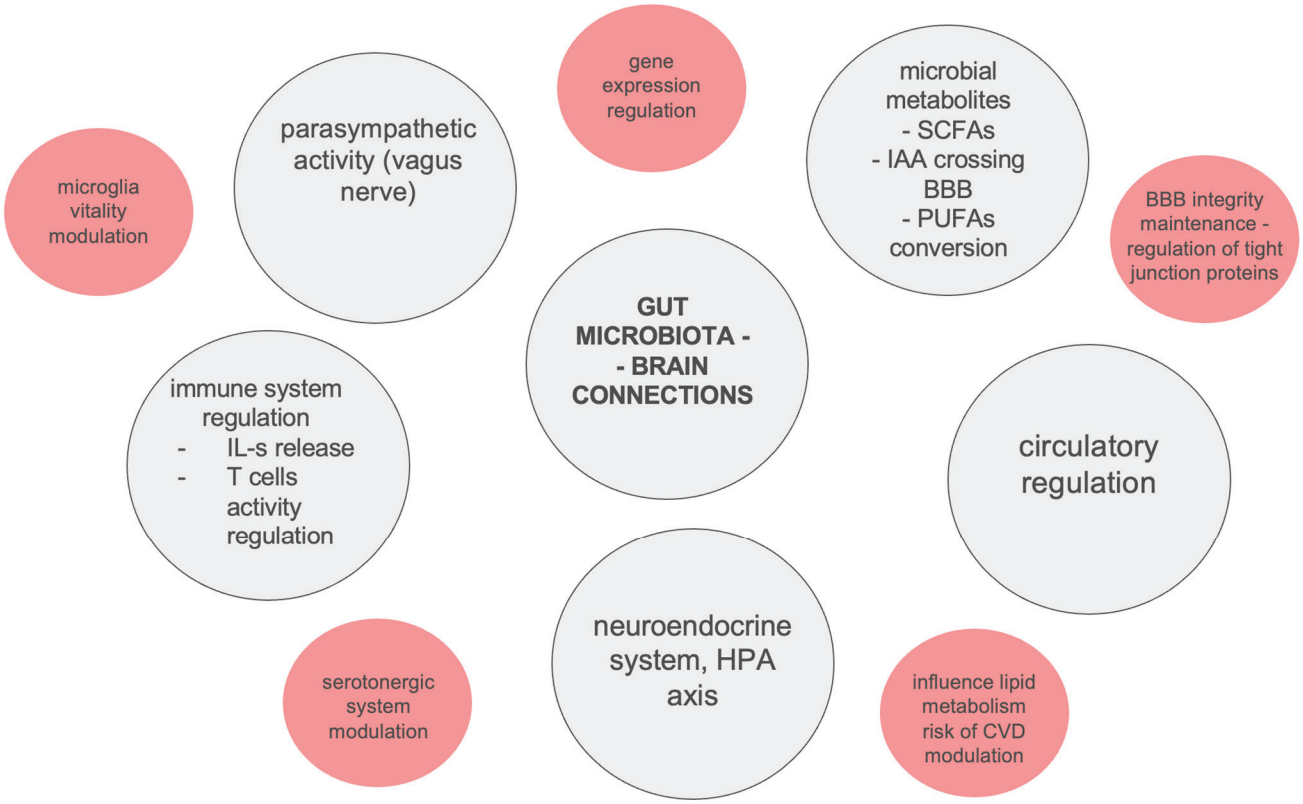


Figure 2. Potential connections between gut microbiota and neurodegeneration. BBB—Blood–Brain Barrier, CVD—Cardiovascular Disease, HPA—Hypothalamic–Pituitary–Adrenal axis, IAA—Isoamylamine, IL-s—Interleukins, PUFAs—Polyunsaturated Fatty Acids, SCFAs—Short-Chain Fatty Acids.

5. Role of the Intestinal Microbiota in Future Diagnostic Processes and Treatments

In the context of the innovative idea of personalized medicine, there is still a need to identify readily available biological materials and highly specific markers with the aim of providing effective diagnostic approaches and successful treatments. Fecal investigations assessing abnormal concentrations of metabolites linked with riboflavin and biotin synthesis or carbohydrate-active enzymes (CAZymes) activity, which are responsible for carbohydrate degradation, or detecting a set of 11 genera with significant indications in PD using qPCR or 16S rRNA sequencing, could serve as examples of the abovementioned personalized approaches [139–141]. Metabolic alterations involving butyrate production, lipoic or alpha-linolenic acids, and glycerophospholipid metabolism are also linked with precise modifications in concrete bacterial species concentrations, which is considered to act as a potential determinant of more personal approaches for the diagnosis and treatment

of PD [141]. Measurement of αSyn aggregation in the terminal ileum in combination with peripheral inflammation markers has also been underlined as a potential novel strategy for the identification of PD in its prodromal phase [142].

Elevated levels of peripheral αSyn could result in mitochondrial disruption, acting as a trigger for microglial activation and neuronal loss. Furthermore, the role of bacterial infection leading to an autoimmune mitochondria-specific response has also been underlined as a potential factor contributing to the development of PD, and it is considered that the mitochondrial lipid cardiolipin could induce enhanced oligomerization of pathological αSyn and intensify neuronal cell death. As different subtypes of Th17 cells are involved in inflammatory processes, it is supposed that bacteria could induce the specific switching between homeostatic Th17 and an inflammatory Th17 cell phenotype. Recent data have underlined the potential role of Bifidobacteria localized in the gut-associated mucosa; furthermore, animal studies have confirmed that an increased level of Enterobacteriacea crossing the intestinal barrier induces chronic inflammation via inflammatory Th17 cell phenotype activation.

Prebiotic/probiotic/synbiotic supplementation and fecal microbiome transplantations have been the most commonly investigated methods of microbial modification in PD trials [124]. Although the effects of FMT in PD have been deeply investigated, there is only one published study concerning its use in APS. So far, FMT in PSP has revealed promising results [126], contributing not only to improved physical activity but also attenuating gastrointestinal and psychiatric symptoms [128].

Prebiotics are molecules that act as substrates for the metabolic processes in which bacteria are directly involved. The most frequently studied prebiotics include dietary fiber (e.g., resistant starch). Most data have suggested PD-related dysbiosis, which led contemporary researchers to assess the effects of bacterial supplementation (in the form of probiotics) on the condition of patients suffering from PD. Recent results have indicated that three months of supplementation with *Lactobacillus acidophilus*, *Bifidobacterium bifidum*, *L. reuteri*, and *L. fermentum* contributed not only to the reduction in pro-inflammatory cytokines in the blood, but also influenced the motor symptoms of PD, as assessed according to the UPDRS scale [143,144]. The results obtained to date indicate that this therapy not only alleviates mild non-motor PD symptoms, but also acts as an immunomodulator, contributing to increased synthesis of SCFAs and reducing the intensity of inflammation—determined, for example, according to the concentration of calprotectin in stool [145,146].

To date, several studies taking into account the effects of probiotics on the clinical condition of patients with PD have been conducted. The mixtures administered most often consisted of *Lactobacillus* and/or *Bifidobacterium* strains; although their concentrations have been described in the literature as being increased in PD, the mechanism that leads to their expansion is not yet fully known [124]. In most cases, probiotic therapy significantly contributed to improved gastrointestinal function, while an improvement in motor skills (determined via UPDRS) was observed in only two of five studies [124]. Unfortunately, not all studies checked the final composition of the microbiota after the end of probiotic therapy. However, it is known that there is an increase in the number of fiber-fermentative bacteria, such as *Ruminococcaceae* and *Lachnospira*, and decreases in *Lactobacillus fermentum* and *Klebsiella oxytoca* [147,148].

Postbiotics are enzymes and substances that are the product of metabolic processes carried out by bacteria, as well as fragments of their cell membranes (e.g., polysaccharides, peptidoglycans, lipoic acid, phosphonic acid, cell surface proteins, cell membrane proteins and extracellular polysaccharides). Interestingly, an animal model study indicated that bacteria-derived lipids could cross the BBB and provide enhanced neurogenesis and in-

flammatory modulation [149]; furthermore, applying postbiotics alone did not reveal the same therapeutic effect as that observed after postbiotic injection [150].

Although there are many postbiotic molecules, most of them possess similar functions, such as reducing the level of oxidative stress, promoting the expression of anti-inflammatory cytokines and promoting neurogenesis [151].

It is worth mentioning that the term "Live Bacteriotherapeutic Products" (LBPs) seems to play a significant role when it comes to descriptions of potential innovative methods for the future treatment of PD [124]. As the field of personalized medicine is still dynamically developing, this term appears to be more appropriate.

The correlation between clinical PD symptoms and concentrations of inflammatory markers under an altered intestinal microbiota due to rifaximin usage has also been investigated [152]. Antibiotic treatment is being investigated in a clinical trial including patients with Parkinson's disease dementia (PDD), who are planned to be treated with ceftriaxone [153]. Research based on animal models has shown that bacteriophage-delivered CRISPR/Cas9 endonuclease could promote the depletion of specific bacterial species and modify the microbiota profile [154].

Supplementation of anti-inflammatory molecules such as biotin or riboflavin, similarly to the insertion of butyrate producers (*B. producta*, inhibiting RAS-related pathways strictly correlated with inflammatory parameters in an animal model), has also been considered as an innovative method for the treatment of PD [139,155]. Interestingly, a mechanism of αSyn accumulation inhibition after *Lactobacillus plantarum*, *Clostridium butyricum* and *Bacillus subtilis* supplementation in an animal model was also underlined, which has not yet been certainly defined [124]. With an increased dietary intake of fiber concurrent with probiotic supplementation (called "synbiotics"), significant clinical changes have been described, such as, i.e., increased gut mobility [124]. Furthermore, intake of maltodextrin—a starch prescribed for the placebo group in one of the PD studies—was related to decreased UPDRS-III and increased MMSE scores [121].

6. Conclusions and Future Directions

APSs are a group of rare diseases with an etiology that has not been fully understood, and for which the methods of treatment developed so far have been ineffective. At present, researchers are still discovering new connections between neurodegeneration and numerous factors, the modification of which could affect the degree of severity of brain tissue damage. Some of the key elements of this complex system are inflammation and the diversity of intestinal microbiota, whose properties and connection with the brain via the bidirectional axis have been studied in the context of many other diseases.

It seems that the intensification of pro-inflammatory reactions, resulting from (among others) intestinal dysbiosis in patients with APSs, may affect the effectiveness of their treatment and constitute a factor that is potentially capable of modifying the course of the disease.

It cannot be absolutely excluded that future microbiome analyses may influence the selection of a proper treatment, or—if a cause–effect relationship was confirmed—that the modification of microbiota species may influence the course of the disease. Although APS and PD share certain similarities, the hypothesis suggesting a link between the gut microbiota and Parkinsonian syndromes is based on the α-synuclein pathology present in the enteric nervous system; therefore, the potential contribution of dysbiosis to tau pathology remains ambiguous.

In the authors' opinion, future studies should focus on potential differences in the gut microbiota among distinct phenotypes of APSs and the exploration of potential connections between dysbiosis, inflammatory patterns and the course of the disease. Potential relation-

ships between the course of the disease and the gut microbiota could initiate a new area of therapeutic approaches focused on non-invasive long-term interventions concerning the diet, probiotics and FMT, among others. Detailed analysis of the potential impacts of dysbiosis on neurodegeneration could lead to individualized treatments focused on the modification of the disease's course; such a therapy could even be tailored to the individual patient, in the case of the importance of specific bacterial strains having been confirmed.

Although promising, all of the above-described hypotheses still require in-depth research for confirmation.

Author Contributions: Conceptualization, N.M.-A.; methodology, D.P., N.M.-A. and P.A.; validation, D.P., N.M.-A. and P.A.; formal analysis, D.P. and N.M.-A.; investigation, D.P.; resources, D.P.; data curation, D.P.; writing—original draft preparation, D.P., N.M.-A. and P.A.; writing—review and editing, D.P., N.M.-A. and P.A.; visualization, D.P.; supervision, N.M.-A.; project administration, N.M.-A. All authors have read and agreed to the published version of the manuscript.

Funding: This research received no external funding.

Conflicts of Interest: The authors declare no conflict of interest.

References

1. Przewodowska, D.; Marzec, W.; Madetko, N. Novel Therapies for Parkinsonian Syndromes-Recent Progress and Future Perspectives. *Front. Mol. Neurosci.* **2021**, *14*, 720220. [CrossRef]
2. Deutschländer, A.B.; Ross, O.A.; Dickson, D.W.; Wszolek, Z.K. Atypical parkinsonian syndromes: A general neurologist's perspective. *Eur. J. Neurol.* **2018**, *25*, 41–58. [CrossRef]
3. Khan, I.; De Jesus, O. Frontotemporal Lobe Dementia. In *StatPearls*; StatPearls Publishing LLC: Treasure Island, FL, USA, 2025.
4. McFarland, N.R.; Hess, C.W. Recognizing Atypical Parkinsonisms: "Red Flags" and Therapeutic Approaches. *Semin. Neurol.* **2017**, *37*, 215–227. [PubMed]
5. Wenning, G.K.; Stankovic, I.; Vignatelli, L.; Fanciulli, A.; Calandra-Buonaura, G.; Seppi, K.; Palma, J.A.; Meissner, W.G.; Krismer, F.; Berg, D.; et al. The Movement Disorder Society Criteria for the Diagnosis of Multiple System Atrophy. *Mov. Disord.* **2022**, *37*, 1131–1148. [CrossRef] [PubMed]
6. Rana, A.Q.; Qureshi, A.R.; Siddiqui, O.; Sarfraz, Z.; Rana, R.; Shtilbans, A. Prevalence of pain in atypical parkinsonism: A systematic review and meta-analysis. *J. Neurol.* **2019**, *266*, 2093–2102. [CrossRef]
7. Alster, P.; Migda, B.; Madetko-Alster, N. The Significance of High-Density Lipoprotein-Derived Inflammatory Parameters in Atypical Parkinsonisms—Pilot Study. *J. Clin. Med.* **2025**, *14*, 2212. [CrossRef]
8. Lo, R.Y. Epidemiology of atypical parkinsonian syndromes. *Tzu Chi Med. J.* **2022**, *34*, 169–181. [CrossRef]
9. Su, D.; Cui, Y.; He, C.; Yin, P.; Bai, R.; Zhu, J.; Lam, J.S.T.; Zhang, J.; Yan, R.; Zheng, X.; et al. Projections for prevalence of Parkinson's disease and its driving factors in 195 countries and territories to 2050: Modelling study of Global Burden of Disease Study 2021. *BMJ* **2025**, *388*, e080952. [CrossRef] [PubMed]
10. Lamptey, R.N.L.; Chaulagain, B.; Trivedi, R.; Gothwal, A.; Layek, B.; Singh, J. A Review of the Common Neurodegenerative Disorders: Current Therapeutic Approaches and the Potential Role of Nanotherapeutics. *Int. J. Mol. Sci.* **2022**, *23*, 1851. [CrossRef]
11. Koziorowski, D.; Figura, M.; Milanowski, Ł.M.; Szlufik, S.; Alster, P.; Madetko, N.; Friedman, A. Mechanisms of Neurodegeneration in Various Forms of Parkinsonism-Similarities and Differences. *Cells* **2021**, *10*, 656. [CrossRef]
12. Rietdijk, C.D.; Perez-Pardo, P.; Garssen, J.; van Wezel, R.J.; Kraneveld, A.D. Exploring Braak's Hypothesis of Parkinson's Disease. *Front. Neurol.* **2017**, *8*, 37. [CrossRef] [PubMed]
13. Horsager, J.; Andersen, K.B.; Knudsen, K.; Skjærbæk, C.; Fedorova, T.D.; Okkels, N.; Schaeffer, E.; Bonkat, S.K.; Geday, J.; Otto, M.; et al. Brain-first versus body-first Parkinson's disease: A multimodal imaging case-control study. *Brain* **2020**, *143*, 3077–3088. [CrossRef] [PubMed]
14. Horsager, J.; Knudsen, K.; Sommerauer, M. Clinical and imaging evidence of brain-first and body-first Parkinson's disease. *Neurobiol. Dis.* **2022**, *164*, 105626. [CrossRef]
15. Rauf, A.; Badoni, H.; Abu-Izneid, T.; Olatunde, A.; Rahman, M.M.; Painuli, S.; Semwal, P.; Wilairatana, P.; Mubarak, M.S. Neuroinflammatory Markers: Key Indicators in the Pathology of Neurodegenerative Diseases. *Molecules* **2022**, *27*, 3194. [CrossRef]
16. Kalyan, M.; Tousif, A.H.; Sonali, S.; Vichitra, C.; Sunanda, T.; Praveenraj, S.S.; Ray, B.; Gorantla, V.R.; Rungratanawanich, W.; Mahalakshmi, A.M.; et al. Role of Endogenous Lipopolysaccharides in Neurological Disorders. *Cells* **2022**, *11*, 4038. [CrossRef] [PubMed]

17. Madetko-Alster, N.; Otto-Ślusarczyk, D.; Wiercińska-Drapało, A.; Koziorowski, D.; Szlufik, S.; Samborska-Ćwik, J.; Struga, M.; Friedman, A.; Alster, P. Clinical Phenotypes of Progressive Supranuclear Palsy-The Differences in Interleukin Patterns. *Int. J. Mol. Sci.* **2023**, *24*, 15135. [CrossRef]
18. Li, F.; Weng, G.; Zhou, H.; Zhang, W.; Deng, B.; Luo, Y.; Tao, X.; Deng, M.; Guo, H.; Zhu, S.; et al. The neutrophil-to-lymphocyte ratio, lymphocyte-to-monocyte ratio, and neutrophil-to-high-density-lipoprotein ratio are correlated with the severity of Parkinson's disease. *Front. Neurol.* **2024**, *15*, 1322228. [CrossRef]
19. Madetko, N.; Migda, B.; Alster, P.; Turski, P.; Koziorowski, D.; Friedman, A. Platelet-to-lymphocyte ratio and neutrophil-tolymphocyte ratio may reflect differences in PD and MSA-P neuroinflammation patterns. *Neurol. Neurochir. Pol.* **2022**, *56*, 148–155. [CrossRef]
20. Rinninella, E.; Raoul, P.; Cintoni, M.; Franceschi, F.; Miggiano, G.A.D.; Gasbarrini, A.; Mele, M.C. What is the Healthy Gut Microbiota Composition? A Changing Ecosystem across Age, Environment, Diet, and Diseases. *Microorganisms* **2019**, *7*, 14. [CrossRef]
21. Risely, A. Applying the core microbiome to understand host-microbe systems. *J. Anim. Ecol.* **2020**, *89*, 1549–1558. [CrossRef]
22. van de Guchte, M.; Blottière, H.M.; Doré, J. Humans as holobionts: Implications for prevention and therapy. *Microbiome* **2018**, *6*, 81. [CrossRef] [PubMed]
23. Barichella, M.; Severgnini, M.; Cilia, R.; Cassani, E.; Bolliri, C.; Caronni, S.; Ferri, V.; Cancello, R.; Ceccarani, C.; Faierman, S.; et al. Unraveling gut microbiota in Parkinson's disease and atypical parkinsonism. *Mov. Disord.* **2019**, *34*, 396–405. [CrossRef] [PubMed]
24. Wu, M.; Li, P.; Li, J.; An, Y.; Wang, M.; Zhong, G. The Differences between Luminal Microbiota and Mucosal Microbiota in Mice. *J. Microbiol. Biotechnol.* **2020**, *30*, 287–295. [CrossRef]
25. Missiego-Beltrán, J.; Beltrán-Velasco, A.I. The Role of Microbial Metabolites in the Progression of Neurodegenerative Diseases-Therapeutic Approaches: A Comprehensive Review. *Int. J. Mol. Sci.* **2024**, *25*, 10041. [CrossRef]
26. Romano, S.; Savva, G.M.; Bedarf, J.R.; Charles, I.G.; Hildebrand, F.; Narbad, A. Meta-analysis of the Parkinson's disease gut microbiome suggests alterations linked to intestinal inflammation. *NPJ Park. Dis.* **2021**, *7*, 27. [CrossRef]
27. Zhu, X.; Shen, J.; Feng, S.; Huang, C.; Wang, H.; Huo, F.; Liu, H. Akkermansia muciniphila, which is enriched in the gut microbiota by metformin, improves cognitive function in aged mice by reducing the proinflammatory cytokine interleukin-6. *Microbiome* **2023**, *11*, 120. [CrossRef]
28. Li, Z.; Lu, G.; Li, Z.; Wu, B.; Luo, E.; Qiu, X.; Guo, J.; Xia, Z.; Zheng, C.; Su, Q.; et al. Altered Actinobacteria and Firmicutes Phylum Associated Epitopes in Patients with Parkinson's Disease. *Front. Immunol.* **2021**, *12*, 632482. [CrossRef] [PubMed]
29. Yao, Y.; Han, W. Proline Metabolism in Neurological and Psychiatric Disorders. *Mol. Cells* **2022**, *45*, 781–788. [CrossRef]
30. Zhang, K.; Paul, K.C.; Jacobs, J.P.; Chou, H.L.; Duarte Folle, A.; Del Rosario, I.; Yu, Y.; Bronstein, J.M.; Keener, A.M.; Ritz, B. Parkinson's Disease and the Gut Microbiome in Rural California. *J. Parkinsons Dis.* **2022**, *12*, 2441–2452. [CrossRef]
31. Zuo, S.; Wang, H.; Zhao, Q.; Tang, J.; Wang, M.; Zhang, Y.; Sang, M.; Tian, J.; Wang, P. High levels of Bifidobacteriaceae are associated with the pathogenesis of Parkinson's disease. *Front. Integr. Neurosci.* **2022**, *16*, 1054627. [CrossRef]
32. Hokari, R.; Tomioka, A. The role of lymphatics in intestinal inflammation. *Inflamm. Regen.* **2021**, *41*, 25. [CrossRef] [PubMed]
33. Rahman, M.M.; Islam, F.; -Or-Rashid, M.H.; Mamun, A.A.; Rahaman, M.S.; Islam, M.M.; Meem, A.F.K.; Sutradhar, P.R.; Mitra, S.; Mimi, A.A.; et al. The Gut Microbiota (Microbiome) in Cardiovascular Disease and Its Therapeutic Regulation. *Front. Cell Infect. Microbiol.* **2022**, *12*, 903570. [CrossRef]
34. Barnhart, M.M.; Chapman, M.R. Curli biogenesis and function. *Annu. Rev. Microbiol.* **2006**, *60*, 131–147. [CrossRef]
35. Sjöbring, U.; Pohl, G.; Olsén, A. Plasminogen, absorbed by *Escherichia coli* expressing curli or by Salmonella enteritidis expressing thin aggregative fimbriae, can be activated by simultaneously captured tissue-type plasminogen activator (t-PA). *Mol. Microbiol.* **1994**, *14*, 443–452. [CrossRef]
36. Castellino, F.J.; Ploplis, V.A. Structure and function of the plasminogen/plasmin system. *Thromb. Haemost.* **2005**, *93*, 647–654. [PubMed]
37. Chen, S.G.; Stribinskis, V.; Rane, M.J.; Demuth, D.R.; Gozal, E.; Roberts, A.M.; Jagadapillai, R.; Liu, R.; Choe, K.; Shivakumar, B.; et al. Exposure to the Functional Bacterial Amyloid Protein Curli Enhances Alpha-Synuclein Aggregation in Aged Fischer 344 Rats and Caenorhabditis elegans. *Sci. Rep.* **2016**, *6*, 34477. [CrossRef] [PubMed]
38. Singh, A.A.; Khan, F.; Song, M. Biofilm-Associated Amyloid Proteins Linked with the Progression of Neurodegenerative Diseases. *Int. J. Mol. Sci.* **2025**, *26*, 2695. [CrossRef]
39. DeWolf, S.E.; Kasimsetty, S.G.; Hawkes, A.A.; Stocks, L.M.; Kurian, S.M.; McKay, D.B. DAMPs Released from Injured Renal Tubular Epithelial Cells Activate Innate Immune Signals in Healthy Renal Tubular Epithelial Cells. *Transplantation* **2022**, *106*, 1589–1599. [CrossRef]
40. Shannon, K.M. Gut-Derived Sterile Inflammation and Parkinson's Disease. *Front. Neurol.* **2022**, *13*, 831090. [CrossRef]

41. Singh, V.; Lee, G.; Son, H.; Koh, H.; Kim, E.S.; Unno, T.; Shin, J.H. Butyrate producers, "The Sentinel of Gut": Their intestinal significance with and beyond butyrate, and prospective use as microbial therapeutics. *Front. Microbiol.* **2022**, *13*, 1103836. [CrossRef]
42. Rodríguez-Leyva, I.; Chi-Ahumada, E.G.; Carrizales, J.; Rodríguez-Violante, M.; Velázquez-Osuna, S.; Medina-Mier, V.; Martel-Gallegos, M.G.; Zarazúa, S.; Enríquez-Macías, L.; Castro, A.; et al. Parkinson disease and progressive supranuclear palsy: Protein expression in skin. *Ann. Clin. Transl. Neurol.* **2016**, *3*, 191–199. [CrossRef]
43. Sun, Y.; Zhang, M.; Chen, C.C.; Gillilland, M., 3rd; Sun, X.; El-Zaatari, M.; Huffnagle, G.B.; Young, V.B.; Zhang, J.; Hong, S.C.; et al. Stress-induced corticotropin-releasing hormone-mediated NLRP6 inflammasome inhibition and transmissible enteritis in mice. *Gastroenterology* **2013**, *144*, 1478–1487.e8. [CrossRef]
44. Li, Y.; Chen, Y.; Jiang, L.; Zhang, J.; Tong, X.; Chen, D.; Le, W. Intestinal Inflammation and Parkinson's Disease. *Aging Dis.* **2021**, *12*, 2052–2068. [CrossRef]
45. Nie, S.; Jing, Z.; Wang, J.; Deng, Y.; Zhang, Y.; Ye, Z.; Ge, Y. The link between increased Desulfovibrio and disease severity in Parkinson's disease. *Appl. Microbiol. Biotechnol.* **2023**, *107*, 3033–3045. [CrossRef]
46. Walker, A.; Czyz, D.M. Oh my gut! Is the microbial origin of neurodegenerative diseases real? *Infect. Immun.* **2023**, *91*, e0043722. [CrossRef] [PubMed]
47. Huynh, V.A.; Takala, T.M.; Murros, K.E.; Diwedi, B.; Saris, P.E.J. Desulfovibrio bacteria enhance alpha-synuclein aggregation in a Caenorhabditis elegans model of Parkinson's disease. *Front. Cell. Infect. Microbiol.* **2023**, *13*, 1181315. [CrossRef] [PubMed]
48. Andersen, K.K.; Vad, B.S.; Kjaer, L.; Tolker-Nielsen, T.; Christiansen, G.; Otzen, D.E. Pseudomonas aeruginosa rhamnolipid induces fibrillation of human α-synuclein and modulates its effect on biofilm formation. *FEBS Lett.* **2018**, *592*, 1484–1496. [CrossRef] [PubMed]
49. Bleffert, F.; Granzin, J.; Gohlke, H.; Batra-Safferling, R.; Jaeger, K.E.; Kovacic, F. Pseudomonas aeruginosa esterase PA2949, a bacterial homolog of the human membrane esterase ABHD6: Expression, purification and crystallization. *Acta Crystallogr. F Struct. Biol. Commun.* **2019**, *75 Pt 4*, 270–277. [CrossRef]
50. Han, Q.W.; Yuan, Y.H.; Chen, N.H. The therapeutic role of cannabinoid receptors and its agonists or antagonists in Parkinson's disease. *Prog. Neuropsychopharmacol. Biol. Psychiatry* **2020**, *96*, 109745. [CrossRef]
51. Romo-Vaquero, M.; Fernández-Villalba, E.; Gil-Martinez, A.L.; Cuenca-Bermejo, L.; Espín, J.C.; Herrero, M.T.; Selma, M.V. Urolithins: Potential biomarkers of gut dysbiosis and disease stage in Parkinson's patients. *Food Funct.* **2022**, *13*, 6306–6316. [CrossRef]
52. Sun, C.Y.; Li, J.R.; Wang, Y.Y.; Lin, S.Y.; Ou, Y.C.; Lin, C.J.; Wang, J.D.; Liao, S.L.; Chen, C.J. p-Cresol Sulfate Caused Behavior Disorders and Neurodegeneration in Mice with Unilateral Nephrectomy Involving Oxidative Stress and Neuroinflammation. *Int. J. Mol. Sci.* **2020**, *21*, 6687. [CrossRef]
53. Singh, Y.; Trautwein, C.; Romani, J.; Salker, M.S.; Neckel, P.H.; Fraccaroli, I.; Abeditashi, M.; Woerner, N.; Admard, J.; Dhariwal, A.; et al. Overexpression of human alpha-Synuclein leads to dysregulated microbiome/metabolites with ageing in a rat model of Parkinson disease. *Mol. Neurodegener.* **2023**, *18*, 44. [CrossRef]
54. Ashurst, J.V.; Nappe, T.M. Isopropanol Toxicity. In *StatPearls*; StatPearls Publishing LLC: Treasure Island, FL, USA, 2025.
55. Mathew, A.R.; Di Matteo, G.; La Rosa, P.; Barbati, S.A.; Mannina, L.; Moreno, S.; Tata, A.M.; Cavallucci, V.; Fidaleo, M. Vitamin B12 Deficiency and the Nervous System: Beyond Metabolic Decompensation—Comparing Biological Models and Gaining New Insights into Molecular and Cellular Mechanisms. *Int. J. Mol. Sci.* **2024**, *25*, 590. [CrossRef]
56. Wang, C.; Yang, M.; Liu, D.; Zheng, C. Metabolic rescue of α-synuclein-induced neurodegeneration through propionate supplementation and intestine-neuron signaling in *C. elegans*. *Cell Rep.* **2024**, *43*, 113865. [CrossRef] [PubMed]
57. Proano, A.C.; Viteri, J.A.; Orozco, E.N.; Calle, M.A.; Costa, S.C.; Reyes, D.V.; German-Montenegro, M.; Moncayo, D.F.; Tobar, A.C.; Moncayo, J.A. Gut Microbiota and Its Repercussion in Parkinson's Disease: A Systematic Review in Occidental Patients. *Neurol. Int.* **2023**, *15*, 750–763. [CrossRef]
58. Xie, J.; Li, L.F.; Dai, T.Y.; Qi, X.; Wang, Y.; Zheng, T.Z.; Gao, X.Y.; Zhang, Y.J.; Ai, Y.; Ma, L.; et al. Short-Chain Fatty Acids Produced by *Ruminococcaceae* Mediate α-Linolenic Acid Promote Intestinal Stem Cells Proliferation. *Mol. Nutr. Food Res.* **2022**, *66*, e2100408. [CrossRef] [PubMed]
59. Yang, Q.; Wei, C.; Guo, S.; Liu, J.; Tao, Y. Cloning and characterization of a L-lactate dehydrogenase gene from *Ruminococcaceae* bacterium CPB6. *World J. Microbiol. Biotechnol.* **2020**, *36*, 182. [CrossRef] [PubMed]
60. Teng, Y.; Mu, J.; Xu, F.; Zhang, X.; Sriwastva, M.K.; Liu, Q.M.; Li, X.; Lei, C.; Sundaram, K.; Hu, X.; et al. Gut bacterial isoamylamine promotes age-related cognitive dysfunction by promoting microglial cell death. *Cell Host Microbe* **2022**, *30*, 944–960.e8. [CrossRef]
61. Tao, Y.; Zhu, X.; Wang, H.; Wang, Y.; Li, X.; Jin, H.; Rui, J. Complete genome sequence of *Ruminococcaceae* bacterium CPB6: A newly isolated culture for efficient n-caproic acid production from lactate. *J. Biotechnol.* **2017**, *259*, 91–94. [CrossRef]
62. Zhu, Y.; Li, Y.; Zhang, Q.; Song, Y.; Wang, L.; Zhu, Z. Interactions Between Intestinal Microbiota and Neural Mitochondria: A New Perspective on Communicating Pathway from Gut to Brain. *Front. Microbiol.* **2022**, *13*, 798917. [CrossRef]

63. Wei, Y.; Gao, J.; Kou, Y.; Liu, M.; Meng, L.; Zheng, X.; Xu, S.; Liang, M.; Sun, H.; Liu, Z.; et al. The intestinal microbial metabolite desaminotyrosine is an anti-inflammatory molecule that modulates local and systemic immune homeostasis. *FASEB J.* **2020**, *34*, 16117–16128. [CrossRef] [PubMed]
64. Palacios, N.; Hannoun, A.; Flahive, J.; Ward, D.; Goostrey, K.; Deb, A.; Smith, K.M. Effect of Levodopa Initiation on the Gut Microbiota in Parkinson's Disease. *Front. Neurol.* **2021**, *12*, 574529. [CrossRef] [PubMed]
65. Chu, C.; Yu, L.; Li, Y.; Guo, H.; Zhai, Q.; Chen, W.; Tian, F. Lactobacillus plantarum CCFM405 against Rotenone-Induced Parkinson's Disease Mice via Regulating Gut Microbiota and Branched-Chain Amino Acids Biosynthesis. *Nutrients* **2023**, *15*, 1737. [CrossRef]
66. Lee, Y.Z.; Cheng, S.H.; Chang, M.Y.; Lin, Y.F.; Wu, C.C.; Tsai, Y.C. Neuroprotective Effects of Lactobacillus plantarum PS128 in a Mouse Model of Parkinson's Disease: The Role of Gut Microbiota and MicroRNAs. *Int. J. Mol. Sci.* **2023**, *24*, 6794. [CrossRef]
67. Rosario, D.; Boren, J.; Uhlen, M.; Proctor, G.; Aarsland, D.; Mardinoglu, A.; Shoaie, S. Systems Biology Approaches to Understand the Host-Microbiome Interactions in Neurodegenerative Diseases. *Front. Neurosci.* **2020**, *14*, 716. [CrossRef] [PubMed]
68. Andoh, A. Physiological Role of Gut Microbiota for Maintaining Human Health. *Digestion* **2016**, *93*, 176–181. [CrossRef]
69. Flint, H.J. Gut microbial metabolites in health and disease. *Gut Microbes* **2016**, *7*, 187–188. [CrossRef]
70. Dalile, B.; Van Oudenhove, L.; Vervliet, B.; Verbeke, K. The role of short-chain fatty acids in microbiota-gut-brain communication. *Nat. Rev. Gastroenterol. Hepatol.* **2019**, *16*, 461–478. [CrossRef]
71. Martin-Gallausiaux, C.; Marinelli, L.; Blottière, H.M.; Larraufie, P.; Lapaque, N. SCFA: Mechanisms and functional importance in the gut. *Proc. Nutr. Soc.* **2021**, *80*, 37–49. [CrossRef]
72. Yao, Y.; Cai, X.; Fei, W.; Ye, Y.; Zhao, M.; Zheng, C. The role of short-chain fatty acids in immunity, inflammation and metabolism. *Crit. Rev. Food Sci. Nutr.* **2022**, *62*, 1–12. [CrossRef]
73. Silva, Y.P.; Bernardi, A.; Frozza, R.L. The Role of Short-Chain Fatty Acids From Gut Microbiota in Gut-Brain Communication. *Front. Endocrinol.* **2020**, *11*, 25. [CrossRef] [PubMed]
74. Hsiao, E.Y.; McBride, S.W.; Hsien, S.; Sharon, G.; Hyde, E.R.; McCue, T.; Codelli, J.A.; Chow, J.; Reisman, S.E.; Petrosino, J.F.; et al. Microbiota modulate behavioral and physiological abnormalities associated with neurodevelopmental disorders. *Cell* **2013**, *155*, 1451–1463. [CrossRef]
75. Bermudez-Martin, P.; Becker, J.A.J.; Caramello, N.; Fernandez, S.P.; Costa-Campos, R.; Canaguier, J.; Barbosa, S.; Martinez-Gili, L.; Myridakis, A.; Dumas, M.E.; et al. The microbial metabolite p-Cresol induces autistic-like behaviors in mice by remodeling the gut microbiota. *Microbiome* **2021**, *9*, 157. [CrossRef] [PubMed]
76. O'Mahony, S.M.; Clarke, G.; Borre, Y.E.; Dinan, T.G.; Cryan, J.F. Serotonin, tryptophan metabolism and the brain-gut-microbiome axis. *Behav. Brain Res.* **2015**, *277*, 32–48. [CrossRef]
77. Kigerl, K.A.; Ankeny, D.P.; Garg, S.K.; Wei, P.; Guan, Z.; Lai, W.; McTigue, D.M.; Banerjee, R.; Popovich, P.G. System x_c^- regulates microglia and macrophage glutamate excitotoxicity in vivo. *Exp. Neurol.* **2012**, *233*, 333–341. [CrossRef]
78. Pavek, P. Pregnane X Receptor (PXR)-Mediated Gene Repression and Cross-Talk of PXR with Other Nuclear Receptors via Coactivator Interactions. *Front. Pharmacol.* **2016**, *7*, 456. [CrossRef]
79. Lavelle, A.; Sokol, H. Gut microbiota-derived metabolites as key actors in inflammatory bowel disease. *Nat. Rev. Gastroenterol. Hepatol.* **2020**, *17*, 223–237. [CrossRef]
80. Ağagündüz, D.; Yılmaz, B.; Şahin, T.; Güneşliol, B.E.; Ayten, Ş.; Russo, P.; Spano, G.; Rocha, J.M.; Bartkiene, E.; Özogul, F. Dairy Lactic Acid Bacteria and Their Potential Function in Dietetics: The Food-Gut-Health Axis. *Foods* **2021**, *10*, 3099. [CrossRef] [PubMed]
81. Pham, L.; Baiocchi, L.; Kennedy, L.; Sato, K.; Meadows, V.; Meng, F.; Huang, C.K.; Kundu, D.; Zhou, T.; Chen, L.; et al. The interplay between mast cells, pineal gland, and circadian rhythm: Links between histamine, melatonin, and inflammatory mediators. *J. Pineal Res.* **2021**, *70*, e12699. [CrossRef]
82. Chambers, E.S.; Viardot, A.; Psichas, A.; Morrison, D.J.; Murphy, K.G.; Zac-Varghese, S.E.; MacDougall, K.; Preston, T.; Tedford, C.; Finlayson, G.S.; et al. Effects of targeted delivery of propionate to the human colon on appetite regulation, body weight maintenance and adiposity in overweight adults. *Gut* **2015**, *64*, 1744–1754. [CrossRef]
83. Agnihotri, N.; Mohajeri, M.H. Involvement of Intestinal Microbiota in Adult Neurogenesis and the Expression of Brain-Derived Neurotrophic Factor. *Int. J. Mol. Sci.* **2022**, *23*, 15934. [CrossRef] [PubMed]
84. Müller, P.; Duderstadt, Y.; Lessmann, V.; Müller, N.G. Lactate and BDNF: Key Mediators of Exercise Induced Neuroplasticity? *J. Clin. Med.* **2020**, *9*, 1136. [CrossRef]
85. Guillemin, G.J. Quinolinic acid, the inescapable neurotoxin. *FEBS J.* **2012**, *279*, 1356–1365. [CrossRef] [PubMed]
86. Kaisar, M.M.M.; Pelgrom, L.R.; van der Ham, A.J.; Yazdanbakhsh, M.; Everts, B. Butyrate Conditions Human Dendritic Cells to Prime Type 1 Regulatory T Cells via both Histone Deacetylase Inhibition and G Protein-Coupled Receptor 109A Signaling. *Front. Immunol.* **2017**, *8*, 1429. [CrossRef]

87. Rosser, E.C.; Piper, C.J.M.; Matei, D.E.; Blair, P.A.; Rendeiro, A.F.; Orford, M.; Alber, D.G.; Krausgruber, T.; Catalan, D.; Klein, N.; et al. Microbiota-Derived Metabolites Suppress Arthritis by Amplifying Aryl-Hydrocarbon Receptor Activation in Regulatory B Cells. *Cell Metab.* **2020**, *31*, 837–851.e10. [CrossRef]
88. Varela, R.B.; Valvassori, S.S.; Lopes-Borges, J.; Mariot, E.; Dal-Pont, G.C.; Amboni, R.T.; Bianchini, G.; Quevedo, J. Sodium butyrate and mood stabilizers block ouabain-induced hyperlocomotion and increase BDNF, NGF and GDNF levels in brain of Wistar rats. *J. Psychiatr. Res.* **2015**, *61*, 114–121. [CrossRef] [PubMed]
89. Barker, R.A.; Björklund, A.; Gash, D.M.; Whone, A.; Van Laar, A.; Kordower, J.H.; Bankiewicz, K.; Kieburtz, K.; Saarma, M.; Booms, S.; et al. GDNF and Parkinson's Disease: Where Next? A Summary from a Recent Workshop. *J. Park. Dis.* **2020**, *10*, 875–891. [CrossRef]
90. Selma-Royo, M.; Tarrazó, M.; García-Mantrana, I.; Gómez-Gallego, C.; Salminen, S.; Collado, M.C. Shaping Microbiota During the First 1000 Days of Life. *Adv. Exp. Med. Biol.* **2019**, *1125*, 3–24.
91. Garcia-Mantrana, I.; Selma-Royo, M.; Alcantara, C.; Collado, M.C. Shifts on Gut Microbiota Associated to Mediterranean Diet Adherence and Specific Dietary Intakes on General Adult Population. *Front. Microbiol.* **2018**, *9*, 890. [CrossRef]
92. Fusco, W.; Lorenzo, M.B.; Cintoni, M.; Porcari, S.; Rinninella, E.; Kaitsas, F.; Lener, E.; Mele, M.C.; Gasbarrini, A.; Collado, M.C.; et al. Short-Chain Fatty-Acid-Producing Bacteria: Key Components of the Human Gut Microbiota. *Nutrients* **2023**, *15*, 2211. [CrossRef]
93. Vacca, M.; Celano, G.; Calabrese, F.M.; Portincasa, P.; Gobbetti, M.; De Angelis, M. The Controversial Role of Human Gut Lachnospiraceae. *Microorganisms* **2020**, *8*, 573. [CrossRef] [PubMed]
94. Maturana, J.L.; Cárdenas, J.P. Insights on the Evolutionary Genomics of the Blautia Genus: Potential New Species and Genetic Content Among Lineages. *Front. Microbiol.* **2021**, *12*, 660920. [CrossRef]
95. Nie, K.; Ma, K.; Luo, W.; Shen, Z.; Yang, Z.; Xiao, M.; Tong, T.; Yang, Y.; Wang, X. Roseburia intestinalis: A Beneficial Gut Organism from the Discoveries in Genus and Species. *Front. Cell. Infect. Microbiol.* **2021**, *11*, 757718. [CrossRef] [PubMed]
96. Zaplana, T.; Miele, S.; Tolonen, A.C. Lachnospiraceae are emerging industrial biocatalysts and biotherapeutics. *Front. Bioeng. Biotechnol.* **2023**, *11*, 1324396. [CrossRef]
97. Palmnäs-Bédard, M.S.A.; Costabile, G.; Vetrani, C.; Åberg, S.; Hjalmarsson, Y.; Dicksved, J.; Riccardi, G.; Landberg, R. The human gut microbiota and glucose metabolism: A scoping review of key bacteria and the potential role of SCFAs. *Am. J. Clin. Nutr.* **2022**, *116*, 862–874. [CrossRef] [PubMed]
98. Ramakrishna, B.S. Role of the gut microbiota in human nutrition and metabolism. *J. Gastroenterol. Hepatol.* **2013**, *28* (Suppl. 4), 9–17. [CrossRef]
99. Loh, J.S.; Mak, W.Q.; Tan, L.K.S.; Ng, C.X.; Chan, H.H.; Yeow, S.H.; Foo, J.B.; Ong, Y.S.; How, C.W.; Khaw, K.Y. Microbiota-gut-brain axis and its therapeutic applications in neurodegenerative diseases. *Signal Transduct. Target. Ther.* **2024**, *9*, 37.
100. Nysten, J.; Van Dijck, P. Can we microbe-manage our vitamin acquisition for better health? *PLoS Pathog.* **2023**, *19*, e1011361. [CrossRef]
101. Magnúsdóttir, S.; Ravcheev, D.; de Crécy-Lagard, V.; Thiele, I. Systematic genome assessment of B-vitamin biosynthesis suggests co-operation among gut microbes. *Front. Genet.* **2015**, *6*, 148. [CrossRef]
102. Hossain, K.S.; Amarasena, S.; Mayengbam, S. B Vitamins and Their Roles in Gut Health. *Microorganisms* **2022**, *10*, 1168. [CrossRef]
103. Peterson, C.T.; Rodionov, D.A.; Osterman, A.L.; Peterson, S.N. B Vitamins and Their Role in Immune Regulation and Cancer. *Nutrients* **2020**, *12*, 3380. [CrossRef] [PubMed]
104. Uebanso, T.; Shimohata, T.; Mawatari, K.; Takahashi, A. Functional Roles of B-Vitamins in the Gut and Gut Microbiome. *Mol. Nutr. Food Res.* **2020**, *64*, e2000426. [CrossRef]
105. Javanmardi, S.; Rezaei Tavabe, K.; Rosentrater, K.A.; Solgi, M.; Bahadori, R. Effects of different levels of vitamin B(6) in tank water on the Nile tilapia (*Oreochromis niloticus*): Growth performance, blood biochemical parameters, intestine and liver histology, and intestinal enzyme activity. *Fish. Physiol. Biochem.* **2020**, *46*, 1909–1920. [CrossRef] [PubMed]
106. Feng, C.; Yan, J.; Luo, T.; Zhang, H.; Zhang, H.; Yuan, Y.; Chen, Y.; Chen, H. Vitamin B12 ameliorates gut epithelial injury via modulating the HIF-1 pathway and gut microbiota. *Cell. Mol. Life Sci.* **2024**, *81*, 397. [CrossRef] [PubMed]
107. Ge, Y.; Zadeh, M.; Mohamadzadeh, M. Vitamin B12 coordinates ileal epithelial cell and microbiota functions to resist Salmonella infection in mice. *J. Exp. Med.* **2022**, *219*, e20220057. [CrossRef]
108. Roth, W.; Mohamadzadeh, M. Vitamin B12 and gut-brain homeostasis in the pathophysiology of ischemic stroke. *EBioMedicine* **2021**, *73*, 103676. [CrossRef]
109. Karl, J.P.; Meydani, M.; Barnett, J.B.; Vanegas, S.M.; Barger, K.; Fu, X.; Goldin, B.; Kane, A.; Rasmussen, H.; Vangay, P.; et al. Fecal concentrations of bacterially derived vitamin K forms are associated with gut microbiota composition but not plasma or fecal cytokine concentrations in healthy adults. *Am. J. Clin. Nutr.* **2017**, *106*, 1052–1061. [CrossRef]
110. Pan, M.H.; Maresz, K.; Lee, P.S.; Wu, J.C.; Ho, C.T.; Popko, J.; Mehta, D.S.; Stohs, S.J.; Badmaev, V. Inhibition of TNF-α, IL-1α, and IL-1β by Pretreatment of Human Monocyte-Derived Macrophages with Menaquinone-7 and Cell Activation with TLR Agonists In Vitro. *J. Med. Food* **2016**, *19*, 663–669. [CrossRef]

111. Dihingia, A.; Ozah, D.; Baruah, P.K.; Kalita, J.; Manna, P. Prophylactic role of vitamin K supplementation on vascular inflammation in type 2 diabetes by regulating the NF-κB/Nrf2 pathway via activating Gla proteins. *Food Funct.* **2018**, *9*, 450–462. [CrossRef]
112. Dai, L.; Mafra, D.; Shiels, P.G.; Hackeng, T.M.; Stenvinkel, P.; Schurgers, L.J. Vitamin K and Hallmarks of Ageing: Focus on Diet and Gut Microbiome. *Nutrients* **2023**, *15*, 2727. [CrossRef] [PubMed]
113. Popa, D.S.; Bigman, G.; Rusu, M.E. The Role of Vitamin K in Humans: Implication in Aging and Age-Associated Diseases. *Antioxidants* **2021**, *10*, 566. [CrossRef] [PubMed]
114. Shiels, P.G.; Painer, J.; Natterson-Horowitz, B.; Johnson, R.J.; Miranda, J.J.; Stenvinkel, P. Manipulating the exposome to enable better ageing. *Biochem. J.* **2021**, *478*, 2889–2898. [CrossRef] [PubMed]
115. Bonakdar, M.; Czuba, L.C.; Han, G.; Zhong, G.; Luong, H.; Isoherranen, N.; Vaishnava, S. Gut commensals expand vitamin A metabolic capacity of the mammalian host. *Cell Host Microbe* **2022**, *30*, 1084–1092.e5. [CrossRef]
116. Bourke, C.D.; Berkley, J.A.; Prendergast, A.J. Immune Dysfunction as a Cause and Consequence of Malnutrition. *Trends Immunol.* **2016**, *37*, 386–398. [CrossRef]
117. Zhu, Y.; Self, W.K.; Holtzman, D.M. An emerging role for the gut microbiome in tauopathy. *Neurotherapeutics* **2024**, *21*, e00423. [CrossRef] [PubMed]
118. Mossad, O.; Batut, B.; Yilmaz, B.; Dokalis, N.; Mezö, C.; Nent, E.; Nabavi, L.S.; Mayer, M.; Maron, F.J.M.; Buescher, J.M.; et al. Gut microbiota drives age-related oxidative stress and mitochondrial damage in microglia via the metabolite N(6)-carboxymethyllysine. *Nat. Neurosci.* **2022**, *25*, 295–305. [CrossRef]
119. Buchon, N.; Broderick, N.A.; Chakrabarti, S.; Lemaitre, B. Invasive and indigenous microbiota impact intestinal stem cell activity through multiple pathways in Drosophila. *Genes. Dev.* **2009**, *23*, 2333–2344. [CrossRef]
120. Lei, H.; Crawford, M.S.; McCole, D.F. JAK-STAT Pathway Regulation of Intestinal Permeability: Pathogenic Roles and Therapeutic Opportunities in Inflammatory Bowel Disease. *Pharmaceuticals* **2021**, *14*, 840. [CrossRef]
121. Zhao, J.; Bang, S.; Furutani, K.; McGinnis, A.; Jiang, C.; Roberts, A.; Donnelly, C.R.; He, Q.; James, M.L.; Berger, M.; et al. PD-L1/PD-1 checkpoint pathway regulates hippocampal neuronal excitability and learning and memory behavior. *Neuron* **2023**, *111*, 2709–2726.e9. [CrossRef]
122. Zhou, Y.; Liu, Z.; Chen, T. Gut Microbiota: A Promising Milestone in Enhancing the Efficacy of PD1/PD-L1 Blockade Therapy. *Front. Oncol.* **2022**, *12*, 847350. [CrossRef]
123. Chen, X.; Firulyova, M.; Manis, M.; Herz, J.; Smirnov, I.; Aladyeva, E.; Wang, C.; Bao, X.; Finn, M.B.; Hu, H.; et al. Microglia-mediated T cell infiltration drives neurodegeneration in tauopathy. *Nature* **2023**, *615*, 668–677. [CrossRef] [PubMed]
124. Hamilton, A.M.; Krout, I.N.; White, A.C.; Sampson, T.R. Microbiome-based therapeutics for Parkinson's disease. *Neurotherapeutics* **2024**, *21*, e00462. [CrossRef]
125. DuPont, H.L.; Suescun, J.; Jiang, Z.D.; Brown, E.L.; Essigmann, H.T.; Alexander, A.S.; DuPont, A.W.; Iqbal, T.; Utay, N.S.; Newmark, M.; et al. Fecal microbiota transplantation in Parkinson's disease—A randomized repeat-dose, placebo-controlled clinical pilot study. *Front. Neurol.* **2023**, *14*, 1104759. [CrossRef]
126. Cheng, Y.; Tan, G.; Zhu, Q.; Wang, C.; Ruan, G.; Ying, S.; Qie, J.; Hu, X.; Xiao, Z.; Xu, F.; et al. Efficacy of fecal microbiota transplantation in patients with Parkinson's disease: Clinical trial results from a randomized, placebo-controlled design. *Gut Microbes* **2023**, *15*, 2284247. [CrossRef]
127. Scheperjans, F.; Levo, R.; Bosch, B.; Lääperi, M.; Pereira, P.A.B.; Smolander, O.P.; Aho, V.T.E.; Vetkas, N.; Toivio, L.; Kainulainen, V.; et al. Fecal Microbiota Transplantation for Treatment of Parkinson Disease: A Randomized Clinical Trial. *JAMA Neurol.* **2024**, *81*, 925–938. [CrossRef] [PubMed]
128. Tian, H.; Wang, J.; Feng, R.; Zhang, R.; Liu, H.; Qin, C.; Meng, L.; Chen, Y.; Fu, Y.; Liang, D.; et al. Efficacy of faecal microbiota transplantation in patients with progressive supranuclear palsy-Richardson's syndrome: A phase 2, single centre, randomised clinical trial. *EClinicalMedicine* **2023**, *58*, 101888. [CrossRef] [PubMed]
129. Forloni, G. Alpha Synuclein: Neurodegeneration and Inflammation. *Int. J. Mol. Sci.* **2023**, *24*, 5914. [CrossRef] [PubMed]
130. Wijeyekoon, R.S.; Kronenberg-Versteeg, D.; Scott, K.M.; Hayat, S.; Kuan, W.L.; Evans, J.R.; Breen, D.P.; Cummins, G.; Jones, J.L.; Clatworthy, M.R.; et al. Peripheral innate immune and bacterial signals relate to clinical heterogeneity in Parkinson's disease. *Brain Behav. Immun.* **2020**, *87*, 473–488. [CrossRef]
131. Su, Y.; Shi, C.; Wang, T.; Liu, C.; Yang, J.; Zhang, S.; Fan, L.; Zheng, H.; Li, X.; Luo, H.; et al. Dysregulation of peripheral monocytes and pro-inflammation of alpha-synuclein in Parkinson's disease. *J. Neurol.* **2022**, *269*, 6386–6394. [CrossRef]
132. La Vitola, P.; Balducci, C.; Baroni, M.; Artioli, L.; Santamaria, G.; Castiglioni, M.; Cerovic, M.; Colombo, L.; Caldinelli, L.; Pollegioni, L.; et al. Peripheral inflammation exacerbates α-synuclein toxicity and neuropathology in Parkinson's models. *Neuropathol. Appl. Neurobiol.* **2021**, *47*, 43–60. [CrossRef]
133. Reddy, K.; Dieriks, B.V. Multiple system atrophy: α-Synuclein strains at the neuron-oligodendrocyte crossroad. *Mol. Neurodegener.* **2022**, *17*, 77. [CrossRef]
134. Holec, S.A.M.; Lee, J.; Oehler, A.; Batia, L.; Wiggins-Gamble, A.; Lau, J.; Ooi, F.K.; Merz, G.E.; Wang, M.; Mordes, D.A.; et al. The E46K mutation modulates α-synuclein prion replication in transgenic mice. *PLoS Pathog.* **2022**, *18*, e1010956. [CrossRef] [PubMed]

135. Pan, L.; Li, C.; Meng, L.; Tian, Y.; He, M.; Yuan, X.; Zhang, G.; Zhang, Z.; Xiong, J.; Chen, G.; et al. Tau accelerates α-synuclein aggregation and spreading in Parkinson's disease. *Brain* **2022**, *145*, 3454–3471. [CrossRef]
136. Engen, P.A.; Dodiya, H.B.; Naqib, A.; Forsyth, C.B.; Green, S.J.; Voigt, R.M.; Kordower, J.H.; Mutlu, E.A.; Shannon, K.M.; Keshavarzian, A. The Potential Role of Gut-Derived Inflammation in Multiple System Atrophy. *J. Park. Dis.* **2017**, *7*, 331–346. [CrossRef] [PubMed]
137. Tan, A.H.; Chong, C.W.; Song, S.L.; Teh, C.S.J.; Yap, I.K.S.; Loke, M.F.; Tan, Y.Q.; Yong, H.S.; Mahadeva, S.; Lang, A.E.; et al. Altered gut microbiome and metabolome in patients with multiple system atrophy. *Mov. Disord.* **2018**, *33*, 174–176. [CrossRef] [PubMed]
138. Wan, L.; Zhou, X.; Wang, C.; Chen, Z.; Peng, H.; Hou, X.; Peng, Y.; Wang, P.; Li, T.; Yuan, H.; et al. Alterations of the Gut Microbiota in Multiple System Atrophy Patients. *Front. Neurosci.* **2019**, *13*, 1102. [CrossRef]
139. Nagoya University. New Research Shows Link Between Gut Microbiota and Parkinson's Disease. 2024. Available online: https://www.labmanager.com/new-research-shows-link-between-gut-microbiata-and-parkinson-s-disease-32393 (accessed on 20 January 2025).
140. Nishiwaki, H.; Ueyama, J.; Ito, M.; Hamaguchi, T.; Takimoto, K.; Maeda, T.; Kashihara, K.; Tsuboi, Y.; Mori, H.; Kurokawa, K.; et al. Meta-analysis of shotgun sequencing of gut microbiota in Parkinson's disease. *NPJ Park. Dis.* **2024**, *10*, 106. [CrossRef]
141. Zhao, Z.; Chen, J.; Zhao, D.; Chen, B.; Wang, Q.; Li, Y.; Chen, J.; Bai, C.; Guo, X.; Hu, N.; et al. Microbial biomarker discovery in Parkinson's disease through a network-based approach. *NPJ Park. Dis.* **2024**, *10*, 203. [CrossRef]
142. Munoz-Pinto, M.F.; Candeias, E.; Melo-Marques, I.; Esteves, A.R.; Maranha, A.; Magalhães, J.D.; Carneiro, D.R.; Sant'Anna, M.; Pereira-Santos, A.R.; Abreu, A.E.; et al. Gut-first Parkinson's disease is encoded by gut dysbiome. *Mol. Neurodegener.* **2024**, *19*, 78. [CrossRef]
143. Borzabadi, S.; Oryan, S.; Eidi, A.; Aghadavod, E.; Daneshvar Kakhaki, R.; Tamtaji, O.R.; Taghizadeh, M.; Asemi, Z. The Effects of Probiotic Supplementation on Gene Expression Related to Inflammation, Insulin and Lipid in Patients with Parkinson's Disease: A Randomized, Double-blind, PlaceboControlled Trial. *Arch. Iran. Med.* **2018**, *21*, 289–295.
144. Tamtaji, O.R.; Taghizadeh, M.; Daneshvar Kakhaki, R.; Kouchaki, E.; Bahmani, F.; Borzabadi, S.; Oryan, S.; Mafi, A.; Asemi, Z. Clinical and metabolic response to probiotic administration in people with Parkinson's disease: A randomized, double-blind, placebo-controlled trial. *Clin. Nutr.* **2019**, *38*, 1031–1035. [CrossRef] [PubMed]
145. Becker, A.; Schmartz, G.P.; Gröger, L.; Grammes, N.; Galata, V.; Philippeit, H.; Weiland, J.; Ludwig, N.; Meese, E.; Tierling, S.; et al. Effects of Resistant Starch on Symptoms, Fecal Markers, and Gut Microbiota in Parkinson's Disease—The RESISTA-PD Trial. *Genom. Proteom. Bioinform.* **2022**, *20*, 274–287. [CrossRef]
146. Hall, D.A.; Voigt, R.M.; Cantu-Jungles, T.M.; Hamaker, B.; Engen, P.A.; Shaikh, M.; Raeisi, S.; Green, S.J.; Naqib, A.; Forsyth, C.B.; et al. An open label, non-randomized study assessing a prebiotic fiber intervention in a small cohort of Parkinson's disease participants. *Nat. Commun.* **2023**, *14*, 926. [CrossRef] [PubMed]
147. Sun, H.; Zhao, F.; Liu, Y.; Ma, T.; Jin, H.; Quan, K.; Leng, B.; Zhao, J.; Yuan, X.; Li, Z.; et al. Probiotics synergized with conventional regimen in managing Parkinson's disease. *NPJ Park. Dis.* **2022**, *8*, 62. [CrossRef]
148. Yang, X.; He, X.; Xu, S.; Zhang, Y.; Mo, C.; Lai, Y.; Song, Y.; Yan, Z.; Ai, P.; Qian, Y.; et al. Effect of Lacticaseibacillus paracasei strain Shirota supplementation on clinical responses and gut microbiome in Parkinson's disease. *Food Funct.* **2023**, *14*, 6828–6839. [CrossRef] [PubMed]
149. Loeffler, D.A. Influence of Normal Aging on Brain Autophagy: A Complex Scenario. *Front. Aging Neurosci.* **2019**, *11*, 49. [CrossRef]
150. Ahmed, S.; Busetti, A.; Fotiadou, P.; Vincy Jose, N.; Reid, S.; Georgieva, M.; Brown, S.; Dunbar, H.; Beurket-Ascencio, G.; Delday, M.I.; et al. In vitro Characterization of Gut Microbiota-Derived Bacterial Strains with Neuroprotective Properties. *Front. Cell Neurosci.* **2019**, *13*, 402. [CrossRef]
151. Głowacka, P.; Oszajca, K.; Pudlarz, A.; Szemraj, J.; Witusik-Perkowska, M. Postbiotics as Molecules Targeting Cellular Events of Aging Brain-The Role in Pathogenesis, Prophylaxis and Treatment of Neurodegenerative Diseases. *Nutrients* **2024**, *16*, 2244. [CrossRef]
152. Tanner, C. Microbiota Intervention to Change the Response of Parkinson's Disease. 2019. Available online: https://clinicaltrials.ucsf.edu/trial/NCT03575195 (accessed on 20 January 2025).
153. Ho, J. To Assess the Efficacy and Safety of Ceftriaxone in Patients with Mild to Moderate Parkinson's Disease Dementia. 2019. Available online: https://clinicaltrial.be/nl/details/69615?per_page=100&only_recruiting=0&only_eligible=0&only_active=0 (accessed on 20 January 2025).

154. Wang, J.Y.; Doudna, J.A. CRISPR technology: A decade of genome editing is only the beginning. *Science* **2023**, *379*, eadd8643. [CrossRef]
155. Liu, J.; Lv, X.; Ye, T.; Zhao, M.; Chen, Z.; Zhang, Y.; Yang, W.; Xie, H.; Zhan, L.; Chen, L.; et al. Microbiota-microglia crosstalk between Blautia producta and neuroinflammation of Parkinson's disease: A bench-to-bedside translational approach. *Brain Behav. Immun.* **2024**, *117*, 270–282. [CrossRef]

Disclaimer/Publisher's Note: The statements, opinions and data contained in all publications are solely those of the individual author(s) and contributor(s) and not of MDPI and/or the editor(s). MDPI and/or the editor(s) disclaim responsibility for any injury to people or property resulting from any ideas, methods, instructions or products referred to in the content.

International Journal of
Molecular Sciences

MDPI

Review

Update on the Symptomatic Treatment of Huntington's Disease: From Pathophysiology to Clinical Practice

Gonzalo Olmedo-Saura [1,2,3,4,5,†], Eugenio Bernardi [2,†], Lidia Bojtos [2,3,4,5], Saül Martínez-Horta [1,2,3,4,5], Javier Pagonabarraga [1,2,3,4], Jaime Kulisevsky [1,2,3,4,5,*] and Jesús Pérez-Pérez [1,2,3,4,5,*]

1 Medicine Department, Universitat Autònoma de Barcelona (UAB), 08193 Barcelona, Spain
2 Movement Disorders Unit, Neurology Department, Hospital de la Santa Creu i Sant Pau, 08041 Barcelona, Spain
3 Institut d'Investigacions Biomèdiques-Sant Pau (IIB-Sant Pau), 08041 Barcelona, Spain
4 Centro de Investigación Biomédica en Red-Enfermedades Neurodegenerativas (CIBERNED), 28029 Madrid, Spain
5 European Huntington's Disease Network (EHDN), 89081 Ulm, Germany
* Correspondence: jaime.kulisevsky@uab.cat (J.K.); jperezp@santpau.cat (J.P.-P.); Tel.: +34-93-5565986 (J.K.); Fax: +34-93-5565748 (J.K.)
† These authors contributed equally to this work.

Abstract: Huntington's disease (HD) is the most common autosomal dominant neurodegenerative disorder, characterized by a triad of motor dysfunction, cognitive decline, and psychiatric disturbances. While recent efforts have focused on developing disease-modifying therapies, no treatment has yet demonstrated clinical efficacy. As a result, symptomatic treatment remains the cornerstone of care. However, high-quality evidence from large randomized trials is limited, and therapeutic decisions must rely on clinical expertise and extrapolation from other neurological or psychiatric conditions. This narrative review provides a comprehensive and practical overview of symptomatic treatment strategies for HD with emphasis on the pathophysiological underpinnings of each symptom and the molecular mechanisms of available and emerging therapies, aiming to support rational, individualized management. Finally, we highlight the critical role of non-pharmacological interventions and the need for multidisciplinary approaches to optimize patient outcomes and quality of life.

Keywords: Huntington disease; chorea; movement disorders; cognitive dysfunction; psychiatric symptoms; pathophysiology

1. Introduction

Huntington's disease (HD) is the most common autosomal dominant neurodegenerative disorder, with an estimated prevalence of 10–12 cases per 100,000 individuals of European ancestry [1–3]. It is caused by an expansion of ≥36 CAG repeats (>39 for full penetrance) in the *HTT* gene [4], which encodes the huntingtin protein (HTT) [5,6]. The typical age at onset ranges from 30 to 60 years, with earlier onset and greater disease severity associated with longer expansions [7]. In addition to its well-characterized genetic basis, the clinical diagnosis and staging of HD have evolved from traditional motor-based criteria to a more biologically grounded framework. Classically, diagnosis is established in individuals with a pathogenic *HTT* expansion or positive family history who develop unequivocal motor signs, corresponding to a score of 4 (≥99% confidence) on the Diagnostic Confidence Level (DCL) of the Unified Huntington's Disease Rating Scale (UHDRS) [5]. More recently, the Huntington's Disease Integrated Staging System (HD-ISS) has been proposed for individuals with ≥40 CAG repeats. It defines four stages: stage 0 (gene expansion

carriers without detectable disease-related changes), stage 1 (evidence of neurodegeneration, typically caudate and/or putaminal atrophy), stage 2 (emergence of motor and/or cognitive signs based on UHDRS-Total Motor Score (TMS) and Symbol Digit Modalities Test thresholds), and stage 3 (functional decline).

Although the pathophysiology of HD is not fully elucidated, it is established that the expanded CAG repeat results in the production of abnormal and unstable HTT species, including full-length mutant HTT (mHTT), exon 1 fragments, and products of repeat-associated non-ATG (RAN) translation [8,9]. These species promote neurodegeneration through toxic gain-of-function mechanisms, including protein misfolding, aggregation, RNA-mediated toxicity, and dysregulation of other cellular processes [10–12]. A key modulator of disease onset and progression is somatic instability of the CAG repeat expansion [13–15], particularly within vulnerable cell populations as the striatal medium spiny neurons (MSNs). This process is modulated by several DNA repair pathways, with strong evidence implicating mismatch repair genes as PMS1, MLH1, MSH3, PMS2, FAN1, LIG1 [6,14–16].

Clinically, HD is characterized by a triad of motor, cognitive, and psychiatric manifestations that reflect the progressive disruption of cortico-striato-thalamo-cortical circuits including the motor, associative, and limbic loops [17].

While numerous disease-modifying therapies are under development—with several already being evaluated in ongoing phase 1 and 2 clinical trials, and some projected to soon enter phase 3 [10,18]—the treatment of HD remains entirely symptomatic. The general guiding principle is to prioritize the most disruptive symptoms reported by patients and caregivers, while carefully accounting for comorbidities and the side effects (especially considering the heightened sensitivity of HD patients to medication side effects). Notably, most pharmacological interventions have not been evaluated in large-scale randomized clinical trials (RCTs), limiting the robustness of the evidence supporting their use. Consequently, an optimal therapeutic approach requires a careful balance between clinical expertise and evidence-based medicine [19].

The aim of this review is to provide an updated, comprehensive and practical overview of symptomatic treatment strategies for HD. Emphasis is placed on the pathophysiological rationale, mechanisms of action, and real-world applicability of pharmacological and non-pharmacological interventions across the motor, cognitive, and psychiatric domains of the disease. Disease-modifying therapies are beyond the scope of this review.

2. Search Strategy

For this narrative review, we conducted a non-systematic literature search of peer-reviewed articles published in English up to March 2025. The search was performed using the PubMed database. The following search strategy was used: (“Huntington Disease” [Title] OR “Huntington’s Disease” [Title] OR “Huntington*” [Title]) AND (“treatment” [Title/Abstract] OR “therapy” [Title/Abstract] OR “management” [Title/Abstract] OR “pharmacological” [Title/Abstract] OR “non-pharmacological” [Title/Abstract]) AND Humans [Mesh]. Additional references were identified by manually screening the reference lists of included articles and relevant reviews. Studies considered pertinent to the scope of this review were selected for inclusion.

3. Symptomatic Treatment of Huntington’s Disease

3.1. Motor Symptoms

HD was first described by George Huntington in 1872 as “hereditary chorea” [20]. However, the motor phenotype is more complex and evolves with disease progression,

encompassing dystonia, gait abnormalities, motor impersistence, myoclonus, oculomotor disturbances and in advanced stages bradykinesia and rigidity.

These motor manifestations reflect the progressive disruption of basal ganglia circuits:

In early stages, there is preferential degeneration of D2-expressing GABAergic MSNs of the indirect pathway. These neurons, which contain enkephalin and project to the external globus pallidus (GPe), normally inhibit thalamocortical drive. Their loss leads to disinhibition of thalamic output and increased cortical excitability, resulting in hyperkinetic features such as chorea [17,21–23].

As neurodegeneration progresses to involve D1-expressing MSNs of the direct pathway and those that contain substance P and project to the internal globus pallidus (GPi), parkinsonian symptoms including bradykinesia and rigidity become more prominent [17,21–23].

Juvenile-onset HD or juvenile-HD (defined as onset before 21 years) accounts for 4–10% of cases [24] and typically presents with parkinsonism and dystonia as the initial motor symptoms, rather than chorea. This distinct phenotype, with more rapid progression, requires adapted symptomatic approaches [25–27].

This section will review the most clinically relevant motor symptoms of adult-onset HD individually, highlighting their pathophysiological basis and therapeutic management. Brief comments on juvenile HD are included where appropriate.

3.1.1. Chorea

Chorea is the hallmark motor feature of HD and often the earliest observed manifestation. It is also the symptom for which the greatest number of targeted interventions have been studied and are currently available. It refers to involuntary, irregular, purposeless, nonrhythmic, abrupt, rapid, unsustained movements that seem to flow from one part of the body to another [28,29]. The key for differentiating from other hyperkinetic movements is its randomness in timing, direction, and distribution [28,30].

In early stages, chorea typically begins in the facial muscles, especially the forehead, later spreads to the distal extremities and progressively involves more proximal areas such as the trunk. Other hyperkinetic phenomena may co-occur, including athetosis (irregular writhing movements predominantly involving distal extremities), choreo-dystonia, and ballism (large, proximal choreatic movements) [29,31]. Nocturnal choreatic movements may represent one of the earliest motor manifestations [32,33]. Despite being visibly evident, patients frequently lack awareness of their movements, with anosognosia being common and clinically significant [34,35].

As previously described, chorea in HD results from underactivation of the indirect basal ganglia pathway due to early degeneration of D2-expressing MSNs [36,37]. Although simplified, a useful framework for understanding treatment strategies is that activation of D2 receptors (e.g., by endogenous dopamine) exacerbates chorea by suppressing the indirect pathway, whereas D2 antagonism can restore inhibitory tone and reduce hyperkinetic symptoms.

Clinical Management

Chorea does not always require treatment. In mild or non-disabling cases, supportive interventions such as patient and caregiver education, environmental modifications and adaptive tools may be enough. Pharmacologic therapy is generally reserved for cases causing functional impairment, loss of balance, discomfort, or leads to social stigma [30,38,39]. The goal of treatment is to reduce the severity of chorea—not to eliminate it completely—while minimizing side effects and improving quality of life.

Several therapeutic options are available; however, monotherapy should be prioritized, with combination therapy reserved for refractory cases, given the lack of robust evidence [38] and the increased risk of additive adverse events (e.g., QTc prolongation, neuroleptic malignant syndrome, sedation, cognitive worsening). A therapeutic decision-making algorithm for the treatment of chorea in HD is presented in Figure 1.

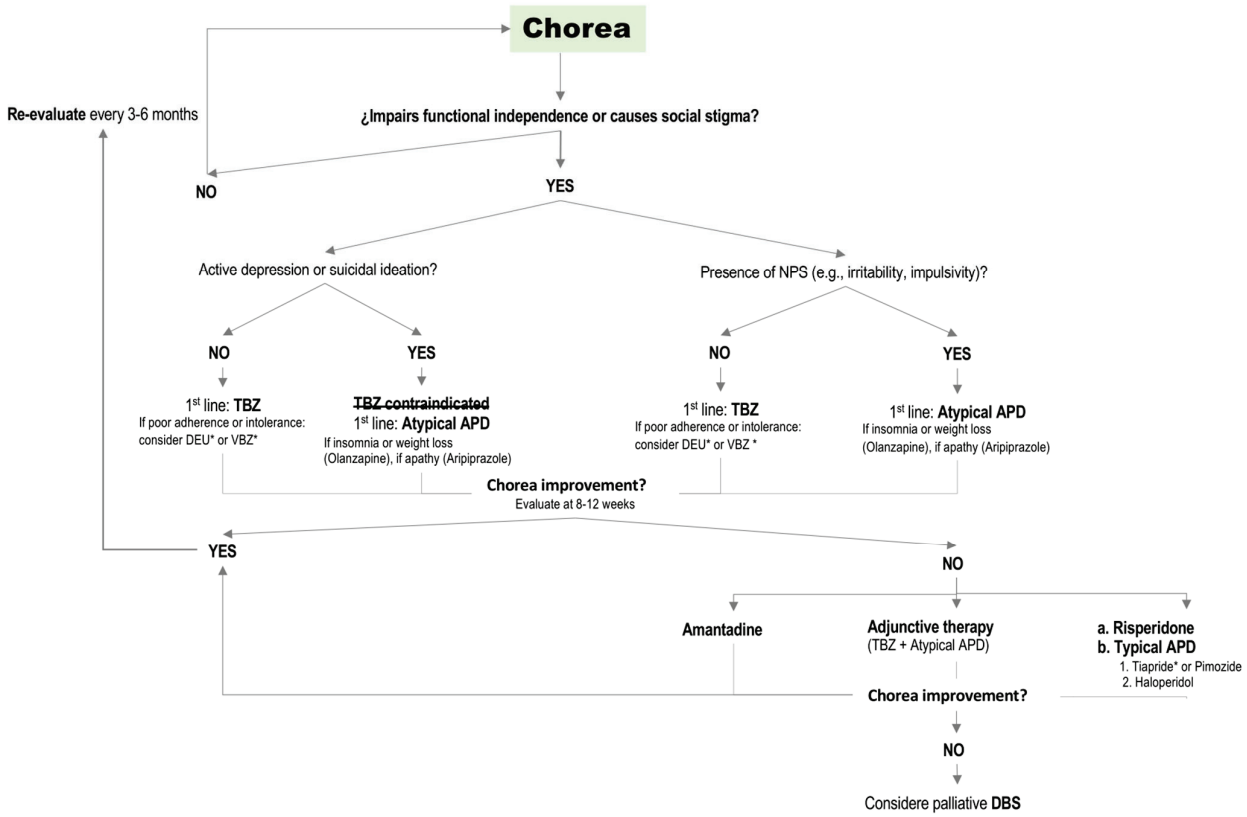


Figure 1. Flowchart illustrating the decision tree for recommended treatments in Huntington's disease (HD). * If available. Abbreviations: NPS, neuropsychiatric symptoms; TBZ, tetrabenazine; DEU, Deutetrabenazine; VBZ, Valbenazine; VMAT2, vesicular monoamine transporter type 2 inhibitors; APD, antipsychotic drugs; DBS, deep brain stimulation.

A. Vesicular Monoamine Transporter type 2 (VMAT2) inhibitors

The first pharmacological approach for chorea was reserpine [40], which reduced involuntary movements through irreversible VMAT inhibition but caused significant peripheral (VMAT type 1) and central (VMAT type 2) side effects due to non-selective blockade [41]. VMATs load monoamines—dopamine, serotonin, noradrenaline, and histamine—into synaptic vesicles and its inhibition reduces vesicular storage, diminished synaptic release, and increased cytosolic degradation.

This led to the development of tetrabenazine (TBZ), a reversible and selective VMAT2 inhibitor, which preferentially reduces dopaminergic signaling [42,43] and became the first drug specifically approved for HD chorea following its demonstrated efficacy in the TETRA-HD pivotal trial [44]. Evidence from open-label studies supports its long-term benefit and tolerability [45–47]. Potential side effects, often idiosyncratic and dose-dependent, include sedation, parkinsonism, akathisia, insomnia and particularly depression and suicidal ideation, with one complete suicide reported in the TETRA-HD study. TBZ is therefore contraindicated in individuals with poorly controlled depression or active suicidal ideation, and close psychiatric monitoring is advised [48]. Due to its short half-life (5–8 h), TBZ requires three daily doses, starting low (e.g., 12.5 mg/day) and titrating every 1–2 weeks

to a maximum of 75 mg/day [49,50]; in carefully selected patients, higher doses up to 200 mg/day may be used [51]. Once clinical improvement is achieved, periodic reassessment is recommended to determine the need for ongoing therapy and gradual dose reduction should be considered [29]. The posology, including recommended starting and maximal doses of the most commonly used drugs for the treatment of chorea in HD, is presented in Table 1.

Table 1. Summary of pharmacological treatments commonly used for chorea in Huntington's disease, including recommended starting dose, maximal dose, availability, and estimated cost. * Maximum dose of VMAT2 inhibitors may vary depending on CYP2D6 metabolizer status and tolerability. † In very selected clinical cases, TBZ doses until 200 mg/day could be considered with close monitoring. Cost classification: low—generic medication widely available; estimated cost < EUR 20/month; low–moderate—estimated cost EUR 20–100/month; high—specialty drugs with limited access or requiring prior authorization; estimated cost >EUR 500/month. Abbreviations: VMAT2 inhibitors, vesicular monoamine transporter 2 inhibitors; APDs, antipsychotic drugs; NMDA, N-methyl-D-aspartate; QD, once daily; BID, twice daily; TID, three times daily.

Mechanism	Drug Name	Recommended Starting Dose	Recommended Maximal Dose	Availability	Estimated Price
VMAT 2 INHIBITORS	**Tetrabenazine (TBZ)**	12.5–25 mg (QD or BID)	*,† 75 mg/d (TID)	Worldwide	Low–moderate
	Deutetrabenazine (DEU)	12 mg (BID)	* 48 mg/d (BID)	USA, Canada, Australia, selected European countries	High
	Valbenazine (VBZ)	40 mg (QD)	* 80 mg/d (QD)	USA	High
ATYPICAL APDs	**Olanzapine**	2.5–5 mg (QD or BID)	20 mg/d (BID)	Worldwide	Low–moderate
	Aripiprazole	2–15 mg (QD or BID)	30 mg/d (BID)	Worldwide	Low–moderate
	Risperidone	0.5–2 mg (QD or BID)	16 mg/d (BID)	Worldwide	Low
TYPICAL APDs	**Tiapride**	50–200 mg (QD or BID)	900 mg/d (TID)	Europe	Low
	Pimozide	1 mg (QD)	2–4 mg/d (QD)	Worldwide (limited availability)	Low
	Haloperidol	0.5–2 mg (QD or BID)	10 mg/d (BID)	Worldwide	Low
NMDA ANTAGONIST RECEPTOR	**Amantadine**	100–200 mg (QD or BID)	400 mg (BID)	Worldwide	Low

TBZ and all VMAT2 inhibitors are metabolized via the cytochrome P450 2D6 (CYP2D6). Polymorphisms and co-administration of strong CYP2D6 inhibitors (e.g., paroxetine, fluoxetine, fluvoxamine) can raise plasma levels, increasing the risk of adverse events [52]. Genotyping is not routinely necessary [48].

Deutetrabenazine (DEU) is a deuterated analogue of TBZ, in which key hydrogen atoms are replaced by deuterium (a heavy hydrogen isotype). This modification slows CYP2D6 metabolism, prolongs the half-life of active metabolites, and results in more stable plasma concentrations, allowing for twice-daily dosing and potentially improved tolerability [49,53]. DEU demonstrated efficacy and safety in the FIRST-HD trial, showing significant chorea reduction and improved quality of life with no increase in depression or suicidality compared to a placebo [54]. Long-term benefit was confirmed in the ARC-HD open-label extension [55]. The recommended maximum dose is 48 mg/day, or 36 mg/day in poor CYP2D6 metabolizers, or when using strong CYP2D6 inhibitors [56].

Valbenazine (VBZ), a valine-ester prodrug of an active DEU metabolite, offers once-daily dosing due to extended half-life. In the KINECT-HD trial, VBZ was efficacious in reducing HD chorea severity and was well tolerated, with somnolence as the most common side effect [57]. The recommended dose is 80 mg/day, and although VBZ is not yet widely available, it is considered a promising agent for patients requiring simplified regimens [49,58].

There are no head-to-head studies comparing VMAT2 inhibitors. The main differences are expected to be pharmacokinetic, with DEU and VBZ offering more practical dosing [58]. An indirect comparison of TBZ and DEU suggested that DEU may be associated with a lower incidence of depressive symptoms and somnolence, although these findings require confirmation [59]. Additionally, a small open-label study reported that switching from TBZ to DEU led to improved chorea control [55].

B. Antipsychotic Drugs (APDs)/Neuroleptics

APDs are the most prescribed drugs in HD clinical practice [60]. Although data from RCTs are limited, in expert surveys they are often selected as the first-line treatment for chorea, especially when accompanied by psychiatric symptoms such as irritability, aggression, or psychosis [38,61]. Neuroleptics vary considerably in their pharmacodynamics, particularly between typical (first-generation) and atypical (second-generation) agents. Their anti-choreic effect is mainly attributed to D2 receptor antagonism, which enhances the indirect pathway. However, D2 receptor antagonism carries the risk of extrapyramidal side effects, including parkinsonism, tardive dyskinesia and akathisia, as well as apathy and cognitive dysfunction, which are particularly concerning in HD [48].

First-generation (typical) APDs, such as haloperidol, pimozide and benzamides (e.g., tiapride, amisulpride, and sulpiride), exhibit strong D2 antagonism relative to 5-HT2A binding. It offers higher potency but also a higher risk of tardive dyskinesia, parkinsonism, sedation, and akathisia [62], which limits their use in modern practice.

Their use is based on limited evidence from small open-label studies and small trials [63–68]; moreover, methodological limitations preclude strong conclusions [69]. Tiapride remains in use in several European countries due to its relatively benign profile and is included as a first-line recommendation in recent German guidelines [70], despite its unavailability in North America. Pimozide may be reserved for refractory cases, though its evidence is largely anecdotal and its primary indication remains Tourette syndrome [68]. Haloperidol, although it has important side effects, is a practical option specially in resource-limited settings due to low cost [71].

Their use is supported by limited evidence from small open-label studies and underpowered clinical trials [63–68]; however, significant methodological limitations preclude definitive conclusions [69]. Tiapride remains in clinical use in several European countries due to its relatively favorable tolerability profile and is endorsed as a first-line treatment in recent German guidelines [70], although it is not available in North America. Pimozide may be considered in refractory cases, although supporting evidence is largely anecdotal and its primary indication remains Tourette syndrome [68]. Despite its adverse effect profile, haloperidol continues to be a practical choice in resource-limited settings due to its low cost [71].

Second-generation (atypical) antipsychotics offer a more favorable tolerability profile due to the fact that they combine moderate D2 antagonism with 5-HT2A and histaminergic modulation.

Risperidone is considered one of the most effective, likely due to its higher affinity for D2/D3 receptors. However, it is more frequently associated with extrapyramidal symptoms [72–75]. Olanzapine showed a favorable effect in two out of three small open studies [76], and is known to induce weight gain and sedation—mainly through H1 receptor

antagonism. Interestingly, both effects can be beneficial in HD [77–81]. Aripiprazole is a partial agonist at D2 and 5HT1A, and antagonist at 5HT2A receptors [82] with preferential mesolimbic activity, and stabilizing effect on dopaminergic tone. Small clinical studies and case reports support its efficacy in chorea reduction, with additional potential benefits for apathy, sedation, and sleepiness [69,83–85]. An analysis from the Enroll-HD database suggests that risperidone and olanzapine may be at least as effective as TBZ in controlling chorea [74].

Other agents such as quetiapine [86,87] and clozapine [88,89] have also been used, but are less effective for chorea due to their low D2 receptor affinity.

C. Amantadine

Amantadine is a weak, noncompetitive N-methyl-D-aspartate (NMDA) receptor antagonist, originally developed as an antiviral agent, and later serendipitously found to improve dyskinesias in Parkinson's disease. It modulates glutamatergic transmission in the basal ganglia and interacts with sigma-1, nicotinic, and 5-HT3 serotonin receptors, which may further influence dopaminergic tone and cortical excitability [90].

Clinical data are conflicting. One trial using oral amantadine up to 300 mg over two weeks found no significant changes in objective chorea scores, though some participants reported subjective benefit [91]. In contrast, a trial with doses up to 400 mg showed a 36% reduction in UHDRS chorea scores [92] without evidence of cognitive side effects, and another crossover study demonstrated benefit following both intravenous and oral administration [93]. Additionally, a small open-label study reported sustained efficacy with oral amantadine over one year of follow-up [94]. However, a Cochrane meta-analysis concluded that existing trials were underpowered and heterogeneous, and do not support consistent efficacy [76]. Nonetheless, some clinicians consider it a reasonable alternative when first-line options are not tolerated or contraindicated [38]. Common adverse effects include agitation, insomnia, peripheral edema, and livedo reticularis, particularly at higher doses.

D. Other Agents with Limited Evidence

Memantine, a low-affinity, non-competitive NMDA receptor antagonist that modulates glutamatergic excitotoxicity, showed potential benefits in a small open-label study [95], though this finding requires replication.

Riluzole is a glutamatergic modulator that inhibits presynaptic glutamate release. Initial small studies yielded inconsistent results [96,97]. However, a three-year RCT failed to demonstrate significant benefit on motor symptoms [98], and based on available evidence, it is not currently recommended for HD chorea.

Pridopidine is a small molecule with a complex mechanism of action. Initially developed as a dopamine stabilizer, it primarily acts as a highly selective sigma-1 receptor (S1R) agonist [99], a mechanism believed to underlie its proposed neuroprotective and homeostatic effects on intracellular signaling and mitochondrial function. Despite promising previous data [100–102], the PRIDE-HD and PROOF-HD trials did not meet primary motor endpoints [103]. Post hoc analyses, however, suggested possible motor benefit in patients not receiving concurrent dopamine-blocking agents [104]. As a strong CYP2D6 inhibitor, it may interact with VMAT2 inhibitors [105].

Other agents such as levetiracetam, valproate and clonazepam have been described in case series or case reports, though their use remains anecdotal [106–108].

E. Deep Brain Stimulation (DBS)

DBS targeting the pallidum has been explored as an option for patients with severe and medically refractory HD chorea. Available data from case reports, open-label studies,

and small trials suggest that DBS can lead to a sustained reduction in chorea severity in carefully selected individuals, without significant deterioration in cognition or mood. However, its uncertain impact on the overall HD motor symptoms, variability in outcomes, and the progressive nature of HD remain important limitations [109–119]. A large international, multicenter RCT (NCT02535884) has recently been completed, and results are pending publication.

Alternative pallidal targets have been explored. One study reported greater chorea reduction with ventral GPi stimulation compared to the classical dorsal GPi target [120], while other small studies have evaluated GPe stimulation with promising results [37,119]. Further research is needed to clarify optimal targeting and patient selection criteria.

F. Non-Pharmacological Interventions

Motor rehabilitation, including physical and occupational therapy, may help reduce the functional impact of chorea through safety-focused strategies and environmental adaptations (e.g., grab bars, weighted utensils). These interventions can support daily function and mitigate the psychosocial burden of involuntary movements [121–123].

Ongoing Research

Bevantolol, a non-selective β-adrenergic antagonist initially developed as an antihypertensive, has recently gained attention as a potential anti-choreic therapy following the discovery of its VMAT2 inhibitory properties. In a recent proof-of-concept study, Bevantolol demonstrated a modest but consistent reduction in chorea severity, with a favorable tolerability profile [124]. Two phase IIb clinical trials—SOM3355 (NCT03575676 and NCT05475483)—have been completed, and results are pending publication.

Authors Recommendations

Pharmacological treatment should only be considered when chorea significantly interferes with function or causes social distress and therapy must be individualized based on severity and comorbidities.

TBZ remains the first-line treatment unless contraindicated by active depression or suicidality. DEU and VBZ are emerging alternatives with at least more favorable pharmacokinetic profile. Second-generation antipsychotics, especially aripiprazole or olanzapine, are appropriate when neuropsychiatric symptoms (NPSs) such as irritability or psychosis coexist, or when VMAT2 inhibitors are poorly tolerated. In patients with mild chorea or intolerance to first-line therapies, amantadine may be considered, though evidence is limited. Importantly, the clinical impact of anti-choreic therapy may become evident after 4 to 8 weeks of treatment. In severe, refractory cases, typical antipsychotics such as pimozide, tiapride or haloperidol should be considered or even pallidal DBS may be used as a palliative strategy in selected patients.

3.1.2. Motor Impersistence

Motor impersistence is a core motor feature of HD, defined as the inability to maintain a voluntary muscle contraction at a constant level [17] resulting in a difficulty to sustain postures or continuous movements [125,126]. This leads to frequent compensatory repositioning or postural collapse that may affect oculomotor, facial, axial or limb musculature. It may be highly disabling, contributing to manipulation difficulties, impaired autonomous gait, and even dysphagia [17,127].

Unlike chorea, motor impersistence progresses steadily over the course of the disease, making it a possible surrogate marker of disease severity [17,128]. In addition to its functional consequences, it underlies characteristic exploratory signs, including tongue

impersistence, the "milkmaid's grip" in the hands [28,125], or the "rubbery gait" caused by loss of postural tone in the trunk and lower extremities [129].

It was firstly described in patients with right hemispheric stroke [130], and it has also been reported in PSP [131] and in moderate or severe dementia stages of Alzheimer's Disease [132]. Although often described clinically as a form of "negative chorea", it reflects a distinct and incompletely understood pathophysiological substrate: impaired sustained output from basal ganglia–thalamocortical circuits driven by progressive degeneration of D1- and D2-receptor-expressing MSNs, and further exacerbated by altered skeletal muscle excitability [133,134].

Clinical Management and Author's Recommendations

There are no approved or specifically targeted pharmacological treatments for motor impersistence. The symptom is understudied, in part due to the lack of standardized, sensitive clinical tools to quantify its severity and monitor treatment response. A small, randomized, crossover study evaluated the effect of apomorphine in five patients and demonstrated transient improvement in motor persistence as assessed by the tongue protrusion subitem of the UHDRS-TMS. However, the absence of a clear pathophysiological rationale to explain this effect, the limited sample size and short-lasting effect do not preclude any therapeutic recommendation [135].

In clinical practice, it is often empirically managed with the same agents used for chorea, especially when both symptoms coexist. VMAT2 inhibitors, APD, or amantadine may offer indirect benefits, although specific efficacy for motor impersistence has not been systematically studied.

3.1.3. Dystonia

Dystonia is reported in over 90% of HD patients, with its severity correlating positively with disease progression, and overall motor and cognitive impairment [136–138]. It may also be exacerbated by antidopaminergic medications.

It is defined as sustained or intermittent involuntary muscle contractions that result in twisting, repetitive movements (so called-dystonic movements, when lasting several seconds) or abnormal postures (so called-dystonic postures, when they last minutes to hours). Unlike chorea, dystonic movements are patterned and repeatedly involve the same group of muscles [28,29].

In adult-onset HD, dystonia is typically mild, generalized, and often coexists with chorea. It becomes evident during voluntary motor tasks such as tandem gait. Common manifestations include sustained fist clenching, excessive trunk or knee flexion, and abnormal arm posturing (e.g., "handbagging"). As the disease progresses, dystonia tends to become more persistent and functionally limiting [17]. Segmental and focal fixed dystonia forms are less frequent but may occur. In juvenile-onset HD, dystonia is often an early and prominent symptom.

The pathophysiology of dystonia in HD is multifactorial. Progressive degeneration of striatal MSNs, affecting both the direct and indirect pathways, leads to dysregulated output from the GPi and GPe reducing tonic inhibition of the thalamus and resulting in excessive activation of premotor areas. This is accompanied by abnormal cortical motor processing, including impaired movement preparation, hyperexcitability in premotor and supplementary motor areas, disorganized sensorimotor integration, and loss of inhibitory mechanisms. Emerging evidence also suggests the involvement of cerebellar and cortico-striato-thalamo-cortical loops, which may further impair motor program execution. Together, these alterations disrupt agonist–antagonist coordination and promote persistent dystonic motor patterns [28].

Clinical Management

There are no approved pharmacological treatments specifically developed for dystonia in HD. In most adult-onset cases, dystonia is mild and does not require targeted treatment. As a first step, medications that may aggravate dystonia should be reduced or discontinued. When treatment is needed, management generally follows the same principles as for isolated generalized or segmental dystonia.

Oral anticholinergics such as trihexyphenidyl have shown efficacy [139], but in HD, their use is generally discouraged due to poor tolerability and cognitive adverse effects. Baclofen, a GABA-B receptor agonist, may offer modest benefit orally, but stronger evidence supports intrathecal or intraventricular infusion in severe, refractory cases—particularly in juvenile-onset HD [140]. Long-acting benzodiazepines, such as clonazepam and diazepam, can offer symptomatic relief owing to their central muscle relaxant and anxiolytic properties, but sedation frequently limits their use. Tizanidine, an α2-adrenergic agonist, has been reported to confer modest benefits [141].

Focal dystonias, particularly those causing pain or interfering with hygiene and function in advanced stages (e.g., hand closure, cervical posturing), may respond well to botulinum toxin A injections [142,143].

Non-pharmacological interventions including active and passive physiotherapy, stretching exercises, and postural re-education are essential to maintain range of motion and prevent contractures in advanced stages or juvenile-onset HD [30,141]

DBS targeting the GPi and, more recently, the subthalamic nucleus (STN), has shown potential benefits in reducing dystonia severity and improving quality of life in small case series of juvenile-onset HD with severe, generalized, refractory dystonia. However, responses are variable, and the procedure carries non-negligible risks, particularly in the context of cognitive decline and progressive neurodegeneration [144,145].

Ongoing Research

Post hoc FIRST-HD trial analyses suggested that DEU may contribute to dystonia improvement, although this was not a primary endpoint [54]. Supporting this possibility, a recent open-label pilot study reported good tolerability, and potential symptomatic benefit in patients with isolated dystonia, particularly with blepharospasm [146].

Author's Recommendations

In adult-onset HD, dystonia is frequent but often non-disabling during the early and mid-stages and no targeted intervention is required. In advanced or juvenile-onset HD cases, systemic agents such as benzodiazepines or baclofen may be used empirically, with caution regarding sedation and cognitive effects. In juvenile-onset HD, severe, refractory cases, intrathecal baclofen or DBS may be considered, although patient selection must account for overall disease progression and cognitive status.

3.1.4. Parkinsonism

Parkinsonism is a near-universal motor feature in advanced stages of HD, manifesting with rigidity, bradykinesia, and postural instability [147]. It is worth noting that impairments in finger-tapping rhythm and speed can appear early in the disease course, reflecting deficits in fine motor control rather than true bradykinesia.

In juvenile-onset HD, as previously mentioned, parkinsonism, often accompanied by dystonia, is usually the predominant motor phenotype [25,26]. A similar phenotype, though rare, can also appear in very-late-onset HD.

The development of parkinsonism result from the progressive spread of neurodegeneration to D1-expressing MSNs, particularly those projecting to the GPi and substantia

nigra pars reticulata (SNr), leading to underactivation of the direct pathway and excessive thalamic inhibition.

Clinical Management

When parkinsonian features emerge, it is essential to review the patient's current medications, as commonly used drugs—including neuroleptics and VMAT2 inhibitors—can contribute to bradykinesia and rigidity.

In patients with functionally limiting symptoms, especially in juvenile-onset HD, levodopa may offer partial and transient benefits [30,148] although chorea or NPS may worsen or re-emerge. Case reports support the use of dopamine agonists [149], amantadine [150] and MAO-B inhibitors, which may also positively affect mood and apathy [151]. Importantly, MAO-B inhibitors should be avoided in patients receiving VMAT-2 due to the risk of hypertensive crisis and serotonin syndrome.

As in dystonia physiotherapy focused on joint mobility, stretching, postural training, and relaxation techniques can help mitigate stiffness, improve mobility, and prevent contractures [30].

Author's Recommendations

In adult-onset HD, parkinsonism typically appears in advanced stages or is secondary to medication. In such cases, the priority is to reduce or discontinue contributing drugs, and dopaminergic therapy is rarely needed.

In contrast, parkinsonism is often a core and early manifestation of juvenile-onset HD, frequently accompanied by disabling dystonia. In these patients, levodopa or amantadine may be considered. In highly selected patients with severe treatment-refractory parkinsonism, DBS as for dystonia has been explored as a palliative strategy.

3.1.5. Gait and Balance Disorders

Gait disorders in HD are complex and multifactorial, with heterogeneous clinical presentations, arising from dysfunction across striatal, cortical, cerebellar, and postural control circuits [152–154].

They are not solely attributable to chorea [67], but may also reflect motor impersistence, dystonia, impaired motor planning, loss of dual-tasking ability, bradykinesia, and postural instability [129].

Clinical Management

There are no approved pharmacological treatments specifically targeting gait dysfunction. While anti-choreic therapies may lead to modest improvements in selected patients, they may also worsen gait when used at higher doses by inducing parkinsonism or freezing of gait.

Therefore, management is primarily based on non-pharmacological strategies. Specialized physiotherapy programs [155,156], including proprioceptive training, postural transitions, and coordination exercises, combined with home-based exercise regimens [157,158] and early introduction of assistive devices—such as walkers or wheelchairs—have shown benefit in maintaining ambulation and reducing fall risk [159].

Ongoing Research

Although, as previously mentioned, the PRIDE-HD and PROOF-HD trials did not meet primary motor endpoints, some exploratory analyses have suggested a possible benefit of pridopidine on gait and balance subitems in early HD stages [160].

Author's Recommendations

Early, sustained specialized physiotherapy, and the early use of assistive devices is the cornerstone of gait management. Control of chorea may help in some cases, but caution is advised with high-dose anti-choreic therapy, as it may paradoxically impair gait.

3.1.6. Other Motor Manifestations

Akathisia is characterized by a subjective feeling of inner restlessness combined with involuntary, purposeless movements and an inability to remain still [29]. While it can be mistaken for chorea, it is typically iatrogenic, most often induced by TBZ, APD, or selective serotonin reuptake inhibitors (SSRIs) [51]. Management involves withdrawing the causative agent. Benzodiazepines or beta-blockers may help in refractory cases [30].

Myoclonus is more frequently observed in juvenile-onset HD where it may coexist with epilepsy. It typically presents as sudden, jerky, stimulus-sensitive movements, reflecting their cortical origin in HD [161]. When prominent, it may interfere with motor function and contribute to gait instability and falls. First-line treatment options include levetiracetam, clonazepam, and valproic acid [70,162].

Motor and phonic tics, including grunting, snorting, or guttural sounds, may be present in HD and can be difficult to differentiate from chorea [163]. Specific treatment is rarely required; when necessary, individualized management should generally follow an approach similar to that used for chorea.

Dysphagia is a common and clinically significant symptom in advanced stages. It increases the risk of aspiration pneumonia (the leading cause of death) and contributes to malnutrition and cachexia [164]. Management should include regular evaluation of swallowing function by a speech-language pathologist or swallowing therapist [30] and caregivers should be trained to recognize early signs of aspiration, such as coughing during meals or voice changes [30]. Management includes dietary texture modifications (e.g., pureed foods, thickened liquids) and compensatory swallowing techniques [165]. When oral intake becomes unsafe or insufficient, percutaneous endoscopic gastrostomy (PEG) feeding should be considered. Early discussion of this topic with the patient and caregivers is essential to align decisions with patient preferences [30]. Although no medications directly improve dysphagia, reducing pharyngeal chorea may indirectly facilitate safer swallowing.

Weight loss is multifactorial and highly prevalent in HD, resulting from hyperkinetic movements, reduced intake (due to psychiatric symptoms or dysphagia), and increased basal metabolic rate (linked to hypothalamic or mitochondrial dysfunction). A multidisciplinary approach with regular nutritional assessment and high-calorie, high-protein supplementation (if necessary) is essential [166]. H1 antagonist agents should be considered, particularly when weight loss is associated with chorea (e.g., olanzapine) or with depression or insomnia (e.g., mirtazapine).

A summary of current recommendations for the clinical management of motor symptoms other than chorea is provided in Table 2.

Table 2. Treatment recommendations for motor symptoms (other than chorea) in Huntington's disease: insights from published literature, expert consensus, and clinical experience. Abbreviations: TBZ, tetrabenazine; APDs, antipsychotic drugs; JHD, juvenile-onset Huntington's disease; GPi/STN-DBS, internal globus pallidus or subthalamic nucleus deep brain stimulation; SSRIs, selective serotonin reuptake inhibitors; BZDs, benzodiazepines; LEV, levetiracetam; CZP, clonazepam; VPA, valproic acid; TS, Tourette syndrome; CBT, cognitive behavioral therapy; PEG, percutaneous endoscopic gastrostomy; H1 antagonist agents, histamine H1 receptor antagonist agents.

Motor Symptom	Special Considerations	Pharmacological Interventions	Non-Pharmacological Interventions
MOTOR IMPERSISTENCE	May be highly disabling.	No approved therapies. Empirical use of TBZ, amantadine, or APD (especially when coexists with chorea).	No specific evidence available; physiotherapy and task-specific motor training may help.
DYSTONIA	Often mild and action-induced; specific pharmacological treatment is rarely needed. • Severe or fixed forms are frequent in JHD.	First step: reduce antidopaminergic medication if present. Second step: Same management as for idiopathic dystonias. • JHD: Intrathecal baclofen or GPi/STN-DBS in refractory cases.	Active/passive physiotherapy, stretching, and postural re-education.
PARKINSONISM	Typically emerges in late-stage or as drug-induced; specific pharmacological treatment is rarely needed. • Prominent and disabling in JHD.	First step: reduce antidopaminergic medication if present. Step step: consider levodopa or amantadine (especially if chorea coexists).	Same as for dystonia.
GAIT DISTURBANCES	Multifactorial origin; not solely attributable to chorea.	No approved therapies. Treat contributing factors (e.g., chorea, dystonia, motor impersistence) if present and functionally impairing.	Specialized physiotherapy, postural training, proprioceptive strategies, and early use of assistive devices (e.g., walker, wheelchair).
AKATHISIA	Mostly iatrogenic (TBZ, APD or SSRIs)	First step: identify and reduce or withdraw causative agent. Alternatives: Beta-blockers, BZD.	No specific evidence available; management is primarily pharmacological.
MYOCLONUS	Treatment only required if functionally disabling. • Common in JHD.	First step: LEV, CZP Alternatives: VPA	No specific evidence available; management is primarily pharmacological.
TICS	Specific treatment is rarely needed.	Usually managed similarly to chorea.	If intervention is required, follow TS management principles: behavioral therapy (CBT/habit reversal), education, reassurance.
DYSPHAGIA	Clinically significant in advanced stages. Early discussions about PEG placement are essential to align care with patient preferences.	Consider treating contributing factors (e.g., pharyngeal chorea or tics).	Regular swallowing evaluations by specialists; caregiver training to detect early signs; dietary texture modifications; PEG when indicated.
WEIGHT LOSS	Highly prevalent and multifactorial.	High-calorie, high-protein nutritional supplementation. Consider H1 antagonist agents particularly when weight loss is associated with chorea (e.g., olanzapine), or with depression or insomnia (e.g., mirtazapine).	Regular nutritional assessment.

3.2. Cognitive Symptoms

Cognitive impairment is a core feature of HD, often emerging years before motor onset, and progressing steadily throughout the disease course [17]. The predominant pattern is a dysexecutive syndrome, reflecting early degeneration of fronto-striatal circuits—especially the caudate nucleus and its projections to the dorsolateral prefrontal cortex [167–170]. Clinically, this manifests as slowed information processing, reduced working memory, impaired planning, cognitive inflexibility, and deficits in social cognition [167–170]. Importantly, as previously mentioned, anosognosia is frequent and clinically significant, often impairing engagement with care and compromising safety [171,172].

As the disease advances, posterior cortical involvement becomes more prominent leading to a progressive, predominantly non-amnestic dementia [168], with early visuospatial impairment (such as impaired mental rotation) [173], and language disintegration including syntactic errors, anomia, and poor discourse cohesion [174,175]. Some cognitive alterations, such as perseverative ideation, are discussed in the neuropsychiatric section due to their overlap with behavioral symptoms.

3.2.1. Clinical Management

No pharmacological agent has convincingly demonstrated efficacy in reversing, delaying or improving cognitive decline in HD. It is essential to minimize medications with potential cognitive side effects. Recent Enroll-HD data indicate that VMAT2 inhibitors and APD are associated with worsening cognitive performance, particularly processing speed, and accelerated functional decline [176].

Although degeneration of cortical cholinergic transmission has been proposed, clinical trials with cholinesterase inhibitors have yielded inconclusive or negative results. Early open-label studies with rivastigmine suggested modest benefit [177–179], but later trials failed to replicate these findings [180]. Galantamine [181] and donepezil [182] showed either no benefit or worsened symptoms—donepezil, in particular, was associated with increased chorea, falls, irritability, and anxiety [183]. Memantine also failed to show Efficacy [95]. A systematic review concluded that the current evidence does not support the routine use of cholinesterase inhibitors or memantine in HD [76]. Still, up to 3.2% of patients—mainly in North America—receive these agents in clinical practice [60].

Psychostimulants such as modafinil or methylphenidate have been used off-label to enhance alertness, motivation, or processing speed, but evidence remains limited [184] and caution is required due to potential side effects.

Though, the cornerstone of cognitive management remains non-pharmacological. Cognitive stimulation strategies—including computerized executive training, group-based cognitive therapy, and external memory aids (e.g., agendas, reminder apps)—may offer temporary benefits and possibly slow decline [185,186]. A recent RCT demonstrated that both computerized cognitive training and music therapy improved global cognition, functional outcomes, and fronto-striatal connectivity [187]. In advanced stages, care should focus on structured, low-stimulus environments with clear routines, as HD patients are especially vulnerable to sensory overload and disorganization [30].

3.2.2. Ongoing Research

Several compounds targeting glutamatergic or dopaminergic transmission have been evaluated with limited success. Amantadine showed modest benefits in small studies [92], while cariprazine, a dopamine D3/D2 partial agonist, was associated with cognitive improvement in a small controlled study using the Addenbrooke's Cognitive Examination [188]. Conversely, ketamine proved to be harmful in HD [189], and dalzanemdor (SAGE-718), a novel NMDA positive allosteric modulator, failed to meet its primary endpoints in a phase 2 trial despite initial safety and tolerability signals [190]. Other agents such as latrepirdine, a multi-target molecule (mitochondrial pore blockade, NMDA/AMPA modulation, and calcium channel inhibition) initially developed for Alzheimer's disease and pridopidine, failed to improve cognition in HD clinical trials [99,103,160,191–193]. Similarly, SSRIs failed to improve cognition in non-depressed HD patients [194,195].

3.2.3. Author's Recommendations

It is essential to avoid, whenever possible, medications that may worsen cognitive function, such as VMAT2 inhibitors or APD particularly in advanced stages. In cases where comorbid depression may further impair cognition, the use of vortioxetine—given its favorable cognitive

profile—should be considered. In very selected cases, psychostimulants may also be explored, particularly in patients with prominent apathy or slowed processing speed.

3.3. Behavioral and Neuropsychiatric Symptoms (NPS)

NPS are nearly universal in HD, often emerging years before motor onset and significantly contributing to impair functional independence, cause emotional distress, and reduce quality of life for both patients and caregivers [196–199]. Their expression is heterogeneous, fluctuating, and poorly correlated with disease stage, which contributed to their exclusion from the HD-ISS biological staging system [200].

These symptoms arise from progressive neurodegeneration—particularly of frontostriatal and limbic circuits—but also reflect psychological responses to disease awareness, functional loss, or the burden of being a gene expansion carrier. Moreover, certain HD medications, particularly those targeting motor symptoms, may exacerbate psychiatric features such as apathy or depression [201].

Importantly, no pharmacological treatment has been approved for any psychiatric symptom in HD. Current management strategies are largely extrapolated from other conditions, with limited supporting evidence from case reports, or small open-label studies in HD [19,70,201]. Nonetheless, the need for targeted, symptom-specific, and individualized approaches are essential, combining pharmacological strategies with non-pharmacological interventions.

This section reviews the most clinically relevant NPS in HD (Table 3), many of which are captured by the Problem Behaviors Assessment—short version (PBA-s). Less frequent symptoms such as hallucinations or disorientation, although included in the PBA-s, are not addressed in dedicated sections due to the lack of HD-specific treatment strategies and their frequent overlap with broader cognitive or psychiatric syndromes.

Table 3. Treatment recommendations for behavioral and neuropsychiatric symptoms in Huntington's disease (HD), based on published literature, expert consensus, and clinical experience. When applicable, the first-line treatment recommended by the authors is indicated in parentheses. Abbreviations: NPS, neuropsychiatric symptoms; SSRIs, selective serotonin reuptake inhibitors; SNRIs, serotonin–norepinephrine reuptake inhibitors; VPA, valproic acid; CBZ, carbamazepine; LTG, lamotrigine; ECT, electroconvulsive therapy; BZDs, benzodiazepines; APDs, antipsychotic drugs; CBT, cognitive behavioral therapy; TBZ, tetrabenazine.

NPS	Special Considerations	Pharmacological Interventions	Non-Pharmacological Interventions
DEPRESSION	Treatment should be tailored to coexisting symptoms (e.g., irritability, apathy, insomnia).	First step: SSRIs (sertraline, citalopram) or SNRIs (venlafaxine, duloxetine). In severe or recurrent cases: consider mood stabilizers (VPA, CBZ, LTG).	Psychotherapy and/or CBT. Consider ECT in selected treatment-resistant cases.
ANXIETY	May be exacerbated by comorbidities or medications.	First step: address comorbid conditions. Second step: SSRIs or SNRIs • Consider BZD for acute anxiety episodes or during SSRI/SNRI titration.	Structured routines, relaxation techniques, psychoeducation (for patients and caregivers).
APATHY	One of the most disabling and underrecognized NPS.	**No approved therapies**. First step: review and reduce potentially aggravating medications. Second step: Consider SSRIs (if depression is present), or activating agents (methylphenidate, modafinil).	Structured daily routines, and tailored social or physical activities to enhance motivation.

Table 3. *Cont.*

NPS	Special Considerations	Pharmacological Interventions	Non-Pharmacological Interventions
IRRITABILITY AND AGGRESSIVENESS	Treatment should be guided by symptom severity and coexisting psychiatric features.	First step: High-dose SSRIs (sertraline and escitalopram). Second step: APD (aripiprazole or olanzapine). Consider adjunctive mood stabilizers in refractory cases.	Behavioral strategies: avoid confrontation, de-escalate early signs, and use distraction techniques.
PERSEVERATIVE IDEATION AND OCD	Perseveration is much more common.	Perseveration: SSRIs or APD (olanzapine or risperidone). OCD: High-dose SSRIs or clomipramine.	CBT and psychoeducation (for patients and caregivers).
PSYCHOSIS	Important to rule out and treat comorbid medical conditions that may trigger or worsen psychosis.	First step: APD (olanzapine, risperidone or aripiprazole). If no response, consider other APDs such as clozapine.	Consider ECT in severe treatment-resistant cases.
SUICIDAL IDEATION	**Suicide risk should be systematically assessed.** May occur independently of major depression.	First step: Prompt identification and management of contributing factors (depression, impulsivity or perseveration) or withdraw possible contributing medications (e.g., TBZ) Second step: Consider APD (olanzapine)	Ensure caregiver involvement, prevent social isolation. Consider psychiatric hospitalization if safety is compromised.
IMPULSIVITY	Treatment should be tailored to symptom profile.	If comorbid depression or irritability: SSRIs. If impulsive aggressivity: atypical APD. Consider adjunctive mood stabilizers.	Psychoeducation (for patients and caregivers) to provide insight and reduce triggers.

3.3.1. Depression

Depression affects up to 50% of individuals with HD across all the disease course [202]. The pathophysiology involves degeneration of fronto-limbic circuits, basal ganglia, and prefrontal cortex, alongside serotonergic dysregulation [203].

Clinical Management

As with other NPS in HD, available evidence is scarce, mostly based on case reports, open-label studies, or post hoc analyses, and lacks high-quality randomized trials [204]. SSRIs and serotonin-norepinephrine reuptake inhibitors (SNRIs) are the most commonly used pharmacological options in clinical practice [19,205] with small studies supporting the use of venlafaxine [206] and citalopram [195]. Treatment selection is often guided by the associated symptom profile: sertraline or escitalopram in cases with prominent irritability [207] or obsessive–compulsive symptoms [208]; mirtazapine (a noradrenergic and specific serotoninergic molecule) when insomnia or weight loss is present [209], and duloxetine in cases with concurrent neuropathic pain.

In patients with severe or recurrent depression, adjunctive use of mood stabilizers such as valproate, lamotrigine [210], lithium [211], or carbamazepine may be considered to reduce relapse risk [30]. Electroconvulsive therapy (ECT) has shown efficacy in treatment-resistant cases but should be reserved for exceptional situations due to the risk of short-term memory impairment [212–215].

Non-pharmacological interventions such as cognitive behavioral therapy (CBT), and supervised physical activity may improve depressive symptoms [201].

Author's Recommendations

Antidepressant selection should be symptom-driven. We recommend avoiding tricyclic antidepressants, paroxetine, and fluvoxamine due to their higher anticholinergic burden and potential for cognitive side effects.

3.3.2. Anxiety

Anxiety is common in HD but often underrecognized or misattributed to other behavioral changes. It frequently coexists with depression and may manifest as generalized worry, somatic tension, panic attacks, or anticipatory anxiety. It is frequently reactive to disease awareness, functional decline, and social or economic stressors [201].

Neurobiologically, it has been associated with dysregulation in fronto-limbic circuits, including the amygdala, insula, and anterior cingulate cortex, with serotonergic dysfunction likely contributing to symptom expression.

Clinical Management and Author's Recommendations

Initial steps include identifying and treating psychiatric or medical comorbidities that may worsen anxiety [201]. SSRIs or SNRIs are first-line treatments, which offer anxiolytic effects while addressing concurrent depressive symptoms, with some evidence supporting fluoxetine [195]. Benzodiazepines may be considered for short-term or situational relief, particularly during SSRI/SNRI initiation, but their long-term use should be avoided due to the risk of sedation, falls, and cognitive impairment.

Non-pharmacological interventions are essential and should include structured daily routines, relaxation techniques, caregiver education, and—when cognitively feasible—CBT.

3.3.3. Apathy

Apathy affects up to 90% of HD patients, is among the most disabling NPS, and the NPS most consistently associated with disease progression in large cohort studies such as TRACK-HD [196,216,217]. While insight into this symptom may be preserved in early stages, it often diminishes as the disease progresses [218].

It is defined as a state of decreased motivation resulting in reduced goal-directed activities, not explained by cognitive impairment, emotional distress, or reduced consciousness, although it often overlaps with depression and cognitive impairment [218–220]. Neural correlates include dysfunction in the dorsolateral, orbitofrontal and ventromedial prefrontal cortices, as well as the anterior cingulum, amygdala and ventral tegmental area [221–223].

Clinical Management

No pharmacological treatment has proven effective for apathy in the general population or HD population. Initial steps include reviewing and reducing potentially aggravating medications and addressing comorbid depression if present [201].

Non-pharmacological interventions—such as structured daily routines, caregiver coaching, and personalized social or physical engagement—are the cornerstone of management, and should be adapted to the patient's cognitive status [201].

Ongoing Research

Bupropion (a norepinephrine–dopamine reuptake inhibitor) [224], aripiprazole [225], modafinil [184], and cariprazine [188] have shown signals of potential benefit in small studies, although none demonstrated clear efficacy in larger trials. SRX246 (a vasopressin V1a receptor antagonist) failed to meet endpoints in a phase 2 trial.

Author's Recommendations

Based on clinical experience, if depressive symptoms are present, an SSRI should be trialed. In non-depressed but severely apathetic individuals, activating agents like modafinil or methylphenidate may be considered. Medications that may worsen apathy should be reduced or replaced by agents with a more activating profile, such as aripiprazole.

3.3.4. Irritability and Aggressiveness

Irritability is defined as a proneness to anger, which can unfortunately lead to an outburst of rage and even verbal or physical aggression. Its significantly contributes to social isolation, caregiver burden and, in advanced stages, institutionalization.

It has been associated with dysfunction in fronto-limbic circuitry, including the striatum, amygdala, pulvinar and prefrontal cortex, with impaired serotonergic signaling and reduced structural integrity affecting emotional regulation and inhibitory control [226–228].

Clinical Management

SSRIs—particularly sertraline, escitalopram, and fluoxetine—are considered first-line treatments, even in non-depressed patients, as they have shown to reduce irritability and aggression, and are generally well tolerated [195,207,229–231]. Their efficacy may depend on reaching moderate-to-high doses, which downregulate presynaptic 5-HT1A autoreceptors and enhance serotonergic transmission in fronto-limbic circuits involved in affect regulation [231]. High-dose paroxetine and fluvoxamine should be avoided due to unfavorable adverse effects [229].

Atypical neuroleptics should be considered in severe cases that result in aggressive behavior or when chorea coexists [78,232,233]. Aripiprazole, in particular, may offer additional benefit due to its dopaminergic modulation and relatively favorable side effect profile [225,234]. In cases with emotional lability or poor behavioral control, mood stabilizers such as valproate or carbamazepine should be considered as adjunctive therapy [19,210,235].

Non-pharmacological strategies should be prioritized, even before pharmacological treatment. Behavioral interventions include avoiding confrontations, de-escalating early signs of irritability, using distraction techniques, and ensuring a structured, low-stimulus environment to reduce emotional reactivity. Measures must also ensure the safety and well-being of family members, especially when children are involved.

Ongoing Research

SRX246 showed good tolerability in the STAIR phase 2a trial [236], with exploratory analyses suggesting possible benefit in aggressive behavior [237]. Dextromethorphan/quinidine, used to treat pseudobulbar affect in ALS, failed to show improvement in irritability in a proof-of-concept study on 20 HD patients [238].

Author's Recommendations

For mild to moderate irritability, SSRIs remain the preferred first-line treatment, often requiring doses at the higher end of the therapeutic range. In partial responders, adjunctive therapy with agents such as mirtazapine may be helpful, particularly when comorbid insomnia or weight loss is present. For severe irritability or overt aggression, atypical APDs are indicated. Treatment must always be guided by a careful risk–benefit analysis, as these symptoms may endanger the safety of the patient or others, occasionally requiring hospitalization.

3.3.5. Perseverative Ideation and Obsessive–Compulsive Disorder (OCD)

Perseverative ideation and conduct are very common in HD, tend to increase as functional capacity declines, correlating with lower Total Functional Capacity (TFC) scores [196]. Perseverative cognition has been linked to increased risk of suicidal ideation, especially when combined with other NPS. This symptomatology is thought to arise from frontal–striatal circuit degeneration, particularly affecting cognitive flexibility [239].

Classic OCD is less frequent, though still more common than in the general population [196]. A key clinical distinction lies in the lack of intrusive distress: whereas OCD typically involves ego-dystonic, anxiety-provoking thoughts, perseverative patterns in HD tend to be ego-syntonic and reflect cognitive rigidity rather than true compulsivity.

Clinical Management and Author's Recommendations

When pharmacological intervention is needed, SSRIs are generally considered the first-line treatment, particularly when symptoms coexist with anxiety or depression. Sertraline has shown benefit in case reports for obsessive symptoms [208]. In more severe cases, especially when symptoms are accompanied by strong irritability or poor behavioral control, adjunctive treatment with atypical antipsychotics such as olanzapine or risperidone may be useful [240].

In patients meeting criteria for classical OCD, high-dose SSRIs may be necessary. If inadequate response, clomipramine—a tricyclic antidepressant with strong serotonergic activity—may be cautiously trialed, although its anticholinergic burden and potential interactions with VMAT2 inhibitors warrant careful monitoring [241].

Non-pharmacological approaches, though also understudied, are crucial. CBT, when cognitive capacity allows, may help manage intrusive thoughts or compulsive behaviors. Psychoeducation for caregivers is essential to differentiate between behavioral rigidity and psychiatric compulsions, promoting more appropriate management strategies [30].

3.3.6. Psychosis

Psychotic symptoms are relatively uncommon in HD, yet recent findings from large cohorts such as ENROLL-HD suggest a higher prevalence than classically reported [242]. Surprisingly, it has been associated with lower CAG repeat counts but younger age at diagnosis [243], and is often present in the context of prominent cognitive impairment [244].

Clinical Management

First-line treatment consists of atypical APD, though data supporting their use in HD are limited to small case series, observational studies and small trials [69,77–79,81,83,84,232,233]. To date, there is no evidence that favors one drug over another, although risperidone [75], olanzapine and aripiprazole [84] are the most commonly prescribed. Clozapine may be considered in pharmacoresistant cases or in patients who develop disabling parkinsonism or dystonia given its more favorable extrapyramidal side-effect profile.

ECT has been shown to be effective in selected cases, particularly when psychotic symptoms are severe, treatment-resistant, or coexist with mood disturbances or suicidality [212,213].

Author's Recommendations

Firstly, it is essential to identify and treat comorbid medical conditions that may precipitate acute psychotic episodes, including infections, metabolic disturbances, substance use, or medication effects. In patients with established psychosis, we recommend initiating atypical antipsychotics, selecting the agent based on comorbid features, titrating slowly with close monitoring of psychiatric and motor status.

3.3.7. Suicidal Ideation

Suicidality represents a major concern in HD, with suicide rates 2–6 times higher than in the general population [245–247]. Risk is elevated throughout the disease course but is especially high around genetic diagnosis, the initial appearance of symptoms, and when functional dependency begins [248,249]. Contributing factors include psychiatric

comorbidities (e.g., depression, anxiety, impulsivity), reduced insight, social stressors, and existential distress [48]. Importantly, suicidal ideation may occur independently of major depression, often driven by impulsivity and perseverative cognition.

Clinical Management and Author's Recommendations

Suicide risk should be systematically assessed in all patients with HD, regardless of disease stage. Prevention involves prompt identification and treating risk factors such as underlying depression, impulsivity, and social isolation [30]. As previously noted, some drugs such as TBZ may worsen mood or induce suicidality in vulnerable individuals [250], warranting close monitoring during dose titration.

Although evidence is limited, one open-label study suggested a reduction in suicidal ideation following treatment with olanzapine [240]. In high-risk scenarios, caregivers' involvement in safety planning is essential, and hospitalization should be considered when safety cannot be assured.

3.3.8. Impulsivity

Impulsivity refers to the tendency to act prematurely without adequate forethought, often leading to socially inappropriate comments, emotional outbursts, compulsive shopping, disinhibited sexual behavior, or other high-risk actions. When combined with irritability, perseveration or depression, impulsivity may increase the risk of harmful behaviors, including suicide attempts. This symptom is thought to reflect orbitofrontal cortex dysfunction and its connections with the ventral striatum and limbic structures, leading to a loss of cortical inhibitory control.

Clinical Management and Author's Recommendations

Impulsivity is often addressed indirectly by treating comorbid conditions. SSRIs are used when impulsivity occurs in the context of depression or irritability, while atypical APDs are indicated in cases of impulsive aggressivity. Mood stabilizers such as valproate or carbamazepine may also be helpful in flattening affective instability and reducing emotionally driven impulsive episodes [30].

Psychoeducation is essential to help caregivers understand that impulsive behavior is a neuropsychiatric symptom—not simply inappropriate conduct—and to provide them with strategies to reduce environmental triggers.

3.3.9. Other NPSs

Sleep disorders affect two-thirds of HD patients and may include insomnia, circadian rhythm disruption, fragmented sleep, or hypersomnia [251,252]. They result from a combination of neurodegenerative changes, psychiatric comorbidities (e.g., depression, anxiety), or side effects of medications. Management should begin with identifying and addressing the underlying cause (e.g., mood disorder, nighttime movements, pain), followed by implementation of sleep hygiene measures. When necessary, short-acting hypnotics or sedative antidepressants such as mirtazapine or trazodone may be used, always with caution in patients at risk of falls or cognitive impairment. Melatonin is a pharmacologic option particularly when there is pattern of circadian rhythm disordered sleep [201].

Sexual disorders range from reduced libido (often associated with depression or SSRIs) to disinhibited or hypersexual behavior, which may be part of a broader impulse control disturbance. As in other symptoms, treatment should be individualized and consider psychiatric comorbidities, family distress, and the patient's safety and dignity.

4. Conclusions

Symptomatic management remains the cornerstone of care in HD, despite recent advances in disease-modifying therapies. A deeper understanding of HD's phenotypic heterogeneity and underlying pathophysiology is essential to develop effective, patient-centered treatments. Chorea is the only symptom with specifically approved pharmacological options—VMAT2 inhibitors—though their use is limited by psychiatric adverse effects. Neuroleptics are commonly prescribed, especially when psychiatric symptoms coexist, but may exacerbate cognitive and motor dysfunction. In contrast, other disabling motor features, such as motor impersistence, remain underexplored and lack targeted therapies. No pharmacological intervention has demonstrated clear efficacy in treating cognitive impairment, and psychiatric symptoms are managed based on extrapolation from other disorders, primarily using SSRIs and atypical antipsychotics. Special attention must be given to the emergence of suicidal ideation, and psychological support should be provided to both patients and their families. Overall, given the modest efficacy and frequent side effects of available medications, non-pharmacological and multidisciplinary approaches are essential to preserve function and enhance quality of life. Symptomatic care in HD must remain proactive, person-centered, and responsive to the complex and evolving needs of each individual and their families.

Author Contributions: Conceptualization, G.O.-S. and J.P.-P.; methodology, G.O.-S., E.B. and J.P.-P.; writing—original draft preparation, G.O.-S., E.B. and J.P.-P.; writing—review and editing, L.B., S.M.-H., J.P. and J.K.; visualization, G.O.-S. and J.P.-P. All authors have read and agreed to the published version of the manuscript.

Funding: This research received no external funding.

Institutional Review Board Statement: Not applicable.

Informed Consent Statement: Not applicable.

Data Availability Statement: All data are included in the publication.

Acknowledgments: G.O.-S. acknowledges support from a Río Hortega Fellowship (CM24/00023) from the Carlos III Health Institute.

Conflicts of Interest: The authors declare no conflicts of interest for this work.

Abbreviations

APDs: Antipsychotic Drugs; CBT: Cognitive Behavioral Therapy; CNS: Central Nervous System; DBS: Deep Brain Stimulation; DEU: Deutetrabenazine; ECT: Electroconvulsive Therapy; GPe: External Globus Pallidum; GPi: Internal Globus Pallidum; HD: Huntington's Disease; HD-ISS: Huntington's Disease Integrated Staging System; HTT: Huntingtin Protein; MAO: Monoamine Oxidase; mHTT: Mutant Huntingtin Protein; MSNs: Medium Spiny Neurons; NMDAR: N-methyl-D-aspartate Receptor; NPS: Neuropsychiatric Symptoms; OCD: Obsessive–Compulsive Disorder; PBA-s: Problem Behaviors Assessment—short version; PEG: Percutaneous Endoscopic Gastrostomy; RAN: Repeat-Associated Non-ATG; RCTs: Randomized Control Trials; S1R: Sigma-1 Receptor; SNr: Substantia Nigra Pars Reticulata; SNRIs: Serotonin-Norepinephrine Reuptake Inhibitors; SSRIs: Selective Serotonin Reuptake Inhibitors; STN: Subthalamic Nucleus; TBZ: Tetrabenazine; TFC: Total Functional Capacity; TMS: Total Motor Score; UHDRS: Unified Huntington Disease Rating Scale; VBZ: Valbenazine; VMAT2: Vesicular Monoamine Transporter Type 2.

References

1. Evans, S.J.; Douglas, I.; Rawlins, M.D.; Wexler, N.S.; Tabrizi, S.J.; Smeeth, L. Prevalence of adult Huntington's disease in the UK based on diagnoses recorded in general practice records. *J. Neurol. Neurosurg. Psychiatry* **2013**, *84*, 1156–1160. [CrossRef] [PubMed]
2. Medina, A.; Mahjoub, Y.; Shaver, L.; Pringsheim, T. Prevalence and Incidence of Huntington's Disease: An Updated Systematic Review and Meta-Analysis. *Mov. Disord.* **2022**, *37*, 2327–2335. [CrossRef]
3. Rawlins, M.D.; Wexler, N.S.; Wexler, A.R.; Tabrizi, S.J.; Douglas, I.; Evans, S.J.; Smeeth, L. The Prevalence of Huntington's Disease. *Neuroepidemiology* **2016**, *46*, 144–153. [CrossRef]
4. Macdonald, M. A novel gene containing a trinucleotide repeat that is expanded and unstable on Huntington's disease chromosomes. *Cell* **1993**, *72*, 971–983. [CrossRef]
5. Bates, G.P.; Dorsey, R.; Gusella, J.F.; Hayden, M.R.; Kay, C.; Leavitt, B.R.; Nance, M.; Ross, C.A.; Scahill, R.I.; Wetzel, R.; et al. Huntington Disease. *Nat. Rev. Dis. Primers* **2015**, *1*, 15005. [CrossRef]
6. Scahill, R.I.; Farag, M.; Murphy, M.J.; Hobbs, N.Z.; Leocadi, M.; Langley, C.; Knights, H.; Ciosi, M.; Fayer, K.; Nakajima, M.; et al. Somatic CAG repeat expansion in blood associates with biomarkers of neurodegeneration in Huntington's disease decades before clinical motor diagnosis. *Nat. Med.* **2025**, *31*, 807–818. [CrossRef]
7. Langbehn, D.R.; Brinkman, R.; Falush, D.; Paulsen, J.; Hayden, M.R.; on behalf of an International Huntington's Disease Collaborative Group. A new model for prediction of the age of onset and penetrance for Huntington's disease based on CAG length. *Clin. Genet.* **2004**, *65*, 267–277. [CrossRef]
8. Saudou, F.; Humbert, S. The Biology of Huntingtin. *Neuron* **2016**, *89*, 910–926. [CrossRef]
9. Romo, L.; Mohn, E.S.; Aronin, N. A Fresh Look at Huntingtin mRNA Processing in Huntington's Disease. *J. Huntington's Dis.* **2018**, *7*, 101–108. [CrossRef]
10. Tabrizi, S.J.; Estevez-Fraga, C.; van Roon-Mom, W.M.C.; Flower, M.D.; Scahill, R.I.; Wild, E.J.; Muñoz-Sanjuan, I.; Sampaio, C.; Rosser, A.E.; Leavitt, B.R. Potential disease modifying therapies for Huntington's disease, lessons learned and future opportunities. *Lancet Neurol.* **2022**, *21*, 645–658. [CrossRef]
11. Tabrizi, S.J.; Flower, M.D.; Ross, C.A.; Wild, E.J. Huntington disease: New insights into molecular pathogenesis and therapeutic opportunities. *Nat. Rev. Neurol.* **2020**, *16*, 529–546. [CrossRef] [PubMed]
12. Ross, C.A.; Tabrizi, S.J. Huntington's disease: From molecular pathogenesis to clinical treatment. *Lancet Neurol.* **2011**, *10*, 83–98. [CrossRef] [PubMed]
13. Moss, D.J.H.; Pardiñas, A.F.; Langbehn, D.; Lo, K.; Leavitt, B.R.; Roos, R.; Durr, A.; Mead, S.; TRACK-HD Investigators; REGISTRY Investigators; et al. Identification of genetic variants associated with Huntington's disease progression: A genome-wide association study. *Lancet Neurol.* **2017**, *16*, 701–711. [CrossRef]
14. Lee, J.-M.; Wheeler, V.C.; Chao, M.J. Identification of Genetic Factors that Modify Clinical Onset of Huntington's Disease. *Cell* **2015**, *162*, 516–526. [CrossRef]
15. Lee, J.-M.; Correia, K.; Loupe, J.; Kim, K.-H.; Barker, D.; Hong, E.P.; Chao, M.J.; Long, J.D.; Lucente, D.; Vonsattel, J.P.G.; et al. CAG Repeat Not Polyglutamine Length Determines Timing of Huntington's Disease Onset. *Cell* **2019**, *178*, 887–900.e14. [CrossRef]
16. Handsaker, R.E.; Kashin, S.; Reed, N.M.; Tan, S.; Lee, W.-S.; McDonald, T.M.; Morris, K.; Kamitaki, N.; Mullally, C.D.; Morakabati, N.R.; et al. Long somatic DNA-repeat expansion drives neurodegeneration in Huntington's disease. *Cell* **2025**, *188*, 623–639.e19. [CrossRef]
17. Walker, F.O. Huntington's disease. *Lancet* **2007**, *369*, 218–228. [CrossRef]
18. Estevez-Fraga, C.; Tabrizi, S.J.; Wild, E.J. Huntington's Disease Clinical Trials Corner: March 2024. *J. Huntington's Dis.* **2024**, *13*, 1–14. [CrossRef]
19. Killoran, A.; Biglan, K.M. Current therapeutic options for Huntington's disease: Good clinical practice versus evidence-based approaches? Mov. *Disord.* **2014**, *29*, 1404–1413. [CrossRef]
20. Lanska, D.J. George Huntington (1850–1916) and Hereditary Chorea. *J. Hist. Neurosci.* **2000**, *9*, 76–89. [CrossRef]
21. Rubinsztein, D.C. Molecular Biology of Huntington's Disease (HD) and HD-Like Disorders. In *Genetics of Movement Disorders*; Elsevier: Amsterdam, The Netherlands, 2003; pp. 365–383.
22. Waldvogel, H.J.; Kim, E.H.; Tippett, L.J.; Vonsattel, J.-P.G.; Faull, R.L.M. The Neuropathology of Huntington's Disease. In *Behavioral Neurobiology of Huntington's Disease and Parkinson's Disease*; Nguyen, H.H.P., Cenci, M.A., Eds.; Springer: Berlin/Heidelberg, Germany, 2015; pp. 33–80.
23. Obeso, J.A.; Rodriguez-Oroz, M.C.; Stamelou, M.; Bhatia, K.P.; Burn, D.J. The expanding universe of disorders of the basal ganglia. *Lancet* **2014**, *384*, 523–531. [CrossRef]
24. Quarrell, O.; O'DOnovan, K.L.; Bandmann, O.; Strong, M. The Prevalence of Juvenile Huntington's Disease: A Review of the Literature and Meta-Analysis. *PLoS Curr.* **2012**, *4*, 149–161. [CrossRef] [PubMed]

25. Oosterloo, M.; on behalf of the Pediatric Huntington Disease Working Group of the European Huntington Disease Network; Touze, A.; Byrne, L.M.; Achenbach, J.; Aksoy, H.; Coleman, A.; Lammert, D.; Nance, M.; Nopoulos, P.; et al. Clinical Review of Juvenile Huntington's Disease. *J. Huntington's Dis.* **2024**, *13*, 149–161. [CrossRef]
26. Bakels, H.S.; Roos, R.A.; van Roon-Mom, W.M.; de Bot, S.T. Juvenile-Onset Huntington Disease Pathophysiology and Neurodevelopment: A Review. *Mov. Disord.* **2021**, *37*, 16–24. [CrossRef] [PubMed]
27. Stout, J.C. Juvenile Huntington's disease: Left behind? *Lancet Neurol.* **2018**, *17*, 932–933. [CrossRef]
28. Goldman, J.G. *Principles and Practice of Movement Disorders*, 3rd ed.; Elsevier: Amsterdam, The Netherlands, 2022. [CrossRef]
29. Jankovic, J. Treatment of hyperkinetic movement disorders. *Lancet Neurol.* **2009**, *8*, 844–856. [CrossRef]
30. Bachoud-Lévi, A.-C.; Ferreira, J.; Massart, R.; Youssov, K.; Rosser, A.; Busse, M.; Craufurd, D.; Reilmann, R.; De Michele, G.; Rae, D.; et al. International Guidelines for the Treatment of Huntington's Disease. *Front. Neurol.* **2019**, *10*, 710. [CrossRef]
31. Bhidayasiri, R.; Truong, D.D. Chorea and related disorders. *Postgrad. Med. J.* **2004**, *80*, 527–534. [CrossRef]
32. Goodman, A.O.G.; Rogers, L.; Pilsworth, S.; McAllister, C.J.; Shneerson, J.M.; Morton, A.J.; Barker, R.A. Asymptomatic Sleep Abnormalities Are a Common Early Feature in Patients with Huntington's Disease. *Curr. Neurol. Neurosci. Rep.* **2010**, *11*, 211–217. [CrossRef]
33. Fish, D.R.; Sawyers, D.; Allen, P.J.; Blackie, J.D.; Lees, A.J.; Marsden, C.D. The Effect of Sleep on the Dyskinetic Movements of Parkinson's Disease, Gilles de la Tourette Syndrome, Huntington's Disease, and Torsion Dystonia. *Arch. Neurol.* **1991**, *48*, 210–214. [CrossRef]
34. Hergert, D.C.; Sanchez-Ramos, J.; Cimino, C.R. Awareness of Chorea in Huntington's Disease. *J. Huntington's Dis.* **2020**, *9*, 99–103. [CrossRef]
35. Isaacs, D.; Gibson, J.S.; Stovall, J.; Claassen, D.O. The Impact of Anosognosia on Clinical and Patient-Reported Assessments of Psychiatric Symptoms in Huntington's Disease. *J. Huntington's Dis.* **2020**, *9*, 291–302. [CrossRef] [PubMed]
36. DeLong, M.R. The basal ganglia. In *Principles of Neural Science*; Kandel, E.R., Schwartz, J.H., Jessell, T.M., Eds.; The McGraw-Hill Companies: New York, NY, USA, 2000; pp. 853–867.
37. Ligot, N.; Krystkowiak, P.; Simonin, C.; Goldman, S.; Peigneux, P.; Van Naemen, J.; Monclus, M.; Lacroix, S.F.; Devos, D.; Dujardin, K.; et al. External Globus Pallidus Stimulation Modulates Brain Connectivity in Huntington's Disease. *J. Cereb. Blood Flow Metab.* **2010**, *31*, 41–46. [CrossRef] [PubMed]
38. Burgunder, J.-M.; Guttman, M.; Perlman, S.; Goodman, N.; van Kammen, D.P.; Goodman, L. An International Survey-based Algorithm for the Pharmacologic Treatment of Chorea in Huntington's Disease. *PLoS Curr.* **2011**, *3*, RRN1260. [CrossRef] [PubMed]
39. Ferreira, J.J.; Rodrigues, F.B.; Duarte, G.S.; Mestre, T.A.; Bachoud-Levi, A.; Bentivoglio, A.R.; Burgunder, J.; Cardoso, F.; Claassen, D.O.; Landwehrmeyer, G.B.; et al. An MDS Evidence-Based Review on Treatments for Huntington's Disease. *Mov. Disord.* **2021**, *37*, 25–35. [CrossRef]
40. Wu, D.; Chen, Q.; Yu, Z.; Huang, B.; Zhao, J.; Wang, Y.; Su, J.; Zhou, F.; Yan, R.; Li, N.; et al. Transport and inhibition mechanisms of human VMAT2. *Nature* **2023**, *626*, 427–434. [CrossRef]
41. Curzon, G. How reserpine and chlorpromazine act: The impact of key discoveries on the history of psychopharmacology. *Trends Pharmacol. Sci.* **1990**, *11*, 61–63. [CrossRef]
42. Dalton, M.P.; Cheng, M.H.; Bahar, I.; Coleman, J.A. Structural mechanisms for VMAT2 inhibition by tetrabenazine. *eLife* **2024**, *12*, RP91973. [CrossRef]
43. Koch, J.; Shi, W.-X.; Dashtipour, K. VMAT2 inhibitors for the treatment of hyperkinetic movement disorders. *Pharmacol. Ther.* **2020**, *212*, 107580. [CrossRef]
44. Huntington Study Group. Tetrabenazine as antichorea therapy in Huntington disease: A randomized controlled trial. *Neurology* **2006**, *66*, 366–372. [CrossRef]
45. Fasano, A.; Cadeddu, F.; Guidubaldi, A.; Piano, C.; Soleti, F.; Zinzi, P.D.; Bentivoglio, A.R. The Long-term Effect of Tetrabenazine in the Management of Huntington Disease. *Clin. Neuropharmacol.* **2008**, *31*, 313–318. [CrossRef] [PubMed]
46. Jankovic, J.; Beach, J. Long-term effects of tetrabenazine in hyperkinetic movement disorders. *Neurology* **1997**, *48*, 358–362. [CrossRef] [PubMed]
47. Kenney, C.; Hunter, C.; Jankovic, J. Long-term tolerability of tetrabenazine in the treatment of hyperkinetic movement disorders. *Mov. Disord.* **2006**, *22*, 193–197. [CrossRef]
48. Frank, S. Treatment of Huntington's Disease. *Neurotherapeutics* **2014**, *11*, 153–160. [CrossRef]
49. Gibson, J.S.; Claassen, D.O. State-of-the-art pharmacological approaches to reduce chorea in Huntington's disease. *Expert Opin. Pharmacother.* **2021**, *22*, 1015–1024. [CrossRef]
50. Reilmann, R. Pharmacological treatment of chorea in Huntington's disease–good clinical practice versus evidence-based guideline. *Mov. Disord.* **2013**, *28*, 1030–1033. [CrossRef]
51. Frank, S. Tetrabenazine as anti-chorea therapy in Huntington Disease: An open-label continuation study. Huntington Study Group/TETRA-HD Investigators. *BMC Neurol.* **2009**, *9*, 62. [CrossRef]

52. Kenney, C.; Hunter, C.; Davidson, A.; Jankovic, J. Short-term effects of tetrabenazine on chorea associated with Huntington's disease. *Mov. Disord.* **2007**, *22*, 10–13. [CrossRef]
53. Schneider, F.; Stamler, D.; Bradbury, M.; Loupe, P.S.; Hellriegel, E.; Cox, D.S.; Savola, J.; Gordon, M.F.; Rabinovich-Guilatt, L. Pharmacokinetics of Deutetrabenazine and Tetrabenazine: Dose Proportionality and Food Effect. *Clin. Pharmacol. Drug Dev.* **2021**, *10*, 647–659. [CrossRef]
54. Huntington Study Group; Frank, S.; Testa, C.M.; Stamler, D.; Kayson, E.; Davis, C.; Edmondson, M.C.; Kinel, S.; Leavitt, B.; Oakes, D.; et al. Effect of Deutetrabenazine on Chorea Among Patients With Huntington Disease. *JAMA* **2016**, *316*, 40–50. [CrossRef]
55. Frank, S.; Testa, C.; Edmondson, M.C.; Goldstein, J.; Kayson, E.; Leavitt, B.R.; Oakes, D.; O'neill, C.; Vaughan, C.; Whaley, J.; et al. The Safety of Deutetrabenazine for Chorea in Huntington Disease: An Open-Label Extension Study. *CNS Drugs* **2022**, *36*, 1207–1216. [CrossRef] [PubMed]
56. Frank, S.; Testa, C.M.; Goldstein, J.; Kayson, E.; Leavitt, B.R.; Oakes, D.; O'nEill, C.; Whaley, J.; Gross, N.; Chaijale, N.; et al. Safety and Efficacy of Deutetrabenazine at High versus Lower Daily Dosages in the ARC-HD Study to Treat Chorea in Huntington Disease. *CNS Drugs* **2025**, *39*, 185–195. [CrossRef] [PubMed]
57. Stimming, E.F.; Claassen, D.O.; Kayson, E.; Goldstein, J.; Mehanna, R.; Zhang, H.; Liang, G.S.; Haubenberger, D.; Adams, J.; Beck, C.; et al. Safety and efficacy of valbenazine for the treatment of chorea associated with Huntington's disease (KINECT-HD): A phase 3, randomised, double-blind, placebo-controlled trial. *Lancet Neurol.* **2023**, *22*, 494–504. [CrossRef]
58. Patino, J.; Stimming, E.F.; Testa, C.M.; Mehanna, R. Valbenazine for the treatment of chorea associated with Huntington's disease. *Expert Opin. Pharmacother.* **2024**, *26*, 127–132. [CrossRef]
59. Rodrigues, F.B.; Duarte, G.S.; Costa, J.; Ferreira, J.J.; Wild, E. Tetrabenazine Versus Deutetrabenazine for Huntington's Disease: Twins or Distant Cousins? *Mov. Disord. Clin. Pract.* **2017**, *4*, 582–585. [CrossRef]
60. Feleus, S.; Skotnicki, L.E.; Roos, R.A.; de Bot, S.T. Medication Use and Treatment Indications in Huntington's Disease; Analyses from a Large Cohort. *Mov. Disord. Clin. Pr.* **2024**, *11*, 1530–1541. [CrossRef]
61. Priller, J.; Ecker, D.; Landwehrmeyer, B.; Craufurd, D. A Europe-wide assessment of current medication choices in Huntington's disease. *Mov. Disord.* **2008**, *23*, 1788. [CrossRef]
62. Martino, D.; Karnik, V.; Osland, S.; Barnes, T.R.E.; Pringsheim, T.M. Movement Disorders Associated With Antipsychotic Medication in People With Schizophrenia: An Overview of Cochrane Reviews and Meta-Analysis. *Can. J. Psychiatry* **2018**, *63*, 730–739. [CrossRef]
63. Deroover, J.; Baro, F.; Bourguignon, R.P.; Smets, P. Tiapride versus placebo: A double-blind comparative study in the management of Huntington's chorea. *Curr. Med Res. Opin.* **1984**, *9*, 329–338. [CrossRef]
64. Quinn, N.; Marsden, C.D. A double blind trial of sulpiride in Huntington's disease and tardive dyskinesia. *J. Neurol. Neurosurg. Psychiatry* **1984**, *47*, 844–847. [CrossRef]
65. Leonard, D.P.; Kidson, M.A.; Brown, J.G.E.; Shannon, P.J.; Taryan, S. A Double Blind Trial of Lithium Carbonate and Haloperidol in Huntington's Chorea. *Aust. N. Z. J. Psychiatry* **1975**, *9*, 115–118. [CrossRef] [PubMed]
66. Barr, A.N.; Fischer, J.H.; Roller, W.C.; Spunt, A.L.; Singhal, A. Serum haloperidol concentration and choreiform movements in Huntington's disease. *Neurology* **1988**, *38*, 84. [CrossRef]
67. Koller, W.C.; Trimble, J. The gait abnormality of Huntington's disease. *Neurology* **1985**, *35*, 1450. [CrossRef]
68. Girotti, F.; Carella, F.; Scigliano, G.; Grassi, M.P.; Soliveri, P.; Giovannini, P.; Parati, E.; Caraceni, T. Effect of neuroleptic treatment on involuntary movements and motor performances in Huntington's disease. *J. Neurol. Neurosurg. Psychiatry* **1984**, *47*, 848–852. [CrossRef]
69. Unti, E.; Mazzucchi, S.; Palermo, G.; Bonuccelli, U.; Ceravolo, R. Antipsychotic drugs in Huntington's disease. *Expert Rev. Neurother.* **2016**, *17*, 227–237. [CrossRef]
70. Saft, C.; Burgunder, J.-M.; Dose, M.; Jung, H.H.; Katzenschlager, R.; Priller, J.; Nguyen, H.P.; Reetz, K.; Reilmann, R.; Seppi, K.; et al. Symptomatic treatment options for Huntington's disease (guidelines of the German Neurological Society). *Neurol. Res. Pr.* **2023**, *5*, 1–10. [CrossRef]
71. Benchoua, A.; Trioulier, Y.; Diguet, E.; Malgorn, C.; Gaillard, M.-C.; Dufour, N.; Elalouf, J.-M.; Krajewski, S.; Hantraye, P.; Déglon, N.; et al. Dopamine determines the vulnerability of striatal neurons to the N-terminal fragment of mutant huntingtin through the regulation of mitochondrial complex II. *Hum. Mol. Genet.* **2008**, *17*, 1446–1456. [CrossRef]
72. Duff, K.; Beglinger, L.J.; O'ROurke, M.E.; Nopoulos, P.; Paulson, H.L.; Paulsen, J.S. Risperidone and the Treatment of Psychiatric, Motor, and Cognitive Symptoms in Huntington's Disease. *Ann. Clin. Psychiatry* **2008**, *20*, 1–3. [CrossRef]
73. Johnston, T.G. Risperidone long-acting injection and Huntington's disease: Case series with significant psychiatric and behavioural symptoms. *Int. Clin. Psychopharmacol.* **2011**, *26*, 114–119. [CrossRef]
74. Schultz, J.L.; Kamholz, J.A.; Nopoulos, P.C.; Killoran, A. Comparing Risperidone and Olanzapine to Tetrabenazine for the Management of Chorea in Huntington Disease: An Analysis from the Enroll-HD Database. *Mov. Disord. Clin. Pr.* **2018**, *6*, 132–138. [CrossRef]

75. Erdemoglu, A.K.; Boratav, C. Risperidone in chorea and psychosis of Huntington's disease. *Eur. J. Neurol.* **2002**, *9*, 182–183. [CrossRef] [PubMed]
76. Mestre, T.; Ferreira, J.; Coelho, M.M.; Rosa, M.; Sampaio, C. Cochrane Movement Disorders Group Therapeutic interventions for disease progression in Huntington's disease. *Cochrane Database Syst. Rev.* **2009**, *2009*, CD006455. [CrossRef] [PubMed]
77. Bogelman, G.; Hirschmann, S.; Modai, I. Olanzapine and Huntington's Disease. *J. Clin. Psychopharmacol.* **2001**, *21*, 245–246. [CrossRef] [PubMed]
78. Laks, J.; Rocha, M.; Capitão, C.; Domingues, R.C.; Ladeia, G.; Lima, M.; Engelhardt, E. Functional and motor response to low dose olanzapine in huntington's disease: Case report. *Arq. Neuro-Psiquiatr.* **2004**, *62*, 1092–1094. [CrossRef]
79. Bonelli, R.M.; Mahnert, F.A.; Niederwieser, G. Olanzapine for Huntington's Disease: An Open Label Study. *Clin. Neuropharmacol.* **2002**, *25*, 263–265. [CrossRef]
80. Dipple, H.C. The use of olanzapine for movement disorder in Huntington's disease: A first case report. *J. Neurol. Neurosurg. Psychiatry* **1999**, *67*, 123–124. [CrossRef]
81. Grove, V.E.J.; Quintanilla, J.; DeVaney, G.T. Improvement of Huntington's Disease with Olanzapine and Valproate. *N. Engl. J. Med.* **2000**, *343*, 973–974. [CrossRef]
82. Shapiro, D.A.; Renock, S.; Arrington, E.; Chiodo, L.A.; Liu, L.-X.; Sibley, D.R.; Roth, B.L.; Mailman, R. Aripiprazole, A Novel Atypical Antipsychotic Drug with a Unique and Robust Pharmacology. *Neuropsychopharmacology* **2003**, *28*, 1400–1411. [CrossRef]
83. Yavuz, K.; Ulusoy, S.; Alnıak, İ. Aripiprazole Treatment for Choreoathetoid and Psychotic Symptoms of Huntington's Disease. *J. Neuropsychiatry* **2013**, *25*, E31. [CrossRef]
84. Lin, W.-C.; Chou, Y.-H. Aripiprazole Effects on Psychosis and Chorea in a Patient with Huntington's Disease. *Am. J. Psychiatry* **2008**, *165*, 1207–1208. [CrossRef]
85. Brusa, L.; Orlacchio, A.; Moschella, V.; Iani, C.; Bernardi, G.; Mercuri, N.B. Treatment of the symptoms of Huntington's disease: Preliminary results comparing aripiprazole and tetrabenazine. *Mov. Disord.* **2009**, *24*, 126–129. [CrossRef] [PubMed]
86. Bonelli, R.M.; Niederwieser, G. Quetiapine in Huntington's disease: A first case report. *J. Neurol.* **2002**, *249*, 1114–1115. [CrossRef] [PubMed]
87. Seitz, D.P.; Millson, R.C. Quetiapine in the Management of Psychosis Secondary to Huntington's Disease: A Case Report. *Can. J. Psychiatry* **2004**, *49*, 413. [CrossRef]
88. The trial use of clozapine for abnormal involuntary movement disorders. *Am. J. Psychiatry* **1979**, *136*, 317–320. [CrossRef]
89. van Vugt, J.P.P.; Siesling, S.; Vergeer, M.; van der Velde, E.A.; Roos, R.A.C. Clozapine versus placebo in Huntington's disease: A double blind randomised comparative study. *J. Neurol. Neurosurg. Psychiatry* **1997**, *63*, 35–39. [CrossRef]
90. Danysz, W.; Dekundy, A.; Scheschonka, A.; Riederer, P. Amantadine: Reappraisal of the timeless diamond—Target updates and novel therapeutic potentials. *J. Neural Transm.* **2021**, *128*, 127–169. [CrossRef]
91. O'Suilleabhain, P.; Dewey, R.B., Jr. A Randomized Trial of Amantadine in Huntington Disease. *Arch. Neurol.* **2003**, *60*, 996. [CrossRef]
92. Metman, L.V.; Morris, M.J.; Farmer, C.; Gillespie, M.; Mosby, K.; Wuu, J.; Chase, T.N. Huntington's disease. *Neurology* **2002**, *59*, 694–699. [CrossRef]
93. Lucetti, C.; Del Dotto, P.; Gambaccini, G.; Agnello, G.D.; Bernardini, S.; Rossi, G.; Murri, L.; Bonuccelli, U. IV amantadine improves chorea in Huntington's disease An acute randomized, controlled study. *Neurology* **2003**, *60*, 1995–1997. [CrossRef]
94. Lucetti, C.; Gambaccini, G.; Bernardini, S.; Dell'AGnello, G.; Petrozzi, L.; Rossi, G.; Bonuccelli, U. Amantadine in Huntington's disease: Open-label video-blinded study. *Neurol. Sci.* **2002**, *23*, s83–s84. [CrossRef]
95. Ondo, W.G.; Mejia, N.I.; Hunter, C.B. A pilot study of the clinical efficacy and safety of memantine for Huntington's disease. *Park. Relat. Disord.* **2007**, *13*, 453–454. [CrossRef] [PubMed]
96. Huntington Study Group. Dosage effects of riluzole in Huntington's disease: A multicenter placebo-controlled study. *Neurology* **2003**, *61*, 1551–1556. [CrossRef] [PubMed]
97. Seppi, K.; Mueller, J.; Bodner, T.; Brandauer, E.; Benke, T.; Weirich-Schwaiger, H.; Poewe, W.; Wenning, G.K. Riluzole in Huntington's disease (HD): An open label study with one year follow up. *J. Neurol.* **2001**, *248*, 866–869. [CrossRef]
98. Landwehrmeyer, G.B.; Dubois, B.; de Yébenes, J.G.; Kremer, B.; Gaus, W.; Kraus, P.H.; Przuntek, H.; Dib, M.; Doble, A.; Fischer, W.; et al. Riluzole in Huntington's disease: A 3-year, randomized controlled study. *Ann. Neurol.* **2007**, *62*, 262–272. [CrossRef]
99. Waters, S.; Tedroff, J.; Ponten, H.; Klamer, D.; Sonesson, C.; Waters, N. Pridopidine: Overview of Pharmacology and Rationale for its Use in Huntington's Disease. *J. Huntington's Dis.* **2018**, *7*, 1–16. [CrossRef]
100. Garcia-Miralles, M.; Geva, M.; Tan, J.Y.; Yusof, N.A.B.M.; Cha, Y.; Kusko, R.; Tan, L.J.; Xu, X.; Grossman, I.; Orbach, A.; et al. Early pridopidine treatment improves behavioral and transcriptional deficits in YAC128 Huntington disease mice. *J. Clin. Investig.* **2017**, *2*, e95665. [CrossRef]
101. Geva, M.; Kusko, R.; Soares, H.; Fowler, K.D.; Birnberg, T.; Barash, S.; -Wagner, A.M.; Fine, T.; Lysaght, A.; Weiner, B.; et al. Pridopidine activates neuroprotective pathways impaired in Huntington Disease. *Hum. Mol. Genet.* **2016**, *25*, 3975–3987. [CrossRef]

102. Naia, L.; Ly, P.; Mota, S.I.; Lopes, C.; Maranga, C.; Coelho, P.; Gershoni-Emek, N.; Ankarcrona, M.; Geva, M.; Hayden, M.R.; et al. The Sigma-1 Receptor Mediates Pridopidine Rescue of Mitochondrial Function in Huntington Disease Models. *Neurotherapeutics* **2021**, *18*, 1017–1038. [CrossRef]
103. Reilmann, R.; McGarry, A.; Grachev, I.D.; Savola, J.-M.; Borowsky, B.; Eyal, E.; Gross, N.; Langbehn, D.; Schubert, R.; Wickenberg, A.T.; et al. Safety and efficacy of pridopidine in patients with Huntington's disease (PRIDE-HD): A phase 2, randomised, placebo-controlled, multicentre, dose-ranging study. *Lancet Neurol.* **2019**, *18*, 165–176. [CrossRef]
104. Geva, M.; Reilmann, R.; Feigin, A.; Rosser, A.; Kostyk, S.; Chen, K.; Mehra, M.; Cohen, Y.; Goldberg, P.; Hayden, M. Analyses of the Phase 3 Trial of Pridopidine's Outcome on Function in Huntington Disease (PROOF-HD) Demonstrates Efficacy in Participants Without Antidopaminergic Medications (S30.002). *Neurology* **2024**, *102*, 6964. [CrossRef]
105. Goldberg, Y.P.; Navon-Perry, L.; Cruz-Herranz, A.; Chen, K.; Hecker-Barth, G.; Spiegel, K.; Cohen, Y.; Niethammer, M.; Tan, A.M.; Schuring, H.; et al. The Safety Profile of Pridopidine, a Novel Sigma-1 Receptor Agonist for the Treatment of Huntington's Disease. *CNS Drugs* **2025**, *39*, 485–498. [CrossRef] [PubMed]
106. de Tommaso, M.; Di Fruscolo, O.; Sciruicchio, V.; Specchio, N.; Cormio, C.; De Caro, M.F.; Livrea, P. Efficacy of Levetiracetam in Huntington Disease. *Clin. Neuropharmacol.* **2005**, *28*, 280–284. [CrossRef] [PubMed]
107. Zesiewicz, T.A.; Sullivan, K.L.; Hauser, R.A.; Sanchez-Ramos, J. Open-label pilot study of levetiracetam (Keppra) for the treatment of chorea in Huntington's disease. *Mov. Disord.* **2006**, *21*, 1998–2001. [CrossRef] [PubMed]
108. Peiris, J.B.; Boralessa, H.; Lionel, N.D. Clonazepam in the treatment of choreiform activity. *Med. J. Aust.* **1976**, *1*, 225–227.
109. Biolsi, B.; Cif, L.; El Fertit, H.; Gil Robles, S.; Coubes, P. Long-term follow-up of Huntington disease treated by bilateral deep brain stimulation of the internal globus pallidus. *J. Neurosurg.* **2008**, *109*, 130–132. [CrossRef]
110. Bonomo, R.; Elia, A.E.; Bonomo, G.; Romito, L.M.; Mariotti, C.; Devigili, G.; Cilia, R.; Giossi, R.; Eleopra, R. Deep brain stimulation in Huntington's disease: A literature review. *Neurol. Sci.* **2021**, *42*, 4447–4457. [CrossRef]
111. Edwards, T.C.; Zrinzo, L.; Limousin, P.; Foltynie, T. Deep brain stimulation in the treatment of chorea. *Mov. Disord.* **2011**, *27*, 357–363. [CrossRef]
112. Fasano, A.; Mazzone, P.; Piano, C.; Quaranta, D.; Soleti, F.; Bentivoglio, A.R. GPi-DBS in Huntington's disease: Results on motor function and cognition in a 72-year-old case. *Mov. Disord.* **2008**, *23*, 1289–1292. [CrossRef]
113. Gonzalez, V.; Cif, L.; Biolsi, B.; Garcia-Ptacek, S.; Seychelles, A.; Sanrey, E.; Descours, I.; Coubes, C.; de Moura, A.-M.R.; Corlobe, A.; et al. Deep brain stimulation for Huntington's disease: Long-term results of a prospective open-label study. *J. Neurosurg.* **2014**, *121*, 114–122. [CrossRef]
114. Kang, G.A.; Heath, S.; Rothlind, J.; Starr, P.A. Long-term follow-up of pallidal deep brain stimulation in two cases of Huntington's disease. *J. Neurol. Neurosurg. Psychiatry* **2010**, *82*, 272–277. [CrossRef]
115. Moreno, J.L.L.-S.; García-Caldentey, J.; Regidor, I.; del Álamo, M.; de Yébenes, J.G. A 5-year follow-up of deep brain stimulation in Huntington's disease. *Park. Relat. Disord.* **2014**, *20*, 260–261. [CrossRef] [PubMed]
116. Moro, E.; Lang, A.E.; Strafella, A.P.; Poon, Y.W.; Arango, P.M.; Dagher, A.; Hutchison, W.D.; Lozano, A.M. Bilateral globus pallidus stimulation for Huntington's disease. *Ann. Neurol.* **2004**, *56*, 290–294. [CrossRef]
117. Spielberger, S.; Hotter, A.; Wolf, E.; Eisner, W.; Müller, J.; Poewe, W.; Seppi, K. Deep brain stimulation in Huntington's disease: A 4-year follow-up case report. *Mov. Disord.* **2012**, *27*, 806–807. [CrossRef] [PubMed]
118. Steinhardt, J.; Zittel, S.; Tadic, V.; Tronnier, V.; Moll, C.; Bäumer, T.; Münchau, A.; Rasche, D.; Brüggemann, N. GPi/GPe borderland– a potential sweet spot for deep brain stimulation for chorea in Huntington's disease? *Neurol. Res. Pr.* **2024**, *6*, 1–3. [CrossRef]
119. Wojtecki, L.; Groiss, S.J.; Ferrea, S.; Elben, S.; Hartmann, C.J.; Dunnett, S.B.; Rosser, A.; Saft, C.; Südmeyer, M.; Ohmann, C.; et al. A Prospective Pilot Trial for Pallidal Deep Brain Stimulation in Huntington's Disease. *Front. Neurol.* **2015**, *6*, 177. [CrossRef]
120. Delorme, C.; Rogers, A.; Lau, B.; Francisque, H.; Welter, M.-L.; Vidal, S.F.; Yelnik, J.; Durr, A.; Grabli, D.; Karachi, C. Deep brain stimulation of the internal pallidum in Huntington's disease patients: Clinical outcome and neuronal firing patterns. *J. Neurol.* **2015**, *263*, 290–298. [CrossRef]
121. Thompson, J.A.; Cruickshank, T.M.; Penailillo, L.E.; Lee, J.W.; Newton, R.U.; Barker, R.A.; Ziman, M.R. The effects of multi-disciplinary rehabilitation in patients with early-to-middle-stage Huntington's disease: A pilot study. *Eur. J. Neurol.* **2012**, *20*, 1325–1329. [CrossRef]
122. Busse, M.; Quinn, L.; Debono, K.; Jones, K.; Collett, J.; Playle, R.; Kelly, M.; Simpson, S.; Backx, K.; Wasley, D.; et al. A Randomized Feasibility Study of a 12-Week Community-Based Exercise Program for People With Huntington's Disease. *J. Neurol. Phys. Ther.* **2013**, *37*, 149–158. [CrossRef]
123. Quinn, L.; Playle, R.; Drew, C.J.; Taiyari, K.; Williams-Thomas, R.; Muratori, L.M.; Hamana, K.; Griffin, B.A.; Kelson, M.; Schubert, R.; et al. Physical activity and exercise outcomes in Huntington's disease (PACE-HD): Results of a 12-month trial-within-cohort feasibility study of a physical activity intervention in people with Huntington's disease. *Park. Relat. Disord.* **2022**, *101*, 75–89. [CrossRef]

124. Gamez, J.; Calopa, M.; Muñoz, E.; Ferré, A.; Huertas, O.; McAllister, K.; Reig, N.; Scart-Grès, C.; Insa, R.; Kulisevsky, J. A proof-of-concept study with SOM3355 (bevantolol hydrochloride) for reducing chorea in Huntington's disease. *Br. J. Clin. Pharmacol.* **2022**, *89*, 1656–1664. [CrossRef]
125. Gordon, A.M.; Quinnc, L.; Reilmannab, R.; Marderd, K. Coordination of Prehensile Forces during Precision Grip in Huntington's Disease. *Exp. Neurol.* **2000**, *163*, 136–148. [CrossRef] [PubMed]
126. Kojović, M.; Bhatia, K.P. Bringing order to higher order motor disorders. *J. Neurol.* **2018**, *266*, 797–805. [CrossRef]
127. Reilmann, R.; Bohlen, S.; Klopstock, T.; Bender, A.; Weindl, A.; Saemann, P.; Auer, D.P.; Ringelstein, E.B.; Lange, H.W. Tongue force analysis assesses motor phenotype in premanifest and symptomatic Huntington's disease. *Mov. Disord.* **2010**, *25*, 2195–2202. [CrossRef] [PubMed]
128. Reilmann, R.; Kirsten, F.; Quinn, L.; Henningsen, H.; Marder, K.; Gordon, A.M. Objective assessment of progression in Huntington's disease: A 3-year follow-up study. *Neurology* **2001**, *57*, 920–924. [CrossRef]
129. Termsarasab, P.; Frucht, S.J. The "Stutter-Step": A Peculiar Gait Feature in Advanced Huntington's Disease and Chorea-Acanthocytosis. Mov. *Disord. Clin. Pract.* **2018**, *5*, 223–224. [CrossRef]
130. Fisher, M. Left hemiplegia and motor impersistence. *J. Nerv. Ment. Dis.* **1956**, *123*, 201–218. [CrossRef]
131. Cambier, J.; Masson, M.; Viader, F.; Limodin, J.; Strube, A. Le syndrome frontal de la paralysie supranucléaire progressive [Frontal syndrome of progressive supranuclear palsy]. *Rev Neurol* **1985**, *141*, 528–536. [PubMed]
132. Lopez, O.L.; Becker, J.T.; Boller, F. Motor Impersistence in Alzheimer's Disease. *Cortex* **1991**, *27*, 93–99. [CrossRef]
133. Gantois, I.; Fang, K.; Jiang, L.; Babovic, D.; Lawrence, A.J.; Ferreri, V.; Teper, Y.; Jupp, B.; Ziebell, J.; Morganti-Kossmann, C.M.; et al. Ablation of D1 dopamine receptor-expressing cells generates mice with seizures, dystonia, hyperactivity, and impaired oral behavior. *Proc. Natl. Acad. Sci. USA* **2007**, *104*, 4182–4187. [CrossRef]
134. Miranda, D.R.; Reed, E.; Jama, A.; Bottomley, M.; Ren, H.; Rich, M.M.; Voss, A.A. Mechanisms of altered skeletal muscle action potentials in the R6/2 mouse model of Huntington's disease. *Am. J. Physiol. Physiol.* **2020**, *319*, C218–C232. [CrossRef]
135. Albanese, A.; Cassetta, E.; Carretta, D.; Bentivoglio, A.R.; Tonali, P. Acute Challenge with Apomorphine in Huntington's Disease. *Clin. Neuropharmacol.* **1995**, *18*, 427–434. [CrossRef] [PubMed]
136. van de Zande, N.A.; Massey, T.H.; McLauchlan, D.; Roberts, A.P.; Zutt, R.; Wardle, M.; Payne, G.C.; Clenaghan, C.; Tijssen, M.A.J.; Rosser, A.E.; et al. Clinical characterization of dystonia in adult patients with Huntington's disease. *Eur. J. Neurol.* **2017**, *24*, 1140–1147. [CrossRef] [PubMed]
137. Louis, E.D.; Lee, P.; Quinn, L.; Marder, K. Dystonia in Huntington's disease: Prevalence and clinical characteristics. *Mov Disord.* **1999**, *14*, 95–101. [CrossRef] [PubMed]
138. Achenbach, J.; von Hein, S.M.; Saft, C. Functional and cognitive capacity differ in dystonic motor subtypes when compared to choreatic and hypokinetic-rigid motor subtypes in Huntington's disease. *Brain Behav.* **2020**, *10*, e01704. [CrossRef]
139. Burke, R.E.; Fahn, S.; Marsden, C.D. Torsion dystonia: A double-blind, prospective trial of high-dosage trihexyphenidyl. *Neurology* **1986**, *36*, 160. [CrossRef]
140. Motta, F.; Antonello, C.E. Analysis of complications in 430 consecutive pediatric patients treated with intrathecal baclofen therapy: 14-year experience: Clinical article. *J. Neurosurg. Pediatr.* **2014**, *13*, 301–306. [CrossRef]
141. Balint, B.; Mencacci, N.E.; Valente, E.M.; Pisani, A.; Rothwell, J.; Jankovic, J.; Vidailhet, M.; Bhatia, K.P. Dystonia. *Nat. Rev. Dis. Prim.* **2018**, *4*, 1–23. [CrossRef]
142. Dressler, D. Botulinum toxin for treatment of dystonia. *Eur. J. Neurol.* **2010**, *17*, 88–96. [CrossRef]
143. Jankovic, J. Botulinum toxin: State of the art. *Mov. Disord.* **2017**, *32*, 1131–1138. [CrossRef]
144. Cislaghi, G.; Capiluppi, E.; Saleh, C.; Romano, L.; Servello, D.; Mariani, C.; Porta, M. Bilateral Globus Pallidus Stimulation in Westphal Variant of Huntington Disease. *Neuromodul. Technol. Neural Interface* **2013**, *17*, 502–505. [CrossRef]
145. Ferrea, S.; For the Surgical Approaches Working Group of the European Huntington's Disease Network (EHDN); Groiss, S.J.; Elben, S.; Hartmann, C.J.; Dunnett, S.B.; Rosser, A.; Saft, C.; Schnitzler, A.; Vesper, J.; et al. Pallidal deep brain stimulation in juvenile Huntington's disease: Local field potential oscillations and clinical data. *J. Neurol.* **2018**, *265*, 1573–1579. [CrossRef] [PubMed]
146. Deik, A.; Aamodt, W.; Cadet, C.; Lasker, A.; Oliver, A.; Spindler, M.; Tropea, T.F.; Vaswani, P.; Siderowf, A. An Open-Label Pilot Study to Examine the Safety, Tolerability and Efficacy of Deutetrabenazine in Isolated Dystonia. *Mov. Disord. Clin. Pr.* **2025**, *12*, 504–509. [CrossRef]
147. Reilmann, R. Parkinsonism in Huntington's disease. In *International Review of Neurobiology*; Elsevier: Amsterdam, The Netherlands, 2019; pp. 299–306.
148. Racette, B.A.; Perlmutter, J.S. Levodopa responsive parkinsonism in an adult with Huntington's disease. *J. Neurol. Neurosurg. Psychiatry* **1998**, *65*, 577–579. [CrossRef]
149. Bonelli, R.M.; Niederwieser, G.; Diez, J.; Gruber, A.; Költringer, P. Pramipexole Ameliorates Neurologic and Psychiatric Symptoms in a Westphal Variant of Huntington's Disease. *Clin. Neuropharmacol.* **2002**, *25*, 58–60. [CrossRef]

150. Magnet, M.K.; Bonelli, R.M.; Kapfhammer, H.-P. Amantadine in the Akinetic-Rigid Variant of Huntington's Disease. *Ann. Pharmacother.* **2004**, *38*, 1194–1196. [CrossRef]
151. Pérez-Pérez, J.; Martínez-Horta, S.; Pagonabarraga, J.; Carceller, M.; Kulisevsky, J. Rasagiline for the treatment of parkinsonism in Huntington's disease. *Park. Relat. Disord.* **2015**, *21*, 340–342. [CrossRef]
152. Casaca-Carreira, J.; Temel, Y.; van Zelst, M.; Jahanshahi, A. Coexistence of Gait Disturbances and Chorea in Experimental Huntington's Disease. *Behav. Neurol.* **2015**, *2015*, 1–6. [CrossRef]
153. Heikkinen, T.; Bragge, T.; Bhattarai, N.; Parkkari, T.; Puoliväli, J.; Kontkanen, O.; Sweeney, P.; Park, L.C.; Munoz-Sanjuan, I.; Li, Y. Rapid and robust patterns of spontaneous locomotor deficits in mouse models of Huntington's disease. *PLoS ONE* **2020**, *15*, e0243052. [CrossRef]
154. Vuong, K.; Canning, C.G.; Menant, J.C.; Loy, C.T. Gait, balance, and falls in Huntington disease. In *Handbook of Clinical Neurology*; Elsevier: Amsterdam, The Netherlands, 2018; pp. 251–260.
155. Quinn, L.; Kegelmeyer, D.; Kloos, A.; Rao, A.K.; Busse, M.; Fritz, N.E. Clinical recommendations to guide physical therapy practice for Huntington disease. *Neurology* **2020**, *94*, 217–228. [CrossRef]
156. Quinn, L.; Busse, M. The role of rehabilitation therapy in Huntington disease. In *Handbook of Clinical Neurology*; Elsevier: Amsterdam, The Netherlands, 2017; pp. 151–165.
157. Kloos, A.D.; Fritz, N.E.; Kostyk, S.K.; Young, G.S.; Kegelmeyer, D.A. Video game play (Dance Dance Revolution) as a potential exercise therapy in Huntington's disease: A controlled clinical trial. *Clin. Rehabil.* **2013**, *27*, 972–982. [CrossRef]
158. Khalil, H.; Quinn, L.; van Deursen, R.; Dawes, H.; Playle, R.; Rosser, A.; Busse, M. What effect does a structured home-based exercise programme have on people with Huntington's disease? A randomized, controlled pilot study. *Clin. Rehabil.* **2013**, *27*, 646–658. [CrossRef] [PubMed]
159. Kegelmeyer, D.A.; Kostyk, S.K.; Fritz, N.E.; Scharre, D.W.; Young, G.S.; Tan, Y.; Schubert, R.; Reilmann, R.; Kloos, A.D. Immediate effects of treadmill walking in individuals with Lewy body dementia and Huntington's disease. *Gait Posture* **2021**, *86*, 186–191. [CrossRef] [PubMed]
160. de Yebenes, J.G.; Landwehrmeyer, B.; Squitieri, F.; Reilmann, R.; Rosser, A.; Barker, R.A.; Saft, C.; Magnet, M.K.; Sword, A.; Rembratt, Å.; et al. Pridopidine for the treatment of motor function in patients with Huntington's disease (MermaiHD): A phase 3, randomised, double-blind, placebo-controlled trial. *Lancet Neurol.* **2011**, *10*, 1049–1057. [CrossRef] [PubMed]
161. Caviness, J.N.; Kurth, M. Cortical myoclonus in huntington's disease associated with an enlarged somatosensory evoked potential. *Mov. Disord.* **1997**, *12*, 1046–1051. [CrossRef]
162. Saft, C.; Lauter, T.; Kraus, P.H.; Przuntek, H.; Andrich, J.E. Dose-dependent improvement of myoclonic hyperkinesia due to Valproic acid in eight Huntington's Disease patients: A case series. *BMC Neurol.* **2006**, *6*, 11. [CrossRef]
163. Jankovic, J.; Ashizawa, T. Tourettism associated with Huntington's disease. *Mov. Disord.* **1995**, *10*, 103–105. [CrossRef]
164. Pizzorni, N.; Pirola, F.; Ciammola, A.; Schindler, A. Management of dysphagia in Huntington's disease: A descriptive review. *Neurol. Sci.* **2020**, *41*, 1405–1417. [CrossRef]
165. Leopold, N.A.; Kagel, M.C. Dysphagia in Huntington's Disease. *Arch. Neurol.* **1985**, *42*, 57–60. [CrossRef]
166. Cubo, E.; Rivadeneyra, J.; Armesto, D.; Mariscal, N.; Martinez, A.; Camara, R.J.; Spanish Members of the European Huntington Disease Network. Relationship between Nutritional Status and the Severity of Huntington's Disease. A Spanish Multicenter Dietary Intake Study. *J. Huntingt. Dis.* **2015**, *4*, 78–85. [CrossRef] [PubMed]
167. Peavy, G.M.; Jacobson, M.W.; Goldstein, J.L.; Hamilton, J.M.; Kane, A.; Gamst, A.C.; Lessig, S.L.; Lee, J.C.; Corey-Bloom, J. Cognitive and functional decline in Huntington's disease: Dementia criteria revisited. *Mov. Disord.* **2010**, *25*, 1163–1169. [CrossRef]
168. Martinez-Horta, S.; Sampedro, F.; Horta-Barba, A.; Perez-Perez, J.; Pagonabarraga, J.; Gomez-Anson, B.; Kulisevsky, J. Structural brain correlates of dementia in Huntington's disease. *NeuroImage Clin.* **2020**, *28*, 102415. [CrossRef] [PubMed]
169. Puig-Davi, A.; Martinez-Horta, S.; Sampedro, F.; Horta-Barba, A.; Perez-Perez, J.; Campolongo, A.; Izquierdo-Barrionuevo, C.; Pagonabarraga, J.; Gomez-Anson, B.; Kulisevsky, J. Cognitive and Affective Empathy in Huntington's Disease. *J. Huntington's Dis.* **2021**, *10*, 323–334. [CrossRef] [PubMed]
170. Mason, S.L.; Schaepers, M.; Barker, R.A. Problems with Social Cognition and Decision-Making in Huntington's Disease: Why Is it Important? *Brain Sci.* **2021**, *11*, 838. [CrossRef] [PubMed]
171. McCusker, E.; Loy, C.T. The Many Facets of Unawareness in Huntington Disease. *Tremor Hyperkin. Mov.* **2014**, *4*, 257. [CrossRef]
172. McCusker, E.A.; Gunn, D.G.; Epping, E.A.; Loy, C.T.; Radford, K.; Griffith, J.; Mills, J.A.; Long, J.D.; Paulsen, J.S.; On behalf of the PREDICT-HD Investigators of the Huntington Study Group. Unawareness of motor phenoconversion in Huntington disease. *Neurology* **2013**, *81*, 1141–1147. [CrossRef]
173. Duff, K.; Paulsen, J.; Mills, J.; Beglinger, L.J.; Moser, D.J.; Smith, M.M.; Langbehn, D.; Stout, J.; Queller, S.; Harrington, D.L.; et al. Mild cognitive impairment in prediagnosed Huntington disease. *Neurology* **2010**, *75*, 500–507. [CrossRef]
174. Hinzen, W.; Rosselló, J.; Morey, C.; Camara, E.; Garcia-Gorro, C.; Salvador, R.; de Diego-Balaguer, R. A systematic linguistic profile of spontaneous narrative speech in pre-symptomatic and early stage Huntington's disease. *Cortex* **2018**, *100*, 71–83. [CrossRef]

175. Puig-Davi, A.; Franch-Marti, C.; Ruiz-Barrio, I.; Sampedro, F.; Perez-Perez, J.; Matias-Guiu, J.A.; Cuetos, F.; Olmedo-Saura, G.; Perez-Carasol, L.; Horta-Barba, A.; et al. Early Language Impairment as an Integral Part of the Cognitive Phenotype in Huntington's Disease. *Ann. Clin. Transl. Neurol.* **2025**, *12*, 1201–1213. [CrossRef]
176. Geva, M.; Goldberg, Y.P.; Schuring, H.; Tan, A.M.; Long, J.D.; Hayden, M.R. Antidopaminergic Medications and Clinical Changes in Measures of Huntington's Disease: A Causal Analysis. *Mov. Disord.* **2025**, *40*, 928–937. [CrossRef]
177. de Tommaso, M.; Specchio, N.; Sciruicchio, V.; Difruscolo, O.; Specchio, L.M. Effects of rivastigmine on motor and cognitive impairment in Huntington's disease. *Mov. Disord.* **2004**, *19*, 1516–1518. [CrossRef]
178. de Tommaso, M.; Difruscolo, O.; Sciruicchio, V.; Specchio, N.; Livrea, P. Two Years' Follow-up of Rivastigmine Treatment in Huntington Disease. *Clin. Neuropharmacol.* **2007**, *30*, 43–46. [CrossRef] [PubMed]
179. Rot, U.; Kobal, J.; Sever, A.; Pirtošek, Z.; Mesec, A. Rivastigmine in the treatment of Huntington's disease. *Eur. J. Neurol.* **2002**, *9*, 689–690. [CrossRef] [PubMed]
180. Sešok, S.; Bolle, N.; Kobal, J.; Bucik, V.; Vodušek, D.B. Cognitive function in early clinical phase huntington disease after rivastigmine treatment. *Psychiatr. Danub.* **2014**, *26*, 239–248. [PubMed]
181. Petrikis, P.; Andreou, C.; Piachas, A.; Bozikas, V.; Karavatos, A. Treatment of Huntington's disease with galantamine. *Int. Clin. Psychopharmacol.* **2004**, *19*, 49–50. [CrossRef]
182. Fernandez, H.H.; Friedman, J.H.; Grace, J.; Beason-Hazen, S. Donepezil for Huntington's disease. *Mov. Disord.* **2000**, *15*, 173–176. [CrossRef]
183. Cubo, E.; Shannon, K.M.; Tracy, D.; Jaglin, J.A.; Bernard, B.A.; Wuu, J.; Leurgans, S.E. Effect of donepezil on motor and cognitive function in Huntington disease. *Neurology* **2006**, *67*, 1268–1271. [CrossRef]
184. Blackwell, A.D.; Paterson, N.S.; Barker, R.A.; Robbins, T.W.; Sahakian, B.J. The effects of modafinil on mood and cognition in Huntington's disease. *Psychopharmacology* **2008**, *199*, 29–36. [CrossRef]
185. Piira, A.; van Walsem, M.R.; Mikalsen, G.; Nilsen, K.H.; Knutsen, S.; Frich, J.C. Effects of a One Year Intensive Multidisciplinary Rehabilitation Program for Patients with Huntington's Disease: A Prospective Intervention Study. *PLoS Curr.* **2013**, *5*. [CrossRef]
186. Cruickshank, T.M.; Thompson, J.A.; Domínguez D, J.F.; Reyes, A.P.; Bynevelt, M.; Georgiou-Karistianis, N.; Barker, R.A.; Ziman, M.R. The effect of multidisciplinary rehabilitation on brain structure and cognition in Huntington's disease: An exploratory study. *Brain Behav.* **2015**, *5*, e00312. [CrossRef]
187. Moreu-Valls, A.; Puig-Davi, A.; Martinez-Horta, S.; Kulisevsky, G.; Sampedro, F.; Perez-Perez, J.; Horta-Barba, A.; Olmedo-Saura, G.; Pagonabarraga, J.; Kulisevsky, J. A randomized clinical trial to evaluate the efficacy of cognitive rehabilitation and music therapy in mild cognitive impairment in Huntington's disease. *J. Neurol.* **2025**, *272*, 1–14. [CrossRef]
188. Molnar, M.J.; Molnar, V.; Fedor, M.; Csehi, R.; Acsai, K.; Borsos, B.; Grosz, Z. Improving Mood and Cognitive Symptoms in Huntington's Disease With Cariprazine Treatment. *Front. Psychiatry* **2022**, *12*, 825532. [CrossRef] [PubMed]
189. Murman, D.L.; Giordani, B.; Mellow, A.M.; Johanns, J.R.; Little, R.A.; Hariharan, M.; Foster, N.L. Cognitive, behavioral, and motor effects of the NMDA antagonist ketamine in Huntington's disease. *Neurology* **1997**, *49*, 153–161. [CrossRef] [PubMed]
190. Koenig, A.; Lewis, M.; Wald, J.; Li, S.; Varoglu, M.; Dai, J.; Sankoh, A.; Paumier, K.; Doherty, J.; Quirk, M. Dalzanemdor (SAGE-718), a novel, investigational N-methyl-D-aspartate receptor positive allosteric modulator: Safety, tolerability, and clinical pharmacology in randomized dose-finding studies in healthy participants and an open-label study in participants with Huntington's disease. *Clin. Transl. Sci.* **2024**, *17*, e13852. [CrossRef]
191. Available online: https://investor.sagerx.com/news-releases/news-release-details/sage-therapeutics-announces-topline-results-phase-2-dimension (accessed on 15 April 2025).
192. HORIZON Investigators of the Huntington Study Group; European Huntington's Disease Network. A Randomized, Double-blind, Placebo-Controlled Study of Latrepirdine in Patients With Mild to Moderate Huntington Disease. *JAMA Neurol.* **2013**, *70*, 25. [CrossRef]
193. Lundin, A.; Dietrichs, E.; Haghighi, S.; Göller, M.-L.; Heiberg, A.; Loutfi, G.; Widner, H.; Wiktorin, K.; Wiklund, L.; Svenningsson, A.; et al. Efficacy and Safety of the Dopaminergic Stabilizer Pridopidine (ACR16) in Patients With Huntington's Disease. *Clin. Neuropharmacol.* **2010**, *33*, 260–264. [CrossRef]
194. Beglinger, L.J.; Adams, W.H.; Langbehn, D.; Fiedorowicz, J.G.; Jorge, R.; Biglan, K.; Caviness, J.; Olson, B.; Robinson, R.G.; Kieburtz, K.; et al. Results of the citalopram to enhance cognition in Huntington disease trial. *Mov. Disord.* **2013**, *29*, 401–405. [CrossRef]
195. Como, P.G.; Rubin, A.J.; O'BRien, C.F.; Lawler, K.; Hickey, C.; Rubin, A.E.; Henderson, R.; McDermott, M.P.; McDermott, M.; Steinberg, K.; et al. A controlled trial of fluoxetine in nondepressed patients with Huntington's disease. *Mov. Disord.* **1997**, *12*, 397–401. [CrossRef]
196. van Duijn, E.; Craufurd, D.; Hubers, A.A.M.; Giltay, E.J.; Bonelli, R.; Rickards, H.; Anderson, K.E.; van Walsem, M.R.; van der Mast, R.C.; Orth, M.; et al. Neuropsychiatric symptoms in a European Huntington's disease cohort (REGISTRY). *J. Neurol. Neurosurg. Psychiatry* **2014**, *85*, 1411–1418. [CrossRef]

197. Epping, E.A.; Kim, J.-I.; Craufurd, D.; Brashers-Krug, T.M.; Anderson, K.E.; McCusker, E.; Luther, J.; Long, J.D.; Paulsen, J.S.; PREDICT-HD Investigators; et al. Longitudinal Psychiatric Symptoms in Prodromal Huntington's Disease: A Decade of Data. *Am. J. Psychiatry* **2016**, *173*, 184–192. [CrossRef]
198. Ho, A.K.; Gilbert, A.S.; Mason, S.L.; Goodman, A.O.; Barker, R.A. Health-related quality of life in Huntington's disease: Which factors matter most? *Mov. Disord.* **2009**, *24*, 574–578. [CrossRef]
199. Martinez-Horta, S.; Perez-Perez, J.; van Duijn, E.; Fernandez-Bobadilla, R.; Carceller, M.; Pagonabarraga, J.; Pascual-Sedano, B.; Campolongo, A.; Ruiz-Idiago, J.; Sampedro, F.; et al. Neuropsychiatric symptoms are very common in premanifest and early stage Huntington's Disease. *Park. Relat. Disord.* **2016**, *25*, 58–64. [CrossRef] [PubMed]
200. Tabrizi, S.J.; Schobel, S.; Gantman, E.C.; Mansbach, A.; Borowsky, B.; Konstantinova, P.; Mestre, T.A.; Panagoulias, J.; Ross, C.A.; Zauderer, M.; et al. A biological classification of Huntington's disease: The Integrated Staging System. *Lancet Neurol.* **2022**, *21*, 632–644. [CrossRef] [PubMed]
201. Anderson, K.E.; van Duijn, E.; Craufurd, D.; Drazinic, C.; Edmondson, M.; Goodman, N.; van Kammen, D.; Loy, C.; Priller, J.; Goodman, L.V. Clinical Management of Neuropsychiatric Symptoms of Huntington Disease: Expert-Based Consensus Guidelines on Agitation, Anxiety, Apathy, Psychosis and Sleep Disorders. *J. Huntington's Dis.* **2018**, *7*, 355–366. [CrossRef]
202. Slaughter, J.R.; Martens, M.P.; Slaughter, K.A. Depression and Huntington's Disease: Prevalence, Clinical Manifestations, Etiology, and Treatment. *CNS Spectr.* **2001**, *6*, 306–308, 325–326. [CrossRef]
203. Jellinger, K.A. The pathobiology of depression in Huntington's disease: An unresolved puzzle. *J. Neural Transm.* **2024**, *131*, 1511–1522. [CrossRef]
204. Zadegan, S.A.; Ramirez, F.; Reddy, K.S.; Sahin, O.; Rocha, N.P.; Teixeira, A.L.; Stimming, E.F. Treatment of Depression in Huntington's Disease: A Systematic Review. *J. Neuropsychiatry* **2024**, *36*, 283–299. [CrossRef]
205. Phillips, W.; Shannon, K.M.; Barker, R.A. The current clinical management of Huntington's disease. *Mov. Disord.* **2008**, *23*, 1491–1504. [CrossRef]
206. Holl, A.K.; Wilkinson, L.; Painold, A.; Holl, E.M.; Bonelli, R.M. Combating depression in Huntington's disease: Effective antidepressive treatment with venlafaxine XR. *Int. Clin. Psychopharmacol.* **2010**, *25*, 46–50. [CrossRef]
207. Ranen, N.G.; Lipsey, J.R.; Treisman, G.; Ross, C.A. Sertraline in the treatment of severe aggressiveness in Huntington's disease. *J. Neuropsychiatry* **1996**, *8*, 338–340. [CrossRef]
208. Patzold, T.; Brüne, M. Obsessive compulsive disorder in huntington disease: A case of isolated obsessions successfully treated with sertraline. *Cogn. Behav. Neurol.* **2002**, *15*, 216–219.
209. Bonelli, R.M. Mirtazapine in Suicidal Huntington's Disease. *Ann. Pharmacother.* **2003**, *37*, 452. [CrossRef] [PubMed]
210. Shen, Y.-C. Lamotrigine in motor and mood symptoms of Huntington's disease. *World J. Biol. Psychiatry* **2008**, *9*, 147–149. [CrossRef] [PubMed]
211. Raja, M.; Soleti, F.; Bentivoglio, A.R. Lithium Treatment in Patients With Huntington Disease and Suicidal Behavior. *J. Clin. Psychopharmacol.* **2013**, *33*, 819–821. [CrossRef] [PubMed]
212. Adrissi, J.; Nadkarni, N.A.; Gausche, E.; Bega, D. Electroconvulsive Therapy (ECT) for Refractory Psychiatric Symptoms in Huntington's Disease: A Case Series and Review of the Literature. *J. Huntington's Dis.* **2019**, *8*, 291–300. [CrossRef]
213. Cusin, C.; Franco, F.B.; Fernandez-Robles, C.; DuBois, C.M.; Welch, C.A. Rapid improvement of depression and psychotic symptoms in Huntington's disease: A retrospective chart review of seven patients treated with electroconvulsive therapy. *Gen. Hosp. Psychiatry* **2013**, *35*, 678.e3–678.e5. [CrossRef]
214. Ranen, N.G.; Peyser, C.E.; Folstein, S.E. ECT as a treatment for depression in Huntington's disease. *JNP* **1994**, *6*, 154–159.
215. Mughal, M.R.; Baharani, A.; Chigurupati, S.; Son, T.G.; Chen, E.; Yang, P.; Okun, E.; Arumugam, T.; Chan, S.L.; Mattson, M.P. Electroconvulsive shock ameliorates disease processes and extends survival in huntingtin mutant mice. *Hum. Mol. Genet.* **2010**, *20*, 659–669. [CrossRef]
216. Paulsen, J.S.; Ready, R.E.; Hamilton, J.M.; Mega, M.S.; Cummings, J.L. Neuropsychiatric aspects of Huntington's disease. *J. Neurol. Neurosurg. Psychiatry* **2001**, *71*, 310–314. [CrossRef]
217. Tabrizi, S.J.; Scahill, R.I.; Owen, G.; Durr, A.; Leavitt, B.R.; Roos, R.A.; Borowsky, B.; Landwehrmeyer, B.; Frost, C.; Johnson, H.; et al. Predictors of phenotypic progression and disease onset in premanifest and early-stage Huntington's disease in the TRACK-HD study: Analysis of 36-month observational data. *Lancet Neurol.* **2013**, *12*, 637–649. [CrossRef]
218. Atkins, K.J.; Andrews, S.C.; Chong, T.T.; Stout, J.C. Multidimensional Apathy: The Utility of the Dimensional Apathy Scale in Huntington's Disease. *Mov. Disord. Clin. Pr.* **2021**, *8*, 361–370. [CrossRef]
219. De Paepe, A.E.; Garcia-Gorro, C.; Martinez-Horta, S.; Perez, J.P.; Kulisevsky, J.; Rodriguez-Dechicha, N.; Vaquer, I.; Subira, S.; Calopa, M.; Santacruz, P.; et al. Delineating apathy profiles in Huntington's disease with the short-Lille Apathy Rating Scale. *Park. Relat. Disord.* **2022**, *105*, 83–89. [CrossRef] [PubMed]
220. Connors, M.H.; Teixeira-Pinto, A.; Loy, C.T. Apathy and Depression in Huntington's Disease: Distinct Longitudinal Trajectories and Clinical Correlates. *J. Neuropsychiatry* **2023**, *35*, 69–76. [CrossRef] [PubMed]

221. Levy, R.; Dubois, B. Apathy and the Functional Anatomy of the Prefrontal Cortex–Basal Ganglia Circuits. *Cereb. Cortex* **2006**, *16*, 916–928. [CrossRef] [PubMed]
222. Martínez-Horta, S.; Perez-Perez, J.; Sampedro, F.; Pagonabarraga, J.; Horta-Barba, A.; Carceller-Sindreu, M.; Gomez-Anson, B.; Lozano-Martinez, G.A.; Lopez-Mora, D.A.; Camacho, V.; et al. Structural and metabolic brain correlates of apathy in Huntington's disease. *Mov. Disord.* **2018**, *33*, 1151–1159. [CrossRef]
223. De Paepe, A.E.; Sierpowska, J.; Garcia-Gorro, C.; Martinez-Horta, S.; Perez-Perez, J.; Kulisevsky, J.; Rodriguez-Dechicha, N.; Vaquer, I.; Subira, S.; Calopa, M.; et al. White matter cortico-striatal tracts predict apathy subtypes in Huntington's disease. *NeuroImage Clin.* **2019**, *24*, 101965. [CrossRef]
224. Gelderblom, H.; Wüstenberg, T.; McLean, T.; Mütze, L.; Fischer, W.; Saft, C.; Hoffmann, R.; Süssmuth, S.; Schlattmann, P.; van Duijn, E.; et al. Bupropion for the treatment of apathy in Huntington's disease: A multicenter, randomised, double-blind, placebo-controlled, prospective crossover trial. *PLoS ONE* **2017**, *12*, e0173872. [CrossRef]
225. Sassone, J.; Mencacci, N.; Colciago, C.; Squitieri, F.; Silani, V.; Poletti, B.; Ciarmiello, A.; Ciarmiello, R. Aripiprazole in the treatment of Huntington's disease: A case series. *Neuropsychiatr. Dis. Treat.* **2008**, *5*, 1–4. [CrossRef]
226. Martinez-Horta, S.; Sampedro, F.; Horta-Barba, A.; Perez-Perez, J.; Pagonabarraga, J.; Gomez-Anson, B.; Kulisevsky, J. Structural brain correlates of irritability and aggression in early manifest Huntington's disease. *Brain Imaging Behav.* **2020**, *15*, 107–113. [CrossRef]
227. Stock, J.V.D.; De Winter, F.; Ahmad, R.; Sunaert, S.; Van Laere, K.; Vandenberghe, W.; Vandenbulcke, M. Functional brain changes underlying irritability in premanifest Huntington's disease. *Hum. Brain Mapp.* **2015**, *36*, 2681–2690. [CrossRef]
228. Labuschagne, I.; Jones, R.; Callaghan, J.; Whitehead, D.; Dumas, E.M.; Say, M.J.; Hart, E.P.; Justo, D.; Coleman, A.; Santos, R.C.D.; et al. Emotional face recognition deficits and medication effects in pre-manifest through stage-II Huntington's disease. *Psychiatry Res.* **2013**, *207*, 118–126. [CrossRef]
229. De Marchi, N.; Daniele, F.; Ragone, M.A. Fluoxetine in the treatment of Huntington's disease. *Psychopharmacology* **2001**, *153*, 264–266. [CrossRef]
230. Van Duijn, E. Treatment of Irritability in Huntington's Disease. *Curr. Treat. Options Neurol.* **2010**, *12*, 424–433. [CrossRef]
231. Andrade, C.; Rao, N.s.K. How antidepressant drugs act: A primer on neuroplasticity as the eventual mediator of antidepressant efficacy. *Indian J. Psychiatry* **2010**, *52*, 378. [CrossRef]
232. Alpay, M.; Koroshetz, W.J. Quetiapine in the Treatment of Behavioral Disturbances in Patients With Huntington's Disease. *Psychosomatics* **2006**, *47*, 70–72. [CrossRef]
233. Paleacu, D.; Anca, M.; Giladi, N. Olanzapine in Huntington's disease: Olanzapine in Huntington's disease. *Acta Neurol. Scand.* **2002**, *105*, 441–444. [CrossRef]
234. Habibi, N.; Dodangi, N.; Nazeri, A. Efficacy and Safety of Aripiprazole for Treatment of Irritability in Children with Autistic Disorder: An Open-Label Study. *Iran. J. Med. Sci.* **2015**, *40*, 548–549.
235. Fisher, C.A.; Sewell, K.; Brown, A.; Churchyard, A. Aggression in Huntington's Disease: A Systematic Review of Rates of Aggression and Treatment Methods. *J. Huntington's Dis.* **2014**, *3*, 319–332. [CrossRef]
236. Brownstein, M.J.; Simon, N.G.; Long, J.D.; Yankey, J.; Maibach, H.T.; Cudkowicz, M.; Coffey, C.; Conwit, R.A.; Lungu, C.; Anderson, K.E.; et al. Safety and Tolerability of SRX246, a Vasopressin 1a Antagonist, in Irritable Huntington's Disease Patients—A Randomized Phase 2 Clinical Trial. *J. Clin. Med.* **2020**, *9*, 3682. [CrossRef]
237. Maibach, H.T.; Brownstein, M.J.; Hersch, S.M.; Anderson, K.E.; Itzkowitz, D.E.; Damiano, E.M.; Simon, N.G. The Vasopressin 1a Receptor Antagonist SRX246 Reduces Aggressive Behavior in Huntington's Disease. *J. Pers. Med.* **2022**, *12*, 1561. [CrossRef]
238. Furr-Stimming, E.; Zadegan, S.; Murillas, J.P.; Dongarwar, D.; Rocha, N.P. A Pilot Study to Evaluate the Efficacy of Dextromethorphan/Quinidine in Treating Irritability in Huntington's Disease (P6-3.008). *Neurology* **2024**, *102*, 6940. [CrossRef]
239. Oosterloo, M.; Craufurd, D.; Nijsten, H.; van Duijn, E. Obsessive-Compulsive and Perseverative Behaviors in Huntington's Disease. *J. Huntington's Dis.* **2019**, *8*, 1–7. [CrossRef] [PubMed]
240. Squitieri, F.; Cannella, M.; Porcellini, A.; Brusa, L.; Simonelli, M.; Ruggieri, S. Short-term effects of olanzapine in Huntington disease. *Cogn. Behav. Neurol.* **2001**, *14*, 69–72.
241. Anderson, K.; Craufurd, D.; Edmondson, M.C.; Goodman, N.; Groves, M.; van Duijn, E.; van Kammen, D.P.; Goodman, L. An International Survey-based Algorithm for the Pharmacologic Treatment of Obsessive-Compulsive Behaviors in Huntington's Disease. *PLoS Curr.* **2011**, *3*, RRN1261. [CrossRef] [PubMed]
242. Jaini, A.; Yomtoob, J.; Yeh, C.; Bega, D. Understanding HD Psychosis: An Analysis from the ENROLL-HD Database. *Tremor Other Hyperkinetic Mov.* **2020**, *10*, 16. [CrossRef]
243. Rocha, N.P.; Mwangi, B.; Candano, C.A.G.; Sampaio, C.; Stimming, E.F.; Teixeira, A.L. The Clinical Picture of Psychosis in Manifest Huntington's Disease: A Comprehensive Analysis of the Enroll-HD Database. *Front. Neurol.* **2018**, *9*, 930. [CrossRef]
244. Connors, M.H.; Teixeira-Pinto, A.; Loy, C.T. Psychosis and longitudinal outcomes in Huntington disease: The COHORT Study. *J. Neurol. Neurosurg. Psychiatry* **2019**, *91*, 15–20. [CrossRef]

245. Schoenfeld, M.; Myers, R.H.; Cupples, L.A.; Berkman, B.; Sax, D.S.; Clark, E. Increased rate of suicide among patients with Huntington's disease. *J. Neurol. Neurosurg. Psychiatry* **1984**, *47*, 1283–1287. [CrossRef]
246. Di Maio, L.; Squitieri, F.; Napolitano, G.; Campanella, G.; Trofatter, J.A.; Conneally, P.M. Suicide risk in Huntington's disease. *J. Med Genet.* **1993**, *30*, 293–295. [CrossRef]
247. Baliko, L.; Csala, B.; Czopf, J. Suicide in Hungarian Huntington's Disease Patients. *Neuroepidemiology* **2004**, *23*, 258–260. [CrossRef]
248. Fiedorowicz, J.G.; Mills, J.A.; Ruggle, A.; Langbehn, D.; Paulsen, J.S. PREDICT-HD Investigators of the Huntington Study Group. Suicidal Behavior in Prodromal Huntington Disease. *Neurodegener Dis.* **2011**, *8*, 483–490. [CrossRef]
249. Wesson, M.; Boileau, N.R.; Perlmutter, J.S.; Paulsen, J.S.; Barton, S.K.; McCormack, M.K.; Carlozzi, N.E. Suicidal Ideation Assessment in Individuals with Premanifest and Manifest Huntington Disease. *J. Huntington's Dis.* **2018**, *7*, 239–249. [CrossRef] [PubMed]
250. van Duijn, E.; Fernandes, A.R.; Abreu, D.; Ware, J.J.; Neacy, E.; Sampaio, C. Incidence of completed suicide and suicide attempts in a global prospective study of Huntington's disease. *BJPsych Open* **2021**, *7*, e158. [CrossRef] [PubMed]
251. Arnulf, I.; Nielsen, J.; Lohmann, E.; Schieffer, J.; Wild, E.; Jennum, P.; Konofal, E.; Walker, M.; Oudiette, D.; Tabrizi, S.; et al. Rapid Eye Movement Sleep Disturbances in Huntington Disease. *Arch. Neurol.* **2008**, *65*, 482–488. [CrossRef] [PubMed]
252. Bellosta Diago, E.; Perez Perez, J.; Santos Lasaosa, S.; Viloria Alebesque, A.; Martinez Horta, S.; Kulisevsky, J.; Lopez Del Val, J. Circadian rhythm and autonomic dysfunction in presymptomatic and early Huntington's disease. *Park. Relat. Disord.* **2017**, *44*, 95–100. [CrossRef]

Disclaimer/Publisher's Note: The statements, opinions and data contained in all publications are solely those of the individual author(s) and contributor(s) and not of MDPI and/or the editor(s). MDPI and/or the editor(s) disclaim responsibility for any injury to people or property resulting from any ideas, methods, instructions or products referred to in the content.

International Journal of
Molecular Sciences

MDPI

Article

Impact of HSV-1 Infection on Alzheimer's Disease Neurodegeneration Markers: Insights from LUHMES 2D and 3D Neuronal Models

María Martín-Rico [1,2], Blanca Salgado [1,2], Inés Beamonte [1], Isabel Sastre [1,2], María J. Bullido [1,2,3,*] and Jesús Aldudo [1,2,3,*]

[1] Centro de Biologia Molecular Severo Ochoa (CBM), CSIC—Universidad Autonoma de Madrid, 28049 Madrid, Spain; maria.martin@cbm.csic.es (M.M.-R.); bsalgado@cbm.csic.es (B.S.); inesbp04@gmail.com (I.B.); isastre@cbm.csic.es (I.S.)
[2] CIBER de Enfermedades Neurodegenerativas, Instituto de Salud Carlos III, 28031 Madrid, Spain
[3] Instituto de Investigacion Sanitaria del Hospital Universitario La Paz—IdiPAZ, 28046 Madrid, Spain
* Correspondence: mjbullido@cbm.csic.es (M.J.B.); jaldudo@cbm.csic.es (J.A.)

Abstract

Herpes simplex virus type 1 (HSV-1) has been proposed as an environmental risk factor for Alzheimer's disease (AD). Viral infection of neuronal cells can reproduce hallmark pathological features of AD, including intracellular beta-amyloid (Aβ) accumulation, tau hyperphosphorylation, and lysosomal dysfunction. However, the molecular mechanisms underlying these alterations remain unclear, partly due to limitations of existing experimental models. Here, we established both two-dimensional (2D) and three-dimensional (3D) LUHMES neuronal cultures—a human mesencephalic-derived neural cell line that differentiates rapidly into mature neurons—to investigate HSV-1-induced AD-associated markers. Our results demonstrate that HSV-1 infection induces key features of AD, including intracellular accumulation of Aβ peptides and hyperphosphorylation of tau protein. Moreover, we observed disruptions in the autophagy–lysosome pathway, characterized by increased LC3-II levels, reduced cathepsin activity, and impaired lysosomal burden. Notably, these AD-like alterations were reproduced in 3D LUHMES neuronal aggregates, confirming their susceptibility to productive HSV-1 infection. Collectively, these findings indicate that HSV-1 not only triggers AD-like neuropathological markers but also disrupts cellular clearance mechanisms that may contribute to neuronal dysfunction and degeneration. This study validates the 3D LUHMES system as a useful human neuronal model to study virus-induced neurodegeneration and its mechanistic links to AD pathology.

Keywords: HSV-1; Alzheimer's disease; LUHMES cells; 3D neuronal cultures; beta-amyloid; phosphorylated tau; neurodegeneration; lysosomal alterations

1. Introduction

Alzheimer's disease (AD) is the most common cause of dementia, characterized by progressive neurodegeneration and cognitive impairment [1]. Despite extensive research efforts, its exact etiology remains elusive, and current therapeutic strategies only provide limited symptomatic relief [2]. Although senile plaques—primarily composed of beta-amyloid (Aβ) peptides—and neurofibrillary tangles (NFTs)—formed by hyperphosphorylated tau protein—have been recognized as key features of AD for over a century [3],

the molecular mechanisms driving the progression of the disorder are still not fully understood. Historically, the amyloid cascade hypothesis has dominated AD research, proposing that accumulation of Aβ peptides initiates a cascade of pathological events culminating in neuronal death [4]. However, accumulating evidence suggests that multiple factors, including infectious agents, significantly contribute to the complexity and progression of AD pathology [5].

Herpes simplex virus type 1 (HSV-1) is a highly prevalent human pathogen that infects a large proportion of the global population, typically during early life [6]. It is primarily associated with orolabial lesions but has the capacity to infect neurons and establish lifelong latency within the peripheral nervous system, particularly in sensory ganglia. Periodic reactivation of the virus can lead to recurrent symptoms and viral shedding [7]. Beyond its classical clinical presentations, growing evidence suggests that HSV-1 may exert long-term effects on the central nervous system (CNS). The virus is neurotropic and capable of invading the brain, where it may persist in a latent or low-grade replicative state [8]. Reactivation or chronic infection in the CNS has been implicated in various neurological disorders, including encephalitis, and more recently, neurodegenerative diseases such as AD [9,10]. In this context, understanding HSV-1's mechanisms of neuroinvasion, latency, reactivation, and the cellular pathways it disrupts—particularly in neuronal cells—is essential for elucidating its potential role in neurodegeneration.

A growing number of studies suggest a possible association between chronic HSV-1 infection and an increased risk of developing AD. Epidemiological studies have consistently identified associations between HSV-1 and a higher risk of AD, particularly among individuals carrying the APOE-ε4 allele [11–14]. Neuropathological analyses have revealed that HSV-1 DNA is frequently detected in the brains of AD patients, especially in brain regions severely affected by the disease, i.e., the hippocampus/limbic system [15]. Furthermore, experimental studies demonstrate that HSV-1 infection can directly induce hallmark AD features, such as Aβ accumulation [16], tau hyperphosphorylation [17], neuroinflammation [18] and synaptic dysfunction [19]. However, the detailed molecular and cellular mechanisms linking HSV-1 infection to AD pathology remain to be fully elucidated.

Emerging evidence also highlights the critical involvement of the autophagy–lysosomal system in both AD pathology and viral infections [20,21]. In AD, impaired autophagic flux and lysosomal dysfunction lead to the accumulation of toxic protein aggregates, including Aβ and phosphorylated tau, thereby contributing to neuronal stress and degeneration [20,22]. Likewise, several neurotropic viruses—including HSV-1—are known to interfere with autophagy and lysosomal pathways to favor their replication and persistence within host cells [21,23]. Thus, disruption of the autophagy–lysosomal system represents a convergent mechanism linking HSV-1 infection to AD-like neurodegenerative processes.

Advanced cellular models capable of recapitulating key aspects of human brain physiology offer invaluable tools for investigating virus-induced neurodegenerative processes. LUHMES (Lund human mesencephalic) is a human dopaminergic neuronal progenitor cell line derived from embryonic mesencephalic precursor cells, conditionally immortalized through the integration of the *v-myc* oncogene controlled by a tetracycline-regulated system. These cells exhibit a remarkable capacity for proliferation and, upon controlled suppression of the oncogene, differentiate rapidly into mature neurons that display physiological and morphological properties characteristic of the human nervous system [24]. Importantly, LUHMES cells differentiate exclusively into post-mitotic neurons under these conditions. Numerous foundational studies have demonstrated that differentiated LUHMES cultures form highly homogeneous neuronal populations, and do not give rise to glial cells of any lineage, including astrocytes, oligodendrocytes or microglia [24–26]. A key advantage of the LUHMES cellular model is its ability to maintain homogeneous and stable neuronal

https://doi.org/10.3390/ijms27020642

differentiation in long-term cultures, providing consistent cell lines for reproducible studies. This makes them particularly valuable for large-scale pharmacological screening assays and investigations into genetic and environmental factors involved in neurodegenerative diseases. Additionally, LUHMES cells are suitable for modeling neurological disorders in both two-dimensional (2D) and three-dimensional (3D) culture systems [25,27,28], enabling the generation of models that more closely replicate the spatial and cellular complexity of the human brain environment. Furthermore, these cells have been successfully used to study the effects of infectious and toxic agents on neuronal physiology [29,30], thereby facilitating an understanding of the mechanisms underlying the onset and progression of CNS pathologies. To date, only a few studies have explored HSV-1 infection in LUHMES cultures, and most have focused on the establishment and maintenance of viral latency in 2D cultures [30–32]. The effects of productive lytic infection on AD-related markers have not been characterized in this model.

Considering the above-mentioned advantages of LUHMES cells, mainly their growing capacity and ability to differentiate into a homogeneous neuronal phenotype, the present study aimed to develop and characterize a 3D LUHMES-based model of HSV-1 infection to investigate the molecular mechanisms leading to virus-induced neurodegeneration. We demonstrate that HSV-1 infection in this system reproduces AD-like alterations, including intracellular Aβ accumulation, tau hyperphosphorylation, and lysosomal dysfunction. Collectively, these findings provide new insights into the potential role of HSV-1 in AD pathogenesis and establish a human neuronal platform suitable for mechanistic studies to dissect the interplay between viral infection and neurodegeneration.

2. Results

2.1. LUHMES Cells Efficiently Differentiate into a Homogeneous Neuronal Population

LUHMES cells are a human neuronal precursor cell line derived from embryonic mesencephalon that can be terminally differentiated into post-mitotic dopaminergic-like neurons under defined culture conditions. In their proliferative state, LUHMES cells exhibit a compact and rounded morphology. As reported in earlier studies, withdrawal of growth factors combined with tetracycline exposure induces rapid neuronal differentiation, with neurite outgrowth visible within 2–3 days and a pronounced neuronal morphology by day 5. By this time, cells form dense neuronal networks clearly observable under phase-contrast microscopy (Figure 1A).

Immunocytochemical analysis revealed that proliferating LUHMES cells express neural progenitor and proliferation markers, including nestin—a neuroepithelial stem cell marker involved in cytoskeletal organization—and Ki-67, a proliferation marker associated with DNA replication (Figure 1B). Upon differentiation, these markers were downregulated, whereas the expression of mature neuronal markers such as βIII-tubulin, microtubule-associated protein 2 (MAP2) and neuronal nuclei antigen (NeuN) was strongly upregulated (Figure 1C). Unlike other neural stem cell models, LUHMES cells do not give rise to glial lineages such as astrocytes or oligodendrocytes, highlighting their suitability for studies focused exclusively on neuronal biology.

Protein and gene expression analysis by Western blot and reverse transcription followed by quantitative PCR (RT-qPCR) further confirmed the transition from a progenitor to a neuronal phenotype. A marked decrease in nestin, SOX2—a transcription factor essential for embryonic development—and Ki-67 (*MKI67*) was accompanied by strong upregulation of neuronal markers including βIII-tubulin, MAP2, synapsin 1 (*SYN1*), synaptophysin (*SYP*), and D2 dopamine receptor (*DRD2*) (Figure 1D, E). Overall, these findings demonstrate the rapid and efficient neuronal differentiation of LUHMES cells into a homogeneous

https://doi.org/10.3390/ijms27020642

population of post-mitotic human neurons, providing a robust in vitro system to investigate cellular and molecular mechanisms underlying neurodegeneration.

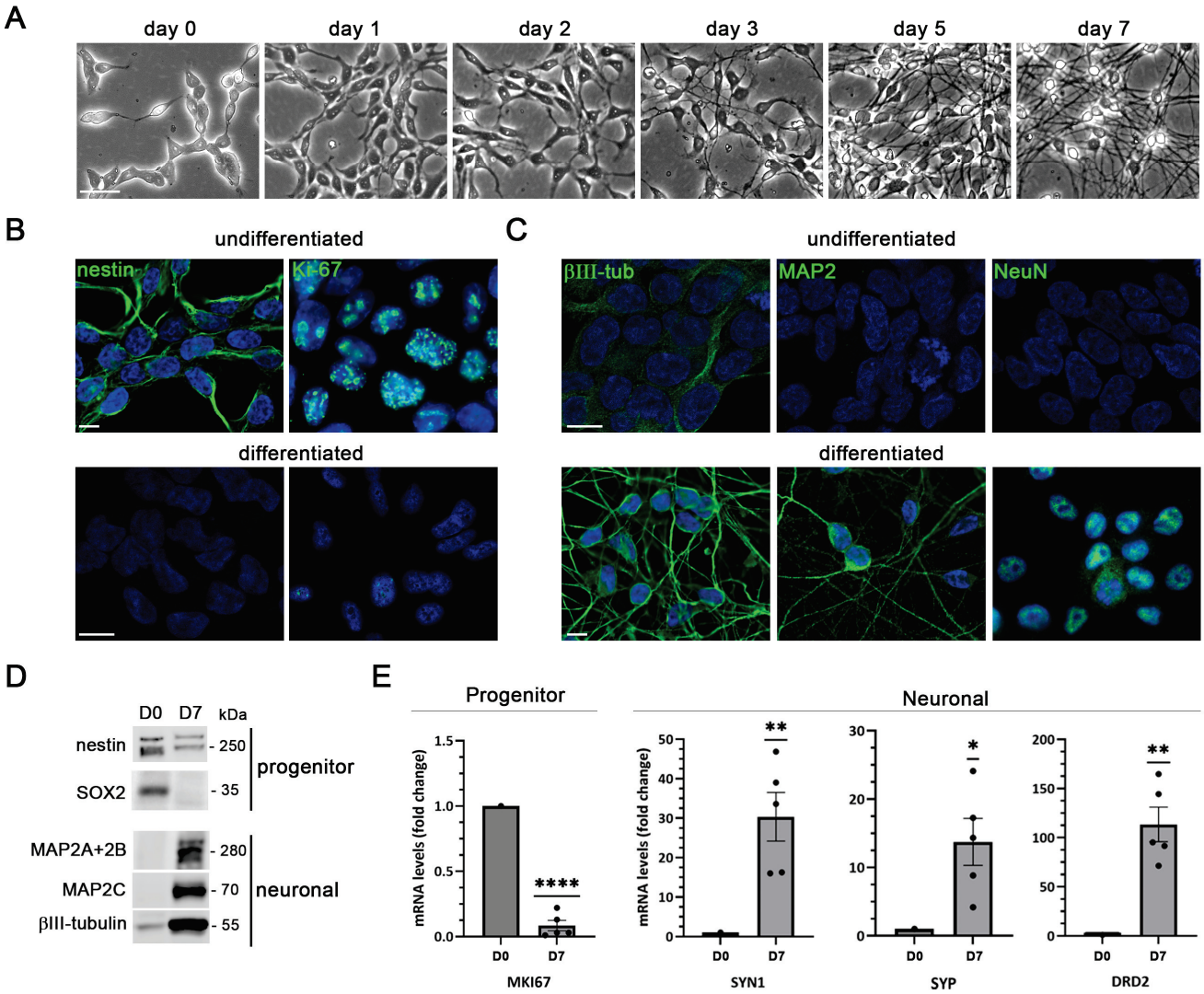


Figure 1. Differentiation of LUHMES cells into post-mitotic neurons in 2D cultures. (**A**) Representative phase-contrast images of LUHMES cells at different days of differentiation. Scale bar: 50 µm. (**B**) Immunofluorescence staining of the proliferation marker Ki-67 and the neural progenitor marker nestin in undifferentiated and 7-day-differentiated LUHMES cells. Scale bar: 10 µm. (**C**) Immunofluorescence images of neuronal markers (βIII-tubulin (βIII-tub), microtubule-associated protein 2 (MAP2) and neuronal nuclei antigen (NeuN) in undifferentiated and 7-day-differentiated LUHMES cells. DAPI-stained nuclei are also shown. Scale bar: 10 µm. (**D**) Western blot analysis of neural progenitor (nestin and SOX2) and neuronal (βIII-tub and MAP2 isoforms) marker levels in undifferentiated (D0) and 7-day-differentiated (D7) LUHMES cells. (**E**) Analysis of gene expression of proliferation (*MKI67*) and neuronal (synapsin I (*SYN1*), synaptophysin (*SYP*) and D2 dopamine receptor (*DRD2*)) markers by reverse transcription followed by quantitative PCR (RT-qPCR) in undifferentiated (D0) and 7-day differentiated cells (D7). Graph data show the mean ± standard error of the mean (SEM) of 5 independent experiments ($n = 5$) (one-sample *t*-test; * $p < 0.05$; ** $p < 0.01$; **** $p < 0.0001$).

2.2. LUHMES Cells Are Permissive to HSV-1 Infection in Both Proliferative and Differentiated States

To evaluate HSV-1 permissiveness in LUHMES cells, we first analyzed infection dynamics in proliferative cultures. In this undifferentiated state, LUHMES cells displayed a

https://doi.org/10.3390/ijms27020642

rounded morphology and exhibited a rapid lytic response upon HSV-1 exposure, characterized by progressive cell detachment and cytopathic effects visible at 18 h post-infection (hpi) (Supplementary Figure S1A). Western blot analysis confirmed the expression of HSV-1 proteins representative of distinct kinetic classes, including the immediate early protein ICP4, the early protein ICP8, and the true-late glycoprotein gC, all of which increased in a viral dose-dependent manner (Figure 2A). To assess the extent of infection, immunofluorescence analysis using an anti-gC antibody was performed, revealing a dose-dependent increase in the proportion of infected cells. At a multiplicity of infection (MOI) of 3 for 18 h, nearly all cells (>90%) displayed strong gC immunoreactivity (Figure 2B). qPCR further demonstrated a dose-dependent increase in HSV-1 DNA copy number (Figure 2C), consistent with active viral genome replication. Finally, viral titer assays confirmed the release of infectious viral particles into the culture supernatants, indicating that LUHMES progenitor cells efficiently support productive lytic replication of HSV-1 (Figure 2D).

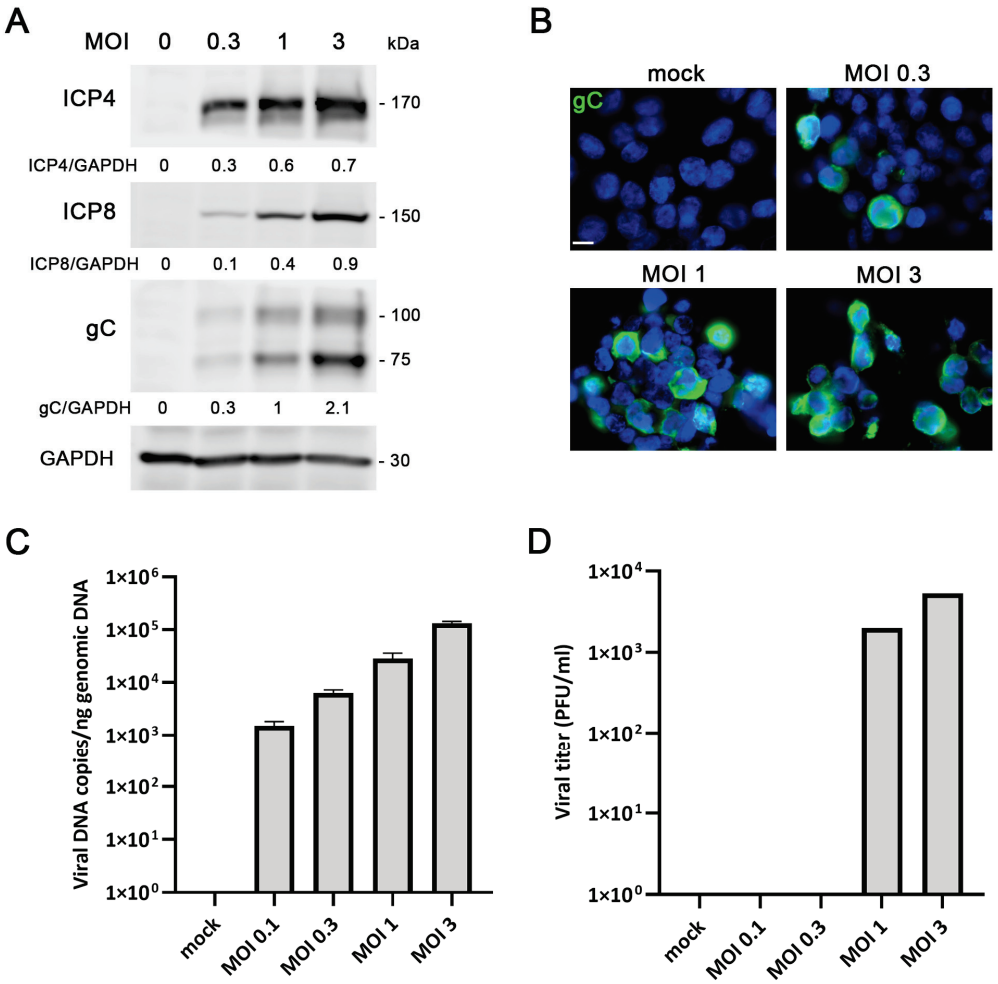


Figure 2. Characterization of Herpes simplex virus type 1 (HSV-1) infection in proliferative LUHMES cells in 2D cultures. (**A**–**D**) Proliferative LUHMES cells were uninfected (mock) or infected with HSV-1 at different multiplicities of infection (MOI) for 18 h (hpi), and the infection efficiency was monitored. (**A**) Analysis of ICP4, ICP8 and gC viral protein levels by Western blot. A GAPDH blot to ensure equal loading is also shown. The ratio of viral proteins to GAPDH of a representative experiment, obtained by densitometry analysis, is shown below the blots. (**B**) Immunofluorescence images of gC viral protein. Cell nuclei were stained with DAPI. Scale bar: 10 µm. (**C**) Viral DNA levels were determined by qPCR. The graph shows the data of a representative experiment (mean + standard deviation (SD) of technical replicates). (**D**) Extracellular viral titers were determined by plaque assays. The graph shows the data of a representative experiment (PFU: plaque-forming units).

https://doi.org/10.3390/ijms27020642

To characterize HSV-1 infection in LUHMES neurons, cultures were differentiated for 7 days prior to viral exposure. At 24 hpi, neurons began to exhibit cytopathic effects, including initial signs of neurite fragmentation. By 48 hpi, neurons had lost their characteristic branched morphology, appeared rounded, and started to detach from the culture surface (Supplementary Figure S1B). Western blot analysis demonstrated the expression of HSV-1 proteins corresponding to distinct kinetic phases—ICP4 (immediate-early) and gC (late)—in differentiated neurons at 24 hpi and 48 hpi, showing a clear dependence on viral dose and infection time (Figure 3A). Consistently, immunofluorescence revealed nuclear localization of ICP4 and prominent staining of viral glycoproteins gB and gD at 24 and 48 hpi. At MOI 1, about 50% of cells expressed viral proteins, increasing to over 90% at MOI 3 (Figure 3B). qPCR confirmed active viral genome replication (Figure 3C), and titer assays detected the release of infectious particles into the culture supernatant (Figure 3D). Notably, viral yields were lower, and the appearance of extracellular virus was delayed compared with proliferative LUHMES cultures.

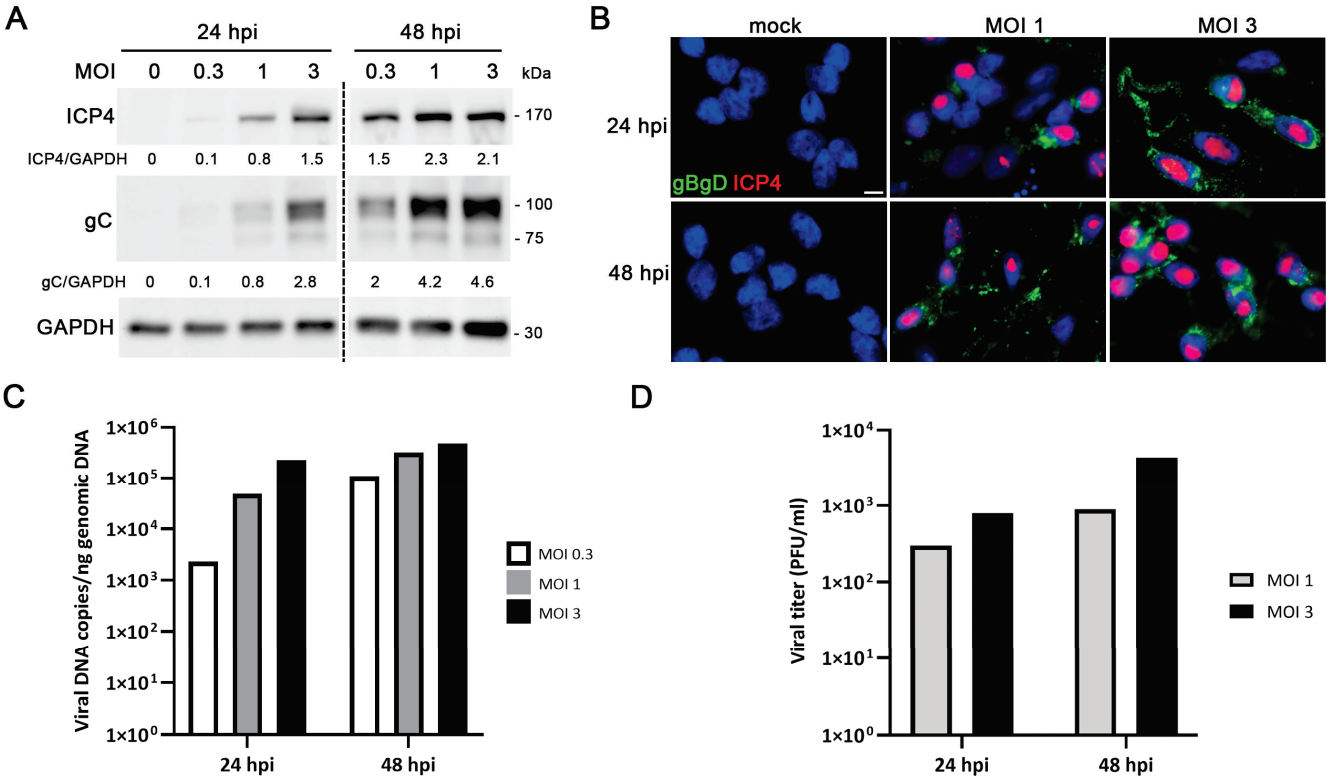


Figure 3. Characterization of HSV-1 infection in differentiated LUHMES neurons in 2D cultures. (**A**–**D**) LUHMES neurons differentiated for 7 days were infected with HSV-1 at different MOI for 24 and 48 h, and the infection efficiency was evaluated. (**A**) Western blot analysis of ICP4 and gC levels. A GAPDH blot to ensure equal loading is also shown. The ratio of viral proteins to GAPDH of a representative experiment is shown below the blots. (**B**) Immunofluorescence analysis using antibodies that recognize ICP4 and glycoproteins B and D. Cell nuclei were stained with DAPI. Scale bar: 10 µm. (**C**) Quantification of viral DNA levels using qPCR. The graph shows the data of a representative experiment. (**D**) Extracellular viral titers were quantified by plaque assays. The graph shows the data of a representative experiment.

Together, these findings demonstrate that LUHMES cells are permissive to HSV-1 infection in both proliferative and post-mitotic neuronal states. In addition, we selected 18 hpi for proliferative LUHMES cells and 24 hpi for differentiated neurons, as these time points yielded robust and reproducible detection of viral DNA and proteins while still

https://doi.org/10.3390/ijms27020642

preserving sufficient cellular integrity for quantitative analyses. Likewise, a MOI of 3 was chosen because it provided homogeneous infection in both proliferative and differentiated cultures without inducing excessive cytotoxicity. Overall, these parameters were identified as the optimal conditions for reliably assessing HSV-1–induced AD-related molecular alterations (Aβ accumulation, tau phosphorylation and autophagy–lysosome dysfunction) in the LUHMES model.

2.3. HSV-1 Induces AD-Related Molecular Markers in LUHMES Cells

Accumulation of Aβ peptides, which aggregate to form senile plaques, represents a major hallmark of AD. HSV-1 infection has been shown to promote intracellular Aβ accumulation by disrupting the non-amyloidogenic amyloid precursor protein (APP) processing pathway and reducing the secretion of Aβ peptides [16]. LUHMES cells have been reported to express endogenous APP [33,34]. We confirmed APP expression in LUHMES cells by Western blot analysis (Supplementary Figure S2A). To evaluate whether HSV-1 infection modulates Aβ levels in proliferative LUHMES cells, immunofluorescence analysis was performed. In uninfected cultures (mock), no intracellular Aβ was detected with any of the anti-Aβ antibodies tested. In contrast, following HSV-1 exposure, a pronounced accumulation of Aβ was observed, as revealed by immunolabeling with Aβ40- and Aβ42-specific antibodies (Figure 4A). The extracellular Aβ content in the conditioned media of LUHMES cells was subsequently quantified by ELISA assays. A viral dose-dependent reduction in secreted Aβ40 and Aβ42 levels was observed in HSV-1-infected cultures relative to mock-infected cultures (Figure 4B). In mock-infected cultures, Aβ40 and Aβ42 peptides are efficiently secreted, which may explain why their intracellular levels remain below the detection threshold of our immunofluorescence settings. Overall, these findings suggest that HSV-1 infection impairs Aβ secretion, thereby promoting intracellular Aβ accumulation in proliferative LUHMES cells.

Tau, a microtubule-associated protein, undergoes hyperphosphorylation in AD, leading to the formation of NFTs, another defining neuropathological feature of the disease. To assess whether HSV-1 infection affects tau phosphorylation in proliferative LUHMES cells, immunofluorescence assays were carried out using antibodies recognizing tau phosphorylated at residues Thr205 and Ser422, both of which are typically associated with NFTs. In non-infected cells, no phosphorylated tau was detected. Upon HSV-1 infection, strong accumulation of phosphorylated tau was evident at 18 hpi (Figure 4C). Western blot analysis further confirmed a significant increase in tau phosphorylation at epitopes Ser202 and Thr231, which are also present in NFTs (Figure 4D).

To determine whether the effects of HSV-1 observed in proliferative LUHMES cells were also present in mature neuronal cultures, LUHMES cells were differentiated to obtain post-mitotic neurons and subsequently infected with HSV-1. Similar to what was observed in proliferative LUHMES cells, HSV-1 infection induced a marked intracellular accumulation of Aβ in differentiated neurons. In mock-infected cultures, Aβ immunoreactivity was virtually absent, whereas HSV-1–infected neurons displayed a strong intracellular Aβ signal detected with antibodies specific to both Aβ40 and Aβ42 (Figure 5A). Consistent with these observations, ELISA quantification of conditioned media revealed a significant, dose-dependent reduction in secreted Aβ40 levels in HSV-1–infected neuronal cultures compared with non-infected controls. Although the decrease in secreted Aβ42 levels did not reach statistical significance, a clear downward trend was observed (Figure 5B). These results indicate that viral infection compromises Aβ secretion, leading to its intracellular retention in LUHMES neurons.

https://doi.org/10.3390/ijms27020642

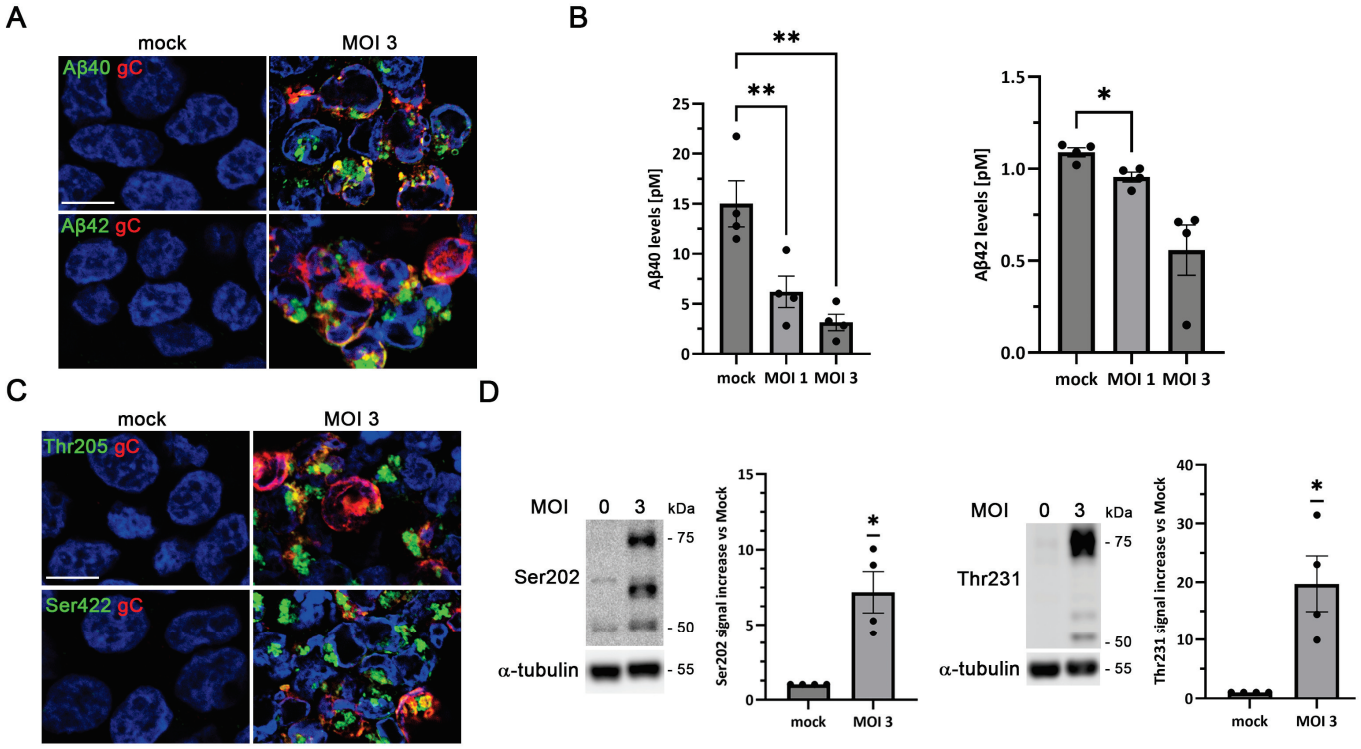


Figure 4. HSV-1 infection induces Alzheimer's disease (AD)-like markers in proliferative LUHMES cells. (**A**–**D**) Proliferative LUHMES cells were infected with HSV-1 at MOI 1 or 3 for 18 h, and the beta-amyloid (Aβ) and phosphorylated tau levels were assessed. (**A**) Immunofluorescence analysis of Aβ40 and Aβ42 in HSV-1–infected and control cultures. Infection was monitored by gC staining. DAPI-stained nuclei are also shown. Scale bar: 10 µm. (**B**) Quantification of extracellular Aβ40 and Aβ42 by ELISA. The graph data represent the mean ± SEM of 4 independent experiments ($n = 4$; One-way ANOVA and Dunnett's test; * $p < 0.05$; ** $p < 0.01$). (**C**) Immunostaining of phosphorylated tau using the phosphorylation-sensitive antibodies Thr205 and Ser422. Infection was monitored by gC staining. DAPI-stained nuclei are also shown. Scale bar: 10 µm. (**D**) Western blot analysis of phosphorylated tau (Ser202 and Thr231) levels. α-Tubulin was used as a loading control. The graph data represent the mean ± SEM of ratios of phosphorylated tau to α-tubulin obtained by densitometry analysis ($n = 4$; one-sample *t*-test; * $p < 0.05$).

We next examined whether HSV-1 infection alters tau phosphorylation in these neuronal cultures. Immunofluorescence analysis revealed that, in control neurons, phosphorylated tau (Thr205 and Ser422) was barely detectable. In contrast, infected neurons exhibited widespread phospho-tau staining throughout the soma and neuritic processes at 24 hpi (Figure 5C). Western blot analysis further confirmed a significant increase in tau phosphorylation at the Ser202 and Thr231 epitopes in HSV-1-infected neuronal cultures (Figure 5D). In contrast to the increase in phospho-tau levels, HSV-1 infection induced a reduction in total tau protein levels in both undifferentiated cells and differentiated LUHMES neurons (Supplementary Figure S2B). This decrease is consistent with the global host protein shutoff associated with lytic HSV-1 infection and indicates that the increase in phospho-tau signal is not merely a consequence of elevated total tau levels, but rather reflects a genuine increase in tau phosphorylation. Finally, to exclude the possibility that the detected phospho-tau signals corresponded to viral proteins, we performed a control Western blot in which only the viral preparation was loaded (Supplementary Figure S2C). Under these conditions, no bands corresponding to phospho-tau epitopes (Ser202 or Thr231) were detected, confirming the specificity of the antibodies used.

https://doi.org/10.3390/ijms27020642

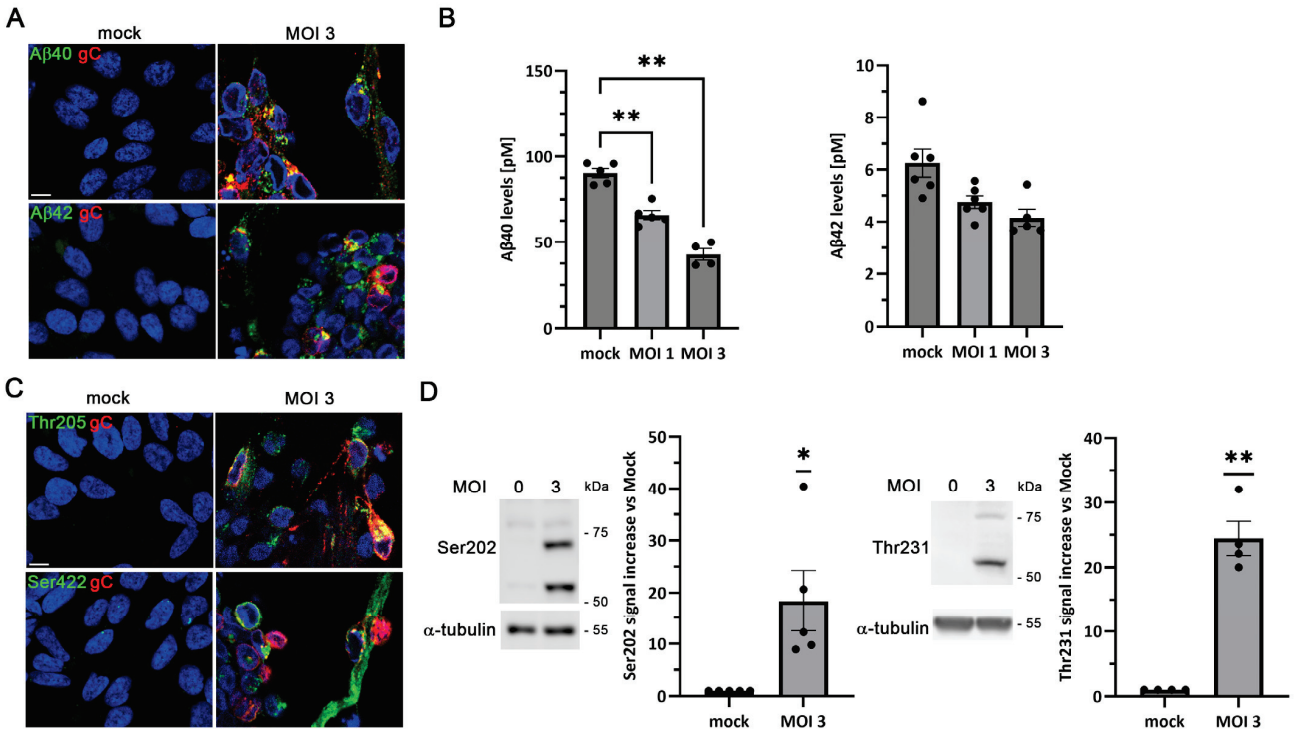


Figure 5. HSV-1 infection induces AD-like markers in LUHMES neurons. (**A**–**D**) 7-day-differentiated LUHMES cells were infected with HSV-1 at MOI 1 or 3 for 24 h, and the Aβ and phosphorylated tau levels were monitored. (**A**) Immunofluorescence staining of Aβ40 and Aβ42. Infection was monitored by gC staining. DAPI-stained nuclei are also shown. Scale bar: 10 µm. (**B**) Quantitative analysis of secreted Aβ40 and Aβ42 levels in conditioned medium by ELISA assays. The graph data represent the mean ± SEM of 5 (Aβ40) or 6 (Aβ42) independent experiments ($n = 5$ or $n = 6$; Mixed-effects model and Dunnett's test; ** $p < 0.01$). (**C**) Tau phosphorylated levels were assessed by immunofluorescence using the phosphorylation-sensitive antibodies Thr205 and Ser422. Infected cells were stained with a gC antibody. DAPI-stained nuclei are also shown. Scale bar: 10 µm. (**D**) Analysis of phosphorylated tau levels by Western blot using antibodies specific for the phosphorylated epitopes Ser202 and Thr231. α-Tubulin was used as a loading control. The graph data represent the mean ± SEM of ratios of phosphorylated tau to α-tubulin obtained by densitometry analysis ($n = 5$; one-sample *t*-test; * $p < 0.05$, ** $p < 0.01$).

Collectively, these results demonstrate that HSV-1 infection recapitulates hallmark AD-like pathological features—intracellular Aβ accumulation and tau hyperphosphorylation—not only in proliferative LUHMES cells but also in differentiated LUHMES-derived neurons. These findings underscore the capacity of HSV-1 to alter the metabolism of amyloid peptides and the phosphorylation of tau protein across different stages of neuronal maturation, thereby strengthening the potential of this human neuronal model for investigating the pathogenic link between viral infection and AD-related alterations.

2.4. HSV-1 Alters Markers of the Autophagy–Lysosome Pathway in LUHMES Cells

Another neuropathological mechanism associated with AD and reported to be affected by HSV-1 infection involves the dysfunction of the autophagy–lysosome pathway. Among numerous lines of evidence supporting this relationship, we have reported alterations in this axis in human neuroblastoma cells [35]. During autophagy activation, the cytosolic form of LC3 (LC3-I) undergoes lipidation to form LC3-II, which binds to autophagic membranes and remains associated with autophagosomes throughout their maturation. To determine whether HSV-1 alters this pathway in LUHMES cells, we first analyzed LC3 expression levels and distribution in proliferative cultures. Immunofluorescence analysis

https://doi.org/10.3390/ijms27020642

revealed a marked accumulation of LC3 in HSV-1-infected cells, whereas LC3 staining was nearly undetectable in mock-infected cultures (Figure 6A). The punctate LC3 staining pattern was consistent with the accumulation of autophagosomes. Western blot analysis corroborated these observations, showing a viral dose-dependent increase in LC3-II levels (Figure 6B).

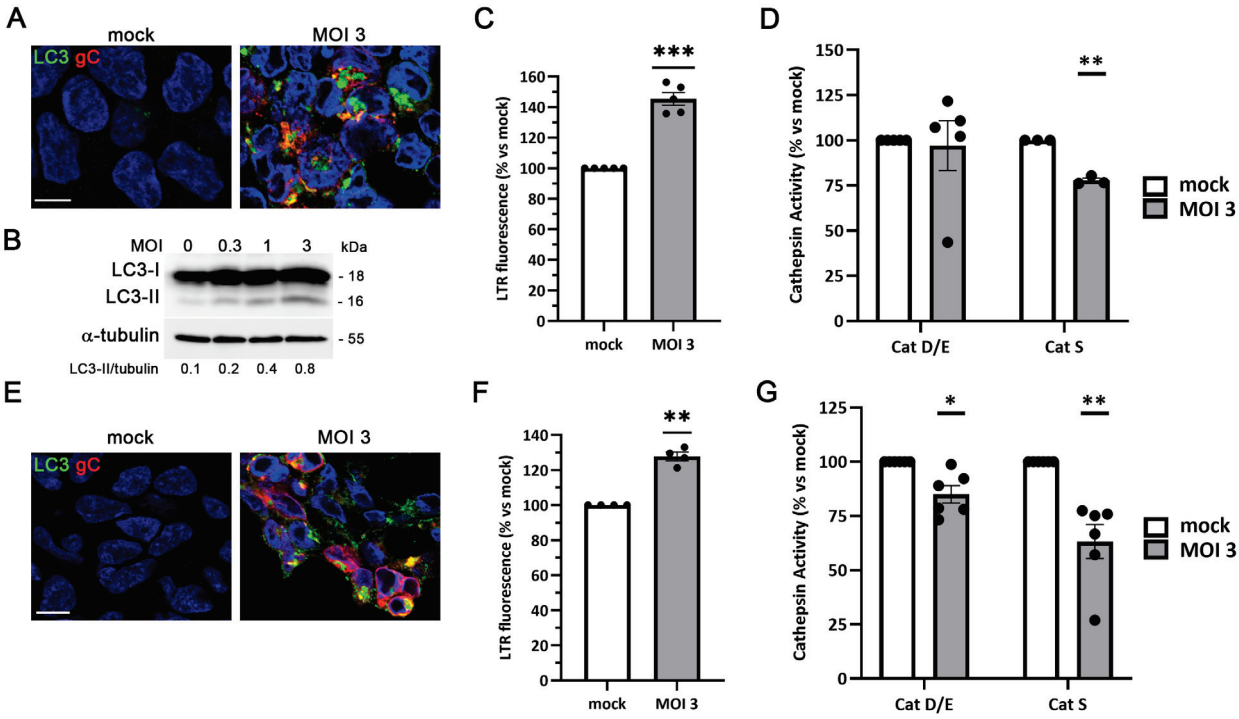


Figure 6. Lysosomal alterations induced by HSV-1 in proliferative and differentiated LUHMES cells. (**A**–**D**) LUHMES proliferative cells were infected with HSV-1 at different MOI for 18 h. (**A**) Immunofluorescence images of intracellular LC3 accumulation in infected cells (MOI 3) are shown. Infection was monitored by gC staining. DAPI-stained nuclei are also shown. Scale bar: 10 µm. (**B**) Western blot analysis of LC3 in LUHMES cell lysates after HSV-1 infection at different viral doses. An α-tubulin blot to ensure equal loading is also shown. The ratio of LC3-II to tubulin of a representative experiment, obtained by densitometric analysis, is shown below the blots. (**C**) Analysis of lysosomal load by quantification of the LysoTracker Red (LTR) fluorescence in LUHMES cells infected with HSV-1 at MOI 3. The graph data show the mean ± SEM of 5 independent experiments ($n = 5$; one-sample *t*-test; *** $p < 0.001$). (**D**) The relative enzymatic activities of cathepsins D/E and S were quantified in LUHMES cells after HSV-1 infection (MOI 3). Graph data show the mean ± SEM of 3 (Cat S) or 5 (Cat D/E) independent experiments ($n = 3$ or $n = 5$; one-sample *t*-test; ** $p < 0.01$). (**E**–**G**) LUHMES neurons, differentiated for 7 days, were infected with HSV-1 at an MOI of 3 for 24 h, and lysosomal alterations were analyzed. (**E**) Immunofluorescence images of intracellular LC3. Infection was monitored with an antibody specific for gC. Cell nuclei were stained with DAPI. Scale bar: 10 µm. (**F**) Lysosomal load was determined by quantifying LTR fluorescence. The graph data show the mean ± SEM of 4 independent experiments ($n = 4$; one-sample *t*-test; ** $p < 0.01$). (**G**) Lysosomal activity of cathepsins D/E and S was measured. The graph data show the mean ± SEM of 6 independent experiments ($n = 6$; one-sample *t*-test; * $p < 0.05$, ** $p < 0.01$).

To further explore the effects of HSV-1 on lysosomal integrity and function, we evaluated the lysosomal load using the lysosomotropic dye LysoTracker Red (LTR), as well as the enzymatic activity of several lysosomal hydrolases (cathepsins D/E and S). LTR fluorescence intensity was significantly higher in HSV-1–infected LUHMES cultures than in non-infected controls, reflecting an increased lysosomal burden upon infection (Figure 6C). Moreover, while cathepsin D/E activity was not affected by infection, the activity of lysoso-

https://doi.org/10.3390/ijms27020642

mal cathepsin S was significantly reduced in HSV-1–infected LUHMES cells (Figure 6D), suggesting a defect in lysosomal proteolytic function. Together, these data indicate that HSV-1 disrupts the autophagy–lysosome pathway in proliferative LUHMES cells, suggesting altered autophagic processing and lysosomal degradation, although additional flux-specific assays would be required to definitively distinguish enhanced autophagy induction from impaired clearance.

We next investigated whether similar alterations occurred in LUHMES cells differentiated into mature neurons. Immunofluorescence analysis revealed an accumulation of LC3 in HSV-1-infected neurons (Figure 6E), consistent with an accumulation of autophagosomes as observed in proliferative LUHMES cells. In contrast to mock-infected controls, differentiated neurons exposed to HSV-1 exhibited a pronounced increase in LTR fluorescence intensity (Figure 6F), indicating that viral infection also enhances lysosomal content in mature neuronal cultures. Furthermore, lysosomal enzymatic activity measured using fluorogenic substrates for cathepsins D, E, and S showed a significant decrease in all tested enzymes in infected neuronal cultures (Figure 6G). These results indicate that HSV-1 infection compromises both the autophagic process and lysosomal proteolytic activity in LUHMES-derived neurons.

Together, these findings suggest that HSV-1-induced alterations of the autophagy and lysosome machineries may represent a relevant mechanism underlying the appearance of AD-related markers in the infected neurons.

2.5. Development of a 3D Neuronal Model Using Differentiated LUHMES Cells

Building on these findings, we next sought to determine whether HSV-1 infection induces similar AD-like alterations within a more structured 3D neuronal environment. To this end, we first generated and optimized LUHMES-based 3D neuronal cultures. Following a previously described protocol for the establishment of 3D LUHMES neuronal cultures [26], we adapted and refined the procedure to fit our experimental conditions (Figure 7A). Briefly, LUHMES cells were seeded in low-adhesion plates containing differentiation medium and maintained under constant orbital agitation. Under these conditions, the cells spontaneously aggregated into free-floating spherical structures (Figure 7B). To ensure appropriate oxygen and nutrient diffusion and to prevent the formation of necrotic cores, the aggregate diameter was kept below 350 μm. Continuous monitoring of cultures up to day 14 of differentiation revealed stable aggregate morphology, with an average diameter of approximately 300 μm (Figure 7C).

To assess the proliferation rate within 3D LUHMES cultures, we analyzed the expression of Ki-67, a well-established proliferation marker, in undifferentiated cells and at 4, 7, 10, and 14 days of differentiation. Immunofluorescence analysis revealed a clear Ki-67 signal at day 4, with Ki-67–positive cells distributed throughout the aggregates, indicating the presence of actively dividing cells. As differentiation progressed, the number of Ki-67-positive cells markedly decreased and became nearly undetectable by day 10 (Figure 7D), consistent with a progressive inhibition of proliferation during neuronal maturation.

To further characterize the differentiation status of the 3D LUHMES cultures, RT-qPCR analysis was performed to quantify the expression of neuronal and progenitor markers throughout the differentiation process. The expression levels of the proliferation marker gene *MKI67* and the neuronal genes *DRD2*, *SYN1*, and *SYP* were analyzed relative to those in undifferentiated cells. Consistent with the immunofluorescence data, Ki-67 mRNA levels progressively declined during differentiation, indicating the loss of proliferative and progenitor features. In contrast, neuronal markers were upregulated, reflecting the acquisition of a mature neuronal phenotype. By day 14 of differentiation, expression of neuronal genes reached maximal levels, while *MKI67* expression was strongly downregulated (Figure 7E).

https://doi.org/10.3390/ijms27020642

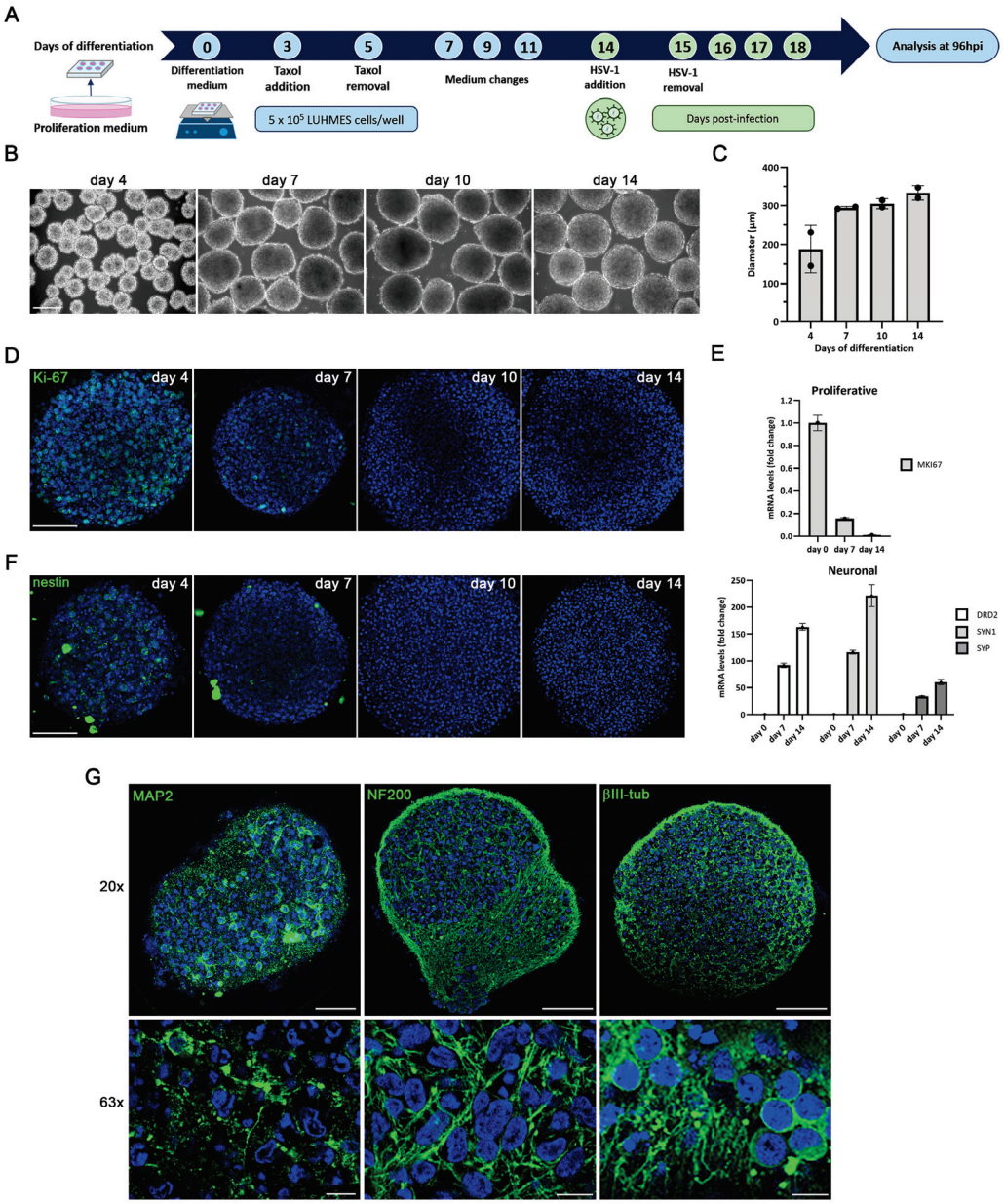


Figure 7. Characterization of three-dimensional (3D) LUHMES neuronal cultures. (**A**) The two-dimensional (2D) differentiation protocol was adapted for 3D culture by maintaining the single-cell suspension under continuous gyratory shaking. The infection with HSV-1-UL46-GFP was added at day 14 of differentiation, and 3D aggregates were processed at 96 hpi. (**B**) Phase-contrast microscopy images of 3D LUHMES neuronal cultures at different days of differentiation. Scale bar: 200 µm. (**C**) Quantification of the diameter of 3D aggregates at days 4, 7, 10 and 14 of differentiation. The graph shows the mean ± SD of the diameter of at least 50 3D aggregates per condition. (**D**) Immunofluorescence analysis of 3D neuronal cultures showing Ki-67–positive cells at differentiation days 4, 7, 10, and 14. DAPI-stained nuclei are also shown. Scale bar: 100 µm. (**E**) Analysis of gene expression of progenitor (*MKI67*) and neuronal (*DRD2*, *SYN1* and *SYP*) genes by RT-qPCR in undifferentiated (day 0) and 7 and 14-day LUHMES differentiated cells. Graph data show the mean ± SD of a representative experiment. (**F**) Immunofluorescence images of 3D LUHMES cultures at differentiation days 4, 7, 10 and 14, stained with an antibody against the neural progenitor cell marker nestin. Scale bar: 100 µm. (**G**) Immunofluorescence images showing neuronal markers (MAP2, neurofilament heavy chain (NF200), and βIII-tub) in 14-day differentiated 3D LUHMES cultures. Higher-magnification micrographs are also shown. Cell nuclei were stained with DAPI. Scale bars: 100 µm (20×) and 10 µm (63×).

https://doi.org/10.3390/ijms27020642

Consistent with these transcriptional data, immunofluorescence analysis further confirmed neuronal differentiation within 3D aggregates. Staining for the neural progenitor marker nestin revealed a marked reduction in its expression as differentiation progressed, indicating the loss of precursor characteristics (Figure 7F). In contrast, mature neuronal markers such as MAP2, neurofilament heavy chain (NF200), and βIII-tubulin showed strong and widespread expression throughout the aggregates, consistent with a well-established neuronal phenotype. High-magnification images highlighted extensive neuritic arborization and the presence of long, branching neurites characteristic of mature neurons, confirming the proper neuronal maturation achieved in the 3D cultures (Figure 7G).

These findings demonstrate that by day 14, LUHMES cells within 3D aggregates acquire a mature neuronal phenotype characterized by increased neuronal gene expression, extensive neurite formation, and an almost complete loss of proliferative markers.

2.6. Development of a 3D LUHMES-Based Model of HSV-1 Infection

One of the main objectives of this study was to establish a model of HSV-1 infection in 3D LUHMES neuronal cultures. To optimize infection conditions, we used a fluorescent HSV-1 strain expressing the tegument protein VP11/12—encoded by the UL46 gene—as a GFP fusion protein (UL46-GFP). 3D LUHMES cultures were initially infected with increasing doses of the UL46-GFP strain for 24 h, and infection efficiency was assessed by fluorescence microscopy. A dose-dependent increase in both the extent and intensity of GFP fluorescence within the 3D aggregates was observed, indicating the progressive spread of infection throughout the cultures (Figure 8A).

Subsequently, the expression of viral proteins representative of different stages of the viral replication cycle was quantified: ICP4 (an immediate-early gene), UL42 (a leaky late gene), and gC (a true late gene). Western blot analysis showed a dose-dependent increase in all three viral proteins, reaching a plateau at a viral dose of 5×10^6 plaque-forming units (PFU) (Figure 8B). To further confirm active viral replication, viral DNA levels were quantified by qPCR, demonstrating that the UL46-GFP strain replicates efficiently in 3D LUHMES neuronal cultures (Figure 8C). Taken together, these results confirm the susceptibility of 3D LUHMES cultures to HSV-1 infection and allowed the optimization of experimental parameters, establishing 5×10^6 PFU as the optimal viral dose for subsequent assays.

To further assess the ability of the virus to penetrate the 3D aggregates, confocal optical sections corresponding to the central regions of the spheroids were analyzed at different post-infection time points. Confocal microscopy images revealed that the viral signal became detectable in the inner layers of the aggregates at 18 hpi and progressively increased over time (Figure 8D). These observations confirm that HSV-1 efficiently spreads throughout the entire 3D structure, resulting in a homogeneous infection across the aggregates.

Finally, immunofluorescence assays were performed to confirm the expression and localization of viral proteins within 3D LUHMES aggregates after 96 h of infection. Confocal microscopy images showed the presence of ICP4 and the glycoproteins gB, gC and gD distributed throughout the aggregates. High-magnification images revealed the characteristic nuclear localization of ICP4 within viral replication compartments, while gB, gC, and gD were detected predominantly in the cytoplasm (Figure 8E). These observations confirm that HSV-1 undergoes a complete and efficient infection in 3D LUHMES neuronal cultures.

Altogether, we determined that infection of 3D LUHMES aggregates with 5×10^6 PFU and analysis at 96 hpi provided the most consistent and homogeneous viral infection while preserving sufficient aggregate integrity to evaluate HSV-1–induced neurodegeneration-related markers. These parameters were therefore selected as the optimal conditions for the 3D model.

https://doi.org/10.3390/ijms27020642

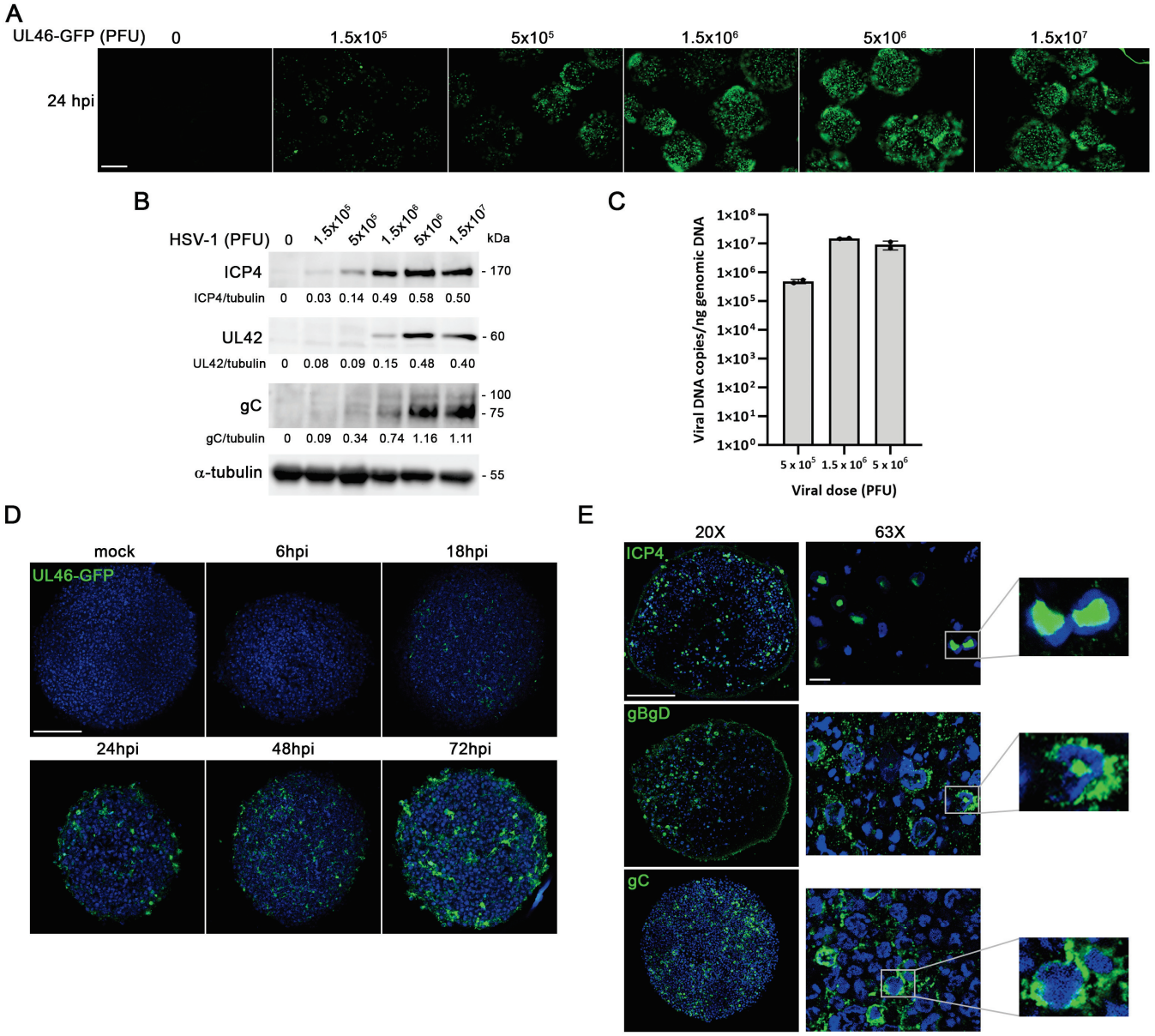


Figure 8. Analysis of HSV-1 infection in LUHMES neuronal aggregates. (**A**) Fluorescence microscopy images of LUHMES 3D cultures infected for 24 h with increasing doses of the fluorescent HSV-1 strain UL46-GFP. Scale bar: 200 µm. (**B**,**C**) LUHMES 3D neuronal cultures differentiated for 14 days were infected for 96 h with increasing doses of UL46-GFP strain. (**B**) Analysis of ICP4, UL42, and gC viral protein levels by Western blot. An α-tubulin blot to ensure equal loading is also shown. The ratio of viral proteins to α-tubulin of a representative experiment is shown below the blots. (**C**) Viral DNA levels were quantified by qPCR. Data represent the mean ± SD of a representative experiment. (**D**) 14 day-differentiated 3D LUHMES cultures were infected with 5×10^6 PFU of UL46-GFP strain for different time periods. Confocal microscopy images corresponding to the center of the 3D aggregates illustrate the time-dependent penetration of HSV-1 infection. Cell nuclei were stained with DAPI. Scale bar: 100 µm. (**E**) Immunofluorescence analysis using antibodies against ICP4 and viral glycoproteins B, D and C in 14-day-differentiated 3D LUHMES cultures infected with 5×10^6 PFU for 96 h. Higher-magnification images show the nuclear localization of ICP4 and the cytosolic distribution of viral glycoproteins. Cell nuclei were stained with DAPI. Scale bars: 100 µm (20×) and 10 µm (63×). In all panels, spheroids were optically cleared and imaged using confocal z-stacks. Panels show central optical sections.

https://doi.org/10.3390/ijms27020642

2.7. HSV-1 Triggers AD-like Alterations in 3D LUHMES Neuronal Cultures

Our next aim was to determine whether the pathological effects of HSV-1 observed in proliferative and differentiated 2D LUHMES cultures were recapitulated in 3D neuronal aggregates. To this end, we analyzed the accumulation and secretion of Aβ peptides, as well as the phosphorylation state of tau.

In non-infected 3D cultures, no detectable signal for Aβ or phosphorylated tau was observed. In contrast, HSV-1-infected cultures exhibited clear intracellular Aβ accumulation, as revealed by immunofluorescence using antibodies specific for Aβ40 and Aβ42. Higher magnification images showed that Aβ accumulation occurred in ICP4-positive cells, indicating its association with active viral infection (Figure 9A). ELISA quantification of extracellular Aβ confirmed a strong reduction in secreted Aβ40 and Aβ42 levels, which was statistically significant in the case of Aβ40 (Figure 9B). Furthermore, immunostaining with phospho-tau-specific antibodies revealed a robust accumulation of phosphorylated tau at Thr205 and Ser422 epitopes in infected neurons, forming a punctate cytoplasmic pattern similar to that previously described in 2D LUHMES cultures (Figure 9C). Consistently, Western blot analysis revealed a significant increase in tau phosphorylation at the Ser202 and Thr231 epitopes in HSV-1–infected 3D neuronal cultures (Figure 9D), further supporting the induction of AD-like pathological features by the virus.

To investigate whether the lysosomal dysfunction previously detected in 2D LUHMES neurons also occurs under 3D conditions, we examined markers of the autophagy–lysosome pathway in infected aggregates. Immunofluorescence analysis showed a pronounced accumulation of LC3 in infected neurons, suggesting altered autophagosome dynamics (Figure 9E). In parallel, a significant decrease in LTR fluorescence was detected, suggesting a loss of lysosomal acidity and/or reduced lysosomal quantity (Figure 9F). Consistent with these observations, the enzymatic activity of lysosomal cathepsins D, E and S was markedly decreased in infected 3D cultures compared with controls, indicating impaired proteolytic capacity (Figure 9G). Collectively, these findings demonstrate that HSV-1 infection disrupts lysosomal function in differentiated 3D LUHMES neurons, mirroring the alterations previously identified in 2D models and supporting a conserved mechanism of virus-induced lysosomal dysfunction.

In summary, the 3D LUHMES neuronal model faithfully recapitulates the AD-like neuropathological alterations induced by HSV-1, providing a useful human neuronal system to study HSV-1–induced AD-related molecular mechanisms. These data further strengthen the hypothesis that HSV-1 may act as an environmental factor contributing to AD pathogenesis by disrupting neuronal homeostasis and protein clearance mechanisms.

https://doi.org/10.3390/ijms27020642

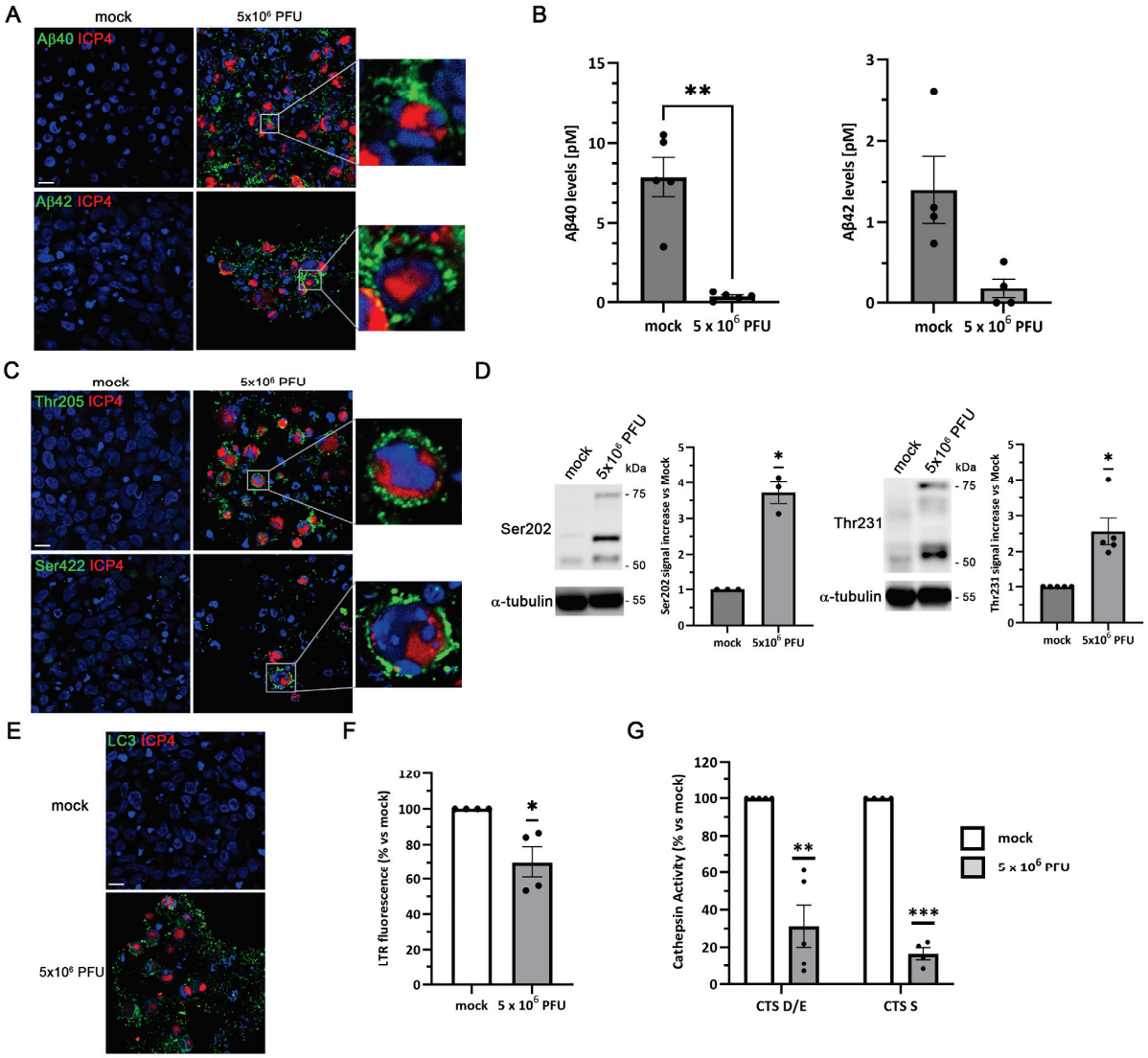


Figure 9. HSV-1 infection triggers Aβ accumulation, tau hyperphosphorylation, and lysosomal dysfunction in 3D LUHMES neuronal cultures. LUHMES 3D neuronal cultures were infected with 5×10^6 PFU of HSV-1 for 96 h, and Aβ levels, tau phosphorylation, and lysosomal alterations were assessed. (**A**) Immunofluorescence analysis of Aβ40 and Aβ42 accumulation in HSV-1–infected and control cultures. Infection was monitored by ICP4 staining. Higher-magnification images show Aβ staining in infected cells. Nuclei were counterstained with DAPI. Scale bar: 10 µm. (**B**) Quantification of extracellular Aβ40 and Aβ42 levels by ELISA. Data represent the mean ± SEM of 4 (Aβ42) or 5 (Aβ40) independent experiments ($n = 4$ or $n = 5$; Student's *t*-test; ** $p < 0.01$). (**C**) Immunostaining of phosphorylated tau using phosphorylation-sensitive antibodies Thr205 and Ser422. Infection was monitored by ICP4 staining. Higher-magnification images show phosphorylated tau staining in infected cells. Nuclei were counterstained with DAPI. Scale bar: 10 µm. (**D**) Western blot analysis of phosphorylated tau (Ser202 and Thr231) levels. An α-tubulin blot is shown as a loading control. The graph data represent the mean ± SEM of ratios of phosphorylated tau to α-tubulin obtained by densitometry analysis ($n = 3$ for Ser202 and $n = 5$ for Thr231; one-sample *t*-test; * $p < 0.05$). (**E**) Immunofluorescence images of intracellular LC3 accumulation. Infection was monitored with an antibody specific for ICP4. Cell nuclei were stained with DAPI. Scale bar: 10 µm. (**F**) Lysosomal load was determined by quantifying LTR fluorescence. The graph data show the mean ± SEM of 4 independent experiments ($n = 4$; one-sample *t*-test; * $p < 0.05$). (**G**) Enzymatic activity of cathepsins D/E and S was measured. The graph data show the mean ± SEM of 4 (Cat S) or 5 (Cat D/E) independent experiments ($n = 4$ or $n = 5$; one-sample *t*-test; ** $p < 0.01$; *** $p < 0.001$). In all immunofluorescence panels, spheroids were optically cleared and imaged using confocal z-stacks. Panels show central optical sections.

https://doi.org/10.3390/ijms27020642

3. Discussion

AD is the most common cause of dementia and represents an increasing global health challenge. Despite extensive research, the precise mechanisms underlying AD pathogenesis remain incompletely understood, and effective disease-modifying therapies are still lacking. The growing prevalence of AD highlights the urgent need for experimental models that more faithfully reproduce the complexity of the human disease and overcome the limitations of current research systems. The present study provides significant insights into the potential link between HSV-1 infection and AD-related molecular alterations, specifically emphasizing the value of LUHMES-derived neuronal models in understanding this relationship. Our results reinforce the growing body of evidence positioning HSV-1 as a meaningful environmental risk factor contributing to AD pathogenesis.

The LUHMES cell line, derived from human embryonic mesencephalic precursor cells, offers critical advantages for studying infection-associated neurodegeneration. These cells exhibit both proliferative and neuronal differentiation states [24], enabling the examination of infection from initial viral entry to mature neuronal dysfunction. Their stable and homogeneous differentiation into neuron-like cells under defined conditions provides high reproducibility—an essential feature for mechanistic dissection and pharmacological screening.

Despite dopaminergic neurons have been extensively studied in the context of other neurodegenerative diseases, such as Parkinson's disease, alterations in dopaminergic midbrain have recently gained interest for AD research [36]. Moreover, the trigeminal ganglia—one of the entry paths to the CNS proposed for HSV-1—is also connected to the brainstem, suggesting a plausible way for the virus to access and impair the dopaminergic system. In fact, a recent study investigated the spatial pattern of HSV-1 infection in mice, and reported the presence of viral antigens in different brain regions, including brainstem's neuromodulatory centers [37]. Thus, dopaminergic nature of LUHMES neurons seems also adequate to assess the role of HSV-1 in AD.

Another major strength of the LUHMES model is its adaptability to both 2D and 3D culture systems [26]. While 2D cultures facilitate high-throughput exploration of viral and host responses, 3D cultures more closely reproduce the spatial organization, cell–cell communication, and cell-matrix interactions that take place in the human brain. Nevertheless, these platforms still lack other components that are essential for modelling brain pathophysiology, such as glial cells, which are involved in neuroinflammation. In this regard, we are currently working with neuro-glial models of HSV-1 infection and neurodegeneration [38], which could provide a complementary view to the tools presented in this work.

The LUHMES neuronal model also provides an effective human platform for studying how neurotropic viruses disrupt neuronal homeostasis. Previous studies have demonstrated that LUHMES neurons can be efficiently infected by HSV-1, supporting both lytic and latent infection modes in 2D systems [31,39]. Beyond HSV-1, LUHMES progenitors and differentiated neurons are also permissive to other neurotropic viruses, including hemorrhagic fever and Zika viruses [30], further validating the model's versatility for studying virus–neuron interactions.

One of the main goals of this study was to establish a model of lytic HSV-1 infection in 3D LUHMES neuronal cultures. Using an orbital shaking-based method originally developed for human induced pluripotent stem cells (iPSCs)-derived neurons [26,40], we generated uniform spheroidal aggregates that mimic key features of neuronal architecture. The results obtained from the evaluation of various viral parameters demonstrated the ability of HSV-1 to efficiently infect different types of LUHMES cultures, including both 2D proliferative and differentiated cells, as well as 3D neuronal aggregates. First, a dose-

https://doi.org/10.3390/ijms27020642

dependent increase in the expression of viral proteins was observed. Since these proteins are expressed at distinct stages of the viral replication cycle (ICP4 is an α gene expressed at the immediate-early stage; gB is a β gene expressed during the early phase; and gC and gD are "true late" γ2 genes whose expression strictly depends on viral DNA replication), these findings suggest that the virus is capable of completing its full replication cycle in 3D aggregates. Second, qPCR analysis revealed the presence of HSV-1 DNA in the 3D neuronal cultures, confirming the replicative capacity of the virus. Finally, immunofluorescence assays detected the expression of ICP4 and the viral glycoproteins gC and gB/gD throughout the entire 3D aggregates. Collectively, these data demonstrate the ability of HSV-1 to efficiently infect and replicate in 3D cultures of LUHMES-derived neurons, underscoring the model's potential for studying virus–induced neurodegeneration.

We further show that HSV-1 infection elicits hallmark AD-like alterations in proliferative and differentiated LUHMES cells across both 2D and 3D culture systems, including intracellular Aβ accumulation and robust tau hyperphosphorylation. These findings extend our previous observations in other neuronal cell systems [16,17,38,41], and strengthen the concept that HSV-1 can simultaneously disrupt Aβ metabolism and tau regulation—two central drivers of AD pathology. These observations are consistent with epidemiological studies and neuropathological analyses identifying HSV-1 DNA in brain regions significantly affected by AD [15,42]. The accumulation of Aβ peptides accompanied by a reduction in their extracellular secretion, suggests that HSV-1 interferes with the proteolytic processing of APP, potentially through the modulation of α-, β- and γ-secretase activity. The inhibition of Aβ secretion could underlie the intracellular accumulation of Aβ induced by HSV-1, as observed in other cellular models of infection [16]. Given the proposed antimicrobial function of Aβ [43], this buildup may initially reflect an innate antiviral response that, if chronically activated, could contribute to neurotoxicity and plaque formation.

In parallel, the marked increase in tau phosphorylation at multiple AD-related epitopes (Ser202, Thr205, Thr231, and Ser422) highlights the ability of HSV-1 to disturb tau homeostasis. This extensive pattern of hyperphosphorylation suggests broad dysregulation of kinase activity, and is compatible with the involvement of several tau-related kinases described in the literature (e.g., GSK3β, CDK5, p38 MAPK) [44]. However, because kinase activation was not directly assessed in this study, the contribution of specific signaling pathways remains hypothetical and will require further investigation. Notably, our group previously demonstrated that inhibitors of several CDKs were able to reverse tau phosphorylation at Ser396, Ser404, and Ser409 epitopes in an HSV-1 infection model using the human neuroblastoma cell line SK-N-MC [17], further supporting the involvement of CDK-related pathways in HSV-1–induced tau dysregulation. Similar phosphorylation profiles in both proliferative and differentiated LUHMES cells indicate that this disruption is independent of maturation stage, reflecting a generalized perturbation of tau regulation by HSV-1.

Beyond classical neuropathological markers, our results reveal HSV-1-induced impairment of autophagy–lysosome function, evidenced by LC3-II accumulation, impaired lysosomal burden, and reduced cathepsin activity. These data are consistent with a possible alteration in autophagosome maturation and/or lysosomal acidification/enzymatic function, although LC3-II accumulation alone cannot distinguish impaired clearance from enhanced initiation of autophagy. Because autophagic flux was not directly measured in this study, interpretations regarding impaired autophagosome clearance must be made with caution. The combination of LC3-II accumulation, reduced cathepsin activity and altered lysosomal markers suggests lysosomal dysfunction, but does not by itself establish a definitive block in autophagic flux. Consistent with this, our group previously reported that HSV-1 infection in human neuroblastoma cells leads to inhibition of late stages of the autophagic process and profound dysfunction of the lysosomal pathway, reinforcing the

https://doi.org/10.3390/ijms27020642

notion that this virus profoundly interferes with cellular degradative systems [35,41]. Such alterations are known to occur early in AD and provide a mechanistic link between defective proteostasis, Aβ accumulation, and tau dysregulation [20]. Thus, HSV-1 may not only mimic but also accelerate the neurodegenerative cascade through sustained impairment of cellular clearance pathways.

Taken together, our findings demonstrate that HSV-1 can reproduce core AD-like pathological signatures across different stages of neuronal differentiation. The ability of the virus to modulate both APP processing and tau phosphorylation highlights its potential role as a multifactorial driver of neurodegeneration. These data support the growing body of evidence linking latent or recurrent HSV-1 infection to the molecular events underlying sporadic AD [45–47]. Further investigation using 3D LUHMES-based cultures and single-cell transcriptomic approaches will help elucidate the cellular pathways and signaling networks through which HSV-1 contributes to neurodegenerative processes in the human brain. It is important to note that this study is based on an acute, high-dose lytic infection paradigm, which does not replicate the chronic, latent, or intermittently reactivating HSV-1 infection scenario proposed to contribute to AD over decades. Therefore, the alterations described here should be interpreted as acute neuronal responses to lytic infection, and their long-term relevance to latent or recurrent HSV-1 infection will require further investigation.

To date, only a few studies have employed LUHMES cells to investigate HSV-1 infection, and most of these have focused on establishing and characterizing latent infection in conventional 2D cultures [31,32,39]. Consequently, the effects of productive HSV-1 infection and its impact on neuronal integrity, protein homeostasis, and AD-like pathological hallmarks have not been explored. Although several 3D models of HSV-1 infection have been previously reported in different human neuronal systems [48–50], to our knowledge, this work reports for the first time the establishment of a 3D LUHMES model of HSV-1 infection, which recapitulates major AD-related features in a human neuronal context. This represents a step forward in modelling HSV-1-induced neurodegenerative mechanisms in a controlled human neuronal system. A priority for future work in our group is to expand this system to model HSV-1 latency and reactivation. HSV-1 latency has been successfully established in 2D LUHMES neuronal cultures [31]. Although a few studies have described latent HSV-1 infection in 3D brain organoids derived from human iPSCs [49,51], these models often display high complexity and heterogeneity, which may limit mechanistic analyses. To our knowledge, no 3D model of latent HSV-1 infection has yet been developed using LUHMES-derived neurons, to investigate the latent state or to evaluate how reactivation contributes to neuronal dysfunction and neurodegeneration. The implementation of such a 3D latency model would represent a valuable tool for elucidating the molecular mechanisms by which HSV-1 persistence leads to progressive neuronal damage and AD-related pathology.

In conclusion, our study underscores the potential of LUHMES-derived neuronal models as a translational platform to elucidate the interplay between HSV-1 infection and AD pathology. The ability to simulate key neuropathological features of AD in response to HSV-1 infection within these human-derived neuronal cells provides a powerful framework for future research. Ultimately, insights derived from these models may significantly advance our understanding of virus-induced neurodegeneration, uncover potential therapeutic targets, and guide the development of effective interventions to mitigate HSV-1-associated neurodegenerative processes.

Limitations of the Study

While this study establishes LUHMES cells as a robust human neuronal platform to investigate HSV-1–induced AD-related molecular alterations, several limitations should be acknowledged.

https://doi.org/10.3390/ijms27020642

First, although LUHMES cells differentiate into homogeneous populations of post-mitotic human neurons, they are of mesencephalic dopaminergic origin and therefore do not fully recapitulate the cortical or hippocampal neuronal subtypes primarily affected in AD. Nevertheless, increasing evidence supports a role for dopaminergic midbrain alterations in disease development, and the trigeminal ganglia—one of the proposed HSV-1 entry routes into the central nervous system—are connected to the brainstem, providing a plausible pathway for viral access to dopaminergic circuits. In addition, the LUHMES model lacks other central nervous system cell types, including astrocytes, microglia, oligodendrocytes, vascular and immune cells, which are known to modulate neurodegenerative processes in vivo. Consequently, this system does not aim to reproduce full brain complexity but rather offers a reductionist neuronal framework to study virus-induced molecular alterations under controlled conditions.

Second, the experimental paradigm employed relies on acute lytic HSV-1 infection, whereas the epidemiological association between HSV-1 and Alzheimer's disease is more plausibly linked to lifelong latent infection with intermittent reactivation. Although acute infection is a widely used and informative approach to uncover virus-driven molecular pathways, the present study does not address latency, reactivation cycles or chronic low-grade infection, which represent important directions for future research.

Third, while multiple AD-related markers were analyzed—including intracellular Aβ accumulation, tau phosphorylation and autophagy–lysosome pathway alterations—the study focuses primarily on molecular and cellular readouts. Functional neuronal outcomes, such as electrophysiological activity, synaptic integrity or network connectivity, were not assessed and therefore neurodegeneration is inferred at the molecular level rather than demonstrated through functional impairment.

Finally, although the LUHMES system offers practical advantages in terms of reproducibility, scalability and suitability for both 2D and 3D cultures, the findings presented here should be interpreted as mechanistic and exploratory, rather than directly translatable to clinical settings. Further validation in more complex human-based models—such as brain organoids, co-culture systems including glial cells, or in vivo models—will be required to assess the broader physiological and clinical relevance of HSV-1–induced alterations described in this study.

Despite these limitations, the LUHMES-based platform described here provides a valuable and accessible human neuronal model to dissect virus-induced molecular mechanisms relevant to neurodegenerative processes and to support future mechanistic and translational studies.

4. Materials and Methods

4.1. Cell Culture and Differentiation

LUHMES human neuronal precursor cells (BioCat GmbH, Heidelberg, Germany) were cultured as previously described [24]. Briefly, cells were maintained in Nunclon Delta-treated culture plates (ThermoFisher Scientific, Waltham, MA, USA) pre-coated with 50 µg/mL poly-L-ornithine (Sigma-Aldrich, St. Louis, MO, USA) and 1 µg/mL fibronectin (Sigma-Aldrich). Cells were cultured in proliferation medium composed of Advanced DMEM/F12 supplemented with GlutaMAX^{TM} (Gibco, Waltham, MA, USA), 1% N2 supplement (Gibco), 50 µg/mL gentamicin and 40 ng/mL recombinant basic fibroblast growth factor (bFGF; R&D Systems, Minneapolis, MN, USA). Cell passages were performed every 3–4 days.

Neuronal differentiation of LUHMES cultures was performed following previously established protocols [25,26]. For 2D differentiation, cells were switched to differentiation medium containing Advanced DMEM/F12 supplemented with GlutaMAX^{TM}, 1% N2 supplement, 50

https://doi.org/10.3390/ijms27020642

μg/mL gentamicin and 2 μg/mL tetracycline (Sigma-Aldrich), and maintained for 7 days with medium changes every 2–3 days. For 3D differentiations, 5×10^5 LUHMES cells were seeded in 6-well non-treated plates (ThermoFisher Scientific) containing differentiation medium and cultured under orbital agitation at 90 rpm (Celltron shaker system; INFORS HT, Bottmingen, Switzerland). The medium was renewed every 2–3 days. To inhibit residual proliferation, taxol (10 nM; paclitaxel, Sigma-Aldrich) was added on day 3 of differentiation and removed two days later. 3D neuronal aggregates were maintained in differentiation medium for 14 days. After 7 days in 2D cultures and 14 days in 3D cultures, neuronal maturation was assessed by phase-contrast microscopy and by evaluating marker expression using RT-qPCR, Western blot, and immunofluorescence assays.

All LUHMES cultures were incubated at 37 °C in a humidified atmosphere containing 5% CO_2.

4.2. HSV-1 Infection

2D LUHMES cultures were infected with the wild-type HSV-1 strain KOS 1.1 (kindly provided by Dr. L. Carrasco) at different MOI and for various time points as indicated in each experiment. Cells were incubated in a viral solution for 1 h at 37 °C. Then, the unbound virus was removed and replaced with fresh culture medium. Cells were maintained at 37 °C until their collection. Differentiated 2D cultures were infected after 7 days of differentiation.

3D LUHMES aggregates were infected after 14 days of differentiation using different viral doses and incubation times, as specified in each experiment. A fluorescent HSV-1 strain expressing GFP fused to the UL46 tegument protein (UL46-GFP) [52] was also used in selected assays. At 18 hpi, the culture medium was replaced to remove residual extracellular virus, and samples were collected at 4 days post-infection.

Control cultures (mock) were incubated with virus-free suspensions and processed using identical procedures. Both HSV-1 strains were propagated and purified from Vero cells, as previously described [53]. Viral titers in cell culture supernatants were determined by plaque assays as previously described [54].

4.3. Viral DNA Quantification

Total DNA was purified using the NZY Tissue gDNA Isolation kit (NZYtech, Lisbon, Portugal) following the manufacturer's instructions. HSV-1 DNA levels were quantified by real-time qPCR using a CFX-384 Real-Time PCR System (Bio-Rad, Hercules, CA, USA) and a custom-designed TaqMan assay targeting the US12 viral gene (forward primer: 5′-CGTACGCGATGAGATCAATAAAAGG-3′; reverse primer: 5′-GCTCCGGGTCGTGCA-3′; TaqMan probe: 5′-AGGCGGCCAGAACC-3′). Viral DNA content was normalized to the amount of human genomic DNA using a predesigned TaqMan assay for the 18S rRNA gene (Hs9999991_s1; Applied Biosystems, Waltham, MA, USA). Data were analyzed using Bio-Rad CFX maestro 2.2. software. Quantification results are expressed as the number of HSV-1 DNA copies per ng of genomic DNA.

4.4. Immunofluorescence Analysis

4.4.1. 2D Cultures

Cells grown on glass coverslips were fixed in 4% paraformaldehyde (PFA) and permeabilized with blocking solution containing 2% foetal calf serum and 0.2% Triton X-100 in phosphate buffer saline (PBS). Coverslips were then incubated with the corresponding primary antibodies, followed by Alexa Fluor-coupled secondary antibodies, both diluted in blocking solution (Table 1). Finally, nuclei were counterstained with 4,6-diamino-2-phenylindole (DAPI; Merck, Rahway, NJ, USA) in PBS and mounted on glass slides using Mowiol mounting medium (Sigma-Aldrich). All procedures were carried out at room temperature (RT) with samples protected from light.

https://doi.org/10.3390/ijms27020642

Table 1. List of antibodies used in Western blot (WB) and immunofluorescence (IF) analysis.

	Target	Dilution			Reference	Manufacturer
		WB	IF			
			2D	3D		
Primary antibodies	NF200			1:1000	N4142	Sigma (St. Louis, MO, USA)
	βIII-Tub	1:10,000	1:1000	1:1000	ab18207	Abcam (Cambridge, UK)
	MAP2 (2A+2B)	1:250	1:250	1:500	M 1406	Sigma
	MAP2 (2A+2B+2C)	1:250			sc-74421	Santa Cruz (Dallas, TX, USA)
	NeuN		1:250		ab104224	Abcam
	Nestin	1:1000	1:250	1:500	656801	BioLegend (San Diego, CA, USA)
	APP	1:4000			MAB348	Millipore (Burlington, MA, USA)
	Total Tau	1:1000			NB100-82247	Bio-Techne (Abingdon, UK)
	P-Tau Thr205		1:100	1:250	44-738G	ThermoFisher Scientific (Waltham, MA, USA)
	P-Tau Ser422		1:100	1:250	44-764G	ThermoFisher Scientific
	P-Tau Ser202	1:250			ab9674	Sigma
	P-Tau Thr231	1:250			44-746G	ThermoFisher Scientific
	Aβ40		1:250	1:500	44-348A	ThermoFisher Scientific
	Aβ42		1:250	1:500	44-344	ThermoFisher Scientific
	ICP4	1:1000		1:1000	ab6514	Abcam
	ICP8	1:1000			sc-51906	Santa Cruz
	UL42	1:1000			sc-53329	Santa Cruz
	gC	1:3000	1:1000	1:1000	ab6509	Abcam
	gB/gD			1:1000	Provided by Dr. Tabares	---
	LC3/LC3-II	1:1000	1:250	1:500	L7543	Sigma
	Ki-67		1:500	1:500	ab16667	Abcam
	SOX2	1:1000			ab79351	Abcam
	GAPDH	1:1000			sc-51906	Santa Cruz
	α-tubulin	1:10,000			T5168	Sigma
Secondary antibodies	Anti-Mouse-POD	1:25,000			PI-2000	Vector (Newark, CA, USA)
	Anti-Rabbit-POD	1:25,000			GAR/IgG (H+L)/PO	Nordic (Susteren, The Netherlands
	Alexa-488 anti-mouse		1:1000	1:500	A-21202	ThermoFisher Scientific
	Alexa-555 anti-mouse		1:1000	1:500	A-31570	ThermoFisher Scientific
	Alexa-647 anti-mouse		1:1000	1:500	A-31571	ThermoFisher Scientific
	Alexa-488 anti-rabbit		1:1000	1:500	A-21206	ThermoFisher Scientific
	Alexa-555 anti-rabbit		1:1000	1:500	A-31572	ThermoFisher Scientific
	Alexa-647 anti-rabbit		1:1000	1:500	A-31573	ThermoFisher Scientific

4.4.2. 3D Cultures

LUHMES 3D aggregates were collected in 1.5 mL tubes, and immunofluorescence analysis was performed as previously described [26]. Briefly, aggregates were washed once with cold PBS and fixed with 2% PFA for 1 h at 4 °C. After fixation, samples were permeabilized with blocking buffer containing 10% foetal calf serum, 1% bovine serum albumin (BSA) and 0.15% saponin in PBS for 1 h at 4 °C under gentle agitation. Primary antibody incubation was performed in 4-well or 24-well plates for 96 h at 4 °C under agitation, using antibodies diluted in blocking buffer. Then, samples were incubated with Alexa Fluor-coupled secondary antibodies for 72 h at 4 °C under the same conditions. Nuclei were counterstained with DAPI for 1 h at RT with agitation. Finally, after immunostaining, 3D LUHMES aggregates were cleared using RapiClear™ 1.49 (Sunjin Lab, Hsinchu City, Taiwan) to ensure uniform antibody penetration and optical transparency. Aggregates were mounted using 0.25 mm iSpacers (Sunjin Lab) adhered to microscope slides. Aggregates were placed within the iSpacers with minimal PBS, and the chamber was filled with

https://doi.org/10.3390/ijms27020642

RapiClear 1.49 before sealing with a coverslip. Slides were left to dry overnight at RT and stored at 4 °C in the dark until imaging.

4.4.3. Fluorescence and Confocal Microscopy

Sample visualization was carried out using an inverted Axiovert 200M widefield microscope (ZEISS, Jena, Germany) coupled to a PCO edge 4.2 bi camera and a laser scanning ZEISS LSM900 confocal vertical system coupled to an Axio Imager 2 upright microscope (ZEISS). Images were acquired using 40× or 63× oil immersion objectives for cellular visualization and a 20× objective to capture complete 3D aggregates. For 3D cultures, images at 20× magnification were obtained from the central optical plane after acquiring a complete z-stack through the aggregate. In each experiment, 3–5 fields per condition (30–50 cells/field) were imaged, resulting in 150–400 cells analysed per experiment, and all experiments were repeated at least three times independently. Immunofluorescence images were acquired using Metamorph 7.10.5.476 or ZEN Blue 3.4 imaging software and subsequently processed with Fiji/ImageJ v1.54r and Adobe Photoshop 22.1.1.

4.5. Cell Lysates and Western Blot Analysis

Cell lysates were prepared by incubating samples in the radioimmunoprecipitation assay (RIPA) buffer (10 mM Tris-HCl pH 7.5, 50 mM NaCl, 1% Nonidet P-40, 0.2% sodium deoxycholate, 0.1% sodium dodecyl sulphate (SDS), and 1 mM EDTA) supplemented with protease (CompleteTM Mini, EDTA-free Protease Inhibitor Cocktail, Roche, Basel, Switzerland) and phosphatase (PhosSTOPTM, Roche) inhibitors. Protein concentrations in the cell lysates were determined by bicinchoninic acid assay (BCA, ThermoFisher Scientific) according to the manufacturer's instructions. Equal amounts of protein were resolved by Laemmli discontinuous SDS–polyacrylamide gel electrophoresis (SDS-PAGE) and transferred onto nitrocellulose membranes. Membranes were blocked with either 3% BSA and 0.2% Tween 20 in PBS or 5% non-fat milk and 0.2% Tween 20 in PBS. Incubations with primary and peroxidase-coupled secondary antibodies (Table 1) were performed for 1 h at RT. Finally, protein bands were detected using enhanced chemiluminescence reagents (ECL, Amersham Biosciences, Amersham, UK) according to the manufacturer's instructions. Densitometric quantification of protein bands was performed using Image Lab 6.0.1 software (Bio-Rad).

4.6. Quantification of mRNA Levels

mRNA expression levels were determined by RT-qPCR. Total RNA was isolated using the NZY Total RNA Isolation kit (NZYtech). Complementary DNA (cDNA) was synthesized from total RNA using the High-Capacity RNA-to-cDNA Kit (Applied Biosystems). cDNAs were amplified by PCR using primers specific for neural progenitor and neuronal genes (Table 2). Gene expression values were normalized to β-actin, used as a reference gene due to its stable expression across experimental conditions. Real-time qPCR assays were performed in a CFX-384 Real-Time PCR System (Bio-Rad), and data were analyzed using BioRad CFX maestro 2.2. software.

Table 2. List of primers used in RT-qPCR analysis of LUHMES cells differentiation.

Genes *		Forward Primer	Reverse Primer
Proliferation	*MKI67*	5′-ATCGTCCCAGGTGGAAGAGTT-3′	5′-ATAGTAACCAGGCGTCTCGTGG-3′
Neuronal differentiation	*SYN1*	5′-TCAGACCTTCTACCCCAATCA-3′	5′-GTCCTGGAAGTCATGCTGGT-3′
	SYP	5′-CGAGGTCGAGTTCGAGTA CC-3′	5′-AATTCGGCTGACGAGGAGTA-3′
	DRD2	5′-GCCGGGTTGGCAATGATGCA-3′	5′-ACGGCGAGCATCCTGAACTT-3′
Reference	*ACTB*	5′-AGTGTGACGTGGACATCCGCAAAG-3′	5′-ATCCACATCTGCTGGAAGGTGGAC-3′ 5′-GTCCACCTTCCAGCAGATGTGGAT-3′

* *MKI67* (Ki-67); *SYN1* (synapsin I); *SYP* (synaptophysin); *DRD2* (D2 dopamine receptor); *ACTB* (β-actin).

https://doi.org/10.3390/ijms27020642

4.7. Secreted Aβ Measurements

Conditioned media from control and HSV-1-infected samples were assayed for human Aβ40 and Aβ42 levels using commercial sandwich enzyme-linked immunosorbent assay (ELISA) kits (Wako, Tokyo, Japan), following the manufacturer's instructions. Culture media were first collected and inactivated by ultraviolet exposure. After centrifugation, supernatants were stored at −70 °C until use. Prior to analysis, samples were concentrated by lyophilization and resuspended in PBS. An 8-fold concentration was applied for LUHMES 2D cultures and a 4-fold concentration for 3D LUHMES aggregate media. Detection was based on a colorimetric reaction generated by the anti-Aβ detection antibody, and absorbance was measured at 450 nm using a Model 680 microplate reader (Bio-Rad). Final concentrations of Aβ40 and Aβ42 were expressed as picomoles per liter (pM) of culture medium.

4.8. Quantification of Lysosome Load

Lysosomal load was assessed using the acidotropic probe LTR (ThermoFisher Scientific), which freely diffuses across cell membranes and accumulates in acidic organelles. One hour before the end of the treatment period, cells were incubated with 0.5 μM LTR in culture medium for 1 h at 37 °C and subsequently washed with PBS. Cells were then lysed in RIPA buffer and centrifuged at 13,000× *g* for 10 min. Protein concentration in the lysates was determined using the BCA assay. LTR fluorescence intensity in the cell lysates was measured using a FLUOstar OPTIMA microplate reader (BMG LABTECH, Saitama, Japan) with excitation and emission wavelengths of 560 nm and 590 nm, respectively.

4.9. Cathepsin Activity Assays

The enzymatic activity of cathepsins was determined as previously described, with minor modifications [55]. Briefly, cells were lysed under gentle shaking in 50 mM sodium acetate buffer (pH 5.5) containing 0.1 M NaCl, 1 mM EDTA, and 0.2% Triton X-100. Lysates were clarified by centrifugation, and the supernatants were immediately used for the determination of proteolytic activity. A total of 25 μg (cathepsin D/E assay) or 100 μg (cathepsin S assay) of protein from each lysate was incubated for 30 min at 37 °C with the following fluorogenic substrates (Enzo Life Sciences, Farmingdale, NY, USA): Z-VVR-7-amino-4-methylcoumarin (Z-VVR-AMC; 20 μM), a specific substrate for cathepsin S, and Mca-GKPILFFRLK (Dnp)-D-Arg-NH_2 (10 μM), a fluorogenic substrate for cathepsins D and E. Fluorescence resulting from substrate cleavage was measured using a Spark® multimode microplate reader (Tecan, Männedorf, Switzerland) with excitation/emission wavelengths of 360/430 nm for cathepsin S substrate and 320/400 nm for the cathepsin D/E substrate.

4.10. Statistical Analysis

Statistical differences between groups were analyzed pairwise using a two-tailed Student's *t*-test, or a One-sample *t*-test when data were expressed as relative values. ANOVA and multiple comparisons (Dunnet's test) were applied to quantitative data obtained from ELISA. When needed, mixed-effects model was used instead of ANOVA. Statistical significance was set at $p < 0.05$ (*), $p < 0.01$ (**), $p < 0.001$ (***), and $p < 0.0001$ (****). The statistical analyses were performed using Microsoft Excel and GraphPad software 10.5.0.

Supplementary Materials: The following supporting information can be downloaded at: https://www.mdpi.com/article/10.3390/ijms27020642/s1.

Author Contributions: Conceptualization, J.A. and M.J.B.; methodology, M.M.-R., J.A. and M.J.B.; validation, J.A. and M.J.B.; formal analysis, M.M.-R. and J.A.; investigation, M.M.-R., J.A., B.S., I.B. and I.S.; resources, J.A. and M.J.B.; data curation, J.A.; writing—original draft preparation, M.M.-R. and J.A.; writing—review and editing, M.M.-R., B.S., J.A. and M.J.B.; visualization, M.M.-R. and J.A.;

https://doi.org/10.3390/ijms27020642

supervision, J.A. and M.J.B.; project administration, J.A. and M.J.B.; funding acquisition, M.J.B. All authors have read and agreed to the published version of the manuscript.

Funding: This work was funded by the Spanish Ministerio de Ciencia, Innovacion y Universidades (PID2020-113921RB-I00 and PID2024-155549OB-I00). Blanca Salgado is a recipient of a Predoctoral Research Contract from the Spanish Ministerio de Universidades (FPU21/06616).

Institutional Review Board Statement: Not applicable.

Informed Consent Statement: Not applicable.

Data Availability Statement: The original contributions presented in this study are included in the article/Supplementary Materials. Further inquiries can be directed to the corresponding authors.

Acknowledgments: The UL46-GFP HSV-1 strain was kindly provided by Jose A. Lopez-Guerrero (Universidad Autonoma de Madrid), and the anti-gBgD antibody by E. Tabares (Universidad Autonoma de Madrid). Institutional grants from the Fundación Ramón Areces and Banco de Santander to the Centro de Biología Molecular Severo Ochoa are also acknowledged. In addition, we acknowledge the Advanced Light Microscopy Facility (SMOA) at the Centro de Biologia Molecular Severo Ochoa.

Conflicts of Interest: The authors declare no conflicts of interest.

Abbreviations

2D	Two-dimensional
3D	Three-dimensional
AD	Alzheimer's disease
APP	Amyloid precursor protein
Aβ	Beta-amyloid
BCA	Bicinchoninic acid assay
BSA	Bovine serum albumin
cDNA	Complementary DNA
CNS	Central nervous system
DAPI	4,6-diamino-2-phenylindole
ELISA	Sandwich enzyme-linked immunosorbent assay
hpi	Hours post-infection
iPSCs	Induced pluripotent stem cells
HSV-1	Herpes simplex virus type 1
LTR	LysoTracker Red
MAP2	Microtubule-associated protein 2
MOI	Multiplicities of infection
NeuN	Neuronal nuclei antigen
NF200	Neurofilament heavy chain
NFTs	Neurofibrillary tangles
PBS	Phosphate buffer saline
PFA	Paraformaldehyde
PFU	Plaque forming units
RIPA	Radioimmunoprecipitation assay
RT	Room temperature
SD	Standard deviation
SDS	Sodium dodecyl sulphate
SEM	Standard error of the mean
UL46-GFP	HSV-1 strain expressing GFP fused to the UL46 tegument protein

References

1. Dementia. Available online: https://www.who.int/news-room/fact-sheets/detail/dementia (accessed on 4 December 2025).

https://doi.org/10.3390/ijms27020642

2. Breijyeh, Z.; Karaman, R. Comprehensive Review on Alzheimer's Disease: Causes and Treatment. *Molecules* **2020**, *25*, 5789. [CrossRef]
3. Long, J.M.; Holtzman, D.M. Alzheimer Disease: An Update on Pathobiology and Treatment Strategies. *Cell* **2019**, *179*, 312–339. [CrossRef] [PubMed]
4. Herrup, K. The Case for Rejecting the Amyloid Cascade Hypothesis. *Nat. Neurosci.* **2015**, *18*, 794–799. [CrossRef] [PubMed]
5. AmeliMojarad, M.; AmeliMojarad, M.; Cui, X. An Overview on the Impact of Viral Pathogens on Alzheimer's Disease. *Ageing Res. Rev.* **2024**, *104*, 102615. [CrossRef] [PubMed]
6. Herpes Simplex Virus. Available online: https://www.who.int/news-room/fact-sheets/detail/herpes-simplex-virus (accessed on 4 December 2025).
7. Marcocci, M.E.; Napoletani, G.; Protto, V.; Kolesova, O.; Piacentini, R.; Li Puma, D.D.; Lomonte, P.; Grassi, C.; Palamara, A.T.; De Chiara, G. Herpes Simplex Virus-1 in the Brain: The Dark Side of a Sneaky Infection. *Trends Microbiol.* **2020**, *28*, 808–820. [CrossRef] [PubMed]
8. Pinchera, B.; Di Filippo, I.; Cuccurullo, F.; Salvatore, E.; Gentile, I. Alzheimer's Disease and Herpes Viruses: Current Events and Perspectives. *Rev. Med. Virol.* **2024**, *34*, e2550. [CrossRef]
9. Duarte, L.F.; Farías, M.A.; Álvarez, D.M.; Bueno, S.M.; Riedel, C.A.; González, P.A. Herpes Simplex Virus Type 1 Infection of the Central Nervous System: Insights Into Proposed Interrelationships with Neurodegenerative Disorders. *Front. Cell Neurosci.* **2019**, *13*, 46. [CrossRef]
10. Chauhan, P.; Begum, M.Y.; Narapureddy, B.R.; Gupta, S.; Wadhwa, K.; Singh, G.; Kumawat, R.; Sharma, N.; Ballal, S.; Jha, S.K.; et al. Unveiling the Involvement of Herpes Simplex Virus-1 in Alzheimer's Disease: Possible Mechanisms and Therapeutic Implications. *Mol. Neurobiol.* **2024**, *62*, 5850–5874. [CrossRef]
11. Itzhaki, R.F.; Lin, W.R.; Shang, D.; Wilcock, G.K.; Faragher, B.; Jamieson, G.A. Herpes Simplex Virus Type 1 in Brain and Risk of Alzheimer's Disease. *Lancet* **1997**, *349*, 241–244. [CrossRef]
12. Tzeng, N.-S.; Chung, C.-H.; Lin, F.-H.; Chiang, C.-P.; Yeh, C.-B.; Huang, S.-Y.; Lu, R.-B.; Chang, H.-A.; Kao, Y.-C.; Yeh, H.-W.; et al. Anti-Herpetic Medications and Reduced Risk of Dementia in Patients with Herpes Simplex Virus Infections-a Nationwide, Population-Based Cohort Study in Taiwan. *Neurotherapeutics* **2018**, *15*, 417–429. [CrossRef]
13. Vestin, E.; Boström, G.; Olsson, J.; Elgh, F.; Lind, L.; Kilander, L.; Lövheim, H.; Weidung, B. Herpes Simplex Viral Infection Doubles the Risk of Dementia in a Contemporary Cohort of Older Adults: A Prospective Study. *J. Alzheimers Dis.* **2024**, *97*, 1841–1850. [CrossRef]
14. Liu, Y.; Johnston, C.; Jarousse, N.; Fletcher, S.P.; Iqbal, S. Association between Herpes Simplex Virus Type 1 and the Risk of Alzheimer's Disease: A Retrospective Case-Control Study. *BMJ Open* **2025**, *15*, e093946. [CrossRef] [PubMed]
15. Wozniak, M.A.; Mee, A.P.; Itzhaki, R.F. Herpes Simplex Virus Type 1 DNA Is Located within Alzheimer's Disease Amyloid Plaques. *J. Pathol.* **2009**, *217*, 131–138. [CrossRef] [PubMed]
16. Santana, S.; Recuero, M.; Bullido, M.J.; Valdivieso, F.; Aldudo, J. Herpes Simplex Virus Type I Induces the Accumulation of Intracellular β-Amyloid in Autophagic Compartments and the Inhibition of the Non-Amyloidogenic Pathway in Human Neuroblastoma Cells. *Neurobiol. Aging* **2012**, *33*, 430.e19–430.e33. [CrossRef] [PubMed]
17. Alvarez, G.; Aldudo, J.; Alonso, M.; Santana, S.; Valdivieso, F. Herpes Simplex Virus Type 1 Induces Nuclear Accumulation of Hyperphosphorylated Tau in Neuronal Cells. *J. Neurosci. Res.* **2012**, *90*, 1020–1029. [CrossRef]
18. Wang, Z.; Liu, J.; Han, J.; Zhang, T.; Li, S.; Hou, Y.; Su, H.; Han, F.; Zhang, C. Herpes Simplex Virus 1 Accelerates the Progression of Alzheimer's Disease by Modulating Microglial Phagocytosis and Activating NLRP3 Pathway. *J. Neuroinflammat.* **2024**, *21*, 176. [CrossRef]
19. Acuña-Hinrichsen, F.; Covarrubias-Pinto, A.; Ishizuka, Y.; Stolzenbach, M.F.; Martin, C.; Salazar, P.; Castro, M.A.; Bramham, C.R.; Otth, C. Herpes Simplex Virus Type 1 Neuronal Infection Triggers the Disassembly of Key Structural Components of Dendritic Spines. *Front. Cell Neurosci.* **2021**, *15*, 580717. [CrossRef]
20. Nixon, R.A.; Rubinsztein, D.C. Mechanisms of Autophagy-Lysosome Dysfunction in Neurodegenerative Diseases. *Nat. Rev. Mol. Cell Biol.* **2024**, *25*, 926–946. [CrossRef]
21. Choi, Y.; Bowman, J.W.; Jung, J.U. Autophagy during Viral Infection—A Double-Edged Sword. *Nat. Rev. Microbiol.* **2018**, *16*, 341–354. [CrossRef]
22. Chou, C.-C.; Vest, R.; Prado, M.A.; Wilson-Grady, J.; Paulo, J.A.; Shibuya, Y.; Moran-Losada, P.; Lee, T.-T.; Luo, J.; Gygi, S.P.; et al. Proteostasis and Lysosomal Repair Deficits in Transdifferentiated Neurons of Alzheimer's Disease. *Nat. Cell Biol.* **2025**, *27*, 619–632. [CrossRef]
23. Ripa, I.; Andreu, S.; López-Guerrero, J.A.; Bello-Morales, R. Interplay between Autophagy and Herpes Simplex Virus Type 1: ICP34.5, One of the Main Actors. *Int. J. Mol. Sci.* **2022**, *23*, 13643. [CrossRef] [PubMed]
24. Scholz, D.; Pöltl, D.; Genewsky, A.; Weng, M.; Waldmann, T.; Schildknecht, S.; Leist, M. Rapid, Complete and Large-Scale Generation of Post-Mitotic Neurons from the Human LUHMES Cell Line. *J. Neurochem.* **2011**, *119*, 957–971. [CrossRef] [PubMed]

https://doi.org/10.3390/ijms27020642

25. Smirnova, L.; Harris, G.; Delp, J.; Valadares, M.; Pamies, D.; Hogberg, H.T.; Waldmann, T.; Leist, M.; Hartung, T. A LUHMES 3D Dopaminergic Neuronal Model for Neurotoxicity Testing Allowing Long-Term Exposure and Cellular Resilience Analysis. *Arch. Toxicol.* **2016**, *90*, 2725–2743. [CrossRef] [PubMed]
26. Harris, G.; Hogberg, H.; Hartung, T.; Smirnova, L. 3D Differentiation of LUHMES Cell Line to Study Recovery and Delayed Neurotoxic Effects. *Curr. Protoc. Toxicol.* **2017**, *73*, 11.23.1–11.23.28. [CrossRef]
27. Beliakov, S.V.; Blokhin, V.; Surkov, S.A.; Ugrumov, M.V. LUHMES Cells: Phenotype Refinement and Development of an MPP+-Based Test System for Screening Antiparkinsonian Drugs. *Int. J. Mol. Sci.* **2023**, *24*, 733. [CrossRef]
28. Zhang, X.-M.; Yin, M.; Zhang, M.-H. Cell-Based Assays for Parkinson's Disease Using Differentiated Human LUHMES Cells. *Acta Pharmacol. Sin.* **2014**, *35*, 945–956. [CrossRef]
29. Tong, Z.-B.; Huang, R.; Braisted, J.; Chu, P.-H.; Simeonov, A.; Gerhold, D.L. 3D-Suspension Culture Platform for High Throughput Screening of Neurotoxic Chemicals Using LUHMES Dopaminergic Neurons. *SLAS Discov.* **2024**, *29*, 100143. [CrossRef]
30. Whisnant, A.W.; Clark, S.E.; Aguilar-Briseño, J.A.; Durnell, L.A.; Grothey, A.; Miller, A.M.; Varga, S.M.; Meier, J.L.; Grose, C.; Sinn, P.L.; et al. A More Rapid Method for Culturing LUHMES-Derived Neurons Provides Greater Cell Numbers and Facilitates Studies of Multiple Viruses. *Viruses* **2025**, *17*, 1001. [CrossRef]
31. Edwards, T.G.; Bloom, D.C. Lund Human Mesencephalic (LUHMES) Neuronal Cell Line Supports Herpes Simplex Virus 1 Latency In Vitro. *J. Virol.* **2019**, *93*, e02210-18. [CrossRef]
32. Grams, T.R.; Edwards, T.G.; Bloom, D.C. A Viral lncRNA Tethers HSV-1 Genomes at the Nuclear Periphery to Establish Viral Latency. *J. Virol.* **2023**, *97*, e0143823. [CrossRef]
33. Scholz, D.; Chernyshova, Y.; Leist, M. Control of Aβ Release from Human Neurons by Differentiation Status and RET Signaling. *Neurobiol. Aging* **2013**, *34*, 184–199. [CrossRef] [PubMed]
34. Scholz, D.; Chernyshova, Y.; Ückert, A.-K.; Leist, M. Reduced Aβ Secretion by Human Neurons under Conditions of Strongly Increased BACE Activity. *J. Neurochem.* **2018**, *147*, 256–274. [CrossRef] [PubMed]
35. Santana, S.; Bullido, M.J.; Recuero, M.; Valdivieso, F.; Aldudo, J. Herpes Simplex Virus Type I Induces an Incomplete Autophagic Response in Human Neuroblastoma Cells. *J. Alzheimers Dis.* **2012**, *30*, 815–831. [CrossRef] [PubMed]
36. D'Amelio, M.; Puglisi-Allegra, S.; Mercuri, N. The Role of Dopaminergic Midbrain in Alzheimer's Disease: Translating Basic Science into Clinical Practice. *Pharmacol. Res.* **2018**, *130*, 414–419. [CrossRef]
37. Niemeyer, C.S.; Merle, L.; Bubak, A.N.; Baxter, B.D.; Gentile Polese, A.; Colon-Reyes, K.; Vang, S.; Hassell, J.E.; Bruce, K.D.; Nagel, M.A.; et al. Olfactory and Trigeminal Routes of HSV-1 CNS Infection with Regional Microglial Heterogeneity. *J. Virol.* **2024**, *98*, e00968-24. [CrossRef]
38. Salgado, B.; Sastre, I.; Bullido, M.J.; Aldudo, J. Herpes Simplex Virus Type 1 Induces AD-like Neurodegeneration Markers in Human Progenitor and Differentiated ReNcell VM Cells. *Microorganisms* **2023**, *11*, 1205. [CrossRef]
39. Barrozo, E.R.; Nakayama, S.; Singh, P.; Neumann, D.M.; Bloom, D.C. Herpes Simplex Virus 1 MicroRNA miR-H8 Is Dispensable for Latency and Reactivation In Vivo. *J. Virol.* **2021**, *95*, e02179-20. [CrossRef]
40. Hogberg, H.T.; Bressler, J.; Christian, K.M.; Harris, G.; Makri, G.; O'Driscoll, C.; Pamies, D.; Smirnova, L.; Wen, Z.; Hartung, T. Toward a 3D Model of Human Brain Development for Studying Gene/Environment Interactions. *Stem Cell Res. Ther.* **2013**, *4*, S4. [CrossRef]
41. Kristen, H.; Sastre, I.; Muñoz-Galdeano, T.; Recuero, M.; Aldudo, J.; Bullido, M.J. The Lysosome System Is Severely Impaired in a Cellular Model of Neurodegeneration Induced by HSV-1 and Oxidative Stress. *Neurobiol. Aging* **2018**, *68*, 5–17. [CrossRef]
42. Jamieson, G.A.; Maitland, N.J.; Wilcock, G.K.; Craske, J.; Itzhaki, R.F. Latent Herpes Simplex Virus Type 1 in Normal and Alzheimer's Disease Brains. *J. Med. Virol.* **1991**, *33*, 224–227. [CrossRef]
43. Eimer, W.A.; Vijaya Kumar, D.K.; Navalpur Shanmugam, N.K.; Rodriguez, A.S.; Mitchell, T.; Washicosky, K.J.; György, B.; Breakefield, X.O.; Tanzi, R.E.; Moir, R.D. Alzheimer's Disease-Associated β-Amyloid Is Rapidly Seeded by Herpesviridae to Protect against Brain Infection. *Neuron* **2018**, *99*, 56–63.e3; Correction in *Neuron* **2018**, *100*, 1527–1532. [CrossRef] [PubMed]
44. D'Mello, S.R. When Good Kinases Go Rogue: GSK3, P38 MAPK and CDKs as Therapeutic Targets for Alzheimer's and Huntington's Disease. *Int. J. Mol. Sci.* **2021**, *22*, 5911. [CrossRef] [PubMed]
45. Martin, C.; Aguila, B.; Araya, P.; Vio, K.; Valdivia, S.; Zambrano, A.; Concha, M.I.; Otth, C. Inflammatory and Neurodegeneration Markers during Asymptomatic HSV-1 Reactivation. *J. Alzheimers Dis.* **2014**, *39*, 849–859. [CrossRef] [PubMed]
46. De Chiara, G.; Piacentini, R.; Fabiani, M.; Mastrodonato, A.; Marcocci, M.E.; Limongi, D.; Napoletani, G.; Protto, V.; Coluccio, P.; Celestino, I.; et al. Recurrent Herpes Simplex Virus-1 Infection Induces Hallmarks of Neurodegeneration and Cognitive Deficits in Mice. *PLoS Pathog.* **2019**, *15*, e1007617. [CrossRef]
47. Cairns, D.M.; Smiley, B.M.; Smiley, J.A.; Khorsandian, Y.; Kelly, M.; Itzhaki, R.F.; Kaplan, D.L. Repetitive Injury Induces Phenotypes Associated with Alzheimer's Disease by Reactivating HSV-1 in a Human Brain Tissue Model. *Sci. Signal.* **2025**, *18*, eado6430. [CrossRef]

https://doi.org/10.3390/ijms27020642

48. Rybak-Wolf, A.; Wyler, E.; Pentimalli, T.M.; Legnini, I.; Oliveras Martinez, A.; Glažar, P.; Loewa, A.; Kim, S.J.; Kaufer, B.B.; Woehler, A.; et al. Modelling Viral Encephalitis Caused by Herpes Simplex Virus 1 Infection in Cerebral Organoids. *Nat. Microbiol.* **2023**, *8*, 1252–1266. [CrossRef]
49. D'Aiuto, L.; Bloom, D.C.; Naciri, J.N.; Smith, A.; Edwards, T.G.; McClain, L.; Callio, J.A.; Jessup, M.; Wood, J.; Chowdari, K.; et al. Modeling Herpes Simplex Virus 1 Infections in Human Central Nervous System Neuronal Cells Using Two- and Three-Dimensional Cultures Derived from Induced Pluripotent Stem Cells. *J. Virol.* **2019**, *93*, e00111-19. [CrossRef]
50. Cairns, D.M.; Rouleau, N.; Parker, R.N.; Walsh, K.G.; Gehrke, L.; Kaplan, D.L. A 3D Human Brain-like Tissue Model of Herpes-Induced Alzheimer's Disease. *Sci. Adv.* **2020**, *6*, eaay8828. [CrossRef]
51. Cairns, D.M.; Itzhaki, R.F.; Kaplan, D.L. Potential Involvement of Varicella Zoster Virus in Alzheimer's Disease via Reactivation of Quiescent Herpes Simplex Virus Type 1. *J. Alzheimers Dis.* **2022**, *88*, 1189–1200. [CrossRef]
52. Willard, M. Rapid Directional Translocations in Virus Replication. *J. Virol.* **2002**, *76*, 5220–5232. [CrossRef]
53. Carrascosa, A.L.; Santarén, J.F.; Viñuela, E. Production and Titration of African Swine Fever Virus in Porcine Alveolar Macrophages. *J. Virol. Methods* **1982**, *3*, 303–310. [CrossRef]
54. Santana, S.; Sastre, I.; Recuero, M.; Bullido, M.J.; Aldudo, J. Oxidative Stress Enhances Neurodegeneration Markers Induced by Herpes Simplex Virus Type 1 Infection in Human Neuroblastoma Cells. *PLoS ONE* **2013**, *8*, e75842. [CrossRef]
55. Porter, K.; Nallathambi, J.; Lin, Y.; Liton, P.B. Lysosomal Basification and Decreased Autophagic Flux in Oxidatively Stressed Trabecular Meshwork Cells: Implications for Glaucoma Pathogenesis. *Autophagy* **2013**, *9*, 581–594. [CrossRef]

Disclaimer/Publisher's Note: The statements, opinions and data contained in all publications are solely those of the individual author(s) and contributor(s) and not of MDPI and/or the editor(s). MDPI and/or the editor(s) disclaim responsibility for any injury to people or property resulting from any ideas, methods, instructions or products referred to in the content.

https://doi.org/10.3390/ijms27020642

MDPI AG
Grosspeteranlage 5
4052 Basel
Switzerland
Tel.: +41 61 683 77 34

International Journal of Molecular Sciences Editorial Office
E-mail: ijms@mdpi.com
www.mdpi.com/journal/ijms



Disclaimer/Publisher's Note: The title and front matter of this reprint are at the discretion of the Guest Editor. The publisher is not responsible for their content or any associated concerns. The statements, opinions and data contained in all individual articles are solely those of the individual Editor and contributors and not of MDPI. MDPI disclaims responsibility for any injury to people or property resulting from any ideas, methods, instructions or products referred to in the content.





Academic Open
Access Publishing

mdpi.com

ISBN 978-3-7258-9276-1